

Ivo Häring

Risk Analysis and Management: Engineering Resilience

Risk Analysis and Management: Engineering Resilience

Ivo Häring

Risk Analysis and Management: Engineering Resilience



Springer

@Seismicisolation

Ivo Häring
Fraunhofer Ernst-Mach-Institut
Efringen-Kirchen
Germany

ISBN 978-981-10-0013-3
DOI 10.1007/978-981-10-0015-7

ISBN 978-981-10-0015-7 (eBook)

Library of Congress Control Number: 2015952989

Springer Singapore Heidelberg New York Dordrecht London
© Springer Science+Business Media Singapore 2015

This work is subject to copyright. All rights are reserved by the Publisher, whether the whole or part of the material is concerned, specifically the rights of translation, reprinting, reuse of illustrations, recitation, broadcasting, reproduction on microfilms or in any other physical way, and transmission or information storage and retrieval, electronic adaptation, computer software, or by similar or dissimilar methodology now known or hereafter developed.

The use of general descriptive names, registered names, trademarks, service marks, etc. in this publication does not imply, even in the absence of a specific statement, that such names are exempt from the relevant protective laws and regulations and therefore free for general use.

The publisher, the authors and the editors are safe to assume that the advice and information in this book are believed to be true and accurate at the date of publication. Neither the publisher nor the authors or the editors give a warranty, express or implied, with respect to the material contained herein or for any errors or omissions that may have been made.

Printed on acid-free paper

Springer Science+Business Media Singapore Pte Ltd. is part of Springer Science+Business Media
(www.springer.com)

@Seismicisolation

Acknowledgments

The preparation of this textbook has been partially supported by the Federal Ministry of Education and Research (BMBF) within the Federal Government—German Federal State competition “Advancement through Education: Open Universities.”



Contents

1	Introduction, Overview and Acknowledgements	1
1.1	Introduction	1
1.2	Selected Features of Text	2
1.3	Background and Research Programs	3
1.4	Structure of Text	5
	References	8
2	Introduction to Risk Analysis and Risk Management Processes	9
2.1	Overview	9
2.2	Fundamental Definitions	11
2.2.1	Threat Scenario Type, Hazard Events	11
2.2.2	Risk	11
2.2.3	Classification of Risk.	13
2.2.4	Risk Management and Risk Analysis	13
2.2.5	Overview	14
2.3	Examples for Risk Management and Risk Analysis Schemes.	14
2.3.1	Loading-Based Assessment	14
2.3.2	Scenario-Based Assessment	14
2.3.3	5-Step Risk Management Scheme	15
2.3.4	Risk Management Schemes for Explosive Safety Scenarios	16
2.4	Attributes of the Risk Analysis and Risk Management Processes	19
2.5	Risk Analysis and Management Process.	19
2.6	Typical Dependencies of Risk Management Steps	23
2.7	Summary and Outlook.	24
2.8	Questions	25
2.9	Answers.	26
	References	26

3	Introduction to Database Analysis of Terroristic Events	27
3.1	Overview	27
3.2	Database Analysis Scheme	28
3.3	Mathematical Notations	30
3.4	Spotting Data and Data Acquisition	30
3.4.1	Definition of Events	30
3.4.2	Sources for Data Gathering	33
3.4.3	Automation of Data Spotting and Gathering	34
3.4.4	Clustering	34
3.5	Adjustment	35
3.6	Database Design	36
3.7	The Database	41
3.8	Data Selection	42
3.9	Data Preparation	43
3.10	Selection and Application of Simple Statistical Methods	44
3.10.1	Total Numbers of Events/Attribute	44
3.10.2	Sums Over Time Intervals	45
3.10.3	Sums Over Other Classes of Attributes	46
3.10.4	Computing Frequencies	46
3.11	Selection of Visualization Methods and Visualization	51
3.12	Use of Database Analysis in the Risk Management Process	51
3.13	Summary and Outlook	53
3.14	Questions	53
3.15	Answers	55
	References	58
4	More Elaborate Database Analysis for Risk and Resilience Analysis	61
4.1	Overview	61
4.2	F-N Curves	62
4.2.1	Selection and Application of the Method	62
4.2.2	Selection of the Visualization Method	64
4.3	Time Series	64
4.3.1	Definition of Time Series	64
4.3.2	Smoothing	65
4.3.3	Correlation	65
4.3.4	Autocorrelation	67
4.3.5	Trend	68
4.3.6	Cycles	70
4.3.7	Forecast	71
4.3.8	Matching this Section with the Diagram from Chap. 3	75
4.3.9	More about Time Series Analysis	76
4.4	Risk Maps	76

4.5	Summary and Outlook	79
4.6	Questions	79
4.7	Answers	81
	References	88
5	Event Analysis: Initial Situation and Hazard Source	91
5.1	Overview	91
5.2	Event Analysis in the Risk Management Process	93
5.3	Event Analysis of Representative Terror Events on Airports	94
5.4	Hazards and Scenarios for the Numerical Simulation of the Risk of Progressive Collapse of a Building	97
5.5	Scenario Analysis in the Project “Urban Risk Analysis”	101
5.5.1	The Project	101
5.5.2	Fatal Accident Rate	101
5.5.3	Database Analysis	102
5.5.4	Event Frequency	105
5.5.5	Extent of Damage	107
5.5.6	Risk Map	107
5.5.7	Summary	108
5.6	Analysis of Future Threats to Civil Aviation	109
5.6.1	Categorization of Present and Future Threats	110
5.6.2	Prioritization of the Threats	110
5.7	Summary and Outlook	111
5.8	Questions	111
5.9	Answers	112
	References	112
6	Hazard Propagation I: Explosions and Blast	115
6.1	Overview	115
6.2	Characterization of Explosions	117
6.2.1	Natural Versus Man-Made	117
6.2.2	Surrounding Media and Explosive Material	117
6.2.3	Intentional Explosions	117
6.2.4	Accidental Explosions	119
6.2.5	Terroristic Explosions	120
6.3	Overview of Physical Consequences and Damage Due to Explosions	120
6.4	Explosions in Air and Their Characteristics: Physical Consequences	123
6.4.1	General Definition of Explosion	123
6.4.2	Ideal Explosions, Point Source	124
6.5	Build-up of Blast Wave from Point Source	125
6.6	Blast Hazard Characterization: Pressure-Time History, Overpressure, Blast Impulse	127

6.7	Scaling Laws	128
6.8	Limiting Cases of the Blast Loading of a Single Degree of Freedom Model: Static Loading, Impulsive Loading and Quasi-Static Loading	130
6.9	Summary and Outlook	133
6.10	Questions	133
	References	134
7	Hazard Source Characterization and Propagation II: Fragments	137
7.1	Overview	137
7.2	General Description and Assumptions	138
7.3	Coordinate Systems	139
7.3.1	Polar Geocentric Coordinates	139
7.3.2	Cartesian Coordinates	139
7.4	Convex Hull and the Cauchy Theorem	141
7.5	Fragment Matrix	143
7.6	Fragment Trajectories	145
7.7	Experimental Assessment of Debris Launch Conditions	146
7.8	Fragment Density	148
7.9	Summary and Outlook	150
7.10	Questions	151
	References	153
8	Hazard Propagation III: Free Field Blast and Complex Blast: Empirical-Analytical Expressions and Scaled Experiments	155
8.1	Overview	155
8.2	Free Field Side-On Overpressure and Blast Impulse for TNT: Kingery and Bulmash Parameterizations	156
8.3	TNT Equivalent for Overpressure and Blast: Examples of the Computation of Overpressure and Blast Impulse	158
8.4	Determination of Complex Blast Hazard with Scaled Experiments	160
8.4.1	Determination of Complex Blast Engineering Scaling Factors from Scaled Experiments	162
8.5	Summary and Outlook	164
8.6	Questions	165
	References	165
9	Mathematical Basics for Hazard and Damage Analysis	167
9.1	Overview	167
9.2	Probability Theory	168
9.2.1	One-dimensional Density Functions: Empirical Density Function and Probability Density Function	168
9.2.2	Probabilities	170

9.2.3	Expectation/Mean and Standard Deviation	171
9.2.4	Examples for Density Functions	172
9.3	Vectors, Planes and Angles in \mathbb{R}^3	172
9.3.1	Sums, Scalar Product and Angle	172
9.3.2	Straight Lines	174
9.3.3	Planes and Normal Vectors	174
9.3.4	Matrices	177
9.3.5	Rotation Matrices	178
9.4	Euler Angles	179
9.5	Summary and Outlook	180
9.6	Questions	180
9.7	Answers	181
	References	185
10	Damage Analysis I: Probit Functions and Probability Distributions	187
10.1	Overview	187
10.2	Direct and Indirect Damage Analysis	189
10.3	Probit Functions or Normal Distribution from Binary Choice	192
10.4	Probit Distribution and Probit Function	194
10.5	Application of the Probit Approach to Damage Assessment in Terms of Overpressure and Scaled Distance	196
10.6	Examples for Probit Functions for Damage Analysis of Non-explosive Events	198
10.7	Alternative Distributions for Parameterizations for Blast and Fragment Effects	198
	10.7.1 Damage Analysis in the Literature	198
	10.7.2 Other Distributions for Damage Analysis	199
	10.7.3 Free Parameterizations in Terms of Several Parameters	200
10.8	Fragment Effects on Personal	200
	10.8.1 Critical Values	200
	10.8.2 Example for Probability Distributions	201
	10.8.3 Probit Function from Range Commander Council	201
	10.8.4 Free Parameterizations: Model by Mercx	202
10.9	Summary and Outlook	202
	References	202
11	Damage Analysis II: Selection of Distributions and Determination of Parameters	205
11.1	Overview	205
11.2	Overview: Determination of Probability Distributions	206
11.3	Graphical Method for Parameter Estimation	207
	11.3.1 Normal Distribution	207

11.3.2	Lognormal Distribution	207
11.3.3	Weibull Distribution	207
11.4	Normal and Weibull Distribution for Damage Assessment of Blast Effects: Case Study for Damage Assessment Using Resampling	209
11.5	Literature About Statistical Methods	212
11.6	Summary and Outlook	213
11.7	Questions	213
	References	214
12	Damage Analysis III: Object Densities, Presented Surfaces Based on Exposure, Geometry and Damage Models	215
12.1	Overview	215
12.2	Areal Object Density for Quantifying Exposure	217
12.3	Presented Surface	218
12.3.1	Presented Surface of a Cuboid	218
12.3.2	Other Presented Surfaces	221
12.4	Monte Carlo Computation of Presented Surfaces	223
12.4.1	Motivation	223
12.4.2	The Model	224
12.4.3	Monte Carlo Methods	226
12.4.4	Discretization of the Relevant Surface	228
12.5	Relevant Presented Surface	230
12.6	Summary and Outlook	232
	References	232
13	Hazard Event Frequency, Distribution of Objects and Success Frequency of Avoiding Hazards	233
13.1	Overview	233
13.2	Hazard Event Frequency	235
13.2.1	Event Frequencies from the Historical Record	236
13.2.2	Event Frequencies from Fault Tree Analysis	237
13.3	Discrete Distribution of Objects	237
13.3.1	Example: The “Real World Scenario”	239
13.3.2	The Scenario in More Detail	240
13.3.3	Individual Exposure	241
13.3.4	Individual Local and Non-local Risk	242
13.3.5	Average Presence	243
13.3.6	Formalization	246
13.4	Success Frequency of Avoiding Hazards	248
13.5	Summary and Outlook	249
	References	249
14	Risk Computation and Visualization	251
14.1	Overview	251
14.2	Individual Versus Collective Risk	252

14.3	Risk Computation	255
14.3.1	Individual Local Risks Due to Single Stationary Hazard Source and Combination of Damage Effects.	255
14.3.2	Possible Event Locations Distributed on 3D Line: F-N Curve Generation	257
14.3.3	Local Annual Risk in Case of Multiple Threats: Object-Wise Empirical-Analytical Approach	257
14.3.4	Local Risk in Case of Multiple Possible Event Types and Locations	258
14.4	Examples for Risk Mapping	260
14.5	Risk Matrix	261
14.6	Risk Graph.	262
14.7	Summary and Outlook.	264
	References.	269
15	Simple Examples of Risk Analysis	271
15.1	Overview	271
15.2	Database Analysis: Terrorist Threat to Underground Traffic Systems.	272
15.2.1	Database Analysis for Worldwide Underground Traffic Systems.	272
15.2.2	Quantitative Risk Evaluation.	274
15.2.3	Potential Risks and Derived Scenarios	274
15.2.4	The Given Example and the Risk Management Process	275
15.3	Credit Card Example	276
15.3.1	The Given Example and the Risk Management Process	276
15.4	Summary and Outlook.	278
15.5	Questions	279
15.6	Answers.	279
	References.	280
16	Risk Analysis and Management Example for Increasing Harbour Security in Case of Bulk Scanning of Containers	281
16.1	Overview	281
16.2	Event Analysis	284
16.2.1	Database Analysis	284
16.2.2	Table of Hazards.	286
16.2.3	Derived Scenarios	287
16.3	Hazard Analysis	287
16.3.1	Explosions Under Free Field Conditions	287
16.3.2	Blast Hazard.	288
16.3.3	Side-on and Reflected Pressure and Impulse.	289

16.3.4	TNT Equivalent	290
16.3.5	Overpressure	290
16.3.6	Projection Hazard: Debris Throw	292
16.3.7	Hazard Through Thermal Radiation	295
16.3.8	Radioactive Material After an Explosion	297
16.4	Damage Analysis	298
16.4.1	Blast in Explosions Under Free Field Conditions	298
16.4.2	Damage to Persons by Thermal Radiation	301
16.4.3	Damage to Persons by Propagation of Radioactive Material	302
16.5	Damage Analysis of the Scenarios	306
16.6	Risk Analysis	306
16.6.1	Probability of Occurrence	307
16.6.2	Damage	307
16.6.3	Collective Risk (Societal Risk)	308
16.7	Summary	309
16.8	Questions	310
	References	310
17	Risk Acceptance Criteria	313
17.1	Overview	313
17.2	Concepts and Methods	315
17.2.1	Three Principles of Defining Risk Acceptance Criteria	316
17.2.2	Individual and Collective Risks Based on the Classical Formula of Risks	317
17.2.3	Fatal Accident Rate	317
17.2.4	Lost Life-Years	318
17.2.5	Localized Individual Risk and Risk Contours	319
17.2.6	ALARP	319
17.2.7	F-N Curves	319
17.2.8	Construction of an F-N Curve in Practice	320
17.2.9	Risk Map/Matrix	326
17.3	Health and Safety Executive Boundaries	326
17.4	Examples for Risk Criteria by Sectors	328
17.4.1	Risks for Landslides	328
17.4.2	Risks for Liquefied Natural Gas Crew	328
17.4.3	Risks for Ammunition Storage Workers	330
17.4.4	Risk Criteria by Proske	330
17.4.5	Examples for Risk Criteria by Country	332
17.5	Risk Criteria for Humanitarian Demining	337
17.6	Risk Evaluation and Communication	338
17.7	Summary	339

Contents	xv
17.8 Questions	339
17.9 Answers	340
References	341
18 Risk Mitigation and Chance Enhancement Measures for Improving Resilience	343
18.1 Overview	343
18.2 Organizational Mitigation Measures	344
18.3 Building Design	345
18.4 Barriers (Far-Out and Close-In)	346
18.5 Secondary Facades: Multifunctional Hulls	347
18.6 Structural Reinforcement Systems	348
18.7 What Do the Mitigation Measures Reduce?	349
18.8 Decisive Factors	350
18.9 Secondary Risks	351
18.10 Summary and Outlook	351
References	352
Index	353

Abbreviations

AFNOR	Association Française de Normalisation
ANSI	American National Standards
BB	Birnbaum
BFA	Bouncing failure analysis
BSI	British Standard Institute
C	Consequences
D	Column of the FMEA in relation to legal requirements
DC	Diagnostic coverage
DFM	Double failure matrix
DFTA	Dynamic fault tree analysis
DIN	Deutsches Institut für Normung
e.g.	For example
E/E/PE	Electrical/electronic/programmable electronic
ECT	Estimated number of computing operations (estimated computing time)
EMM	European media monitor
EN	European norm
EPS	Emergency power system
ES	Exposed site
ESQRA-GE	German explosive safety quantitative risk analysis
ETA	Event tree analysis
EUC	Equipment under control
EZRT	Entwicklungszentrum für Röntgentechnik
FEM	Finite element method
FHA	Fault hazard analysis
FIT	Failure in time
FIT	Failures in time
FMEA	Failure modes and effects analysis
FMECA	Failure modes and criticality analysis
FMEDA	Failure modes, effects, and diagnostic coverage analysis
F-N-curve	Frequency–number curve

f-N-curve	Frequency–number curve
FSQRA	Fuze Safety Quantitative Risk Analysis
FTA	Fault tree analysis
FV	Fussell-Vesely
GTD	Global Terrorism Database
HL	Hazard log
i.e.	That is
IBD	Internal block diagram
IEC	International Electrotechnical Commission
IED	Improvised explosive device
IEV	International Electrotechnical Vocabulary
INS	Immediate, necessary, and sufficient
ISO	International Organization for Standardization
JRC	Joint Research Center
LPG	Liquefied petroleum gas
MIPT	Memorial Institute for the Prevention of Terrorism
MOB	Multiple occurring branch
MOE	Multiple occurring event
MTTF	Mean in time to the next failure
NASA	National Aeronautics and Space Administration
NEQ	Net explosive quantity
O&SHA	Operating and support hazard analysis
ON	Österreichisches Normeninstitut
P	Probability
PC	Parts count
PD	Probability of default
PES	Potential explosive site
PFD	Probability of failure on demand
PFH	Probability of failure per hour
PHA	Preliminary hazard analysis
PHL	Preliminary hazard list
PSC	Preliminary, secondary, and command
R	Risk
RADC	Rome Air Development Center
RAF	Red Army Faction
RAW	Risk achievement worth
Rem	Roentgen equivalent in man
RF	Risk factor
RPN	Risk priority number
RPZ	Risikoprioritätszahl
RRSE	Root relative square error
RRW	Risk reduction worth
SD	Sequence diagram
SDOF	Single degree of freedom
SFF	Safe failure fraction

SHA	System hazard analysis
SIL	Safety integrity level
SMA	Simple moving average
SMD	State machine diagram
SNV	Schweizerische Normenvereinigung
SQL	Structured Query Language
SRS	Software requirements specification
SSHA	Subsystem hazard analysis
SS-SC	State of system–state of component
START	National Consortium for the Study of Terrorism and Responses to Terrorism
Sv	Sievert
SysML	Systems Modeling Language
TED	Terror event database
TEDAS	Terror Event Database Analysis software
TM	Team member
TNT	Trinitrotoluene
TS-FTA	Takagi-Sugeno fault tree analysis
UK	United Kingdom
UML	Unified Modeling Language
UNI	Ente Nazionale Italiano di Unification
V	Verification and validation
VBIED	Vehicle-born improvised explosive device
VDA	Verband der Automobilindustrie

Mathematical Notations

π	Adjustment factor
\wedge	And
ω	Angular frequency
\bar{x}	Arithmetic mean
$\rho(k)$	Autocorrelation function
$\hat{\gamma}(k)$	Autocovariance
ρ_k	Autocovariance coefficient
$ A $	Cardinality of A
\overline{A}	Complement of A
Ω	Complete space
$P(B A)$	Conditional probability of B given A
C	Consequences
r_{xy}	Correlation coefficient
R_{crit}	Critical risk quantity
D	Detection rating
\emptyset	Empty set
\cup_{ex}	Exclusive union
$E(t)$	Expected value
$f(t)$	Failure density
$F(t)$	Failure probability
$\lambda(t)$	Failure rate
F	Feasibility rating
f	Frequency
I	Impulse
\cap	Intersection
\tilde{x}	Median
\mathbb{N}_0	Nonnegative integers
\neg	Not
$\#$	Number of
O	Occurrence rating

\vee	Or
T	Period
\mathbb{N}	Positive integers
P, p	Pressure
P	Probability
Pr	Probit
Rb	Reliability
R	Risk
S	Severity rating
α	Smoothing constant
$\Delta\Omega$	Solid angle surface element
s_x	Standard deviation
\subseteq	Subset
\cup	Union
s_x^2	Variance
\setminus	Without

List of Figures

Figure 2.1	Blaise Pascal. © Juulijs—Fotolia	12
Figure 2.2	First scheme of the risk management and risk analysis process	14
Figure 2.3	The scenario that a suitcase bomb is being placed next to a building	15
Figure 2.4	Catchwords and pictograms for the 5-step risk management scheme	16
Figure 2.5	ESQRA-GE risk management scheme (Radtke et al. 2011)	17
Figure 2.6	Overview of hazard and risk analysis modeling steps (Häring et al. 2009). Reprinted from Reliability and System Safety Engineering, Vol. 94, Issue 9, I. Häring, M. Schönherr, C. Richter, Quantitative hazard and risk analysis for fragments of high explosive shells in air, pp. 1461–1470, Copyright 2009, with permission from Elsevier	17
Figure 2.7	AASTP 4—scheme to develop a risk-based decision approach (AASTP-4 Ed. 1 2011). Reprinted from Allied Ammunition Storage and Transport Publication: Manual on explosives safety risk analysis (AASTP-4 Ed.1), Nato Standardization Organization, 2011	18
Figure 2.8	AASTP 4—scheme to apply a risk-based decision aid. The scheme uses the abbreviations for potential explosive site (<i>PES</i>) and exposed site (<i>ES</i>) (AASTP-4 Ed. 1 2011). Reprinted from Allied Ammunition Storage and Transport Publication: Manual on explosives safety risk analysis (AASTP-4 Ed.1), Nato Standardization Organization, 2011	19
Figure 2.9	First scheme of the risk management and risk analysis process	22
Figure 2.10	Second scheme of the risk management and risk analysis process	23

Figure 3.1	Scheme for database analysis.	29
Figure 3.2	Scheme for modular software architecture to cluster data (Kleb 2006)	35
Figure 3.3	Scheme of the terror event database (<i>TED</i>) (Siebold 2007)	37
Figure 3.4	Number of events in France per quarter (Siebold 2007)	43
Figure 3.5	Events in Germany per quarter from 1968 to 2004 (Siebold 2007).	46
Figure 3.6	Percentage of fatalities per group in Northern Ireland from 1968 to 2004, absolute numbers of fatalities can be found in the legend (Siebold 2007)	50
Figure 3.7	Number of events per country (Siebold 2007)	51
Figure 3.8	Frequencies of the different attack types in Brazil from 1970 to 2010.	58
Figure 4.1	Collective risk criteria for the UK (<i>blue line</i>), the Netherlands (<i>orange</i>), and Czechoslovakia (<i>red</i>) (Schönherr 2009)	63
Figure 4.2	Simple moving average ($k = 3$)	66
Figure 4.3	Simple moving average ($k = 15$)	66
Figure 4.4	Weighted moving average ($k = 3$) with weights 0.25, 0.5 and 0.25	67
Figure 4.5	Exponential smoothing ($\alpha = 0.3$)	67
Figure 4.6	Scattergram: Number of casualties and fatalities per quarter in France from 1968 to 2004 and the regression line (Siebold 2007)	68
Figure 4.7	Typical correlograms for a trend, b white noise, c cycles, d trend + cycles, e cycles + white noise, f trend + white noise, g trend + cycles + white noise, where “+” means that the time series were added (Siebold 2007)	69
Figure 4.8	Polynomial trend for $k = 6$ for events in Germany between 1968 and 2004 per quarter (Siebold 2007)	70
Figure 4.9	Polynomial trend for $k = 2$ for events in Germany between 1968 and 2004 per quarter (Siebold 2007)	70
Figure 4.10	Periodograms of artificial time series for a trend, b white noise, c cycles, d trend + cycles, e cycles + white noise, f trend + white noise, g trend + cycles + white noise, where “+” means that the time series were added (Siebold 2007)	72

Figure 4.11	Bartlett 2 Window for the number of events in Germany per quarter from a 1968 to 1997 and b 1998 to 2004, and after (multiplicatively) removing a linear trend for c 1968 to 1997 and d 1998 to 2004 (Siebold 2007)	73
Figure 4.12	Averaged rrse as a function of the smoothing constant α from (Siebold 2007)	74
Figure 4.13	Risk map worldwide, consequences over frequency diagram: costs per event over events per year from terror event database (Brombacher 2005)	76
Figure 4.14	Extension of Fig. 4.13 by lines showing the risk R (Brombacher 2005)	77
Figure 4.15	Extension of Fig. 4.14 by a categorization by colors into low (<i>green</i>) and high (<i>red</i>) risks (Brombacher 2005)	77
Figure 4.16	Correlogram for a Chile and b Italy, 1968–2004 (Siebold 2007)	80
Figure 4.17	Time series of injuries in Great Britain for terroristic attacks, 1970–2010, with data from (National Consortium for the Study of Terrorism and Responses to Terrorism (START) 2011)	82
Figure 4.18	Time series after smoothing with SMA	83
Figure 4.19	Time series after exponential smoothing	84
Figure 4.20	Correlogram for the time series of injuries in Great Britain, 1970–2010	84
Figure 4.21	Periodogram for the time series of injuries in Great Britain, 1970–2010	84
Figure 4.22	Recognition of cycles in the time series	85
Figure 4.23	Polynomial trend function of order 3	86
Figure 4.24	Linear trend function of order 1	87
Figure 5.1	Worldwide distribution of attacks on airports from 1968 to 2007 (Ziehm et al. 2010)	95
Figure 5.2	Used attacks from 1968 to 2007 (Ziehm et al. 2010)	96
Figure 5.3	Scheme of attack locations at European airports (1968–2007). For 16 attacks no description of their location is available (Ziehm et al. 2010)	97
Figure 5.4	Distribution of attacks by target categories with information from TED (Rinder et al. 2011)	98
Figure 5.5	Development of terrorist attacks from 1968 to 2007 for the three target categories “ministry”, “finance/insurance” and “energy” (Rinder et al. 2011). The development is shown in per cent of the total number over the time span. The attack types are	

listed on the right. The percentage is taken from the total number of attacks on the three target categories. E.g. 100 % corresponding to 3622 events for explosives are obtained by summing up the percentages for the 8 data points representing 5 years, respectively.....	99
Figure 5.6 Distribution of 130 researched events with complete or partial collapse by building types (Rinder et al. 2011).....	100
Figure 5.7 Percentage breakdown of the attacks on the first level of target resolution in per cent. The regarded time period is 1965–2004 (Mayrhofer 2010).	103
Figure 5.8 Percentage breakdown of the attacks on the second level of target resolution. The regarded time period is 1965–2004 (Mayrhofer 2010)	103
Figure 5.9 Absolute number of attacks on the third level of target resolution. The regarded time period is 1965–2004 (Mayrhofer 2010).	104
Figure 5.10 Percentage breakdown of the attacks on the first level of target resolution for different time periods. The regarded time period is 1965–2004 (Mayrhofer 2010).....	105
Figure 5.11 Comparison of percentage breakdown of attacks worldwide for resolution level 2 for target (<i>dark</i>) and in Europe (<i>light</i>). The regarded time period is 1965–2004 (Mayrhofer 2010).	106
Figure 5.12 Risk map for building damage. The regarded time period is 1965–2004. The x-axis shows “Event/year/building in the category in Europe”, the y-axis “Million Euros/event” (Mayrhofer 2010)	108
Figure 5.13 Number of terrorist attacks on airports, worldwide by year, created with TED (Ziehm et al. 2012).	109
Figure 5.14 Graphical presentation of likelihood and impact of different threats (Ziehm et al. 2012)	110
Figure 6.1 Top view of an explosive test site after 3 explosive test events, taken with an aerial drone. Visible are the crater in the center, crater throw (ejections) and some of the large fragments of the car (direction 01:00 and 07:00). A close look reveals radial marking lines, which are used to locate fragments and debris within 5° sectors. The farthest thrown visible fragment is a turquoise colored engine hood (direction 07:30), ca.	

100 m away from the explosion site. Source: Technical test center WTD 91 (Technical test center WTD 91 2014)	121
Figure 6.2 Fireball, fragments and effects of blast expansion in case of car bomb explosion of 100 kg PETN ignited on the floor between front seat and rear bench. The sudden pressure rise generates the condensation disc on the ground. Diameter of fireball: ca. 10 m, time after ignition: 37 ms. Minor first fragments are visible in the left half of the picture (Technical test center WTD 91 2014)	121
Figure 6.3 Fragment launch distribution snapshot after a free field car bomb explosion, 1.1 s after the ignition. Besides the detonation products, dust of the sandy ground is visible over ground zero. The air is filled with thousands of larger and smaller fragments on all types of trajectories: from flat to very steep flight paths. Some characteristic fragments can be identified in videos, respectively on the picture. As an example, the two front shock absorbers with wheels attached are marked with red circles on their flat flight paths. In the corresponding video they first bounce to the ground, before, bouncing and rolling, they leave the visible area of the camera (Technical test center WTD 91 2013).	122
Figure 6.4 Overview of selected consequences of explosions (Dörr and Rübarsch 2005).	122
Figure 6.5 Near-field pressure-distance curve (Klomfass and Thoma 1997a, p. 2, Fig. 1.1).	125
Figure 6.6 Far-field pressure-distance curve (Klomfass and Thoma 1997a, p. 3, Fig. 1.2).	125
Figure 6.7 Separation of blast wave from detonation products for ground burst. Picture likely to be taken during ESKIMO test series, see (Weals 1973) for ESKIMO I test series	126
Figure 6.8 Examples of pressure-time histories produced by the burst of a frangible glass sphere containing high pressure air or argon (Baker et al. 1983, p. 136, Fig. 2.11). With permission from Elsevier.	126
Figure 6.9 Energy distribution in a blast wave as a function of time after the explosion (Strehlow and Baker 1976; Baker et al. 1983). With permission from Elsevier	127
Figure 6.10 Ideal blast wave structure (Baker et al. 1983, p. 111, Fig. 2.1). With permission from Elsevier.	128

Figure 6.11	Hopkinson-Cranz blast wave scaling (Baker et al. 1983, p. 116, Fig. 2.2). With permission from Elsevier	129
Figure 6.12	Example for Sachs-scaling of overpressure (Baker et al. 1983, p. 120, Fig. 2.4). With permission from Elsevier	130
Figure 6.13	a Linear-/ elasticplastic- and arctangent response model. b Piecewise linear response model. c Response functional (Fischer and Häring 2009) With permission from Elsevier	131
Figure 7.1	Illustration of how the three axes of the Cartesian coordinate system are related to the polar geocentric coordinate system	140
Figure 7.2	Examples of smaller car fragments: at the <i>top</i> an electric motor (ca. 3 cm diameter) as used for the windscreens wiper or as window winder; beneath are other metallic fragments, some of them are bent by the explosion (Technical test center WTD 52 2013)	142
Figure 7.3	Examples of car bomb fragments: parts of the front suspension and crash structure of the car stopped by a measurement box; just behind the box a wheel with the shock absorber; other fragments are distributed over the ground (Technical test center WTD 52 2013)	142
Figure 7.4	Example of the convex hull (Aschmoneit 2011)	143
Figure 7.5	Projections of a cuboid in two different positions (Aschmoneit 2011)	144
Figure 7.6	Drag coefficient c_w in terms of the Mach number v/c . The <i>blue line</i> are natural fragments, the <i>rectangles</i> display rather round fragments, <i>triangles</i> long fragments and the <i>diamonds</i> flat fragments (Dörr et al. 2003)	146
Figure 7.7	Detection and localization of fragments after 2 test explosions. This <i>picture</i> shows a part of the test site that is 80 to 120 m apart from ground zero. The subdivision in 5° angular sectors is clearly visible, was well as some medium and smaller fragments. The biggest fragment is the turquoise colored engine hood of one of the car bombs in der lower right part of the picture. This fragment was torn apart in one piece from the car. It is interesting that it is not much twisted like many other fragments. Such fragments are candidates for rather irregular distribution due to sailing effects. The composed aerial pictures allow to zoom in the pictures (Technical test center WTD 91 2014)	147

Figure 7.8	Car loaded with 50 kg PETN behind the front seats in a simulated gateway of an asset. On the <i>right</i> and <i>left</i> hand sides there are gabions (hesco bastions) filled with stones with a diameter of 5 to 15 cm, height 2 m, width 1 m and length 10 m. The supermini car has a dry weight of 790 kg. All liquids and window glasses have been removed before the experiment (Technical test center WTD 52 2013).	148
Figure 7.9	Gateway as shown in Fig. 7.8 after the explosive event. The gabions are seriously damaged near the original location of the car bomb. Some of the gabions at the <i>right</i> hand side tumbled back in the direction of the hazard source, because behind them a further test vehicle was located for damage assessment. The crater is comparatively small because of the rocky ground. In the <i>middle</i> of the picture, fragments of the car and protective structures for the filming and measuring equipment are visible. For instance, a massive fragment lies just straight ahead. Also the radial segment markings for locating the fragments are visible, see the thin white lines that originate from the explosive source location (Technical test center WTD 52 2013).	149
Figure 7.10	Debris throw due to an explosion. This <i>picture</i> shows the same scenario as Fig. 7.8 during the explosion of the car bomb. The burst of the gabions and the resulting debris throw is clearly visible. The debris in this scenario consists mainly of rock pieces used to fill the structures besides the mesh wire that hold it. On the <i>right</i> hand side fragments of the car fly in driving direction. The cloud is mainly due to the crater dust (Technical test center WTD 52 2013)	150
Figure 7.11	Crater formation after car bomb free field explosion with 120 kg TNT. The ground persists of sand and topsoil and comprised only few stones. Behind the crater, fragments of the car are visible. The biggest fragment consists of the rear suspension, crash structure and a wheel. Smaller parts are widespread across the test site. In the middle of the background, a protective structure for the filming is visible (Technical test center WTD 91 2012).	151
Figure 7.12	Free field test site after two car bomb explosions with 100 kg PETN. It was taken with an aerial drone flying in a height of 30 m above ground zero. The crater and	

some big fragments are clearly visible. The big fragments consist mostly of the rear suspension, the crash structure and parts of the frame. Smaller parts are widespread across whole parts of the test site. The test site was subdivided in 72 angular sectors, each 5° wide. The <i>orange</i> poles and <i>yellow</i> ropes close to the crater are visible on the <i>right</i> side of the picture. This test arrangement improved the localization and classification of the fragments as well as the analysis of the aerial photos. The first 20 m around ground zero are excluded, because of the high explosive loading (Technical test center WTD 91 2014)	152
Figure 7.13 The scheme of the discretized launching sphere that is used in the methodology of EMI's software solutions ESQRA, FSQRA and RAFOB-RAM (Salhab 2012)	153
Figure 8.1 Side-on overpressure over scaled distance in double-logarithmic scale (Aschmoneit et al. 2009) according to (Kingery and Bulmash 1984; Swisdak 1994, 2001)	157
Figure 8.2 Scaled blast impulse over scaled distance in double-logarithmic scale (Aschmoneit et al. 2009) according to (Kingery and Bulmash 1984; Swisdak 1994, 2001)	158
Figure 8.3 Street crossing geometry with buildings along the street frontage. The load is placed at the beginning of a straight street. The measurement gauge is placed after the street crossing. Close to the load heavy model components are used to prevent them from being blown away by the blast. The scaling factor was 1:40 (Dörr and Frick 2006).	161
Figure 8.4 Pressure time history at selected pressure gauge. See Fig. 8.3	161
Figure 8.5 Straight street with separated building blocks. The <i>grey box</i> is instrumented. The load is located in front of the building (Brombacher et al. 2009)	161
Figure 8.6 The position of the gauges is indicated by the <i>symbols</i> . Crosses with a <i>vertical</i> and a <i>horizontal line</i> are at the front of the building, crosses with two <i>diagonal lines</i> are at the two sides, and <i>filled circles</i> are at the back of the cuboid.	162
Figure 8.7 Measure gauge at bottom of front side. See Fig. 8.6 for the geometry. Three experimental curves are depicted showing the reproducibility of the results: x-axis shows time, y-axis pressure	163

Figure 8.8	Measure gauge at top of front side. See Fig. 8.6 for the geometry. <i>Axes</i> show time and pressure	163
Figure 8.9	Measure gauge at center of right hand side. See Fig. 8.6 for the geometry. <i>Axes</i> show time and pressure	164
Figure 8.10	Measure gauge at bottom of back side. See Fig. 8.6 for the geometry. <i>Axes</i> show time and pressure	164
Figure 9.1	Result of an optimal experiment: empirical density (Häring 2005)	169
Figure 9.2	Lognormal density functions (Wikipedia 2005), letters in the legend are modified	169
Figure 9.3	Cosine function	174
Figure 9.4	Two vectors and the two angles.	174
Figure 9.5	Illustration of (9.22)	175
Figure 9.6	Counter-clockwise rotation around the z-axis, see e.g. (Wikipedia 2013b)	178
Figure 9.7	The <i>arrows</i> indicate how a figure can be rotated around three angles to get into any arbitrary position, picture modified from Wikipedia (2013a). Here the first angle describes the rotation around the z-axis, then around the new x-axis and last around the new z-axis. It is called the z-x-z convention of Euler angles.	179
Figure 10.1	Difference between the direct (<i>bottom row</i>) and the indirect (<i>top row</i>) approach, from the presentation of Aschmoneit et al. (2009)	189
Figure 10.2	Physics based damage analysis, from the presentation of Aschmoneit et al. (2009)	190
Figure 10.3	Direct damage analysis, from the presentation of Aschmoneit et al. (2009)	190
Figure 10.4	Example for a probit function using physical hazard input data (direct or empirical damage assessment): probability of minor ear drum damage in terms of blast overpressure James et al. (1982)	191
Figure 10.5	Probit functions from binary choice, from the presentation of Aschmoneit et al. (2009)	192
Figure 10.6	Normal distribution, modified from Wikipedia (2013)	193
Figure 10.7	Visualization of the normal and lognormal distributions. P is the overpressure, QD the scaled distance, from the presentation of Aschmoneit et al. (2009)	197
Figure 10.8	Example for <i>Bowen curve</i> Lethality of a standing person in front of a reflecting wall due to blast effects. Taken from Dörr et al. (2003) and based on Bowen	

et al. (1968). The criterion is given in terms of the maximum overpressure P_s and the blast duration t_s	200
Figure 10.9 Probability of AIS level injury in dependence of the kinetic energy. Taken from Dörr et al. (2005), based on ATP Research (2004) and Feinstein et al. (1986)	201
Figure 11.1 Overview of the determination of probability distributions: (1) raw data; (2) preprocessing; (3) selection of distribution; (4) parameter determination; (5) error estimation for parameters; (6) goodness of fit test; (7) final probability distribution	206
Figure 11.2 Weibull parameter estimation with the graphic method, see presentation of (Aschmoneit et al. 2009a)	208
Figure 11.3 Cumulated lognormal distribution determined with point, moment and graphic estimator (Aschmoneit et al. 2009b)	211
Figure 11.4 Cumulated normal distribution determined with point, moment and graphic estimator (Aschmoneit et al. 2009b)	211
Figure 11.5 Cumulated Weibull distribution determined with point, moment and graphic estimator (Aschmoneit et al. 2009b)	212
Figure 11.6 Distribution with the best fit as found as determined by the Kolmogorow-Smirnow test (Aschmoneit et al. 2009b)	212
Figure 12.1 Scheme of the distribution of identical box-shaped objects on a three-dimensional surface (Häring 2005)	217
Figure 12.2 Two-dimensional plot of the three dimensional situation. The surface is three-dimensional and the line representing the tangent plane normally is a plane. The normal vector would look the same in a three-dimensional plot (Häring 2005)	217
Figure 12.3 The green lines show some exemplary presented surfaces (Häring 2005)	218
Figure 12.4 A cuboid with side lengths a , b and c (Häring 2005)	218
Figure 12.5 Two of the six normal vectors of a cuboid (Häring 2005)	219
Figure 12.6 The vector v can be described as the vector $(0, 0, 1)$ that is rotated around the z-axis and the y-axis (Häring 2005)	219

Figure 12.7	The presented surface of the <i>upper side</i> of the cuboid	220
Figure 12.8	A cylinder with the corresponding notation (Häring 2005)	222
Figure 12.9	Computation of the presented surface of a cylinder	222
Figure 12.10	Shading effects in the computation of the presented surface of a simplified truck	223
Figure 12.11	The idea behind the computation of the presented surface with Monte Carlo simulation	224
Figure 12.12	The labeling of the cuboid R_i (Häring 2005)	224
Figure 12.13	Idea of Monte Carlo integration in a simple example	227
Figure 12.14	Presented surface of a cube with side length 1 m (Häring 2005)	229
Figure 12.15	Approximated presented surface of a cube with side length 1 m (Häring 2005)	229
Figure 12.16	The idea of relevant presented surfaces (Häring 2005)	230
Figure 13.1	Procedure for predicting incident likelihood from the historical record and the alternative way of fault tree analysis (American Institute of Chemical Engineers 1999, p. 299)	238
Figure 13.2	Living situation in the “real-world scenario” (not true to scale) (Rübarsch 2003)	239
Figure 13.3	Location of the objects (Rübarsch 2003)	240
Figure 14.1	Explosion and different levels of damage effects depending on the distance from the explosion	253
Figure 14.2	Two situations with the same individual risk but different collective risks	254
Figure 14.3	Two situations with the same collective risk but different individual risks	254
Figure 14.4	3D model and empirical frequencies of terror events on the Water Haven site plan at Waterford City, Ireland (courtesy Bolster Group) (Riedel et al. 2015)	260
Figure 14.5	Local event frequency distributed in a quarter normalized to 1: what-if event distribution (Riedel et al. 2015): The vicinity of the conference hotel and the international cooperation shows increased frequency (susceptibility), also for neighboring urban assets	261
Figure 14.6	Quantitative what-if risks in case of a terroristic explosive event within the quarter (Riedel et al. 2015). a Glazing damage risk. b Local fatality risk	

outside buildings. c Progressive collapse risk of buildings. d Overall average monetary risk due to local traffic delays caused by road damage, taking into account repair times.	262
Figure 14.7 Risk graph: general scheme (International Electrotechnical Commission 2010, part 5, p. 33). Reprinted from IEC 61508-5 with permission of IEC (Geneva), transferred through the division DKE of the VDE e.V. Relevant are the standards with the latest date of issue, which can be purchased at www.iecnormen.de . The German translation is published as DIN EN 61508-5 (VDE 0803-5) and can be purchased at www.iec-normen.de	263
Figure 14.8 Risk graph—example (illustrates general principles only) (International Electrotechnical Commission 2010, part 5, p. 34). Reprinted from IEC 61508-5 with permission of IEC (Geneva), transferred through the division DKE of the VDE e.V. Relevant are the standards with the latest date of issue, which can be purchased at www.iec-normen.de . The German translation is published as DIN EN 61508-5 (VDE 0803-5) and can be purchased at www.iec-normen.de	264
Figure 15.1 Number of events per quarter on tunnels and bridges, worldwide (Fischer and Millon 2010)	273
Figure 15.2 Sort of attack on bridges worldwide between 1997 and 2007	273
Figure 15.3 Example for risk analysis in the case of fraud with debit cards	277
Figure 16.1 Number of attacks on harbors per year from 1970 to 2006 (Ziehm et al. 2011)	284
Figure 16.2 Distribution of the attacks on harbors by continent (Ziehm et al. 2011). The classification of the continents follows (Ziehm 2009)	285
Figure 16.3 Explosion hazards (Ziehm et al. 2011)	287
Figure 16.4 Example of a pressure-time curve or history $p(t)$ (<i>red curve</i>) for an explosion under free field conditions. Pressure of the surrounding P_0 , overpressure P_s , suction, underpressure or negative phase, specific blast impulse I (<i>hatched area</i>) and duration of the positive overpressure phase T_s	289
Figure 16.5 <i>Upper diagram:</i> Measurement for the “side-on”-pressure P_s and “side-on”-impulse I_s . <i>Lower diagram:</i> Measurement for reflected pressure P_r and reflected	

	impulse I_r . $V_{blast\ wind}$ velocity of the blast wind, $V_{blast\ front}$ velocity of the blast front (Ziehm et al. 2011)	290
Figure 16.6	Average velocity of the side wall of a container after an explosion at the container ground in the center. Taken from Robert T. Conway, John Tatom. ISO Container Source Function Development for the Klotz Group Engineering Tool. DDESB, Explosives Safety Seminar. Portland. USA. With permission	292
Figure 16.7	The number of fragments over their mass for different fitted models for three tests with an ISO container (1000 kg NEQ). Taken from Robert T. Conway, John Tatom. ISO Container Source Function Development for the Klotz Group Engineering Tool. DDESB, Explosives Safety Seminar. Portland. USA. With permission	293
Figure 16.8	Different functions describing the mass distribution as a function of the NEQ. Taken from Robert T. Conway, John Tatom. ISO Container Source Func- tion Development for the Klotz Group Engineering Tool. DDESB, Explosives Safety Seminar. Portland. USA. With permission	294
Figure 16.9	Horizontal angle distribution of fragments for a container explosion (4000 kg NEQ) on a truck (<i>in the middle</i>) with a distance of more than 100 m. Taken from Robert T. Conway, John Tatom. ISO Container Source Function Development for the Klotz Group Engineering Tool. DDESB, Explosives Safety Sem- inar. Portland. USA. With permission.	295
Figure 16.10	Horizontal angle distribution of fragments for a container explosion (4000 kg NEQ) on a truck (<i>in the middle</i>) with a distance of more than 250 m. Taken from Robert T. Conway, John Tatom. ISO Container Source Function Development for the Klotz Group Engineering Tool. DDESB, Explosives Safety Sem- inar. Portland. USA. With permission.	296
Figure 16.11	Degree of injury from different models with regard to the incident thermal flux and the exposure time (Hymes 1983). Reprinted from Ian Hymes, The physiological and pathological effects of thermal radiation, Report N. SRD R 275, UK Atomic Energy Authority, Warrington, UK, with permission of Nuclear Decommissioning Authority	302

Figure 17.1	Three lines of reasoning as visualized by Johansen (2010). The y-axis is abstract and can be any reasonable measure of risks, for example €/year or injuries/year	316
Figure 17.2	Sample for empirical F-N curve. Display of the data in Table 17.1.	321
Figure 17.3	Display of the cumulative probabilities without forming classes	322
Figure 17.4	fN diagram belonging to Table 17.1.	322
Figure 17.5	Modified illustration of the classification of risk by van Breugel (2001)	323
Figure 17.6	Example of an FN-curve and a criterion line (both axes in logarithmic scale)	325
Figure 17.7	Comparison of F-N-curve and f-N-curve. The <i>thin red line</i> shows that the fN-curve is not a straight line in double-log scale.	325
Figure 17.8	Interim societal risk tolerance criteria (Geotechnical Engineering Office 1998). With permission	329
Figure 17.9	Societal risk acceptance for crew (Vanem et al. 2008). With permission from Elsevier	330
Figure 17.10	Comparison of F-N curves generated from the risk criteria presented in his paper (Trbojevic 2005). R2P2 = (Health and Safety Executive 2001), COMAH = (Health and Safety Executive 2004)	334
Figure 17.11	Proposed individual risk criteria (Trbojevic 2005)	335
Figure 17.12	Proposed societal risk criteria (Trbojevic 2005)	335
Figure 17.13	Comparison of individual risk criteria (Cornwell 2015). EPA = Environmental Protection Agency (Cornwell and meyer 1997). With permission from Quest Consultants	337
Figure 18.1	Advantageous (<i>upper row</i>) and disadvantageous (<i>lower row</i>) building shapes in the case of an explosion (Mayrhofer 2010)	345
Figure 18.2	Example of a barrier (Stolz 2012)	347
Figure 18.3	Example for a structural damping mitigation measure (Brenneis and Millon 2012)	349
Figure 18.4	Evaluation of risk mitigation measures (Siebold et al. 2015)	350
Figure 18.5	Overview of overall risk management as generated by the tool IDAS: objectives, risks (including their color-coded evaluation), measures (including their color coded assessment), secondary risks and measures (Siebold et al. 2015). With permission from Taylor and Francis	351

List of Tables

Table 2.1	Complementary attributes of risk and chance analysis and management processes	20
Table 2.2	Placement of the 14 risk management steps of Sect. 2.4 in the 5-step risk management scheme of Sect. 2.3.3	24
Table 2.3	Dependencies of the different risk management steps on each other	25
Table 3.1	Advantages and disadvantages of the different approaches to the database analysis scheme	30
Table 3.2	Mathematical notation and formulas	31
Table 3.3	Sources for data acquisition	33
Table 3.4	Translation of the vocabulary in Fig. 3.3	38
Table 3.5	Detailed list of the relation “ <i>anschlaege</i> ”	39
Table 3.6	Overview of the mathematical and database notation	40
Table 3.7	Data of 5 attacks in Germany in 1985 (Siebold 2007)	44
Table 3.8	Examples for probabilities and frequencies with corresponding graphics (Häring et al. 2005)	47
Table 3.9	Allocation of the database analysis methods of this chapter and Chap. 2 to the steps of the risk management process	52
Table 3.10	Overview of database notation	56
Table 3.11	The structure of GTD	57
Table 3.12	Frequencies of the different attack types in Brazil from 1970 to 2010	58
Table 4.1	Risk map from AOP-15 (AOP-15 2009) with four severity classes and six probability/frequency levels. Risk levels are low (<i>green</i>), medium (<i>yellow</i>) and high (<i>red</i>). Reprinted from AOP-15 Edition 3, Nato Standardization Agency (NSA), 2009	78

Table 4.2	Computations for displaying a time series of injuries in Great Britain for terroristic attacks, 1970–2010	82
Table 4.3	Computations for smoothing the time series	83
Table 4.4	Computations for smoothing the time series	83
Table 4.5	Computation of the coefficients for the trend function	86
Table 4.6	Coefficients for the trend function	86
Table 4.7	Forecasting with Microsoft Excel	87
Table 4.8	rrse for forecasting with Microsoft Excel	88
Table 5.1	Clustering of different building types in the database (Mayrhofer 2010)	102
Table 6.1	Type of energy release of explosive source and theoretical models describing the sources. Explosion type (Baker et al. 1983, p. 107, Table 2.1). With permission from Elsevier	118
Table 7.1	The polar geocentric coordinates	140
Table 7.2	Transformation between polar geocentric and Cartesian coordinates	141
Table 7.3	Structure of a typical fragment matrix (Salhab et al. 2011b). Reprinted from Advances in Safety, Reliability and Risk Management. ESREL 2011 Annual Conference Proceedings	144
Table 7.4	Example of a typical fragment matrix (Salhab et al. 2011a). Reprinted from Advances in Safety, Reliability and Risk Management. ESREL 2011 Annual Conference Proceedings	145
Table 8.1	Parameters for side-on overpressure (Swisdak 1994)	156
Table 8.2	Parameters for blast impulse (Swisdak 1994)	157
Table 8.3	TNT equivalent weight factors for free air effects (AASTP-1 2010), based on (NATO Group of Experts on the Safety Aspects of Transportation and Storage of Mil. Ammo and Explosives 1976; USA WES/CoE 1986; Drake et al. 1989)	159
Table 10.1	Overview of the definitions of variables	192
Table 10.2	Probit value and matching percentage (Rübarsch and Gürke 2001)	194
Table 10.3	Overview of literature: kind of consequences from blast and fragments, kind of parameterization	199
Table 10.4	Abbreviated Injury Scale (AIS): injury levels	201
Table 11.1	Sample data for alternative distribution functions: blast injury probability of dummies at a given distance (Gürke 2002; Aschmoneit et al. 2009a)	210
Table 11.2	Parameter values for the lognormal- and the normal distribution (Rinne 1997; Meyna and Pauli 2003)	210

Table 11.3	Parameter values for the Weibull distribution	211
Table 11.4	Literature about statistical methods for parameter estimation	213
Table 13.1	Definition of basic situations in 1 week = 168 h (Rübärsch 2003)	241
Table 13.2	Description of the 12 types of persons	242
Table 13.3	Number of persons of the different types	244
Table 13.4	Number of persons present at objects at different times of the day and at different days during the week (local exposure)	244
Table 14.1	Explanation of the parameters in Fig. 14.8 (International Electrotechnical Commission 2010, part 5, p. 34). Reprinted from IEC 61508-5 with permission of IEC (Geneva), transferred through the division DKE of the VDE e.V. Relevant are the standards with the latest date of issue, which can be purchased at www.iec-normen.de . The German translation is published as DIN EN 61508-5 (VDE 0803-5) and can be purchased at www.iec-normen.de	265
Table 14.2	Example of data relating to risk graph (Fig. 14.8) (International Electrotechnical Commission 2010, part 5, p. 35). Reprinted from IEC 61508-5 with permission of IEC (Geneva), transferred through the division DKE of the VDE e.V. Relevant are the standards with the latest date of issue, which can be purchased at www.iec-normen.de . The German translation is published as DIN EN 61508-5 (VDE 0803-5) and can be purchased at www.iec-normen.de	265
Table 14.3	Example of calibration of the general purpose risk graph (International Electrotechnical Commission 2010, part 5, p. 36)	267
Table 14.4	Overview of norms and standards treating risk graphs, translated extract of Table 10.3 in Thielsch (2012)	269
Table 15.1	Example how a defined scenario can be analyzed with the risk management process	276
Table 15.2	Comparison of the credit card example and the risk management process	278
Table 15.3	Examples for missing risk analysis and management steps in the credit card example	278
Table 16.1	General explanations of the content of the hazard table, translated from (Ziehm et al. 2011)	286
Table 16.2	TNT equivalents of some explosives for overpressure (Ziehm et al. 2011)	291

Table 16.3	Constants c_j in dependence of the interval Z lies in Swisdak (1994)	292
Table 16.4	Damage classes for residential buildings and other buildings in lightweight construction	299
Table 16.5	Damage classes for reinforced concrete frame construction	300
Table 17.1	Original accident data including frequencies and number of fatalities (Proske 2008) based on Ball and Floyd (2001). With permission of Springer Science and Business Media	320
Table 17.2	Sorted accident data with respect to number of fatalities, corresponding cumulative frequencies and the contributing events (Proske 2008) based on Ball and Floyd (2001). With permission of Springer Science and Business Media.	321
Table 17.3	Rearranged accident data (Proske 2008) based on Ball and Floyd (2001). With permission of Springer Science and Business Media.	321
Table 17.4	Computation of an f-N-curve from an F-N-curve: spreadsheet application example	326
Table 17.5	Annual risk of death from industrial accidents to employees for various industry sectors (Health and Safety Executive 2001)	327
Table 17.6	Average annual risk of injury as a consequence of an activity (Health and Safety Executive 2001)	327
Table 17.7	Tolerable risks for engineered slopes (Australian Geomechanics Society 2000)	328
Table 17.8	Individual risk acceptance criteria for LNG crew (Vanem et al. 2008), based on Skjøng et al. (2005)	329
Table 17.9	Extract from Table 3.19 in Proske (2008)	332
Table 17.10	Risk contours in Land use Planning (Z = zone) (Okstad and Hokstad 2001)	333
Table 17.11	Comparison of individual risk criteria (Trbojevic 2005)	334
Table 17.12	Risk criteria in Häring et al. (2009) © With permission from Elsevier	336
Table 18.1	Exemplary categorization of mitigation measures (Fischer and Stolz 2011)	349

Abstract

The text introduces basic risk concepts and proceeds to risk management and analysis processes and steps. Risk management is essential for improving resiliency in all resilience management steps: preparation, prevention, protection, response, and recovery. The main emphasis is on methods that fulfill the requirements of one or several risk management steps, including statistical–empirical analyses, probabilistic and parametrized models, and engineering approaches, e.g., for fragment and blast propagation or hazard densities in case of terroristic threat events.

The methods investigate the kind of events and scenarios, as well as frequency, exposure, avoidance, hazard propagation, damage and risks of events. Further methods are presented for context assessment, risk visualization, communication, comparison, and assessment as well as the selection of mitigation measures. The processes and methods are exemplified with detailed results and overviews on security research projects, in particular in application domains such as transport, aviation, explosive threats, and urban security.

The text addresses advanced bachelor, master, and doctoral students as well as scientists, researchers, and developers in academia, industry, and small and medium enterprises that work in the emerging field of security and safety engineering.

Examples of interest include sufficient control of emerging and novel hazards and risks, occupational safety, identification of minimum (functional) safety requirements, engineering methods for countering malevolent or terroristic events, security research challenges, interdisciplinary approaches to risk control and management, change and improvement management, and support of rational decision making.

Chapter 1

Introduction, Overview and Acknowledgements

This chapter contains some introductory material ranging from a general introduction (Sect. 1.1) to selected key features and aims of the text (Sect. 1.2) to an overview of the build up of the overall text and each chapter (Sect. 1.4). Section 1.3 on the main research projects that contributed to the present textbook as well as most of the acknowledgement text provide good insight into the background and context of the text.

1.1 Introduction

The lecture notes on risk analysis introduce fundamental risk concepts, detailed risk management and analysis steps and processes and a multitude of proven methods to implement the processes and steps. They show how engineering approaches provide risk assessment and input for risk communication, evaluation and mitigation. The application cases, sample processes and methods cover security and safety scenarios due to man-made, natural and natural-technical threats. Examples include land transport, harbor and airport security as well as terroristic and accidental events, in particular explosions.

The reader is empowered to design, tailor and interconnect risk and chance management processes as well as methods. All application cases draw from a pool of research and development projects in the domain of applied security and safety research in a German national and mainly European international context. Methods introduced include historical-statistical analyses, e.g. based on terror event data, engineering methods for the characterization of hazard sources and hazard propagation, e.g. blast and fragments, as well as engineering and probabilistic damage modeling. They provide input for the computation of individual, local, collective (group) risks and risk comparison quantities.

From resilience management perspective, the text focuses on improving preparation, prevention and protection rather than response and recovery. From a risk management perspective, the focus is on risk identification and assessment taking into account the given context rather than risk evaluation and mitigation as

an activity. However, the effect of mitigation measures in terms of risk reduction is assessed. For each chapter, it is shown how the presented approach links with typical resilience management phases. In a similar way one could link it with (technical) resilience capabilities, e.g. sense, model, infer, act, lean and adapt.

The text covers most of the risk analysis steps in detail: analysis of scenarios, events, hazard sources, physical hazard potential including its propagation in space and time, probabilities including frequency of damage event, exposition of objects, avoidance frequency, consequences including damaging effects for persons and objects. The probability and consequence quantities are combined to various risk quantities, including individual local risks, individual risk, collective local risks and collective total risks. Also FN-curves are defined for various applications. The text focuses on the application of risk management and analysis approaches to new domains or on extending the depth of analysis in existing application domains.

The lecture notes address advanced graduate, master and doctoral students as well as engineers and scientists working in the field of security and safety research, engineering and technical development, in academia and a broad range of industry. It is of introductory nature, but also contains detailed case studies that are expected to be of interest also for experts in the security research domain, in particular the summaries of project and case study results.

1.2 Selected Features of Text

The detailed risk management schemes introduced at the very beginning of the text and exemplified with methods along the whole text are believed to be of general interest since it allows to structure and parallelize the development and application of risk management processes from an engineering perspective.

For instance, geographical urban geometry and population distributions are typically independent of potential threats, damage assessment depends only on the physical hazard potential rather than all details of the hazard source, damage evaluation models can be the same for different types of physical hazards, or the range of risk visualization options are rather independent of the type of risks. In most cases, the application examples for the methods presented reach state of the art of current applied research.

The field of risk engineering and science for improving security has emerged rather recently, triggered, challenged and constantly questioned by the 9/11 events in New York and similar events before and thereafter, e.g. the 13/11 events in Paris. It is not yet a technical scientific field per se. However, contours of such a field are emerging showing its interdisciplinary character involving multiple technical and societal fields. It can be considered as a part of security and safety research or resilience engineering research and has to be benchmarked by its relevance for real-world applications and end users, the consideration of the citizens' needs as well as its well-founded scientific, interdisciplinary and methodical approach.

The text places engineering and science risk management approaches and results at least in a minimum context of societal processes and evaluations. It emphasizes the need for input from the societal domain, even at the level of engineering risk assessments. For instance, the risk engineer has to decide which information is relevant for risk decision making before endeavoring in expensive engineering analyses.

The present text aims at showing how far engineering-driven approaches carry in selected domains of security and resilience engineering research. It also shows the emerging challenges even when implementing rather simple approaches in this domain, e.g., often already starting with the selection of appropriate definitions and aims of analysis. The reader is encouraged to gain such inputs from his application context. In the present text, such inputs have often been generated by appropriate composition of research consortia and input of partners.

The application of the presented risk management process and methods is not limited to the security domain. It is also of relevance for the quantitative assessment of hazards and risks in the context of occupational safety and functional safety. For instance, quantitative risk analysis methods can be used to determine minimum functional safety requirements. The textbook mainly contributes to assessing and improving the prevention of and protection from hazardous disruptive events. In this sense it links the prevention phase to the probability assessment of chance and risk management and analysis and the protection to its consequence and damage assessment.

1.3 Background and Research Programs

The textbook rests on the results of a few dozens of research projects in the civil or societal security research domain. Most of them were funded by the German Ministry for Education and Research (BMBF) and the European Commission (EC). In some of the projects similar approaches have been employed within a novel non-military civil and societal security research application domain as in the case of projects funded by the German Ministry of Defense (BMVg). However, only if the methods were already documented in the public scientific literature. Most of the approaches and project results presented in the present text involve malicious events (terror events) and man-made events in particular in urban, transport, airport and humanitarian demining scenarios.

The presented processes and methods have been mainly developed and/or applied within the security research programs of the European Commission (EC) and the German Ministry for Education and Research (BMBF). The text also owes most of its application examples to the efficient collaboration within these projects. Most of the projects address possible risks for citizens and critical infrastructure (critical infrastructure protection). In particular in the transport, public urban space and aviation domain. Mainly addressed are man-made malicious (terroristic) and accidental hazards. The results of the following research projects contributed most to the present text:

- End-user driven demo for CBRNE (EDEN, European Union (EU) project) (EDEN 2015)
- ENOUNTER, Explosive Neutralization and Mitigation Countermeasures for improvised explosive devices in Urban/Civil Environments (ENCOUNTER, EU project) (Encounter 2015)
- Comprehensive toolbox for humanitarian clearing of large civil areas from anti-personal landmines (D-BOX, EU project) (D-BOX 2015)
- Vulnerability Identification Tools for Resilience Enhancements of Urban Environments (VITRUV, EU project) (VITRUV 2014)
- Increase of container security by applying contactless inspections in port terminals (ECSIT, BMBF project) (ECSIT 2013)
- Protection of critical bridges and tunnels in the course of roads (SKRIBT, SKRIBT+, BMBF Projects) (SKRIBT 2011; SKRIBT Plus 2012)
- Project on the hazard and risk assessment of improvised explosive devices (German Ministry of the Interior (BMI))
- Airport security system (FluSs, BMBF project) (Bundesministerium für Bildung und Forschung 2014)

The lecture notes significantly extend lectures held at the University of Applied Science Furtwangen (HFU) in the Bachelor and Master degree program on safety and security engineering as well a lecture held at the Baden-Württemberg Cooperative State University (DHBW) Lörrach.

The main resources for developing the present text originate from the German Ministry of Education and Research (BMBF): the Fraunhofer Ernst-Mach-Institute (EMI), supported by the University of Freiburg, developed continuous academic education in the security and resilience research domain.

Within the BMBF project “Windows for continuing education”, which is one project within the Federal Government—German Federal State competition “Advancement through Education: Open Universities” (Bundesministerium für Bildung und Forschung 2015; Federal Ministry of Education and Research 2015), the University of Freiburg provided technical and didactic support, drawing on its strong background in the development of online master courses in the technical domain. Fraunhofer EMI was responsible for the development of the scientific content and didactic materials, in particular resulting in the present lecture notes. The two courses developed in the risk management and analysis domain Risk Analysis I and II comprise 10 European Credit Transfer System (ECTS) points equivalent to approximately 300 h of work, including presence days and the preparation and presentation of a final project. The present text condenses the generated lecture note material.

Most of the approaches presented within the text have been implemented in application software tools in the security and safety domain. For example for the empirical-statistical assessment of historic terroristic events with respect to kind of events, frequency of events, damage effects and object-specific risks, in particular resolving the quantities with a high level with respect to the kind of damage and of objects affected. Another major set of tools comprises hazard and risk analysis tools for hazardous sources that are supported by 3D visualizations.

A key objective of the text is to guide readers to select, tailor and extend existing approaches and methods to their scenario-specific requirements. The idea is that such informed and efficient application of existing approaches can occur at different levels, including the definition of a risk management and analysis scheme, the selection of methods for each step, the tailoring and extension of the methods, as well as the definition of interfaces between the methods and beyond steps. This is supported by the introduction of a set of flexible definitions that are adhered to throughout the text. Furthermore, the application methods and example refer to the conceptual framework introduced, repeating again key definitions, including possible modifications.

1.4 Structure of Text

The chapters of the text are structured according to risk management schemes. We use a 5 step and 14 step scheme and variations thereof. Often single methods can be used in more than one step. Hence an additional alternative ordering principle, which has not been adhered to, is the kind of methods discussed ranging from qualitative-heuristic, statistical-empirical, analytical-empirical, to engineering approaches as well as numerical simulation approaches.

In a similar way, the development of software application tools including data management, interface development and visualizations can be viewed as separate activities that have to be covered by several risk management phases. In summary, the text aligns risk management methods within risk management steps rather than showing the coverage of risk management phases by risk management methods. This results in a modular presentation that follows the risk analysis or management phases that have to be covered in real applications.

Each chapter comprises the introduction, which relates the chapter content to the other chapters and gives an overview of the content of the chapter. For an overview, it is recommended to read all the chapter introductions before starting to read the main bodies of the chapters.

After the introduction which positions the chapter within the overall text, the main content sections of the chapters follow. They typically start with definitions and overviews and either proceed from examples to general considerations or vice versa. Another ordering scheme is to deal with key concepts of the chapter in separate sections, respectively. Some chapters consist of several case studies, typically one per section. The length of the chapters varies rather significantly, as well as the number of chapters per risk management step. This is due to the focus on risk management steps that can be covered with engineering and natural science methods, the selected methods that are presented in detail and the selected application cases.

Each chapter has a summarizing section and a section with questions. For questions answers are given, in case they are believed to support the chapter text.

All questions aim at operationalizing the contents of the chapters rather than asking for knowledge.

Complementing the introductory remarks also the summary sections of each chapter are recommended as a further starting point for gaining an overview of the text. The text uses a rather rich section structure that also aims at providing a good overview. For increasing the usability of the text, the text is indexed. In particular, the first definition of key technical terms is marked.

Acknowledgements According to the thematic focus on applied risk management and analysis driven by physical-engineering methods in the application domain of security and resiliency research, there is a broad range of persons and bodies to be thanked.

The University of Applied Science Furtwangen (HFU) invited the Fraunhofer Ernst-Mach-Institute to support the establishment of its bachelor and master degree program in security and safety engineering. Numerous students provided feedback to details as well as the general structure of parts the text. This also holds true for the students of the Baden-Wuerttemberg Cooperative State University (DHBW).

Thanks also goes to the following bachelor, diploma or master students at Fraunhofer EMI, who the present author was happy to attract and to supervise internally. They contributed to research projects in the risk analysis and management domain, key results of which are summarized in the present text. In particular, the text is often based on theses, conference and journal papers that resulted from their work: R.G. Salhab (Master thesis, external supervisor: Prof. T. Filk, University of Freiburg), P. Thielisch (Bachelor, external supervisor: Prof. U. Weber, HFU Furtwangen), S. Kipping (Master, external supervisor: Prof. Dirk Reichelt, HS Zittau-Görlitz), S. Scheler (Diploma, external supervisor: Prof. T. Wieland, HS Coburg), P. Ettwein (Diploma, external supervisor: Prof. H. Winter, HFT Stuttgart), F. Schubert (Diploma, external supervisor: Prof. M. Hahne, RFH Köln), M. Rottenkolber (Diploma, external supervisor: Prof. A. Fritsch, MUAS München), F. Suhrke (Diploma, external supervisor: Prof. F. Kuypers, OTHR Regensburg), T. Aschmoneit (Diploma, external supervisor: Prof. S. Helwig, HMUAS Mittweida), M. Loos (Diploma, external supervisor: Prof. G. Ringwelski, HSZG Zittau/Görlitz), M. Schönher (Master, external supervisor: Prof. G. Radons, TU Chemnitz), C. Richter (Diploma, external supervisor: Prof. F. Häußler, FH Berlin), K.-U. Fischer (Diploma, external supervisor: Prof. M. Kschischio, FH Koblenz), U. Siebold (Diploma, External Supervisors: Prof. W. Burgard, Dr. A. Karwath, University Freiburg), N. Kübler (Diploma, external supervisor: Prof. B. Laschinger, HFU Furtwangen), S. Kubicki (Diploma, external supervisor: Prof. A. Sikora, DHBW Lörrach), T. Pfanner (Diploma, external supervisor: Prof. H. Martin, FHNW Basel), J. Kleb (Diploma, external supervisor: Prof. L. Piepmeyer, HFU Furtwangen).

The text also benefited from the experience of the University of Freiburg in particular its technical faculty in providing master online courses in the technical domain. Within the German Ministry for Education and Research (BMBF) project “Windows for continuous academic education” that aims at the generation and implementation of academic continuous education courses of Universities, the Fraunhofer Ernst-Mach-Institute (EMI) lead the sub project “Security and Safety systems technologies”. The present text profited in particular from the experience and exchange with the co-subprojects “Embedded Systems” led by Prof. Bernd Becker, “Solar Energy Engineering” led by Prof. Leonhard Reindl and “Freiburg Academy for Science and Technology (FAST)” led by Prof. Ingo Krossing as well as the Fraunhofer Institute for Solar Energy Systems (ISE) co subproject “Energy systems technology” led by Dr. Thomas Schlegel. Also the broad technical and didactic support of the University of Freiburg is highly appreciated. The text also incorporates numerous feedbacks of the students participating in the continuous academic training courses.

The text implemented valuable feedback from scientists of the department of Security technologies and structural protection at Fraunhofer Ernst-Mach-Institute (EMI), in particular J. Weissbrodt, J. Schäfer, K. Fischer, W. Niklas and G. Vogelbacher. Thanks also goes to the head

of the group Hazard and risk analysis Dr. Malte von Ramin, the former heads of this group Dr. Frank Radtke and Dipl.-Ing. Andreas Dörr, Dr.-Ing. Uli Siebold the head of the group “Safety and efficiency analysis”, Stefan Ebenböhch of the group “Reliable systems” and Dr.-Ing. Oliver Millon of the group “Security of buildings” as well as feedback of the former heads of department Dr.-Ing. Christoph Mayrhofer and Dipl.-Phys. Gerhard Gürke, the head of the department Dr.-Ing. Alexander Stolz and the deputy head of the department Prof. Dr.-Ing. Werner Riedel.

Many of the topics covered in the present text have only come to the attention of a broader scientific, social science, natural science and engineering community due to the massive research programs on national and EU scale under the label security and resilience research, triggered and challenged by 9/11 and many similar events thereafter. The former head of the Fraunhofer EMI, Prof. Klaus Thoma, as well as the current head of the institute, Prof. Stefan Hiermaier, enabled and contributed with their scientific backgrounds to numerous working groups and steering committees, thus envisioning, preparing and enabling many of the contents that are detailed in the present text. They also gave critical feedback to the present text. Many of the projects referred to in the text have been initiated or made accessible to Fraunhofer EMI by the deputy head of the institute, Dr. Tobias Leismann and coworkers, in particular the head of the strategic management Daniel Hiller.

The generation as well as the iteration of the text at Fraunhofer EMI was very much supported by the scientific lector work of Sina Rathjen who compiled first versions of the text based on outlines by the author and content materials provided by selected sources. Thanks also goes to the librarian staff and the media and publishing team at the institute: Brigitta Soergel, Jessica Helbling, Ulrike Galena, Birgit Bindnagel and Johanna Holz.

The following institutions and persons contributed most to the publishing licenses of figures and tables, in alphabetical order:

APT-Research;

Bienz, Kummer & Partner;

J. Beard;

R. T. Conway;

J. B. Cornwell;

DKE, the German Commission for Electrical, Electronic & Information Technologies of DIN and VDE;

Elsevier Books;

Geotechnical Engineering Office and the Director of the Civil Engineering and Development, the Government of the Hong Kong Special Administrative Region;

German Federal Office of Civil Protection and Disaster Assistance (BBK);

German technical centers WTD 52 and WTD 91;

Health and Safety Executive (HSE) Books UK;

Information Request Team AWE;

I. J. Johansen;

P. Kummer; Nato Standardization Organization (NSO);

Nuclear Decommissioning Authority UK;

D. Proske;

Quest Consultants;

M. Steyerer;

M. M. Swisdack;

J. Tatom;

Taylor and Francis UK;

Wiley UK.

Last but not least, the text owes much to the thorough support of the team at Springer publishing house, in particular Dr. Christoph Baumann, senior editor engineering Springer Singapore,

Carmen Wolf editorial assistant Springer Heidelberg, Balaji Muthukumaraswamy project coordinator (books) and Ramasubramaniyan Velu from Scientific Publishing Services Springer Chennai.

References

- Bundesministerium für Bildung und Forschung. (2014). *FluSs: Flughafen-Sicherungssystem*. Retrieved August 20, 2015, from <http://www.bmbf.de/de/22446.php>
- Bundesministerium für Bildung und Forschung. (2015). *Bund-Länder-Wettbewerb "Aufstieg durch Bildung: offene Hochschulen"*. Retrieved August 25, 2015, from <http://www.wettbewerb-offene-hochschulen-bmbf.de/>
- D-BOX. (2015). *Welcome to the D-BOX website*. Retrieved August 20, 2015, from <https://d-boxproject.eu/>
- ECSIT. (2013). *ECSIT—Erhöhung der ContainerSicherheit durch berührungslose Inspektion im Hafen-Terminal*. Retrieved August 20, 2015, from www.ecsit-security.de
- EDEN. (2015). *Welcome to EDEN—End-user driven DEmo for cbrNE*. Retrieved August 20, 2015, from <https://eden-security-fp7.eu/>
- Encounter. (2015). *Encounter*. Retrieved August 20, 2015, from www.encounter-fp7.eu
- Federal Ministry of Education and Research. (2015). *Continuing Academic Education*. Retrieved August 25, 2015, from <http://www.bmbf.de/en/349.php>
- SKRIBT. (2011). *SKRIBT—what does it mean?* Retrieved August 20, 2015, from <http://www.skribt.org/home.htm>
- SKRIBT Plus. (2012). *SKRIBT plus*. Retrieved August 20, 2015, from <http://skribt.org/skribtplus/index.htm>
- VITRUV. (2014). *VITRUV vulnerability identification tools for resilience enhancements of urban environments*. Retrieved August 20, 2015, from <http://www.vitruv-project.eu/>

Chapter 2

Introduction to Risk Analysis and Risk Management Processes

2.1 Overview

This chapter defines basic terms of risk and equivalently chance analysis: risk (chance) event, frequency of event, exposure, hazard propagation, consequence and damage analysis. It introduces the classical notion of risk being proportional to a measure for probability of events and measure for consequences of an event. It is distinguished between risk computation, visualization, comparison and evaluation. In particular, different sample risk criteria are discussed.

This chapter motivates and introduces phases (steps) for risk and chance management and analysis by discussing state-of-practice schemes, before defining a fine resolved risk management process in 14 steps, which includes risk analysis. Attributes of risk management processes and phases are introduced as well typical dependencies of phases. It also discusses different simplifying versions or tailoring of the processes. For instance, if the initial scenario and all threats are known, it sometimes suffices to consider only few threat events within well-defined settings.

In terms of resilience (catastrophe) management (response) cycle, the risk management steps related to frequency of event, exposure and prevention probability relate most to the prevention phase of the resilience management scheme. The hazard source characterization, the hazard propagation and the damage determination relate mainly to the resilience management protection phase. However, depending on which objectives are chosen within the risk management scheme, also the resilience management phases response, recovery and preparation can be assessed using classical risk/chance management and analysis.

All methods and examples in Chaps. 3–18 can be related to this chapter, since they contribute to fulfill one or more phases of risk management and analysis. This chapter adopts a management perspective when compared to the remaining chapters, since it focuses on top level requirements for the process and the steps rather than showing how to conduct the analyses. This top perspective is very useful to

structure risk management tasks, since it is likely that all the phases have to be covered.

This chapter is also useful for identifying where interdisciplinary boundaries and responsibilities within risk management projects arise, as well as for structuring engineering, scientific, computer science or implementation boundaries and interfaces.

In the following, besides the further introductory Chap. 3, most of the chapters focus on single methods and their application or at least sets of methods that can be used within one or several risk management phases. The categorization along different methods can also be used for structuring risk analysis and management processes as well as projects. However, likely drawbacks include that limitations of the method and discipline will also limit the coverage of all risk management phases as well as that interfaces between steps are not well defined, since within a single method there is much less need to distinguish between steps, which limits the reusability of risk management steps/phases.

The main advantage of using a step-wise risk analysis and management approach is that in this case often most of the steps can be reused in an informed way, for instance, exposure distributions of persons are almost completely independent for different types of whole sets of hazardous events.

For instance, the statistical quality of empirical-historical data is rather strong when predicting average annual rates of events when compared to predicting an average consequence measure. Consequences for defined scenarios can alternatively be computed using engineering and simulation methods. However, even event probability estimates can be strongly improved when using in addition scenario input, which cannot be drawn from historical-statistical data.

The chapter introduces risk/chance analysis and management. It gives a first impression of the general ideas before going into details throughout the following chapters. It also shows how to divide the analysis into steps.

Section 2.2 describes the scope of this book in terms of the sample hazard events we mainly regard in this book, namely high explosive and impact events. It introduces the fundamental definitions risk, risk analysis and risk management. It also explains the term risk in more detail and ends with a scheme that provides an overview of the definitions in this chapter.

Section 2.3 gives examples of risk analysis and risk management schemes from the literature, one of them being the standard 5-step risk management scheme. Section 2.4 continues with a list of properties of risk management processes based on the preceding schemes and the literature.

Section 2.4 lists the steps of a risk analysis process in more detail and embeds the risk analysis process in the risk management process. The overview scheme of Sect. 2.2 is extended to a larger scheme including the steps that are explained in Sect. 2.4. Section 2.5 presents typical dependencies of the steps of the risk management process.

Fraunhofer EMI sources used for this chapter are (Klomfass and Thoma 1997b; Klomfass and Thoma 1997a; Häring, Schönher et al. 2009; Radtke, Stacke et al. 2011).

2.2 Fundamental Definitions

2.2.1 Threat Scenario Type, Hazard Events

We mainly consider risk scenarios where either impact or high explosive events are involved, can be used for sufficient modeling or play a major role in the analysis. The focus will be broadened in order to include terrorist threat scenarios as well as natural catastrophes.

High explosive events are characterized by very fast and localized energy release (Klomfass and Thoma 1997, p. 1). In case of high explosions a fast moving detonation front separates the initial material and the detonation products. Examples for high explosives are dynamite or TNT. High explosions do not comprise fast burnings, combustions, the transformation of pyrotechnics, and slow propellants.

An impact is a “sudden time-dependent load” (Bangash 2009). *Impact events* involve fragments generated by high explosions. Impact events also include events with tube launched projectiles, events where debris is generated by explosions or where system components impact the earth’s surface.

2.2.2 Risk

Risk considers a measure for the frequency/probability of events and a measure for the consequences. There are different definitions of risk in the literature. Some examples are:

- “Risk is the combination of probability and the extent of consequences” (Ale 2002)
- Risk is the “effect of uncertainty on objectives” (ISO 2009).

Most definitions do not ask for a special relation between probability and consequences on the one hand and risk on the other hand. The classical definition of risk has the strong requirement of proportionality (Dörr and Häring 2006, 2008; Mayrhofer 2010):

“Risk should be proportional to the probability of occurrence as well as to the extent of damage.” Blaise Pascal (1623–1662), see Fig. 2.1.

Formalized this reads as follows:

Classical definition of risk: *Risk is proportional to a measure for the probability P of an event (frequency, likelihood) and the consequences C of an event (impact, effect on objectives):*

$$R = PC. \quad (2.1)$$

We work with this definition and generalizations thereof for the computation of risks.

Fig. 2.1 Blaise Pascal.
© Juulijis—Fotolia



Negligible risks are called *de minimis risks* (Proske 2004). In the assessment of risks we go beyond just requiring that

$$PC \leq R_{crit}, \quad (2.2)$$

where R_{crit} is a critical risk quantity, for example the classical annual de minimis risk of fatalities is $10^{-6}a^{-1}$ (Proske 2004). We typically ask for more inequalities to hold, for example

$$\begin{aligned} P &\leq f_1(P, C), \\ C &\leq f_2(P, C), \end{aligned} \quad (2.3)$$

which requires that the frequencies and consequences obey inequalities which depend on both the frequency and consequences, respectively.

In generalization of (2.2), it is also possible to bound the risk by a more complex function than the constant value R_{crit} :

$$PC \leq f_3(P, C). \quad (2.4)$$

2.2.3 Classification of Risk

Risk can be classified by different attributes of risk. Examples for classifications are:

- local versus non-localized risks,
- risks per event, in case of an event (conditional risks), per time interval, or per life cycle,
- risks on demand versus continuous risks,
- individual versus collective (group) risks,
- voluntary versus involuntary risks,
- perceived or subjective risks versus objective risks,
- risks based on (semi-)quantitative estimates versus quantitative risk computations,
- statistical historic risks versus risks based on models,
- source of risk: man-made, technical, natural, natural-technical,
- objects, persons or body parts at risk: risk for machinery, personnel, third party, health, lung, etc. affected by the risk, e.g. Proske distinguishes between natural risks, technical risks, risks for the health, and social risks (Proske 2004).

Examples of risks which match these classifications are:

- local individual annual risk of injury due to terroristic explosions,
- total average fatal collective annual risk of a given scenario,
- Collective total risk expressed using a frequency-number curve (F-N-curve): frequency of one or more injuries per year, frequency of ten or more injuries per year due to an explosive storage site.

2.2.4 Risk Management and Risk Analysis

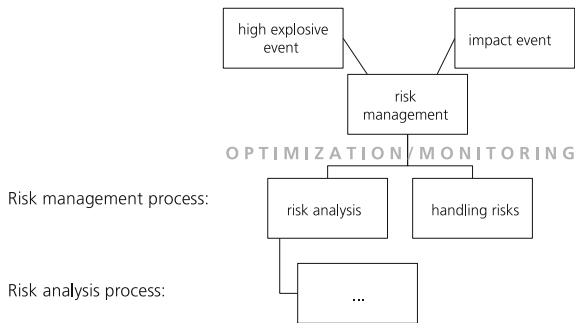
Definition of risk analysis: *Risk analysis* is the determination of risks in a given context.

Definition of risk management: *Risk management* consists of risk analysis and the handling (mitigation) of risks, including changing the context.

Definition of risk analysis and risk management process: Risk analysis and risk management can be divided into different steps. The iterative or incremental execution of these steps together with communication between the steps is *the risk analysis/risk management process*.

Remark The risk analysis and the risk management process are often described in schemes, see Sect. 2.3.

Fig. 2.2 First scheme of the risk management and risk analysis process



2.2.5 Overview

The terms that have been defined so far can be summarized in the scheme in Fig. 2.2.

2.3 Examples for Risk Management and Risk Analysis Schemes

2.3.1 Loading-Based Assessment

In *loading-based assessment* a predetermined dynamic or static loading is analyzed that the building has to stand in addition to the classical loadings. These classical loadings include loadings due to the structures itself, the working load, and the natural environmental loads like wind, snow, and earth quakes. Obviously this approach already assumes that the threat is well known and can be reduced to characteristic loads. This approach fits well into structural engineering processes in particular when assuming in addition that high-dynamic loading can be reduced to equivalent static loads.

Remark An even simpler approach is to increase the safety factors of constructional engineering by a defined factor.

2.3.2 Scenario-Based Assessment

Slightly more general than the known-loading approach is *scenario-based assessment*. In this case a few well defined scenarios are assumed, for example (among



Fig. 2.3 The scenario that a suitcase bomb is being placed next to a building

others), a suitcase bomb with 10 kg net explosive quantity at a distance of 10 m, see Fig. 2.3.

In terms of the more comprehensive risk management and risk analysis schemes of Sects. 2.3.3–2.4 the loading- and scenario-based approach do not make all analysis steps explicit. Typical questions that are not covered in a systematic way include: Are all possible loadings/scenarios considered in the given context (completeness)? How are the assessment criteria derived? Are there mitigation measures beyond structural target enhancement?

2.3.3 5-Step Risk Management Scheme

A standard scheme for the risk management process is the *5-step risk management scheme*. It can be found in many applications. The versions vary slightly, but essentially look like this scheme, based on (Ale et al. 2009):

- (1) **Establish context:** Describe the initial situation, define aims such as safety or health.
- (2) **Identify hazards/risks:** Define damage scenarios. This involves describing the hazard source and the exposure of persons or objects.
- (3) **Analyze/compute risks:** Estimate or specify the probabilities and consequences of events.
- (4) **Evaluate/rank/prioritize/assess risks:** Judge whether risks are acceptable or not. This can involve a comparison of the levels of risk with predefined criteria or a comparison of costs and benefits.
- (5) **Treat/mitigate risks:** For risks that are not acceptable, change the initial situation or find external solutions such as insurance.

The steps are linked by an iterative or incremental (optimization and) monitoring process. Consultations and communication take place between the steps.

See Fig. 2.4 for a graphical version of the 5-step risk management scheme.

Remark An actual decision process also involves subjective perception and cultural or ethical aspects. This is not displayed in this scheme.

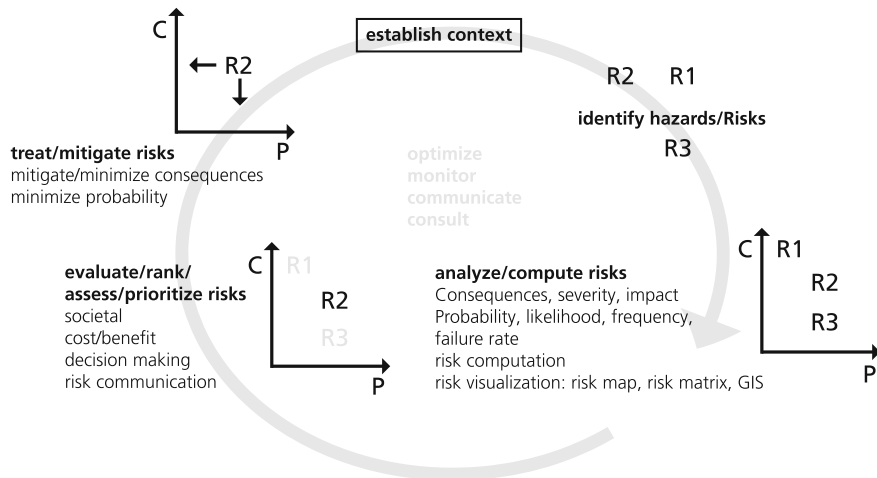


Fig. 2.4 Catchwords and pictograms for the 5-step risk management scheme

2.3.4 Risk Management Schemes for Explosive Safety Scenarios

The German explosive safety quantitative risk analysis (ESQRA-GE) tool uses the scheme from Fig. 2.5 (Radtke et al. 2011). It is applied to ammunition storage scenarios, the disposal of improvised explosive devices (IEDs) in case of terrorist threats and explosive ordnance disposal (EOD) in case of explosive remnants of war (ERW) or again terrorist threats.

Figure 2.6 gives a graphical visualization of the risk analysis steps of the assessment of overhead/overflight scenarios involving moving hazard sources, for example high explosive rounds or rounds with illumination subsystems. The scheme shows the risk analysis steps of the Fuze Safety Quantitative Risk Analysis Software (FSQRA) by grouping them into five steps (Häring et al. 2009).:

- (1) Scenario analysis
- (2) Physical consequence analysis
- (3) Damage analysis
- (4) Probability analysis
- (5) Risk analysis

The schemes in Figs. 2.7 and 2.8 are from (AASTP-4 Ed. 1 2011). The AASTP (Allied Ammunition Storage and Transport Publication) describes in rather general terms how to apply mainly the quantitative risk analysis and management approach to military ammunition storage sites. Its Part 4 Manual on explosives safety risk analysis is an overview designed for use by policy makers, safety professionals, and analysts. It supports the continued growth and utilization of risk-based methods. It

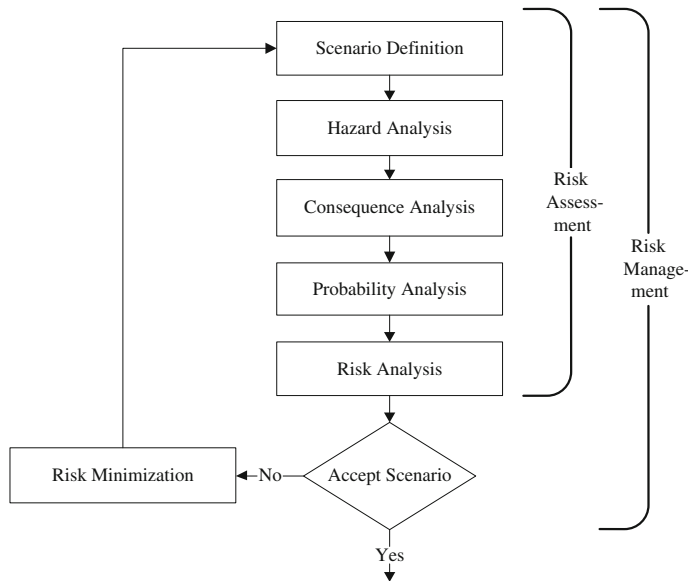


Fig. 2.5 ESQRA-GE risk management scheme (Radtke et al. 2011)

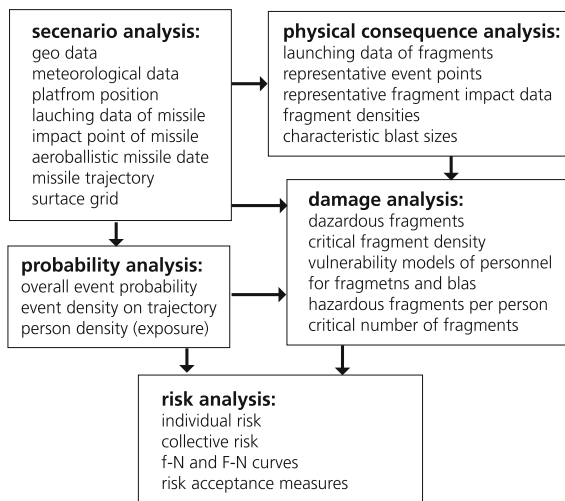


Fig. 2.6 Overview of hazard and risk analysis modeling steps (Häring et al. 2009). Reprinted from Reliability and System Safety Engineering, Vol. 94, Issue 9, I. Häring, M. Schönherr, C. Richter, Quantitative hazard and risk analysis for fragments of high explosive shells in air, pp. 1461–1470, Copyright 2009, with permission from Elsevier

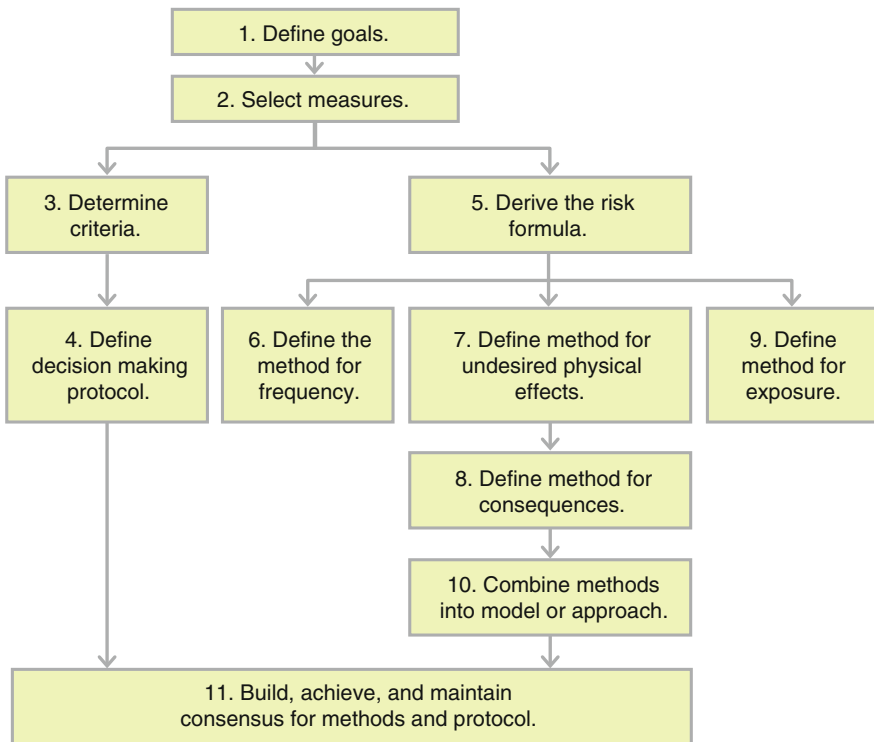


Fig. 2.7 AASTP 4—scheme to develop a risk-based decision approach (AASTP-4 Ed. 1 2011)
Reprinted from Allied Ammunition Storage and Transport Publication: Manual on explosives safety risk analysis (AASTP-4 Ed.1), Nato Standardization Organization, 2011

is designed to assist in developing and using new applications and to provide examples of current international uses. Towards these purposes, it

- “Provides guidance in the establishment of risk-based decision methods,
- Describes existing risk-based methods in use by the participating nations,
- Identifies common features of risk-based approaches, so that assessments done by individual nations in multinational operations may be understood and, if appropriate, used by other countries” (AASTP-4 Ed. 1 2008).

During the last 15 years this approach was implemented in various NATO countries including associated non-NATO states like Norway and Singapore. Similar approaches can also be used for non-military high explosive sources, e.g. improvised explosive devices (IEDs) as well as for related scenarios like impacting threats.

We note that the schemes of Figs. 2.5, 2.6, and 2.8 all distinguish between physical effects and damage effects. The determination of these steps seems to require more effort than the steps covering the determination of the frequency/probability quantities. Comparing the 5-step-scheme of Fig. 2.4 and the schemes of Figs. 2.7 and 2.8 we find that the risk computation step is much extended.

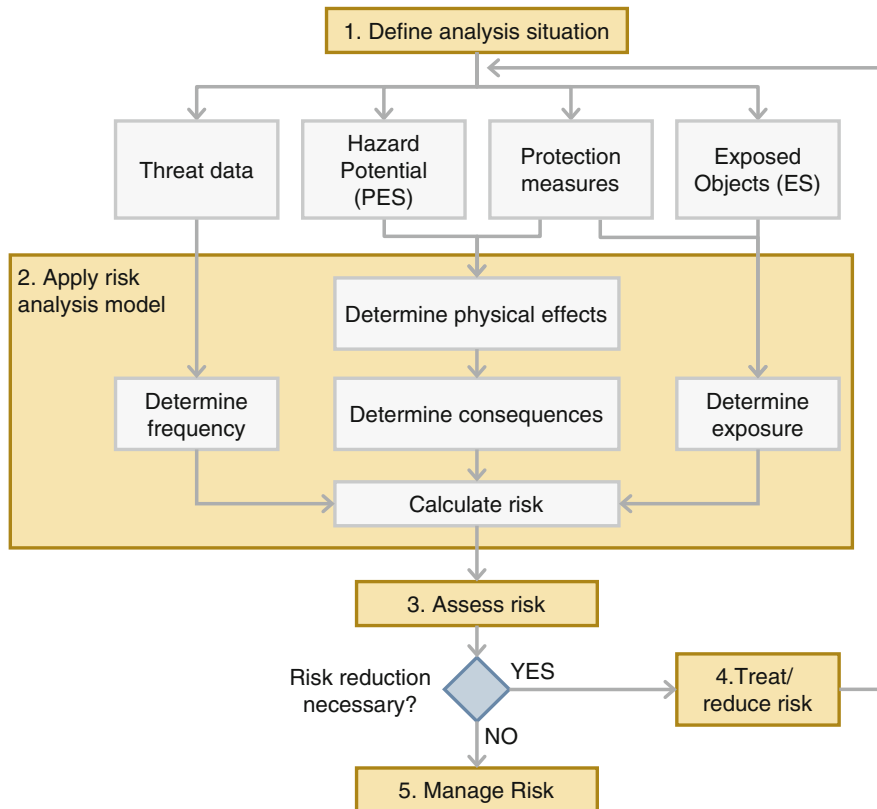


Fig. 2.8 AASTP 4—scheme to apply a risk-based decision aid. The scheme uses the abbreviations for potential explosive site (*PES*) and exposed site (*ES*) (AASTP-4 Ed. 1 2011). Reprinted from Allied Ammunition Storage and Transport Publication: Manual on explosives safety risk analysis (AASTP-4 Ed.1), Nato Standardization Organization, 2011

2.4 Attributes of the Risk Analysis and Risk Management Processes

Comparing the schemes from Sect. 2.3 we find that the processes and their describing schemes have different properties. Table 2.1 lists those and some further attributes.

2.5 Risk Analysis and Management Process

We now give a more detailed description of the **risk analysis process** that will be used in the following chapters. It divides into 9 steps that are connected by an iterative or incremental optimization and monitoring process. We start the

Table 2.1 Complementary attributes of risk and chance analysis and management processes

Implicit	Explicit
With software support	Without software support
Graphical description/visualization	Textual description
Coarse process steps	Refined process steps
Standardized, formalized	Ad hoc, situation/scenario driven
Described from decision maker perspective	Described from end-user perspective
Time critical process steps	Not time critical process steps
Real time risk analysis, risk management for decision support	Preventive risk analysis, ex-post risk analysis, forensic risk analysis
Virtual environment to exchange information	Exchange information in person
Multidisciplinary	One discipline
Multiple stakeholders	One stakeholder
Multinational	National
Based on existing database	Collect data by oneself
Threat assessment focusing on Consequences or likelihood	Threat assessment based on risk (i.e. consequences and likelihood)
Considering only first order effects (effects on health and first actions)	Considering also second and third order effects (effects on society, economy, and politics)
Scenario-based	Covering multiple scenarios
Focusing on worst-case scenario	Considering a broader range of scenarios
Application to real scenarios (ex-post, for validation purposes)	Application to fictitious scenarios (preventive analysis)

enumeration with (2) to add another step in front of it when we treat the risk management process.

- (2) **Initial situation without hazard source:** All information needed to apply hazard and damage schemes is being collected. This includes geometrical, geographical, meteorological, and topological data and information about materials and meteorological conditions.
- (3) **Description of the hazard source:** The description includes geometry, mass, position, orientation, and velocity of the hazard source as well as mitigation measures close to the hazard source.
- (4) **Hazard propagation/hazard analysis:** This includes the potential dispersion, distribution, and impact load distribution of the physical hazard.
- (5) **Damage/consequence analysis/modeling:** Here the effects of the physical hazard potential on objects like persons, vehicles, buildings, and infrastructure are determined.
- (6) **Analysis of hazard event frequency:** It is analyzed how often the hazard source becomes active. This is determined by considering, for example, the frequency of the hazard source being present, the frequency of an unintended

event within the hazard source and the frequency of a failure of the containment. This step also covers location-dependent event frequencies.

- (7) **Distribution of objects:** The distribution describes how many and where objects of interest are located in the area. Exposition/exposure describes that they are actually exposed to the damaging effects.
- (8) **Success frequency of avoiding hazard event consequences:** This step considers the success frequency of organizational and training measures, of spontaneous reactions (for example flight) as well as the success rates of placing passive, reactive, or active physical barriers.
- (9) **Risk computation and visualization:** This involves the computation of various risk quantities. The visualization options include risk maps, risk tables, and F-N-diagrams.
- (10) **Risk comparison with criteria:** The risk quantities are compared to risk assessment criteria, for example risk matrices, critical values, and F-N criteria. For example, one checks whether the nonlocal annual individual risk is smaller than the de minimis risk.

To describe **the risk management process**, the following steps are added.

- (1) **Background/Context:** This includes information about the country where the event is located, the cultural and ethical background, the legal and technical requirements, and the types of scenarios that are considered.
- (11) **Risk assessment:** Risk assessment is the combination of the previous step (10) with other steps that enables to make a final risk evaluation. In particular, legal, social, and psychological effects on the assessment of risks are considered.
- (12) **Risk communication** focuses on the communication of risks to experts, responders, the public, and third party. For instance, risks comparable to the risks that are to be assessed are named. This should be risks the persons addressed can relate to. An emotional link to the risk should be created.
- (13) **Evaluate risk:** Taking the steps (10)–(12) into account, It is being judged whether risks are acceptable or not.
- (14) **Mitigation measures:** There are mitigation measures that reduce the frequency, mitigation measures that reduce the physical hazards, mitigation measures that reduce the consequences of events, and mixed mitigation measures. We also count feasible changes of the background among mitigation measures.

Figure 2.9 extends the first overview of the risk management process from Fig. 2.2. The iterative or incremental (optimization and) monitoring process between the steps is indicated as well.

Figure 2.10 and Table 2.2 show how the 5-step risk management scheme of Fig. 2.4 and the 14-step risk analysis and management scheme from this section Fig. 2.9 relate to each other.

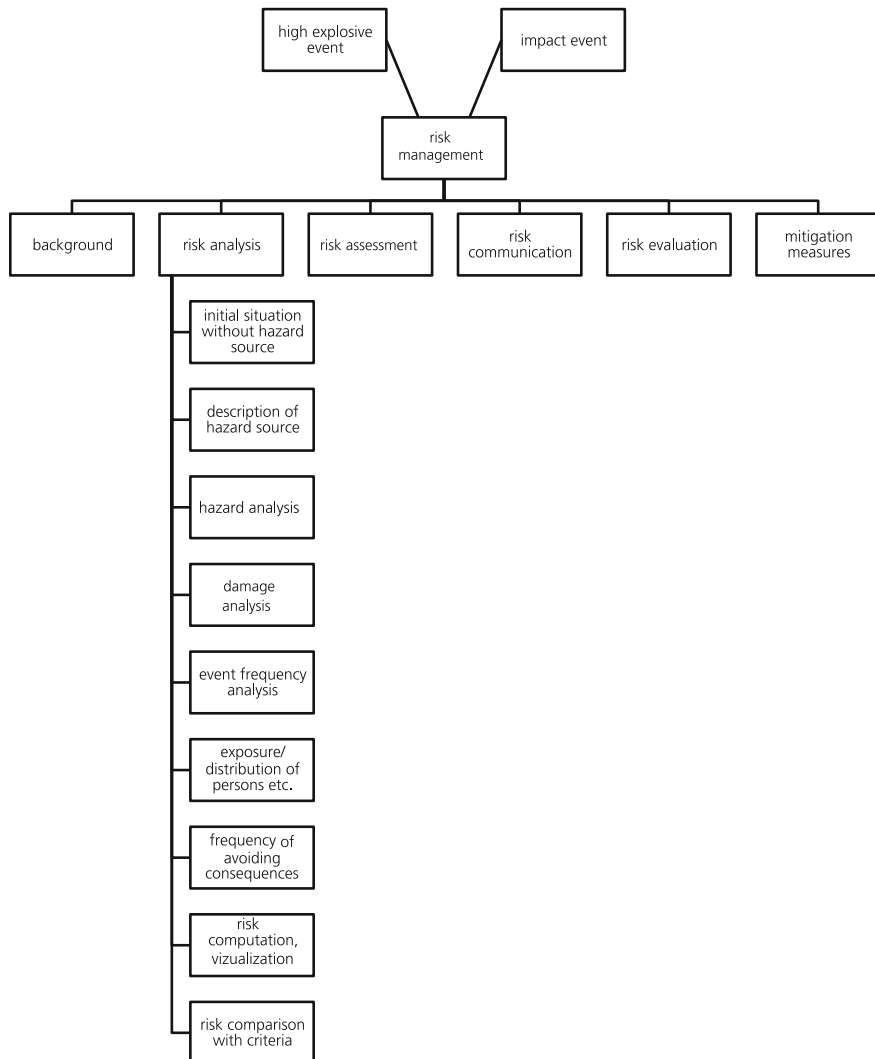


Fig. 2.9 First scheme of the risk management and risk analysis process

Table 2.2 reads as follows: Take for example step 3 in the left column (“Description of the hazard source”). The black “X” in the column “(2) Identify risk/hazards” means that step 3 can definitely be assigned to the second step of the 5-step scheme. The gray “X” in the column “(1) Establish context” means that some aspects of step 3 can also be assigned to the first step of the 5-step scheme.

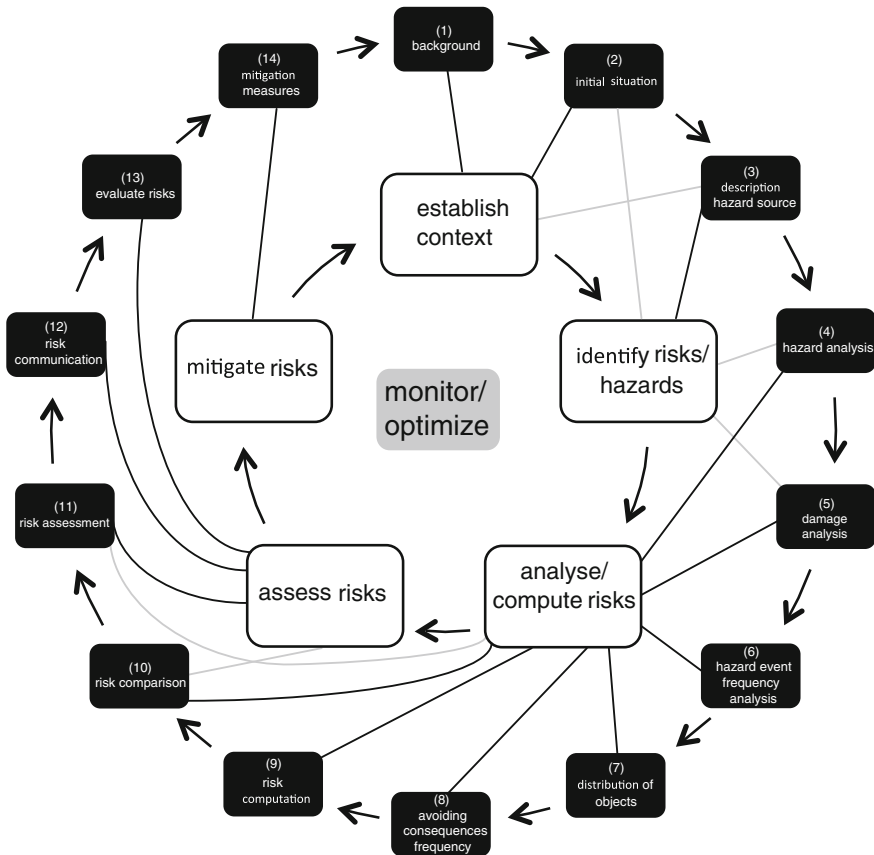


Fig. 2.10 Second scheme of the risk management and risk analysis process

2.6 Typical Dependencies of Risk Management Steps

Table 2.3 shows how the different risk management steps depend on each other in the process. Example for how to read the table: Take a look at the line where it says step 7 in the column furthest on the right and where there are “x” in the columns for input steps 1, 2, 6, 12, and 14. The line should be read in the following way: The steps 1, 2 and 6 should be executed before step 7 and the results of step 7 should be reconsidered after finishing steps 12 and 14.

Remark Remember that the risk management model it is an iterative model. The reconsidering can be understood as being part of a complete redoing of all steps after step 14.

Table 2.2 Placement of the 14 risk management steps of Sect. 2.4 in the 5-step risk management scheme of Sect. 2.3.3

	(1) Establish context	(2) Identify risk/hazards	(3) Analyze/compute risks	(4) Access risks	(5) Mitigate risks
(1) Background	X				
(2) Initial situation without hazard source	X	X			
(3) Description of the hazard source	X	X			
(4) Hazard propagation/hazard analysis		X	X		
(5) Damage analysis/modeling		X	X		
(6) Analysis of hazard event frequency			X		
(7) Distribution of objects			X		
(8) Success frequency of avoiding hazard event consequences			X		
(9) Risk computation and visualization			X		
(10) Risk comparison with criteria			X	X	
(11) Risk assessment			X	X	
(12) Risk communication				X	
(13) Evaluate risk				X	
(14) Mitigation measures					X

2.7 Summary and Outlook

This chapter introduced different risk analysis and management processes and schemes to represent them.

In the following we focus on the 14-step risk management process of Sect. 2.4. After analyzing the dependencies of the different steps in Sect. 2.5, the most appropriate scheme for the risk management process appears to be the one from Fig. 2.10 while keeping in mind that it is possible to go around the circle several times and to leave out steps on the way. We note that the steps 10–13 are rather elaborate to allow for societal input in the decision process.

Table 2.3 Dependencies of the different risk management steps on each other

Steps relevant for input/output														Step
1	2	3	4	5	6	7	8	9	10	11	12	13	14	
													x	1
x												x		2
x	x											x		3
	x	x										x		4
	x		x			x						x		5
x	x	x				x						x		6
x	x				x					x			x	7
x	x				x					x		x		8
		x	x	x	x	x						x		9
x	x						x					x		10
x							x	x				x		11
x	x							x	x			x		12
x	x						x	x	x	x		x		13
x	x	x									x			14

After two chapters on database analysis to have the necessary tools at hand, the steps of the 14-steps risk management process will be explained in more detail, focusing, in particular, on the nine steps of the risk analysis process.

2.8 Questions

- (1) How is risk analysis defined?
- (2) The broadly acceptable level of risk in the UK is the individual annual risk of fatalities: $10^{-6} a^{-1}$ (Proske 2008).
 - (a) How can this information be used in a risk management process?
 - (b) In which step of the 14-step risk management process can it be used?
- (3) Must the steps of the 5-step risk management scheme happen in the presented order? If yes, why is this necessary? If no, why would one go back to a previous step?
- (4) For what type of building could the scenario-based assessment be interesting?
- (5) Which boxes in Fig. 2.5 can be related to which of the steps of the 5-step risk management scheme of Fig. 2.4?
- (6) Which of the steps of the 14-step risk management scheme in Fig. 2.10 are covered by the scheme in Fig. 2.7?
- (7) Which definition of risk do you use at your work place? Which other definitions can you find in the literature? Discuss the differences and advantages or disadvantages.

2.9 Answers

- (1) See Sect. 2.2.4.
- (2) (a) As R_{crit} in (2.2).
 (b) In step (10), see Sect. 2.4.
- (3) No, the incremental optimization and monitoring process might ask for a reconsideration of a previous step, see Sect. 2.3.3.
- (4) E.g. an embassy, bank building, headquarter of a company, house of a public person, ...
- (5) Scenario definition -> 1, hazard analysis -> 2, consequence analysis, probability analysis and risk analysis -> 3, accept scenario yes, no -> 4, risk minimization -> 5.

References

- AASTP-4 Ed. 1. (2008). Manual on explosives safety risk analysis—Part 4. Nato Standardization Organization. Brussels: NATO.
- AASTP-4 Ed. 1. (2011). Manual on explosives safety risk analysis—Part 4. Nato Standardization Organization. Brussels: NATO.
- Ale, B. J. M. (2002). Risk assessment practices in The Netherlands. *Safety Science*, 40(1–4), 105–126.
- Ale, B., Aven, T., & Jongejan, R. (2009). Review and discussion of basic concepts and principles in integrated risk management. *ESREL (European Safety and Reliability Conference)*, Prag. London: Taylor and Francis Group.
- Bangash, M. Y. H. (2009). *Shock, impact and explosion—Structural analysis and design*. Berlin: Springer.
- Dörr, A., & Häring, I. (2006). Einführung in die Risikoanalyse 2. In N. Gebbeken, M. Keuser, M. Klaus, I. Mangerig & K. Thoma (Eds.), *Workshop Bau-Protect 2006*.
- Dörr, A., & Häring, I. (2008). Introduction to methods applied in hazard and risk analysis 3. In N. Gebbeken (Ed.), *Workshop Bau-Protect*.
- Häring, I., Schönherr, M., & Richter, C. (2009). Quantitative hazard and risk analysis for fragments of high explosive shells in air. *Reliability and System Safety Engineering*, 94(9), 1461–1470.
- ISO. (2009). *ISO Guide 73: Risk management vocabulary*. Geneva: International Organization for Standardization.
- Klomfass, A., & Thoma, K. (1997). *Ausgewählte Kapitel der Kurzzeitdynamik Teil 1 – Explosionen in Luft*. Freiburg: Fraunhofer Institut für Kurzzeitdynamik, Ernst-Mach-Institut.
- Mayrhofer, C. (2010). Städtebauliche Gefährdungsanalyse - Abschlussbericht Fraunhofer Institut für Kurzzeitdynamik, Ernst-Mach-Institut, EMI, Bundesamt für Bevölkerungsschutz und Katastrophenhilfe. http://www.emi.fraunhofer.de/fileadmin/media/emi/geschaeftsfelder/Sicherheit/Downloads/FiB_7_Webdatei_101011.pdf
- Proske, D. (2004). *Katalog der Risiken, Risiken und ihre Darstellung*. Dresden: Eigenverlag.
- Proske, D. (2008). *Catalogue of risks—Natural, technical, social and health risks*. Berlin: Springer.
- Radtke, F. K. F., Stacke, I., & Häring, I. (2011). Extension of the German explosive safety quantitative risk analysis tool ESQRA-GE. *14th ISIEMS*. Seattle, USA.

Chapter 3

Introduction to Database Analysis of Terroristic Events

3.1 Overview

The chapter introduces data-driven analysis for risk/chance analysis and management. The main aim is to show that even rather simple event data can be used for assessments. Examples are event type analysis (scenario analysis), frequency, consequence and risk analysis.

The chapter introduces a data management scheme that is aligned to the risk management and analysis process. This allows the application of the approach to related domains. It also helps to reduce the data-gathering effort. Data selection and preparation is necessary before the application of analysis methods. It is shown how to implement such an approach using standard database management technology.

The identification of suitable data sources for historic-statistical analysis is discussed along with basic approaches and a rather advanced option to overcome the lack of data, namely the systematic gathering and clustering of news texts related to risk events of interest. Ultimately, the data gathering has also to operationalize a sharp definition of risk events of interest.

The controlled selection of data for later data analysis is key for proper analysis, for instance threats of a certain type, in certain regions on certain types of infrastructure are of interest. It is shown which types of event attributes are typically of interest and how to implement them using a relational database scheme and standard database management schemes.

This chapter also introduces a variety of basic methods, diagram types and visualizations to represent event types, risks and the time dependency of different event characteristics (attributes), for instance frequency and severity of events.

Furthermore, this chapter emphasizes the need for a well-informed definition of risk quantities. For instance, data-driven risk quantities should be comparable on absolute scales: extensive quantities that increase in case of a larger raw data body should be avoided as well as meaningless scales, e.g. when employing

semi-quantitative scales only, since they prevent the comparison with more advanced approaches.

Database-driven analysis typically contributes to the resilience engineering of resilience management and analysis phases that are related to context and scenario definition and threat characterization. Further steps covered mainly include the identification of types of events, event frequencies and object distributions. However, also damage and risk quantities are accessible. This information can be used for the assessment and improvement of all resilience management phases, in particular prevention and protection.

This chapter gives an introduction to database analysis. Database analysis is an important tool for the risk management process and accompanies the process throughout several steps. This will be shown in detail in Sect. 3.12.

Section 3.2 presents a scheme to illustrate the process that we understand as database analysis. It also describes two approaches to database analysis by interpreting the scheme in two different ways.

Section 3.3 lists the mathematical notations and formulas that are used in this chapter and Chap. 4.

Sections 3.4–3.11 follow the scheme from Sect. 3.2, see Fig. 3.1. Each section explains one or two steps of the database analysis process. Examples are given. Most of them refer to the Terror Event Database (TED) that was designed and populated by the Fraunhofer Ernst-Mach-Institut.

Section 3.12 completes the chapter by drawing connections between database analysis and the 14-step risk management process developed in Chap. 2.

The chapter is mostly based on Siebold (2007) and Siebold et al. (2007). It focuses on databases of terroristic events. Further Fraunhofer EMI sources are Rathmann (2003), Häring et al. (2005), Nahnsen (2005), Kleb (2006). The main author of the EMI sources is U. Siebold supplemented with work by J. Kleb, T. Nahnsen, I. Häring and A. Karwarth.

The goal of this chapter is to have the necessary tools at hand to understand the database analysis and statistical operations in the rest of the course.

3.2 Database Analysis Scheme

“Knowledge Discovery in databases is the non-trivial process of identifying valid, novel, potentially useful, and ultimately understandable patterns in data.” (Fayyad et al. 1996, p. 5)

For an overview on *database analysis*, Fig. 3.1 introduces a scheme that shows the different steps of the process of database analysis. It extends similar schemes given in Fayyad et al. (1996).

There are different approaches to this database analysis process:

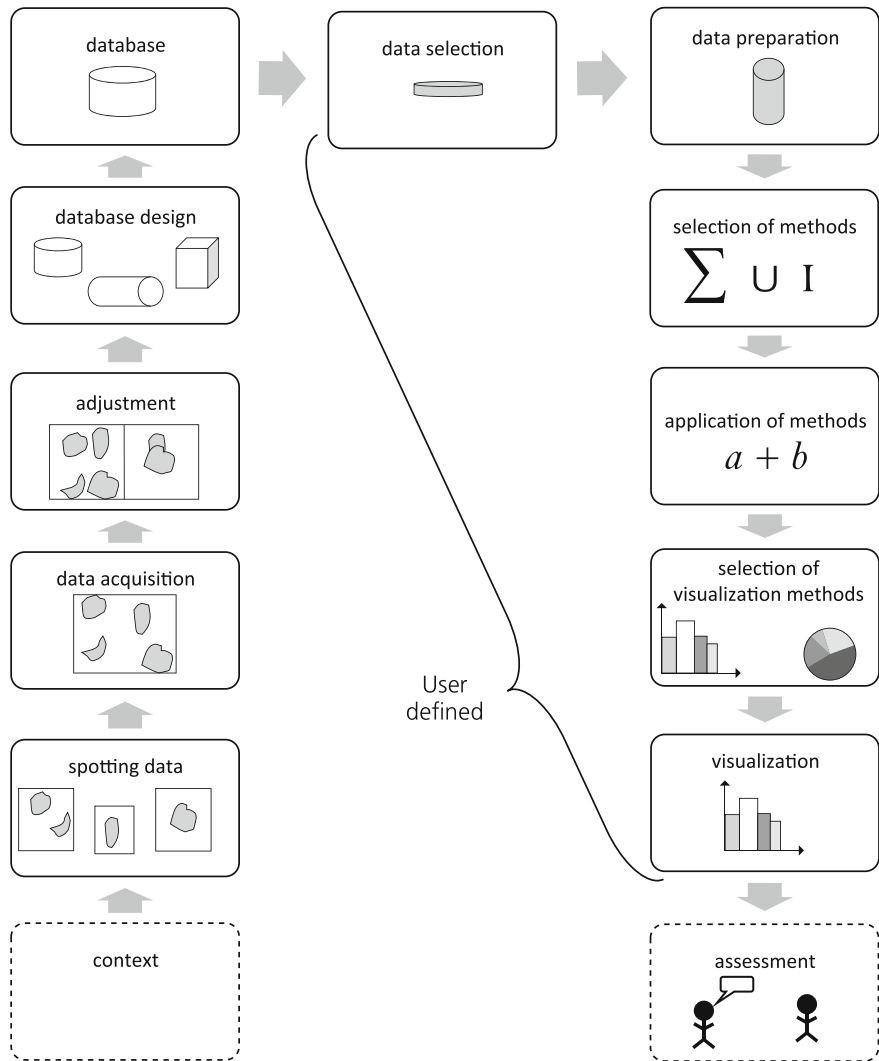


Fig. 3.1 Scheme for database analysis

- (1) **Forwards:** All the data that might be useful is gathered and all the methods that seem reasonable are applied in order to get a broad result that answers the question.
- (2) **Backwards:** The process is read backwards from the desired results. In each backwards step it is analyzed what is needed to get what is wanted. This yields a set of requirements for the data that needs to be collected. Then the forward process is carried out with this data.

Table 3.1 Advantages and disadvantages of the different approaches to the database analysis scheme

Approach	Advantages	Disadvantages
(1) Forwards	The process is only gone through once	It is not clear at the beginning whether the chosen data will yield useful results
(2) Backwards	Work is more focused. There is no collection of unnecessary data and there are no unnecessary calculations	It is not clear at the beginning whether the requirements for the dataset can be fulfilled. The process has to be gone through twice
(3) Mixed, iterative	The approach is very flexible	The process can take a lot of time if one has many iterations

- (3) Mixed/iterative approach: One starts with a data set and analyzes it. If one discovers that it does not yield the desired information, one goes back to change the data set and adapts the analysis to this new data set.

Table 3.1 lists the advantages and disadvantages of the three approaches.

3.3 Mathematical Notations

In order to analyze a database, certain mathematical and statistical background knowledge is necessary. It is assumed that the reader is familiar with mathematical concepts such as union, intersection, and sums. This book also does not give a detailed introduction to elementary statistics. Please refer to Rohatgi and Saleh (2000), Shao (2003) for English and to Kadelka and Henze (2000), Beichelt et al. (2003), Georgii (2004), Irle (2005) for German textbooks on statistics. The mathematical notation and formulas we use can be found in Table 3.2.

3.4 Spotting Data and Data Acquisition

3.4.1 *Definition of Events*

The analysis of information that is transported through magazines, newspapers, and news broadcasts gives the opportunity to build up an archive to selected topics. This archive can be used to generate new and valuable information. Some examples for this are (Kleb 2006, p. 10):

- With an observation of the birthrate one can predict the development of a population.

Table 3.2 Mathematical notation and formulas

Name	Notation/formula	Remark
Positive integers	\mathbb{N}	$\mathbb{N} = \{1, 2, 3, \dots\}$
Non-negative integers	\mathbb{N}_0	$\mathbb{N}_0 = \{0, 1, 2, 3, \dots\}$
Subset	\subseteq	
Intersection	\cap	
Union	\cup	
Exclusive union	$A \cup_{ex} B := (A \cup B) \setminus (A \cap B)$	
Without	\setminus	
And	\wedge	
Or	\vee	
Not x	$\neg x$	The statement x is being negated
Sum	\sum	
Cardinality of A	$ A $	Gives the number of elements of a set
Number of...	#	Used as shorthand verbal notation
(Arithmetic) mean	$\bar{x} := \frac{1}{n} \sum_{i=1}^n x_i$	
Mean in time	$\overline{x_{\text{attacks}/ndays}(t_1, t_2)} := \frac{n}{t_2 - t_1 + 1} \sum_{a \in A} (t_1 \leq a_{[\text{date}]} \leq t_2)_B$	Uses the logic bracket
Logical bracket	$(x)_B := \begin{cases} 1 & \text{if } x \text{ is true/defined,} \\ 0 & \text{otherwise.} \end{cases}$	
Data set	$x = \{x_1, x_2, \dots, x_n\}$	
Variance	$s_x^2 := \frac{1}{n-1} \sum_{i=1}^n (x_i - \bar{x})^2$	
Standard deviation	$s_x := +\sqrt{s_x^2}$	
Median	For $x_1 < x_2 < \dots < x_n$, $\tilde{x} := \begin{cases} x_{(n+1)/2} & \text{if } n \text{ is odd,} \\ \frac{1}{2}(x_{n/2} + x_{n/2+1}) & \text{if } n \text{ is even.} \end{cases}$	
(Pearson's) correlation coefficient between x and y	$r_{xy} = \frac{\frac{1}{n-1} \sum_{j=1}^n (x_j - \bar{x})(y_j - \bar{y})}{s_x s_y}$	
(Empiric) autocovariance	$\hat{\gamma}(k) = \frac{1}{n} \sum_{t=1}^{n-k} (x_{t+k} - \bar{x})(x_t - \bar{x})$	
(Empiric) autocorrelation coefficient	$\rho_k = \frac{\hat{\gamma}(k)}{\hat{\gamma}(0)}$	
Autocorrelation function	$\rho(k) := \rho_k, \quad k \in \mathbb{N}$	The autocorrelation function is a function of the lag k

(continued)

Table 3.2 (continued)

Name	Notation/formula	Remark
<i>Correlogram</i>	Diagram of the autocorrelation function	
Sum of squared residuals/ <i>method of least squares</i>	Minimize $\sum_{j=1}^n (y_i - a - bx_j)^2$ as a function of a and b	
<i>Period</i>	$T = \frac{1}{f} = \frac{2\pi}{\omega}$	f is the frequency, ω the angular frequency
<i>Periodic function</i>	$f(t) = f(t + T)$ for all t	t is the time

- A country's climate is the basis for the estimation of future harvest that is possible in the area.
- With the analysis of terroristic events, models for the risk estimation for future plans related to an area, a country, or a population group can be created.

This text focuses on database analysis of terroristic events.

Before gathering information it has to be specified what an event is, that is, which sorts of incidents are considered and which information about these incidents should be collected. We use the definition from Yun et al. (2003, p. 580):

An *event* is some “(non-trivial) [incident occurring] in a certain place and [at] a certain time”.

For terroristic events we use the specification from Nahnsen (2005) which is based on Yun et al. (2003) and Taylor (2004).

“In particular, an event can be considered to qualify as a *terrorist event* or an attempt of a terrorist event if the terroristic incident occurred at a specific point in time, at a specific location, with specific tactics, and presumably a known extent of the event.” (Nahnsen 2005, p. 14)

He gathers the following attributes for each event:

“Location(s)

Date

Tactics

Attacker(s)

Casualties (killed)

Casualties (wounded)

Organization(s)

Country/Countries in which the attack occurred

Country/Countries being attacked” (Nahnsen 2005, p. 15)

3.4.2 Sources for Data Gathering

Different sources can be used to gather information. Some of them are listed in Table 3.3.

Table 3.3 mentions how the Joint Research Center of the European Commission preprocesses news in EMM. It also gives a brief impression of how data was collected when TED was created and how it is being updated. Those two practices of news gathering are explained in more detail in the following two examples.

Example “At the Joint Research Center (JRC) of the European Commission, the European Media Monitor (EMM; Best 2002) is being developed and maintained. The system monitors selected online newspapers and news wires in order to determine and extract relevant and important information. Currently, several hundred newspapers in several languages including English, German, French, Spanish, and Italian are being monitored. In a first step, news articles are selected from the monitored websites and the actual news text is extracted using a heuristic-based mapping of websites onto a tree structure. In a second step, a finite state machine is currently employed to match approximately 17,000 keywords in 700 categories to the extracted text; the official 2003 report mentions 8000 keywords in 350 categories (Kommission der Europäischen Gemeinschaften 2003). For the category ‘terrorism,’ for instance, representative keywords include “suicide bomb” and “terrorism.” Keywords can be combined in Boolean logic and set operations on categories are possible such as subtracting all entries in one category from the entries in another category.” (Nahnsen 2005, p. 64)

Example Kleb (2006, pp. 10f): The Fraunhofer Ernst-Mach-Institut records terroristic events for TED since 2002. One part of the data is from 22 internet pages, 5 books, and news reports from at least 2 years. The second part was collected manually from the MIPT Terrorism Knowledge Base (MIPT 2007; Siebold 2007). For regular updates, the information is collected by a person by analyzing online news reports about once a month. The person’s work divides into the following steps:

Table 3.3 Sources for data acquisition

Source	Examples
Existing database	TED uses MIPT (2007)
Book	For TED Johnson (1975), Edward et al. (1989), Mickolus et al. (1989), Hoffman (1990, 1991) are used
Website	For TED International Policy Institute for Counter-Terrorism (2007), Terrorism Research Center (2007), Chaveer.de (2007), Rheinzeitung (2007), schlaufuchs.at (2007), Welt.de (2007a, b, c) are used
News report	For TED Tagesschau (2012) is used
Preprocessed news	European Media Monitor (EMM; Best 2002)

- Opening the website of a news magazine.
- Displaying of the day's articles. If the website contains an archive function, this can be used to regard the articles in a weekly or monthly arrangement.
- Subjectively selecting the relevant articles. If there are several articles about the same topic, the newest one is chosen. The selection of an article is done by the title and, if available, the abstract.
- Manual extraction of the information needed for a database entry if the selected article describes a terroristic event.

3.4.3 Automation of Data Spotting and Gathering

“In light of the inherently distributed and unstructured availability of the information in question, [TED’s] current manual approach to gathering information represents a severe bottleneck. In particular, resource requirement and costs are enormous and database-coverage is poor, as it tends to be limited to a comparatively narrow selection of news sources. In other words, under manual database maintenance, record keeping is constrained and forecasting sub-optimal. [...] In order to be able to improve the coverage of the database with respect to the entries’ timeliness and scope, in an intermediate timeframe, the institute seeks computer-aided insertion of terrorist events into the database. In the long-run, it aims for the identification of terrorist events and a combination of multiple news articles on identical events to a single entry in the database, i.e., the institute desires the full automatization of the maintenance and expansion of its database.” (Nahnsen 2005, p. 8)

One step towards this goal is the so called *information extraction*, “the mapping of short natural language texts (such as newswire reports) into predefined, structural representations, or templates, which, when filled, represent and extract [...] key information from the original text” (Gaizauskas and Humphreys 1997, p. 147). For information on this broad field of research see for example Saggion et al. (2003) or Radev and McKeown (1998).

3.4.4 Clustering

One part of data acquisition can be the clustering of data. Kleb (2006) develops an automation for organizing news articles in clusters, ideally matching those articles that describe the same event. The new cluster structure makes the manual extraction of information easier and faster and is hence a big improvement for manually-maintained databases like TED.

Kleb’s *clustering* process that is visualized in Fig. 3.2 divides into the following steps (Kleb 2006):

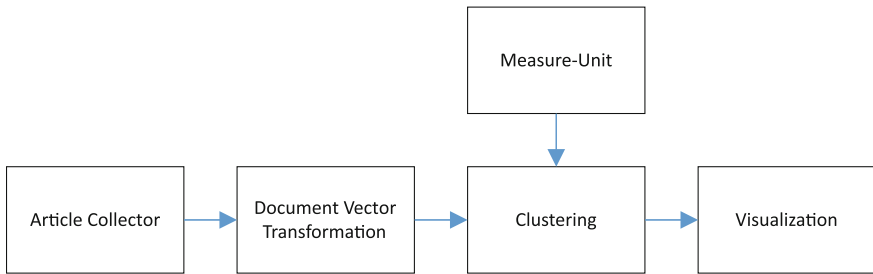


Fig. 3.2 Scheme for modular software architecture to cluster data (Kleb 2006)

- (1) Article Collector: The set of documents is being structured and stored.
- (2) Document Vector Generation: Unstructured text is being transformed into a vector.
- (3) Clustering: Methods to discover similarities between the documents and ways to cluster the documents are being applied.
- (4) Measure Unit: The cluster structure is being evaluated by implemented methods.
- (5) Visualization: Results of the proceeding steps are being graphically presented.

Remark This process also covers the data mining tasks presented in Hand et al. (2001).

Further information about clustering and established algorithms for dividing the document corpus in natural clusters are given in Dubes and Jain (1988), Kaufmann and Rousseeuw (1990), Jain et al. (1999), Ester and Sander (2000), Berkhin (2002), Tan et al. (2005).

3.5 Adjustment

If one collects data, this data comes in very different forms. For example, data from news articles usually contains information about the number of casualties. Data from insurance companies on the other hand rather contains information about the damage sum. So, if one wants to write a table with all the data that has been gathered, one has to decide which information to include in the table and which to leave out. The extreme solution of including all information one has gathered yields a very big table with very many “0”-entries. The other extreme of only including information that appears in (almost) all the sources, might lead to losing important information. Hence, one has to be very careful in the decision process of which information to include.

The same problem occurs if one wants to unify two databases. This can be necessary in different situations. For example, if more information for a specific task is needed than available in the existing database (which is very likely in the

backwards approach described in Sect. 3.2), one has to enlarge the database, for example by including another database. It is also possible that one has two databases and wants to combine them to one to make information included in both more easily accessible and comparable.

Especially for the unification of two databases, it is important to keep the old, complete databases as well and not to only save the new one, as one otherwise loses information that one might need for later projects.

3.6 Database Design

We restrain this section to introducing the coarse structure of TED as an example for how a database is designed. We do not explain the computer scientific methods that are needed to design a database.

Example for an entry in the relation “*anschlaege*” of TED (Rathmann 2003):

Category	Entry
Date (a_datum)	05/07/2002
Target (a_ziel)	Entertainment center (saved as ID)
Category (a_kategorie)	Building for cultural use (saved as ID)
Group (a_gruppe)	Hamas (saved as ID)
Country (a_land)	Israel (saved as ID)
Target country (a_zielland)	Israel (saved as ID)
Tactic (a_taktik)	Suicide attack with explosives (saved as ID)
Tools (a_hilfsmittel)	Suitcase filled with explosives and nails
Injuries/casualties (a_verletzte)	60
Fatalities (a_tote)	16
Damage (a_schaeden)	Collapse of the building
Details (a_details)	A suicide attacker detonates a bomb in a busy pool hall in Israel. The attack takes place in the “Sheffield Club Pool Hall”, on the second floor of a building in Rishon LeTzion (south of Tel-Aviv). The building was located about one block away from the biggest shopping mall in the country

Note that a lot of the information is saved in form of IDs. For these entries, additional information is saved in other relations. For the proceeding example, the ID of “Suicide attack with explosives” leads to the relation “*taktiken*”. In the relation “*taktiken*”, the name “Suicide attack with explosives” is saved under the category *t_name* and a description of the tactic is saved under *t_beschr*.

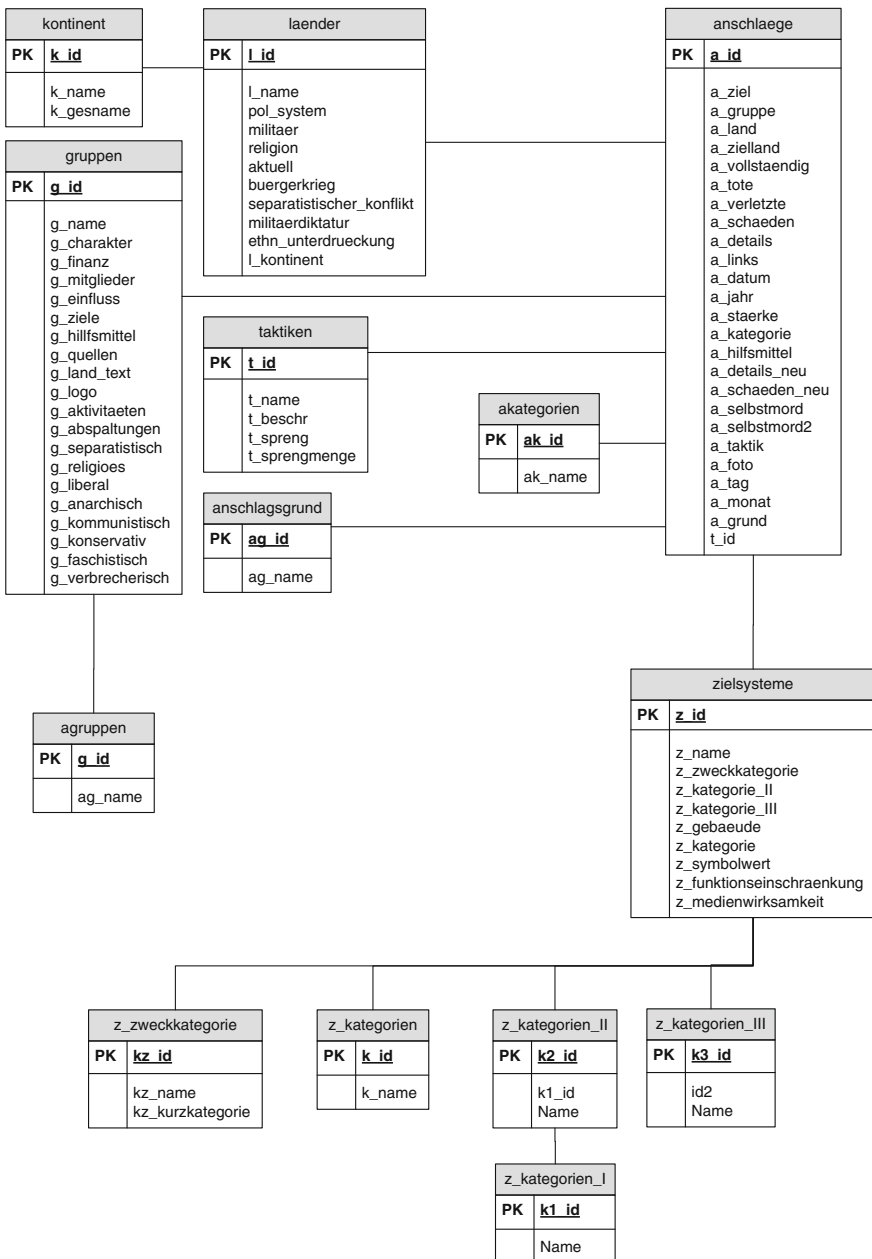


Fig. 3.3 Scheme of the terror event database (TED) (Siebold 2007)

Table 3.4 Translation of the vocabulary in Fig. 3.3

German	English
Anschlaege	Attacks
Laender	Countries
Bevoelkerungszahlen	Population
Kontinent	Continent
Gruppe	Group
Taktik	Tactic
Zielsysteme	Target systems
Kategorien	Categories
Ziel	Target
Land	Country
Zielland	Target country
Vollstaendig	Complete
Tote	Fatalities
Verletzte	Casualties
Schaeden	Damage
Details	Details
Links	Links
Datum	Date
Jahr	Year
Staerke	Strength
Kategorie	Category
Hilfsmittel	Tools
Details_neu	Details_new
Schaeden_neu	Damage_new
Selbstmord	Suicide
Foto	Photo
Tag	Day
Monat	Month
Grund	Reason
Name	Name

TED was realized in Microsoft Access. The structure of TED can be seen in Fig. 3.3. Since the database is in German, the scheme is in German, too. A translation to English is given in Table 3.4.

Events are stored in the relation “*anschlaege*”, see Table 3.5.

Details about the events’ attributes can be found in other relations. For example *a_land* only contains the ID of the country where the event takes place. The associated relation “*laender*” contains details about the country with this ID, for

Table 3.5 Detailed list of the relation “*anschlaege*”

Attribute in <i>anschlaege</i>	Content of the attribute
a_id	Unique ID of the attack
a_ziel	ID of the target system (<i>zielsysteme</i>)
a_gruppe	ID of the group (<i>gruppen</i>)
a_land	ID of the country where the attack took place (<i>laender</i>)
a_zielland	ID of the country that was attacked (<i>laender</i>)
a_vollstaendig	Statement whether data is complete [yes/no]
a_tote	Number of fatalities
a_verletzte	Number of casualties
a_schaeden	Damage (saved as a string)
a_details	Details (saved as a string)
a_links	Links to the internet pages of the attack
a_datum	Date of the attack
a_jahr	Year of the attack
a_staecke	Is not used anymore
a_kategorie	ID of the category of the attack (<i>akategorien</i>)
a_hilfsmittel	Text about used tools
a_details_neu	Details in German
a_schaeden_neu	Damage in German
a_selbstmord	Statement whether it was a suicide [yes/no]
a_selbstmord2	Statement whether it was a suicide [1, 0, -1] (1 = yes, 0 = no, -1 = unknown)
a_taktik	ID of the tactic (<i>taktiken</i>)
a_foto	Number of available photos of the attack
a_tag	Day of the attack
a_monat	Month of the attack
a_grund	ID of the reason for the attack (<i>anschlagsgrund</i>)

A string in brackets says that the attribute links to another relation. Numbers always take values in \mathbb{N}_0 (Siebold 2007)

example its name or continent. This makes the database structure more elegant and compact although the notation, as in Table 3.6, seems complicated at first.

Table 3.6 Overview of the mathematical and database notation

In mathematical notation	In words	In database notation	Remarks
$A = \{e \in anschlaege \mid \text{There were 12 fatalities related to } e\}$	All attacks with 12 casualties	$A = \{e \mid anschlaege(e) \wedge e.a_verletzte = 12\}$	
$B = \{e \in anschlaege \mid e \text{ took place in Germany}\}$	All attacks in Germany	$B = \{e \mid anschlaege(e) \wedge \exists c(\text{laender}(c) \wedge c.l_id = e.a_land \wedge c.l_name = "Deutschland")\}$	a_land contains the ID of Germany, not the word “Germany”. That is why it has to look so complicated
$C = \{e \in anschlaege \mid e \text{ took place in Africa}\}$	All attacks in Africa	$C = \{e \mid anschlaege(e) \wedge \exists c(\text{laender}(c) \wedge c.l_id = e.a_land \wedge c.l_kontinent = "Afrika")\}$	
$A \cap B$ (intersection of A and B)	All attacks in Germany with 12 casualties	$A \cap B = \{e \mid anschlaege(e) \wedge \exists c(\text{laender}(c) \wedge c.l_id = e.a_land \wedge c.l_name = "Deutschland") \wedge e.a_verletzte = 12\}$	This intersection can be empty if there are no attacks in Germany with 12 casualties
$A \cap C$	All attacks in Germany and Africa	$A \cap B = \{e \mid anschlaege(e) \wedge \exists c(\text{laender}(c) \wedge c.l_id = e.a_land \wedge c.l_name = "Deutschland") \wedge c.l_kontinent = "Afrika"\}$	This intersection is always empty because Germany is not part of Africa
$A \cup B$ (union of A and B)	All attacks in Germany with 12 casualties	$A \cup B = \{e \mid anschlaege(e) \wedge \exists c(\text{laender}(c) \wedge c.l_id = e.a_land \wedge c.l_name = "Deutschland") \vee e.a_verletzte = 12\}$	This union is theoretically possible, but is not very likely to be useful in a practical context
$A \cup C$	All attacks in Germany or Africa	$A \cup B = \{e \mid anschlaege(e) \wedge \exists c(\text{laender}(c) \wedge c.l_id = e.a_land \wedge c.l_name = "Deutschland") \vee c.l_kontinent = "Afrika"\}$	This union seems to be of more practical use
$(A \cup C) \cap B$	All attacks in Germany or Africa with 12 casualties	$(A \cup C) \cap B = \{e \mid anschlaege(e) \wedge \exists c(\text{laender}(c) \wedge c.l_id = e.a_land \wedge c.l_name = "Deutschland") \vee c.l_kontinent = "Afrika"\} \wedge e.a_verletzte = 12\}$	It is possible to iteratively combine unions and intersections

(continued)

Table 3.6 (continued)

In mathematical notation	In words	In database notation	Remarks
$A \setminus B$ (A without B)	All attacks with 12 casualties that did not take place in Germany	$B = \{e \mid anschlaege(e) \wedge e.a_verletzte = 12 \wedge \exists c (laender(c) \wedge c.l_id = e.a_land \wedge c.l_name = "Deutschland")\}$	

3.7 The Database

There are several different databases that can be used for the analysis of terroristic events. Some of them are (Siebold 2007):

- Tweed (Skjølberg 2002; Engene 2007) contains data for terroristic events in Western Europe (18 countries) from 1950 to 2004. The database contains 11,245 events and information about 214 terrorist organizations.
- The public database of the Memorial Institute for the Prevention of Terrorism (MIPT 2007) contained data to 32,649 events. It is not available online anymore.
- The work of Dugan, LaFree, and Fogg (Dugan et al. 2006) uses, according to their own report, the most elaborate database of terroristic events with 67,165 recorded events from 1970 to 1997.
- “The Global Terrorism Database (GTD) is an open-source database including information on terrorist events around the world from 1970 through 2010 (with annual updates planned for the future). [...] [The GTD] includes more than 98,000 cases.” (National Consortium for the Study of Terrorism and Responses to Terrorism (START) 2011)

The *Terror Event Database (TED)* that is used for the examples in this chapter has already been introduced. In 2009, TED contained data to 35,525 events with known dates, 172 countries, 1046 terrorist groups, 104 tactics, and 529 target objects (Siebold and Häring 2009). Threats and planned attacks are not part of TED. The data of threats and planned attacks which is used in this chapter is stored in Enders and Sandler (1992). Due to the way the data has been collected, there is a higher number of events between 1998 and 2004 than for the time periods before and after these dates. Hence, the time period from 1998 to 2004 is often regarded separately in the analysis.

3.8 Data Selection

The database analysis that is presented in this chapter is mostly done with the *TED Analysis Software (TEDAS)* that was implemented by Siebold in the framework of his diploma thesis (Siebold 2007).

In the following we denote a tuple from the relation “*anschlaege*” as *event*. It is obvious from the context whether we mean the actual event or whether we mean the tuple. The set of all events in the database is denoted by S . A subset $T \subseteq S$ is called a *selection*.

We denote selections in *tuple calculus*. For example, all events that took place in Germany are

$$B = \{e | \text{anschlaege}(e) \wedge \exists c(\text{laender}(c) \wedge c.l_id = e.a_land \wedge c.l_name = "Deutschland")\} \quad (3.1)$$

in the tuple notation. This set reads as follows: The set contains all events e which can be found in the relation “*anschlaege*” and for which holds: There exists a tuple (country) c in “*laender*” whose unique ID (“ l_id ”) is equal to e ’s value for “ a_land ” and which is called “Deutschland”.

The set is created in the following way: All events would be $\{e | \text{anschlaege}(e)\}$. Asking for e to lie in “*anschlaege*” assures that e is an attack and not a country etc. In “*anschlaege*” the countries are stored in form of IDs. If we knew Germany’s ID, for example suppose it was 123, the set would be $\{e | \text{anschlaege}(e) \wedge e.a_land = 123\}$. Since we do not know Germany’s ID, we go into the relation “*laender*” (countries) and regard the country (that is, $\exists c$ with $\text{laender}(c)$) with the description “Deutschland” (that is, $c.l_name = "Deutschland"$). We take this country’s ID (that is, $c.l_id$ of the c for which $c.l_name = "Deutschland"$) and ask for e to have this country ID (that is, $e.a_land = c.l_id$) in order to lie in B . So the final set is (3.1).

More examples for the notation in tuple calculus can be found in Table 3.6.

Table 3.6 also explains how for two given selections A and B , the elementary set operations

$$\begin{aligned} & A \cup B \text{ (union),} \\ & A \cap B \text{ (intersection),} \\ & A \setminus B \text{ (}A \text{ without } B\text{)} \end{aligned} \quad (3.2)$$

can be written in tuple calculus.

Furthermore, intervals for date, number of fatalities and number of casualties can be selected:

$$\{e | \text{anschlaege}(e) \wedge e.attr \geq a \wedge e.attr \leq b\} \quad (3.3)$$

With these options for combining selections, any selection consisting of terrorist events can be chosen. A single event cannot be intentionally chosen. It is possible that two events have identical dates, number of casualties and fatalities, take place in the same country, and are done by the same group with the same tactic. It might not be resolved, for example, that they take place in different areas of cities.

3.9 Data Preparation

Next we want to preprocess our data by arranging it in three different data types: a set of numbers, a set of tuples with two elements, or a time series.

The simplest form is a set of numbers. This occurs if we are only interested in one attribute of a given selection. For example, if we only want to know the number of casualties in Germany, we choose the set

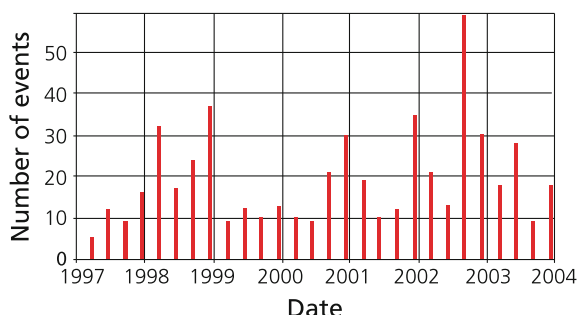
$$\{e.a_verletzte | anschlaege(e) \wedge \exists c(\text{laender}(c) \wedge c.l_id = e.a_land \wedge c.l_name = "Deutschland")\}. \quad (3.4)$$

The generated set is a set of numbers where one cannot see which number belongs to which event. The numbers from such a kind of set can be used for calculating sums or means (see Sect. 3.10).

The second form is a set of tuples with two entries. The entries can be numbers or strings. This form of set is, for example, necessary when presenting data in a pie chart. Numbers for the sizes of the pieces of pie are needed, but also strings for the descriptions. After generating a set of tuples one can organize the tuples in order to merge, for example, all entries for the same country. Typical calculations for numbers from this kind of set are counting the tuples or summing up the entries.

The third form is a time series. “In its simplest form a time series is a collection of numerical observations arranged in a natural order” (Bloomfield 1976). A time series is created similarly to a set of tuples, but the tuples are additionally organized by time. Time series can be used for charts as Fig. 3.4. Time series analysis will be discussed in more detail in Sect. 4.3.

Fig. 3.4 Number of events in France per quarter (Siebold 2007)



3.10 Selection and Application of Simple Statistical Methods

3.10.1 Total Numbers of Events/Attribute

As a first step we want to introduce ways to merge data to get a new data set that can be used to create tables, charts, or other graphical presentations. We first introduce the formulas and then give an example of how they are used.

The total number of events in a selection E is denoted by $|E|$.

The total number of an attribute x in a selection E is defined by

$$S(E_{[x]}) := \sum_{e \in E} e.a_x, \quad (3.5)$$

where $e.a_x$ represents the value of an attribute x of an event e .

For a qualitative measure x such as country, organization, tactic, or target object we sum up how many different types of this measure occur:

$$N(E_{[x]}) := \sum_{t \in T_{[x]}} (\exists e \in E : e.a_x = t)_B. \quad (3.6)$$

Here $T_{[x]} = \{e.a_x | e \in \text{database}\}$. For example, $T_{[\text{country}]}$ is the set of all countries in the database (Siebold 2007).

Example (Example 1 in Siebold 2007):

We regard a set of 5 attacks in Germany in 1985 that are registered in the database. The data is shown in Table 3.7.

In this case we get $|E| = 5$ because there are 5 entries.

Summing up the number of fatalities yields

$$S(E_{[\text{tote}]}) = 1 + 2 + 0 + 3 + 0 = 6 \quad (3.7)$$

and the total number of casualties is

$$S(E_{[\text{verletzte}]}) = 0 + 11 + 0 + 42 + 38 = 91. \quad (3.8)$$

Table 3.7 Data of 5 attacks in Germany in 1985 (Siebold 2007)

<i>a_datum</i>	<i>a_tote</i>	<i>a_verletzte</i>	<i>a_taktik</i>
1985-02-01	1	0	5
1985-08-08	2	11	1
1985-09-06	0	0	4
1985-06-19	3	42	3
1985-11-24	0	38	3

Calculating $S(E_{[taktik]})$ would be useless because we would get the sum of IDs of tactics and not a total number of used tactics.

The total number of used tactics is

$$N(E_{[taktik]}) = \sum_{t=1}^5 (\exists e \in E : e.a_taktik = t)_B = 1 + 0 + 1 + 1 + 1 = 4 \quad (3.9)$$

because 2 is the only tactic that is not used. $N(E_{[tote]})$ and $N(E_{[verletzte]})$ are not well defined because fatalities and casualties are quantitative measures.

3.10.2 Sums Over Time Intervals

Apart from computing total numbers for a selection it is also possible to divide the attributes into classes. For a time series this is done by

$$H(E)_{[t_1, t_2]} := |\{e \in E | e.a_datum \in [t_1, t_2]\}| \quad (3.10)$$

and

$$H(E_{[x]})_{[t_1, t_2]} := \sum_{e \in E, e.a_datum \in [t_1, t_2]} e.a_x. \quad (3.11)$$

Remark In TEDAS this is implemented for $\Delta t := t_2 - t_1 = 1$ day/month/quarter/year.

For our set of tuples with two entries (see Sect. 3.9) we use the middle of the time interval instead of the whole interval as an entry. This yields

$$\left\{ \left(0.5(t_1 + t_2) + i\Delta t, H(E_{[x]})_{[t_1 + i\Delta t, t_2 + i\Delta t]} \right) | i = 0, \dots, n - 1 \right\}. \quad (3.12)$$

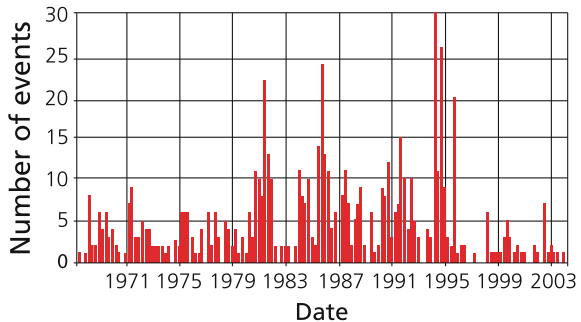
Example (Siebold 2007):

For $e.a_land = \text{Germany's ID}$, $\Delta t = 1$ quarter, and $n = 143$, one gets the tuple set

$$\left\{ \left(1968 + i\Delta t, H(E_{[x]})_{[t_1 + i\Delta t, t_2 + i\Delta t]} \right) | i = 0, \dots, n - 1 \right\} \quad (3.13)$$

which yields Fig. 3.5.

Fig. 3.5 Events in Germany per quarter from 1968 to 2004 (Siebold 2007)



3.10.3 Sums Over Other Classes of Attributes

It is also possible to form classes for other types of attributes. For example, one can calculate the number of events in a selection E with at least b_1 and at most b_2 casualties:

$$N_{[verletzte],[b_1,b_2]}(E) = \sum_{a \in A, b_1 \leq e.a_verletzte \leq b_2} e.a_verletzte. \quad (3.14)$$

3.10.4 Computing Frequencies

So far we have only counted events or computed sums. Now we use these numbers to calculate *probabilities* or *frequencies*. For example, one can calculate the events for one type of building per observed period. This makes it possible to compare data that was collected for time periods of different lengths. One can also go a step further and divide additionally by the number of buildings of this type. An example can be found in Table 3.8.

Probabilities and frequencies allow us to compare data for which the absolute numbers do not yield useful comparisons. On the other hand, it is sometimes difficult to collect the information needed to compute probabilities. For example, the chart in Fig. 3.6 is based on database analysis. A database only has a fixed number of entries. There is no database that contains all terroristic events. So, these numbers can only give estimates of the actual probability or frequency, where the quality of the estimates increases with the size of the database.

Sometimes a total number is not a reasonable measure. For example, if one wants to divide by the total number of tactics, this number can never be known. Even in calculations concerning real objects, like banks or other buildings, the total number is not always known and hard to estimate.

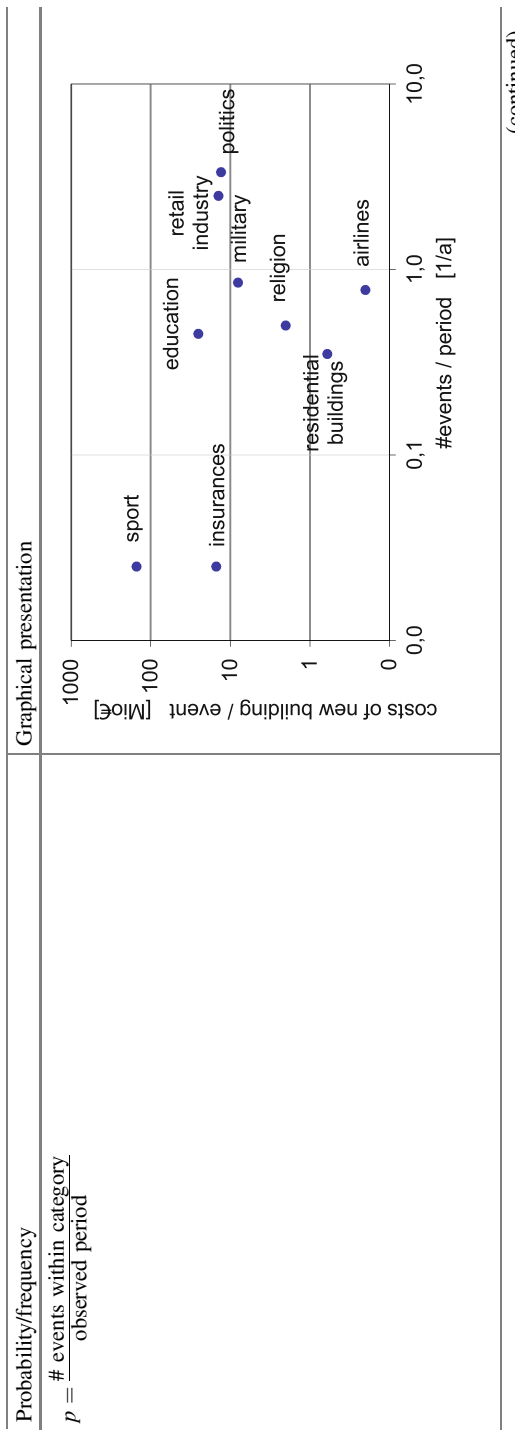
Another risk of the database based calculation of probabilities/ frequencies is that they do not consider important information. For example, the first attempt to

Table 3.8 Examples for probabilities and frequencies with corresponding graphics (Häring et al. 2005)

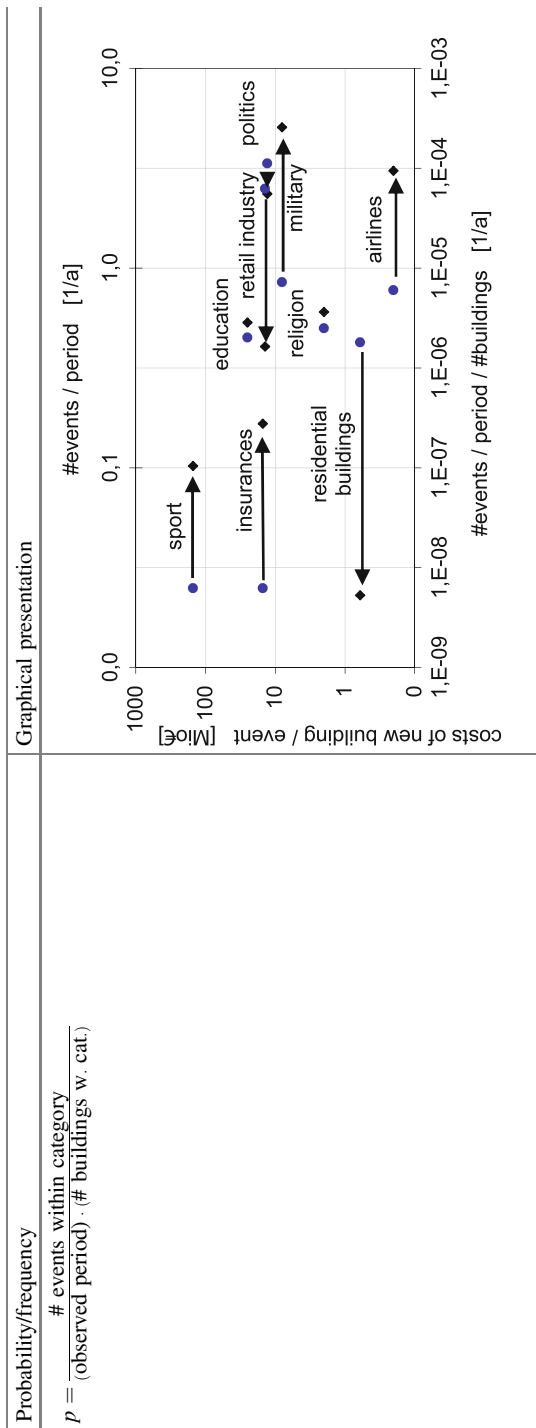
The figure is a horizontal bar chart titled "Graphical presentation" located in the top right corner of the slide. The y-axis is labeled "attacks [%]" and ranges from 0 to 25. The x-axis lists various target categories. The bars are blue.

target	attacks [%]
Storage building	~22
Coining institution	~18
Post office	~15
Cultural centre	~12
Convenience store	~10
Pub	~8
Transportation	~7
Restaurant	~6
Hotel	~5
Factory	~4
Business building	~3
Administrative buildings	~2
Commercial buildings	~1

(continued)

Table 3.8 (continued)

(continued)

Table 3.8 (continued)

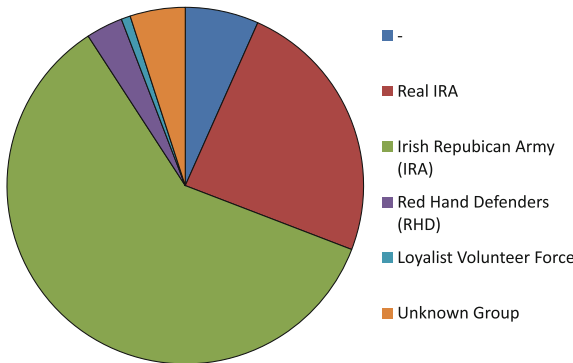


Fig. 3.6 Percentage of fatalities per group in Northern Ireland from 1968 to 2004, absolute numbers of fatalities can be found in the legend (Siebold 2007)

calculate the probability that a terrorist chooses one bank in a given city is to divide 1 by the number of banks. This does not take into consideration that the main bank is more likely to be attacked than a smaller one. Mathematically spoken, one has to choose another probability distribution than the uniform distribution. In general, it is not obvious which distribution is the best choice.

Overall, probabilities and frequencies are helpful for data analysis, but they have to be handled with care.

Example from TED:

- (a) Scenario frequency estimate:

For instance we can compute the frequency of the tactic-target combination explosion and embassy by

$$\text{annual frequency of explosive attacks of embassies in Germany} \\ = \frac{(\text{number of events that use explosives to damage embassies in Germany})}{(\text{number of considered years})(\text{number of embassies})}. \quad (3.15)$$

If there is not sufficient data, we can also replace Germany by Europe.

- (b) Consequence estimate:

For instance we can estimate the average consequences of an attack on an embassy by

$$\text{fatalities per explosive attack on embassies in Europe} \\ = \frac{(\text{number of fatalities due to attacks on embassies in Europe})}{(\text{number of considered years})(\text{number of attacked embassies})}. \quad (3.16)$$

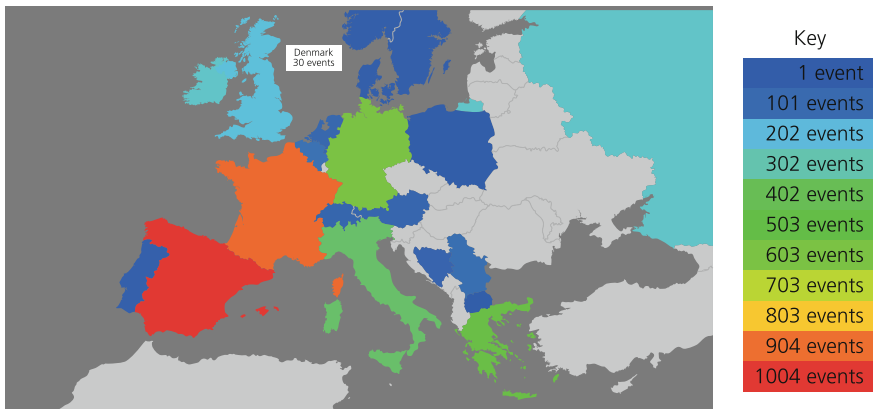


Fig. 3.7 Number of events per country (Siebold 2007)

3.11 Selection of Visualization Methods and Visualization

In practical applications visualization of the data is often the first step of data analysis (Neuhaus and Kreiß 2006). There are several forms of visualization. We have already seen different forms of graphical presentation in Fig. 3.5 and Table 3.8. Another common form of presentation is a *pie chart*. An example for this is Fig. 3.6, which shows the percentage of fatalities per group in Northern Ireland from 1968 to 2004.

Another option is to present data by coloring a map. An example for this is Fig. 3.7 where the online-available tool “Visited Countries Map” (Marcelionis 2006) was used to color countries on a world map. The figure visualizes how many events happened in which country.

3.12 Use of Database Analysis in the Risk Management Process

The methods explained in this and the next chapter are used throughout the whole risk management process. Because the risk management process has seamless transitions between the different steps, and because the same method may be used in several steps, it is not possible to find a clear allocation of the methods to the steps of the risk management process. The intention of Table 3.9 is to deliver a coarse idea of where the methods are typically used and to motivate the study of database analysis.

Table 3.9 Allocation of the database analysis methods of this chapter and Chap. 2 to the steps of the risk management process

Step from risk management process	Section of Chaps. 3 or 4
(1) Background: This includes information about the country where the event is located, the cultural and ethical background, the legal and technical requirements, and the types of scenarios that are considered	3.8, 3.9, 3.10.1–3.10.3 and 4.3
(2) Initial situation without hazard source: All information needed to apply hazard and damage schemes is being collected. This includes geometrical, geographical, meteorological, and topological data and information about materials and meteorological conditions	3.8, 3.9, 3.10.1–3.10.3 and 4.3
(3) Description of the hazard source: The description includes geometry, mass, position, orientation, and velocity of the hazard source as well as mitigation measures close to the hazard source	
(4) Hazard propagation/hazard analysis: This includes the potential dispersion, distribution, and impact load distribution of the physical hazard	
(5) Damage/consequence analysis/modeling: Here the effects of the physical hazard potential on objects like persons, vehicles, buildings, and infrastructure are determined	
(6) Analysis of hazard event frequency: It is analyzed how often the hazard source becomes active. This is determined by considering, for example, the frequency of the hazard source being present, the frequency of an unintended event within the hazard source and the frequency of a failure of the containment	3.10.1–3.10.4 and 4.4
(7) Distribution of objects: The distribution describes how many and where objects of interest are located in the area. Exposition/exposure describes that they are actually exposed to the damaging effects	
(8) Success frequency of avoiding hazard event consequences: This step considers the success frequency of organizational and training measures, of spontaneous reactions (for example flight) as well as the success rates of placing passive, reactive, or active physical barriers	
(9) Risk computation and visualization: This involves the computation of various risk quantities. The visualization options include risk maps, risk tables, and F-N-diagrams	3.11, 4.2 and 4.4
(10) Risk comparison with criteria: The risk quantities are compared to risk assessment criteria, for example risk matrices, critical values, and F-N criteria. For example, one checks whether the nonlocal annual individual risk is smaller than	4.2
(11) Risk assessment: Risk assessment is the combination of the previous step (10) with other steps that enables to make a final risk evaluation. In particular, legal, social, and psychological effects on the assessment of risks are considered	

(continued)

Table 3.9 (continued)

Step from risk management process	Section of Chaps. 3 or 4
(12) Risk communication focuses on the communication of risks to experts, responders, the public, and third party. For instance, risks comparable to the risks that are to be assessed are named. This should be risks the persons addressed can relate to. An emotional link to the risk should be created	3.8, 3.9, results from 4.2 and 4.4
(13) Evaluate risk: Taking the steps (10)–(12) into account, It is being judged whether risks are acceptable or not	
(14) Mitigation measures: There are mitigation measures that reduce the frequency, mitigation measures that reduce the physical hazards, mitigation measures that reduce the consequences of events, and mixed mitigation measures. We also count feasible changes of the background among mitigation measures	

3.13 Summary and Outlook

This chapter has given a first impression of database analysis. The whole database analysis process from spotting data in a news article to visualizing the results has briefly been explained. We have focused on the second half of the scheme in Fig. 3.1, starting with a given database. This part is marked as “user defined” because this part of the scheme is flexible and can be influenced by the type of result the user needs. The flexibility has not been so obvious yet, since we have only presented a very limited numbers of methods. It will become clearer in the next chapter where we present some more methods used in database analysis.

3.14 Questions

- (1) Given the following events:

Event	a_selbstmord	a_grund	a_foto
1	-1	1	10
2	1	2	3
3	1	4	7

- (a) Calculate all reasonable values that can be determined with the methods introduced in the lecture.
- (b) How can a formula from this lecture be modified to determine the total number of (sure) suicides?

- (2) Calculate the following numbers with GTD (<http://www.start.umd.edu/gtd/>):
- (a) frequency of chemical weapons being the used weapon for attacks in Austria,
 - (b) frequency of the target being food/water supply for attacks in Germany,
 - (c) attacks on airports and airlines per year in Germany,
 - (d) attacks per year in Germany.
- (3) What are the advantages of a relational database like TED compared to data in a Microsoft Excel file?
- (4) Which other types of databases besides the relational databases like TED do you know? Give an example for which type of data they are used.
- (5) What are the advantages and disadvantages of using relational databases compared to other database structures?
- (6) Describe a heuristic approach how to find a database scheme for a given set of data.
- (7) Give an overview of the components of database notation.
- (8) Find three other examples to the ones from Sect. 3.4 for the use of database information.
- (9) Make a list of problems that can occur when unifying two databases.
- (10) What would the selection of all events where Germany was attacked except for those between 1970 and 1973 look like in database notation?
- (11) How can one calculate the number of fatalities from attacks by the RAF from 1970 to 1974
 - (a) using formula (3.11)?
 - (b) using formula (3.5)?How is E defined for (a) and (b), respectively?
- (12) Use the Global Terrorism Database (<http://www.start.umd.edu/gtd/>) to answer the following questions:
- (a) When and where was the first attack by RAF listed in GTD?
 - (b) Create a scheme or a table with the structure of GTD.
 - (c) How does the structure of GTD differ from the structure of TED?
- (13) Create a pie chart (for example with Microsoft Excel) that displays the frequencies of the different attack types in Brazil with the data from GTD (<http://www.start.umd.edu/gtd/>).
- (14) The map in Fig. 3.7 makes it possible to see whether there is a connection between where the country is located and the number of attacks. Which other properties besides the geographical location would be interesting aspects in a comparison between countries?

3.15 Answers

- (1) (a) $|E| = 3$, $S(E_{[foto]}) = 20$, and $N(E_{[grund]}) = 3$,
 (b) $S(E_{[selbstmord]}) = \sum_{e \in E} (e.a_selbstmord = 1)_B$
- (2) With the data from GTD from 2012-01-20:
 (a) $1/106 \approx 0.0094$,
 (b) $2/554 \approx 0.0036$,
 (c) $6/(2010 - 1970 + 1) \approx 0.15$,
 (d) $554/(2010 - 1970 + 1) \approx 13.51$.
- (3) Some advantages are

- It is easier to enlarge the structure.
- It is easier to write new entries.
- It is easier to use for other persons.
- Excel sheets are confusing for big data sets.

Unterinformationen (z. B. zu Ländern, Taktiken usw.) können an einem einzigen Ort (nämlich in der entsprechenden Untertabelle) gespeichert werden und müssen nicht in jeder Zeile der Haupttabelle gespeichert werden. Das hat mehrere Vorteile, z. B.:

- geringerer Aufwand bei der Manipulation von Daten (Unterinfos müssen nur an einer Stelle hinzugefügt, geändert bzw. gelöscht werden)
- geringerer Speicherbedarf

- (4) Hierarchical database (family tree), object-oriented database (complex data objects)
- (5) Advantages:

- Data and table structure is more flexible and can be adapted later
- Better processing of big data sets than in object-oriented databases
- ...

Disadvantages:

- Recursive requests are not possible (in contrary to hierarchical structures)
- High resource needs and development costs
- Application-typical behavior of an object cannot be described in the database. So, the description has to be put into the software. This can lead to a redundant implementation if several applications use the same data.
- ...

(Wikipedia 2012)

- (6) See Sect. 3.2.
- (7) See Table 3.10.
- (8) Some further examples are:

- Observation of the population of a city and the surrounding area -> urban and rural development.

Table 3.10 Overview of database notation

Notation	Description
$Category(e)$	e is an element of the category
\wedge, \vee	Combination of different requirements: and, or
$\exists e(\dots)$	There exists an element e with the properties in the breaket
$x_1 \leq e.a_attribute \leq x_2$	The value of the attribute are in the range from x_1 to x_2
\cup, \cap, \setminus	Combination of data sets: union, intersection, without
N, S, H	Sums of attributes/values

- Observation of the age of a country's population -> retirement plans.
- Information about earthquakes -> building of future buildings.

(9) Some problems are:

- The databases might have different categories.
- The databases might have different names for terroristic groups.
- The databases might have contradictory information about an event, for example a different number of casualties.
- The databases might have different designs that do not adapt to the other one easily.

(10) The set would look like

$$B = \{e | anschlaege(e) \wedge \exists c (laender(c) \wedge c.l_id = e.a_zielland \wedge c.l_name = "Deutschland") \wedge (e.a_jahr \leq 1969 \vee e.a_jahr \geq 1974)\} \quad (3.17)$$

or

$$B = \{e | anschlaege(e) \wedge \exists c (laender(c) \wedge c.l_id = e.a_zielland \wedge c.l_name = "Deutschland") \wedge \neg(e.a_jahr \geq 1970 \wedge e.a_jahr \leq 1973)\}. \quad (3.18)$$

(11) (a)

$$E = \{e | anschlaege(e) \wedge \exists k (gruppen(k) \wedge k.g_id = e.a_gruppe \wedge k.g_name = "RAF")\},$$

$$H(E_{[tote]})_{[1.1.1970, 31.12.1974]} = \sum_{\substack{e \in E, \\ e.a_datum \in [1.1.1970, 31.12.1974]}} e.a_tote,$$

(b)

$$E = \{e | anschlaege(e) \wedge \exists k(\text{gruppen}(k) \wedge k.g_id = e.a_gruppe \wedge k.g_name = "RAF" \wedge e.a_datum \geq 1.1.1970 \wedge e.a_datum \leq 31.12.1974)\},$$

$$S(E_{[tote]}) := \sum_{e \in E} e.a_tote.$$

(12) With the data from GTD from 2012-01-20:

- (a) 1977 in Palma de Mallorca, Spain (National Consortium for the Study of Terrorism and Responses to Terrorism (START) 2011).
- (b) The structure of GTD can be seen in Table 3.11.
- (c) TED contains more different information about each attack. With TEDAS there are more implemented analyzing methods. For example, one can not only look at predefined ranges of numbers of fatalities/injuries. GTD is very easy to use. The user does not have to think about database notation, everything can be done with a few clicks.

(13) With the data from GTD from 2012-01-20 (Fig. 3.8 and Table 3.12):

(14) Some other interesting properties are:

- The political system
- The political power

Table 3.11 The structure of GTD

Year	$n \in \mathbb{N}, 1970 \leq n \leq 2010$
Region	Australasia and Oceania, Central America, ...
Country	Afghanistan, Albania, ...
Perpetrator	1 May, 14 K Triad, 14 March Coalition, ...
Weapon type	Biological, chemical, explosives/bombs/dynamite, ...
Attack type	Armed assault, assassination, ...
Target type	Abortion related, airports and airlines, ...
Suicide attack	Yes–no
Non-suicide attack	Yes–no
Criterion I	Yes–no
Criterion II	Yes–no
Criterion III	Yes–no
Ambiguous	Yes–no
Unsuccessful	Yes–no
Injuries and fatalities	$n \in \mathbb{N}_0$, unknown ^a
Injuries only	$n \in \mathbb{N}_0$, unknown ^a
Fatalities only	$n \in \mathbb{N}_0$, unknown ^a

^aIt is possible to ask for ranges 1–10, 11–50, 51–100, 101+

Fig. 3.8 Frequencies of the different attack types in Brazil from 1970 to 2010

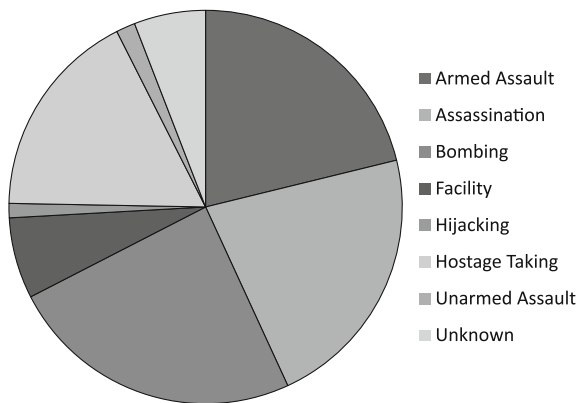


Table 3.12 Frequencies of the different attack types in Brazil from 1970 to 2010

Attack type	# att. of this type	# total attacks	Frequency
Armed assault	54	255	0.211764706
Assassination	56	255	0.219607843
Bombing	62	255	0.243137255
Facility	17	255	0.066666667
Hijacking	3	255	0.011764706
Hostage taking	44	255	0.17254902
Unarmed assault	4	255	0.015686275
Unknown	15	255	0.058823529

- The relationships to other countries
- The economical standard
- The natural resources
- Known terrorist groups within the country
- Immigration statistics

References

- Beichelt, F. E., Montgomery, D. C., Beichelt, F. E., Cheng, S., Christoph, G., Jennings, C. L., et al. (2003). *Teubner-Taschenbuch der Stochastik; Wahrscheinlichkeitstheorie, Stochastische Prozesse, Mathematische Statistik*. Teubner: Stuttgart u.a.
- Berkhin, P. (2002). *Survey of clustering data mining techniques*. Accrue Software, Inc., from <http://www.cc.gatech.edu/~isbell/classes/reading/papers/berkhin02survey.pdf>
- Best, C. (2002). *Europe media monitor*. Retrieved February 10, 2012, from <http://emm.newsbrief.eu/overview.html>
- Bloomfield, P. (1976). *Fourier analysis of time series: An introduction*. New York: Wiley.

- Chaveer.de. (2007). *chaveer.de*. Retrieved March 22, 2007 (Error 404), from www.chaveer.de
- Dubes, R. C., & Jain, A. K. (1988). *Algorithms for clustering data*. Englewood Cliffs: Prentice Hall.
- Dugan, L., LaFree, G., & Fogg, H. (2006). A first look at domestic and international global terrorism events, 1970–1997. *Intelligence and Security Informatics, IEEE International Conference on Intelligence and Security Informatics*. San Diego, USA, Berlin: Springer.
- Edward, F., Mickolus, T. S., & Murdock, Jean M. (1989). *International terrorism in the 1980s: A chronology of events*. Ames: Iowa State University Press.
- Enders, G. F. P. W., & Sandler, T. (1992). A time-series analysis of transnational terrorism: Trends and cycles. *Defence Economics*, 3, 305–320.
- Engene, J. O. (2007). Five decades of terrorism in Europe: The TWEED dataset. *Journal of Peace Research*, 44, 109–121.
- Ester, M., & Sander, J. (2000). *Knowledge discovery in databases - Techniken und Anwendungen*. Berlin: Springer.
- Fayyad, U. M., Piatetsky-Shapiro, G., & Smyth, P. (1996). Knowledge discovery and data mining: Towards a unifying framework. In *2nd International Conference on Knowledge Discovery and Data Mining*. Cambridge: AAAI Press.
- Gaizauskas, R., & Humphreys, K. (1997). Using a semantic network for information extraction. *Natural Language Engineering*, 3(2), 147–169.
- Georgii, H.-O. (2004). *Stochastik Einführung in die Wahrscheinlichkeitstheorie und Statistik*. Berlin, New York: Walter de Gruyter.
- Hand, D., Mannila, H., & Smyth, P. (2001). *Principles of data mining*. Cambridge: The MIT Press.
- Häring, I., Dörr, A. & Brand, C. (2005). Risk analysis methodology for explosions. *14th SRA Europe Annual Meeting 2005*. Como, Italy.
- Hoffman, K. G. B. (1990). *The Rand chronology of international terrorism; 1986*. Santa Monica: RAND.
- Hoffman, K. G. B. (1991). *The Rand chronology of international terrorism for 1987* Santa Monica: RAND.
- International Policy Institute for Counter-Terrorism (2007). ICT. Retrieved March 26, 2007, from <http://ict.org.il>
- Irle, A. (2005). *Wahrscheinlichkeitstheorie und Statistik*. Teubner: Grundlagen - Resultate – Anwendungen.
- Jain, A. K., Murty, M. N., & Flynn, P. K. (1999). Data clustering: A review. *ACM Computer Surveys*, 31, 264–323.
- Johnson, B. M. J. J. (1975). *International terrorism : a chronology, 1968–1974*. Collingdale: Diane Pub Co.
- Kadelka, P.-D. D. D., & Henze, P. D. N. (2000). *Wahrscheinlichkeitstheorie und Statistik für Studierende der Informatik (Skript zur Vorlesung)*.
- Kaufmann, L., & Rousseeuw, P. J. (1990). *Finding groups in data: Introduction to cluster analysis*. Bristol: John and Sons.
- Kleb, J. (2006). *Identifikation von Ereignissen aus Nachrichtentexten - Clustering von Sprachdokumenten*. Furtwangen im Schwarzwald: Diplom, Hochschule Furtwangen University.
- Kommission der Europäischen Gemeinschaften. (2003). *Bericht der Kommission: Jahresbericht der GFS - 2003*. Brussels.
- Marcelionis, A. (2006). *Visited countries map*, from http://www.interactivemaps.org/visited_countries/
- Mickolus, E. F., Sandler, T. & Murdock, J. M. (1989). *International terrorism in the 1980s: A chronology of events 1*. Ames: Iowa State University Press.

- MIPT. (2007). Terrorism knowledge base (TKB). Retrieved March 26, 2007, from www.tkb.org
- Nahnsen, T. (2005). *Event identification and information extraction from natural language text*. Germany: Fraunhofer Ernst-Mach-Institut.
- National Consortium for the Study of Terrorism and Responses to Terrorism (START). (2011). *Global terrorism database [Data file]*. Retrieved January 20, 2012, from <http://www.start.umd.edu/gtd>
- Neuhaus, G., & Kreiß, J.-P. (2006). *Einführung in die Zeitreihenanalyse*. Berlin: Springer.
- Radev, D. R., & McKeown, K. R. (1998). *Generating natural language summaries from multiple on-line sources*.
- Rathmann, E.-M. (2003). *Schutz von Infrastruktur - 2. Zwischenbericht: Konzeptionelle Grundlagen für das Bewertungsverfahren*. Fraunhofer Ernst-Mach-Institut.
- Rheinzeitung. (2007). *rheinzeitung.de*. Retrieved March 22, 2007, from <http://www.rhein-zeitung.de/>
- Rohatgi, V. K., & Saleh, A. K. (2000). *An introduction to probability and statistics*. New York: Wiley.
- Saggion, H., Kuper, J., Cunningham, H., Declerck, T., Wittenburg, P., Puts, M. et al. (2003). Event-co-reference across multiple, multi-lingual sources in the Mumis project. *10th Conference of the European Chapter of the Association for Computational Linguistics (EACL'03, Conference Companion)* (pp. 239–242). Budapest, Hungary: Association for Computational Linguistics. <http://doc.utwente.nl/64347/>
- schlafuchs.at. (2007). *Angaben über terroristische Anschläge*. Retrieved March 22, 2007 (Error 404), from http://www.schlafuchs.at/list/l_terror.htm
- Siebold, U. (2007). *Untersuchung statistischer Auswerteverfahren zur Analyse sicherheitsrelevanter Ereignisse*. Freiburg: Diplom, Albert-Ludwigs-Universität Freiburg.
- Siebold, U., & Häring, I. (2009). Terror event database and analysis software. *Future Security* (pp. 85–92). Karlsruhe, Germany.
- Siebold, U., Häring I., & Karwath, A. (2007). *Statistical and time series analysis of terror event data for prediction and group spreading behavior* (unpublished).
- Shao, J. (2003). *Mathematical statistics*. New York: Springer.
- Skjølberg, J. O. E. K. H.-W. (2002). Data on intrastate terrorism: The TWEED project. *43rd Annual ISA Convention*. New Orleans, LA.
- Tagesschau. (2012). *Die Nachrichten der ARD*. Retrieved February 10, 2012, from <http://www.tagesschau.de>
- Tan, P.-N., Steinbach, M., & Kumar, V. (2005). *Introduction to data mining*. Reading, MA: Addison-Wesley.
- Taylor, S. M. (2004). Information extraction tools: Deciphering human language. *IT Professional November/December*, 28–34.
- Terrorism Research Center, TRC (2007). Retrieved March 26, 2007, from <http://www.homelandsecurity.com>
- Welt.de. (2007a). *Chronik der Anschläge 2000*. Retrieved March 22, 2007 (no content), from <http://www.welt.de/daten/2000/08/14/0814au185346.htm>
- Welt.de. (2007b). *Chronik der Anschläge auf Touristen in Ägypten*. Retrieved March 22, 2007 (Error 404), from <http://www.welt.de/daten/2000/08/14/0814au185346.htm>
- Welt.de. (2007c). *Spirale der Gewalt; Ein Rückblick auf die Entwicklung des Konfliktes zwischen Indien und Pakistan, 1999–2002*. Retrieved March 22, 2007 (Error 404), from <http://www.welt.de/daten/2002/07/15/0715au344452.htm?print=1>
- Wikipedia. (2012). *Relationale Datenbank*. Retrieved April 17, 2012, from http://de.wikipedia.org/wiki/Relationale_Datenbank
- Yun, B.-H., Kim, T.-H., Hwang, Y.-G., Lee, P.-J., & Kang, S.-S. (2003). In A. Gelbukh (Ed), *Event sentence extraction in Korean newspapers computational linguistics and intelligent text processing* (Vol. 2588, pp. 151–153). Berlin/Heidelberg: Springer.

Chapter 4

More Elaborate Database Analysis for Risk and Resilience Analysis

4.1 Overview

This chapter continues with some more advanced database-analysis techniques that can be used for risk analysis and assessment. It uses the notations introduced in Chap. 3.

First, f-N and F-N diagrams are explained. It is indicated how they are generated from historic event data. It is recommended to read this chapter together with Chap. 17, which gives a further example for the determination of F-N diagrams. From statistical perspective, f-N and in particular F-N diagrams are special types of distributions that have proven to be of use in the context of risk assessments and communication.

The main body of this chapter covers the application of time series analysis methods, in particular smoothing, trend detection and its removal, cycle detection using the autocorrelation function and the removal of cycles and the selecting of statistical time series models. The key idea is that only after the removal of trends and cycles, statistical time series models can be selected for the transformed time series.

After taking account of trends and cycles (if any, respectively) different statistical time series models are presented as candidates for prediction and forecasting. Past data is used for training as well as for the assessment of the models. To this end also sample error measures are introduced to assess the goodness of the prediction models.

The identification of correlations between data attributes is also investigated. In this sense the detection of cycles is a special case of correlation. Also the risk diagrams (graphs) are further investigated in this chapter, which have been first introduced in Chap. 3.

Risk diagrams can also be understood as ready-to-use-and-interpret correlation maps using typically original event data, in addition further data is used. For instance, the frequency estimate for risks are taken from the event database and are

combined with information on the objects for which such events are of interest, in particular the number of such objects and the costs of rebuilding, for example. The importance of risk maps is further emphasized by linking the analysis results to the risk assessment matrix (also often called risk map).

In addition to the risk and resilience management phases listed in the overview of Chap. 3, the more elaborate database analysis methods of this chapter contribute to resilience-engineering informed resilience management preparation, event analysis and scenario assessment.

As in Chap. 3, this chapter gives all the formal expressions, such that the approaches can be implemented using standard data management software.

This chapter presents further methods used in database analysis. The methods we have seen so far, such as calculating total numbers or simple frequencies, were very basic. Now we focus on F-N-curves, time series analysis, and risk maps.

Section 4.2 defines F-N curves and gives an example. F-N diagrams as a visualization method for F-N curves are introduced as well.

Section 4.3 explains some details of time series analysis. Starting with the definition of time series, several forms of smoothing are explained and visualized. Statistical methods to detect trend, cycles, or white noise are introduced. Three forecasting methods are also presented and are applied in an example. The section finishes by pointing out in which parts of the database analysis scheme the different aspects of time series analysis occur.

Section 4.4 introduces risks maps. An example for a risk map is given and used to explain two different ways of coloring the areas in a risk map. The problem of how to label the axes is also briefly discussed.

Like the previous chapter the chapter is mostly based on (Siebold 2007) and (Siebold et al. 2007). The latter source is a summary of the first source. Further Fraunhofer EMI sources are (Brombacher 2005; Schönherr 2009). The main author of the EMI sources is U. Siebold supplemented with work by A. Karwarth, B. Brombacher and I. Häring.

The goal of this chapter is to introduce the classical tools of F-N curves, time series analysis, and risk maps that are often used in the risk management process.

4.2 F-N Curves

4.2.1 Selection and Application of the Method

Computed frequencies and the number of fatalities of an event that are stored in TED can be “plotted in either of two fashions:

Non-cumulative frequency basis: For these graphs, called f-N curves, the value plotted on the y-axis is the discrete frequency of experiencing exactly N fatalities.

Cumulative frequency basis: For these graphs, called *F-N curves*, the value plotted on the y-axis is the cumulative frequency of experiencing N or more fatalities” (Center for Chemical Process Safety 2009).

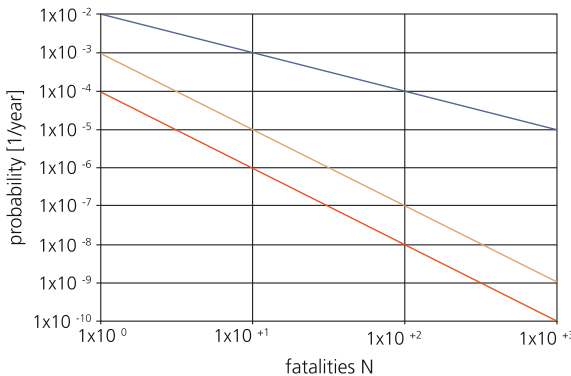


Fig. 4.1 Collective risk criteria for the UK (blue line), the Netherlands (orange), and Czechoslovakia (red) (Schönherr 2009)

The resulting diagram is called an F-N diagram. In F-N diagrams risks can be compared to F-N acceptance measures that take risk aversion into account, see Fig. 4.1. A typical risk aversion criterion reads

$$\begin{aligned} F(N) &= \text{Acceptable probability of } N \text{ or more fatalities} \\ &= aN^{-b}, \end{aligned} \quad (4.1)$$

where $a, b > 0$.

One can compare this risk criterion with single points in the F-N diagram or with a whole F-N curve calculated from data from several given events. “If any portion of the calculated F-N curve exceeds the criterion line, the societal risk is said to exceed that risk criterion” (Center for Chemical Process Safety 2009).

Example for calculating a risk aversion criterion F-N curve: Given two values for a F-N acceptance measure of collective risk in England

$$\begin{aligned} F(10) &= 10^{-3}, \\ F(100) &= 10^{-4}, \end{aligned} \quad (4.2)$$

we can determine the parameters a and b in the risk aversion criterion F-N curve $F(N) = aN^{-b}$.

Substituting the values for N and $F(N)$ in the equation yields

$$\begin{aligned} 10^{-3} &= a \cdot 10^{-b}, \\ 10^{-4} &= a \cdot 100^{-b}. \end{aligned} \quad (4.3)$$

Hence

$$\begin{aligned} a &= 10^{-3+b}, \\ a &= 10^{-4+2b}. \end{aligned} \quad (4.4)$$

Comparing the exponents yields

$$-3 + b = -4 + 2b. \quad (4.5)$$

That is, $b = 1$, $a = 10^{-3+1} = 10^{-2}$ and $F(N) = 10^{-2}N^{-1}$.

The curve is shown as the blue line in Fig. 4.1.

4.2.2 Selection of the Visualization Method

F-N curves can be visualized in so called F-N diagrams as shown in Fig. 4.1.

Remark As risk is defined by $R = PC$, combinations of P and C with the same resulting risk lie on a hyperbola in a coordinate system with N (as a measure of the consequences C) and F (as a measure for P) on the axes. In a double logarithmic scale this becomes a straight line with gradient -1 .

$$\begin{aligned} \text{const} &= NF \\ \Rightarrow F &= \frac{\text{const}}{N} \text{ (hyperbola)} \\ \Rightarrow \log F &= \log \text{const} - \log N \text{ (straight line in double log scale)}. \end{aligned} \quad (4.6)$$

The more general formula $F(N) = aN^{-b}$ becomes a straight line with gradient $-b$ in double logarithmic scale:

$$\begin{aligned} F(N) &= aN^{-b} \\ \Rightarrow F &= \frac{a}{N^b} \text{ (hyperbola)} \\ \Rightarrow \log F &= \log a - b \log N \text{ (straight line in double log scale)}. \end{aligned} \quad (4.7)$$

4.3 Time Series

4.3.1 Definition of Time Series

Definition (Bloomfield 1976): “In its simplest form a *time series* is a collection of numerical observations arranged in a natural order.”

We only regard equidistant time series where two time points within the same time series are one day, month, quarter, or year apart.

4.3.2 Smoothing

If the differences between sequent values in a time series are very big, it can be hard to visually observe characteristics of the data. It often helps to smooth the time series before analyzing it. There are several ways to do this.

The *simple moving average (SMA)* of order k calculates the values for the new, smoothed time series out of n original values $\{x_1, x_2, \dots, x_n\}$ by

$$z_i = \frac{1}{k} \sum_{j=0}^{k-1} x_{i-j}, \quad k \leq i \leq n. \quad (4.8)$$

It is called a *backward SMA* because only previous values are used for the calculation. Adding weights, that is adding w_0, w_1, \dots, w_{k-1} with $\sum_{j=0}^{k-1} w_j = 1$, such that

$$z_i = \sum_{j=0}^{k-1} w_j x_{i-j}, \quad k \leq i \leq n, \quad (4.9)$$

yields the weighted backward SMA. It is possible to have a weighted backward SMA without asking for the sum of the w_j to be 1 (Neuhaus and Kreiß 2006), but TEDAS only considers weights that fulfill the restriction of summing up to 1.

The third method we mention here is *exponential smoothing* (Brown 2004). Its advantage is that it keeps the peaks at the same time points as the original time series. Exponential smoothing is defined recursively by

$$\begin{aligned} z_2 &= x_1 \\ z_i &= \alpha x_{i-1} + (1 - \alpha) z_{i-1} \quad \text{with } 0 < \alpha \leq 1 \text{ and } i \geq 3 \end{aligned} \quad (4.10)$$

(Siebold 2007).

Examples for smoothing results:

Figures 4.2, 4.3, 4.4 and 4.5 show the monthly number of incidents in Germany in the time interval from 1968-01-01 to 2007-12-31 stored in the Terror Event Database and different ways of smoothing the time series.

4.3.3 Correlation

Next we regard the situation where we suspect a statistical connection between two time series with the same time scale (for example between two attributes of the same type of event). For each time point we join the two values that belong to this time point in a 2-tuple. This gives us a set of 2-tuples that we can present in a

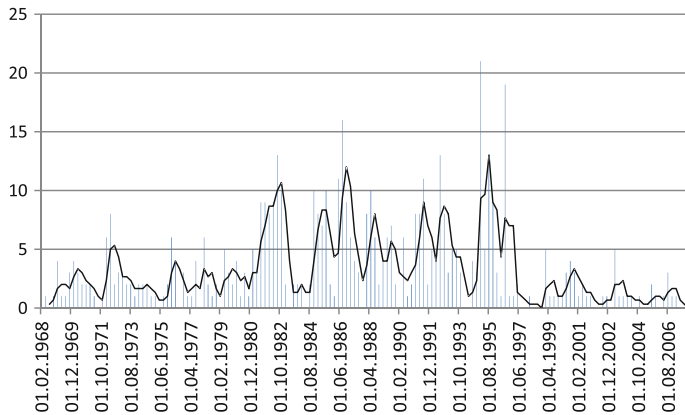


Fig. 4.2 Simple moving average ($k = 3$)

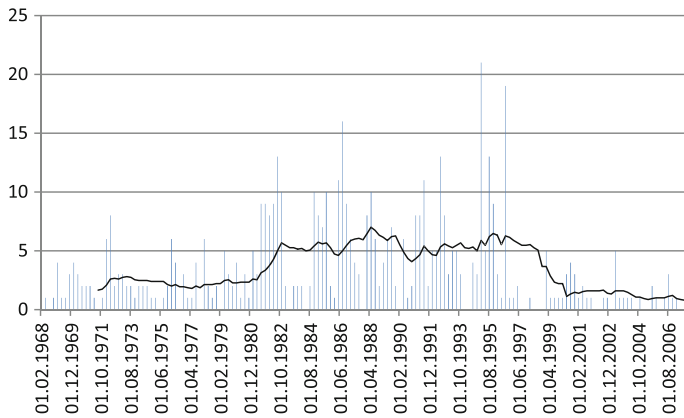


Fig. 4.3 Simple moving average ($k = 15$)

coordinate system, using one axis for each of the two attributes. The resulting diagram is called a *scattergram* (see Fig. 4.6).

If one suspects a linear connection between the two attributes, one can calculate the *regression line* with the method of least squares (see Table 3.2) (Kadelka and Henze 2000). For Fig. 4.6 this is $f(x) = -5, 1 + 11, 4x$. How strong the linear connection between the two attributes is, can be measured with the *correlation coefficient* (see Table 3.2). If its absolute value is close to 1, the linear connection is strong. If it is close to 0, there is no linear statistical connection (Siebold 2007).

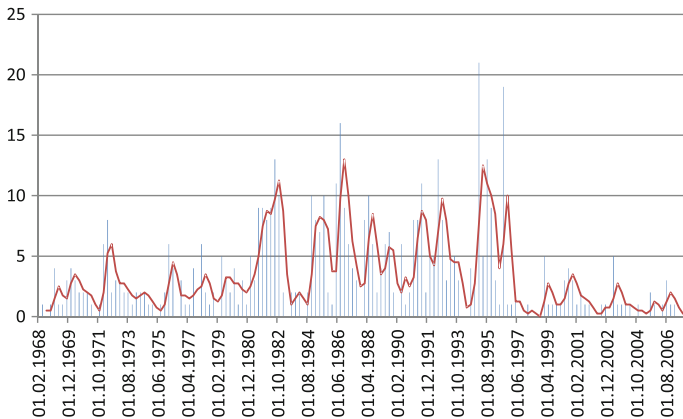


Fig. 4.4 Weighted moving average ($k = 3$) with weights 0.25, 0.5 and 0.25

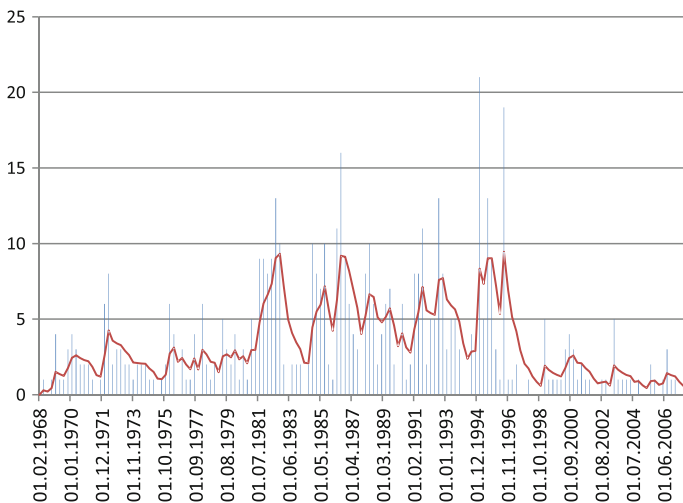


Fig. 4.5 Exponential smoothing ($\alpha = 0.3$)

4.3.4 Autocorrelation

Now we go back to looking at one time series. More specifically, we want to see how strongly the values of a time series that is moved against itself by a lag of k time units and of the original time series are correlated.

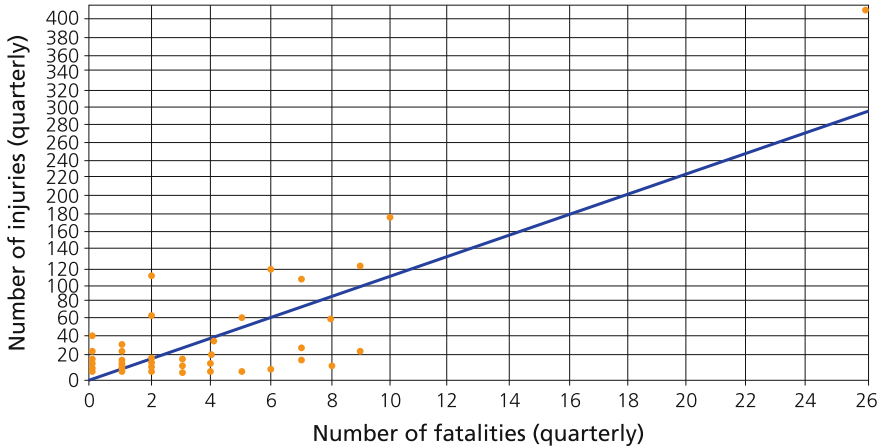


Fig. 4.6 Scattergram: Number of casualties and fatalities per quarter in France from 1968 to 2004 and the regression line (Siebold 2007)

For this we regard the *autocorrelation function*

$$\rho(k) := \rho_k, \quad k \in \mathbb{N} \quad (4.11)$$

where ρ_k is the empiric autocorrelation coefficient for lag k (see Table 3.2 for the definition and the formula). (Jenkins et al. 1994; Beichelt et al. 2003). The resulting diagram is called a correlogram (Gottman 1981; Neuhaus and Kreiß 2006).

Stochastic processes where all autocorrelation coefficients for $k > 0$ are 0, are called *white noise processes*. For practical applications one does not ask for the coefficients to be exactly equal to 0, but allows them to lie in a small interval around 0 in order to call the process a white noise process. We use the *Bartlett Band* (Gottman 1981) as such an interval, that is the interval is $[-2/\sqrt{N}, 2/\sqrt{N}]$ where N is the number of values in our time series.

Figure 4.7 shows typical correlograms (normalized to 1) for artificially generated time series for trend, white noise, cycles, and combinations of those three (Siebold 2007).

4.3.5 Trend

By fitting a trend polynomial of given order to a (smoothed) time series we can identify *trend* behavior. This can be done by setting

$$m(t) = \sum_{i=0}^k a_i m_i(t) \quad \text{for all } t \in \mathbb{N}_0, \quad (4.12)$$

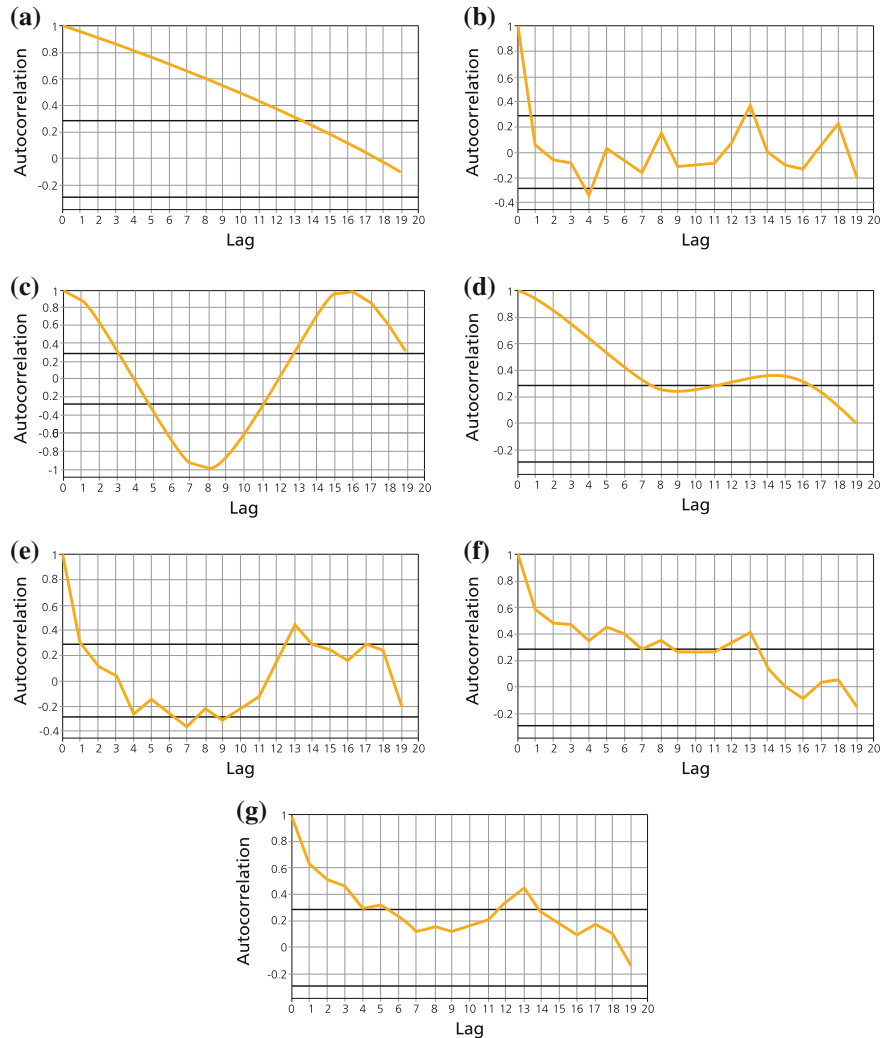


Fig. 4.7 Typical correlograms for **a** trend, **b** white noise, **c** cycles, **d** trend + cycles, **e** cycles + white noise, **f** trend + white noise, **g** trend + cycles + white noise, where “+” means that the time series were added (Siebold 2007)

Fig. 4.8 Polynomial trend for $k = 6$ for events in Germany between 1968 and 2004 per quarter (Siebold 2007)

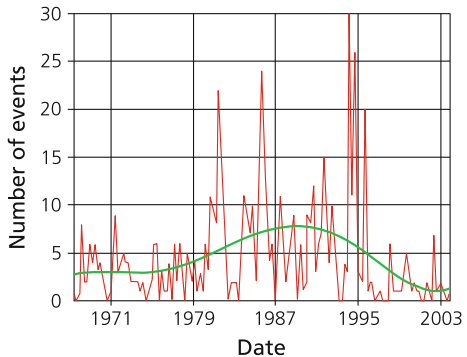
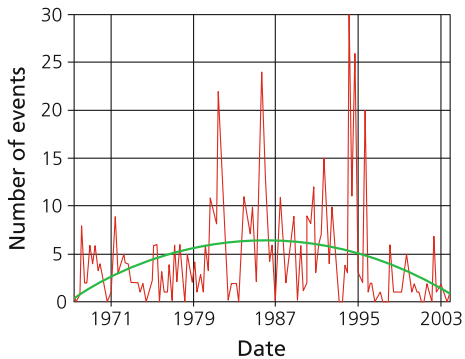


Fig. 4.9 Polynomial trend for $k = 2$ for events in Germany between 1968 and 2004 per quarter (Siebold 2007)



where $m_i(t) = t^i$, $i = 0, \dots, k$ and $a_0, \dots, a_k \in \mathbb{R}$ are chosen by minimizing

$$\sum_{t=1}^n \left(x_t - \sum_{i=0}^k a_i m_i(t) \right)^2 \quad (4.13)$$

(method of least squares) (Neuhaus and Kreiß 2006).

Figure 4.8 shows the polynomial trend for $k = 6$ for events in Germany per quarter from 1968 to 2004. It indicates that the number of events is rising in 2004. One has to be careful with this assumption because it is sinking if we choose $k = 2$ instead (see Fig. 4.9).

4.3.6 Cycles

One can expect that cycles exist in time series of terroristic events, for example because terroristic activity can be related to tourism which increases or decreases during certain times of the year.

We demonstrate a method to find *cycles* in a time series that is more precise than the optical interpretation of the correlogram as in Fig. 4.7. In particular, graphical analysis is difficult if there is white noise in the time series. Then this new method, the so called *periodogram*, is a useful tool. It also shows trend behavior because trend can be seen as cyclic behavior with an infinite period.

The periodogram is a function of the autocovariances of the time series. It shows the frequencies of a time series, which indicate trend or cycles. We use a smoothed periodogram, the so called Bartlett 2 window,

$$f_B(\lambda) = \frac{1}{2\pi} \left(\hat{\gamma}(0) + 2 \sum_{k=1}^m \hat{\gamma}(k) w_k \cos(\lambda k) \right) \quad (4.14)$$

for frequency $0 \leq \lambda \leq \pi$ (where $2\pi/\lambda = t$) and with weights $w_k = 1 - k/m$.

One can present the periodogram in a diagram with the frequency on the abscissa and the spectral density on the ordinate. If the periodogram has a high spectral density for very small frequencies, this indicates trend behavior. If it has a peak, we can expect a cycle (see also Fig. 4.10) (Siebold 2007).

Sometimes it is necessary to (additively or multiplicatively) remove a linear or quadratic trend before one can see cyclic behavior. An example for this is given in Fig. 4.11.

Remark It is also possible to decompose the time series into trend, cycles, and white noise. This can happen additively or multiplicatively.

4.3.7 Forecast

There are several methods to forecast a time series. We concentrate on three simple methods and on numerical forecasts. It is, for example, also possible to use the decomposition we have mentioned for forecasts or to use the methods that are explained here to do binary forecasts (Siebold 2007).

Given a time series $x_1, x_2, x_3, \dots, x_{n-1}$ we adapt our model to these values and predict the value \hat{x}_n with our forecasting method.

To judge how good our forecast is we use the *root relative square error* (*rrse*) that is defined by

$$\text{rrse} = \frac{\sqrt{\sum_{i=2}^n (x_i - \hat{x}_i)^2}}{\sqrt{\sum_{i=2}^n (x_i - \bar{x})^2}} \quad (4.15)$$

where \bar{x} is the mean of our time series.

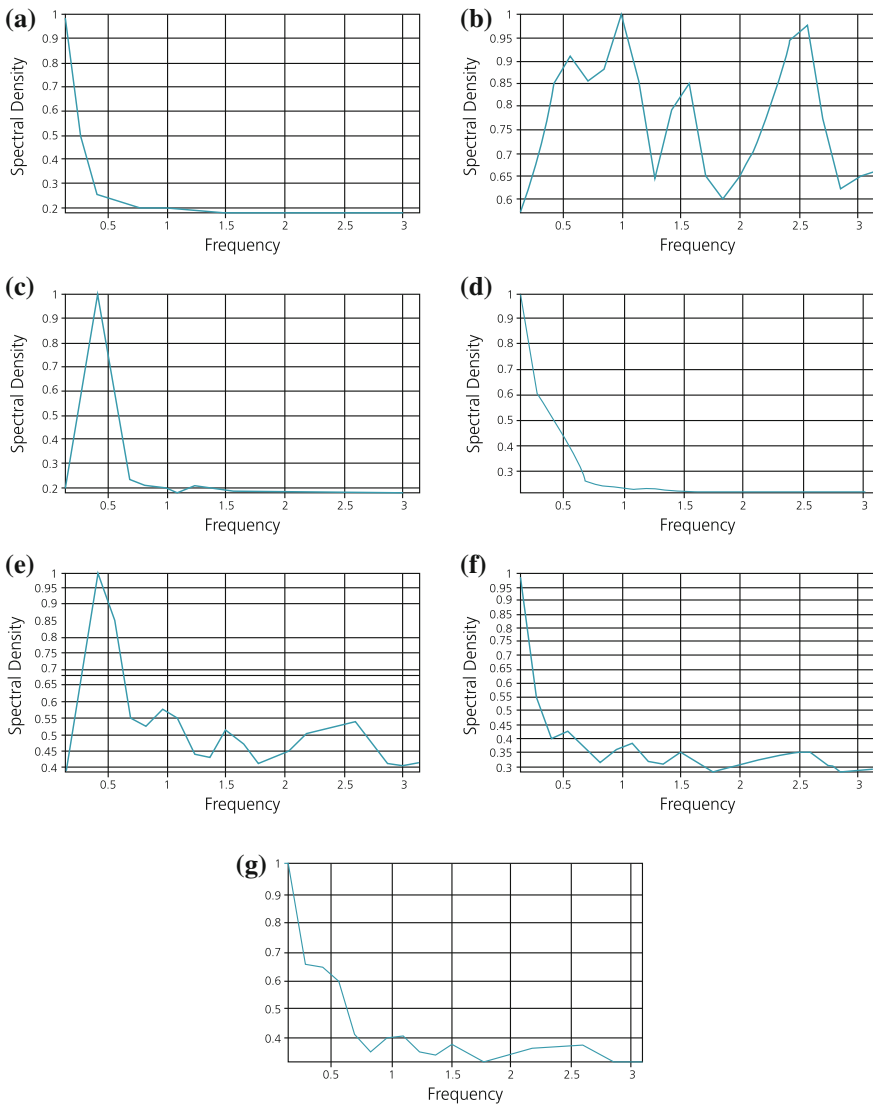


Fig. 4.10 Periodograms of artificial time series for **a** trend, **b** white noise, **c** cycles, **d** trend + cycles, **e** cycles + white noise, **f** trend + white noise, **g** trend + cycles + white noise, where “+” means that the time series were added (Siebold 2007)

Next we present our three forecasting methods. In every forecasting method values are rounded to integers.

Zero-forecast: The same value is being predicted for every time point, for example the value that appears most often in the given time series: $\hat{x}_n = a$ for all n .

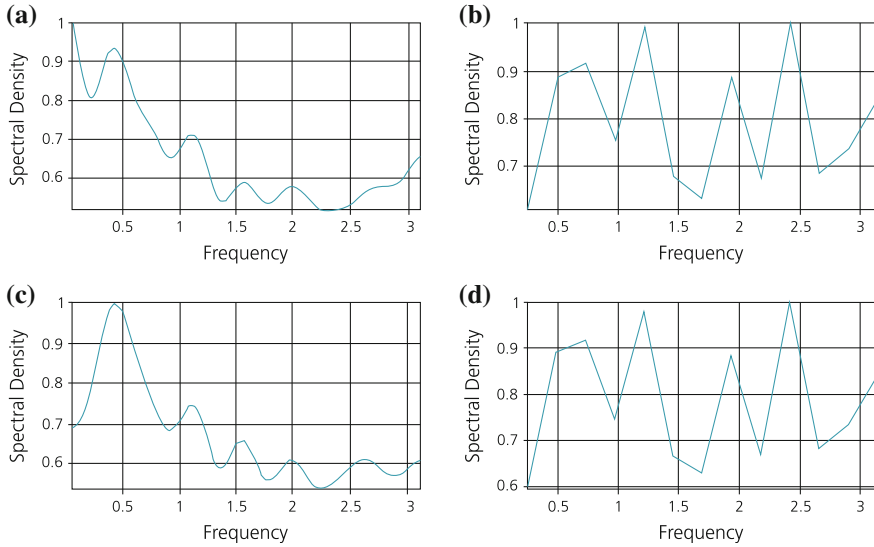


Fig. 4.11 Bartlett 2 Window for the number of events in Germany per quarter from **a** 1968 to 1997 and **b** 1998 to 2004, and after (multiplicatively) removing a linear trend for **c** 1968 to 1997 and **d** 1998 to 2004 (Siebold 2007)

Method 1: The current value is being used to predict the next one: $\hat{x}_n = x_{n-1}$.

Forecast with exponential smoothing:

Algorithm 1 shows the forecasting algorithm from TEDAS with the help of exponential smoothing. The smoothing constant α is set by the user.

Algorithm 1: `forecast_exp (time series d)`

// Forecast with exponential smoothing.

Initial $0 < \alpha \leq 1$

```

01: val = d[0]
02: i = 1
03: while i < d.size do
04:   val =  $\alpha \cdot d[i] + (1 - \alpha) \cdot val$ 
05:   i = i + 1
06: end while
07: return  $\alpha \cdot d[i-1] + (1 - \alpha) \cdot val$ 

```

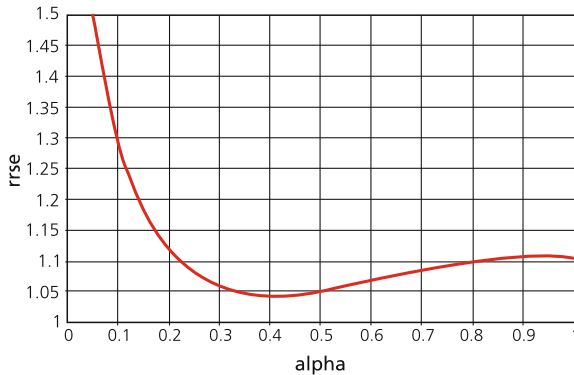


Fig. 4.12 Averaged rrse as a function of the smoothing constant α from (Siebold 2007)

In our notation $d[0] = x_1, d[1] = x_2, \dots, d[n - 2] = x_{n-1}$, and $\hat{x}_n = \alpha \cdot d[d.size - 1] + (1 - \alpha) \cdot val$, the returned value from line 06.

It is possible to optimize the smoothing constant α numerically. This is done by using the constant α that minimizes the rrse over the previous time points in the time series. For the example from (Siebold 2007) this is shown in Fig. 4.12 (Siebold 2007).

Example Given the time series

$$x_1 = 1, x_2 = 2, x_3 = 4, x_4 = 2, x_5 = 1, x_6 = 3, x_7 = 5$$

with $\bar{x} \approx 2.57$, we demonstrate the three forecasting methods.

(a) **Zero-forecast:** $\hat{x}_2 = \hat{x}_3 = \hat{x}_4 = \hat{x}_5 = \hat{x}_6 = \hat{x}_7 = \hat{x}_8 = 2$.

$$\begin{aligned} rrse &= \frac{\sqrt{(2-2)^2 + (4-2)^2 + (2-2)^2 + (1-2)^2 + (3-2)^2 + (5-2)^2}}{\sqrt{(2-2.57)^2 + (4-2.57)^2 + (2-2.57)^2 + (1-2.57)^2 + (3-2.57)^2 + (5-2.57)^2}} \\ &\approx 1.16. \end{aligned}$$

(b) **Method 1:** $\hat{x}_2 = 1, \hat{x}_3 = 2, \hat{x}_4 = 4, \hat{x}_5 = 2, \hat{x}_6 = 1, \hat{x}_7 = 3, \hat{x}_8 = 5$.

$$\begin{aligned} rrse &= \frac{\sqrt{(2-1)^2 + (4-2)^2 + (2-4)^2 + (1-2)^2 + (3-1)^2 + (5-3)^2}}{\sqrt{(2-2.57)^2 + (4-2.57)^2 + (2-2.57)^2 + (1-2.57)^2 + (3-2.57)^2 + (5-2.57)^2}} \\ &\approx 1.26. \end{aligned}$$

(c) **Forecast with exponential smoothing** for $\alpha = 0.3$:

$$\begin{aligned}\hat{x}_2 &= 1, \\ \hat{x}_3 &= 0.3 \cdot 2 + 0.7 \cdot 1 = 1.3 \approx 1, \\ \hat{x}_4 &= 0.3 \cdot 4 + 0.7 \cdot 1 = 1.9 \approx 2, \\ \hat{x}_5 &= 0.3 \cdot 2 + 0.7 \cdot 2 = 2, \\ \hat{x}_6 &= 0.3 \cdot 1 + 0.7 \cdot 2 = 1.7 \approx 2, \\ \hat{x}_7 &= 0.3 \cdot 3 + 0.7 \cdot 2 = 2.3 \approx 2, \\ \hat{x}_8 &= 0.3 \cdot 5 + 0.7 \cdot 2 = 2.9 \approx 3.\end{aligned}$$

$$\begin{aligned}rrse &= \frac{\sqrt{(2-1)^2 + (4-1)^2 + (2-2)^2 + (1-2)^2 + (3-2)^2 + (5-2)^2}}{\sqrt{(2-2.57)^2 + (4-2.57)^2 + (2-2.57)^2 + (1-2.57)^2 + (3-2.57)^2 + (5-2.57)^2}} \\ &\approx 1.37.\end{aligned}$$

Remark Our example shows unusual results. In (Siebold 2007) bigger example time series were used and the errors behave in the way one would expect: Forecasting with exponential smoothing has the smallest error, Method 1 has the second smallest error of those three methods and the zero-forecast is the worst forecasting method in that test. One reason why the exponential smoothing method does not yield good results in our example is that we chose α arbitrarily instead of optimizing it.

Remark Even though the exponential smoothing method has a lower rrse in the calculations in (Siebold 2007) than in our example, Siebold concludes that the method is not satisfying without additional information such as news, historic events, or background knowledge about terror organizations. These methods implemented in TEDAS are however a good assisting tool for forecasts done by persons.

4.3.8 Matching this Section with the Diagram from Chap. 3

In the process from Fig. 3.1 time series analysis appears in every step from data selection to visualization. In the step of data selection, the attributes are chosen that should be represented in the time series. They are saved as a time series (as mentioned in Sect. 3.9) in the step of data preparation. The steps selection and application of methods are the most present, as smoothing, regression lines, correlation coefficients, autocorrelation functions, trend polynomials, periodograms, and forecast methods can be counted as methods. The selection and application of visualization methods are not always explicitly mentioned, but all the diagrams in this section represent visualization methods.

4.3.9 More about Time Series Analysis

This chapter covers basic concepts of time series analysis. Siebold shows in (Siebold 2007) that these methods already only apply to certain data sets (for example, certain analysis methods only provide results for a few countries) and that one has to be very careful in using them for interpretations and forecasts. Therefore, applying more complex methods for more detailed analysis does not promise more results. For more complex time series analysis methods and applications in different research areas see for example (Ao 2010).

4.4 Risk Maps

Risk maps (also called risk matrices or risk graphs) are diagrams in coordinate systems with frequencies on the abscissa and consequences on the ordinate where parts of the coordinate system are colored to indicate whether the risk is seen as high, low, acceptable, or non-acceptable. Examples for risk maps are given in Figs. 4.13, 4.14, 4.15 and Table 4.1.

In Fig. 4.14 F-N curves like in Sect. 4.2 are used as a classification for high and low risks. It is also common to color the rectangles as the ones that can be seen in Fig. 4.15 as well to distinguish between high and low risks.

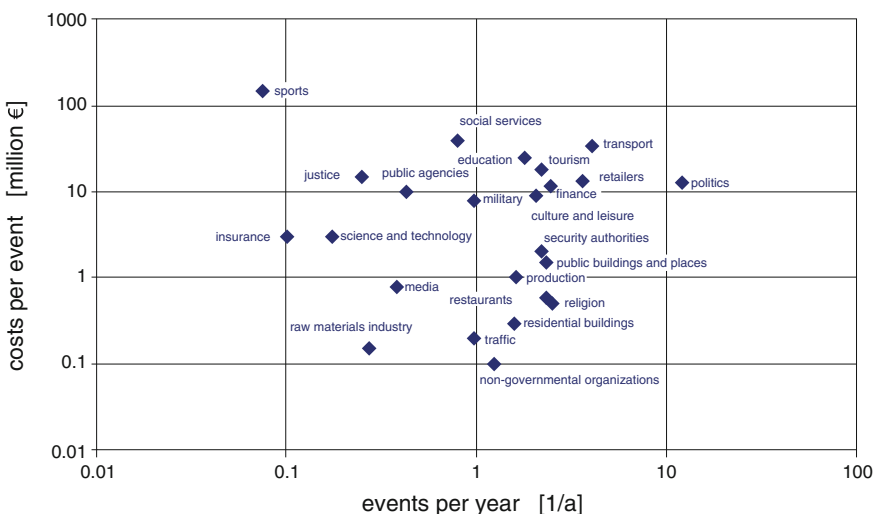


Fig. 4.13 Risk map worldwide, consequences over frequency diagram: costs per event over events per year from terror event database. (Brombacher 2005)

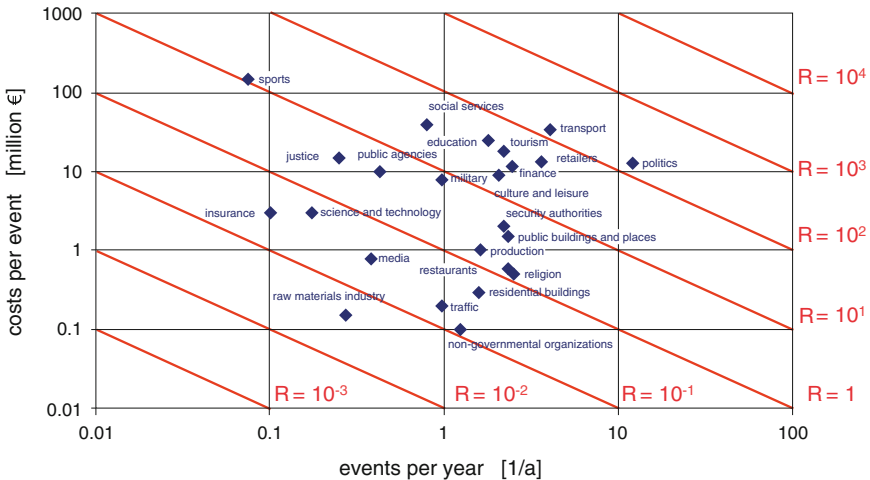


Fig. 4.14 Extension of Fig. 4.13 by lines showing the risk R (Brombacher 2005)

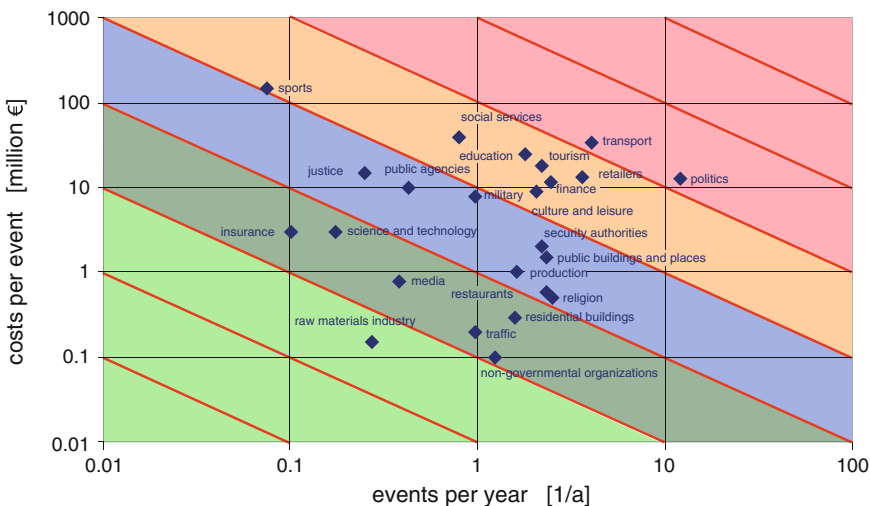


Fig. 4.15 Extension of Fig. 4.14 by a categorization by colors into low (green) and high (red) risks (Brombacher 2005)

It is important to clearly label the axes. Otherwise the risk map seems informative but does not actually help for the risk analysis process. For example the description from “low” over “moderate” to “high” for the likelihood or impact can mean anything if it is not further specified (WEKA Business Media AG 2012). Axes labeled with numbers on the other hand (like in Fig. 4.13) cannot be interpreted in several ways and are therefore more meaningful.

Table 4.1 Risk map from AOP-15 (AOP-15 2009) with four severity classes and six probability/frequency levels. Risk levels are low (*green*), medium (*yellow*) and high (*red*). Reprinted from AOP-15 Edition 3, Nato Standardization Agency (NSA), 2009

Level of probability	Probability of occurrence per lifetime	Probability of occurrence per hour of operation	Catastrophic	Critical	Limited	Insignificant
			I	II	III	IV
Frequent A	$P > 10^{-1}$	To be determined project-specifically	I-A	II-A	III-A	IV-A
Probable B	$10^{-1} \geq P > 10^{-2}$		I-B	II-B	III-B	IV-B
Occasional C	$10^{-2} \geq P > 10^{-3}$		I-C	II-C	III-C	IV-C
Low D	$10^{-3} \geq P > 10^{-6}$		I-D	II-D	III-D	IV-D
Improbable E	$10^{-6} \geq P > 10^{-7}$		I-E	II-E	III-E	IV-E
Noncredible F	$10^{-7} \geq P$		I-F	II-F	III-F	IV-F

4.5 Summary and Outlook

In this chapter we have seen several different aspects of time series analysis. It was shown how one can get very interesting results such as trend behavior with rather simple statistic methods. Additionally, F-N curves and diagrams as well as risk maps have been introduced. Those are very crucial for risk management, as they help to decide whether risks are acceptable, and will appear often throughout the next chapters.

4.6 Questions

- (1) What is the difference between f-N-curves and F-N-curves?
- (2) Consider the time series $\{3, 4, 4, 6, 5, 2\}$. What is the smoothed time series with
 - (a) SMA, $k = 2$,
 - (b) SMA, $k = 3$,
 - (c) weighted SMA, $k = 2$, $w_0 = 1/3$, $w_1 = 2/3$,
 - (d) exponential smoothing with $\alpha = 0.2$.

Does the peak move in one of those cases? If yes, does it move to the left or to the right and does it always move into that direction?

How do you have to choose w_0 and w_1 to get the same results in (c) as in (a)?

- (3) Given $F(10) = 10^{-6}$ and $F(1000) = 10^{-10}$.
 - (a) Determine the risk aversion criterion $F(N) = aN^{-b}$. Sketch the F-N-curve in double-log scale.
 - (b) If you regard the sketch from (a) as a risk map where the area inside the triangle created by the F-N-curve and the axes is considered as acceptable risk, is a frequency of $3 \cdot 10^{-6}$ for $N = 5$ acceptable or not?
- (4) Given the following correlograms (Fig. 4.16):

What kind of behavior do they show?
- (5) Use Microsoft Excel to analyze a time series (without regarding that all numbers should be integers):
 - (a) Create a time series of successful attacks on Great Britain from 1970 to 2010 using GTD (<http://www.start.umd.edu/gtd/>) and Microsoft Excel and display it in a diagram.
 - (b) Compute the smoothed time series for SMA with $k = 3$, SMA with $k = 8$, and weighted SMA with $k = 3$ and $w_0 = 0.5$, $w_1 = 0.25$, and $w_2 = 0.25$, and display them in a diagram together with the original time series.
 - (c) Compute the exponentially smoothed time series for $\alpha = 0.3$, $\alpha = 0.05$, $\alpha = 0.0005$, and $\alpha = 0.99$ and display it in a diagram together with the original time series.

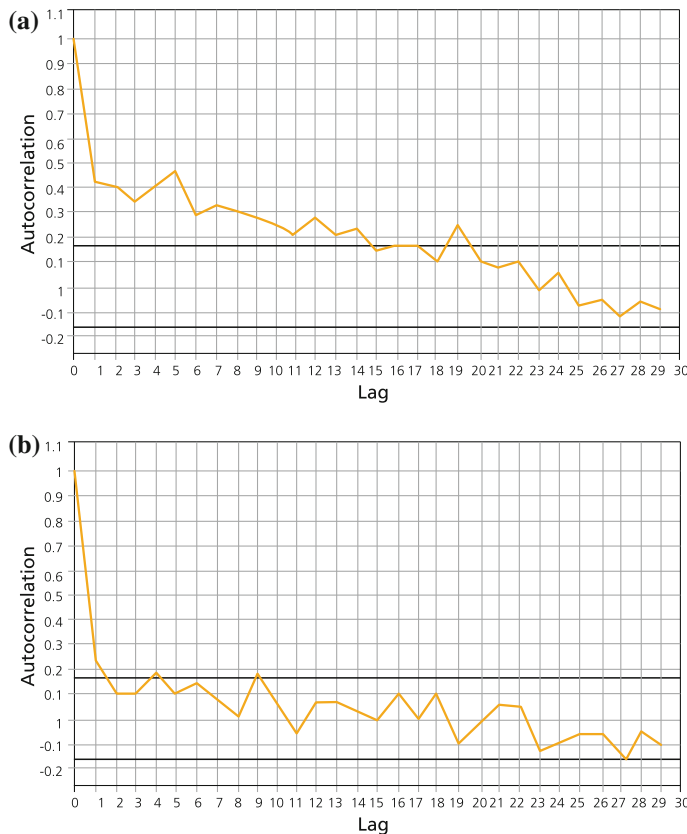


Fig. 4.16 Correlogram for **a** Chile and **b** Italy, 1968–2004 (Siebold 2007)

- (d) Create and interpret a correlogram for the given time series for $k = 0, 1, 2, \dots, 20$.
- (e) After again reading Sect. 4.3.6: Create and interpret a periodogram for the given time series for $m = 20$ and λ in steps of 0.1. Relate it to the diagram from (a).
- (f) Compute the injuries per year for Great Britain from 1970 to 2010.
- (g) Use Microsoft Excel to compute the linear and the polynomial trend function of degree three (that is, $k = 3$) for the given time series. Compare it to the trend function that Microsoft Excel generates, if you choose the option to include a trend function in a diagram.
- (h) Compute the forecasted series $\hat{x}_1, \hat{x}_2, \dots, \hat{x}_n$ to the given time series with zero-forecast with $a = 0$ and $a = 70$, with Method 1 and by exponential smoothing with $\alpha = 0.06$ and $\alpha = 0.3$. Compare the five rrse's. What do you notice?
- (i) Which value would you choose for \hat{x}_{n+1} based on your analysis from (h)?

4.7 Answers

- (1) For the f-N curve, the y-values are the frequencies of experiencing exactly N fatalities. For the F-N curve, the y-values are the frequencies of experiencing N or more fatalities (see Sect. 4.2.1).
- (2) See Sect. 4.3.2.
 - (a) $z_2 = 0.5(x_2 + x_1) = 3.5$, $z_3 = 0.5(x_3 + x_2) = 4$, $z_4 = 5$, $z_5 = 5.5$, $z_6 = 3.5$.
 - (b) $z_3 = 1/3 \cdot (x_3 + x_2 + x_1) = 11/3$, $z_4 = 1/3 \cdot (x_4 + x_3 + x_2) = 14/3$, $z_5 = 5$, $z_6 = 13/3$.
 - (c) $z_2 = 1/3 \cdot x_2 + 2/3 \cdot x_1 = 4/3 + 6/3 = 10/3$, $z_3 = 4$, $z_4 = 14/3$, $z_5 = 17/3$, $z_6 = 4$.
 - (d) $z_1 = 3$, $z_2 = 0.2x_1 + 0.8z_1 = 3$, $z_3 = 0.2 \cdot 4 + 0.8 \cdot 3 = 3.2 \approx 3$, $z_4 = 0.2 \cdot 4 + 0.8 \cdot 3 = 3.2 \approx 3$, $z_5 = 0.2 \cdot 6 + 0.8 \cdot 3 = 3.6 \approx 4$, $z_6 = 0.2 \cdot 5 + 0.8 \cdot 4 = 4.2 \approx 4$.

The peak moves in some cases. It can only move to a later time point. It moves if the value/values after the peak are bigger than before.

One has to choose $w_0 = w_1 = 0.5$. This can be seen by comparing the formulas for z_2 in (a) and (c).

- (3) The graph can be drawn with a mathematical computer program. Here we only give the formulas.

$$10^{-6} = a \cdot 10^{-b}, \quad 10^{-10} = a \cdot 1000^{-b}.$$

$$\begin{aligned} \text{(a)} \quad & \Rightarrow 10^{-6+b} = 10^{-10+3b} \\ & \Rightarrow b = 2, \quad a = 10^{-4}. \end{aligned}$$

That is, $F(N) = 10^{-4}N^{-2}$ (see Sect. 4.2.1).

- (b) $3 \cdot 10^{-6} < 4 \cdot 10^{-6} = 10^{-4} \cdot 5^{-2} = F(5)$. Hence, the point $(5/3 \cdot 10^{-6})$ lies under the F-N-curve which means that the risk is acceptable.

- (4) In correlogram (a) one can see an almost linear decline, indicating trend behavior (This does not mean that there cannot also be cyclic behavior in the time series). In correlogram (b) one can see white noise, as the graph stays inside the Bartlett Band.
- (5) To determine the answers, a German version of Microsoft Excel was used. Translations of the functions can, for example, be found under <http://www.hlt-steyr.ac.at/~morg/pcinfo/Excel/exce9uxx.htm>. Only extracts from the tables are shown here.

- (a) Searching for successful attacks in Great Britain from 1970 to 2010 yields 413 incidents. (National Consortium for the Study of Terrorism and Responses to Terrorism (START) 2011)
Sorting them by injuries and copying the part of the table into Microsoft Excel where the number of injuries is not 0 or unknown, leaves 122 incidents to work with.

Remark Cleaning this data is not part of the task. Hence, the computations are based on the data as it comes from the database, including, for example, the event in 1974 with 101 injuries twice.

In Microsoft Excel the following steps prepare the data for displaying it in a diagram:

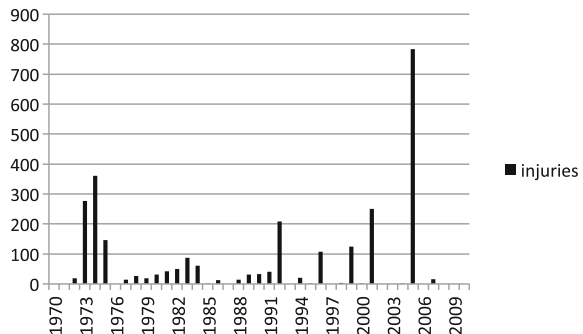
- Deletion of all columns which are not needed.
- “=BRTEILJAHRE(“01.01.1970”; B2)” and “=GANZZAHL(D2 + 1970)” change the date into a year. (A few dates have to be adapted manually because they are saved in a form Excel does not recognize.)
- Assume the injuries are saved in (F2:F124) and the matching year in (G2: G124), Table 4.2 is created in the following way (add a “=” in front of the functions) where “year” is written in I2:

Table 4.2 Computations for displaying a time series of injuries in Great Britain for terroristic attacks, 1970–2010

Year	1970	1971
Injuries	SUMME(J4:J126)	SUMME(K4:K126)
	WENN(\$G2 = J\$2;\$F2;0)	WENN(\$G2 = K\$2;\$F2;0)
	WENN(\$G3 = J\$2;\$F3;0)	WENN(\$G3 = K\$2;\$F3;0)

- Presenting the first two rows in a diagram (Fig. 4.17):

Fig. 4.17 Time series of injuries in Great Britain for terroristic attacks, 1970–2010, with data from (National Consortium for the Study of Terrorism and Responses to Terrorism (START) 2011)

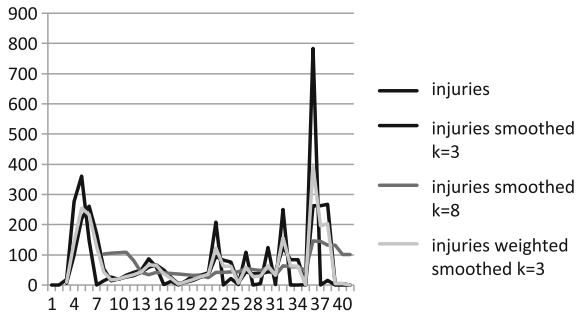


- (b) The smoothed time series can be computed as in the following Table 4.3 (again add “=” in front of functions/computations) where “year” is written in B129:

Table 4.3 Computations for smoothing the time series

Year	1970	1971	1972
Injuries	0	0	19
Injuries smoothed k = 3			$1/3 \times (E130 + D130 + C130)$
Injuries smoothed k = 8			
Injuries weighted smoothed k = 3			$1/2 \times E130 + 1/4 \times D130 + 1/4 \times C130$

The resulting diagrams are shown in Fig. 4.18.

**Fig. 4.18** Time series after smoothing with SMA

- (c) The smoothed time series can be computed as in the following Table 4.4 (again add “=” in front of functions/computations) where “year” is written in B129:

Table 4.4 Computations for smoothing the time series

Year	1970	1971
Injuries	0	0
Injuries exp. a = 0.3	C130	$0.3 \times C130 + (1-0.3) \times C131$
Injuries exp. a = 0.05	C130	$0.05 \times C130 + (1-0.05) \times C132$
Injuries exp. a = 0.0005	C130	$0.0005 \times C130 + (1-0.0005) \times C133$
Injuries exp. a = 0.99	C130	$0.99 \times C130 + (1-0.99) \times C134$

The resulting diagrams are shown in Fig. 4.19.

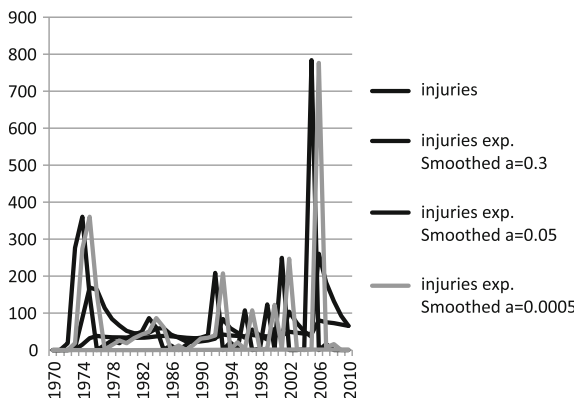
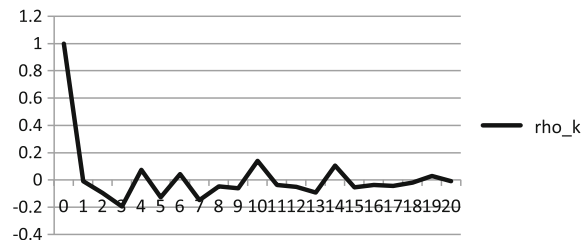


Fig. 4.19 Time series after exponential smoothing

(d) The correlogram looks like this (Fig. 4.20):

Fig. 4.20 Correlogram for the time series of injuries in Great Britain, 1970–2010



The boundaries of the Bartlett Band for this time series are $\pm 2/\sqrt{41} \approx \pm 0.3123$. The autocorrelation function stays inside the Bartlett Band which indicates white noise behavior.

(e) The periodogram looks like this (Fig. 4.21):

Fig. 4.21 Periodogram for the time series of injuries in Great Britain, 1970–2010

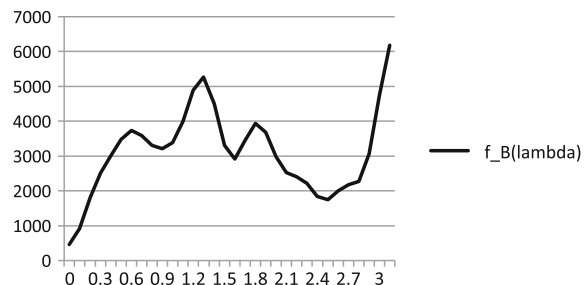
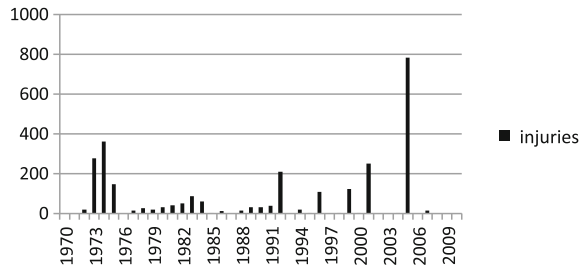


Fig. 4.22 Recognition of cycles in the time series



It has a peak for $\lambda \approx 1.3$. This indicates a cyclic behavior with a period of $2\pi/\lambda \approx 4.8$ years. This can also be recognized in the diagram of our time series (see Fig. 4.22), where the distance between the peaks is either this or twice as big. It is not very clearly noticeable though, which is not surprising. Only 41 time points are regarded which yields a rather short time series. Additionally, the correlogram mostly shows white noise behavior and the periodogram does not have a very clear peak.

- (f) Adding all the numbers of injuries and dividing by $2010 - 1970 + 1 = 41$ yields that there were 68,024 injuries per year in Great Britain from 1970 to 2010.
- (g) To calculate $m(t) = \sum_{i=0}^k a_i m_i(t)$ one has to minimize

$$\sum_{t=1}^n \left(x_t - \sum_{i=0}^k a_i m_i(t) \right)^2. \quad (4.16)$$

For $k = 3$ this is

$$\sum_{t=1}^n \left(x_t - a_0 - a_1 t - a_2 t^2 - a_3 t^3 \right)^2. \quad (4.17)$$

Differentiating with respect to a_i and setting it equal to 0 yields

$$0 = 2 \sum_{t=1}^n x_t t^i - 2a_0 \sum_{t=1}^n t^i - 2a_1 \sum_{t=1}^n t^{i+1} - 2a_2 \sum_{t=1}^n t^{i+2} - 2a_3 \sum_{t=1}^n t^{i+3}. \quad (4.18)$$

Hence, one has 4 equations with the 4 variables a_0 , a_1 , a_2 , and a_3 . In Table 4.5 the necessary values are computed.

Table 4.5 Computation of the coefficients for the trend function

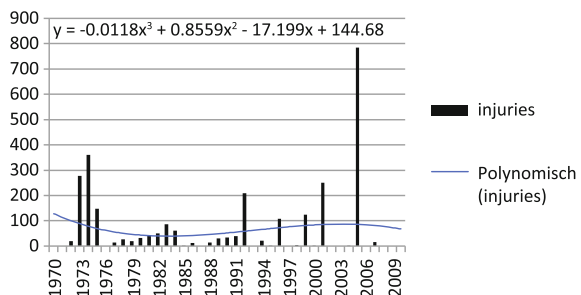
	t	1	...	41	
	Year	1970	...	2010	
	x_t	0	...	0	$2 \times \text{summe}_1^n(x_t \times t^i)$
0	$x_t \times t^0$	C\$201 × C\$199 ^{\$A202}	...	0	2 × SUMME(C202:AQ202)
1	$x_t \times t^1$	C\$201 × C\$199 ^{\$A203}	...	0	119,646
2	$x_t \times t^2$	C\$201 × C\$199 ^{\$A204}	...	0	3,493,246
3	$x_t \times t^3$	C\$201 × C\$199 ^{\$A205}	...	0	112,448,946
4	$x_t \times t^4$	0	...	0	3,758,540,470
5	$x_t \times t^5$	0	...	0	1.28142E+11
6	$x_t \times t^6$	0	...	0	4.42424E+12
0	t^0	C\$199 ^{\$A209}	...	1	2 × SUMME(C209:AQ209)
1	t^1	C\$199 ^{\$A210}	...	41	1720
2	t^2	1	...	1681	47,642
3	t^3	1	...	68,921	1,482,642
4	t^4	1	...	2,825,761	49,214,186
5	t^5	1	...	1.16E+08	1,701,578,802
6	t^6	1	...	4.75E+09	60,510,015,722

The computed coefficients for the system of equations are shown in Table 4.6

Table 4.6 Coefficients for the trend function

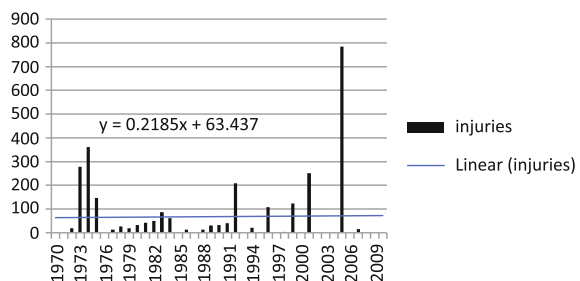
a_0	a_1	a_2	a_3	Right side
82	1722	47,642	1,482,642	5578
1722	47,642	1,482,642	49,214,186	119,646
47,642	1,482,642	49,214,186	1,701,578,802	3,493,246
1,482,642	49,214,186	1,701,578,802	6.051E + 10	112,448,946

Solving the system yields the trend polynomial (Fig. 4.23).

Fig. 4.23 Polynomial trend function of order 3

This is the same trend function as the tool in Microsoft Excel generates. The linear case (Fig. 4.24) can be derived from the previous one by only regarding parts of the table.

Fig. 4.24 Linear trend function of order 1



(h) The forecasts can be calculated as in Table 4.7 where “t” is written in B238.

Table 4.7 Forecasting with Microsoft Excel

t	1	2
Year	1970	1971
x_t	0	0
Zero-forecast with the constant value 0		
$x_t \text{ hat}$	\$F\$243	0
$(x_t \text{ hat} - x_t)^2$	$(C\$240-C244)^2$	0
$(x_t - \text{average})^2$	$(C\$240-\$AQ\$164)^2$	4627.31767
Method 1		
$x_t \text{ hat}$	0	C240
$(x_t \text{ hat} - x_t)^2$	$(C\$240-C249)^2$	$(D\$240-D249)^2$
Exp. Smoothing with $a = 0.06$		
$x_t \text{ hat}$	0	C240
$(x_t \text{ hat} - x_t)^2$	$(C\$240-C249)^2$	$(D\$240-D249)^2$
rrse =	$\text{WURZEL}(\text{SUMME}(C245:AQ245))/$ $\text{WURZEL}(\text{SUMME}(C246:AQ246))$	

The resulting rrse's are shown in Table 4.8.

Table 4.8 rrse for forecasting with Microsoft Excel

Method	rrse
Zero $a = 0$	1.11099084
Zero $a = 70$	1.00009881
Method 1	1.4164343
Exp $a = 0.06$	1.05164464
Exp $a = 0.3$	1.1175021

One notices that the rrse for the zero-forecast and the forecast with exponential smoothing depends very much on how we choose a and α , respectively. For the Zero-Method, the rrse is small for a close to the arithmetic mean of the time series. For exponential forecasts the rrse is small for α close to the optimal α which we did not calculate for this time series but which seems to be close to $\alpha = 0.06$ by trying out different values for α .

If one looks at the values the methods predict for \hat{x}_{n+1} , they vary extremely. On the other hand, the values for the two methods with the smallest rrse are not too far apart with $\hat{x}_{n+1} = 70$ for the zero-forecast with $a = 70$ and $\hat{x}_{n+1} = 66.123$ for the forecast with exponential smoothing with $\alpha = 0.06$. With the intuitive method of predicting the arithmetic mean of the time series up to this point, $\bar{x} = 68.0244$, one would be in the middle of those two forecasts. Hence, based on our forecasts, $\hat{x}_{n+1} = \bar{x}$ is a reasonable choice.

References

- Ao, S.-I. (2010). *Applied time series analysis and innovative computing* (p. 59). Dordrecht: Springer Science + Business Media B.V.
- AOP-15. (2009). 3 Edn. Nato Standardization Agency (NSA). Retrieved 2014-02-17, from <http://www2.fhi.nl/plot2012/archief/2010/images/aop-15e.pdf>
- Beichelt, F. E., Montgomery, D. C., Beichelt, F. E., Cheng, S., Christoph, G., Jennings, C. L., et al. (2003). *Teubner-Taschenbuch der Stochastik; Wahrscheinlichkeitstheorie, Stochastische Prozesse, Mathematische Statistik*. Stuttgart u.a.: Teubner.
- Bloomfield, P. (1976). *Fourier analysis of time series: An introduction*. Hoboken: Wiley.
- Brombacher, B. (2005). Bedrohung durch Internationalen Terrorismus. *Carl Cramz Seminar*. Efringen-Kirchen, Germany, Fraunhofer EMI.
- Brown, R.G. (2004). *Smoothing forecasting and prediction of discrete time series*. Mineola: Dover Publications.
- Center for Chemical Process Safety. (2009). In Appendix A: Understanding and Using F-N Diagrams. *Guidelines for developing quantitative safety risk criteria*. NJ, USA: Wiley, Inc. Hoboken. doi: [10.1002/9780470552940.app1](https://doi.org/10.1002/9780470552940.app1)
- Gottman, J. M. (1981). *Time-series analysis. A comprehensive introduction for social scientists*. Cambridge: Cambridge University Press.
- Jenkins, G.M., Box, G.E.P., & Reinsel, G.C. (1994). *Time series analysis: forecasting and control*. Upper Saddle River: Prentice Hall.

- Kadelka, D., & Henze, N. (2000). *Wahrscheinlichkeitstheorie und Statistik für Studierende der Informatik (Skript zur Vorlesung)*.
- National Consortium for the Study of Terrorism and Responses to Terrorism (START). (2011). *Global terrorism database [data file]*. Retrieved 2012-01-20, from <http://www.start.umd.edu/gtd>
- Neuhaus, G., & Kreiß, J.-P. (2006). *Einführung in die Zeitreihenanalyse*. Berlin: Springer.
- Schönherr, M. (2009). *Optimization of trajectory-based risk analyses*. Master Master Thesis, TU Chemnitz.
- Siebold, U. (2007). *Untersuchung statistischer Auswerteverfahren zur Analyse sicherheitsrelevanter Ereignisse*. Diplom, Albert-Ludwigs-Universität Freiburg.
- Siebold, U., Häring, I., & Karwath, A. (2007). Statistical and time series analysis of terror event data for prediction and group spreading behavior (unpublished).
- WEKA Business Media AG. (2012). "Bereits akzeptiert, kaum hinterfragt - Risk Maps als Instrument im Risikocontrolling." Retrieved 2012-01-25, from http://www.weka-finanzen.ch/praxisreport_view.cfm?nr_praxisreport=879

Chapter 5

Event Analysis: Initial Situation and Hazard Source

5.1 Overview

This chapter presents approaches to characterize the initial scenario and to identify types of threat events (threats) which should be considered within risk analysis and management. The challenge is to separate this scenario and event analysis from any further and much more specific analyses.

Typically it is this analysis step in which background information and possible events are missed or mixed resulting in a non-modular and incomplete analysis. Therefore, this chapter stresses the difference between information that is independent of threats and information that characterizes potential threats.

This chapter heavily draws on the empirical-statistical analysis methods introduced in Chap. 4 and this chapter, for instance event type ratio analysis. This chapter shows how the empirical-statistical analysis can be used to generate absolute frequencies of events which are relevant for specific examples of critical infrastructure, e.g. airports or special types of buildings.

It is shown how a subset of an existing rather generic threat event database is extended with further information, in particular to allow for an analysis of likely threat locations. This example also shows that even historic event data for a specific application opens up a rather broad set of possible threat events, all of which have to be considered within a complete risk management process.

This chapter also uses empirical-statistical analysis for the preselection of scenario sets to be dealt with exemplarily with more elaborate methods. This is an example for a typical scenario-based risk analysis and management process which uses classical engineering approaches, see also Chap. 2. Since engineering approaches are time-consuming, a restriction to a manageable representative or parametrized set of scenarios is necessary.

The identification of likely events in urban areas is a further application example presented in this chapter. It is shown how the database example of Chaps. 3 and 4 is applied to identify at different levels of abstraction likely combinations of threats

and objects at risk. Frequency, consequence and risk quantities are defined which are relevant for the assessment in urban contexts. In particular risk maps are developed for urban terroristic threat assessment.

As in the example discussed in the text paragraph before, this is again an example of a rather complete empirical-historical risk assessment using additional data. Again, the context was that only critical risks were further investigated using more elaborate methods. From a risk management process perspective, such a preselection of risks is critical, since formally all risks should be assessed using comparable scales to achieve a complete risk analysis. However, in informed and practical applications it suffices or is often necessary to exclude certain scenarios using rather coarse and conservative assessments.

Finally, this chapter presents an expert-based categorization of possible existing, emerging and new threat events. This example covers most genuinely the idea of pre-event scenario analysis and threat event identification. In its complexity and broadness, it is an example for the need of a variety of risk management and in particular analysis methods for risks.

The probability of event pre-assessment discussed in this chapter, will in parts be taken up again in Chaps. 14–18.

Before analyzing a potentially hazardous event it has to be clearly defined. In many situations, it is not possible to analyze all possible situations and circumstances. Here it is especially important to define appropriate scenarios. Since the quality of the subsequent risk analysis depends heavily on the choice of the scenarios, this step in the risk analysis process is very important. Within the event analysis all credible hazard events have to be considered that are possible given the context framework. The exclusion of hazard events (scenarios) takes place in later steps.

If it is intended that the scenarios are rather well defined or even predetermined, this should be clearly stated within the context of the risk management process.

Section 5.2 relates event analysis to the risk management process steps and gives an idea what it comprises depending on the project.

Sections 5.3–5.6 give four examples of the event analysis in research and development projects at Fraunhofer EMI: airport security, building security, urban security and aviation security, respectively.

In each case, mainly past (terror) event data is used to select the most relevant threat scenarios. In some of the examples, selected scenarios are assessed further by adding additional past event information. Event analysis identifies all scenarios relevant for risk analysis and management for improving resiliency. In particular it allows to focus more elaborate approaches and methods of risk analysis and resilience engineering on an informed selection of scenarios.

The main Fraunhofer EMI sources of this chapter are (Mayrhofer 2010; Ziehm et al. 2010, 2012; Rinder et al. 2011). A further Fraunhofer EMI source is (Leismann and Hasberg 2013). The main authors of the EMI sources are J. Weissbrodt (published under her birth name Ziehm) supplemented with work by O. Herzog, C. Roller, M. Voss, I. Häring, F. K. F. Radtke and T. Leismann, T. Rinder supplemented with work by A. Stolz, K. Fischer and F. Schäfer, and Chr. Mayrhofer supplemented with work by C. Brand, B. Brombacher, A. Dörr, J. Frick, S. Sutter and M. Voss.

5.2 Event Analysis in the Risk Management Process

Taking the context into account and considering the initial situation without threat event, the main purpose of the event analysis is to identify all credible hazard events including chains of events. The purpose of the event analysis is not to reduce the list of possible events from the very beginning.

Means of identification of credible hazard events include expert knowledge, structured brain storming, analysis of historic events, and methods of forecasting.

The term scenario can be used at least in two different ways. First, as a rather detailed description of a potential hazardous event with sufficient information for the risk management process. Second, as a group of similar hazard events in a given setting, e.g. stabbing in urban areas. Throughout the present text we use the first rather specific definition. We may broaden it e.g. by allowing for parameter ranges in given scenarios, e.g. net explosive quantity ranges.

In the risk management process we defined the steps 2 and 3 as follows (see Sect. 2.4):

(2) Initial situation without hazard source: All information needed to apply hazard and damage schemes is being collected. This includes geometrical, geographical, meteorological, and topological data and information about materials and meteorological conditions.

Remark It excludes probabilistic information on distribution of persons and objects. However, the step collects sufficient information to conduct person and object distribution information. In a similar way it excludes hazard propagation data.

(3) Description of the hazard source: The description includes geometry, mass, position, orientation, and velocity of the hazard source as well as mitigation measures close to the hazard source.

The steps of defining and describing the initial situation and the hazard source can take very different amounts of time and effort and depend strongly on the task. Compare the two exemplary tasks:

- (a) A company has a gas tank on its facility. They want to determine the risk for their workers due to possible gas tank explosions, including expected injuries and financial damage for the company.
- (b) A government body wants to analyze the risk of terrorist attacks on bridges and reduce it with appropriate measures if necessary.

Case (a) is comparably simple because the scenario is rather fix. The hazard source and its surroundings are clearly defined. In the two steps of the risk management process necessary data is collected, for example the structural data on the facility in the vicinity of the tank as part of the initial situation analysis, as well as measurements of the tank, the chemical properties of the gas as part of the hazard source description, etc.

Case (b) is more complicated. In Germany there are approximately 120,000 major bridges (Bundesministerium für Verkehr 2013), other countries have comparably high numbers. They vary in location, structure, material, age and many other properties.

The forms of terrorist attacks vary, too. Most attacks on bridges will probably use explosives but even with this assumption, the amount of explosive, the location of the explosive and other parameters are still unclear. In this situation, not every bridge and every possible attack can be analyzed. Here it is important to define appropriate scenarios for the later analysis. This scenario definition can be very complex, depending on the problem.

Already at this stage it should be clearly stated if certain credible events are excluded due to limitations of the further analysis methodology as well as limited overall resources. This should be made explicit as part of the context of the risk management process. The arguments also hold true if we take into account that in further risk analysis/management steps most of the events can be excluded due to their very low consequences, or low risk.

5.3 Event Analysis of Representative Terror Events on Airports

In Sect. 5.2 we defined the scope of the event analysis and gave some information on the expected effort depending on the risk management task. We have seen that the event analysis can vary in its length and complexity. In the following Sects. 5.3–5.5 we will show how event analysis was executed in different sample projects.

Before describing the event analysis, we first give a short idea what the project is about: “The project Airport Security System (acronym FluSs – Flughafen Sicherungssystem) is funded by the BMBF(German Federal Ministry for Education and Research) within the call ‘Protection of transport infrastructure’. The aim of FluSs is to prevent and protect the airport infrastructure from the effects of terroristic attacks using a scenario based and integrated management-system taking into account organizational, personal and technical options to enhance the security for people and infrastructure. Besides the scenario-based approach, the project aim is to increase the basic protection of an airport. An integrated security management system will be proposed as well as a demonstrator containing new and optimized security technologies which will be tested at a major airport.” (Ziehm et al. 2010)

The event analysis is part of the scenario-based approach. The result of the event analysis will be three derived scenarios.

The first step is the database analysis as introduced in Chaps. 3 and 4: “Our work starts by setting up a database on terroristic events on airports to get a broad picture of the general threat situation at airports worldwide and to answer questions like: Which tactics are used? Where do the attacks take place and how often do they occur?” (Ziehm et al. 2010).

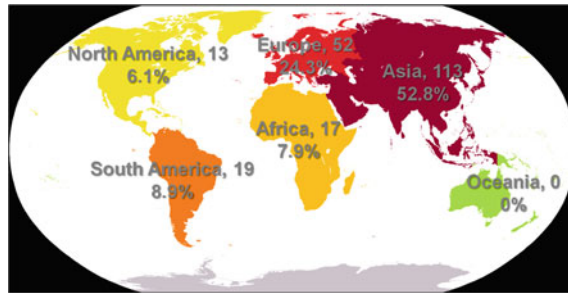


Fig. 5.1 Worldwide distribution of attacks on airports from 1968 to 2007 (Ziehm et al. 2010)

Some results of the database analysis are displayed in Figs. 5.1 and 5.2.

Figure 5.1 shows the worldwide distribution of attacks on airports from 1968 to 2007 by visualizing it on a map. It does not distinguish by countries, only by continents. By adding up the number of attacks that are also displayed in the figure, the total number reads

$$N_{total} = 13 + 19 + 52 + 17 + 113 + 0 = 214. \quad (5.1)$$

Using the total number, the percentages are computed. For example, the fraction of the worldwide attacks that took place in Europe is computed by

$$p_{Europe} = \frac{52}{214} \approx 0.24299 \approx 24.3\%, \quad (5.2)$$

as also shown in the map of Fig. 5.1.

With the information that the numbers relate to the time span from 1968 to 2007 we compute the attacks per year and continent, e.g. the annual attack rate on airports for Europe

$$n_{Europe} = \frac{52}{(2007 - 1968 + 1)a} = \frac{52}{40a} = 1.3 a^{-1}. \quad (5.3)$$

The worldwide annual attack rate reads

$$n_{world} = \frac{214}{(2007 - 1968 + 1)a} = 5.4 a^{-1}. \quad (5.4)$$

Ziehm et al. (2010) summarize: “(Fig. 5.1) shows the continental distribution of historic airport attacks worldwide. Europe is second after Asia hence the threat situation for (German) European airports should not be underestimated. On average there have been five attacks on airports worldwide per year” (Ziehm et al. 2010).

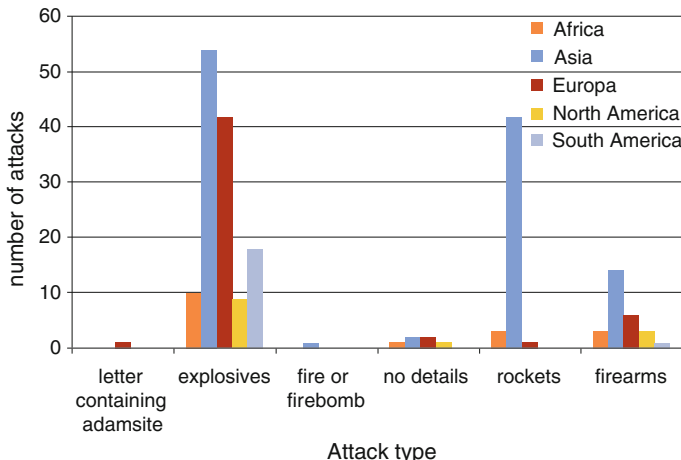


Fig. 5.2 Used attacks from 1968 to 2007 (Ziehm et al. 2010)

The bar chart in Fig. 5.2 shows the different attack types and the number of attacks for each attack type and continent. To get the total number of attacks per type one would have to add the heights of the columns of the different continents for this attack type.

Ziehm et al. (2010) summarize and analyze this as follows: “The weapon type (means of attack) and how often it is used is resolved for continents in (Fig. 5.2). It shows clearly that explosives are the dominant tactic for airports worldwide. The high number of rocket attacks in Asia is due to a high number of attacks on Afghan airports especially since the special situation there after 9/11. Most of the explosive events were carried out by bombs, car or suitcase bombs. This holds true for worldwide as well as for European attacks. The only difference are suicide bombers at airports which did not reach Europe till today” (Ziehm et al. 2010).

For the different attacks, the terrorist event database stores a description of the event. These can be used to analyze the attacks in more detail. In the project, the important question which areas in the airport are the most dangerous was analyzed in this way. The results are shown in Fig. 5.3.

“Figure 5.3 shows an airport scheme with the different attack locations on European airports, basically the same as for worldwide attacks: The terminal is the most affected followed by the different parking areas. Inside the terminal we find that there is almost an equal number of attacks in the controlled and uncontrolled area. This maybe alarming or surprising but one has to consider that we are looking at a dataset of almost 40 years and there have been a lot of changes and improvements to security checks since then. The check-in area inside the terminal is most affected by terrorist attacks supposable because of the crowded place and no security control.” (Ziehm et al. 2010).

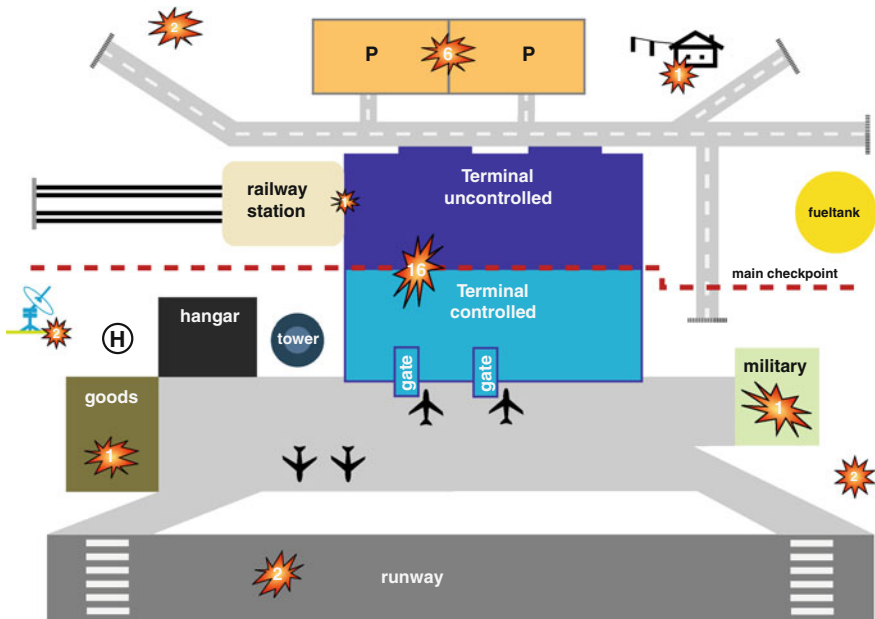


Fig. 5.3 Scheme of attack locations at European airports (1968–2007). For 16 attacks no description of their location is available (Ziehm et al. 2010)

Using the attack types and the locations of the attacks in the database, relevant scenarios were derived:

“Out of the data analysis three main scenarios were deduced:

1. suitcase bomb inside a Terminal (check-in, waiting hall)
2. car bomb in front of a terminal and
3. suicide bomber at a checkpoint” (Ziehm et al. 2010)

This completes the event analysis. The next step in the project was the damage analysis. In this case, each scenario comprises a set of possible events with respect to location and net explosive quantity.

5.4 Hazards and Scenarios for the Numerical Simulation of the Risk of Progressive Collapse of a Building

In the project AURIS (“Autonomes Risiko- und Informationssystem zur Strukturanalyse und Überwachung sicherheitsrelevanter Bauwerke, Autonomous risk and information system for structural analysis and health monitoring of security-relevant buildings”), an innovative building safety management system for the protection of persons in buildings with critical infrastructure is developed and

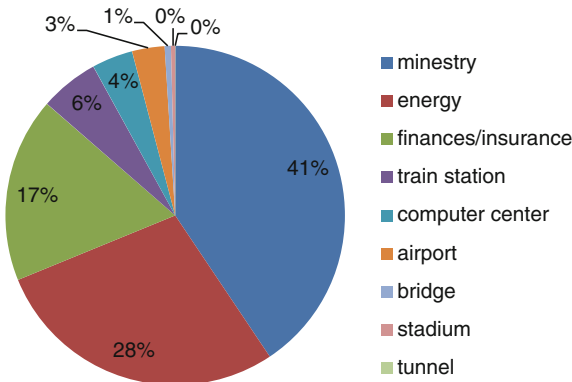


Fig. 5.4 Distribution of attacks by target categories with information from TED (Rinder et al. 2011)

tested (AURIS 2015). For this it was necessary to define a representative damage scenario in the beginning that could be analyzed in the rest of the project.

The event analysis was divided in two parts. The terror event database in the Fraunhofer EMI only contains data on terroristic events. The relevant information was extracted. Additionally, it is possible that non-terroristic events cause progressive collapse. So, as a second field, catastrophic events (collision, fire, earthquake, explosion, flood, overload, extraordinary snow, storm) were analyzed.

This subsection is based on (Rinder et al. 2011). It is a very brief summary of the project results. It does only give an impression of what was considered in the event analysis up to the scenario definition.

For the database analysis, nine target categories were defined: “train station”, “finances and insurance”, “airport”, “ministry”, “computer center”, “stadium”, “bridge”, “energy” and “tunnel”. With these categories the information from the database TED was clustered. Figure 5.4 shows the results of the analysis. To this end, due to the structure of TED, as discussed in Sect. 3.6, for each of the target categories, a list of buildings and structures was defined that belongs to it. For example the target category “finances and insurance” contains banks, stock exchanges, office buildings, post offices and others.

Afterwards, a refinement was done. Instead of regarding all attacks, only structure-damaging attacks were regarded, since those are relevant for the project. For this, the attack types were reduced to explosives and incendiary devices (arson). 74 % of the attacks used explosives, 10 % incendiary devices and 16 % of the attacks did not endanger the structure. The percentages from the pie chart in Fig. 5.4 do not change significantly when only regarding the structure-damaging attacks.

TED does not register the type of building for each attack. Hence, it is not possible to determine the kind of building (e.g. construction, material, size, ...) for

the scenario definition directly from TED. However, it is possible to derive some information from the previous results.

The most endangered target category is ministry (40.6 %), especially for car bombs (80 %). The target category “ministry” has to be considered in the scenario definition and already gives some ideas about the structure of the building.

The second-most endangered category was “energy”. Here it is not distinguished between power plants and office buildings related to this sector. Power plants are due to their dense building structure not very endangered for progressive collapse. Since they are very important for the surrounding population, Rinder et al. (2011) recommend that this should be analyzed in a different project.

The third big category is “finances/insurance”. Computing the average number of injuries and deaths in this category shows that this is also an important category to consider, although the numbers are a lot lower than for the category “ministry”, especially if the attack on the World Trade Center is not considered.

The next step was to find representative building structures for the identified categories. For this, online pictures of typical buildings from the categories “ministry” and “finance/insurance” were searched and analyzed by an expert (structure, used materials, construction, ...).

The last step of the database analysis was a time series (see Fig. 5.5) which shows the increase in the number of attacks in the analyzed time span. The time series can be used to show the need for an improved safety management concept.

As mentioned above, the database TED does not cover all types of events that can cause progressive collapse. So, the second step of the event analysis was an internet research on extraordinary events where buildings were destroyed.

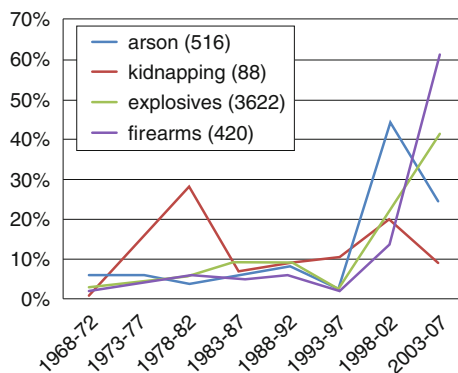


Fig. 5.5 Development of terrorist attacks from 1968 to 2007 for the three target categories “ministry”, “finance/insurance” and “energy” (Rinder et al. 2011). The development is shown in per cent of the total number over the time span. The attack types are listed on the right. The percentage is taken from the total number of attacks on the three target categories. E.g. 100 % corresponding to 3622 events for explosives are obtained by summing up the percentages for the 8 data points representing 5 years, respectively

The medium internet was chosen because encyclopedic and recent literature on this topic was not available. Since there is a lot of wrong information on the internet, some rules were set up, for example:

- (c) the use of information from internet forums was avoided
- (d) Information from small, local newspapers was only used when verified
- (e) Articles on the same topic by different newspapers were compared

The information was stored in a table with predefined categories, that is, a small database was created. In contrary to TED, the newly created database already contained project-specific categories such as the type of building, the building material etc.

The research lead to the definition of 18 typical building types, see Fig. 5.6.

Relevant building types were selected. These were analyzed in terms of cause of collapse (fire, water, wind, earth quake, explosion, ...), number of injuries, construction material, and damaged carrier elements. Several pie charts were created for each of these categories.

The result of the analysis is the definition of two scenarios and one typical building for the rest of the project. It might be surprising that both scenarios are explosive scenarios, one with a big amount of TNT equivalent and one with a smaller amount, since the most frequently occurring destruction was an earthquake. It is explained with the fact that the accelerations in an earthquake are smaller than in an explosion. Hence, a structure analysis system which is developed for countering explosions can also be used for the surveillance of earthquake-endangered buildings. The chosen scenarios can be seen as worst-case estimate and hence make the highest demands, for example on the following tasks in the project.

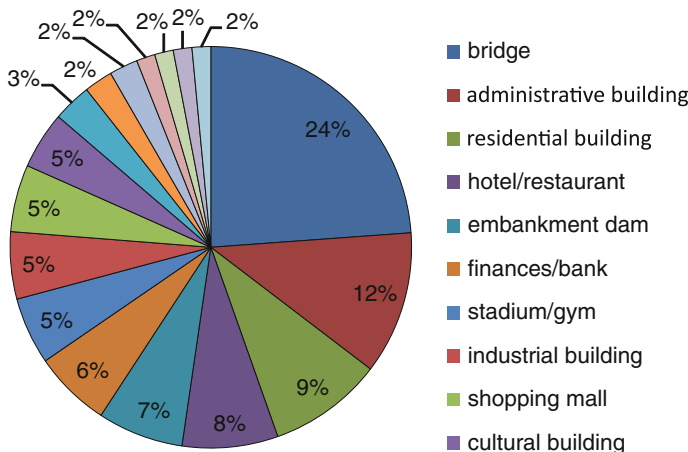


Fig. 5.6 Distribution of 130 researched events with complete or partial collapse by building types (Rinder et al. 2011)

Remark To give an idea of the extent of the analysis and the importance of a detailed event analysis in a project: The total report about the analysis that is summarized here on a couple of pages comprises 60 pages. In many cases, only examples are displayed. Displaying the results of the total event analysis would need many more pages and large Excel sheets.

5.5 Scenario Analysis in the Project “Urban Risk Analysis”

5.5.1 *The Project*

The goal of the project “Urban risk analysis” was to develop a simple tool to display the danger of terroristic events in cities. The project consisted of three parts (Mayrhofer 2010):

- (1) Development of an exemplary 3D-model to display the approximate extent of damage for urban building complexes by single explosions.
- (2) Development of an evaluation system based on the terrorist event database at Fraunhofer EMI to give decision aids to determine endangered (susceptible, exposed) infrastructural buildings.
- (3) Displaying the results of the analysis in a city map to visualize the total situation. Pressure-impulse diagrams are used to determine the destruction of the buildings and the damage is roughly estimated.

With these three steps it should be possible to determine the danger resulting from the existence of certain target systems (e.g. utility services with high media impact) or how the danger changes when these types of buildings are built.

This section summarizes the section scenario analysis in the final report (Mayrhofer 2010) of the project.

The analysis is based on the same definition of risk as we have introduced in Chap. 2. Risk is the product of event frequency and consequences. In the scenario analysis, the risk is estimated using data from the terrorist database and is divided in material and personal risk.

5.5.2 *Fatal Accident Rate*

Apart from the risk as introduced in Sect. 2.2.2, the *Fatal Accident Rate* (FAR), also Fatality Accident Rate, is introduced. In contrary to the usual computation of risk in the unit “per year”, the Fatal Accident Rate is the number of expected fatalities in 100 million operating hours.

Example The following example is taken from (Proske 2008). The annual individual risk of crew members for dying in a plane crash is assumed to be $1.2 \cdot 10^{-3} \text{ a}^{-1}$ and their average flying time to be 1760 h. Hence, the dimensionless Fatal Accident Rate reads

$$FAR = \frac{1.2 \times 10^{-3} \text{ a}^{-1} \cdot a \times 10^8 \text{ h}}{1760 \text{ h}} = 68.2. \quad (5.5)$$

The fatality rate per working (exposure) hour based on the FAR is given by

$$\frac{FAR}{10^8 \text{ h}} = 68.2 \times 10^{-8} \text{ h}^{-1}. \quad (5.6)$$

For comparison: the acceptable FAR for the oil industry is 15. We note that the main difference between the annual accident rate and the FAR is that the FAR only considers the actual exposure time.

5.5.3 Database Analysis

For the project it is important to cluster different types of buildings. This was done in a hierarchical structure with three levels, see Table 5.1.

Diagrams for each level were generated, see Figs. 5.7, 5.8 and 5.9. For the distribution of attacks, it is beneficial to regard also the third level because we obtain the important information that embassies are most endangered only from this chart. The first level chart is so coarse that it does not deliver much information.

Table 5.1 Clustering of different building types in the database (Mayrhofer 2010)

1st level	Government	Industry/economy	Civil
2nd level	Military Politics Security agencies Justice Administration	Finances Retail Travel Insurance Resources Media Manufacture Research Others	Clubs Religion Sports Tourism Catering Culture Social institutions Education Public places Infrastructure Power/water supply Private housing
3rd level	Even more detailed classification than on the 2nd level		

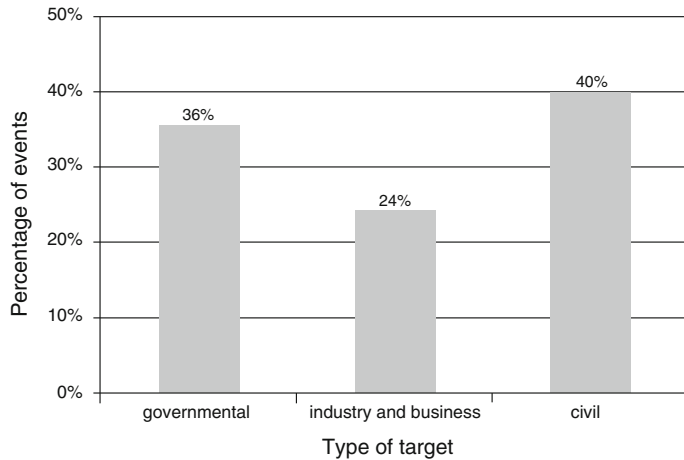


Fig. 5.7 Percentage breakdown of the attacks on the first level of target resolution in per cent. The regarded time period is 1965–2004 (Mayrhofer 2010)

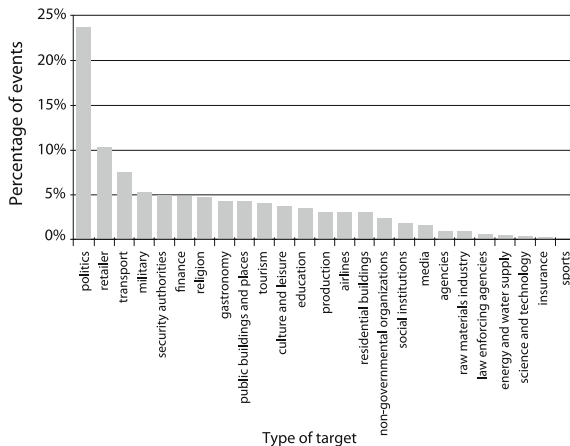


Fig. 5.8 Percentage breakdown of the attacks on the second level of target resolution. The regarded time period is 1965–2004 (Mayrhofer 2010)

For Fig. 5.10 the situation is different. As in Fig. 5.7 only the first level is regarded. This time it is useful because diagrams on higher levels that are additionally divided into time periods would have very many columns. The relatively simple Fig. 5.10 already delivers an important message. Relatively to attacks on all buildings there the number of attack on civil institutions has significantly increased. More than half of the attacks between 2000 and 2004 are against civil institutions.

So far all diagrams referred to the data for worldwide attacks. If a city is analyzed, the user knows the country in which it is located. The question arises

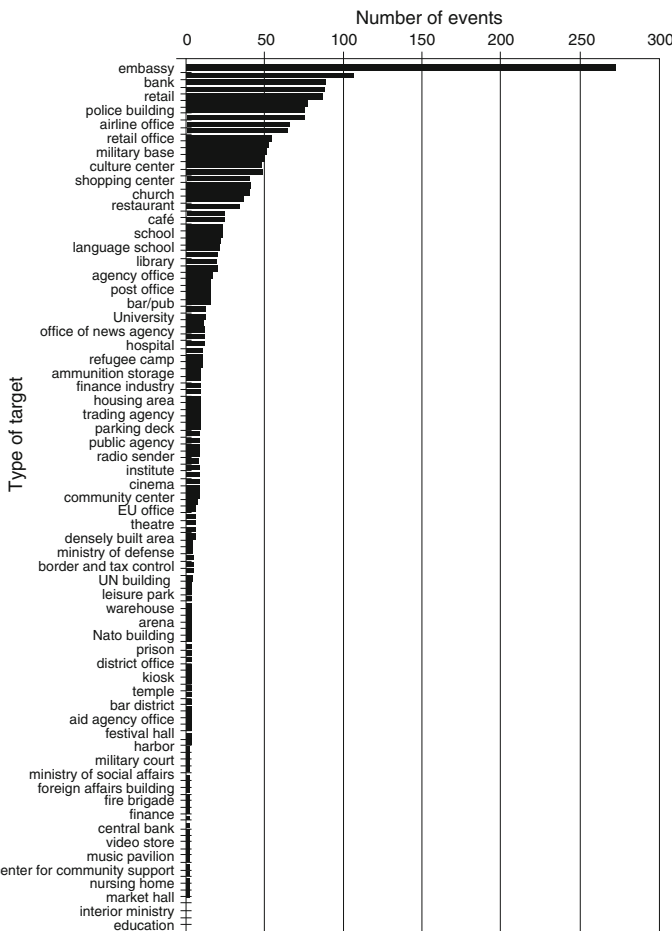


Fig. 5.9 Absolute number of attacks on the third level of target resolution. The regarded time period is 1965–2004 (Mayrhofer 2010)

which database should be used for the analysis. Only considering data from one country leads to a small amount of data. The results of the analysis are strongly influenced by outliers. Considering several countries gives a bigger data base but the different cultural, political, religious, ethical and socio-economical situations in the countries might lead to the use of data that is not relevant for the city/country under consideration. Figure 5.11 shows how the results can vary when choosing data from attacks in Europe or worldwide attacks.

Since there are relevant discrepancies, for example for the areas politics, retail, finances and airlines, both data will be implemented and the user can compare the two results for his defined scenario.

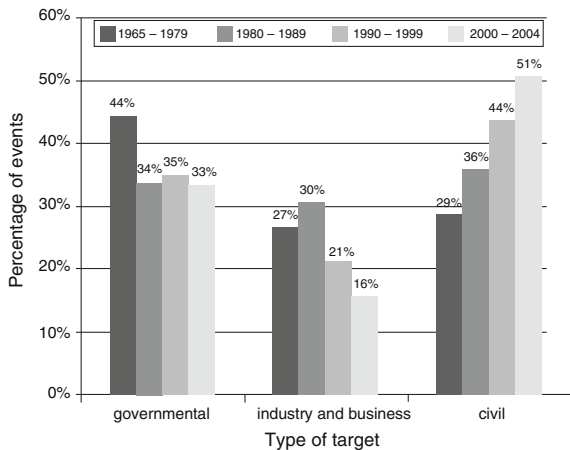


Fig. 5.10 Percentage breakdown of the attacks on the first level of target resolution for different time periods. The regarded time period is 1965–2004 (Mayrhofer 2010)

5.5.4 Event Frequency

The first definition of the event frequency for a type of building or infrastructure (object) being attacked was

$$F = \frac{\text{number of attacks in time interval}}{\text{length of time interval}}, \quad (5.7)$$

which has e.g. the units a^{-1} . The problem with this definition is that it does not consider how many objects exist in that category. If there are 10 attacks on schools and 10 attacks on embassies, they are assigned the same frequency, although there are a lot more schools than embassies. Thinking about a software where frequencies are assigned to buildings on a map, this is not a good definition. Hence, a second definition was introduced:

$$F = \frac{\text{number of attacks}}{(\text{length of time interval})(\text{number of buildings in category})}, \quad (5.8)$$

which again has e.g. the units a^{-1} . This definition is more reasonable. Unfortunately one has to estimate the total number of buildings in the category in Europe or even worldwide. The following estimation was chosen in the project. Berlin as a big city and Lörrach as a small town were chosen as representative cities. For each of the two cities and for each building type, the numbers were determined. This number was extrapolated for the whole world or Europe.

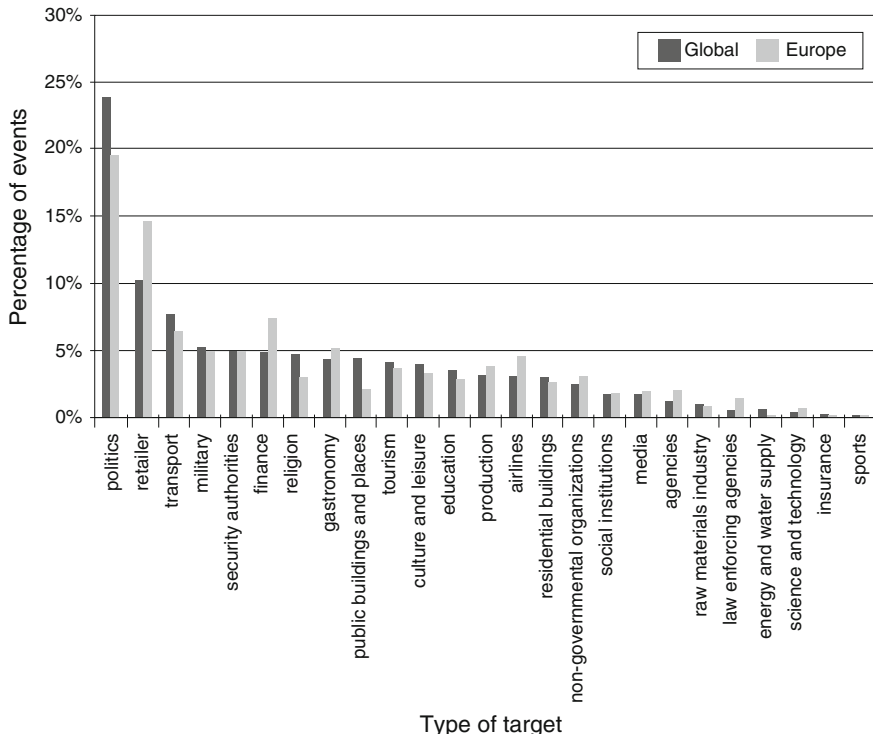


Fig. 5.11 Comparison of percentage breakdown of attacks worldwide for resolution level 2 for target (dark) and in Europe (light). The regarded time period is 1965–2004 (Mayrhofer 2010)

The same was done with the other city and the average of the two numbers was taken as a result.

Example Lörrach has 12 elementary schools and a population of 47,809 people. Berlin has 481 elementary schools and a population of 3,292,365 people. The worldwide urban population is approximately 3.2×10^9 people. With these numbers the estimated number of elementary schools was computed as

$$0.5 \left(\frac{12}{47,809} + \frac{481}{3,292,365} \right) 3.2 \times 10^9 \approx 6.4 \times 10^5. \quad (5.9)$$

The data used in this example is from (Bundeszentrale für politische Bildung 2008; Stadt Berlin 2013; Stadt Lörrach 2013; Zensusdatenbank 2013). The same data is available for all German towns.

We note that the presented type of numbering does not take into account that certain schools have e.g. a much higher symbolic value or are visited by a certain ethical group and might therefore be more susceptible. Such effects can be

considered with scenario specific scaling factors. In this sense (5.7) would be a basic attack frequency rate. The main advantage of expressions like (5.7) is that they can be determined rather objective before adding rather subjective information like symbolic values.

5.5.5 Extent of Damage

The extent of damage depends on the amount of explosive that is used. Since this amount is not known at this point of the analysis, the worst case is assumed where the building is completely destroyed and has to be rebuilt. Different literature was used to collect cost estimates of rebuilding a building. The information was sorted by three types of buildings and averages were computed. The categories were “low” (e.g. barn, garage), “medium” (e.g. private house, store), and “high” (e.g. theater, hospital). For each category the costs are given in euros per square meter.

The danger for persons was estimated in two ways:

- (1) The database was used to compute the average number of injured and dead persons per attack for each of the building categories.
- (2) The user of the software is able to define the number of persons in the building. The computation of the consequences of the attack assumes the worst case that nobody in the building survives the attack.

5.5.6 Risk Map

The event frequencies from Sect. 5.3.3.4 and the consequences from Sect. 5.3.3.5 can be used to compute risks. Since three different definitions of consequences were made, there are also three risks:

- (1) damage in euros per year and building
- (2) fatalities per year and building (based on statistics)
- (3) endangered persons per year and building (depending on the number of persons the user defined)

The risks can be displayed in risk maps, as introduced in Sect. 4.4. Without further information than already determined in this section, it is possible to create a diagram as in Fig. 4.13.

A more meaningful diagram can be created when including F-N-graphs. For F-N-graphs it is necessary to have risks criteria, that is, risks of which it is known that they are seen as small, medium or high. The risks defined here are very problem-specific and relevant criteria could not be found in the literature. The following solution was used: A model town was created in the software. For this, approximately 1,000 buildings were defined and data from the database for events

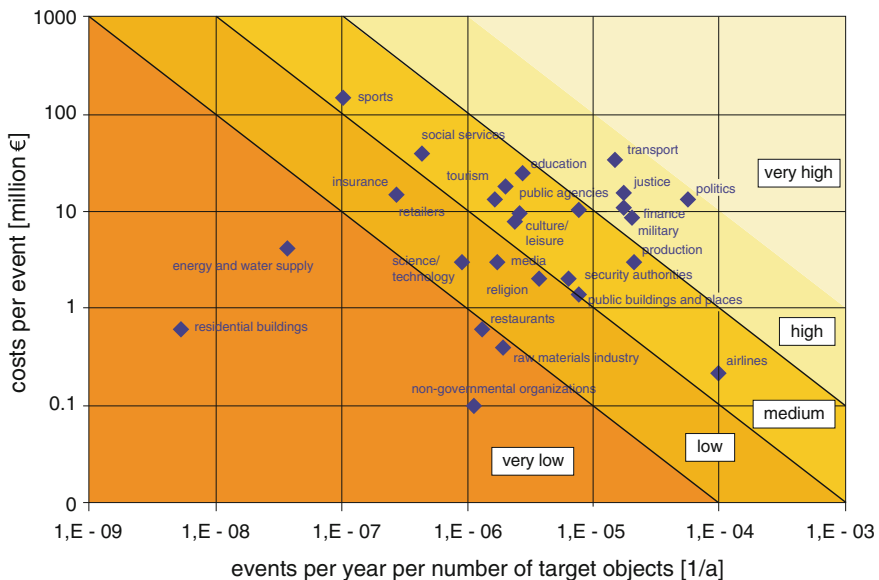


Fig. 5.12 Risk map for building damage. The regarded time period is 1965–2004. The x-axis shows “Event/year/building in the category in Europe”, the y-axis “Million Euros/event” (Mayrhofer 2010)

in this town was entered. The results from the risk computation was used to define the boundaries for “very low”, “low”, “medium”, “high” and “very high” risks. Since everything is based on the model town, the risk classification can never be seen as absolute but only relative to the risks of the model town.

Figure 5.12 shows an exemplary risk map. The risks are computed for structural damage measured in terms of rebuilding costs of the total building for all terror event types with data taken from Europe. The categories “very low”, “low”, etc. are based on the model town.

5.5.7 Summary

Last we want to state how Mayrhofer (2010) summarized his scenario analysis:

“The goal of the appraisal procedure consisted of determining in any city the critical infrastructure. For each building a risk could be computed according to the different use of buildings, the value of a building and the number of persons concerned. The [TED] database of the Ernst-Mach-Institut was categorized, so that for each category from this data base a value in each category was available for the event frequency of attacks on buildings and fatalities per event. The value of a building is calculated by its surface area, floor number and an averaged gross floor area price. Thus a risk can be calculated for each building, regarding the value of

the building, fatalities per event and the maximum damage of all persons concerned. In the program these risks are assigned to a color and the users get demonstrated visually the critical infrastructure. If the user knows, which the threatened buildings are, he could define a scenario and could recognize by the vulnerability and damage analysis the effect of a possible event.

With the Scenario Analysis it is possible to determine from the multiplicity of the infrastructural structures those necessary for the supply of the population which are classified particularly critical due to the events in the past” (Mayrhofer 2010).

5.6 Analysis of Future Threats to Civil Aviation

After 9/11 security measures and regulations for aviation have been steadily increased. At the same time the number of air passengers and flights are expected to double within the next 15 years (Ziehm et al. 2012). “The current security system is close to its limits and cannot be adapted to the future challenges in a cost effective and sufficient way to overcome the continuous increase of terror attacks on the air transport system” (Ziehm et al. 2012), see Fig. 5.13.

“To start a way towards interchanging this purely reactive paradigm by a comprehensive approach the project COPRA aims to devise a research roadmap” (Ziehm et al. 2012). The roadmap shows “drivers and trends in future aviation [,] recommendations and goals for future aviation security concepts [and] recommendations on future research and development” (Leismann and Hasberg 2013).

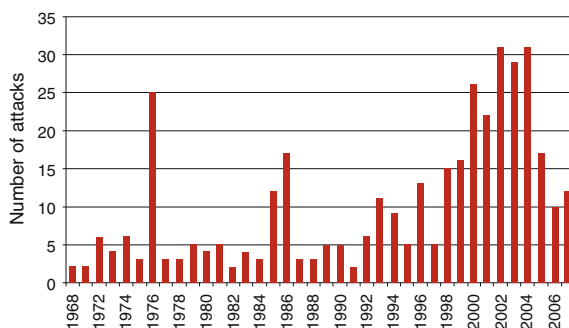


Fig. 5.13 Number of terrorist attacks on airports, worldwide by year, created with TED (Ziehm et al. 2012)

5.6.1 Categorization of Present and Future Threats

The target levels were divided into three categories (Ziehm et al. 2012):

- Aircrafts
- Airport infrastructure
- Auxiliary infrastructure

Threats were divided into (Ziehm et al. 2012):

- Known threats
- Emerging threats
- New threats

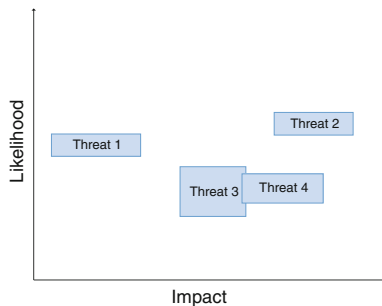
Using a questionnaire among the project partners, 70 threats were collected. The questionnaire also regarded “the destructive impact potential, costs of a threat technology, the availability and the timeframe of availability” (Ziehm et al. 2012).

5.6.2 Prioritization of the Threats

With the information from the questionnaire, threats were prioritized by likelihood (considering cost of threat technology, availability, timeframe of availability) and impact (direct and indirect destructive impact potential), each on a scale from 1 to 5 (Ziehm et al. 2012). The result was displayed in graphs as Fig. 5.14.

The threats were not compared to each other. That is, neither prioritization numbers were assigned nor were criteria lines as in Fig. 5.12 added to the graph of Fig. 5.14. The idea behind it was that “a misleading focus in the following WPs should be avoided” (Ziehm et al. 2012).

Fig. 5.14 Graphical presentation of likelihood and impact of different threats (Ziehm et al. 2012)



Remark The prioritization can be seen as part of the steps “hazard analysis” and “damage analysis” in the risk management process. It is included here to give a broader view on the example.

Remark More information on the project and the roadmap can be found under www.copra-project.eu.

5.7 Summary and Outlook

In this chapter we have seen that the definition of the possible hazard scenarios (hazard/threat events) is important for the following risk analysis and has to be done with care, especially for complex or very general situations.

We discussed four exemplary scenario definitions. In the first case, a database was used to determine the most common forms of terrorist events for the given conditions and three typical scenarios were derived for airports.

In the second example, the database did not contain sufficient data to be the only basis for the scenario definition because for the listed events it did not contain enough details about the buildings and because natural catastrophes were not listed in the database. Therefore, the scenario definition was additionally based on internet research.

The third example also used a database. Here, the scenarios to be analyzed in later parts of the projects were not derived from which scenarios occurred most often but which have the highest risks. This is a different focus than for the two previous examples.

The fourth example shows how scenarios were derived in expert workshops instead of using a database.

Remark The examples in this chapter can also be regarded as empirical frequency and damage analysis. In this sense they could also be assigned to later phases of the risk analysis process.

The next step in the risk analysis process is the hazard analysis. In this context the following chapter treats hazard propagation for explosions.

5.8 Questions

- (1) Find two situations where you would do a risk analysis and explain what you would do in the event analysis.
- (2) How would the scenario analysis in the example situation (b) change if the government wanted to analyze the risk for the Hohenzollernbrücke in Cologne instead of the general risk for bridges. How strongly would the analysis be

influenced by choosing the Deutzer Brücke (bridge for cars) instead of the Hohenzollernbrücke (bridge for trains)?

- (3) Can you confirm the results from Fig. 5.1 with GTD? What are the problems?

5.9 Answers

- (1) Open question
- (2) The structure and material could be analyzed. This depends on the chosen bridge. One is for trains, one for cars. A car bomb would not be possible on the Hohenzollernbrücke, the cathedral is closer to the Hohenzollernbrücke, there are more tourists,...
- (3) Setting “Regardless of doubt”:

North America + Middle Am.	65 + 80	13.2 %
South America	125	11.4 %
North Africa + Middle East	275	25 %
Asia	201	18.3 %
Europe	344	31.4 %
Oceania	6	0.5 %
Total	1096	99.8 %

Problem “Regions” don’t completely match the continents, especially the Middle East is a problem. For the other regions the results are not very similar either. Also, GTD has 5 times as many entries from 1970 to 2007 as TED and many where nobody got hurt.

References

- AURIS. (2015). BMBF project. Retrieved November 9, 2015, from <http://auris-innovation.org/index.php?english>
- Bundeszentrale für politische Bildung. (2008). Städtische Bevölkerung. Retrieved July 24, 2013, from <http://www.bpb.de/gesellschaft/staedte/megastaedte/64736/staedtische-bevoelkerung>
- Bundesministerium für Verkehr, Bau- und Wohnungswesen. (2013). Zahl und Wert der Straßenbrücken in Deutschland. Retrieved July 25, 2013, from <http://www.deutsche-bruecken.de;brueckenbau/>
- Leismann, T., & Hasberg, M. -P. (2013). COPRA aviation security research roadmap (flyer). from www.copra-project.eu

- Mayrhofer, C. (2010). Städtebauliche Gefährdungsanalyse - Abschlussbericht Fraunhofer Institut für Kurzzeitdynamik, Ernst-Mach-Institut, EMI, Bundesamt für Bevölkerungsschutz und Katastrophenhilfe, http://www.emi.fraunhofer.de/fileadmin/media/emi/geschaeftsfelder/Sicherheit/Downloads/FiB_7_Webdatei_101011.pdf
- Proske, D. (2008). *Catalogue of Risks—Natural, Technical, Social and Health Risks*. Berlin, Heidelberg: Springer.
- Rinder, T., Stoltz, A., & Fischer, K. (2011). Bedrohungsanalyse und Szenariodefinition für die rechnerische Simulation des Risikos eines progressiven Gebäudekollapses, Fraunhofer EMI. E 58/11.
- Stadt Berlin. (2013). Berlin. Retrieved July 24, 2013, from <http://www.berlin.de/>
- Stadt Lörrach. (2013). Lörrach. Retrieved July 24, 2013, from <http://www.loerrach.de/>
- Zensusdatenbank. (2013). Zensus 2011. Retrieved July 24, 2013, from <https://ergebnisse.zensus2011.de/#>
- Ziehm, J., Herzog, O., Roller, C., Voss, M., & Häring, I. (2010). Risk analysis of representative terror events on airports within the project FluSs. In *5th Security Research Conference*. Berlin: Fraunhofer Group for Defense and Security.
- Ziehm, J., Radtke, F. K. F., & Leismann, T. (2012). *Analysis of Future Threats to Civil Aviation within the Project COPRA (Comprehensive European Approach to the Protection of Civil Aviation)*. Future Security. Bonn, Germany: Springer.

Chapter 6

Hazard Propagation I: Explosions and Blast

6.1 Overview

This chapter gives a broad overview of the hazard source definition and the hazard potential propagation in case of explosions, in particular detonations. This is a sample hazard type, which is also used *inter alia* in Chaps. 7–18 for illustration of further steps of risk management and analysis.

This chapter shows that even to understand the hazard potential of a single type of threat, a multitude of effects have to be understood for sufficient analysis. It also motivates that even for the sample case explosion only a subset of hazards is used for further illustration. This chapter lists and describes these hazards and focuses on blast (shock wave in air).

The classical categorization of explosions by Baker et al. (1983) is a little extended allowing for malicious (terroristic) explosions, e.g. car bombs. Such events are defined with respect to existing categories of explosions. They are the only type of events which are further discussed in case of explosions.

The explosive type of hazard allows for an initial localization of the hazard source, as in the case of the dispersion of chemicals or biological agents. In particular, natural and technogenic hazards often lack such a straightforward distinction between source and propagation.

For instance, even if earthquakes generate a loading of buildings a little similar to the ground shock loading due to explosions, it is much more difficult to locate the origin of the hazard potential (field). Similar arguments hold true, for instance for strong wind (blast wind) or hail impact. Therefore this chapter distinguishes between the description of the hazard source and the hazard (potential, field) due to the hazard propagation in case of a threat event.

A schematic overview is given which hazards are generated by explosions and how they propagate. Only fragments, debris and fire ball will be further considered in Chaps. 7–12.

For high explosions (detonations), the hazard propagation of blast (shock wave in air) is described for the near and far field. In particular, the parameters are given that describe the hazard potential for most applications: specific blast impulse and overpressure. In a similar way, for other applications local hazard fields can be described.

A deep understanding of the physics of hazard propagation allowed to formulate scaling laws for explosions. Their importance is that they can be used to scale experimental tests for scenario assessment and when carefully employed also for validation of computational approaches. The main reason they are presented in the present text is that they are key for understanding the parameterization of the blast hazard in Chaps. 7 and 8.

A further very illustrative exercise is to exemplarily model the damage effects due to the blast hazard potential using a very simplified single degree of freedom model. It shows that the response of structures due to blast loading is rather different when compared to the empirically much more accessible static loading of structures. This opens up a window to the Chaps. 10–12 on damage assessment.

Understanding and characterizing hazard sources and hazard propagation is important for the prevention, protection, response and recovery in case of events. Examples include the detection of hazard sources, the assessment of the physical hazard potential, the damage assessment, the post event scenario assessment for optimal response and finally the fast recovery based on a through damage and consequence assessment, e.g. reusing parts of the foundations of a construction. Resilience engineering efforts based on the respective knowledge and modelling typically focuses on prevention and protection. It can also be used to improve response and recovery in case of events.

In the risk analysis scheme, Step 4 is described as

- (2) **Hazard propagation/hazard analysis:** This includes the potential dispersion, distribution, and impact load distribution of the physical hazard.

In the case of explosive events, the physical properties of explosions are analyzed. This is done for explosive events in this chapter and Chaps. 7 and 8. This chapter gives an overview of the hazard potential and gives some details for free field blast loading of point sources. Chapter 7 covers point fragment sources. Chapter 8 indicates how to determine complex blast propagation.

In Sect. 6.2 and 6.3 explosions are categorized verbally by selected properties, which are relevant for risk management. Different types of explosions are listed; in particular we define terroristic explosions. It also gives an overview of typical physical consequences of explosions.

In Sect. 6.4–6.8 blast waves of point sources are described with some more formal rigor. We define high explosions and distinguish them from other explosions. We introduce the characteristic pressure-time loading histories after the built-up of the blast wave. We distinguish between different asymptotic loading types of structures due to blast waves. This provides a link to engineering assessment of structural response.

This chapter summarizes parts of Chap. 2 of (Baker et al. 1983). Fraunhofer EMI sources are (Klomfass and Thoma 1997a, b; Dörr and Rübarsch 2005; Häring et al. 2005; Döge and Häring 2006; Fischer and Häring 2009).

6.2 Characterization of Explosions

Explosions can be characterized by different criteria (properties, characteristics). Examples are given in the following subsections. Most of the properties are used for defining the term terroristic (malevolent) explosion in Sect. 6.2.5.

6.2.1 Natural Versus Man-Made

We focus only on explosions occurring in man-made settings. Examples for natural explosions are (Baker et al. 1983, p. 84, Table 2.1)

- lightning,
- volcanic eruptions, and
- meteor impact.

6.2.2 Surrounding Media and Explosive Material

Explosions may occur

- in air (atmospheric explosions)
- in water (underwater explosions), or
- in the earth (underground explosions).

In case of chemical energy release, explosive materials can be solid, liquid or gaseous. Other examples of energy generation are listed in Table 6.1.

We will focus on chemical explosions in air of solid materials.

6.2.3 Intentional Explosions

Intentional explosions or malicious explosions may occur in an industrial or in a military context. Intentional, controlled (tamed) explosions are modern technological achievements.

Table 6.1 Type of energy release of explosive source and theoretical models describing the sources. Explosion types (Baker et al. 1983, p. 107, Table 2.1). Copyright 1983. With permission from Elsevier

Theoretical models	Natural explosions	Intentional explosions	Accidental explosions
Ideal point source:	Lightning	Nuclear weapon explosions	Condensed phase explosions: • Light or no confinement
• Ideal gas	Volcanoes	Condensed phase high explosives:	• Heavy confinement
• Real gas	Meteors		Combustion explosions in enclosures (no prepressure):
Self-similar (infinite source energy)		• Blasting • Military	• Gases and vapors
Bursting sphere		Pyrotechnic separators	• Dusts
Ramp addition (spark)		Vapor phase high explosives (FAE)	Pressure vessels (gaseous contents):
Piston:		Gun powders/propellants:	• Simple failure (inert contents)
• Constant velocity		• Muzzle blast	• Combustion generated failure
• Accelerating		• Recoilless rifle blast	• Failure followed by immediate combustion
• Finite stroke		Exploding spark	• Runaway chemical reaction before failure
Reaction wave:		Exploding wires	• Runaway nuclear reaction before failure
• Deflagration		Laser sparks	
• Detonation		Contained explosions ^a	BLEVE's (Boiling Liquid Expanding Vapor Explosion) (pressure vessel containing a flash-evaporating liquid):
• Accelerating waves			• External heating
• Implosion			– Immediate combustion after release
			– No combustion after release
			• Runaway chemical reaction
			– Immediate combustion after release
			– No combustion after release
			Unconfined vapor cloud explosions Physical vapor explosions

^aContained vessel explosions such as those used in gas and dust explosion engine cylinders are examples

Examples of tamed explosions include [see also (Baker et al. 1983, p. 1)]

- internal combustion engine,
- explosive forming of metal,
- explosive welding of metal,

- separation of stages of launch vehicles (squips),
- cutting of cables and bolts,
- airbag,
- manufacture of industrial diamonds, and
- avalanche blasting.

Examples in the area of mining, earthwork and construction [see also (Baker et al. 1983, p. 1)] are

- blasting in stone quarries,
- earthmoving,
- controlled cratering,
- demolition of buildings and
- drilling.

6.2.4 Accidental Explosions

Accidental explosions may cause unplanned destruction, injuries and death.

Typical industries where accidental explosions occur (see also (Klomfass and Thoma 1997a) and (Baker et al. 1983, pp. 1–2)):

- Manufacture, transportation and storage of explosives
- (Petro) chemical industry
- Sawmills
- Flour mills
- Manufacture of liquefied petroleum gas (LPG)

Typical components that explode due to (process) failure are [see also (Baker et al. 1983, pp. 1–2)]:

- High pressure vessels
- Boilers

Processes that may fail due to explosions include [see also (Baker, Cox, Westine, Kulesz and Strehlow 1983, pp. 1–2)]:

- Molten metal contacting water in foundries
- Fuel gas leakage in buildings
- Manufacture, transport and storage of high vapor pressure or cryogenic fuels
- Cleaning of liquid fuel tanks in tanker vessels
- Manufacture, transport and storage of combustible dusts.

6.2.5 Terroristic Explosions

Terroristic or malicious (malevolent) explosions can be defined as intended explosions that are conducted to harm objects or persons.

From a descriptive point of view terroristic explosions are typically man-made controlled explosions. The intention of an actor cannot be determined with certainty. However, terroristic explosions are in most cases less optimized. They are often improvised. Typically they are conducted in air with solid explosive material.

Terroristic explosions can be very effective, if they are conducted in an environment that allows in addition for accidental explosions, e.g. a car bomb close to a fuel vessel.

Examples for explosive sources or types of bombs are:

- Improvised explosive device (IED),
- Vehicle born IED (VBIED): motorcycle bomb, car bomb, truck bomb,
- Building bomb,
- Suitcase bomb,
- Suicide bomb: any of the sources can be placed by a suicide actor, e.g. suicide car bomb,
- Explosively formed or shaped IED, also termed super bomb.

6.3 Overview of Physical Consequences and Damage Due to Explosions

Physical consequences and damage of explosions include [see also (Baker et al. 1983, p. 2)], see Fig. 6.4 for illustration:

- ground shock
- crater formation
- debris or missile throw generated from earth or covering structures
- fragment throw generated from casing of explosive or material within explosive
- blast for free-field, confined and contained explosions
- fire ball: heat radiation and heat convection
- structural loading caused by blast waves
- impact loading caused by fragments
- far-field blast hazard, e.g. effects from atmospherically reflected or wind-enhanced blast waves

Figure 6.1 gives a top aerial view for the propagation of hazards in case of car bombs as observed in experiments (Technical test center WTD 91 2014).

Figure 6.2 shows the fireball, first fragments and indirectly also the blast expansion (Technical test center WTD 91 2014).



Fig. 6.1 Top view of an explosive test site after 3 explosive test events, taken with an aerial drone. Visible are the crater in the center, crater throw (ejections) and some of the large fragments of the car (direction 01:00 and 07:00). A close look reveals radial marking lines, which are used to locate fragments and debris within 5° sectors. The farthest thrown visible fragment is a turquoise colored engine hood (direction 07:30), ca. 100 m away from the explosion site. Source: Technical test center WTD 91 (Technical test center WTD 91 2014)



Fig. 6.2 Fireball, fragments and effects of blast expansion in case of car bomb explosion of 100 kg PETN ignited on the floor between front seat and rear bench. The sudden pressure rise generates the condensation disc on the ground. Diameter of fireball: ca. 10 m, time after ignition: 37 ms. Minor first fragments are visible in the left half of the picture (Technical test center WTD 91 2014)



Fig. 6.3 Fragment launch distribution snapshot after a free field car bomb explosion, 1.1 s after the ignition. Besides the detonation products, dust of the sandy ground is visible over ground zero. The air is filled with thousands of larger and smaller fragments on all types of trajectories: from flat to very steep flight paths. Some characteristic fragments can be identified in videos, respectively on the picture. As an example, the two front shock absorbers with wheels attached are marked with red circles on their flat flight paths. In the corresponding video they first bounce to the ground, before, bouncing and rolling, they leave the visible area of the camera (Technical test center WTD 91 2013)

Fig. 6.4 Overview of selected consequences of explosions (Dörr and Rübarsch 2005)

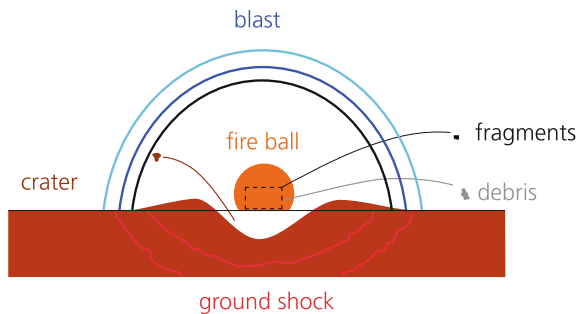


Figure 6.3 shows crater dust ejections, detonation products and fragment throw, in particular of large fragments (Technical test center WTD 91 2013) (Fig. 6.4).

Remarks

- Fragment is the general term that will be used throughout for debris and metal fragments.
- Fragment launch velocities and trajectories can be very inhomogeneous.
- Blast propagation is very unpredictable for non-standard geometries due to venting and confining effects.

6.4 Explosions in Air and Their Characteristics: Physical Consequences

6.4.1 General Definition of Explosion

Strehlow and Baker (1976) define explosions as follows:

"In general, an explosion is said to have occurred in the atmosphere if energy is released over a sufficiently small time and a sufficiently small volume so as to generate a pressure wave of finite amplitude travelling away from the source. This energy may have originally been stored in the system in a variety of forms; these include nuclear, chemical, electrical or pressure energy, for example. However, the release is not considered to be explosive unless it is rapid enough and concentrated enough to produce a pressure wave that one can hear.

Even though many explosions damage their surroundings, it is not necessary that external damage be produced by an explosion. All that is necessary is that the explosion is capable of being heard". (Baker et al. 1983)

The definition of Strehlow and Baker is general and phenomenological enough to comprise all types of explosions which are also termed explosions in colloquial language.

In the following paragraphs we collect some more (parts of) definitions of explosives as well as parts of them. "Explosives may be divided into two categories, high and low. In the former the explosives detonate, in the latter they deflagrate. The difference, according to this classification, lies in that in detonating explosives, such as TNT, the mechanism is based on creating mechanical shock, whereas in deflagrating explosives, the mechanism is thermal in nature" (Astaneh-Asl et al. 2003). An explosion, generally speaking, is an amount of energy released in a very short period of time or the rapid conversion of a solid into a gas with high temperature (Health and Safety Executive 2002). This explosion occurs as a consequence of a chemical reaction.

The last two definitions address that high explosives generate a shock front during the explosion which typically coincides with the transformation of the explosive material to the gaseous phase and the generation of high pressure and temperature. In case of deflagration or fast burning no shock front builds up or if it builds up, it moves not in the order of several thousand meters per second. (Assael and Kakosimos 2010)

The distinction between explosives and propellant from (Rosales 2004) is described also in (Klomfass and Thoma 1997b).

Explosives are materials which have the ability to explode. One further distinguishes between pure explosives and explosive mixtures. The mixtures can be composed of different pure explosives or of explosives and supplements. (Klomfass and Thoma 1997b).

High explosives can cause detonations, which propagate at supersonic speed through a shock wave, which causes a nearly discontinuous change of flow speed, pressure, density and temperature.

Propellants, colloquially also called powder, are materials where the release of chemical energy is detonative but with a smaller detonation speed or through combustion. They are for example used in the automotive industry to quickly fill airbags (Klomfass and Thoma 1997b).

“These definitions are highly conventional, but they are not absolute and enclose some degree of overlapping, and the limits are not as clear as we probably would want. This means that given several conditions of pressure and temperature, a propellant can explode, so it would behave as an explosive even though it is not.” (Rosales 2004)

In the following only chemical detonations are regarded where a fast chemical reaction triggered by a detonation shock front generates the gaseous reaction products.

Explosive atmospheres, pent-up gas and thermonuclear explosions are not regarded.

6.4.2 Ideal Explosions, Point Source

According to the first definition of Sect. 6.4.1 and aiming at the characterization of the explosive source, for example in terms of strength and duration of the explosion, the following quantities are of interest (Baker, Cox, Westine, Kulesz and Strehlow 1983):

- total energy release E of the explosive,
- energy density E/V , where V is the volume of the explosive,
- (average) time rate of energy release (power), $E/\Delta t$, where Δt is the average time of the energy release.

In a distance sufficiently far away from the region where complete destruction is expected and a sufficiently large energy density and sufficiently large time rate of energy release, ideal explosions are only characterized by the total energy release. This finding may also be used for defining ideal explosions.

In the case of solid or liquid high explosives and a sufficiently large total energy release the total energy release is proportional to the volume and hence also mass of the high explosive. In this case it is sufficient to give the TNT equivalent to characterize an ideal high explosive point source.

The TNT equivalent shows which mass of TNT would be necessary to create a blast wave with similar energy. It is influenced by (Klomfass and Thoma 1997b)

- the type of explosive: equivalent mass,
- the geometry of explosive: shape factor and
- the casing of explosive: casing factor.

6.5 Build-up of Blast Wave from Point Source

The following steps may be distinguished:

- Detonation of the high explosive and generation of explosive products
- Very high pressures (order of magnitude 300 kbar = 300,000 bar = 30,000 MPa) localized within the characteristic length scale of the explosive, e.g. radius of sphere, see Fig. 6.5 (Klomfass and Thoma 1997a, pp. 2–3).
- Build-up of shock wave with much less pressures (order of magnitude 1000 kPa = 10,000 hPa = 10 bar), see Fig. 6.6 (Klomfass and Thoma 1997a, pp. 2–3).
- Separation of blast wave from explosive products, see Fig. 6.7.
- Build-up of stable blast wave with dominating first overpressure phase.
- N-like blast wave: overpressure and underpressure phase are of the same order of magnitude. “An ‘N’ wave has a time history somewhat like the letter N. There are two equal shocks, with linear decay from overpressure P_S^+ to

Fig. 6.5 Near-field pressure-distance curve (Klomfass and Thoma 1997a, p. 2, Fig. 1.1)

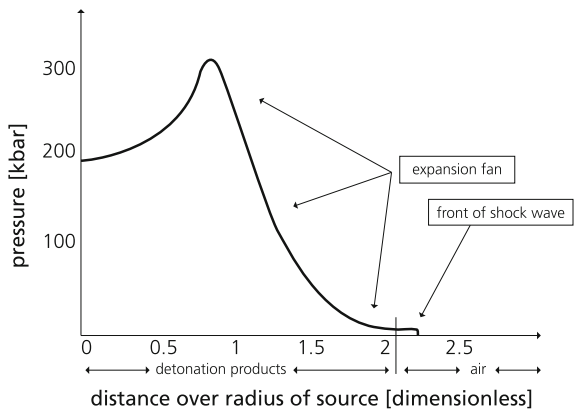


Fig. 6.6 Far-field pressure-distance curve (Klomfass and Thoma 1997a, p. 3, Fig. 1.2)

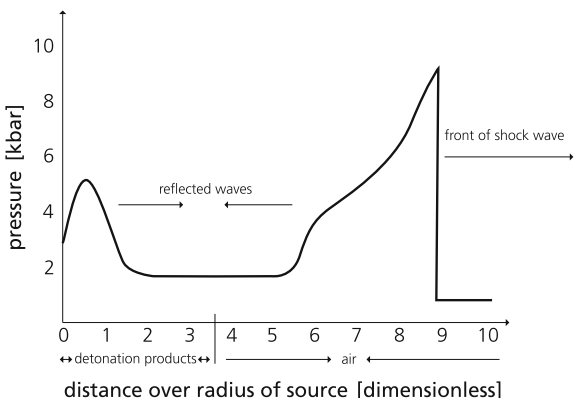
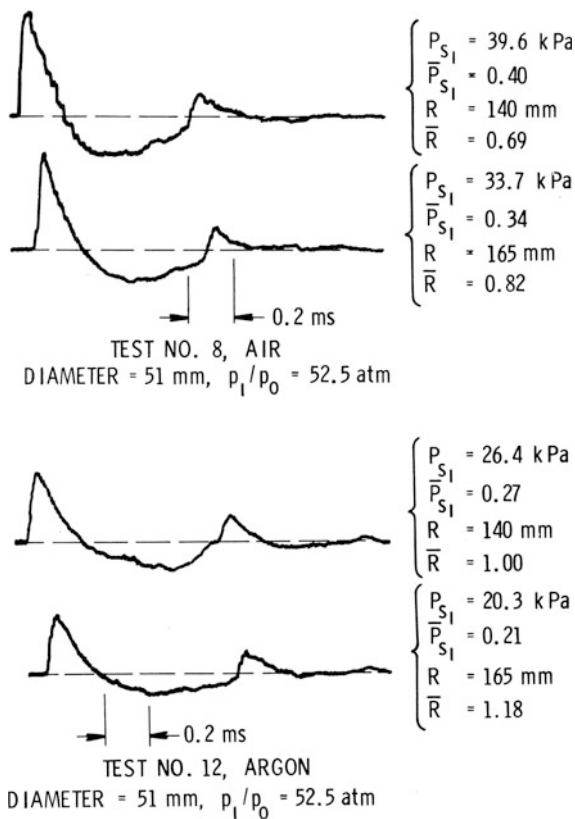




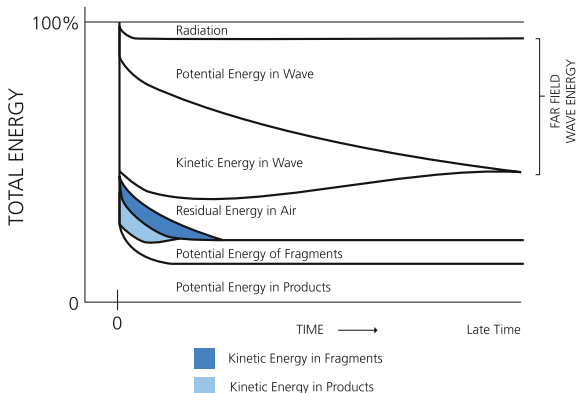
Fig. 6.7 Separation of blast wave from detonation products for ground burst. Picture likely to be taken during ESKIMO test series, see (Weals 1973) for ESKIMO I test series

Fig. 6.8 Examples of pressure-time histories produced by the burst of a frangible glass sphere containing high pressure air or argon (Baker et al. 1983, p. 136, Fig. 2.11). Copyright 1983. With permission from Elsevier



underpressure P_S^- " (Baker et al. 1983). "In the far field region there is theoretical evidence that an 'N' wave must always form and that the blast wave structure in the positive impulse phase is unaffected by the interior flow and is self-sustaining" (Baker et al. 1983) (Fig. 6.8)

Fig. 6.9 Energy distribution in a blast wave as a function of time after the explosion (Strehlow and Baker 1976; Baker et al. 1983). Copyright 1983. With permission from Elsevier



- Non-linear acoustic wave.
- Acoustic wave.

A heuristic energy distribution with respect to time is described in Fig. 6.9, see also Fig. 6.4. Radiation covers heat radiation. The potential energy of the wave covers the compression and tensile energy of the longitudinal shock wave. The kinetic energy covers the energy stored in the particle motion of the shock wave. The residual energy covers energy bound in air, i.e. mainly thermal movement. The potential energy of the fragments and the detonation products is reflected in their gain of height relative to earth's surface.

6.6 Blast Hazard Characterization: Pressure-Time History, Overpressure, Blast Impulse

Overpressure over time measurements (pressure-time histograms, pressure-time graphs) are typically used to characterize blast waves as well as their loading of structures and objects.

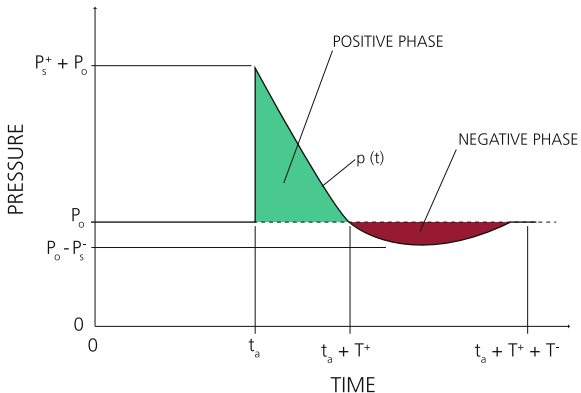
One distinguishes, depending on the position of the overpressure sensor, between

- side-on and reflected (at a certain angle) measurements,
- different positions of the sensor within a geometry (e.g. bottom of structure, top of structure), and
- fixed or movable structures where sensor is mounted (e.g. concrete wall vs. vehicle).

The general geometry setting can also be taken into account:

- free-field, no confinement,
- urban geometries,

Fig. 6.10 Ideal blast wave structure (Baker et al. 1983, p. 111, Fig. 2.1). Copyright 1983. With permission from Elsevier



- confinement with venting, e.g. tunnel structures,
- confinement without venting, e.g. shelter room

An ideal blast wave pressure-time history is given in Fig. 6.10. Important sizes that characterize blast are

- the positive overpressure (peak pressure)

$$P^+ = p(t_a) - p_0 \quad (6.1)$$

- the duration of the overpressure phase T^+
- the specific blast impulse (impulse per area) of the overpressure phase

$$I = \int_{t_a}^{t_a + T^+} [p(t) - p_0] dt \quad (6.2)$$

6.7 Scaling Laws

Well known is the Hopkinson-Cranz scaling, see Fig. 6.11. “An observer located at distance R from the center of an explosive source of characteristic dimension d will be subjected to a blast wave with amplitude of P , duration t_d and a characteristic time history. The integral of the pressure-time history is the impulse i . The Hopkinson-Cranz scaling law then states that an observer stationed at distance λR from the center of a similar explosive source of characteristic dimension λd detonated in the same atmosphere will feel a blast wave of ‘similar’ form with

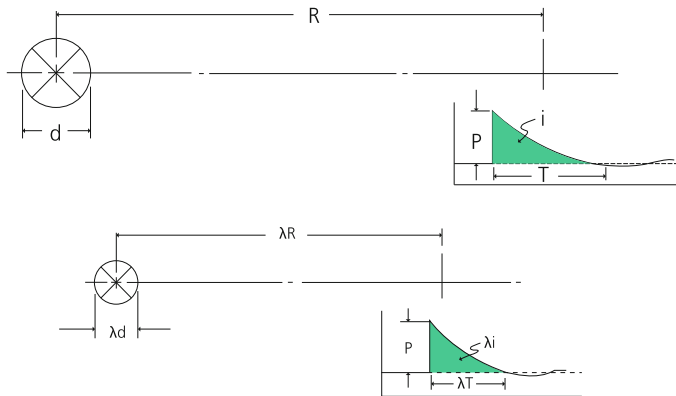


Fig. 6.11 Hopkinson-Cranz blast wave scaling (Baker et al. 1983, p. 116, Fig. 2.2). Copyright 1983. With permission from Elsevier

amplitude P , duration λt_d and impulse λi . All characteristic times are scaled by the same factor as the length scale factor λ " (Conrath et al. 1999).

"The Hopkinson-Cranz scaling law for air blast waves from explosive sources [...] predicts that the entire history of shock loading of a complex structure should scale properly in subscale experiments, provided that:

1. Exact geometric similarity is maintained,
2. All times scale in exactly the same proportion as the geometric (length) scale factor λ ,
3. Types of explosive sources are identical and total source energy E scales as λ^3 , and
4. Initial atmospheric ambient conditions are unchanged." (Hokanson, Esparza et al. 1982)

The Hopkinson-Cranz scaling law is explained in more detail in (Baker et al. 1973).

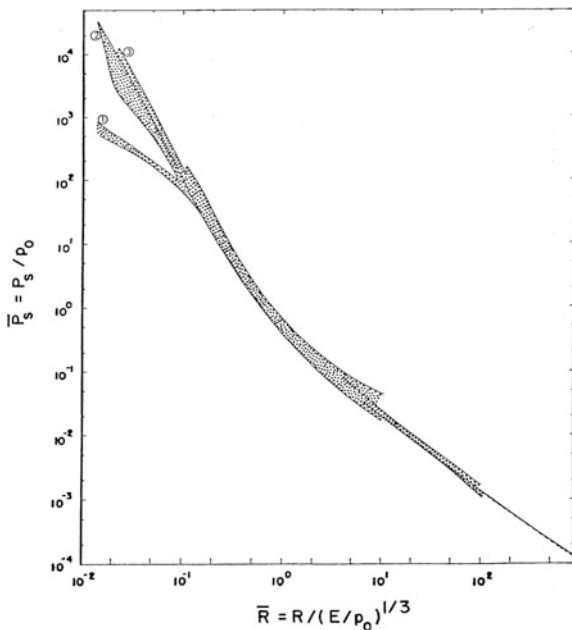
Sach's *scaling law* states that dimensionless overpressure and dimensionless impulse can be expressed as a unique function of a certain dimensionless scaled distance (Baker et al. 1983, p. 117). The dimensionless parameters include quantities which define the ambient atmospheric conditions prior to the explosion, see e.g. Figure 6.12.

However, in practice often the following (simple) scaled distance (skalierter Abstand, Schutzabstand) is used assuming standard atmospheric conditions. This scaled distance is the real distance over the cubic root of the net explosive quantity,

$$x = r/m^{1/3}, \quad [x] = m/kg^{1/3}. \quad (6.3)$$

The cubic root of the mass is proportional to the length scale of the explosive source, e.g. for a cubic source we have $l = V^{1/3} = (m/\rho)^{1/3}$, where V is the

Fig. 6.12 Example for Sachs-scaling of overpressure (Baker et al. 1983, p. 120, Fig. 2.4). Copyright 1983. With permission from Elsevier



volume and ρ is the density of the high explosive source. We further note, that the scaled distance of Fig. 6.12 has also the cubic root dependence on the mass since the released energy is proportional to the explosive mass.

The scaled distance is often used to characterize the damage of explosions.

6.8 Limiting Cases of the Blast Loading of a Single Degree of Freedom Model: Static Loading, Impulsive Loading and Quasi-Static Loading

In this subsection we characterize the high-dynamic blast loading in terms of its effects using asymptotic limiting cases: high-dynamic quasi-static and high-dynamic impulsive Loading. To this end we also compare with static (or very slow dynamic) loading of structures.

To sketch the effects of blast loading of structures we consider the behavior of an ideal-elastic single degree of freedom model without damping. We first consider exponential loading as an analytical approximation to blast loading. We are interested in the shape of the pressure-time history, i.e. the characterization of the hazard potential of the blast.

The response of the structure is modeled by the movement of an ersatz structure consisting of a mass m with loaded area A . The positive x-direction (elongation) is

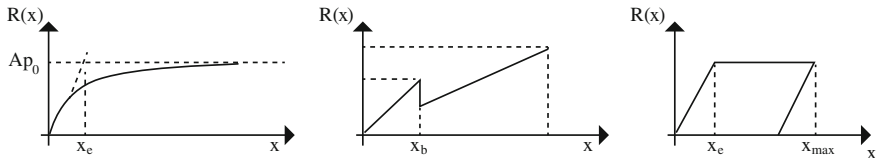


Fig. 6.13 **a** Linear-/ elasticplastic- and arctangent response model. **b** Piecewise linear response model. **c** Response functional (Fischer and Häring 2009). Copyright 2009 With permission from Elsevier

directed in the direction of the movement of the blast wave. The single degree of freedom model has Hook's constant k forcing the mass back to its initial position, see also Fig. 6.13.

The movement of the ersatz structure is defined by the second-order differential equation and its initial conditions

$$\begin{aligned} m \frac{d^2}{dt^2} x(t) &= -kx(t) + AP^+ e^{-t/T}, \\ x(t_0) &= x(0) = 0, \\ v(t_0) &= v(0) = 0. \end{aligned} \quad (6.4)$$

Following Baker et al. (1983), we consider three different types of loading.

First we assume that the pressure rises very slowly to the maximum pressure P^+ , say within a minute (static loading, non-high-dynamic loading). In this case we can use for instance a triangular loading function that starts from zero instead of the exponential loading in (6.4), see e.g. (Fischer and Häring 2009)

$$Ap(t) = \begin{cases} P^+ \left(1 - \frac{t}{T^+}\right) & 0 \leq t \leq T^+ \\ 0 & t > T^+ \end{cases} \quad (6.5)$$

The final deflection is given by

$$\begin{aligned} 0 &= -kx + AP^+, \\ x_{\max} &= \frac{AP^+}{k}. \end{aligned} \quad (6.6)$$

As the second type of loading we assume that we have blast loading with a very long overpressure phase, i.e. we have a sudden pressure rise and a very large T . In this case we equate the strain energy (potential energy of spring) to the work done to obtain the maximum deflection. All the elongation work against the spring force takes place approximately at maximum loading, i.e.

$$\begin{aligned} E_{strain} &= W_{w.d.}, \\ \frac{1}{2}kx^2 &= AP^+ x, \\ x_{max} &= 2\frac{AP^+}{k}. \end{aligned} \quad (6.7)$$

The maximum deflection in (6.7) is doubled when compared to (6.6). The maximum deflection only depends on the maximum overpressure. We call such a loading a pressure loading. In this case during the whole loading process the same overpressure can be assumed.

As a third type of loading we assume a very short loading but with high pressure. In this case the structure has not yet moved significantly at the end of the loading. However, the complete impulse has been transferred. From momentum conservation we obtain the velocity of the ersatz mass

momentum of blast wave = momentum of mass,

$$\begin{aligned} AP^+ T &= mv, \\ v &= \frac{AP^+ T}{m}. \end{aligned} \quad (6.8)$$

Now we assume that the kinetic energy due to the change of momentum of the mass is equal to the strain energy and solve for the maximum deflection

$$\begin{aligned} E_{kin} &= E_{strain}, \\ \frac{1}{2}mv^2 &= \frac{1}{2}m\frac{AP^+ T}{m}\frac{AP^+ T}{m} = \frac{1}{2}kx^2, \\ (AP^+ T)^2 &= kmx^2, \\ x_{max} &= \frac{AP^+ T}{\sqrt{km}}. \end{aligned} \quad (6.9)$$

Since $AP^+ T$ is the impulse (not the specific impulse) of the loading of (6.4), the last line of (6.8) shows that the loading only depends on the blast impulse for a given ersatz structure characterized by its mass and Hook's constant. Hence we call this loading regime impulsive loading. Impulsive loading yields impulsive response. We note that the impulse is proportional to the specific impulse. Thus we must not distinguish between the two when defining the loading regime. For impulsive loading the maximum deflection only depends on the relative blast impulse.

In summary, we distinguish three types of loading. Cases where the

- (1) standard quasi-static slow loading starts from zero loading and the loading time T is long when compared to the response time of the structure, which is of the order of the eigen period of oscillation $T_{eigen} = 2\pi\sqrt{\frac{m}{C}}$. The structure follows the loading.

- (2) dynamic pressure loading, the loading starts suddenly (rise time much less than the eigen period of oscillation) and is long when compared to the response time of the structure: $T \gg T_{eigen}$. The structure accelerates during the loading and also uses kinetic energy for reaching its maximum elongation.
- (3) dynamic impulsive blast loading (starts suddenly and) is short when compared to the response time of the structure: $T \ll T_{eigen}$. The structure is suddenly accelerated and consumes its kinetic energy during the elongation.

Case (3) corresponds to free field explosive loading of smaller explosive quantities. Case (2) corresponds to loading in confined structures and thermonuclear loading.

Further simple examples for the use of single and multiple degree of freedom models for the assessment of structures with respect to explosive loading are given in (Häring et al. 2005; Döge and Häring 2006).

6.9 Summary and Outlook

In this chapter we have seen that one can distinguish between natural and man-made explosions and explosions in different media. A type of explosion that is often in the media are terror explosions, for example the attacks in Boston on April 15, 2013.

In the second part the term explosion is defined and typical equations and graphs for ideal explosions are introduced, for example pressure-distance curves for a point source. The Hopkinson-Cranz scaling is also introduced.

Easily accessible further reading on the topic of this chapter are Chap. 2 (pages 7–14) but also later chapters of (Rosales 2004).

In the next chapter we will see how fragments can be characterized, in terms of their shape, their position in different coordinate systems, fragment matrices and fragment densities.

6.10 Questions

- (1) Which heuristic characterizations of explosions can be made? Give 3 examples for combinations.
- (2) For which steps of the risk analysis process is a phenomenological characterization of explosions helpful?
- (3) In which industrial and technological area do intended explosions occur?
- (4) In which industrial and technological area do accidental explosions occur?
- (5) How would you characterize terrorist explosions?
- (6) For which types of explosions do you expect that risk analyses are performed?

- (7) Name the possible physical consequences of explosions on the ground.
- (8) Name typical damage of explosions on the ground.
- (9) Which physical consequences do you expect from explosions in the air.
- (10) For which phases of the risk management and the risk analysis process is the physical characterization of blast important? Also discuss more unusual risks, e.g. the far-field effect of blast.
- (11) Which sequence of physical processes can be identified for a detonation?
- (12) Which variables and curves characterize blast? Which of them are the most important? (Draw pressure-time graphs and explain)
- (13) What are explosive products (Explosionsschwaden)?
- (14) What is meant by the terms scaling and scaling laws?
- (15) How does one make physical values dimensionless?
- (16) Why does one use scaling to describe physical processes?
- (17) What is a scaled distance? Why is it also called “Schutzabstand” in German?
- (18) Why can the blast impulse be measured more easily than the pressure-time-graph?
- (19) What is a detonation front?

References

- Assael, M. J., & Kakosimos, K. E. (2010). *Fires, Explosions, and Toxic Gas Dispersions*. CRC Press.
- Astaneh-Asl, A., Heydari, C., & Zhao, Q. (2003). Analysis of car-bomb effects on buildings using MSC-Dytran software and protective measures. In *The MSC Software Virtual Product Development Conference*, Dearborn, Michigan.
- Baker, W. E., Cox, P. A., Westine, P. S., Kulesz, J. J., & Strehlow, R. A. (1983). *Explosion hazards and evaluation*. Amsterdam: Elsevier.
- Baker, W. E., Westine, P. S., & Dodge, F. T. (1973). *Similarity Methods in Engineering Dynamics: Theory and Practice of Scale Modeling*. Rochelle Park, New Jersey: Spartan Books.
- Conrath, E. J., Krauthammer, T., Marchand, K. A., & Mlakar, P. F. (1999). *Structural Design for Physical Security: State of the Practice*. Structural Engineering Institute of ASCE.
- Döge, T., & Häring, I. (2006). Bewegungsdifferentialgleichung für Ein- und Mehrmassenschwinger (Differential equations for single and multiple degree of freedom systems). 2. Workshop Bau-Protect (Buildings And Utilities Protection), Sicherheit der baulichen Infrastruktur vor außergewöhnlichen Einwirkungen, München, Universität der Bundeswehr.
- Dörr, A., & Rübarsch, D. (2005). EMI Bericht E 13/05, Fraunhofer EMI.
- Fischer, K.-U., & Häring, I. (2009). SDOF response model parameters from dynamic blast loading experiments. *Engineering Structures*, 31(8), 1677–1686.
- Häring, I., Kranzer, C. & Romani, M. (2005). Generalized single degree of freedom description of generic failure modes due to blast. In *Prepared for the 12th International Symposium on Interaction of the Effects of Munitions with Structures (ISIEMS)*, New Orleans, Louisiana, also EMI report E 16/05.
- Health and Safety Executive. (2002). HID-Safety report assessment guide chemical warehouses: “Hazards”. from <http://www.hse.gov.uk/comah/sragcwh/hazards/images/hazards.pdf>
- Hokanson, J. C., Esparza, E. D., Baker, W. E., & Sandoval, N. R. (1982). Internal Blast Measurements in a Model of the Pantex DWF, Southwest Research Inst San Antonio TX.

- Klomfass, A., & Thoma, K. (1997a). *Ausgewählte Kapitel der Kurzzeitdynamik Teil 1—Explosionen in Luft*. Freiburg: Fraunhofer Institut für Kurzzeitdynamik, Ernst-Mach-Institut.
- Klomfass, A., & Thoma, K. (1997b). *Ausgewählte Kapitel der Kurzzeitdynamik Teil 3—Sprengstoffe*. Freiburg: Fraunhofer-Institut für Kurzzeitdynamik, Ernst-Mach-Institut.
- Rosales, S. A. (2004). Study for development of a blast layer for the virtual range project (Master of Science). from http://etd.fcla.edu/CF/CFE0000190/Rosales_Sergio_A_200412_MS.pdf
- Strehlow, R. A., & Baker, W. E. (1976). The characterization and evaluation of accidental explosions. *Progress in Energy and Combustion Science*, 2(1), 27–60.
- Technical test center WTD 91 (2013). Meppen, Germany.
- Technical test center WTD 91 (2014). Meppen, Germany.
- Weals, F. H. (1973). ESKIMO I Magazine separation test. NWC TP 5430, China Lake.

Chapter 7

Hazard Source Characterization and Propagation II: Fragments

7.1 Overview

This chapter presents a further hazard propagation model. In contrast to the longitudinal compression wave of blast, which almost results in no final displacement of air after an event, in this case material is dispersed. This is somewhat similar as when comparing the hazard propagation loading of earthquakes with the hazard propagation loading due to hail impact.

A basic approach to describe the fragment and debris distribution in case of explosive events, which is often only based on experimental data, is given. It offers the opportunity to (geo-)locate threat trajectories in space. A little similar approaches are of interest when tracing the dispersion of solid agents or fluids.

The assumptions of the presented approach are given, in particular it is not valid for the near field. However, the near field is typically dominated by the blast hazard. This is an example for employing worst case assessment to limit the hazard propagation modeling effort.

This chapter shows how a sufficient hazard source description relates to the hazard propagation modeling: the former should contain sufficient information for the later. This is performed exemplary for explosive hazard sources, however, without showing in detail how the fragment launch conditions are obtained experimentally, by analytical-empirical models or by computational continuum-mechanical simulation.

The modeling and visualization of hazards requires the use of natural coordinate systems: the coordinate system for the hazard source, coordinate systems for objects in the surroundings of the hazard source, for the visualization of earth's surface and for modeling the forces on earth's surface that influence the hazard propagation. This chapter presents a minimum of such coordinate systems and how they are transformed to each other.

For describing the physics of the propagation, geometry properties of the objects propagating and the medium they are propagating through are necessary to

determine the physical forces acting on the propagating objects. It is interesting, that they depend even in this sample case on a large number of assumptions and simplifications, which have to be justified for the application of interest, for example the neglect of wind effects and Coriolis force. Even the decision whether they are conservative or not is not straightforward. For instance, only the combination of mass, initial velocity and shape of fragments allows to assess their criticality rather than one such single parameter.

The definition of various hazard densities of explosions are an example of quantifying parameters for representing the time-dependent 3D hazard field on a surface of interest. It is carefully distinguished between the representation of the hazard potential and its interpretation in terms of potential damage.

This chapter also illustrates that computational simulation and its visualization are a powerful tool to model the propagation of hazards, in particular also allowing to take account of the scenario geometry, e.g. of barriers close to the hazard source or close to objects at risk.

As in the case of Chap. 6, understanding fragment and debris launch conditions and propagation in air contributes to the resilience engineering of prevention and protection, and to a lesser extent to options of improving response and recovery. Examples respectively include the access prevention for potential fragment and debris sources, the prevention of building bombs, appropriate physical counter measures, the optimization of response by using shelters and finally the preparation of recovery means, e.g. efficient removal of primary, secondary and tertiary fragments and debris.

This chapter describes the hazard propagation of fragments generated by explosion. For this the hazard source is defined in Sect. 7.2 and different coordinate systems are introduced in Sect. 7.3.

To simplify the description of objects, the convex hull is introduced in Sect. 7.4. It can be used to simplify a given object, for example a fragment.

Section 7.5 describes the fragments matrix saying in which angles fragments leave.

The last topic are fragment trajectories and fragment densities in Sects. 7.6 and 7.8, respectively.

The main sources of the chapter are Aschmoneit (2011), Salhab et al. (2011a, b). Further Fraunhofer EMI sources are Dörr et al. (2003), Häring and Richter (2009), Salhab (2012). The main authors of the EMI sources are R. Salhab and T. Aschmoneit supplemented with work by I. Häring and R. Salhab supplemented with work by I. Häring and F.K.F. Radtke.

7.2 General Description and Assumptions

In the simplest form, we consider a single explosive source consisting of two materials. Then the hazard source can be described by the tuple

$$\stackrel{H}{\equiv} \left(\vec{r}^{\text{det}}, \{ \vec{e}_i^{\text{det}} \}_{i=1,2,3}, G^{\text{ex}}, \kappa^{\text{ex}}, G^{\text{hull}}, \kappa^{\text{hull}} \right) \quad (7.1)$$

where \vec{r}^{det} is the position of the explosive's geometric center, $\{ \vec{e}_i^{\text{det}} \}_{i=1,2,3}$ are the local Cartesian basis vectors used to describe the explosive source, G^{ex} is the explosive's geometry (in terms of the local coordinate system, including density distributions), κ^{ex} is the type of explosive, G^{hull} the hull's geometry and κ^{hull} the hull's material (Salhab et al. 2011b).

"Especially for fragmentation processes one expects that imperfection of material are very important for modeling, e.g. micro cracks or cavities. The influence can be averaged out by considering multiple models that are statistically generated based on variations of geometry or material properties. Often also in experiment only average effective parameters are determined that already take into account the statistic variations." (Salhab et al. 2011b)

In practice, one normally makes certain assumptions to have manageable experiments and modeling.

The first assumption is homogeneity. This means, that weak points in the structure are neglected and that there are no density fluctuations.

The second usual assumption is the assumption of a point source. In quantitative risk analysis the fragmentation process itself is not interesting and the damage close to the hazard source mostly result from blast. Hence, one assumes that fragments in a sufficient distance can be assumed to originate from one point (Salhab et al. 2011b).

The third assumption is symmetry. One often assumes axial symmetry, which often is correct, for example for pipe bombs. Symmetries reduce the effort to define initial launching conditions.

7.3 Coordinate Systems

7.3.1 Polar Geocentric Coordinates

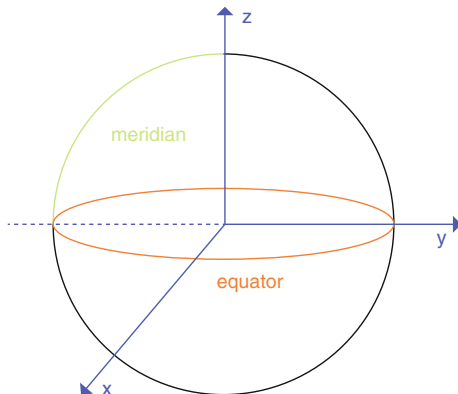
Table 7.1 shows the polar geocentric coordinates φ^{WGSP} and θ^{WGSP} and the parameters needed to transform them into Cartesian coordinates. The degree of latitude is measured up (positive degrees) and down (negative degrees) from the equator. The degree of longitude is measured to the right (positive degrees) and left (negative degrees) from the meridian.

7.3.2 Cartesian Coordinates

The right-handed Cartesian coordinate system with the three perpendicular axes x, y and z is derived from the polar geocentric coordinate system by keeping the origin,

Table 7.1 The polar geocentric coordinates

	Name	Parameter
1	Semi-major axis of ellipse	a
2	Semi-minor axis of ellipse	b
3	Semi-major axis of earth' ellipse (WGS84)	$a_{Earth,WGS84} = 6.3781370 \cdot 10^6 \text{ m}$
4	Semi-minor axis of earth' ellipse (WGS84)	$b_{Earth,WGS84} = 6.3567523 \cdot 10^6 \text{ m}$
5	Height above sea level	H
6	Ellipsoidal height (height above ellipsoid surface)	h
7	Degree of latitude	φ^{WGSP}
8	Degree of longitude	θ^{WGSP}
9	Flattening	$f = \frac{a-b}{a}$
10	Inverse flattening	$\frac{1}{f}$
11	Inverse flattening of earth	$\frac{1}{f_{Earth,WGS84}} = 298.257223563$
12	First numeric eccentricity	$\varepsilon = \sqrt{\frac{a^2-b^2}{a^2}}$
13	First numeric eccentricity of earth	$\varepsilon_{Earth,WGS84}^2 = 0.00669437999013$
14	Transverse radius of curvature	$N = \frac{a}{\sqrt{1-\varepsilon^2 \sin \varphi^{WGSP}}}$

Fig. 7.1 Illustration of how the three axes of the Cartesian coordinate system are related to the polar geocentric coordinate system

letting the negative y-axis go through the intersection of meridian and equator, placing the x-axis perpendicularly to the y-axis also through the equator and the z axis through the north pole. For illustration see Fig. 7.1.

Since the earth is not a sphere, the transformation from polar geocentric to Cartesian coordinates is not as simple as from “regular” polar coordinates to Cartesian coordinates. The transformation is shown in Table 7.2.

Table 7.2 Transformation between polar geocentric and Cartesian coordinates

Transformation from polar geocentric to Cartesian WGS84 coordinates based on Bill (2010)^a	
1	Cartesian coordinate x^{CCS} expressed on polar geocentric coordinates
2	Cartesian coordinate y^{CCS} expressed on polar geocentric coordinates
3	Cartesian coordinate z^{CCS} expressed on polar geocentric coordinates
Transformation from WGS84 Cartesian to polar geocentric coordinates	
4	Latitude expressed in polar geocentric coordinates
5	Longitude expressed in polar geocentric coordinates
6	Height (above ellipsoid surface) expressed in polar geocentric coordinates

^aWGS84 coordinate system as defined in USA Department of Defense (1999) (right-handed CCS, origin at earth center, positive z-axis through geological North Pole, negative y-axis through intersection point of prime meridian and equator)

7.4 Convex Hull and the Cauchy Theorem

Especially natural fragments have all kinds of different shapes, see Figs. 7.2 and 7.3 (Technical test center WTD 52 2013). To compute their trajectories, they are often assumed to be balls. In this case the presented surface that is used within the air drag computation is given by the cross section of the ball, which is independent of the ball's orientation in space.

A more realistic idea is to assume that the fragments tumble in air and that all orientations are equally probable. However, what is the average presented surface (cross section) of such an arbitrary body?

The idea is to first determine the convex hull of a fragment. The convex hull is the smallest convex geometrical body which contains the original body. In a convex body any two points can be connected by a line that completely lies within the body. In the present case, this is no restriction since there is a perspective where the connecting line is perpendicular to a cross section. The convex hull can be used together with the Cauchy Theorem which is introduced later in the section. Depending on the shape of the fragment, the convex hull can be difficult to compute. See Fig. 7.4 for an example of a convex hull.



Fig. 7.2 Examples of smaller car fragments: at the *top* an electric motor (ca. 3 cm diameter) as used for the windscreen wiper or as window winder; beneath are other metallic fragments, some of them are bent by the explosion (Technical test center WTD 52 2013)



Fig. 7.3 Examples of car bomb fragments: parts of the front suspension and crash structure of the car stopped by a measurement box; just behind the box a wheel with the shock absorber; other fragments are distributed over the ground (Technical test center WTD 52 2013)

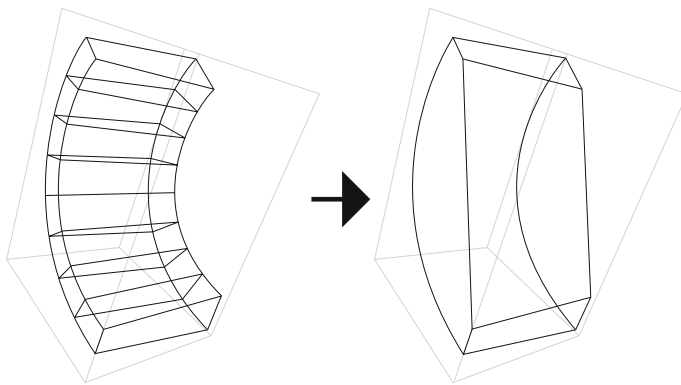


Fig. 7.4 Example of the convex hull (Aschmoneit 2011)

The Cauchy Theorem from the 19th century states that “for an arbitrary convex solid in three dimensions, the average projected area is one-fourth the surface area” (Slepian 2012):

$$A_{rep}^{av} = \frac{1}{4} A_{surface}. \quad (7.2)$$

Example Regard a rectangular cuboid where the sides are 4, 3 and 1 cm long. Figure 7.5 shows two (of infinitely many) different projected areas of the cuboid.

The average projected area of sample cuboids reads, using the Cauchy theorem

$$A_{rep}^{av} = \frac{1}{4} A_{surface} = \frac{1}{4} \cdot 2(3 \text{ cm} \cdot 4 \text{ cm} + 1 \text{ cm} \cdot 3 \text{ cm} + 1 \text{ cm} \cdot 4 \text{ cm}) = 9.5 \text{ cm}^2. \quad (7.3)$$

7.5 Fragment Matrix

In the most general case the following statistical data of a point source is needed:

- Average number of fragments that belong to a given mass interval (mass class) and velocity interval (velocity class) and fly into a given solid angle surface element $\Delta\Omega$,
- The upper bounds of the mass and velocity interval are taken as the representative launching mass and velocity.

In the case of a rotational symmetric body in practice only

- the average number of fragments of a selected mass interval that fly into pre-defined latitude bands (stripes) and
- the average maximum velocity of all fragments of a latitude stripe are given.

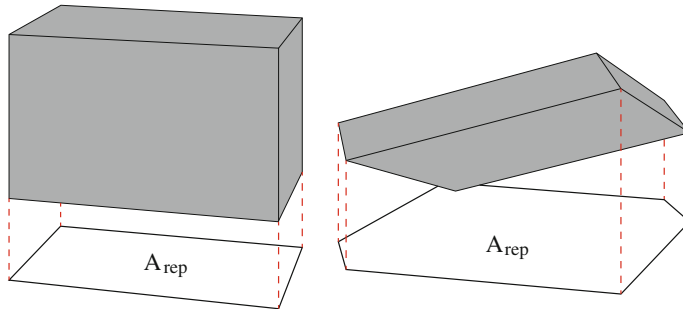


Fig. 7.5 Projections of a cuboid in two different positions (Aschmoneit 2011)

In both cases the interval boundaries and the number of intervals are implicit information that must be available.

In the case of the rotational symmetric body, for practical computations of the fragment hazard, representative fragments for a sufficiently fine launching grid on the unit surface are launched using the following data

- mass: upper bound of mass interval
- velocity: velocity of latitude band.

In the case of a fragment matrix of a rotational symmetric source, each line represents an angle interval. Each column represents a mass interval. Each entry represents the average number of fragments corresponding to the angle interval and the mass interval. The last column shows the average maximum velocities for each latitude band. Hence, they have the form shown in Table 7.3.

In Table 7.3 “ $n_{i,j}$ is the average number of fragments departing within latitude band interval $[\theta_i, \theta_{i+1}]$ and mass interval $[m_j, m_{j+1}]$, if there are $N_\theta - 1$ latitude band intervals and $N_m - 1$ mass intervals in total, and v_i the averaged maximum velocities. A compact [description] is given by

$$\begin{aligned} & N_\theta, N_m, \\ & \{[\theta_i, \theta_{i+1}]\}_{i=0,1,\dots,N_\theta-2}, \{[m_j, m_{j+1}]\}_{j=0,1,\dots,N_m-2}, \\ & \{n_{i,j} = n_{[\theta_i, \theta_{i+1}], [m_j, m_{j+1}]}\}_{i=0,1,\dots,N_\theta-2; j=0,1,\dots,N_m-2}, \\ & \{v_i^{0,frag}\}_{i=0,\dots,N_\theta-1}, \end{aligned} \quad (7.4)$$

where the first two sizes N_θ and N_m are the numbers of latitude band intersections or mass interval intersections, respectively” (Salhab et al. 2011b).

Table 7.3 Structure of a typical fragment matrix (Salhab et al. 2011b). Copyright 2011. With permission from Taylor and Francis

	$[m_0, m_1]$...	$[m_{N_m-2}, m_{N_m-1}]$	
$[\theta_0, \theta_1]$	$n_{0,0}$...	n_{0,N_m-2}	v_0
...
$[\theta_{N_\theta-2}, \theta_{N_\theta-1}]$	$n_{0,N_\theta-2}$...	$n_{N_\theta-2,N_m-2}$	$v_{N_\theta-2}$

Table 7.4 Example of a typical fragment matrix (Salhab et al. 2011a). Reprinted from Advances in Safety, Reliability and Risk Management. ESREL 2011 Annual Conference Proceedings

	[0.1 g, 0.2 g]	...	[56 g, 100 g]	...	v _{max} [m/s]
[0°,10°]	5.6	...	0.78	...	613
...
[90°,100°]	2594.7	...	0	...	1997
...

An example is given in Table 7.4.

Remark Fragment matrices can also be defined for generalized point sources, see Salhab et al. (2011b).

Using a fragment matrix A^{HS} , one can describe a hazard source [compare (7.1)] by

$$H = \left(\vec{r}^{HS}, \{\vec{e}_i^{HS}\}_{i=1,2,3}, Q^{HS}, \left\{ \tau_{\xi}^{HS} \right\}_{\xi}, \beta^{br,HS}, A^{HS} \right) \quad (7.5)$$

where \vec{r}^{HS} is the location, $\{\vec{e}_i^{HS}\}_{i=1,2,3}$ the location basis, Q^{HS} the Net Explosive Quantity, $\left\{ \tau_{\xi}^{HS} \right\}_{\xi}$ are the dimensionless TNT equivalents of the blast characteristics and $\beta^{br,HS}$ is a blast reduction factor (for example due to attenuation) (Salhab et al. 2011a).

7.6 Fragment Trajectories

For (natural) fragment trajectories, in the simplest case, the following forces are considered:

- The gravity force $\vec{F}_{gravity} = m\vec{g}$, where m is the mass of the body and \vec{g} is a constant gravity acceleration vector with an average magnitude of $9.81 \frac{m}{s^2}$.
- The drag force $\vec{F}_{air\,drag} = -\frac{1}{2} \rho A c_w \left(\frac{v}{c}\right) v^2 \frac{\vec{v}}{v}$. Here $c_w \left(\frac{v}{c}\right)$ is the drag coefficient in terms of the Mach number v/c where c is the speed of sound (compare Fig. 7.6), ρ is the density of air which is assumed to be independent of the position, v is the speed of the object, A the cross-sectional area, see also Elert (2013). The area can be computed as in Sect. 7.4.

Figure 7.6 shows some experimental data on empirical c_w curves in terms of the Mach number.

Using Newton's second law $m\vec{a} = \vec{F}$, a two dimensional second order vector differential equation for the fragments can be derived as follows.

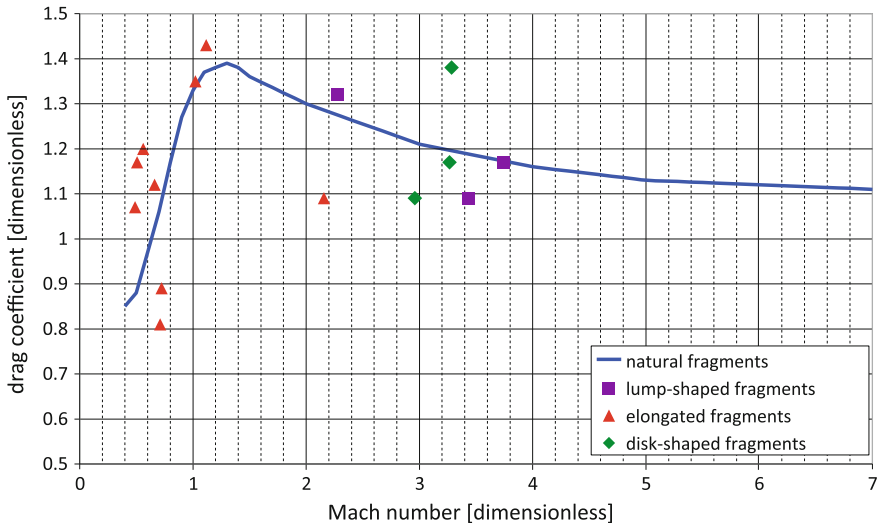


Fig. 7.6 Drag coefficient c_w in terms of the Mach number v/c . The *blue line* are natural fragments, the *rectangles* display rather round fragments, *triangles* long fragments and the *diamonds* flat fragments (Dörr et al. 2003)

$$\begin{aligned}
 m\ddot{\vec{x}} &= \vec{F}; \\
 m\ddot{\vec{x}} &= \vec{F}_{\text{air drag}} + \vec{F}_{\text{gravity}}; \\
 \frac{d^2}{dt^2} \vec{x}(t) &= \frac{d}{dt} \vec{v}(t) = \frac{1}{m} \left(-\frac{1}{2} \rho A c_w (v/c) v^2 \frac{\vec{v}}{v} + m \vec{g} \right); \\
 \vec{x}(t_0) &= \vec{x}_0; \\
 \vec{v}(t_0) &= \vec{v}_0.
 \end{aligned} \tag{7.6}$$

It can be “numerically solved by a Runge-Kutta method with a step size control by Collatz” (Salhab et al. 2011a; see also Wagner 2000).

A typical example that highlights the assumptions made within (7.6) are specially shaped fragments, for instance very elongated or flat fragments. For instance, the turquoise colored engine hood of Fig. 7.7 could have tumbled and sailed (Technical test center WTD 91 2014).

7.7 Experimental Assessment of Debris Launch Conditions

This section gives a qualitative overview on the experimental assessment of debris throw in case of car bombs. The quantification of debris throw in case of containers is discussed exemplarily in Sect. 16.3.8. In this case we adopted the notion that the



Fig. 7.7 Detection and localization of fragments after 2 test explosions. This *picture* shows a part of the test site that is 80 to 120 m apart from ground zero. The subdivision in 5° angular sectors is clearly visible, was well as some medium and smaller fragments. The biggest fragment is the turquoise colored engine hood of one of the car bombs in der lower right part of the picture. This fragment was torn apart in one piece from the car. It is interesting that it is not much twisted like many other fragments. Such fragments are candidates for rather irregular distribution due to sailing effects. The composed aerial pictures allow to zoom in the pictures (Technical test center WTD 91 2014)

hull and framing of a container generates debris, i.e. only the material within or very close to the explosive material generates fragments.

A typical experimental set-up before and after the hazard event are shown in Figs. 7.8 and 7.9, respectively (Technical test center WTD 52 2013). The hazard of interest are the hazard propagation of crater material and material of the barriers.

Figure 7.10 captures the moment where material of the barrier is launching from its initial position (Technical test center WTD 52 2013). In this case, debris generated from the barriers is dominating when compared to carter ejections.

In case of car bombs exploding over softer soil, a much larger crater is generated, see Fig. 7.11. However, in this case, debris throw is not directly observable, see also Figs. 6.2 and 6.3.

Figure 7.12 gives a top view of the crater ejections after a car bomb explosion. For this real-world conditions, a clear pattern is not detectable (Technical test center WTD 91 2014).



Fig. 7.8 Car loaded with 50 kg PETN behind the front seats in a simulated gateway of an asset. On the *right* and *left* hand sides there are gabions (Hesco bastions) filled with stones with a diameter of 5 to 15 cm, height 2 m, width 1 m and length 10 m. The supermini car has a dry weight of 790 kg. All liquids and window glasses have been removed before the experiment (Technical test center WTD 52 2013)

7.8 Fragment Density

Each fragment represents a surface element and is launched in the center of the surface element, see Fig. 7.13. At impact the fragment is weighted according to the average number of fragments that are expected to fly into the selected surface element.

“The fragment density on the ground in the case of a single hazard source is computed as the sum over all representative trajectories hitting the ground volume elements. The weights determine the represented numbers of fragments. The ratios of flight segments (stretches, distances) over the volume of the ground volume element have the dimension one over area and are additional (in general not conservative) weights. The segments are approximated using the entry and exit points, which are computed using straight line approximations between the trajectory points and the scenario geometry data. The idea is that a fragment is hazardous as long as it propagates below a critical height for personnel (height of volume elements).” (Salhab et al. 2011a)



Fig. 7.9 Gateway as shown in Fig. 7.8 after the explosive event. The gabions are seriously damaged near the original location of the car bomb. Some of the gabions at the *right* hand side tumbled back in the direction of the hazard source, because behind them a further test vehicle was located for damage assessment. The crater is comparatively small because of the rocky ground. In the *middle* of the picture, fragments of the car and protective structures for the filming and measuring equipment are visible. For instance, a massive fragment lies just straight ahead. Also the radial segment markings for locating the fragments are visible, see the thin white lines that originate from the explosive source location (Technical test center WTD 52 2013)

The fragment density computed by Salhab et al. (2011a) is

$$\rho_{l,m,n}^{frag} = \sum_{i_{sp}=0}^{N_\theta-2} \sum_{m_{sp}=0}^{N_i^\theta-2} \sum_{l_{sp}=0}^{N_m-2} \sum_{j_{sp}=0}^{N_i^\theta-2} \left(\exists \vec{r}_{\underline{k},l,m}^{en} \left(t_{\underline{k},l,m}^{en} \right) \in V_{l,m} \right) \\ \cdot W_{i_{sp},m_{sp},l_{sp},j_{sp}}^{t_{i_{sp},m_{sp},l_{sp},j_{sp}}^{en}} \frac{\left| \vec{r}_{sp,m_{sp},l_{sp},j_{sp},l,m}^{en} - \vec{r}_{sp,m_{sp},l_{sp},j_{sp},l,m}^{ex} \right|}{\left| V_{l,m}^{gr} \right|}. \quad (7.7)$$

The fragment density from (Häring et al. 2009) is defined as

$$\rho_{impact}(\Delta S_m) = \frac{1}{A(\Delta S_m)} \sum_{h=0}^{N_t-2} \sum_{i=0}^{N_\theta-2} \sum_{i_1=0}^{N_i^\theta-2} \sum_{i_2=0}^{N_i^\theta-2} \sum_{j=0}^{N_m-2} n_{h,i,i_1,i_2,j}^{frag} \\ \cdot \left(\vec{r}_{h,i,i_1,i_2,j}^{impact} \in \Delta S_m \right) \left(E_{h,i,i_1,i_2,j}^{impact} > E_{crit} \right). \quad (7.8)$$



Fig. 7.10 Debris throw due to an explosion. This *picture* shows the same scenario as Fig. 7.8 during the explosion of the car bomb. The burst of the gabions and the resulting debris throw is clearly visible. The debris in this scenario consists mainly of rock pieces used to fill the structures besides the mesh wire that hold it. On the *right* hand side fragments of the car fly in driving direction. The cloud is mainly due to the crater dust (Technical test center WTD 52 [2013](#))

where $n_{h,i,i_1,i_2,j}^{frag}$ is the representative fragment weight, E the energy and $\bar{r}_{h,i,i_1,i_2,j}^{impact}$ the representative fragment impact position data.

Of course, only (7.7) without the last factor is a physical fragment hazard density that can for instance be used to assess the normalization condition of the total number of fragments.

7.9 Summary and Outlook

We distinguished between polar geocentric and Cartesian coordinates.

The convex hull that was introduced is rather technical. Instead one often assumes regular fragments (for example balls).

The fragment matrix, trajectories and density are used to describe how many fragments fly where.

In the next chapter we will still consider hazard propagation but this time with focus on blast.



Fig. 7.11 Crater formation after car bomb free field explosion with 120 kg TNT. The ground persists of sand and topsoil and comprised only few stones. Behind the crater, fragments of the car are visible. The biggest fragment consists of the rear suspension, crash structure and a wheel. Smaller parts are widespread across the test site. In the middle of the background, a protective structure for the filming is visible (Technical test center WTD 91 [2012](#))

7.10 Questions

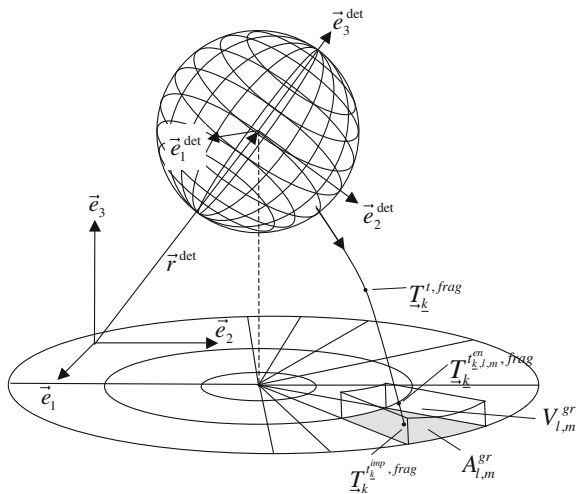
- (1) For which risk analysis steps is the fragment launching data needed?
- (2) What is the difference between natural and performed fragments?
- (3) What is the difference between fragments and debris?
- (4) What is meant by fragment launching conditions?
- (5) What is meant by the assumption of a point source?
- (6) How can data in a fragment matrix for a rotational symmetric body be described verbally? Key words: latitude band intervals, mass intervals, average maximal velocity, average number of fragments.
- (7) How can data in a fragment matrix for a rotational symmetric body be described formally? Key words: latitude band intervals, mass intervals, maximal velocities, average number of fragments.
- (8) Which forces act on the fragments after the acceleration phase?



Fig. 7.12 Free field test site after two car bomb explosions with 100 kg PETN. It was taken with an aerial drone flying in a height of 30 m above ground zero. The crater and some big fragments are clearly visible. The big fragments consist mostly of the rear suspension, the crash structure and parts of the frame. Smaller parts are widespread across whole parts of the test site. The test site was subdivided in 72 angular sectors, each 5° wide. The *orange* poles and *yellow* ropes close to the crater are visible on the *right* side of the picture. This test arrangement improved the localization and classification of the fragments as well as the analysis of the aerial photos. The first 20 m around ground zero are excluded, because of the high explosive loading (Technical test center WTD 91 2014)

- (9) Determine the differential equation that describes the trajectory of the fragments. Key words: $\vec{F}_{drag} = -\frac{1}{2} \rho A c_w (v/c) v^2 \frac{\vec{v}}{v}$
- (10) Why must thousands of trajectories be computed in practice to compute the fragment density on the ground?
- (11) What is the idea behind the usage of representative fragments?
- (12) How can damaging fragments be visualized?
- (13) How can the individual local fatality risk through fragments be computed?

Fig. 7.13 The scheme of the discretized launching sphere that is used in the methodology of EMI's software solutions ESQRA, FSQRA and RAFOB-RAM (Salhab 2012)



References

- Aschmoneit, T. (2011). EMI Bericht E 20/11. Fraunhofer EMI.
- Bill, B. (2010). Grundlagen der Geo-Informations systeme. Wichmann: Berlin.
- Dörr, A., Rübarsch, D., Gürke, G., & Michael, K. (2003). Fraunhofer EMI Bericht E 10/03.
- Elert, G. (2013). *Aerodynamic Drag*. Retrieved August 20, 2013, from <http://physics.info/drag/>
- Häring, I., Schönherr, M., & Richter, C. (2009). Quantitative hazard and risk analysis for fragments of high explosive shells in air. *Reliability and System Safety Engineering*, 94(9), 1461–1470.
- Salhab, R. G. (2012). *Integral expressions for trajectory-based fragment density computations of explosions*. Freiburg im Breisgau: Diplom, Albert-Ludwigs-Universität Freiburg.
- Salhab, R. G., Häring, I. & Radtke, F. K. F. (2011a). Formalization of a quantitative risk analysis methodology for static explosive events. In G. G. S. Bérenguer & G. Soares (Eds.), *ESREL 2011 Annual Conference* (pp. 1311–1320). Troyes, France: Taylor and Francis.
- Salhab, R. G., Häring, I. & Radtke, F. K. F. (2011b). Fragment launching conditions for risk analysis of explosion and impact scenarios. In G. G. S. Bérenguer & G. Soares (Eds.), *ESREL 2011 Annual Conference* (pp. 1579–1587). Troyes, France: Taylor and Francis.
- Slepian, Z. (2012). *The average projected area theorem—Generalization to higher dimensions*. arXiv:1109.0595v4 [math.DG].
- Technical test center WTD 91. (2012). Meppen, Germany.
- Technical test center WTD 52. (2013). Oberjettenberg, Germany.
- Technical test center WTD 91. (2014). Meppen, Germany.
- USA Department of Defense. (1999). Department of Defense World Geodetic System (WGS), National Geospatial-Intelligence Agency.
- Wagner, A. (2000). *Schrittweitenanpassung*. Retrieved August 20, 2013, from <http://www.stellarcom.org/aw/Physik/cp/node39.html>

Chapter 8

Hazard Propagation III: Free Field Blast and Complex Blast: Empirical-Analytical Expressions and Scaled Experiments

8.1 Overview

This chapter, as Chap. 7, takes up the hazard propagation for explosions focusing on blast propagation. Two samples are selected: the propagation in the case of a free field scenario, which is treated using empirically parametrized analytical expressions.

For comparison, scaled free field experiments are used, which cover typical geometries as encountered in urban geometries. These experiments were conducted to determine scaling factors for the characteristic blast hazard quantities introduced in Chap. 6 as well as to validate computational approaches to complex urban blast propagation.

This chapter also takes up the scaling laws introduced in Chap. 6. It becomes obvious how this facilitates experimentation.

Engineering for resiliency of structures and buildings in case of explosions has to take account of possible loading events. The local and overall loading depend on the geography, geometry and topology of the scenarios, for instance of urban geometries and spaces as well as indoor designs. Therefore the modelling and experimental assessment of blast propagation can be used to prevent critical loading regimes as well as protect buildings and infrastructure. Post an disruptive event, the knowledge of the occurred loadings allows to assess optimal response and recovery strategies. Focusing on the resilience engineering of protection means and capabilities is standard when compared to the other also promising options, at least when regarding structural resilience.

Chapter 7 and this chapter comprise examples for hazard source characterization and hazard propagation. The next chapters address the challenge to determine damage quantities given hazard source descriptions or (local) hazard quantities.

This chapter describes how to determine the maximum blast overpressure and the relative blast impulse in case of free field conditions using empirical-analytical expressions (Sect. 8.2). It shows how TNT equivalents are computed for each case,

respectively (Sect. 8.3). The descriptions of the maximum overpressure and the blast impulse follow Kingery and Bulmash (1984).

Section 8.4 describes scaled experiments to determine complex blast for urban street geometries. In Sect. 8.4.1 it is shown how to use such data to compute scaling factors for different urban street geometries.

The main sources used for this chapter include (Swisdak 1994; Dörr et al. 2004; Dörr and Frick 2006; Aschmoneit et al. 2009).

8.2 Free Field Side-On Overpressure and Blast Impulse for TNT: Kingery and Bulmash Parameterizations

The following expressions were obtained from large scale free field experiments using scaling laws. Free field means that hemispherical charges (half sphere) were considered. For TNT the maximum side-on overpressure in terms of the scaled distance $x = r/m^{1/3}$ of (6.3) reads, according to simplified expressions (Kingery and Bulmash 1984; Swisdak 1994, 2001)

$$p_0(x) = \exp\left(\sum_{j=0}^4 c_{ij} \left(\ln\left(\frac{x}{\text{m/kg}^{1/3}}\right)\right)^j\right) \text{kPa}, \quad x \in [a_i, b_i], \quad (8.1)$$

where \ln is the natural logarithm and the interval bounds and coefficients are given in Table 8.1.

Example For $x = 0.524934 \frac{\text{m}}{\text{kg}^{1/3}}$ it is $i = 0$ and $p_0(x) \approx 4519.96 \text{ kPa}$.

From Fig. 8.1 we see that the overpressure is strictly monotonic decreasing with the scaled distance. Thus there is a unique and invertible mapping from the side-on overpressure to the scaled distance.

A typical free field overpressure-time history for a given distance starts with a sudden pressure rise to maximum overpressure, $p(t_a) = p_0 + P_S^+$. Then an exponential decay follows which goes below the ambient pressure and finally the ambient pressure is reached asymptotically from below, compare Fig. 6.10.

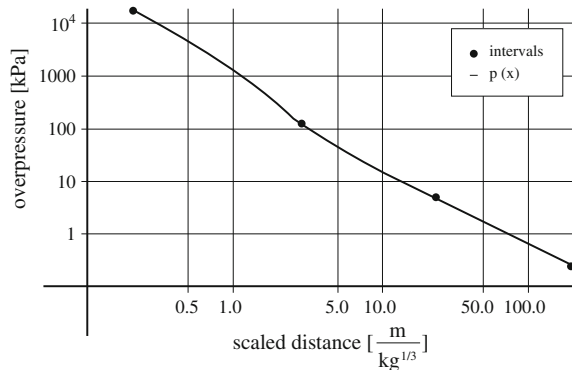
Remark One should keep in mind that all parameters except for the ambient pressure depend on the given scaled distance x .

Integrating the difference between the pressure $p(t)$ and the ambient pressure $p_0 = p(t_a + T^+)$ from the time point of maximum overpressure to the time point of ambient pressure defines the blast impulse (impulse per area, compare with (6.2)):

Table 8.1 Parameters for side-on overpressure (Swisdak 1994)

i	Scaled distance [$\text{m/kg}^{1/3}$]	c_{i0} [-]	c_{i1} [-]	c_{i2} [-]	c_{i3} [-]	c_{i4} [-]
0	[0.2, 2.9]	7.2106	-2.1069	-0.32290	0.1117	0.0685
1	[2.9, 23.8]	7.5938	-3.0523	0.40977	0.0261	-0.01267
2	[23.8, 198.5]	6.0536	-1.4066	0	0	0

Fig. 8.1 Side-on overpressure over scaled distance in double-logarithmic scale (Aschmoneit et al. 2009) according to (Kingery and Bulmash 1984; Swisdak 1994, 2001)



$$I = \int_{t_a}^{t_a + T_+} (p(t) - p_0) dt, \quad [I] = \frac{\text{kg}}{\text{ms}}. \quad (8.2)$$

The blast impulse is the area-specific impulse of the pressure phase and hence has the units of impulse per area.

Remark Again, one should keep in mind that the blast impulse depends on the given scaled distance, that is, I can be seen as a function $I(x)$.

For the scaled blast impulse we have from (Swisdak 1994) the same formal expression as in (8.1), that is,

$$I_s(x) = \exp\left(\sum_{j=0}^4 c_{ij} \left(\ln\left(\frac{x}{\text{m}/\text{kg}^{1/3}}\right)\right)^j\right), \quad x \in [a_i, b_i], [I_s] = \frac{\text{kg}^{2/3}}{\text{ms}}$$

but with coefficients taken from Table 8.2 instead of Table 8.1. From Fig. 8.2 we see that we have locally, with respect to the scaled distance, a unique and invertible relationship between the scaled distance and the scaled blast impulse. In practice, most person damage models work with the overpressure.

For TNT,

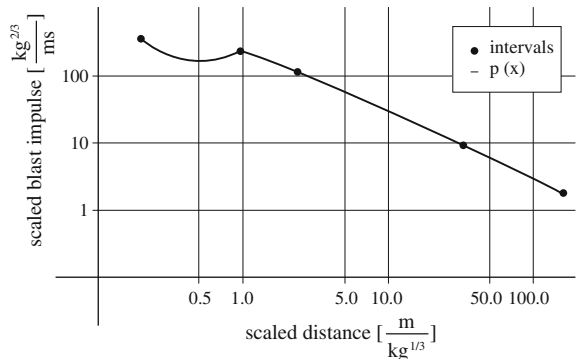
$$I(x) = m^{1/3} I_s(x) \quad [I] = \frac{\text{kg}}{\text{ms}}. \quad (8.3)$$

For other explosives TNT equivalents are necessary, see Sect. 8.3.

Table 8.2 Parameters for blast impulse (Swisdak 1994)

i	Scaled distance [$\text{m}/\text{kg}^{1/3}$]	c_{i0} [-]	c_{i1} [-]	c_{i2} [-]	c_{i3} [-]	c_{i4} [-]
0	[0.2, 0.96]	5.5220	1.1170	0.6000	-0.2920	-0.08700
1	[0.96, 2.38]	5.4650	-0.3080	-1.4640	1.3620	-0.43200
2	[2.38, 33.7]	5.2749	-0.4677	-0.2499	0.0588	-0.00554
3	[33.7, 158.7]	5.9825	-1.0620	0	0	0

Fig. 8.2 Scaled blast impulse over scaled distance in double-logarithmic scale (Aschmoneit et al. 2009) according to (Kingery and Bulmash 1984; Swisdak 1994, 2001)



8.3 TNT Equivalent for Overpressure and Blast: Examples of the Computation of Overpressure and Blast Impulse

If we want to compute the overpressure or blast impulse for a given distance and high explosive other than TNT we use the scaling factors

$$\lambda_{p,\bullet} = m_{p,TNT}/m_\bullet, \quad \lambda_{I,\bullet} = m_{I,TNT}/m_\bullet, \quad (8.4)$$

where m_\bullet is the net explosive quantity of the high explosive, $m_{p,TNT}$ is the *TNT equivalent* mass for overpressure computations and $m_{I,TNT}$ is the TNT equivalent mass for blast impulse computations.

Hence, we have different scaling factors depending whether we want the TNT equivalent for the overpressure or the blast impulse. Scaling factors for some high explosives are given in Table 8.3. For example for 3 kg PETN we obtain for the overpressure in a distance of 2 m

$$\begin{aligned}
 p(x) &= p\left(r/(\lambda_{p,PETN}m_{PETN})^{1/3}\right) \\
 &= p\left(2m/(1.27 \cdot 3 \text{ kg})^{1/3}\right) \\
 &= \exp\left(\sum_{j=0}^4 c_j \left(\ln\left(1.28053 \text{ m/kg}^{1/3}\right)\right)^j\right) \quad i = 0 \\
 &= \exp\left(7.2106 - 2.1069 \cdot \ln(1.28053) - 0.32290 \cdot (\ln(1.28053))^2 \right. \\
 &\quad \left. + 0.1117 \cdot (\ln(1.28053))^3 + 0.0685 \cdot (\ln(1.28053))^4\right) \\
 &= 789.84 \text{ kPa}.
 \end{aligned} \quad (8.5)$$

Equation (8.5) shows that for a given distance and high explosive from Table 8.3 we can compute the overpressure.

Table 8.3 TNT equivalent weight factors for free air effects (AASTP-1 2010), based on (NATO Group of Experts on the Safety Aspects of Transportation and Storage of Mil. Ammo and Explosives 1976; USA WES/CoE 1986; Drake et al. 1989)

Material	Peak pressure equivalent mass	Impulse equivalent mass	Pressure range (MPa)
ANFO (9416 Am/Ni/Fuel oil)	0.82	0.82	0.007–0.700
Composition A-3	1.09	1.07	0.035–0.350
Composition B	1.11	0.98	0.035–0.350
Composition C-4	1.37	1.19	0.070–0.700
Cyclotol 70/30 (RDX/TNT)	1.14	1.09	0.035–0.350
Comp B/TiH ₂ 70/30	1.13	1.13	–
Explosive D	0.85	0.81	–
HBX-1	1.17	1.16	0.035–0.140
HBX-3	1.14	0.97	0.035–0.176
H-6	1.38	1.15	0.035–0.700
Minol II	1.20	1.11	0.021–0.140
Octol 70/30 (HMX/TNT)	1.06	1.06	Estimated
Octol 75/25	1.06	1.06	Estimated
Pentolite	1.42	1.00	0.035–0.700
Pentolite	1.38	1.14	0.035–4.219
PETN	1.27	–	0.035–0.700
Picratol	0.90	0.93	–
RDX	1.14	1.09	–
RDX/5 Wax	1.19	1.16	–
RDX/Wax 98/2	1.19	1.16	–
Tetryl	1.07	–	0.021–0.140
Tetrytol 75/25 (TETRYL/TNT)	1.06	–	Estimated
Tetrytol 70/30	1.06	–	Estimated
Tetrytol 65/35	1.06	–	Estimated
TNETB	1.36	1.10	0.035–0.700
TNT	1.00	1.00	Standard
Torpex II	1.23	1.28	–
TRITONAL 80/20	1.07	0.96	0.035–0.700

For instance, there is also an online tool available to compute blast parameters (United Nations 2015). It is based on (United Nations Department of Economical and Social Affairs 2013).

In summary, for the free field case we can characterize the blast damage hazard in terms of overpressure and blast impulse. These quantities can be computed in real distances as well as in scaled distances.

Most common damage models either depend on overpressure or, much more seldom, blast impulse alone. Hence, we can express such models for the free field geometry in terms of the physical sizes, in terms of the scaled distance or in terms of the real distance and the TNT equivalent masses, taking the discussed inversion options of (6.3) and (8.4) into account.

8.4 Determination of Complex Blast Hazard with Scaled Experiments

Free field conditions as indicated in Fig. 6.4 are not fulfilled in case of urban environments, explosive events within transportation infrastructure or within buildings or vehicles. Such scenarios are typical for terror events with high explosives.

For non-ideal geometries on the one hand one has confinement effects which lead to an increase of overpressure and blast impulse. On the other hand one has venting and shielding effects that lead to a decrease of overpressure and blast. For example, in tunnels the blast overpressure and blast impulse decay much slower than in free field due to the essentially 1D expansion when compared to the 3D expansion.

In addition, superposition of primary and reflected blast waves lead to complex patterns. Also resonance like effects occur. In summary, in case of complex blast increasing distance does not lead to decreasing blast load, at least locally.

For the determination of complex blast loading, the following options exist: full scale experiments, scaled experiments, numerical simulation and engineering approximations.

For rough estimates one often assumes for instance that the blast overpressure increases by a factor of 2 in case of complex geometries.

Figure 8.3 shows a typical experimental set up for scaled experiments. In this case urban geometries were built: straight streets, crossings, T-junctions, and dead-end streets.

For a representative pressure gauge we see a second overpressure phase that is not present in the case of free field propagation, see Fig. 8.4. In summary, the shape of the pressure-time history and the characteristic blast sizes change significantly if the geometry changes from free field to other geometries. Only for special simplified geometries (e.g. tube, free air) again analytical expressions for the loading can be derived. For non-ideal cases, if one is interested in the precise loading, one uses (scaled) experiments or numerical simulation.

Referring to Sect. 6.7, we see that the scaled experiments use Hopkinson-Cranz scaling.

Another example is shown in Fig. 8.5: separated building blocks. Experimental data are:

- Scale 1:20
- TNT equivalent mass 50 g (400 kg) and
- Distance of load in front of center of building to building 1.5 m (30 m)

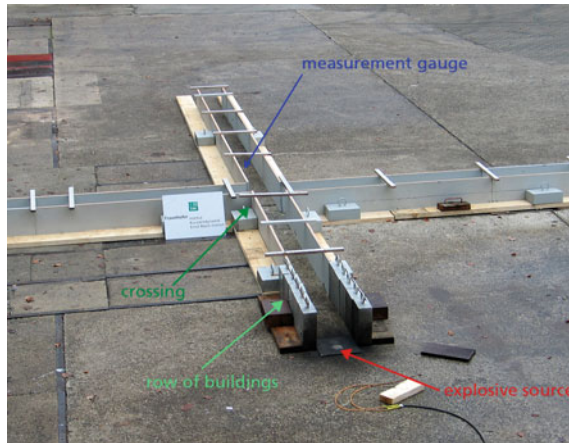


Fig. 8.3 Street crossing geometry with buildings along the street frontage. The load is placed at the beginning of a straight street. The measurement gauge is placed after the street crossing. Close to the load heavy model components are used to prevent them from being blown away by the blast. The scaling factor was 1:40 (Dörr and Frick 2006)

Fig. 8.4 Pressure time history at selected pressure gauge. See Fig. 8.3

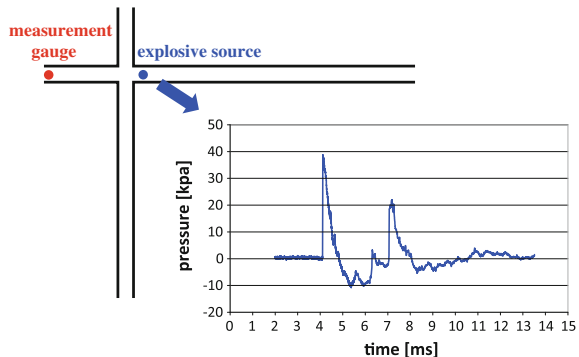
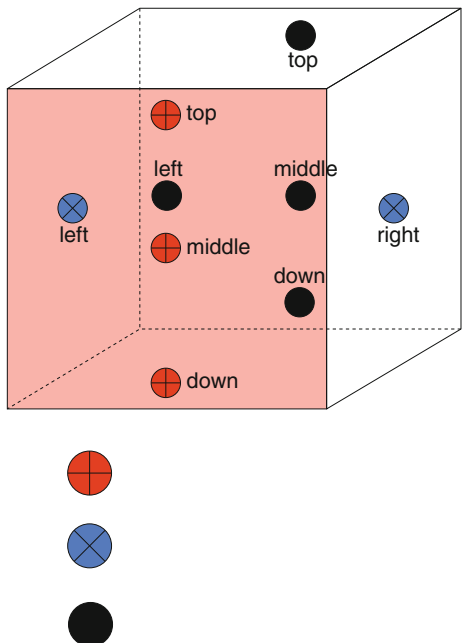


Fig. 8.5 Straight street with separated building blocks. The grey box is instrumented. The load is located in front of the building (Brombacher et al. 2009)



Fig. 8.6 The position of the gauges is indicated by the symbols. Crosses with a vertical and a horizontal line are at the front of the building, crosses with two diagonal lines are at the two sides, and filled circles are at the back of the cuboid



Similar experiments are described in (Dörr et al. 2004). A typical positioning of measurement gauges is shown in Fig. 8.6.

Figures 8.7 and 8.8 show nicely the reflected wave in case of the front side. They show up to one significant second wave. In almost all cases (but the back side wall of Fig. 8.10) the first peak is dominating (Fig. 8.9). Figures 8.6–8.10 are taken from a series of scaled experiments to validate a blast solver, which started with a report by Dörr et al. (2007). The Figures only give an overview for a single selected overall street geometry. In a similar way also much more refined urban local geometries (housing constellations) and indoor scenarios were validated.

8.4.1 Determination of Complex Blast Engineering Scaling Factors from Scaled Experiments

In this section we want to give an example how empirical scaling factors are determined for blast overpressure.

In the project experiments were done where the blast was measured for free field and for urban situations for different distances in 1/40 model tests.

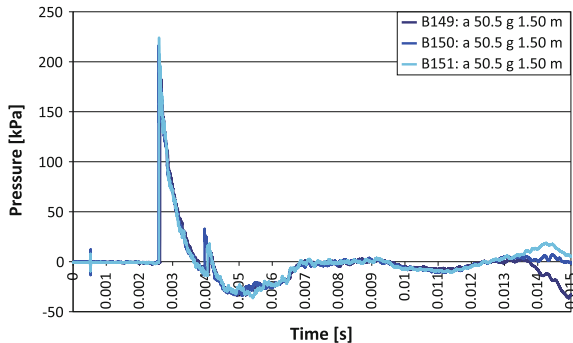


Fig. 8.7 Measure gauge at bottom of front side. See Fig. 8.6 for the geometry. Three experimental curves are depicted showing the reproducibility of the results: x-axis shows time, y-axis pressure

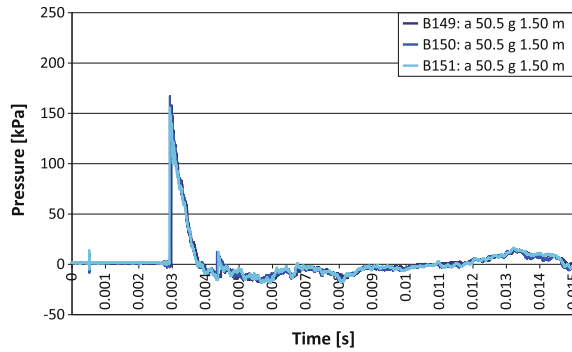


Fig. 8.8 Measure gauge at top of front side. See Fig. 8.6 for the geometry. Axes show time and pressure

“The experimentally measured free field pressure is used to define factors that reproduce the effects of the city environment. These factors are the quotients of the averaged city blast pressure and the averaged free field pressure of each time interval. They are computed for all given geometries, distances and time intervals (Dörr et al. 2004).”

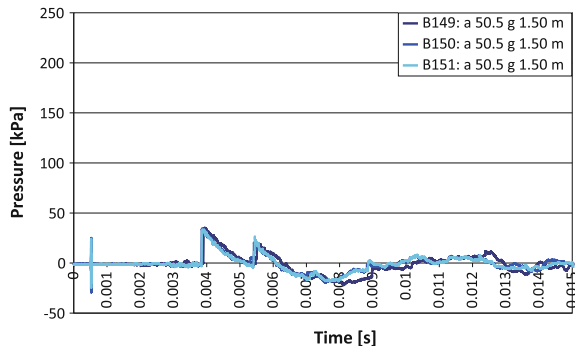


Fig. 8.9 Measure gauge at center of right hand side. See Fig. 8.6 for the geometry. Axes show time and pressure

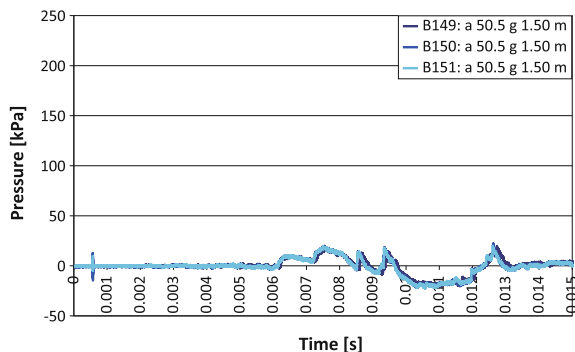


Fig. 8.10 Measure gauge at bottom of back side. See Fig. 8.6 for the geometry. Axes show time and pressure

8.5 Summary and Outlook

In this chapter we have seen an introduction to blast based on a very famous and classical reference, namely (Kingery and Bulmash 1984). For explosions of TNT the maximum overpressure and the blast impulse were expressed in terms of the scaled distance. The TNT equivalent was introduced to use the same formulas for other types of explosives.

Scaled experiments from the Fraunhofer Ernst-Mach-Institute were presented where the blast wave was analyzed in different situations, for example in a street.

In the next chapter we will study the mathematical basics that are needed for the damage analysis. In this way we can concentrate on the analysis itself in the later chapters.

8.6 Questions

- (1) What does free field mean in the context of explosions?
- (2) How does different experimental data for different loads for free field propagation become comparable in one graphic?
- (3) With which methods can one express arbitrary curves with comparably few parameters?
- (4) What are advantage factors and scaling factors used when estimating complex blast effects?
- (5) When does complex blast arise?
- (6) Which geometries are especially critical for focusing effects?
- (7) What is meant by scaled experiments?
- (8) Which methods can be used to quantify complex blast?

References

- AASTP-1 (2010). Manual of NATO Safety Principles for the Storage of Military Ammunition and Explosives, AASTP-1, Edition 1, Change 3. May 2010. Nato Standardization Organization (NSO).
- Aschmoneit, T., Richter, C., Gürke, G., Brombacher, B., Ziehm, J., & Häring, I. (2009). *Parameterization of consequences of explosions: European safety and reliability conference (ESREL), Prague* (pp. 1071–1077). London: Czech Republic., Taylor and Francis Group.
- Brombacher, B., Gürke, G., Brugger, W., & Häring, I. (2009). Experimentelle Validierung des "Blastsolver Modells" 2008. Fraunhofer EMI, E 08/09.
- Drake, J. L., Twisdale, R. A., Frank, W. C., & Dass, C. E. (1989). Protective construction design manual/ESL-TR-87-57 final report. Tyndall AFB, FL, AFESC/Engineering & Services Laboratory.
- Dörr, A., & Frick, J. (2006). Grundlagen der städtebaulichen Gefährdungsanalyse final. Presentation slides.
- Dörr, A., Brombacher, B., & Gürke, G. (2004). Blast behind street junctions... MABS 2004.
- Dörr, A., Gürke, G., & Brugger, W. (2007). Validation experiments for blast solver. Fraunhofer EMI report.
- Kingery, C. N., & Bulmash, G. (1984). *Airblast parameters from TNT spherical air bursts and hemispherical surface bursts*. Maryland, US: Aberdeen Proving Ground.
- Mil. Ammo and Explosives (1976). Manual on NATO safety principles for the storage of ammunition and explosives 1976/77/AC/258-D/258. Brussels, Belgium.
- Swisdak, M. M. Jun. (1994). Simplified Kingery airblast calculations. Proceedings of the 26th Department of Defense (DoD) Explosives Safety Seminar, Miami, Florida, US.
- Swisdak, M. M. (2001). The determination of explosion yield/TNT equivalence from Airblast Data, Indian Head Devision/Naval Surface Warfare Center.

- United Nations. (2015). Kingery-Bulmash Blast Parameter Calculator. Retrieved August 21, 2015 from <http://www.un.org/disarmament/un-saferguard/kingery-bulmash/>
- United Nations Department of Economical and Social Affairs. (2013). Population division, population estimates and projections section. Retrieved June 14, 2013 from <http://esa.un.org/unpd/wpp/unpp/p2k0data.asp>
- USA WES/CoE (1986). TM 5-855-1 Fundamental of protective design. Vicksburg, Mississippi.

Chapter 9

Mathematical Basics for Hazard and Damage Analysis

9.1 Overview

This chapter covers basic notations for probabilistic damage assessment as well as for damage assessment using hazard trajectories as introduced in Chap. 7, which are further used in Chaps. 10–12. The aim is to empower the reader to work with such expressions.

From empirical distributions, probability densities and cumulative probability distributions (probabilities) are derived. Expectation value or mean and standard deviation are defined. For illustration of the introduced notations, the most often used distributions for damage assessment are presented: normal and lognormal.

For later use in Chap. 11, in a basic approach, operations with vectors including the scalar product, line and plane equations as well as different types of rotations are introduced. The definitions of Euler and Cardan angles are only indicated. The latter can be used for describing without singularities the six-dimensional movement of objects. Rotations are also needed when relating the coordinate system that is most suited for describing the hazard source to the coordinate systems that are most suited for describing objects at risk or as used for the visualization.

For the damage analysis in the risk analysis process we use mathematical basics, in particular some probability theory and some linear algebra. They are explained here to be able to focus on the damage analysis itself in the following chapters.

Section 9.2 deals with probability theory, especially probability density function and distributions. It is a summary and partial paraphrasation of Häring (2005). Section 9.3 summarizes the rules for the computation with vectors, angles and matrices in \mathbb{R}^3 . A special focus lies on rotation matrices. We present Euler angles and rotations.

The main Fraunhofer EMI source used for this chapter is Häring (2005) with additional work by S. Rathjen.

9.2 Probability Theory

9.2.1 One-dimensional Density Functions: Empirical Density Function and Probability Density Function

In the simplest case, the damage estimate only depends on a single physical parameter. Two examples (for hearing damage) are:

- the maximum overpressure of a blast wave, and
- the scaled distance in case of a free field scenario.

We have seen in Chap. 5 that the maximum overpressure p_0 is the biggest positive pressure of a blast wave, measured relatively to normal pressure:

$$p_0 = \max_{t, p(t) > 0} p(t), \quad [p_0] = \text{Pa}. \quad (9.1)$$

Empirical formulas are available to compute the maximum overpressure (Baker et al. 1983; Kinney and Graham 1985; Humar 2002), see Sect. 7.1.

The scaled distance used here is the real distance over the cubic root of the net explosive quantity (see Sect. 5.2.5),

$$x = r/m^{1/3}, \quad [x] = \text{m/kg}^{1/3}. \quad (9.2)$$

In the following, we denote both sizes by x . It can be understood as in (9.1) or in (9.2).

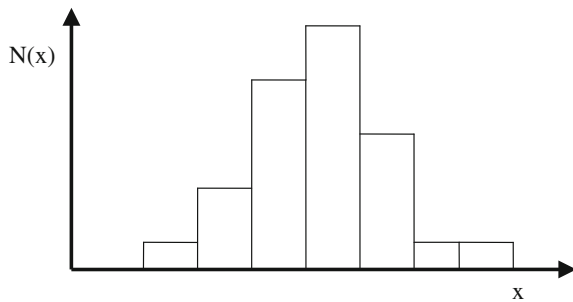
Theoretically, a defined damage level (e.g. structure has to be rebuild, minor ear damage) occurs for an object for a certain minimum value of the physical loading parameter (e.g. maximal overpressure, scaled distance). The maximum information related to a group of objects would be to know this parameter for each object.

In reality, often the best possible information is an interval for the loading parameter the object was exposed to and observed to be damaged according to the selected damage criterion. Note that this does not exclude that it would have been damaged at a lower value of the loading parameter. This of course arises from the typical ex post damage assessment of scenarios. In the following, we assume that the observed damage level belongs to the loading parameter the object was exposed to.

The available information is shown in Fig. 9.1 where for fixed loading parameter intervals the number of damaged objects $N(x)$ is shown. That is, an object is counted in the loading interval the damage can be attributed to. For sufficiently large or low loading parameters, every object will suffer from ear injuries. Hence, adding the heights of the columns yields the total number of objects N_{total} .

If we divide the height of each column in Fig. 9.1 by the total number N_{total} , the resulting step function is a first approximation of the *density function* of the given event (Fisz 1978; Bronstein et al. 1996). A more precise data set would yield a more detailed step function. Imprecisely spoken, the density function can be seen as the

Fig. 9.1 Result of an optimal experiment: empirical density function (Häring 2005)



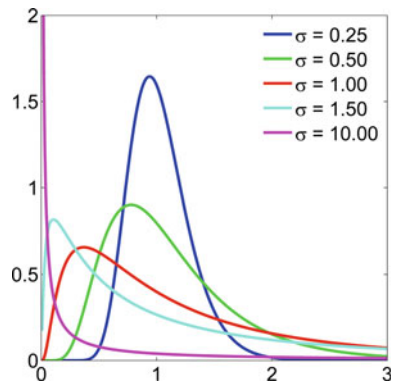
limit of those step functions, which are also called empirical distribution functions, where the length of the loading parameter intervals converges to zero.

From this approach we can already see two properties of the density function. The density function is always non-negative and the integral over all x is 1:

$$\int f(x)dx = 1, \quad f(x) \geq 0. \quad (9.3)$$

Remark From this construction one might wrongly conclude that $f(x) \leq 1$ also holds. This, however, is not true for every density function. Figure 9.2 shows some density functions. Some of them have values bigger than 1. The integral is still one because the interval of the x -axis where the value of the function is bigger than 1 is small enough (in particular, smaller than 1).

Fig. 9.2 Lognormal density functions (Wikipedia 2005), letters in the legend are modified



9.2.2 Probabilities

The density function can be used to compute the probability that x lies in the interval $[a, b]$ by the following equation.

$$P(a \leq x \leq b) = \int_a^b f(x) dx \quad (9.4)$$

In our example,

$$P(0 \leq x \leq b) = \int_0^b f(x) dx \quad (9.5)$$

is the probability that a person has an ear injury for the maximal overpressure b . Often the lower bound of the integral is $-\infty$. Since the maximal overpressure is always positive (see above), this is not necessary here.

Remark An example where the lower bound $-\infty$ is appropriate is the probability that a certain event occurs up to time b .

The probability

$$P(a \leq x \leq \infty) = \int_a^\infty f(x) dx \quad (9.6)$$

can also be interpreted. For this we associate x with the scaled distance. Then (9.6) computes the probability that there is ear damage for a fixed scaled distance a .

Remark We want to emphasize why we use the overpressure in one example and the scaled distance in the other. For the overpressure, if you suffer from ear damage for pressure b , you also suffer from ear damage for any pressure bigger than b . For the scaled distance, it is the opposite: If you suffer from ear damage for scaled distance a , you also suffer from ear damage for any scaled distance smaller than a . Hence, the two different integrals are appropriate.

In general, the integral of the density function from the lower bound of the domain of definition up to a fixed value is called the cumulative distribution function (cdf) (Fisz 1978; Bronstein et al. 1996).

9.2.3 Expectation/Mean and Standard Deviation

In the following chapters the terms expectation or mean and standard deviation will occur several times. The expectation/mean is defined as

$$\mu = \int xf(x)dx \quad (9.7)$$

where we integrate over the whole domain of definition, that is typically from $-\infty$ to ∞ .

The standard deviation is defined as

$$\sigma = \sqrt{\int x^2 f(x)dx - \left(\int xf(x)dx\right)^2}. \quad (9.7)$$

Example The density function for the standard normal distribution is defined as

$$f(x) = \frac{1}{\sqrt{2\pi}} e^{-\frac{x^2}{2}}. \quad (9.8)$$

Computing the mean (first moment) with (9.7) yields

$$\mu = \int_{-\infty}^{\infty} x \frac{1}{\sqrt{2\pi}} e^{-\frac{x^2}{2}} dx = \frac{-1}{\sqrt{2\pi}} \int_{-\infty}^{\infty} -xe^{-\frac{x^2}{2}} dx = \frac{-1}{\sqrt{2\pi}} \left[e^{-\frac{x^2}{2}} \right]_{-\infty}^{\infty} = 0. \quad (9.9)$$

Using the density property $\int f(x)dx = 1$ and integration by parts we compute

$$\begin{aligned} \int_{-\infty}^{\infty} x^2 \frac{1}{\sqrt{2\pi}} e^{-\frac{x^2}{2}} dx &= \int_{-\infty}^{\infty} x \left(x \frac{1}{\sqrt{2\pi}} e^{-\frac{x^2}{2}} \right) dx \\ &= \left[-x \frac{1}{\sqrt{2\pi}} e^{-\frac{x^2}{2}} \right]_{-\infty}^{\infty} - \frac{1}{\sqrt{2\pi}} \int_{-\infty}^{\infty} -e^{-\frac{x^2}{2}} dx = \frac{1}{\sqrt{2\pi}} \int_{-\infty}^{\infty} e^{-\frac{x^2}{2}} dx = 1 \end{aligned} \quad (9.10)$$

for the second moment and with that

$$\sigma = \sqrt{\int_{-\infty}^{\infty} x^2 f(x)dx - \left(\int_{-\infty}^{\infty} xf(x)dx\right)^2} = \sqrt{1 - 0^2} = 1. \quad (9.11)$$

9.2.4 Examples for Density Functions

We list some common examples for density functions

The density function of the *normal* (or *Gaussian*) *distribution* is defined by

$$f_{\mu,\sigma}^N(t) = \frac{1}{\sqrt{2\pi}\sigma} \exp\left(-\frac{(t-\mu)^2}{2\sigma^2}\right). \quad (9.12)$$

The parameters μ and σ are the mean and the standard deviation as defined above. We have seen the special case were $\mu = 0$ and $\sigma = 1$ in the example in Sect. 9.2.3.

The density of the lognormal distribution is defined by

$$f_{a,b}^{LN}(t) = \frac{1}{\sqrt{2\pi}b t} \exp\left(\frac{-(\ln t - a)^2}{2b^2}\right). \quad (9.13)$$

The mean according to Eq. (9.7) is

$$\mu = \exp(a + b^2/2) \quad (9.14)$$

and the standard deviation according to Eq. (9.7) is

$$\sigma = [\exp(2a + 2b^2) - \exp(2a + b^2)]^{1/2}. \quad (9.15)$$

Often the parameters μ and σ are used instead of a and b , respectively. We do not do this here to avoid confusion with the formulas (9.7) and (9.7).

Remark Examples of lognormal density functions were shown in Fig. 9.2.

Further distributions and density functions can for example be found in (Fisz 1978; Bedford and Cooke 2001; Georgii 2004; Klenke 2007) or any (other) introductory book on probability theory.

9.3 Vectors, Planes and Angles in \mathbb{R}^3

9.3.1 Sums, Scalar Product and Angle

A vector in \mathbb{R}^3 is normally expressed by

$$\vec{v} = \begin{pmatrix} v_1 \\ v_2 \\ v_3 \end{pmatrix}. \quad (9.16)$$

The sum of two vectors is computed in the individual components:

$$\vec{v} + \vec{w} = \begin{pmatrix} v_1 \\ v_2 \\ v_3 \end{pmatrix} + \begin{pmatrix} w_1 \\ w_2 \\ w_3 \end{pmatrix} = \begin{pmatrix} v_1 + w_1 \\ v_2 + w_2 \\ v_3 + w_3 \end{pmatrix}. \quad (9.17)$$

The difference is computed similarly.

The multiplication of a number and a vector also happens in the individual components:

$$a \begin{pmatrix} v_1 \\ v_2 \\ v_3 \end{pmatrix} = \begin{pmatrix} av_1 \\ av_2 \\ av_3 \end{pmatrix} \quad (9.18)$$

The length of a vector is computed by

$$|\vec{v}| = \sqrt{v_1^2 + v_2^2 + v_3^2} \quad (9.19)$$

The (standard) scalar product is defined by

$$\langle \vec{v}, \vec{w} \rangle = \left\langle \begin{pmatrix} v_1 \\ v_2 \\ v_3 \end{pmatrix}, \begin{pmatrix} w_1 \\ w_2 \\ w_3 \end{pmatrix} \right\rangle = v_1 w_1 + v_2 w_2 + v_3 w_3. \quad (9.20)$$

Two vectors are orthogonal, that is the angle between them is 90° (or $\pi/2$), if

$$\langle \vec{v}, \vec{w} \rangle = 0. \quad (9.21)$$

In general, the angle between two vectors is computed by

$$\cos \alpha = \frac{\langle \vec{v}, \vec{w} \rangle}{|\vec{v}| |\vec{w}|}. \quad (9.21)$$

Remark $\cos \alpha$ does not yield a unique angle in the interval $[0, 2\pi]$ for $\alpha \neq 0$, compare Figs. 9.3 and 9.4.

In the following, we always take the smaller of the two angles. Then (9.21) is invertible.

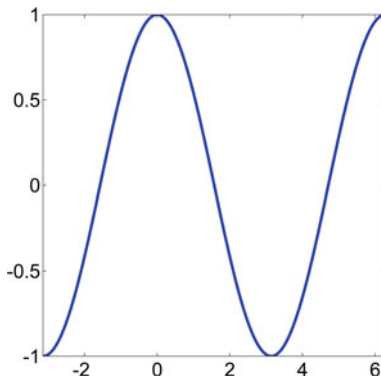


Fig. 9.3 Cosine function

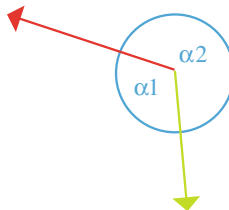


Fig. 9.4 Two vectors and the two angles

9.3.2 Straight Lines

A straight line can be described by

$$\vec{x} = \vec{x}_0 + p\vec{v} \quad (9.22)$$

where \vec{x}_0 is a point in the plane, p a parameter and \vec{v} a vector, see Fig. 9.5.

9.3.3 Planes and Normal Vectors

A plane can be described by

$$E(p, q) = \vec{x}_0 + p\vec{v} + q\vec{w} \quad (9.23)$$

where \vec{x}_0 is a point in the plane, p and q two parameters and \vec{v} and \vec{w} two non-parallel vectors.

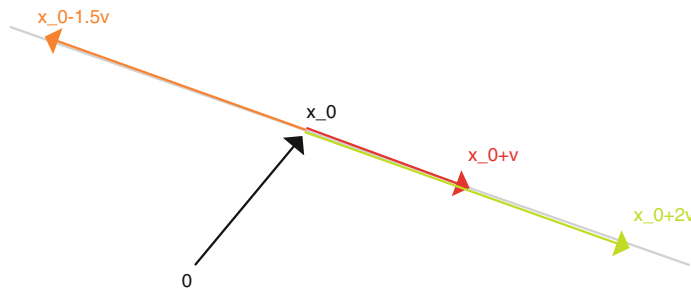


Fig. 9.5 Illustration of (9.22)

A normal vector to the plane is a vector that is orthogonal to the plane, that is, orthogonal to \vec{v} and \vec{w} .

Example A parallel plane to the x-y-plane is

$$E(p, q) = \begin{pmatrix} 3 \\ 4 \\ 2 \end{pmatrix} + p \begin{pmatrix} 1 \\ 0 \\ 0 \end{pmatrix} + q \begin{pmatrix} 0 \\ 1 \\ 0 \end{pmatrix}. \quad (9.24)$$

The vector $\begin{pmatrix} 0 \\ 0 \\ 1 \end{pmatrix}$ is orthogonal to $\begin{pmatrix} 1 \\ 0 \\ 0 \end{pmatrix}$ and $\begin{pmatrix} 0 \\ 1 \\ 0 \end{pmatrix}$ because

$$\left\langle \begin{pmatrix} 1 \\ 0 \\ 0 \end{pmatrix}, \begin{pmatrix} 0 \\ 1 \\ 0 \end{pmatrix} \right\rangle = 1 \cdot 0 + 0 \cdot 0 + 0 \cdot 1 = 0, \quad (9.25)$$

$$\left\langle \begin{pmatrix} 0 \\ 1 \\ 0 \end{pmatrix}, \begin{pmatrix} 0 \\ 0 \\ 1 \end{pmatrix} \right\rangle = 0 \cdot 0 + 1 \cdot 0 + 0 \cdot 1 = 0. \quad (9.26)$$

Hence, $\begin{pmatrix} 0 \\ 0 \\ 1 \end{pmatrix}$ is a normal vector for the plane.

Example The last example was so simple that the solution could be determined by a good guess. This example shows that the computation is only a little more complex for other planes. For this consider

$$E(p, q) = \begin{pmatrix} 3 \\ 5 \\ 4 \end{pmatrix} + p \begin{pmatrix} 6 \\ 3 \\ 2 \end{pmatrix} + q \begin{pmatrix} 8 \\ 1 \\ 7 \end{pmatrix}. \quad (9.27)$$

For a vector orthogonal to the plane the following two equations must hold:

$$\left\langle \begin{pmatrix} 6 \\ 3 \\ 2 \end{pmatrix}, \begin{pmatrix} v_1 \\ v_2 \\ v_3 \end{pmatrix} \right\rangle = 6v_1 + 3v_2 + 2v_3 = 0, \quad (9.28)$$

$$\left\langle \begin{pmatrix} 8 \\ 1 \\ 7 \end{pmatrix}, \begin{pmatrix} v_1 \\ v_2 \\ v_3 \end{pmatrix} \right\rangle = 8v_1 + 1v_2 + 7v_3 = 0 \quad (9.29)$$

Subtracting two times (9.29) from (9.28) yields

$$-18v_1 - 19v_3 = 0, \quad (9.30)$$

that is,

$$v_3 = -\frac{18}{19}v_1. \quad (9.31)$$

Plugging this into (9.28) yields

$$6v_1 + 3v_2 - \frac{18}{19}v_1 = 0, \quad (9.32)$$

that is,

$$v_2 = -1\frac{13}{19}v_1. \quad (9.33)$$

To determine a normal vector, an arbitrary number can be chosen for v_1 . For $v_1 = 1$ the normal vector is

$$\vec{v} = \begin{pmatrix} 1 \\ -1\frac{13}{19} \\ -\frac{18}{19} \end{pmatrix}. \quad (9.34)$$

One often uses normalized normal vectors, that is, a normal vector of length one. It is computed by dividing every component of \vec{v} by the length of \vec{v} , in our case

$$|\vec{v}| = \sqrt{1^2 + \left(-1\frac{13}{19}\right)^2 + \left(-\frac{18}{19}\right)^2} \approx 2.176 \quad (9.35)$$

and

$$\tilde{\vec{v}} = \frac{1}{|\vec{v}|} \vec{v} \approx \frac{1}{2.176} \begin{pmatrix} 1 \\ -1\frac{13}{19} \\ -\frac{18}{19} \end{pmatrix} \approx \begin{pmatrix} 0.460 \\ -0.774 \\ -0.435 \end{pmatrix}. \quad (9.36)$$

Remark The normalized normal vector is not unique, $-\tilde{\vec{v}}$ is the other normal vector of length 1.

9.3.4 Matrices

We will use matrices to describe rotations in \mathbb{R}^3 , see Sect. 9.3.5. In preparation of that section this section is a reminder of how multiplying a matrix with a vector or with another matrix works. Since all matrices will be in \mathbb{R}^3 and since the scheme can be easily extended to bigger matrices, the following matrices will be of size 3×3 .

Let $\overrightarrow{L1}$, $\overrightarrow{L2}$ and $\overrightarrow{L3}$ denote the vectors with the entries of the three lines of the matrix and $\overrightarrow{C1}$, $\overrightarrow{C2}$ and $\overrightarrow{C3}$ the three column vectors. For example regard

$$\begin{pmatrix} 1 & 6 & 3 \\ 4 & 8 & 0 \\ 5 & 2 & 7 \end{pmatrix}, \quad (9.37)$$

Then

$$\begin{aligned} \overrightarrow{L1} &= \begin{pmatrix} 1 \\ 6 \\ 3 \end{pmatrix}, \overrightarrow{L2} = \begin{pmatrix} 4 \\ 8 \\ 0 \end{pmatrix}, \overrightarrow{L3} = \begin{pmatrix} 5 \\ 2 \\ 7 \end{pmatrix}, \overrightarrow{C1} = \begin{pmatrix} 1 \\ 4 \\ 5 \end{pmatrix}, \overrightarrow{C2} = \begin{pmatrix} 6 \\ 8 \\ 2 \end{pmatrix}, \\ \overrightarrow{C3} &= \begin{pmatrix} 3 \\ 0 \\ 7 \end{pmatrix}. \end{aligned}$$

Then the multiplication of a matrix $\underline{\underline{M}}$ and a vector \vec{v} is defined by

$$\underline{\underline{M}}\vec{v} = \begin{pmatrix} \langle \overrightarrow{L1}, \vec{v} \rangle \\ \langle \overrightarrow{L2}, \vec{v} \rangle \\ \langle \overrightarrow{L3}, \vec{v} \rangle \end{pmatrix} \quad (9.38)$$

and the multiplication of two matrices $\underline{\underline{M}}$ and $\underline{\underline{N}}$ is defined by

$$\underline{\underline{MN}} = \begin{pmatrix} \left\langle \overrightarrow{L_M 1}, \overrightarrow{C_N 1} \right\rangle & \left\langle \overrightarrow{L_M 1}, \overrightarrow{C_N 2} \right\rangle & \left\langle \overrightarrow{L_M 1}, \overrightarrow{C_N 3} \right\rangle \\ \left\langle \overrightarrow{L_M 2}, \overrightarrow{C_N 1} \right\rangle & \left\langle \overrightarrow{L_M 2}, \overrightarrow{C_N 2} \right\rangle & \left\langle \overrightarrow{L_M 2}, \overrightarrow{C_N 3} \right\rangle \\ \left\langle \overrightarrow{L_M 3}, \overrightarrow{C_N 1} \right\rangle & \left\langle \overrightarrow{L_M 3}, \overrightarrow{C_N 2} \right\rangle & \left\langle \overrightarrow{L_M 3}, \overrightarrow{C_N 3} \right\rangle \end{pmatrix}. \quad (9.39)$$

Remark The matrix-product is not commutative, that is, $\underline{\underline{MN}} \neq \underline{\underline{NM}}$.

Example Two exemplary multiplications are

$$\begin{pmatrix} 1 & 6 & 3 \\ 4 & 8 & 0 \\ 5 & 2 & 7 \end{pmatrix} \begin{pmatrix} 1 \\ 0 \\ 2 \end{pmatrix} = \begin{pmatrix} 1 \cdot 1 + 6 \cdot 0 + 3 \cdot 2 \\ 4 \cdot 1 + 8 \cdot 0 + 0 \cdot 0 \\ 5 \cdot 1 + 2 \cdot 0 + 7 \cdot 2 \end{pmatrix} = \begin{pmatrix} 7 \\ 4 \\ 19 \end{pmatrix}, \quad (9.40)$$

$$\begin{pmatrix} 1 & 6 & 3 \\ 4 & 8 & 0 \\ 5 & 2 & 7 \end{pmatrix} \begin{pmatrix} 1 & 0 & 1 \\ 0 & 5 & 1 \\ 2 & 0 & 1 \end{pmatrix} = \begin{pmatrix} 1+0+6 & 0+30+0 & 1+6+3 \\ 4+0+0 & 0+40+0 & 4+8+0 \\ 5+0+14 & 0+10+0 & 5+2+7 \end{pmatrix} \quad (9.41) \\ = \begin{pmatrix} 7 & 30 & 10 \\ 4 & 40 & 12 \\ 19 & 10 & 14 \end{pmatrix}.$$

9.3.5 Rotation Matrices

We want to introduce the three matrices that describe the (counter-clockwise, see) rotation around the axes.

$$\underline{\underline{R}} = \begin{pmatrix} \cos \theta & -\sin \theta & 0 \\ \sin \theta & \cos \theta & 0 \\ 0 & 0 & 1 \end{pmatrix} \quad (9.42)$$

describes the rotation around the z-axis (Fig. 9.6).

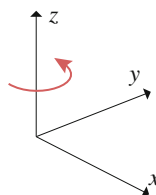


Fig. 9.6 Counter-clockwise rotation around the z-axis, see e.g. (Wikipedia 2013b)

Example If the vector $\begin{pmatrix} 1 \\ 2 \\ 3 \end{pmatrix}$ is rotated by 30° around the z-axis, the resultant vector after the rotation is

$$\begin{pmatrix} \cos 30^\circ & -\sin 30^\circ & 0 \\ \sin 30^\circ & \cos 30^\circ & 0 \\ 0 & 0 & 1 \end{pmatrix} \begin{pmatrix} 1 \\ 2 \\ 3 \end{pmatrix} = \begin{pmatrix} \frac{\sqrt{3}}{2} & -\frac{1}{2} & 0 \\ \frac{1}{2} & \frac{\sqrt{3}}{2} & 0 \\ 0 & 0 & 1 \end{pmatrix} \begin{pmatrix} 1 \\ 2 \\ 3 \end{pmatrix} \approx \begin{pmatrix} -0.134 \\ 2.232 \\ 3 \end{pmatrix}. \quad (9.43)$$

The counter-clockwise rotation around the x-axis is described by

$$\underline{\underline{R}}_x = \begin{pmatrix} 1 & 0 & 0 \\ 0 & \cos \theta & -\sin \theta \\ 0 & \sin \theta & \cos \theta \end{pmatrix} \quad (9.44)$$

and the rotation around the y-axis by

$$\underline{\underline{R}}_y = \begin{pmatrix} \cos \theta & 0 & \sin \theta \\ 0 & 1 & 0 \\ -\sin \theta & 0 & \cos \theta \end{pmatrix}. \quad (9.45)$$

9.4 Euler Angles

Rotation matrices were introduced in Sect. 9.3.5. Also, we have seen that different coordinate systems are useful depending on the context, see Sect. 6.2. In this section we introduce Euler angles and Cardan angles which are related to both.

Euler angles are three angles with which one can describe the rotation of an object into any position (with the same center), see Fig. 9.7.

An introduction to Euler angles is given in University of Arizona (2008b). A variation of Euler angles are the so called Cardan angles or Tait-Bryan angles (University of Arizona 2008a). One can compute Euler angles from a rotation matrix (Slabaugh 2015).

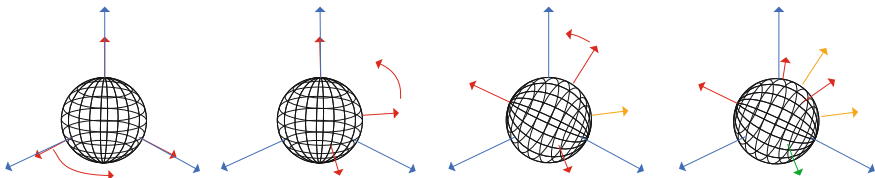


Fig. 9.7 The arrows indicate how a figure can be rotated around three angles to get into any arbitrary position, picture modified from Wikipedia (2013a). Here the first angle describes the rotation around the z-axis, then around the new x-axis and last around the new z-axis. It is called the z-x-z convention of Euler angles

9.5 Summary and Outlook

In this chapter we have seen a selection of mathematical tools. They are not a complete description of the tools available in the discussed area but exactly the ones needed in the following chapters. More precisely, the chapter explained how

- probability densities are defined and constructed,
- probability densities are used to compute means and standard deviations,
- vectors are added and subtracted,
- scalar products and angles are computed,
- orthogonality is defined,
- parameter forms of planes are determined,
- normal vectors are computed,
- a matrix is multiplied with a vector,
- matrices are multiplied with each other,
- rotation matrices are set up and used, and
- Euler and Cardan angles are introduced.

In the next chapter the risk analysis step “damage analysis” is introduced. The focus lies on probability distributions and probit functions.

9.6 Questions

1. Regard the density function $f_{0,1}^{\ln}(t) = \frac{1}{\sqrt{2\pi t}} \exp\left(\frac{-(\ln t)^2}{2}\right)$.
 - (a) Compute the probability $P(0 \leq X \leq 1)$ where X is a random variable distributed according to $f_{0,1}^{\ln}$.
 - (b) Compute the mean μ .
 - (c) Compute the standard deviation σ .
 - (d) Compare your results from (b) and (c) with the Eqs. (9.14) and (9.15).
 - (e) Is the density function ever greater than 1? Compute and compare to Fig. 9.2.
 - (f) Interpret the difference between $f_{0,1}^{\ln}$ and $f_{0,1/8}^{\ln}$ using Fig. 9.2 in the case that the density function describes the injuries in terms of scaled distance.
2. Given two vectors $\vec{w}_1 = \begin{pmatrix} 1 \\ 2 \\ 4 \end{pmatrix}$ and $\vec{w}_2 = \begin{pmatrix} 0 \\ 3 \\ 1 \end{pmatrix}$.
 - (a) Compute $\vec{w}_1 + \vec{w}_2$, $\vec{w}_1 - \vec{w}_2$, $\langle \vec{w}_1, \vec{w}_2 \rangle$ and the angle between \vec{w}_1 and \vec{w}_2 .
 - (b) Which first coordinate would \vec{w}_2 have to have for the angle between the vectors to be 90° ?
 - (c) What is an equation of the plane through the origin that is spanned by \vec{w}_1 and \vec{w}_2 ? What are the two normal vectors to this plane of length 1?

- (d) Which vector does one get by rotating $\begin{pmatrix} 1 \\ 0 \\ 0 \end{pmatrix}$ by 30° around the z-axis and then 45° around the y-axis? Is the result different if one rotates the vector first around the y-axis and then around the z-axis?

9.7 Answers

1.

- (a) By substituting $t = e^z$ one gets

$$\begin{aligned} P(0 \leq X \leq 1) &= \int_0^1 \frac{1}{\sqrt{2\pi t}} \exp\left(\frac{-(\ln t)^2}{2}\right) dt \\ &= \int_{-\infty}^0 \frac{1}{\sqrt{2\pi e^z}} \exp\left(\frac{-z^2}{2}\right) e^z dz = \frac{1}{2} \end{aligned} \tag{9.46}$$

- (b) Again, the substitution $t = e^z$ and $u = z - 1$ are used in the computation.

$$\begin{aligned} \mu &= \int_0^\infty \frac{1}{\sqrt{2\pi}} \exp\left(\frac{-(\ln t)^2}{2}\right) dt \\ &= \int_{-\infty}^\infty \frac{1}{\sqrt{2\pi}} \exp\left(\frac{-z^2}{2}\right) e^z dz \\ &= \int_{-\infty}^\infty \frac{1}{\sqrt{2\pi}} \exp\left(\frac{-z^2 + 2z}{2}\right) dz \\ &= \int_{-\infty}^\infty \frac{1}{\sqrt{2\pi}} \exp\left(\frac{-(z-1)^2 + 1}{2}\right) dz \\ &= \int_{-\infty}^\infty \frac{1}{\sqrt{2\pi}} \exp\left(\frac{-u^2 + 1}{2}\right) du \\ &= e^{1/2} \int_{-\infty}^\infty \frac{1}{\sqrt{2\pi}} \exp\left(\frac{-u^2}{2}\right) du = e^{1/2}. \end{aligned} \tag{9.47}$$

We used that $\frac{1}{\sqrt{2\pi}} \int_{-\infty}^{\infty} \exp\left(\frac{-x^2}{2}\right) dx = 1$ (normal distribution). In order to use this, the method “completing the square” was necessary (from the third to the fourth line).

- (a) σ is computed similarly to μ with the substitutions $t = e^z$ and $u = z - 2$ and the method completing the square.

$$\begin{aligned}
 \sigma &= \sqrt{\int_0^\infty t^2 f(t) dt - \mu^2} \\
 &= \sqrt{\int_0^\infty \frac{t^2}{\sqrt{2\pi t}} \exp\left(\frac{-(\ln t)^2}{2}\right) dt - (e^{1/2})^2} \\
 &= \sqrt{\int_0^\infty \frac{t}{\sqrt{2\pi}} \exp\left(\frac{-(\ln t)^2}{2}\right) dt - e} \\
 &= \sqrt{\int_{-\infty}^\infty \frac{e^z}{\sqrt{2\pi}} \exp\left(\frac{-z^2}{2}\right) e^z dz - e} \\
 &= \sqrt{\int_{-\infty}^\infty \frac{1}{\sqrt{2\pi}} \exp\left(\frac{-z^2 + 4z}{2}\right) dz - \mu^2} \\
 &= \sqrt{\int_{-\infty}^\infty \frac{1}{\sqrt{2\pi}} \exp\left(\frac{-(z-2)^2 + 4}{2}\right) dz - e} \\
 &= \sqrt{\int_{-\infty}^\infty \frac{e^2}{\sqrt{2\pi}} \exp\left(\frac{-u^2}{2}\right) du - e} \\
 &= \sqrt{e^2 - e}
 \end{aligned} \tag{9.48}$$

- (b) The results match with the results from (9.14) and (9.15) for $a = 0$ and $b = 1$.
(c) To find out whether the density function is ever greater than 1, we compute its maximum.

$$\begin{aligned} 0 = f'(t) &= -\frac{1}{\sqrt{2\pi t^2}} e^{-0.5(\ln t)^2} + \frac{1}{\sqrt{2\pi t}} e^{-0.5(\ln t)^2} \left(-\frac{2}{2t} \ln t \right) \\ &= \left(-\frac{1}{\sqrt{2\pi t^2}} - \frac{\ln t}{\sqrt{2\pi t^2}} \right) \underbrace{e^{-0.5(\ln t)^2}}_{\neq 0} \end{aligned} \quad (9.49)$$

So, $-1 - \ln t = 0$ has to hold, that is, $t = e^{-1}$.

$$f(e^{-1}) \approx 0.658 \quad (9.50)$$

and hence smaller than 1.

To show that we computed a maximum (and not a minimum) we compute

$$\begin{aligned} f(e^{-1} - 0.1) &\approx 0.625 \\ f(e^{-1} + 0.1) &\approx 0.639 \end{aligned} \quad (9.51)$$

Remark If Excel is used to compute the function values, one has to compute $-(\dots)^2$ has to be used instead of $-(\dots)^2$ to get correct results because -4^2 is understood as $(-4)^2$ by the software and hence yields an incorrect sign.

2.

$$(a) \quad \vec{w}_1 + \vec{w}_2 = \begin{pmatrix} 1 \\ 5 \\ 5 \end{pmatrix} \quad (9.52)$$

$$\vec{w}_1 - \vec{w}_2 = \begin{pmatrix} 1 \\ -1 \\ 3 \end{pmatrix} \quad (9.53)$$

$$\langle \vec{w}_1, \vec{w}_2 \rangle = 1 \cdot 0 + 2 \cdot 3 + 4 \cdot 1 = 10 \quad (9.54)$$

$$\cos \alpha = \frac{10}{\sqrt{1+4+16}\sqrt{9+1}} = \frac{10}{\sqrt{210}} \quad (9.55)$$

and $\alpha \approx 46.37^\circ$.

$$(b) \quad 1 \cdot x + 2 \cdot 3 + 4 \cdot 1 = 0 \Rightarrow x = -10 \quad (9.56)$$

- (c) The plane has the equation

$$\vec{x} = p \begin{pmatrix} 1 \\ 2 \\ 4 \end{pmatrix} + q \begin{pmatrix} 0 \\ 3 \\ 1 \end{pmatrix} \quad (9.57)$$

The normal vectors are computed by $\left\langle \begin{pmatrix} a \\ b \\ c \end{pmatrix}, \begin{pmatrix} 1 \\ 2 \\ 4 \end{pmatrix} \right\rangle = 0$ and $\left\langle \begin{pmatrix} a \\ b \\ c \end{pmatrix}, \begin{pmatrix} 0 \\ 3 \\ 1 \end{pmatrix} \right\rangle = 0$. They yield the equations

$$\begin{aligned} a + 2b + 4c &= 0 \\ 3b + 1c &= 0 \end{aligned} \quad (9.58)$$

This yields $c = -3b$ and $a = 10b$. A normal vector hence is $\begin{pmatrix} 10 \\ 1 \\ -3 \end{pmatrix}$. The normal vectors of length 1 are $\begin{pmatrix} 10/\sqrt{110} \\ 1/\sqrt{110} \\ -3/\sqrt{110} \end{pmatrix}$ and $\begin{pmatrix} -10/\sqrt{110} \\ -1/\sqrt{110} \\ 3/\sqrt{110} \end{pmatrix}$.

- (d) One has to multiply the vector with the rotation matrices. The rotation matrix of the rotation that should happen first has to stand on the right. Hence, rotating first around the z-axis:

$$\begin{aligned} &\begin{pmatrix} \cos 45^\circ & 0 & \sin 45^\circ \\ 0 & 1 & 0 \\ -\sin 45^\circ & 0 & \cos 45^\circ \end{pmatrix} \begin{pmatrix} \cos 30^\circ & -\sin 30^\circ & 0 \\ \sin 30^\circ & \cos 30^\circ & 0 \\ 0 & 0 & 1 \end{pmatrix} \begin{pmatrix} 1 \\ 0 \\ 0 \end{pmatrix} \\ &= \begin{pmatrix} \cos 45^\circ & 0 & \sin 45^\circ \\ 0 & 1 & 0 \\ -\sin 45^\circ & 0 & \cos 45^\circ \end{pmatrix} \begin{pmatrix} \cos 30^\circ \\ \sin 30^\circ \\ 0 \end{pmatrix} \\ &= \begin{pmatrix} \cos 30^\circ \cos 45^\circ \\ \sin 30^\circ \\ -\cos 30^\circ \sin 45^\circ \end{pmatrix} = \begin{pmatrix} \sqrt{3/8} \\ 1/2 \\ -\sqrt{3/8} \end{pmatrix} \end{aligned} \quad (9.59)$$

First rotating around the y-axis:

$$\begin{aligned}
 & \begin{pmatrix} \cos 30^\circ & -\sin 30^\circ & 0 \\ \sin 30^\circ & \cos 30^\circ & 0 \\ 0 & 0 & 1 \end{pmatrix} \begin{pmatrix} \cos 45^\circ & 0 & \sin 45^\circ \\ 0 & 1 & 0 \\ -\sin 45^\circ & 0 & \cos 45^\circ \end{pmatrix} \begin{pmatrix} 1 \\ 0 \\ 0 \end{pmatrix} \\
 &= \begin{pmatrix} \cos 30^\circ & -\sin 30^\circ & 0 \\ \sin 30^\circ & \cos 30^\circ & 0 \\ 0 & 0 & 1 \end{pmatrix} \begin{pmatrix} \cos 45^\circ \\ 0 \\ -\sin 45^\circ \end{pmatrix} \\
 &= \begin{pmatrix} \cos 30^\circ \cos 45^\circ \\ \sin 30^\circ \cos 45^\circ \\ -\sin 45^\circ \end{pmatrix} = \begin{pmatrix} \sqrt{3/8} \\ \sqrt{1/8} \\ -\sqrt{1/2} \end{pmatrix}.
 \end{aligned} \tag{9.60}$$

The results are not equal and hence the order of the rotations is important.

References

- Baker, W. E., Cox, P. A., Westine, P. S., Kulesz, J. J., & Strehlow, R. A. (1983). *Explosion hazards and evaluation*. Amsterdam: Elsevier.
- Bedford, T., & Cooke, R. (2001). Probabilistic risk analysis: Foundations and methods. Cambridge: Cambridge University Press.
- Bronstein, I. N., Semendjajew, K. A., Grosche, G., Ziegler, V., Ziegler, D., & Zeidler, E. (1996). *Teubner-Taschenbuch der Mathematik*. Stuttgart, Leipzig: B. G. Teubner.
- Fisz, M. (1978). *Wahrscheinlichkeitsrechnung und mathematische Statistik*. Berlin: VEB Deutscher Verlag für Wissenschaften.
- Georgii, H.-O. (2004). *Stochastik Einführung in die Wahrscheinlichkeitstheorie und Statistik*. Berlin, New York: Walter de Gruyter.
- Häring, I. (2005). *EMI Bericht E 15/05*. Ernst-Mach-Institut: Freiburg i. B.
- Humar, J. L. (2002). *Dynamics of structures*. Exton: PA, Balkema Publishers.
- Kinney, G. F., & Graham, K. J. (1985). *Explosive shocks in air*. Berlin: Springer.
- Klenke, A. (2007). Probability theory: A comprehensive course. Berlin: Springer.
- Slabaugh, G. G. (2015). Computing Euler angles from a rotation matrix. Retrieved August 13, 2015 from <http://staff.city.ac.uk/~sbbh653/publications/euler.pdf>
- University of Arizona. (2008a). Bryant Angles. Retrieved August 13, 2015 from <http://www.u.arizona.edu/~pen/ame553/Notes/Lesson%2008-B.pdf>
- University of Arizona. (2008b). Euler angles. Retrieved August 13, 2015 from <http://www.u.arizona.edu/~pen/ame553/Notes/Lesson%2008-A.pdf>
- Wikipedia. (2005). Lognormal distribution. Retrieved July 18, 2013 from https://commons.wikimedia.org/wiki/File:Lognormal_distribution_PDF.png
- Wikipedia. (2013a). Eulersche Winkel. Retrieved December 29, 2013 from http://de.wikipedia.org/wiki/Eulersche_Winkel
- Wikipedia. (2013b). Right-hand rule. Retrieved December 29, 2013 from http://en.wikipedia.org/wiki/Right-hand_rule

Chapter 10

Damage Analysis I: Probit Functions and Probability Distributions

10.1 Overview

This chapter first introduces two distinct concepts for the application of distributions to damage assessment. The main focus is the application of the lognormal distribution (probit approach), which is most often used for damage assessment of explosive effects as well as for other types of damage effects, e.g. flooding.

If distributions are used to compute the damage effects directly from hazard source and geometry information, the approach is called direct. The indirect approach, which is more flexible and modular, is to first compute the physical hazard (field, potential) and then to use distributions or further engineering or simulation damage models to finally compute the damage. For instance, in the case of complex blast propagation, due to lack of data or costs, it would be very challenging to assess the damage from historical data or scaled experiments for different geometries. Very similar arguments hold true for all other types of natural or man-made hazards.

The present textbook uses both approaches, with a strong focus on the indirect stepwise and systematic approach. Chapter 6 covers the hazard source description, Chaps. 7 and 8 the hazard propagation, Chaps. 9–12 the damage assessment. Nevertheless, due to lack of hazard source data and often also scenario data (e.g. types of objects at risk) as well as in case of lack of resources, it is often first choice to use direct damage assessment methods. Direct damage assessment models are also basic benchmarks for damage assessment.

This chapter shows how distributions are used for the indirect approach rather than how to use engineering and simulative approaches, e.g. for the description of the response of structures. For instance it shows how the radial distribution of the maximum overpressure is used as an input for lognormal damage assessment distributions.

Chapter 9 motivates the use of the lognormal distribution (probit) from its suitability for representing empirical data distributions with semi-infinite

arguments. In contrast, this chapter derives the lognormal approach from a standard binary choice approach which uses the normal distribution. It is shown how it can be transformed to a corresponding lognormal distribution.

Formally, the two main application options of the lognormal distributions are cases where the damage increases with increasing argument and where the damage decreases with increasing argument. For both cases application examples are given and the expressions are derived.

This chapter gives further examples for the use of lognormal functions for other types of damage. It also gives examples for other types of distributions, in particular the Weibull and logit distributions. In addition, examples for free parameterizations are given.

As a kind of summary, applying the damage modelling options to a single hazard type, this chapter applies different types of damage models to the fragment hazard. This links to the fragment hazard propagation of Chap. 7. In this case even models simpler than distributions are listed: single critical values. It is seen nicely, that modern distribution models smear out discrete step functions that have their discontinuity at critical values.

Damage analysis and modeling is of high importance to for the resilience engineering of physical protection means close to hazard sources as well as objects at risks, in particular in case of personal protective equipment. Thus damage analysis contributes to the modelling of protection capabilities and the improvement of the protection response of systems.

If potential damage effects are known, a systematic approach to prevention activities is supported, e.g. by prioritizing activities that prevent most critical events.

Potential damage effects are also of high interest for the resilience engineering of the response to disruptive events, for instance for structural or technical systems that support rescue activities. Recovery capabilities and the recovery phase are supported by resilience engineering with respect to potential future disruptive damage effects.

This and the following chapters treat step 5 of the risk analysis process:

- (5) **Damage analysis/modeling:** Here the effects of the physical hazard potential on objects like persons, vehicles, buildings, and infrastructure are determined.

This chapter is a general introduction to damage analysis using probit functions. Chapter 11 extends it to other distributions. Chapter 12 considers a further aspect of damage analysis: The presented surface of objects. Another further aspect, the response of structure to blast, is introduced in a scientific paper as further reading.

The chapter is focused on a mathematical view on damage analysis.

Section 10.2 describes two different approaches to damage analysis: direct and indirect analysis.

We first define the probit distributions (Sects. 10.3 and 10.4) which we later use to describe the damage in terms of overpressure or scaled distance (Sects. 10.5–10.8).

There is a major difference between probit distributions in terms of the physical characteristic blast sizes and the scaled distance. In the first case the cumulated

damage probability increases with the input size. In the second case the damage probability decreases with the scaled distance.

In the case of blast effects the physical quantities that are used to characterize the blast effects are often the blast overpressure and the scaled distance. Both sizes are positive.

The main source of the chapter is Aschmoneit et al. (2009). Further Fraunhofer EMI sources are Dörr, Gürke and Rübarsch (2003), Rübarsch and Gürke (2003). The main author of the EMI sources is T. Aschmoneit supplemented with work by C. Rizzuti, G. Gürke, B. Brombacher, J. Weissbrodt and I. Häring.

10.2 Direct and Indirect Damage Analysis

There are two different approaches to damage analysis. We distinguish between the direct or empirical approach and the indirect approach based on a physical hazard analysis. The difference is illustrated in Fig. 10.1.

The physics based damage analysis consists of three steps (Aschmoneit et al. 2009). First the scenario data have to be determined. Then physical consequences are calculated. Finally damage quantities are estimated using the calculated physical parameters. For instance, the distance r of an object from an explosive mass m is determined as scenario data. The physical consequences include, e.g., the overpressure P at distance r . The damage analysis for the object is the expected damage probability for pressure P .

In case of a direct or empirical damage analysis only two steps are necessary. The difference is that the damage is directly computed from the scenario data. For instance the expected damage could be determined in terms of the scaled distance from empirical data or using a model based on the physical approach. In this case only the TNT equivalent mass m and the distance r enter the damage computation (Aschmoneit et al. 2009).

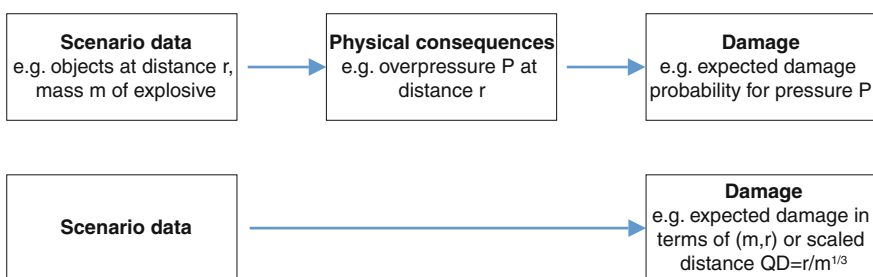


Fig. 10.1 Difference between the direct (bottom row) and the indirect (top row) approach, from the presentation of Aschmoneit et al. (2009)

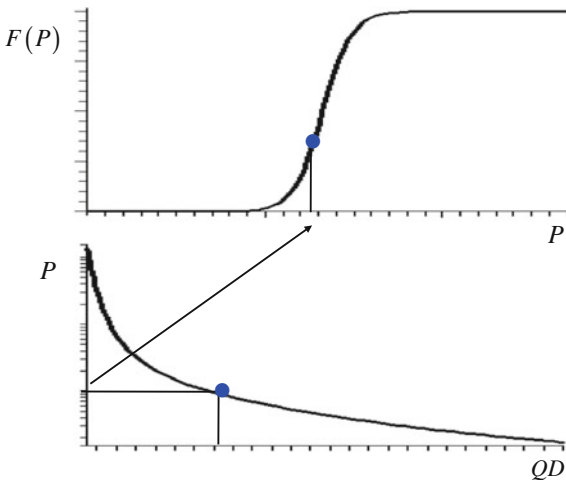


Fig. 10.2 Physics based damage analysis, from the presentation of Aschmoneit et al. (2009)

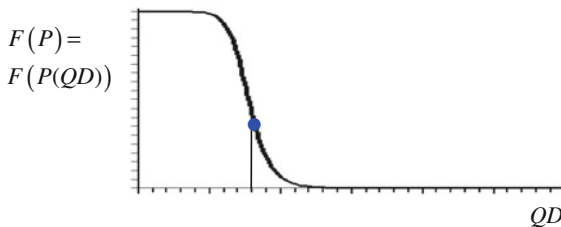


Fig. 10.3 Direct damage analysis, from the presentation of Aschmoneit et al. (2009)

Next we discuss the relation between direct analysis and physics based analysis. Assuming that a physics based damage analysis is available, we show that a direct analysis can be constructed. In particular we show that a cumulative distribution function in terms of the scaled distance can be constructed from a cumulative distribution function in terms of the overpressure P . Let us look at an example of the physics based approach.

First the overpressure P at the distance r is computed. If we assume a free field scenario we can use the Kingery-Bulmash approximations to compute the overpressure P . The Kingery-Bulmash approximations compute the overpressure P in terms of the scaled distance. This is shown in the lower graph of Fig. 10.2. e.g., according to Aschmoneit et al. (2009). Next we compute the expected damage probability in terms of the overpressure P . We use a cumulative distribution function that describes the damage in terms of the overpressure P . This is shown in the upper graph of Fig. 10.2.

Next we show an example for direct damage analysis. In Fig. 10.3 the damage is directly computed from the scaled distance. We note that for small overpressure the

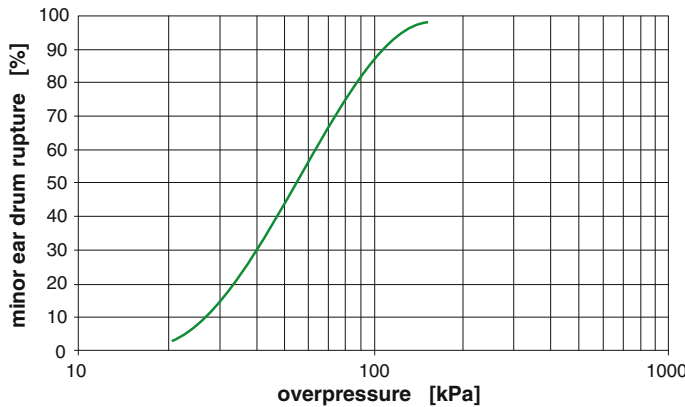


Fig. 10.4 Example for a probit function using physical hazard input data (direct or empirical damage assessment): probability of minor ear drum damage in terms of blast overpressure James et al. (1982)

expected damage is also small, see Fig. 10.2. However, a small scaled distance results in 100 % damage, see Fig. 10.3. Now we are in a position to understand how direct analysis can be constructed from physics based analysis. We assume that the scenario geometry is known and a cumulative distribution function (cdf) in terms of the overpressure for damage analysis is available. Each point of the cdf in terms of the overpressure determines a point of the cdf in terms of the scaled distance. From the scaled distance, that is computed assuming free field scenario, the overpressure is computed and from the overpressure the damage probability.

From the construction principle of the direct damage analysis it becomes obvious that we need a unique mapping from the physical quantity describing the scenario (here: distance or scaled distance) to the physical quantity describing the damage loading (here: overpressure). Referring to the discussion on the free field blast impulse, we note that such mappings do not exist for small scaled distances and the physical loading parameter blast impulse. Such a mapping does also not exist for complex blast scenarios.

Remark If the cdf in terms of the overpressure has a range of validity, also the cdf in terms of the scaled distance has a range of validity. The cdf in terms of the scaled distance is fast and suitable for practical applications of damage analysis.

Figure 10.4 shows the probability of eardrum damage in form of one-dimensional cumulative probability distributions in terms of overpressure. For example, one expects a minor eardrum rupture with a probability of 10 % for a blast overpressure of 40 kPa. Figure 10.4 is an example of the upper graph in Fig. 10.2. The function is called a probit function. It is mathematically derived in the following section.

10.3 Probit Functions or Normal Distribution from Binary Choice

This section motivates the probit approach from a mathematical perspective.

We regard a binary choice situation, that is, we define a variable y that is 1 if there is damage and 0 if there is no damage. The decision whether there is damage is described by the stochastic variable $y_i^* = \alpha - 5 + \beta \ln(x_i) - \varepsilon_i$ where $\varepsilon_i \sim \text{Normal}(0, 1)$ is a normal-distributed random variable and x_i are independent variables. If y_i^* is bigger than or equal to a critical value \tilde{y} , there is damage, otherwise there is none. An overview is given in Table 10.1.

The situation is shown in Fig. 10.5. The red line shows the critical value \tilde{y} . For values above the red line, there is damage, indicated by red dots. Values below the red line represent situations without damage, see black dots. The straight diagonal line is $f(x) = \alpha - 5 + \beta \ln(x)$.

The hardest part to visualize are the normal distributions.

Reminder Figure 10.6 shows a normal distribution. The grey area shows the probability that the random variable is smaller than or equal to k , that is, $p = P(\varepsilon_i \leq k)$.

We have the situation that there is damage if $\varepsilon_i = f(x_i) - y_i^* \leq f(x) - \tilde{y}$. $f(x_i) - \tilde{y}$ is the difference between the diagonal line and the red line at x_i . Regarding Fig. 10.6 and the remark above, we see that $p_i = P(\varepsilon_i \leq f(x) - \tilde{y}) = P(f(x) - \varepsilon_i \geq \tilde{y})$ is the grey area under the turned Gaussian curves in Fig. 10.5. So, with probability p_i , there is damage in situation x_i .

We define the probit function $\Pr(x_i) := \alpha + \beta \ln(x_i)$. From the previous considerations we can conclude

Table 10.1 Overview of the definitions of variables

Damage	$y_i^* \geq \tilde{y}$	$y = 1$
No damage	$y_i^* < \tilde{y}$	$y = 0$

Fig. 10.5 Probit functions from binary choice, from the presentation of Aschmoneit et al. (2009)

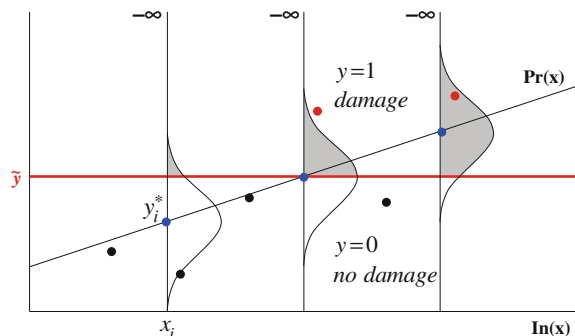
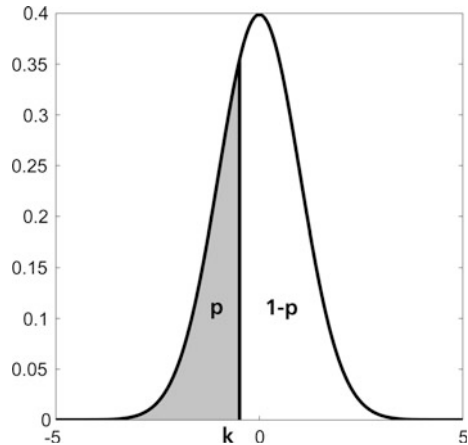


Fig. 10.6 Normal distribution, modified from Wikipedia (2013)



$$\begin{aligned}
 p_i &= P(y_i = 1) \\
 &= P(y_i^* \geq y) \\
 &= P(\alpha - 5 + \beta \ln(x_i) - \varepsilon_i - \tilde{y} \geq 0) \\
 &= P(\varepsilon_i \leq \alpha - 5 + \beta \ln(x_i) - \tilde{y}) \\
 &= F_{0,1}(\alpha + \beta \ln(x_i) - \tilde{y} - 5) \\
 &= F_{0,1}(\Pr(x_i) - \tilde{y} - 5) \\
 &= \int_{-\infty}^{\alpha - 5 + \beta \ln(x_i) - \tilde{y}} \frac{1}{\sqrt{2\pi}} e^{-\frac{t^2}{2}} dt.
 \end{aligned} \tag{10.1}$$

The function $\frac{1}{\sqrt{2\pi}} e^{-\frac{t^2}{2}}$ is the density of the centralized standardized normal distribution.

Remark The random looking 5 is traditional. A reason could be that $\alpha + \beta \ln(x_i) - \tilde{y}$ then only takes positive values in the area where the probability is significantly bigger than 0 because

$$\int_{-\infty}^{-5} \frac{1}{\sqrt{2\pi}} e^{-\frac{t^2}{2}} dt < 10^{-6}. \tag{10.2}$$

To get actual values for the probability, tables like Table 10.2 can be used. The table reads as follows. For a probit value $\Pr(x_i) = 6.13$ and $\tilde{y} = 0$, the related percentage is $p_i = 0.87 = 87\%$. If $\tilde{y} \neq 0$, it has to be subtracted from $\Pr(x_i)$ before looking it up in the table. For example, for $\tilde{y} = 2$ and $\Pr(x_i) = 6.13$, the resulting percentage is between 19 and 20 % (which corresponds to $6.13 - 2 = 4.13$ in the table).

Table 10.2 Probit value and matching percentage (Rübarsch and Gürke 2001)

Percent	0	1	2	3	4	5	6	7	8	9
0	–	2.67	2.95	3.12	3.25	3.36	3.45	3.52	3.59	3.66
10	3.72	3.77	3.82	3.90	3.92	3.96	4.01	4.05	4.08	4.12
20	4.16	4.19	4.23	4.26	4.29	4.33	4.36	4.39	4.42	4.45
30	4.48	4.50	4.53	4.56	4.59	4.61	4.64	4.67	4.69	4.72
40	4.75	4.77	4.80	4.82	4.85	4.87	4.90	4.92	4.95	4.97
50	5.00	5.03	5.05	5.08	5.10	5.13	5.15	5.18	5.20	5.23
60	5.25	5.28	5.31	5.33	5.36	5.39	5.41	5.44	5.47	5.50
70	5.52	5.55	5.58	5.61	5.64	5.67	5.71	5.74	5.77	5.81
80	5.84	5.88	5.92	5.95	5.99	6.04	6.08	6.13	6.18	6.23
90	6.28	6.34	6.41	6.48	6.55	6.64	6.75	6.88	7.05	7.33

Remark It is also possible to use usual tables for normal distributions to determine the percentage. Here, it has to be kept in mind that besides \bar{y} one has to subtract 5 from the probit value to get the upper bound for the integral.

In this simple example, we have seen that we can express the probability that there is damage with the probit function and the normal distribution.

10.4 Probit Distribution and Probit Function

The probit distribution for a quantity z is formulated most often using the probit function

$$\Pr_{\pm}(z) = a \pm b \ln z, \quad (10.3)$$

where a and $b > 0$ are parameters. The cumulated distribution function is then often defined using the standard normal distribution which is readily available in spreadsheet applications (e.g. Snook and Butler 2006) or computer algebra programs (e.g. Wolfram Research 2015; Spillner and Linz 2005; Sommerville 2007):

$$F_{\pm}(z) = F_{\tilde{\mu}=0, \sigma=1}^{\text{Normal}}(\Pr_{\pm}(z) - 5) = \frac{1}{\sqrt{2\pi}} \int_{-\infty}^{\Pr_{\pm}(z)-5} e^{-\frac{t^2}{2}} dt. \quad (10.4)$$

By definition the cumulated distribution function (10.4) increases (decreases) when the probit function (10.3) increases (decreases).

We want to show that assuming the transformations

$$\begin{aligned}-\infty < a = 5 - \mu/\sigma < \infty, \quad b = 1/\sigma > 0, \\ -\infty < \mu = (5 - a)/b < \infty, \quad \sigma = 1/b > 0,\end{aligned}\tag{10.5}$$

the following equations hold:

$$\begin{aligned}F_+(z) &= F_{\bar{\mu}=0, \bar{\sigma}=1}^{\text{Normal}}(\Pr_+(z) - 5) = F_{\mu, \sigma}^{\text{Lognormal}}(z), \\ F_-(z) &= F_{\bar{\mu}=0, \bar{\sigma}=1}^{\text{Normal}}(\Pr_-(z) - 5) = F_{\mu, \sigma}^{\text{Lognormal}}(1/z).\end{aligned}\tag{10.6}$$

Proof Using (10.4) and (10.5) we have

$$\begin{aligned}F_{\pm}(z) &= \frac{1}{\sqrt{2\pi}} \int_{-\infty}^{\Pr_{\pm}(z)-5} e^{-\frac{t^2}{2}} dt \\ &= \frac{1}{\sqrt{2\pi}} \int_{-\infty}^{\alpha \pm \beta \ln z - 5} e^{-\frac{t^2}{2}} dt \\ &= \frac{1}{\sqrt{2\pi}} \int_{-\infty}^{-\frac{\mu \pm 1}{\sigma} \ln z} e^{-\frac{t^2}{2}} dt.\end{aligned}\tag{10.7}$$

By substituting $t = \frac{\ln \tilde{t} - \mu}{\sigma}$, $d\tilde{t} = \sigma dt$, this is

$$F_{\pm}(z) = \frac{1}{\sqrt{2\pi}} \int_0^{\exp(\sigma(-\frac{\mu \pm 1}{\sigma} \ln z) + \mu)} \frac{1}{\sigma t} e^{-\frac{(\ln \tilde{t} - \mu)^2}{2\sigma^2}} d\tilde{t}.\tag{10.8}$$

For the plus case, that is $\Pr_+(z) = \alpha + \beta \ln z$, this is

$$\begin{aligned}F_+(z) &= \frac{1}{\sqrt{2\pi}\sigma} \int_0^z \frac{1}{\tilde{t}} e^{-\frac{(\ln \tilde{t} - \mu)^2}{2\sigma^2}} d\tilde{t} \\ &= F_{\mu, \sigma}^{\log normal}(z)\end{aligned}\tag{10.9}$$

because $\exp(\sigma(-\frac{\mu}{\sigma} \pm \frac{1}{\sigma} \ln z) + \mu) = \exp(-\mu \pm \ln z + \mu) = \exp(\ln z) = z$.

For the minus case, that is $\Pr_-(z) = \alpha - \beta \ln z$, a similar computation yields

$$\begin{aligned}
F_-(z) &= \frac{1}{\sqrt{2\pi}\sigma} \int_0^{z^{-1}} \frac{1}{t} e^{-\frac{(\ln t - \mu)^2}{2\sigma^2}} d\tilde{t} \\
&= F_{\mu,\sigma}^{\log normal} \left(\frac{1}{z} \right).
\end{aligned} \tag{10.10}$$

Equations (10.9) and (10.10) are what we wanted to show.

10.5 Application of the Probit Approach to Damage Assessment in Terms of Overpressure and Scaled Distance

If the cumulated probability depends on a physical size that is by definition only positive and increases with the physical size, in our case the overpressure and the blast impulse, the lognormal density and cumulated distribution function of (10.9) is the right choice. In this case the lognormal density for all physical sizes smaller than z are used to compute the cumulated probability $F_+(z)$. This can be interpreted as considering all damage cases, also for smaller z -values up to the actual z -value.

The case (10.10) cannot be interpreted in terms of the physics involved if we use overpressure or blast impulse. In this case the damage increases as the z -value decreases. This holds true for instance if we consider the damage in terms of the scaled distance. We also want to state it in terms of z and not $1/z$. For this, another substitution, namely $w = \frac{1}{t}$, $dw = -\frac{dt}{w^2}$, is used:

$$\begin{aligned}
F_-(z) &= \frac{1}{\sqrt{2\pi}\sigma} \int_0^{z^{-1}} \frac{1}{t} e^{-\frac{(\ln t - \mu)^2}{2\sigma^2}} d\tilde{t} \\
&= \frac{1}{\sqrt{2\pi}\sigma} \int_{\infty}^w \frac{w}{-w^2} e^{-\frac{(\ln(1/w) - \mu)^2}{2\sigma^2}} dw \\
&= \frac{1}{\sqrt{2\pi}\sigma} \int_w^{\infty} \frac{1}{w} e^{-\frac{(-\ln w - \mu)^2}{2\sigma^2}} dw \\
&= \frac{1}{\sqrt{2\pi}\sigma} \int_w^{\infty} \frac{1}{w} e^{-\frac{(\ln w + \mu)^2}{2\sigma^2}} dw \\
&= 1 - F_{-\mu,\sigma}^{\log normal}(z).
\end{aligned} \tag{10.11}$$

In this case it is actually a survival distribution function.

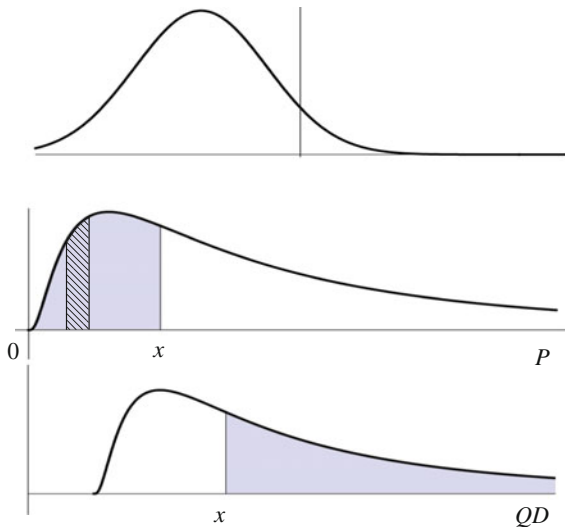


Fig. 10.7 Visualization of the normal and lognormal distributions. P is the overpressure, QD the scaled distance, from the presentation of Aschmoneit et al. (2009)

In summary, we can use a suitable probit distribution interpretation in terms of an integration over the lognormal density in the case that the damage increases with the physical size and in the case of decreasing damage with increasing physical size. Figure 10.7 visualizes the results.

$$\begin{aligned} \varphi(\Pr(x) - 5) &= \frac{1}{\sqrt{2\pi}} e^{-\frac{(\alpha-5+\beta \ln(x)-\tilde{y})^2}{2}} \\ x := \frac{\ln(t) - \mu}{\sigma} \Rightarrow dt &= \sigma t dx, (\mu, \sigma) = \left(\frac{5 + \tilde{y} - \alpha}{\beta}, \frac{1}{\beta} \right) \\ F_+(x) = \Phi(\Pr_+ - 5) &= \frac{1}{\sqrt{2\pi}\sigma} \int_0^x \frac{1}{t} e^{-\frac{(\ln(t) - \mu)^2}{2\sigma^2}} dt \\ F_-(x) = \Phi(\Pr_- - 5) &= \frac{1}{\sqrt{2\pi}\sigma} \int_x^\infty \frac{1}{t} e^{-\frac{(\ln(t) + \mu)^2}{2\sigma^2}} dt. \end{aligned} \quad (10.12)$$

10.6 Examples for Probit Functions for Damage Analysis of Non-explosive Events

For the damage analysis of toxic substances probit functions are used for the combustion products which are generated during fires from burning materials like synthetics, pesticides, synthetic fertilizers (Richmond 2002; Dörr 2003). One can distinguish between local acting substances affecting the respiratory system and the systematically acting substances that penetrate into the blood-circuit thereby leading to damage. Probit functions have been determined from tests with animals and adopted with a safety factor for humans (Green book 1999).

In Cothern (1990) different models (including the probit function) are applied to fit different data from animals (rats, dogs) and humans being exposed to radiation in different ways mostly by accident or lack of knowledge (injected, mining workers, exposed to radon and to atomic bomb explosions).

In the case of biological effects probit functions have been used for example to analyse the activity of a virus, depending on the surrounding temperature, infecting a bug and leading to its death (Sporleder 2008).

10.7 Alternative Distributions for Parameterizations for Blast and Fragment Effects

So far we have only considered the case where the lognormal distribution is appropriate for damage modelling. The lognormal distribution fulfils some properties that we assume for damage modelling and probit function make it easy to compute. However, it is also possible to base the damage analysis on other distribution as shown in this subsection.

10.7.1 Damage Analysis in the Literature

There are many publications that describe blast consequences for personnel. The kind of injuries is classified in lung, ear and whole body damage as well as blow down. The consequences of fragments are divided in damage with and without penetration.

Table 10.3 gives an overview of literature using free parameterizations and the probit function approach. There were no other distributions that allowed an interpretation as one-dimensional probability distribution function other than the probit approach.

“As Table 10.3 shows a lot of authors use probit functions to describe the hazard of explosion effects. Most of the authors use a probit function [and the corresponding lognormal distribution] that can be interpreted [...] according to (10.9).

Table 10.3 Overview of literature: kind of consequences from blast and fragments, kind of parameterization

Nature of the injury	Probit function, probability distribution	Free parameterization
Blast (ear and eardrum)	Eisenberg; Hirsch (1968), James and Burdett (1982), Mercx (1990), Richmond (1992)	–
Blast (lung)	Baker et al. (1983), Mercx (1990), Richmond (1992, 2002), AASTP-4 (2008)	Bowen et al. (1968)—Graph Stumiller (1995), Axelsson and Yelverton (1996)—formula
Blast (whole body)	(Eisenberg)	Bowen et al. (1968), Rytz (1982), Bass et al. (2006)—Graph Zheng (1990), AASTP-4 (2008)—formula
Blast (blow down) (“blow down”)	Fletcher (1968), Petes (1986), AASTP-4 (2008)	Stevens et al. (2003)—formula
Fragments	Eisenberg; Hagipavlou (1986), Gilbert et al. (1994)	Mett (1993)—Graph Walker and Duncan (1967), Mett (1993)—formula

As we have seen in Sect. 10.3 we can derive from such probit functions also probit functions in terms of the scaled distance that can be interpreted according to (10.10) and (10.11).” (Aschmoneit et al. 2009)

10.7.2 Other Distributions for Damage Analysis

Besides the lognormal distributions (based on probit functions), one could also interpret the data from experiments in terms of other distributions. Examples are (presentation of Aschmoneit et al. 2009):

- The logit model $F_L(x) = \frac{1}{1 + e^{-(z + \beta x)}}$
- Weibull distribution $F_W(x) = 1 - e^{-(\frac{x-a}{b})^c}; \quad x \geq a; \quad b, c > 0$
- Normal distribution: $F_N(x) = \int_{-\infty}^x \frac{1}{\sqrt{2\pi}} e^{-\frac{1}{2}\left(\frac{t-\mu}{\sigma}\right)^2} dt; \quad \sigma > 0$

The logit model is very similar to the probit model. It is mentioned for completeness. The Weibull distribution is very often used, because it is very flexible to fit raw data. In Chap. 11 it will be shown how parameters of the Weibull distribution are determined.

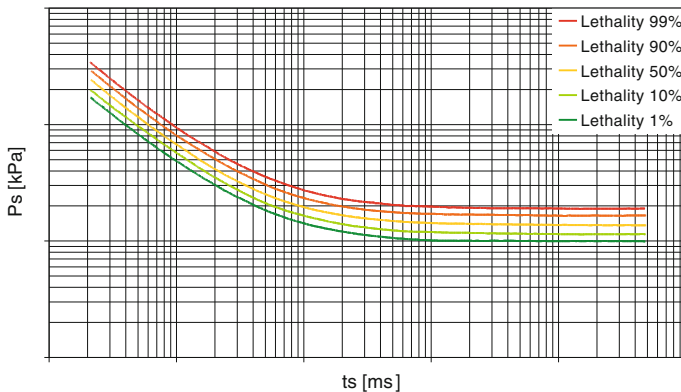


Fig. 10.8 Example for *Bowen curve* Lethality of a standing person in front of a reflecting wall due to blast effects. Taken from Dörr et al. (2003) and based on Bowen et al. (1968). The criterion is given in terms of the maximum overpressure Ps and the blast duration ts

10.7.3 Free Parameterizations in Terms of Several Parameters

Figure 10.8 shows a free graphical parameterization for the lethality assessment of blast, that is the data is connected by a curve and one does not try to find a distribution that matches it particularly well. The damage analysis uses two parameters: duration of freefield overpressure phase (ts) and maximum blast overpressure (Ps). It can be considered as a two dimensional probability distribution.

10.8 Fragment Effects on Personal

10.8.1 Critical Values

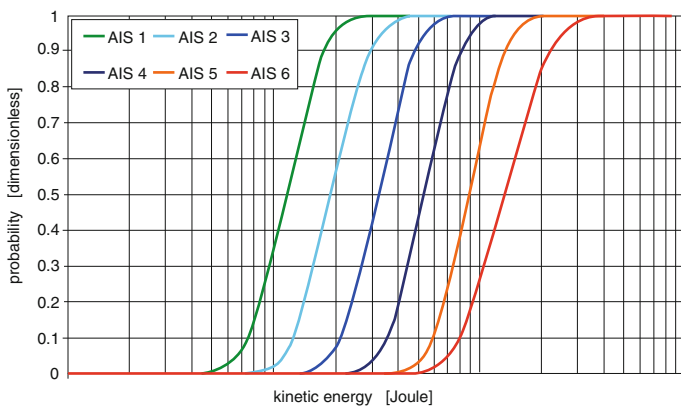
Often the so called NATO criterion is used. It claims that fragments are lethal if their energy is greater than 79 J.

In the literature critical values for fragments are typically given in terms of energy. An example is a study about industrial helmets where Proctor expects serious injuries on the forehead for critical energy values higher than 40–60 J (Proctor 1982). These values are also mentioned in the “Green Book” (1992).

Critical values can also be defined in terms of impulse or velocity.

Table 10.4 Abbreviated Injury Scale (AIS): injury levels

AIS level of injury	Type of injury
0	None
1	Superficial
2	Reversible, medical care necessary
3	Reversible, hospital stay necessary
4	Life threatening, recovery without medical care impossible
5	Life threatening, recovery even with medical care impossible
6	Lethal

**Fig. 10.9** Probability of AIS level injury in dependence of the kinetic energy. Taken from Dörr et al. (2005), based on ATP Research (2004) and Feinstein et al. (1986)

10.8.2 Example for Probability Distributions

Table 10.4 lists the standard Abbreviated Injury Scale (AIS). The probabilities of injuries according to this scale in dependence of the kinetic energy are shown in Fig. 10.9.

10.8.3 Probit Function from Range Commander Council

The following fragment lethality probit model in terms of kinetic energy is taken from the “Range Commander Council”. The model was generated by averaging over all body regions. It uses probit functions as defined in (10.3)

Standing person

$$\text{Pr} = -3.90 + 2.04 \cdot \ln E_{\text{kin}} \quad (10.13)$$

E_{kin} = Kinetic energy [J]

Similar probit functions exist for sitting and lying persons.

10.8.4 Free Parameterizations: Model by Mercx

Another probit function comes from a model by Mercx. Here lethality depends on velocity and mass, see AASTP-4 (2008).

$$\text{Pr} = -38.38 + 2.08 \ln S \quad (10.14)$$

$$S = mV_o^{5.115} \quad (10.15)$$

m = fragment mass [kg]

V_0 = fragment velocity [m/s].

10.9 Summary and Outlook

In this chapter we introduced to concept of probit functions. Probit functions are a widely used method in damage analysis. We tried to give an overview of the mathematical background behind probit functions. To use them in the praxis it often is enough to know the heuristics and the equations.

In the next chapter we will discuss different distributions besides the lognormal distribution that probit functions are based on and their application in damage analysis.

References

- AASTP-4 (2008). Manual on explosives safety risk analysis, Edition 1, Nato Standardization Organization (NSO).
- Aschmoneit, T., Richter, C., Gürke, G., Brombacher, B., Ziehm, J., & Häring, I. (2009). Damage assessment modeling for explosion effects. 13th ISIEMS. Brühl, Germany.
- APT-Research (2004). Injury curves developed for RALCT Phase I. Interagency Coordination Workshop on Injury Modeling. Nellis AFB, Nevada. Retrieved Februar 26–27, 2004
- Axelsson, H., & Yelverton, J. T. (1996). Chest wall velocity as a predictor of non auditory blast injury in a complex wave environment. *The Journal of Trauma, Injury, Infection and Critical Care*, 40(3 Suppl), 31–37.

- Baker, W. E., Cox, P. A., Westine, P. S., Kulesz, J. J., & Strehlow, R. A. (1983). *Explosion hazards and evaluation*. Amsterdam: Elsevier.
- Bass, C.R., Rafaels, K.A., Salzar, R.S. (2006). Pulmonary injury risk assessment for short-duration blasts. In *Proceedings of the 8th Biennial International Symposia on Personal Armour Systems*, Leeds, UK, pp. 233–248, Retrieved Sept 18–22
- Bowen, I. G., Fletcher, E. R., & Richmond, D. R. (1968). Estimate of man's tolerance to the direct effects of air blast. Lovelace Foundation for Medical Education and Research.
- Cothern, C. R., Crawford-Brown, D. J., & Wrenn, M. D. E. (1990). Application of environmental dose-response models to epidemiology and animal data for the effects of ionizing radiation. Environmental International.
- CPR 16E (1989). Methods for the determination of possible damage to people and objects resulting from release of hazardous materials, vol 1.
- Dörr, A., Gürke, G., Häring, I., Michael, K., & Rübärsch, D. (2005). *EMI Bericht E 07/05*. Efringen-Kirchen: Fraunhofer EMI.
- Dörr, A., Gürke, G., & Rübärsch, D. (2003). *EMI Bericht E 46/03*. Efringen Kirchen: Fraunhofer EMI.
- Feinstein, D. J., Heugel, W. F., Kardatzke, M. L., & Weinstock. A. (1968), Personal casualty study final report. IITRI Project No. J6067.
- Fletcher, E. R. (1968). Blast Induced translational effects. New York: New York Academy of Sciences.
- Gilbert, S. M., Lees, F. P., Scilly, N. F. (1994). A model for hazard assessment of the explosion of an explosives vehicle in a built-up area. 26th DDESB explosive safety seminar.
- Hagipavlou, S. C.-H. (1986). A review of the blast casualty rules applicable to UK houses. London: Home Office, Science Research and Development Branch.
- Hirsch, F. G. (1968). Effects of overpressure on the ear- a review. New York:Academy of Sciences.
- James, D. J., & Burdett, K. J. (1982). The Response of the Human Ear to Blast, Part 1: The Effect on the eardrum of a short duration, 'Fast' Rising, Pressure Wave, Joint AWRE/CDE Report No. 0-4/82.
- James, D. J., Pickett, V. C., & Burdett, K. J. (1982). The response of the human ear to blast. JOINT AWRE/CDE Report No. 0-4/82, Ministry of Defence United Kingdom.
- Mercx, W. P. M. (1990). The effects of explosions on humans. Europex Newsletter. Edition 13:2.
- Mett, H. G. (1993). GE amendment of the revision. AASTP-1.
- Petes, J. (1986). Handbook of HE explosion effects. DASIAC-TN-86-15.
- Proctor, T. D. (1982). A review of research relating to industrial helmet design. *Journal of Occupational Accidents* 3.
- Richmond, D. R. J. (1992). Compendium on the biological effects of complex blast waves. Norwegian Defence Construction Service.
- Richmond, D. R. (2002). *Evaluation of Bowen's curves*. Albuquerque, New Mexico: Lovelace Foundation for Medical Education and Research.
- Rübärsch, D. (2003). *EMI Bericht E 36/03*. Efringen-Kirchen: Fraunhofer EMI.
- Rübärsch, D., & Gürke, G. (2001). *EMI Bericht E 41/01*, Fraunhofer EMI.
- Rytz, H. (1982). Building damage due to airblast from an accidental explosion. Defense Technology and procurement group of the Swiss Federal Department of Defense.
- Snook, C., & Butler, M. (2006). UML-B: Formal modeling and design aided by UML. *ACM Transactions on Software Engineering and Methodology*, 15(1), 92–122.
- Sommerville, I. (2007). *Software engineering*. Harlow: Addison-Wesley.
- Spillner, A., & Linz, T. (2005). Basiswissen softwaretest. Heidelberg: Dpunkt.verlag.
- Sporleder, M. E. A. (2008). Effects of temperature on the activity and kinetics of the granulovirus infecting the potato tuber moth. Biological Control.
- Stevens, D., Marchand, K., Young, L. A., Moriarty, R., & Cropsey, L. (2003). Evaluation of structural response and human injury in shock-loaded expeditionary and temporary shelters. Applied Research Associates.

- Stumiller, J. H. (1995). A model of blast overpressure injury to the lung. *The Journal of Biomechanics* 29.
- Green book (1992). Methods for the determination of possible damage to people and objects resulting from release of hazardous materials (1st ed.). *CPR 16E*. Committee for the prevention of disasters. Directorate-General of Labour of the Ministry of Social Affairs and Employment. The Hague.
- Walker, S. H., & Duncan, D. B. (1967). Estimation of the probability of an event as a function of several independent variables. *Biometrika*, 54, 167–178.
- Wikipedia. (2013). Quantil. Retrieved July 08, 2013 from <http://de.wikipedia.org/wiki/Quantil>
- Wolfram Research (2015). “Wolfram Mathematica 10.3”, Retrieved November 23, 2015 from <http://www.wolfram.com>.
- Zheng, L. (1990). Safety distance for a person under action of air shock wave. 24th explosives safety seminar. St. Louis. In AD reports–NTS-AD A. Department of Devense Explosives Safety Board. pp. 949–964.

Chapter 11

Damage Analysis II: Selection of Distributions and Determination of Parameters

11.1 Overview

This chapter addresses the selection of the distribution type and the determination of parameters of analytical distributions. This is challenging, most often due to the lack of data for damage modeling, in particular for personnel.

The determination of the goodness of fit of distributions for the selection of the distribution type, using e.g. the Kolmogorov-Smirnov or the Chi-squared test, is only indicated, as well as almost all standard methods for parameter determination: momentum, likelihood and resampling.

The sample method given for the parameter estimation is the graphical method, applied to the parameter determination of Weibull distributions. It is motivated in detail how the Weibull paper is designed and how to read off the Weibull distribution parameters. It is only indicated how the Weibull paper can be used to assess the correct distribution type.

Due to their relevance for applications, this chapter refers to especially many web pages for further reading, even spreadsheet applications.

With respect to the application areas in terms of the terminology of the resilience management cycle and resilience capabilities, this chapter contributes with probabilistic distribution damage models to damage modelling. Hence as Chap. 10 it mainly is useful for the resilience design and resilience improvement of the prevention and protection phase and corresponding resilience capabilities. To a lesser extent also for the response and recovery phases and capabilities.

The probit approach in Chap. 10 is based on the lognormal distribution. In this chapter we want to take a more general look at probability distributions, especially at the graphical method for their parameter estimation. It is shown how the probabiltiy paper is constructed for the Weibull distribution. In a similar way it can be constructed for other analytical distributions.

In Sect. 11.2 we present a general scheme to determine the probability distribution for a given data set. In Sect. 11.3 we introduce the graphical method for the

parameter estimation of three often-used probability distributions. Section 11.4 applies the normal and the Weibull distribution to damage analysis. Section 11.5 gives suggestions for further reading in the literature about the statistical topics.

The chapter is mostly based on (Aschmoneit et al. 2009a, b) and (Aschmoneit and Häring 2010). Further Fraunhofer EMI sources are (Gürke 2002; Häring and Gürke 2006). The main author of the Fraunhofer EMI sources is T. Aschmoneit supplemented with work by C. Rizzuti, G. Gürke, B. Brombacher, J. Weissbrodt and I. Häring and supplemented with work by G. Gürke.

11.2 Overview: Determination of Probability Distributions

Figure 11.1 summarizes the determination of a probability distribution from raw data in a scheme.

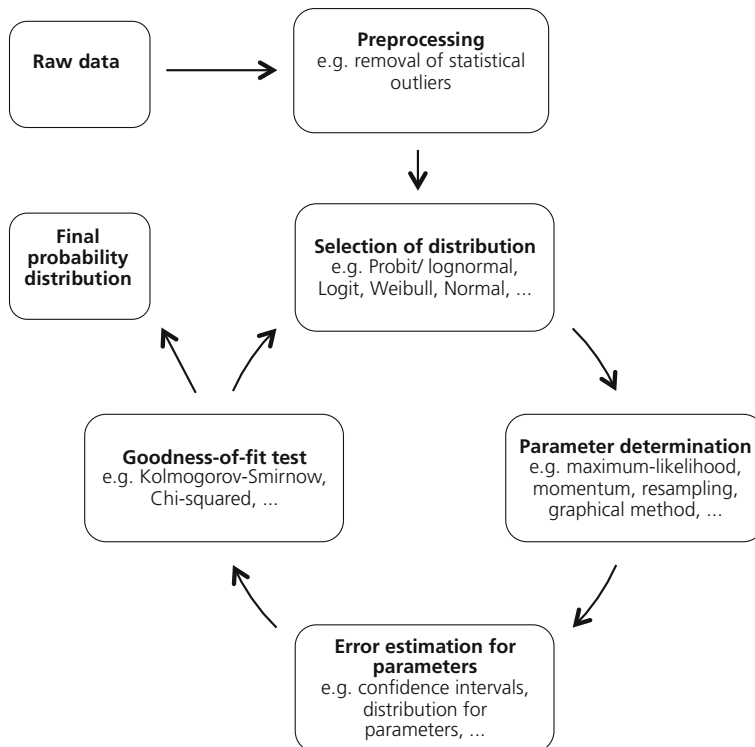


Fig. 11.1 Overview of the determination of probability distributions: (1) raw data; (2) preprocessing; (3) selection of distribution; (4) parameter determination; (5) error estimation for parameters; (6) goodness of fit test; (7) final probability distribution

11.3 Graphical Method for Parameter Estimation

The general idea of the graphical method is to write a data set onto probability paper. If the data lies on a straight line for the distribution belonging to the probability paper, the data is distributed according to that distribution. The straight line through the data can be estimated graphically or the method of least squares is used to compute the regression line $y = mx + n$.

11.3.1 Normal Distribution

Determining normal distributions with probability paper is common. The basic idea is to draw all points from the data set on probability paper for normal distribution. The data belongs to a normal distribution if the points lie on a straight line on the probability paper. If this is the case, the value belonging to the probability 50 % is μ and the value belonging to 84.15 % is $\mu + \sigma$ in

$$F(x) = \frac{1}{\sigma\sqrt{2\pi}} \int_{-\infty}^x e^{-\frac{(t-\mu)^2}{2\sigma^2}} dt. \quad (11.1)$$

A good introduction can for example be found http://reliawiki.org/index.php/The_Normal_Distribution.

11.3.2 Lognormal Distribution

Determining lognormal distributions with probability paper is similar to the normal distribution but a different probability paper is used where the abscissa is scaled logarithmically. See http://reliawiki.org/index.php/The_Lognormal_Distribution#Probability_Planning for more details.

11.3.3 Weibull Distribution

Figure 11.2 shows the choice of the probability paper to determine the Weibull parameters with the graphic method.

Weibull parameter estimation with the graphic method

- Density $f_w(x) = \frac{c}{b} \left(\frac{x-a}{b}\right)^{c-1} e^{-\left(\frac{x-a}{b}\right)^c}; \quad x \geq a; \quad b, c > 0$
- Distribution $F_W(x) = 1 - e^{-\left(\frac{x-a}{b}\right)^c}$

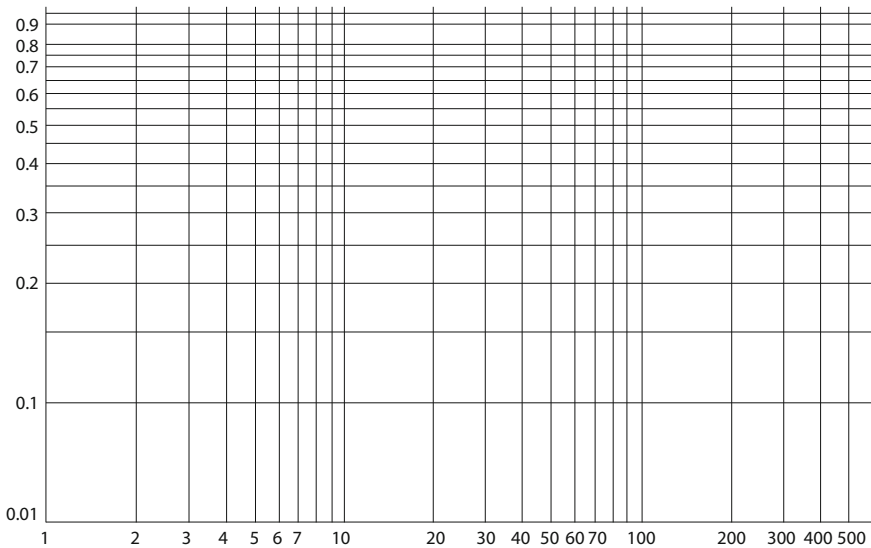


Fig. 11.2 Weibull parameter estimation with the graphic method, see presentation of (Aschmoneit et al. 2009a)

- Scaling of Axes: $\ln(-\ln(1 - F_W(x))) = \frac{c}{\log_{10}(e)} (\log_{10}(x - a) - \log_{10}(b))$
- If the data equates to a Weibull distribution, a stochastic linear correlation follows
- Least-square method (Linear Regression): $y = \hat{m}x + \hat{n}$

The scaling was computed as follows:

$$\begin{aligned}
 F_W(x) &= 1 - e^{-(\frac{x-a}{b})^c} \\
 1 - F_W(x) &= e^{-(\frac{x-a}{b})^c} \\
 \ln(1 - F_W(x)) &= -\left(\frac{x-a}{b}\right)^c \\
 \ln(1 - F_W(x)) &= -e^{c \ln\left(\frac{x-a}{b}\right)} \\
 -\ln(1 - F_W(x)) &= e^{c \ln\left(\frac{x-a}{b}\right)} \\
 \ln(-\ln(1 - F_W(x))) &= c \ln\left(\frac{x-a}{b}\right) \\
 \ln(-\ln(1 - F_W(x))) &= c(\ln(x-a) - \ln(b)) \\
 \ln(-\ln(1 - F_W(x))) &= \frac{c}{\log_{10}(e)} (\log_{10}(x-a) - \log_{10}(b))
 \end{aligned} \tag{11.2}$$

We now want to discuss how the parameters of a Weibull-distribution can be determined from the straight line on the probability paper for the case $a = 0$. On the probability paper the Weibull distribution is shown as

$$Y = \frac{c}{\log_{10}(e)}X - c \frac{\log_{10}(b)}{\log_{10}(e)} \quad (11.3)$$

if the probability paper is scaled as in Fig. 11.2. It is shown as

$$Y = cX - c \ln(b) \quad (11.4)$$

if the axes are scaled according to

$$\ln(-\ln(1 - F_W(x))) = c(\ln(x) - \ln(b)) \quad (11.5)$$

[the second to last line in (11.2)].

We will in the following only consider the case of Eq. (11.4), the other case works analogously.

With

$$Y = mX + n \quad (11.6)$$

we denote the equation of the straight line that we have determined. By looking at the probability paper we can derive the unknown parameters b and c of the Weibull distribution from the known straight line.

By comparing (11.4) and (11.6) we see that $c = m$. On Weibull probability paper one often finds reference lines to determine m .

The point $(b, 1 - e^{-1})$ lies always on the Weibull distribution curve and hence on the straight line in the diagram, because

$$F_W(b) = 1 - e^{-(\frac{b}{b})^c} = 1 - e^{-1}. \quad (11.7)$$

Hence, b can be determined by finding the point on the abscissa belonging to the value $1 - e^{-1}$ on the ordinate.

Remark More details about Weibull distributions, especially about diagrams with Microsoft Excel can be found under <http://www.qualitydigest.com/magazine/1999/jan/article/using-microsoft-excel-weibull-analysis.html>.

A good introduction can be found under http://reliawiki.org/index.php/The_Weibull_Distribution.

11.4 Normal and Weibull Distribution for Damage Assessment of Blast Effects: Case Study for Damage Assessment Using Resampling

Because of the high flexibility as an alternative to the lognormal distribution the Weibull distribution is tested using the high explosive consequence sample data of Table 11.1. We use an empirical dataset of dummies simulating lung blast injuries (Gürke 2002).

Table 11.1 Sample data for alternative distribution functions: blast injury probability of dummies at a given distance (Gürke 2002; Aschmoneit et al. 2009a)

Sample Nr.	Probability (%)
1	15
2	11
3	12
4	13
5	10
6	12
7	8
8	13
9	10
10	12

Table 11.2 Parameter values for the lognormal- and the normal distribution (Rinne 1997; Meyna and Pauli 2003)

Distribution function	Estimator type	μ	σ	Figure	Cite
Lognormal	Point	2.44	0.18	Figure 11.3	Rinne (1997)
	Moment	2.44	0.16	Figure 11.3	Meyna and Pauli (2003)
	Graphic	2.40	0.20	Figure 11.3	Rinne (1997)
Normal	Point	11.60	1.96	Figure 11.4	Rinne (1997)
	Moment	11.60	1.85	Figure 11.4	Rinne (1997)
	Graphic	11.21	2.05	Figure 11.4	Rinne (1997)

The Weibull cumulated distribution is defined as (Meyna and Pauli 2003)

$$F_{a,b,c}^{\text{Weibull}}(x) = 1 - e^{-(\frac{x-a}{b})^c}; \quad x \geq a; \quad b, c > 0 \quad (11.8)$$

In the case of the sample date we can also test whether a normal distribution $F_{\mu,\sigma}^{\text{normal}}(z)$ according to (10.4) is appropriate.

Table 11.2 shows the parameters obtained from different estimators for the lognormal and normal distribution and Table 11.3 for the Weibull distribution using the sample data Table 11.1. In all cases resampling was used.

Figures 11.3, 11.4 and 11.5 show the different graphs with the parameters from Tables 11.2 and 11.3.

For the sample data the Kolmogorow-Smirnow test (Rinne 1997) shows that the Weibull distribution with the moment estimator has the best goodness-of-fit. Figure 11.6 presents this best cumulated distribution function.

Table 11.3 Parameter values for the Weibull distribution

Distribution function	Estimator	a	b	c	Figure	Cite
Weibull	Point	2.44	2.44	0.18	Figure 11.5	Rinne (1997)
	Moment	2.44	2.44	0.16	Figure 11.5	Meyna and Pauli (2003)
	Graphic	2.40	2.40	0.20	Figure 11.5	Rinne (1997)

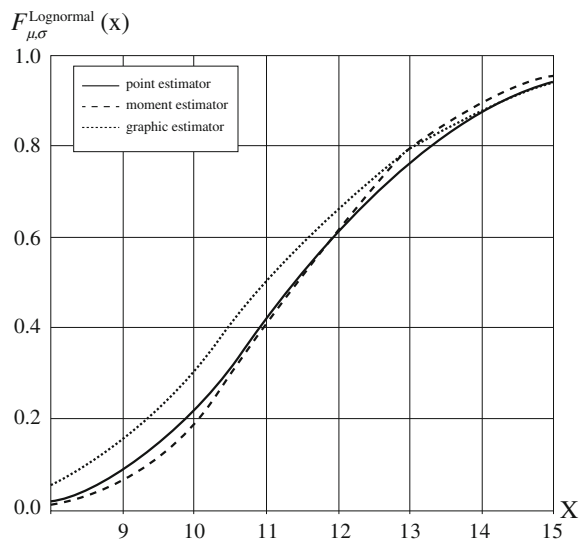
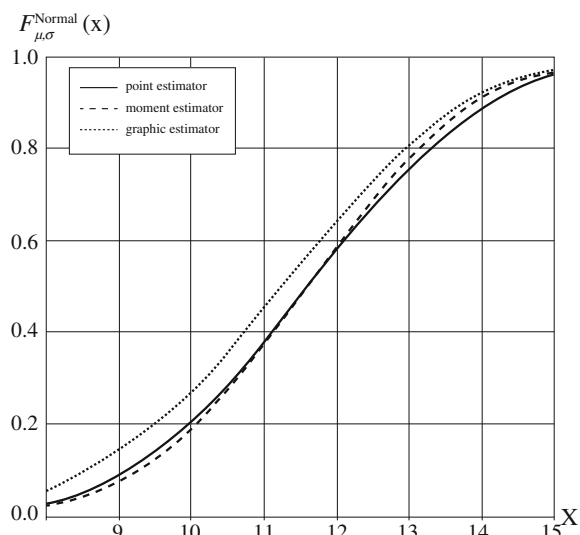
Fig. 11.3 Cumulated lognormal distribution determined with point, moment and graphic estimator (Aschmoneit et al. 2009b)**Fig. 11.4** Cumulated normal distribution determined with point, moment and graphic estimator (Aschmoneit et al. 2009b)

Fig. 11.5 Cumulated Weibull distribution determined with point, moment and graphic estimator (Aschmoneit et al. 2009b)

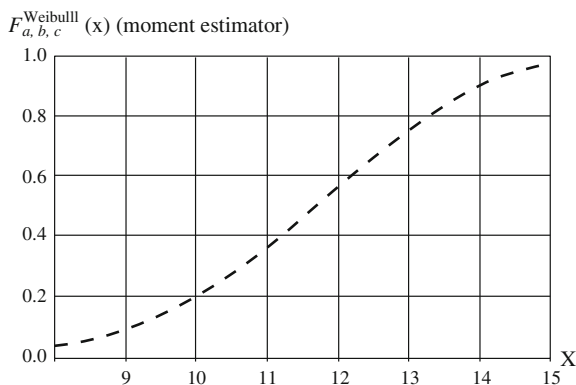
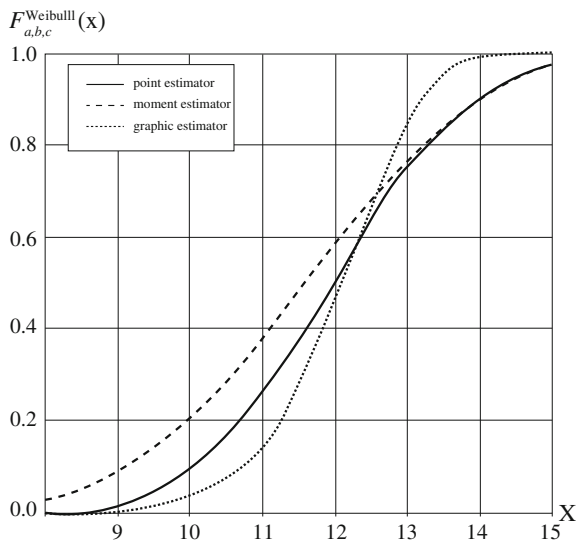


Fig. 11.6 Distribution with the best fit as found as determined by the Kolmogorow-Smirnow test (Aschmoneit et al. 2009b)

11.5 Literature About Statistical Methods

Table 11.4 gives an overview of literature on the statistics used for parameter estimation.

An example for the determination of damage distributions without using analytical distributions (non-parametric approach) in the domain of damage models for explosions is given in (Häring and Gürke 2006). In addition, this example uses expert estimate as data input.

Table 11.4 Literature about statistical methods for parameter estimation

Overview over statistics	Fetzer (1973), Holland (1997), Rinne (1997), Voß (2004)
Goodness of fit tests	Grubbs and Dixon: Dixon (1950; Grubbs 1950; Tukey 1977; Healy 1979) χ^2 -Goodness of fit (Voß 2004) Komogorow-Smirnow goodness of fit (Rinne 1997; Voß 2004)

11.6 Summary and Outlook

In this chapter we have seen:

- Probability distribution functions are useful for direct damage analysis.
- Direct analysis computes the damage from easily accessible scenario data.
- Binary choice modeling explains the often used probit approach.
- From the probit approach lognormal distributions can be derived that can be physically interpreted.
- Many distributions can be used for probabilistic damage modeling.
- The graphical method is an often used for parameter determination.
- The best distribution should be determined using a goodness-of-fit test.

In the next chapter we will see how presented surfaces are computed to determine whether they are hit by fragments.

11.7 Questions

- (1) Which kinds of models to describe the damage by blast do you know?
- (2) What are the advantages and disadvantages of distributions to describe damage in comparison to fixed critical values?
- (3) Which one-dimensional distribution is used to describe the damage through blast?
- (4) How can a one-dimensional probability distribution to describe damage be interpreted physically? Please regard the following cases in simple diagrams:
 - Physical parameter is real
 - Physical parameter is only positive
 - Damage increases with the physical parameter
 - Damage decreases with the physical parameter
- (5) How are the probit function and probit distribution defined? (formula) Which distribution can be used to interpret the probit distribution physically?
- (6) What is meant with “free parameterization”?

- (7) Which steps are necessary if you want to determine a distribution from experiment results?
- (8) Which are the most common methods to determine the parameters of a distribution?
- (9) With which tests can the best kind of distribution from a given set of distributions be chosen? What does significance mean in this context?
- (10) Which physical values are usually used to determine the damage through fragments?
- (11) How can several models be included in one overall model?

References

- Aschmoneit, T., & Häring, I. (2010). Resampling expert estimates for the consequence parameterization of explosions. In B. J. M. Ale, I. A. Papazoglou & E. Zio (Eds.), *European Safety and Reliability Conference (ESREL)*.
- Aschmoneit, T., Richter, C., Gürke, G., Brombacher, B., Ziehm, J., & Häring, I. (2009a). Damage assessment modeling for explosion effects. In *13th ISIEMS*. Brühl, Germany.
- Aschmoneit, T., Richter, C., Gürke, G., Brombacher, B., Ziehm, J., & Häring, I. (2009b). Parameterization of consequences of explosions. In *European Safety and Reliability Conference (ESREL) 2009* (pp. 1071–1077). Prague, London: Czech Republic., Taylor and Francis Group.
- Dixon, W. J. (1950). Analysis of extreme values. *Ann Math Stat*.
- Fetzer, V. (1973). *Einführung in die Grundlagen der mathematischen Statistik*. Hüthig.
- Grubbs, F. E. (1950). Sample criteria for testing outlying observations. *Ann Math Stat*, 27–58.
- Gürke. (2002). Lethality test of a normal distribution. ESQRA Feb02.
- Häring, I., & Gürke, G. (2006). Hazard densities for explosions. In C. G. Soares & E. Zio (Eds.), *Safety and Reliability for Managing Risk, European Safety and Reliability Conference (ESREL) 2006* (Vol. 3, pp. 1987–1994). Valencia, London, Spain: Taylor and Francis Group.
- Healy, M. J. R. (1979). Outliers in clinical chemistry control schemes. *Clinical Chemistry*, 25(5), 675–677.
- Holland, H. (1997). *Grundlagen der Statistik*. Wiesbaden: Gabler.
- Meyna, A., & Pauli, B. (2003). *Taschenbuch der Zuverlässigkeit- und Sicherheitstechnik*. München, Hanser: Quantitative Bewertungsverfahren.
- Rinne. (1997). Taschenbuch der Statistik. Taschenbuch der Statistik (pp. 355–366).
- Tukey, J. W. (1977). *Exploratory data analysis*. Boston: Addison-Wesley.
- Voß, W. (2004). *Taschenbuch der Statistik*. Leipzig: Fachbuchverlag.

Chapter 12

Damage Analysis III: Object Densities, Presented Surfaces Based on Exposure, Geometry and Damage Models

12.1 Overview

This chapter covers basic approaches to the damage assessment modeling in the case of trajectory-based hazard propagation, e.g. fragment and debris impact. In its initial steps, it is an example for the physical-engineering modelling of damage effects, in its final steps it also shows the application of empirical-statistical damage models. The use of distributions for damage modelling is only indicated as well as how to use the presented surfaces in risk analysis approaches. Presented surfaces are used to determine damage probabilities of objects. This information enters risk computations: local and non-local, for individuals and groups.

This chapter uses the basic notions introduced in Chap. 9 for the computation of damage effects. It continues the hazard propagation model introduced in Chap. 7 for fragments and debris.

To avoid as far as possible any object specific modelling, Chap. 10 first uses geometry information only. It is shown how to compute the presented surface, i.e. the surface that could be damaged, in case of explosive fragment and debris impact. The same arguments hold true for other types of impact, e.g. in case of hail or ice rain, objects that are torn from buildings or structures due to heavy wind, or debris generated by (collision) accidents of airplanes or aerial drones (unmanned aerial vehicle or system, UAV or UAS), as well as a set of malicious events in the aerial domain, e.g. aerial drones that discharge objects. The presented surface is computed using analytical and numerical approaches.

In the case of simple geometrical objects, fast analytical approaches are feasible. In the case of more complicated or composed geometries, a Monte Carlo integration approach is employed. This standard approach for numerical integration can for instance also be used to compute fragment propagation using an integral overall formulation as well as for the much simpler computation of cumulated probabilities when using free parameterizations of densities as mentioned in Chap. 10.

This chapter introduces the notion of a relevant surface with respect to a set of criteria. This links presented surfaces with damage models. Typically it suffices to suitably combine a rather small number of damage models for a single object along with their respective different volume and surface elements to obtain a sufficient overall damage model for an object. It is indicated how this is achieved for an object using a discrete damage model for impact energy. It is indicated how to proceed when using other damage quantities, e.g. impulse.

To model unknown positions and orientations of objects, this chapter introduces in detail two concepts. Object exposure densities and the homogeneous integration (averaging) over an unknown orientation parameter. The latter case illustrates under which assumptions unknown parameters can be considered in an adequate way. The former example allows a similar approach at a later risk analysis step. In Chap. 14, when computing exemplarily collective risks, object distributions are used to compute local collective risks as well as overall collective risks. Of course, exposure densities also enter F-N curve computations as introduced in Chap. 17.

Knowing object exposure distributions, object orientation distributions, presented and presented relevant surfaces is a major input for resilience engineering and resilience optimization with respect to prevention, protection, response and recovery capabilities and corresponding resilience response phases. Examples include the assessment of the sufficiency of means of prevention and protection in case of hazard sources that generate object impact (e.g. due to aerial objects, objects thrown from structures and buildings, explosively generated debris and fragments) and the planning of response and recovery, e.g. shelter design, topology and geometry selection.

When computing the damage of objects due to a given hazard potential, e.g. fragment or debris distribution, local physical blast effects or concentration distributions of toxic substances, we need to estimate the density of exposed objects, see Sect. 12.2. Such object densities or local exposures depend on location, time and type of exposed objects as well as their position, e.g. in case of buildings, vehicles and persons.

In case of fragment and debris hazard, corresponding to the trajectory-based hazard propagation, we introduce in Sect. 12.3 presented surfaces to compute the damage effects on objects using simple geometrical 3D bodies (voxel models).

Section 12.4 briefly introduces the Monte-Carlo integration method and applies it to compute presented surfaces of arbitrary geometrical bodies.

The area density of objects and the presented surface areas determine the frequency of the possibility of damage, i.e. the frequency of geometrical impacts, see Sect. 12.5. If we further introduce relevant surfaces with respect to damage criteria we can determine the local frequency of damaging impacts.

The main source of the chapter is (Häring 2005). The main author of the Fraunhofer EMI source is I. Häring.

12.2 Areal Object Density for Quantifying Exposure

The area density used here is the number of objects per area and has the unit 1/area, for example m^{-2} . The area density usually depends on the location on the surface. In the example in Fig. 12.1 the area density is higher towards the middle of the three-dimensional surface.

We may introduce densities that depend on object type, orientation of objects and geometry specifics, etc. For example, for persons it is sometimes useful to distinguish between different positions, e.g. standing and sitting personnel in embassies.

If the standard orientation of the objects is known, local coordinate systems can be defined to describe the objects. For instance the normal vector and the tangent plane in one point of the surface are used to define a local coordinate system for that point, compare Fig. 12.2. In such cases the density is given with respect to such a local coordinate system. Often also an earth-fixed Cartesian coordinate is used.

The three vectors for the local coordinate system are the normal vector and two orthogonal vectors in the tangent plane.

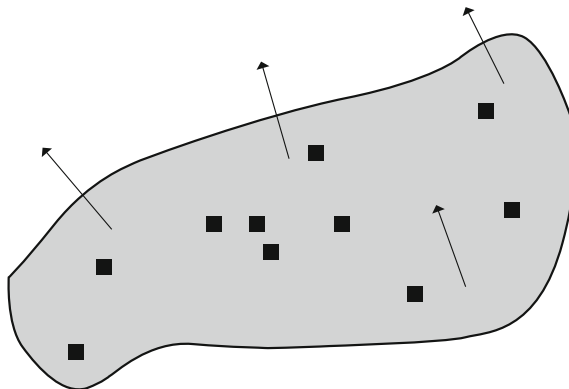


Fig. 12.1 Scheme of the distribution of identical box-shaped objects on a three-dimensional surface (Häring 2005)

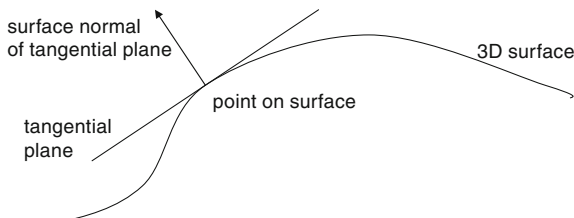


Fig. 12.2 Two-dimensional plot of the three dimensional situation. The surface is three-dimensional and the line representing the tangent plane normally is a plane. The normal vector would look the same in a three-dimensional plot (Häring 2005)

Remark The tangent plane can only be determined if the surface is sufficiently smooth, for example if it is described by a differentiable function. For simulations often the surface is discretized using triangles and for each triangle a local coordinate system is introduced.

12.3 Presented Surface

The presented surface is defined as the projection of the object onto a plane orthogonal to the velocity vector of a fragment impacting the object. Figure 12.3 shows some exemplary presented surfaces in a two-dimensional plot. In a three-dimensional plot the rectangles would be boxes and the lines two-dimensional areas.

12.3.1 Presented Surface of a Cuboid

Figure 12.4 shows a cuboid with side lengths a , b and c and schematically also the vectors (red arrows) representing the angle in which the fragment impacts the cuboid.

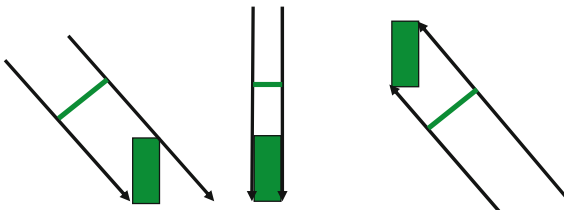
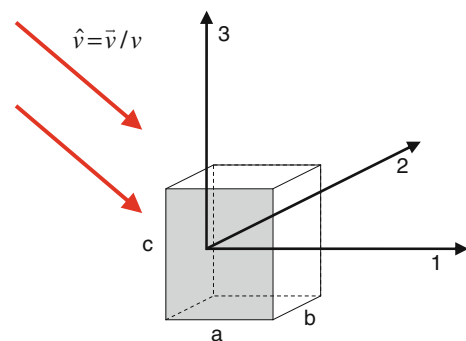


Fig. 12.3 The green lines show some exemplary presented surfaces (Häring 2005)

Fig. 12.4 A cuboid with side lengths a , b and c (Häring 2005)



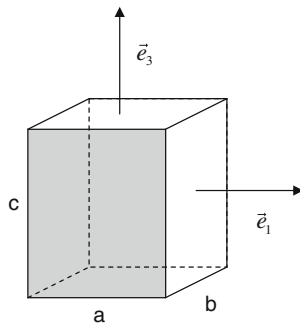


Fig. 12.5 Two of the six normal vectors of a cuboid (Häring 2005)

The normal vectors of the sides (pointing outwards) are

$$\left\{ \begin{pmatrix} 1 \\ 0 \\ 0 \end{pmatrix}, \begin{pmatrix} -1 \\ 0 \\ 0 \end{pmatrix}, \begin{pmatrix} 0 \\ 1 \\ 0 \end{pmatrix}, \begin{pmatrix} 0 \\ -1 \\ 0 \end{pmatrix}, \begin{pmatrix} 0 \\ 0 \\ 1 \end{pmatrix}, \begin{pmatrix} 0 \\ 0 \\ -1 \end{pmatrix} \right\}, \quad (12.1)$$

compare Fig. 12.5.

The vector \hat{v} can be computed by

$$\begin{aligned} \hat{v} &= \begin{pmatrix} \cos \varphi & -\sin \varphi & 0 \\ \sin \varphi & \cos \varphi & 0 \\ 0 & 0 & 1 \end{pmatrix} \begin{pmatrix} \cos \theta & 0 & \sin \theta \\ 0 & 1 & 0 \\ -\sin \theta & 0 & \cos \theta \end{pmatrix} \begin{pmatrix} 0 \\ 0 \\ 1 \end{pmatrix} \\ &= \begin{pmatrix} \cos \theta \cos \varphi & -\sin \varphi & \sin \theta \cos \varphi \\ \cos \theta \sin \varphi & \cos \varphi & \sin \theta \sin \varphi \\ -\sin \theta & 0 & \cos \theta \end{pmatrix} \begin{pmatrix} 0 \\ 0 \\ 1 \end{pmatrix} = \begin{pmatrix} \sin \theta \cos \varphi \\ \sin \theta \sin \varphi \\ \cos \theta \end{pmatrix}. \end{aligned} \quad (12.2)$$

Here, $\theta \in [0, \pi]$ is the angle of the rotation around the y-axis and $\varphi \in [0, 2\pi[$ the angle of the rotation around the z-axis, see Fig. 12.6.

Fig. 12.6 The vector v can be described as the vector $(0, 0, 1)$ that is rotated around the z-axis and the y-axis (Häring 2005)

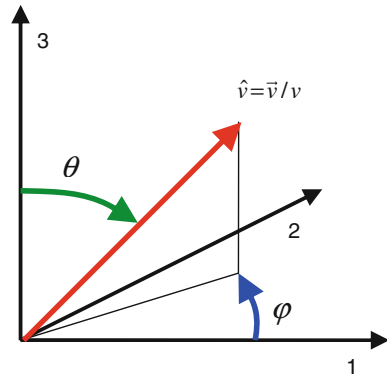
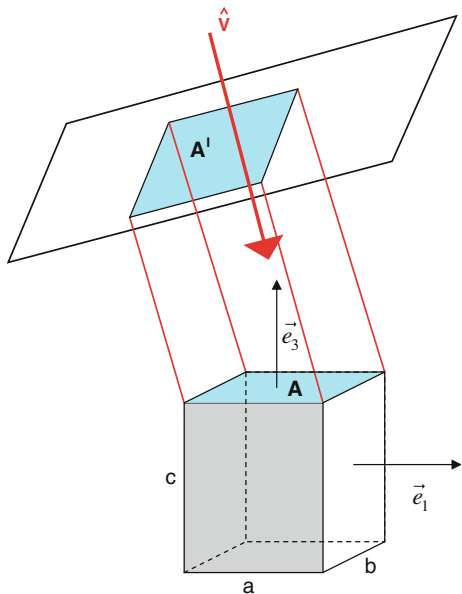


Fig. 12.7 The presented surface of the *upper side* of the cuboid



Remark Here the axes are labeled differently than in Chap. 9 and hence the matrix looks a little different.

We now want to compute the presented surface of the upper side of the cuboid, see Fig. 12.7. For this we regard a plane orthogonal to the vector \hat{v} . The distance of the plane to the cuboid is not relevant for the computation of the presented surface.

The computation of the projected area is similar to the area of an orthogonal projection onto the xy -plane (by rotating the whole system in Fig. 12.7),

$$A' = A |\cos \alpha| \quad (12.3)$$

where A is the original area, A' the projected area and α the angle between the normal vectors of the plane A and the xy -plane, in our case the angle between \hat{v} and e_3 .

We use it in a slightly different version by applying

$$\cos \alpha = \frac{\langle \hat{v}, e_3 \rangle}{|\hat{v}| |e_3|} = \langle \hat{v}, e_3 \rangle. \quad (12.4)$$

We only want to consider situations where the fragment hits the cuboid from the outside, that is, where $\alpha \geq 90^\circ$. For the scalar product this means that

$$\langle \hat{v}, e_3 \rangle \leq 0. \quad (12.5)$$

Combining (12.2) with (12.4) and (12.5) we get

$$\begin{aligned} A' &= A|\cos \alpha| \\ &= A|\langle \hat{v}, e_3 \rangle| \\ &= -A\langle \hat{v}, e_3 \rangle (\langle \hat{v}, e_3 \rangle \leq 0)_B \end{aligned} \quad (12.6)$$

where

$$(x)_B := \begin{cases} 0 & \text{if } x \text{ is true} \\ 0 & \text{otherwise} \end{cases} \quad (12.7)$$

is the logical bracket.

With $A = ab$ we get the final version of (12.6):

$$A' = -ab\langle \hat{v}, e_3 \rangle (\langle \hat{v}, e_3 \rangle \leq 0)_B. \quad (12.8)$$

By applying similar computations for the other five sides of the cuboid one gets

$$\begin{aligned} A'_{cuboid}(e_1, e_2, e_3, a, b, c, \hat{v}) &= -ab\langle \hat{v}, e_3 \rangle (\langle \hat{v}, e_3 \rangle \leq 0)_B \\ &\quad - ab\langle \hat{v}, -e_3 \rangle (\langle \hat{v}, -e_3 \rangle \leq 0)_B \\ &\quad - bc\langle \hat{v}, e_1 \rangle (\langle \hat{v}, e_1 \rangle \leq 0)_B \\ &\quad - bc\langle \hat{v}, -e_1 \rangle (\langle \hat{v}, -e_1 \rangle \leq 0)_B \\ &\quad - ac\langle \hat{v}, e_2 \rangle (\langle \hat{v}, e_2 \rangle \leq 0)_B \\ &\quad - ac\langle \hat{v}, -e_2 \rangle (\langle \hat{v}, -e_2 \rangle \leq 0)_B \\ &= -ab\langle \hat{v}, e_3 \rangle (\langle \hat{v}, e_3 \rangle \leq 0)_B \\ &\quad + ab\langle \hat{v}, e_3 \rangle (\langle \hat{v}, e_3 \rangle \geq 0)_B \\ &\quad - bc\langle \hat{v}, e_1 \rangle (\langle \hat{v}, e_1 \rangle \leq 0)_B \\ &\quad + bc\langle \hat{v}, e_1 \rangle (\langle \hat{v}, e_1 \rangle \geq 0)_B \\ &\quad - ac\langle \hat{v}, e_2 \rangle (\langle \hat{v}, e_2 \rangle \leq 0)_B \\ &\quad + ac\langle \hat{v}, e_2 \rangle (\langle \hat{v}, e_2 \rangle \geq 0)_B. \end{aligned} \quad (12.9)$$

One can see that (due to the contradicting statements in the logical brackets) only 3 terms are added for $\alpha \neq 90^\circ$. For $\alpha = 90^\circ$ there is only one non-zero term and the presented surface is equal to one side of the cuboid.

12.3.2 Other Presented Surfaces

If the orientation of the analyzed object is not known, it is reasonable to compute the presented surface of a sphere. This is easily done as it is the cross-section surface of the sphere, that is, the area of a circle:

$$A'_{sphere}(e_1, e_2, e_3, r, \hat{v}) = \pi r^2 \quad (12.10)$$

where r is the radius of the sphere.

If one axis of the orientation is known, a cylinder is a reasonable assumption, see Fig. 12.8 for the notation.

In the case where $v_1 = 0$ and $v_2 = 0$ in $\hat{v} = \begin{pmatrix} v_1 \\ v_2 \\ v_3 \end{pmatrix}$, the presented surface is the upper side of the cylinder.

For the case where at least one of v_1 and v_2 is not equal to 0, we regard Fig. 12.9 to determine the presented surface. We assume that $v_3 < 0$, the other case is computed similarly. Turning the vector \hat{v} around φ does not change the presented

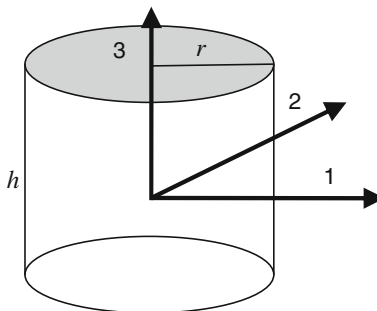


Fig. 12.8 A cylinder with the corresponding notation (Häring 2005)

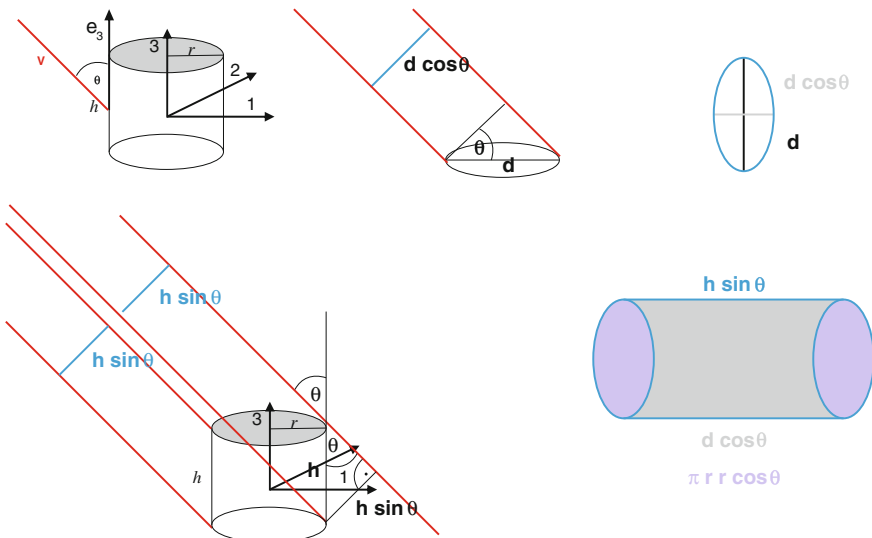


Fig. 12.9 Computation of the presented surface of a cylinder

surface, because the cylinder looks the same from every angle φ . So, the presented surface only depends on the angle between \hat{v} and e_3 . In Fig. 12.9 the angle between $-\hat{v}$ and e_3 is denoted by θ .

The first presented surface we consider is the one of the upper side of the cylinder. The orthogonal projection of a circle is an ellipse with the diagonals d and $d \cos \theta$ as shown in the second and third picture in Fig. 12.9. The lower left picture shows that the height of the cylinder is compressed to $h \sin \theta$. In total the presented surface (lower right picture) is

$$A = \pi r^2 \cos \theta + dh \sin \theta \quad (12.11)$$

for $v_3 < 0$. The only case that changes for $v_3 > 0$ is that the lower instead of the upper side of the cylinder adds to the presented surface. The presented surface stays the same.

12.4 Monte Carlo Computation of Presented Surfaces

12.4.1 Motivation

Section 12.3 showed the computation of presented surfaces for basic objects. A lot of objects can be modeled as a combination of cuboids, for example a truck can be approximated by a bigger cuboid for the trunk compartment and a smaller cuboid for the driving cab. Unfortunately the presented surfaces of the cuboids cannot simply be added because shading effects occur, see Fig. 12.10.

The basic idea for the computation of the presented surface is shown in Fig. 12.11. As before, one regards the vector \hat{v} and a plane orthogonal to \hat{v} . From this plane, rays are sent into the direction of \hat{v} . If they hit the object, the starting point of the ray on the plane is added to the presented surface.

Fig. 12.10 Shading effects in the computation of the presented surface of a simplified truck

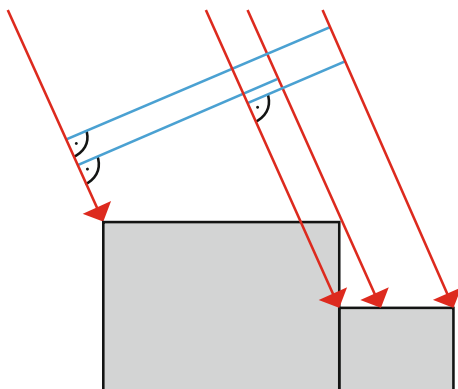
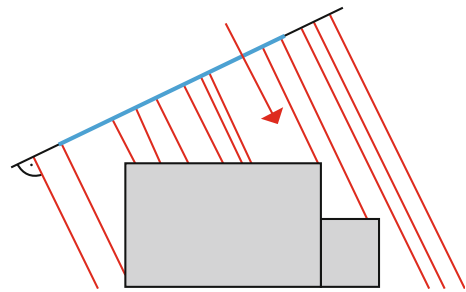


Fig. 12.11 The idea behind the computation of the presented surface with Monte Carlo simulation



12.4.2 The Model

We base the model on the assumption that each three-dimensional object can be modeled with cuboids Q_0, Q_1, \dots, Q_{N-1} where N is the number of cuboids that describe the object and the cuboid Q_i has the eight corners

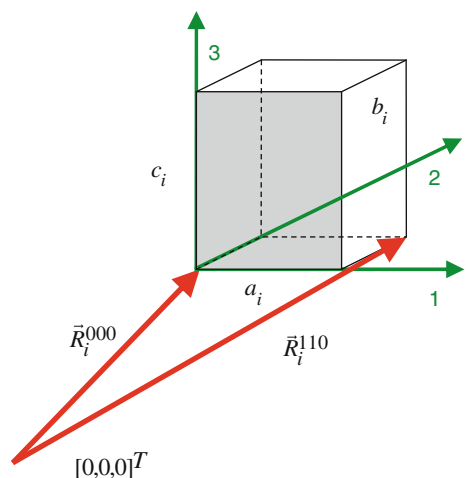
$$R_i^{j,k,l} = R_i + ja_i e_1 + kb_i e_2 + lc_i e_3, \quad j, k, l \in \{0, 1\} \quad (12.12)$$

where a_i, b_i, c_i are the lengths of the edges and R_i one corner of the cuboid. The notation is also shown in Fig. 12.12.

We are only interested in objects with limited size, so we can define

$$R_{\max} = \max_{\substack{i = 0, \dots, N-1 \\ j, k, l \in \{0, 1\}}} |R_i^{jkl}|, \quad (12.13)$$

Fig. 12.12 The labeling of the cuboid R_i (Häring 2005)



that is, the maximal distance of a corner point of one of the cuboids to the origin of the coordinate system. Hence, the whole object is contained in a ball with radius R_{\max} around the origin.

Next we want to determine a plane orthogonal to \hat{v} . From (12.3) we know that

$$\hat{v} = \begin{pmatrix} \sin \theta \cos \varphi \\ \sin \theta \sin \varphi \\ \cos \theta \end{pmatrix}. \quad (12.14)$$

We need two vectors orthogonal to \hat{v} and hence define

$$\hat{w} = \begin{pmatrix} \cos \theta \cos \varphi \\ \cos \theta \sin \varphi \\ -\sin \theta \end{pmatrix} \quad (12.15)$$

and

$$\hat{u} = \begin{pmatrix} -\sin \varphi \\ \cos \varphi \\ 0 \end{pmatrix}. \quad (12.16)$$

Applying

$$\sin^2 \varphi + \cos^2 \varphi = 1 \quad (12.17)$$

it can be seen that all three have norm 1 and that they are orthogonal to each other. Hence, the plane can be described by

$$E(p, q) = -R_{\max} \hat{v} + p \hat{w} + q \hat{u}. \quad (12.18)$$

With this plane, the starting values for a fragment on the plane can be described as

$$\begin{aligned} \vec{r}(t_0) &= -R_{\max} \hat{v} + p \hat{w} + q \hat{u}, \\ \vec{v}(t_0) &= v_0 \hat{v}. \end{aligned} \quad (12.19)$$

For the propagation of the fragment trajectory we use

$$\frac{d}{dt} \begin{bmatrix} \vec{r} \\ \vec{v} \end{bmatrix} = \begin{bmatrix} \vec{v} \\ 0 \end{bmatrix} \quad (12.20)$$

We define the hit function

$$f_{hit}(p, q) = \begin{cases} 1 & \text{if } \exists t \geq t_0 \text{ with } r(t) \in \text{object} \\ 0 & \text{otherwise.} \end{cases} \quad (12.21)$$

It describes whether the fragment hits the object at some point in time. It is numerically computed by defining time points

$$t_j = t_0 + jh, \quad j = 0, 1, 2, \dots \quad (12.22)$$

for sufficiently small h and then computing $\vec{r}(t_j)$.

Let M be the smallest j for which

$$|r_j - r_0| > 2R_{\max}. \quad (12.23)$$

Then the numerical version of the hit function is

$$f_{hit}(p, q) = \begin{cases} 1 & \exists(i, j) : \vec{r}(t_j) \in Q_i \quad i = 0, 1, \dots, N-1, j = 0, 1, \dots, M \\ 0 & \text{otherwise} \end{cases} \quad (12.24)$$

The presented surface is computed by the double integral

$$A(\theta, \varphi) = \int_{-R_{\max}}^{R_{\max}} \int_{-R_{\max}}^{R_{\max}} f_{hit}(p, q) dp dq \quad (12.25)$$

This integral can be computed with any arbitrary Monte Carlo method, see Sect. 12.4.3.

If the orientation of the object is not completely known, for example, if it is known that a truck is standing on its wheels but not in which direction its front is pointing, Monte Carlo methods can also be used to compute the average presented surface for all orientation. In the example that the orientation in the xy-plane is unknown, this would be

$$\begin{aligned} A(\theta) &= \frac{1}{2\pi} \int_0^{2\pi} A(\theta, \varphi) d\varphi \\ &= \frac{1}{2\pi} \int_0^{2\pi} \int_{-R_{\max}}^{R_{\max}} \int_{-R_{\max}}^{R_{\max}} f_{hit}(p, q) dp dq d\varphi \end{aligned} \quad (12.26)$$

12.4.3 Monte Carlo Methods

Monte Carlo integration methods are used to numerically compute integrals, often in higher dimensions. The basic idea is to take an area of known size in which the graph of the integrand lies. Then random points in the area are taken and it is

checked whether they lie under or above the graph of the integrand. The ratio of points under the graph divided by the total number of points multiplied with the size of the known area yields the approximated value of the integral.

Example If one wants to calculate the integral

$$A = \int_{-\sqrt{2}}^{\sqrt{2}} 2 - x^2 dx \quad (12.27)$$

with Monte Carlo, one could choose the box from -2 to 2 on the x-axis and 0 to 2 on the y-axis, see Fig. 12.13.

Random points in the box are taken. If for a point (a, b)

$$b \leq 2 - a^2, \quad (12.28)$$

the point is colored green, otherwise yellow.

The approximated integral value is computed by

$$A_{\text{Monte Carlo}} = \frac{(\text{number of green points})}{(\text{total number of points})} \cdot (\text{size of the box}) = \frac{45}{94} \cdot 8 \approx 3.83. \quad (12.29)$$

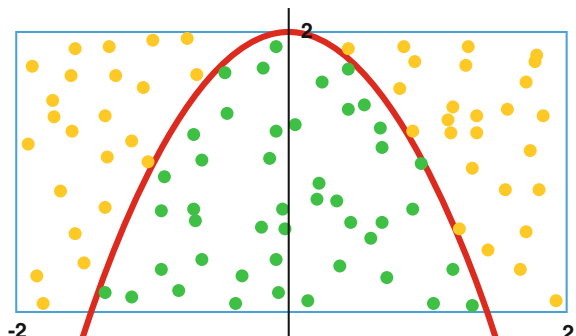
The correct value of the integral is approximately 3.77.

In practical applications one tries to get a sufficiently precise value of the integral together with an error estimate with as few computations of function values as possible.

We want to mention three ideas to reduce the computation effort:

- The area where function values are computed (in Fig. 12.13 this is the blue rectangle) should be as small as possible.
- The area where function values are computed is divided in two (disjoint and well-chosen) parts to reduce the variance of the estimator and hence the error of the integration (Press et al. 2002, pp. 320–331).

Fig. 12.13 Idea of Monte Carlo integration in a simple example



- The points are not distributed randomly but as well-spread as possible with so called quasi-random distributions which “see the gaps” in the already distributed points (Press et al. 2002, pp. 313–319).

Instead of considering randomly generated numbers we next use discrete grids to generate the sample points.

12.4.4 Discretization of the Relevant Surface

With regard to the vertical angle θ and the horizontal angle φ according to Fig. 12.6 we introduce the following net:

$$\theta_i = \frac{\pi i}{N_\theta - 1}, \quad i = 0, 1, \dots, N_\theta - 1, \quad (12.30)$$

$$\varphi_i = \frac{2\pi i}{N_\varphi - 1}, \quad i = 0, 1, \dots, N_\varphi - 1. \quad (12.31)$$

The centers of the angle intervals are

$$\theta_i^c = \frac{\pi(i + \frac{1}{2})}{N_\theta - 1}, \quad i = 0, 1, \dots, N_\theta - 2, \quad (12.32)$$

and

$$\varphi_i^c = \frac{2\pi(i + \frac{1}{2})}{N_\varphi - 1}, \quad i = 0, 1, \dots, N_\varphi - 2. \quad (12.33)$$

The presented surface for an angle pair (θ, φ) is the presented surface of the net grid the angle lies in. To compute the presented surface for a net grid, the center of the grid is used. Formally, this can be written as

$$A(\theta, \varphi) = \sum_{i=0}^{N_\theta^c-2} \sum_{j=0}^{N_\varphi^c-2} (\theta \in [\theta_i, \theta_{i+1}])_B (\varphi \in [\varphi_j, \varphi_{j+1}])_B A(\theta_i^c, \varphi_j^c). \quad (12.34)$$

For the averaged presented surface as in (12.26) this can be written as

$$A(\theta) = \sum_{i=0}^{N_\theta^c-2} (\theta \in [\theta_i, \theta_{i+1}])_B A(\theta_i^c). \quad (12.35)$$

The logical bracket $(\dots)_B$ was introduced in (12.7).

Figures 12.14 and 12.15 compare the results of an analytical and a numerical computation of the presented surface of a cube with side length 1 m. It can be seen

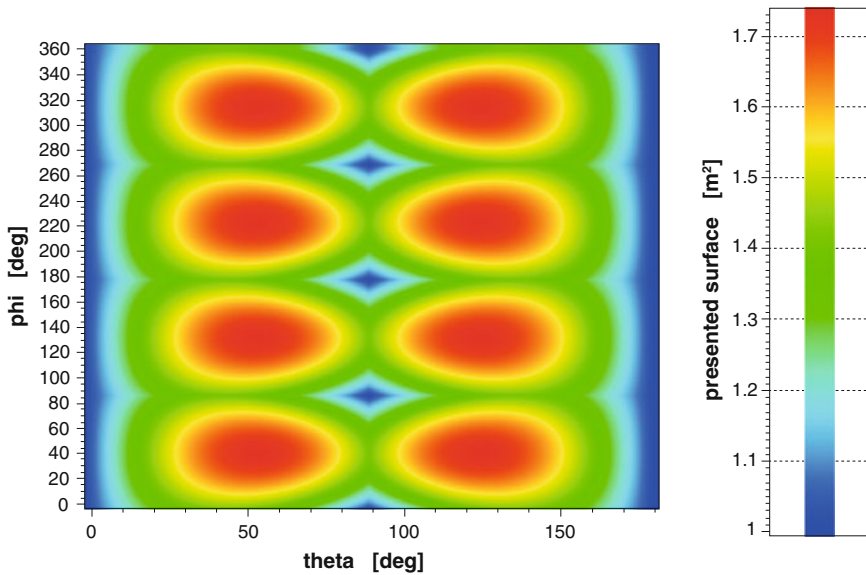


Fig. 12.14 Presented surface of a cube with side length 1 m (Häring 2005)

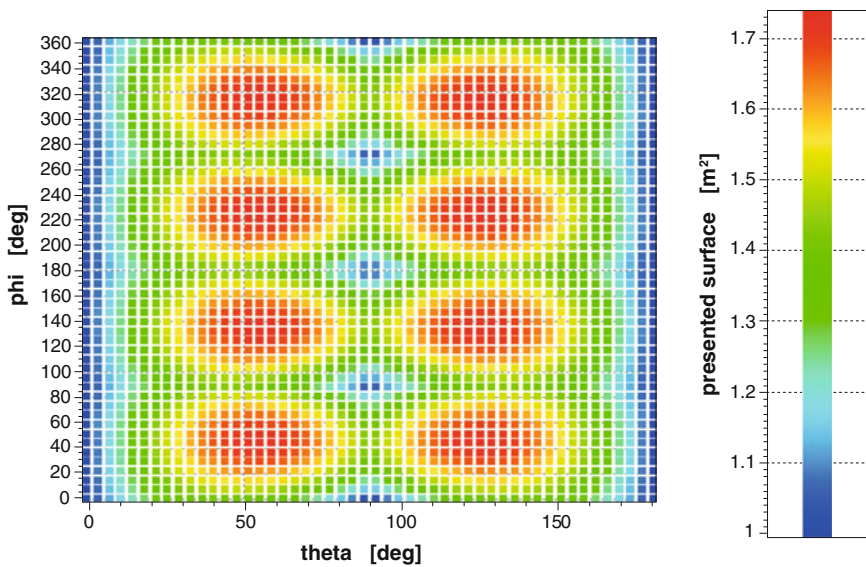


Fig. 12.15 Approximated presented surface of a cube with side length 1 m (Häring 2005)

that the approximation of the hit function and the discretization of the angles yields good results.

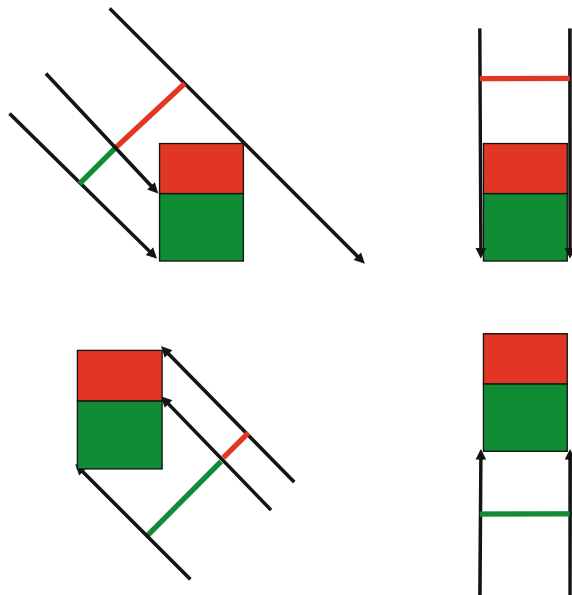
In a similar way, also for much more complicated objects the presented surfaces can be computed.

12.5 Relevant Presented Surface

Not every object is homogeneous. Often, some parts are more sensitive (vulnerable) than others, for example the windows of a building are the weak points in case of fragments impacting buildings. In Fig. 12.16, the more sensitive part of the object is colored red, the less sensitive green. The figure shows the idea of the relevant presented surface.

For example, to compute the relevant presented surface, the impact energy is compared with a critical energy E_{crit} or the impact impulse with a critical impulse, etc. This is used to define a modified hit function which may use different criteria for different parts of the geometry.

Fig. 12.16 The idea of relevant presented surfaces (Häring 2005)



$$f_{hit\ rel.}(p, q, E) = \begin{cases} 1 & \exists(i, j) : \vec{r}(t_j) \in Q_i \text{ and } E_{kin}(t_j) \geq E_{crit}^i \\ & i = 0, 1, \dots, N-1, j = 0, 1, \dots, M \\ 0 & \exists(i, j) : \vec{r}(t_j) \in Q_i \text{ and } E_{kin}(t_j) < E_{crit}^i \\ & i = 0, 1, \dots, N-1, j = 0, 1, \dots, M \\ 0 & \text{otherwise} \end{cases} \quad (12.36)$$

where

$$E_{kin}(t_j) = \frac{1}{2}mv(t_j)^2 \quad (12.37)$$

is the kinetic energy of the fragment, m the mass and $v(t_j)$ the velocity at time t_j .

In Fig. 12.16, the value E_{crit}^i for the red part would be higher than for the green part.

In the same way as in (12.36) also other discrete or probability damage models can be implemented, e.g. with respect to critical impulse transfer or other freely parametrized damage quantities, see Chap. 10.

If the critical energy is the same for every cuboid, that is

$$E_{crit}^i = E_{crit} \quad \text{for all } i, \quad (12.38)$$

the model describes an object where all parts are equally sensitive but only fragments with an energy of at least E_{crit} damage the object.

The relevant presented surface is computed similarly to the presented surface using

$$A(\theta, \varphi, E) = \int_{-R_{max}}^{R_{max}} \int_{-R_{max}}^{R_{max}} f_{hit\ rel.}(p, q, E) dp dq \quad (12.39)$$

or

$$A(\theta, E) = \frac{1}{2\pi} \int_0^{2\pi} \int_{-R_{max}}^{R_{max}} \int_{-R_{max}}^{R_{max}} f_{hit}(p, q, E) dp dq d\varphi \quad (12.40)$$

similarly to (12.25) and (12.26).

Remark Instead of defining critical energies or impulses E_{crit}^i it is also possible to define critical energy densities $(E/A)_{crit}^i$ in the unit $[J/m^2]$. Further examples may be derived also from each of the damage models introduced in Chaps. 10 and 11. We will not consider this here in more detail.

12.6 Summary and Outlook

In this chapter we first introduced exposure densities of objects at risk. They are needed for determining the damage frequency given the hazard potential.

Next we saw how presented surfaces and relevant presented surfaces of objects are computed. For simple objects this can happen analytically, otherwise numerical methods as the Monte Carlo simulation are necessary. Presented surfaces are important when analyzing the damage effects and together with the object densities the damage frequency of fragments.

In the next chapter we describe the response of structures to blast loading using a simple ersatz model.

References

- Häring, I. (2005). *EMI Bericht E 15/05*. Freiburg i. B., Ernst-Mach-Institut.
Press, W. H., Teukolsky, S. A., Vetterling, W. T., & Flannery, B. P. (2002). *Numerical recipes in C++: The art of scientific computing*. Cambridge: Cambridge University Press.

Chapter 13

Hazard Event Frequency, Distribution of Objects and Success Frequency of Avoiding Hazards

13.1 Overview

This chapter comprises a set of approaches for computing overall hazard event scenario probabilities by providing methods to generate event frequency rates (basic event rates), exposure distributions and rates of successful avoidance of hazard events. The last three factors can be understood as sample probabilities (the first one) and conditional probabilities (the last two) that lead to event scenarios.

For instance, when using historical event data for a first estimate, all past influences on overall probabilities of hazard scenarios are already taken account of. Therefore it is difficult to generate event data from historical data that does not already incorporate some type of prevention, protection and even mitigation. For instance, in the case of storage of hazardous goods, very unfavorable storage conditions (e.g. heat, humidity) often are detected and taken account of before actual events. This means that a base rate for major events is hardly empirically accessible.

This chapter reviews a step-wise approach to determine event frequencies from empirical-historical records, which lays more emphasis on control and plausibility checks when compared with the database-driven empirical-historical risk analysis sketched in Chaps. 3 and 4. This also allows to directly link with quantities as defined in Chaps. 3 and 4.

As an alternative approach, the application of fault tree analysis is mentioned. As understood in the present case, this is only an alternative, if the event is due to a technical (sub)system failure that can be quantified using basic failure rates within the deductive fault tree scheme. In the same way, the present text does not discuss attack trees in detail.

This chapter discusses at length a real word scenario, which allows to introduce discrete objects along with local discrete time-dependent exposure quantities for individuals and groups. This approach is a more intuitive approach when compared to the more flexible use of object densities as introduced in Chap. 12. Local

absolute numbers can be first choice, if the number of objects at risks is known and if they are strongly localized.

The use of discrete occupation numbers allows to compute local individual and group risks as well as individual and collective non-local risks, e.g. risks of single persons or groups at a single place or all places visited within one week. Also total average risks are computed.

This hands-on approach shows the need for formalization, which is conducted for the discrete case for illustration. It also shows that average total risks somewhat simplify the results when compared to a set of collective risk numbers, e.g. local collective risks. This is also a motivation for the F-N curve assessment as covered in Chaps. 4 and 17.

In the case of technical safety, when assessing the need for further technical efforts to control risks, in particular when employing safety functions, the options for the reduction of effects of hazards contribute to the overall assessment. This is an example of a risk-driven approach that takes systematically account of the successes frequency of avoiding hazards.

To further clarify the definition of the success (conditional) probability of avoiding hazards, this chapter introduces four examples and discusses their validity.

Chapter 13 contributes to the probability and frequency assessment of risk management and analysis, which is strongly related to the resilience capabilities relevant for prevention and to a lesser extent also for response and recovery resilience capabilities. The frequency and probability quantities enter into the overall assessment of risks of scenarios using various risk quantities. Hence they are also important for the resilience engineering of protection capabilities. For instance, most critical scenarios at an access control point have to take account of the organizational procedures and historic event dates.

This chapter treats three steps of the risk analysis process:

- (6) **Analysis of hazard event frequency:** It is analyzed how often the hazard source becomes active. This is determined by considering, for example, the frequency of the hazard source being present, the frequency of an unintended event within the hazard source and the frequency of a failure of the containment.
- (7) **Distribution of objects:** The distribution describes how many and where objects of interest are located in the area. The exposition/exposure describes that they are actually exposed to the damaging effects.
- (8) **Success frequency of avoiding hazard event consequences:** This step considers the success frequency of organizational and training measures, of spontaneous reactions (for example flight) as well as the success rates of placing passive, reactive, or active physical barriers. It covers success rates due to mitigation or avoidance of physical consequences as well as means to reduce or avoid damage effects.

The aim of steps 6–8 is to determine the probability or frequency of the damage events taking into account the basic event rate (step 6), the exposure (step 7) and other factors (step 8). The steps depend on the context and the hazard source (threat

potential). In general not all steps will be meaningful, e.g. avoidance of consequences in case of a hazard event (active hazard source) is almost impossible for very fast propagating hazards like impacting objects or blast.

Like for all steps, the analysis content of steps 6–8 strongly depends on the context and the threats analyzed, see the scenario steps 1–4 in the risk management process.

Section 13.2 gives two examples to determine hazard event frequencies (basic hazard event rates). In both cases the general approach is illustrated with an example.

Section 13.3 describes in addition to Chap. 12, which covered object densities for computing risks, discrete object distributions and shows how to use them to compute local and non-local individual and collective risks. This section also comprises a basic tabular approach and its formalization for considering object distributions on a set of objects for a set of person types.

Section 13.4 indicates with several examples how to assess avoidance frequencies of consequences of events.

The main source of this chapter is (Rübärsch 2003) with additional work by S. Rathjen. A further Fraunhofer EMI source is (Salhab et al. 2011).

13.2 Hazard Event Frequency

The hazard event frequency describes how often the previously defined hazard occurs in average. The definition is rather easy, to determine the frequency can be difficult. Compare the following two examples:

- Cases of credit card fraud occur in rather high numbers and they are easily comparable. Credit card fraud can be easily defined. The damage is measured in terms of money lost per credit card per time. Statistics can be found online and are easily accessible.
- Cases of terrorist attacks on bridges occur less often. Databases on terrorist events like GTD (National Consortium for the Study of Terrorism and Responses to Terrorism (START) 2011) often also contain ambiguous cases and attack attempts without damage. Statistics are sometimes based on small numbers and therefore not always meaningful. More effort is necessary to determine a reliable event frequency.

Both examples are also very interesting for steps 7 and 8. For instance it is rather reasonable to define these empirical rates as frequencies that already incorporate frequency quantities according to step 7 and 8, if no additional novel means have to be considered, e.g., proven successful early warning systems or novel physical counter measures.

13.2.1 Event Frequencies from the Historical Record

The event frequency can be based on historical records such as databases. The determination of the frequency can be divided into 5 steps (Yoon 2012):

- (1) Define context: “Clear specification of the incidents for which frequency estimates are sought”
- (2) Review source data: “All relevant historical data should be review[e]d for completeness and independence”
- (3) Check data applicability: “Careful review of the source data to confirm applicability”
- (4) Calculate incident frequency: “Historical frequency can be obtained by dividing the number of incidents by the exposed population”
- (5) Validate frequency

“Sample Problem: Estimation of leakage frequencies from a gas pipeline

– Step 1. Define Context

Objective: determine the leakage frequency of proposed 8-in-diameter, 10 mile long, high pressure ethane pipe to be laid in a semi urban area. The proposed pipeline will be seamless, coated and cathodically protected

– Step 2. Review source data

Applicable data is the gas transmission leak report data collected by the U.S. Department of Transportation (Department of Transportation 2014) for the years 1970–1980

– Step 3. Check data applicability

Incorporated pipeline and certain non-relevant incidents must be rejected among all data base

Examples are:

- Pipelines that are not steel
- Pipelines that are installed before 1950
- Incident arising at a longitudinal weld

– Step 4. Calculate likelihood

The pipeline leakage frequencies are derived from the remaining DOT data using following procedure:

- Estimate the base failure for each failure mode
- Modify the base failure rate, where necessary to allow for other condition specific this pipeline” (Yoon 2012)

The event frequency derived from the historical data can be determined with the methods from Sect. 3.10.4, remember for example

annual frequency of explosive attacks of embassies in Germany

$$= \frac{(\text{number of events that use explosives to damage embassies in Germany})}{(\text{number of considered years})(\text{number of embassies})}.$$
(13.1)

13.2.2 Event Frequencies from Fault Tree Analysis

Sometimes there is not enough relevant data to derive the event frequency from historical data. One alternative way to determine the event frequency is the Fault Tree Analysis, see Fig. 13.1.

Fault Tree Analysis is used to derive the probability of an event, the so called top event, from basic events. For example, if the analyzed event is an explosion of a machine due to its failure, the Fault Tree Analysis can be used to decompose the failure into failures of single components of the machine. If the failure rates of the components are known, the event frequency of the explosion can be derived. This approach is well established in the context of system safety analysis.

In the case of security relevant events, e.g., if the event is an improvised explosive device during a sports event, Fault Tree Analysis is much less useful. However, there have been attempts using so-called attack trees (Schneier 1999). They are in particular useful if counter measures are installed and their success can be estimated. In such cases, when assuming a basic rate of attacks and when taking the failure probabilities of the protection measures into account, an overall failure rate can be estimated.

Fault Tree Analysis is not studied in detail here.

13.3 Discrete Distribution of Objects

In the step “distribution of objects”, the area that can be reached by the physical hazard (including its propagation) is analyzed in more detail. This step can include for example the development (or consideration if they already exist) of

- Time sheets in a company (who is working for how long at which side)
- Maps of the area, city, company ground, ...
- Plans of buildings (for example including rooms, escape routes, ...)

This step is rather easy in a precise and narrow scenario, for example for a clearly defined explosive scenario in a given company. It is more difficult if the goal is to define a “typical” scenario to have an analysis that can readily be adapted for similar scenarios.

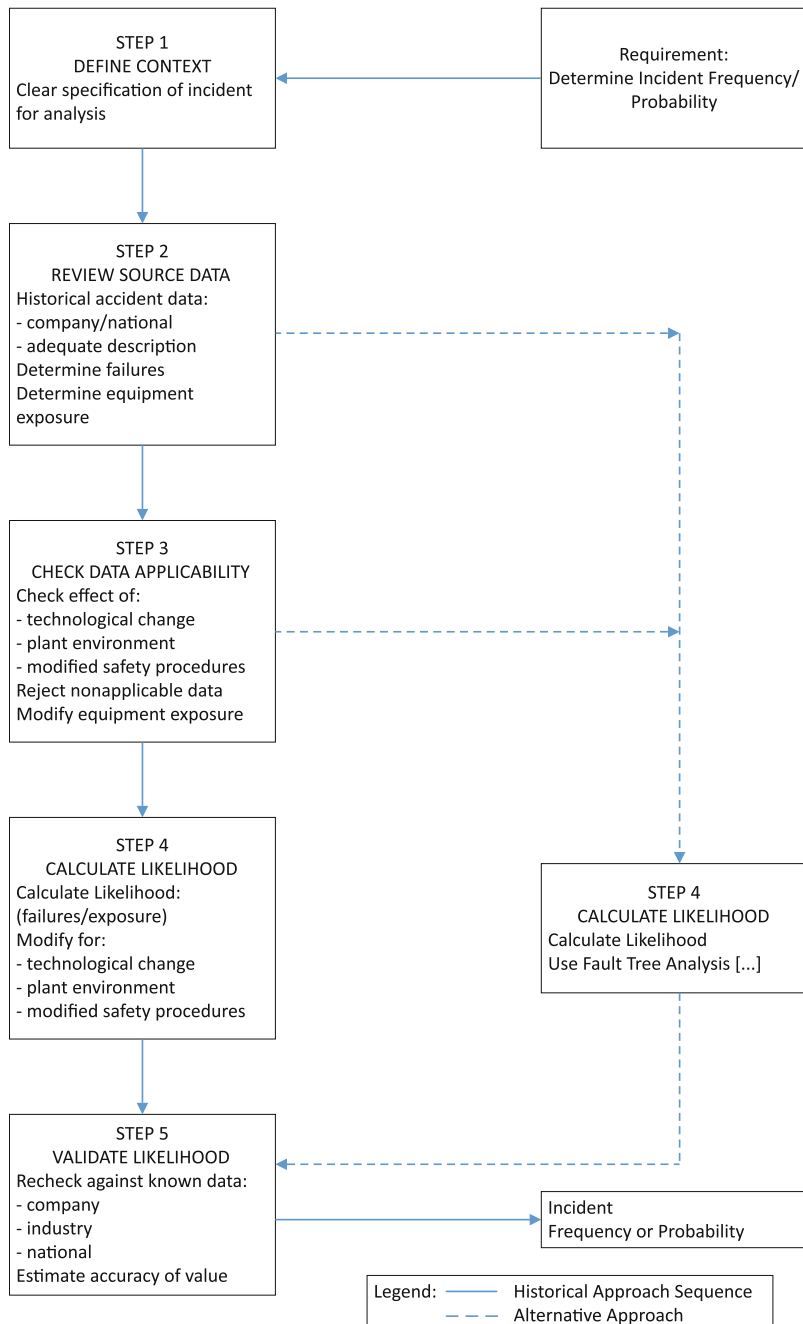


Fig. 13.1 Procedure for predicting incident likelihood from the historical record and the alternative way of fault tree analysis (American Institute of Chemical Engineers 1999, p. 299)

We have treated the exposure of objects also in some detail in Risk Analysis part 3, where object densities were introduced for computing risks. In this section we will further focus on discrete object distributions and associated risks.

13.3.1 Example: The “Real World Scenario”

The so called “real world scenario” was used in a project at Fraunhofer EMI and describes an explosion of 1000 kg net explosive mass in a storage depot (armored concrete) which is located in an urban area ([Rübarsch 2003](#)). The situation is illustrated in Fig. 13.2.

For computations a more formal description of the scenario situation is necessary, see Fig. 13.3.

For each of the objects the shape, the size, the material and the position in the coordinate system have to be described. This is for example necessary to determine the distance to the hazard source or to compute how well a building’s walls protect the people in the inside. In the project at Fraunhofer EMI, the diagram in Fig. 13.3 was accompanied by a list of details for each of the numbered objects.

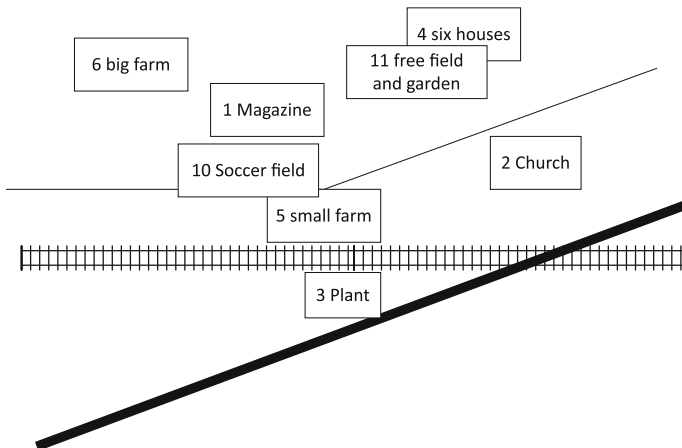


Fig. 13.2 Living situation in the “real-world scenario” (not true to scale) ([Rübarsch 2003](#))

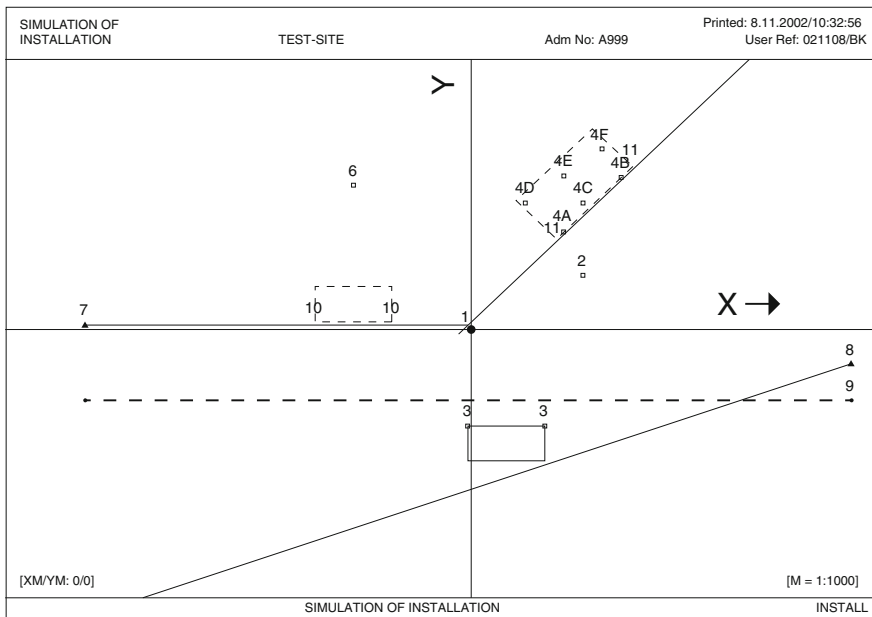


Fig. 13.3 Location of the objects (Rübärsch 2003)

13.3.2 The Scenario in More Detail

The situation in the scenario is a village where 11 objects are defined:

1. Magazine
2. Church
3. Plant
4. 6 houses
5. Small farm
6. Big farm
7. Road
8. Highway
9. Railway
10. Soccer field
11. Free field and garden

Furthermore, the following assumptions are made:

- There is a population of 50 persons in the village. 5 persons live in each of the 6 houses, 4 persons live on the small farm, 15 on the big farm, and the priest lives in the church.
- 2 persons from the houses work in the magazine. 8 persons from the houses go shopping (2 h/week each)

Table 13.1 Definition of basic situations in 1 week = 168 h (Rübarsch 2003)

Basic situation	Short	Time range	Total hours/week	Fractional duration
Night	N	Monday–Friday 21–7 h	74	$SD_N = \frac{74}{168} \approx 0.44$
		Saturday–Sunday 21–9 h		
Working day	D	Monday–Friday 8–17 h	45	$SD_D = \frac{45}{168} \approx 0.27$
Evening and morning	E	Monday–Friday 7–8 h	25	$SD_E = \frac{25}{168} \approx 0.15$
		Monday–Friday 17–21 h		
Weekend day	W	Saturday–Sunday 9–21 h	24	$SD_W = \frac{24}{168} \approx 0.14$

- All people in the village go to church for 2 h every Sunday and there are 150 external visitors from other villages. The priest is in the church all the time.
- 20 persons from the houses and 80 persons from outside the village work in the plant.
- For the road, highway and railway only passing through traffic is considered. To simplify the model, e.g. the highway has no exit in the village, there is no train station and the ways for the people in the village are so short that they can be neglected. Each of the three transport routes is assumed to have a distance of 5 km in the village, the velocities are 60 km/h on the road, 100 km/h on the highway and 80 km/h for the railway. The average amount of vehicles for the road is 100 vehicles/h with an average of 1.5 persons per car. The highway is used by 300 vehicles/h with an average of 2 per vehicle. There are 2 trains per hour with an average of 100 persons in each of them.
- All persons from the houses and the small farm go to soccer practice for 4 h/day in the evening/morning from Monday to Friday. (This also accounts for other outdoor activities.)
- All persons from the houses use the garden for 3 h on the weekend.
- 3 persons from the big farm work on the free field during the working day.
- The persons stay at home whenever they are not busy doing one of the previously defined tasks.

Table 13.1 shows the division into night, working day, evening/morning and weekend.

With the assumptions of the data from Table 13.1 one can distinguish between 12 types of persons, see Table 13.2.

13.3.3 Individual Exposure

Exemplarily we compute the individual presence (individual exposure) of a person of the type “magazine personnel” (see Table 13.2, third line). In the house the person is

Table 13.2 Description of the 12 types of persons

Name	Description of occupation pattern
Priest	Spends 100 % of his time in the church
Magazine personnel	N: 100 % house, D: 100 % magazine, E: 100 % house—4 h/day soccer field, W: 100 % house—2 h church—3 h gardening
Plant worker village	N: 100 % house, D: 100 % plant, E: 100 % house—4 h soccer field, W: 100 % house—2 h church—3 h gardening
Plant worker external	D: 100 % plant, W: 2 h church
Non-working house inhabitants	N: 100 % house, D: 100 % house—2 h/week shopping, E: 100 % house—4 h/day soccer field, W: 100 % house—2 h church—3 h gardening
Small farmers	N: 100 % farm, D: 100 % farm, E: 100 % farm—4 h/day soccer field, W: 100 % farm—2 h church
Big farmers	N: 100 % farm, D: 100 % farm, E: 100 % house, W: 100 % house—2 h church
Big farmers free field	N: 100 % farm, D: 100 % free field, E: 100 % house, W: 100 % house—2 h church
Church visitor	W: 2 h church
Road users	60 km in 1 h -> 5 km in 5 min
Highway users	100 km in 1 h -> 5 km in 3 min
Railway users	80 km in 1 h -> 5 km in 3.75 min

$$100 \% \cdot \frac{74 \text{ h}}{168 \text{ h}} + \frac{25 \text{ h} - 4 \text{ h} \cdot 5}{168 \text{ h}} + \frac{24 \text{ h} - 3 \text{ h} - 2 \text{ h}}{168 \text{ h}} = 58.3 \% \quad (13.1)$$

of the time. Here, the first term shows the 100 % of the night, the second term the evening time without soccer practice, the third term the weekend time without gardening and church.

By a similar computation the person spends $1.0 \cdot \frac{45}{168} = 26.8 \%$ of the time in the magazine, $\frac{4.5}{168} = 11.9 \%$ of the time on the soccer field, $\frac{2}{168} = 1.2 \%$ of the time in the church and $\frac{3}{168} = 1.8 \%$ in the garden.

In summary, given the occupation pattern of Tables 13.1 and 13.2, we can compute the local exposition for each person.

13.3.4 Individual Local and Non-local Risk

What are the numbers from Sect. 13.3.3 relevant for? They can be used to compute the individual risk of persons.

For example, assume the situation where there is an explosion in the plant (which has to be defined more clearly to use it for computations). Numerical models can be used to compute the local pressure and impulse as introduced in Chap. 5 and

the local damage can be analyzed according to Chap. 9. The result is the overall probability of a given damage type (e.g. minor ear damage) taking different locations (building, free field, garden, ...) into account.

With this knowledge it is possible to compute the individual risk of a person of type “magazine personal” by

$$\begin{aligned}
 R_{\text{magazine personal}} = & P(\text{explosion occurs}) \cdot \\
 & (0.268 \cdot P(\text{damage type occurs in house}) \\
 & + 0.119 \cdot P(\text{damage type occurs on soccer field}) \\
 & + 0.012 \cdot P(\text{damage type occurs in church}) \\
 & + 0.018 \cdot P(\text{damage type occurs in garden})).
 \end{aligned} \tag{13.2}$$

The individual risk to suffer from ear injuries in one specific location is computed as the product of the event frequency (probability that explosion occurs) times the probability of local exposition times the probability of the given damage type. This is consistent with the formula

$$R = PC \tag{13.3}$$

from Chap. 1 because the first two factors generate P for each location. To compute the total individual risk, we sum over all locations.

Of course the individual local risk for one location is given by one summand, for example $0.268 \cdot P(\text{damage type occurs in house})$ for the house.

The computation of risks will be treated in more detail in Chap. 14.

13.3.5 Average Presence

Section 13.3.3 concentrated on individual persons and their overall non-local and local risk. This section treats the question how the overall (total) risk of the persons in the village to suffer from ear injuries in case of an explosion in the plant can be determined.

We now use numbers of the scenario that have not been used before: The number of persons of each type, see Table 13.3.

The average number of persons in the scenario is (see Table 13.3)

$$N_{\text{total}} = 50 + 150 \cdot \frac{2 \text{ h}}{168 \text{ h}} + 80 \cdot \frac{45 \text{ h}}{168 \text{ h}} + 12.5 + 30 + 12.5 = 128.21, \tag{13.4}$$

adding the population and the average numbers of external persons in the church, in the plant and on the transportation lines.

Table 13.3 Number of persons of the different types

Name	Number of this type
Priest	1
Magazine personnel	2
Plant worker village	20
Plant worker external	80
Non-working house inhabitants	$30 - 20 - 2 = 8$
Small farmers	4
Big farmers	$15 - 3 = 12$
Big farmers free field	3
Church visitor	150
Road users	There are 100 cars/h and 1 car stays 5 min, that is, in average there are $\frac{100 \text{ cars} \cdot 5 \text{ min}}{60 \text{ min}} = 8.33$ cars with $8.33 \text{ cars} \cdot 1.5 \frac{\text{persons}}{\text{car}} = 12.5$ persons on the road
Highway users	Average: $\frac{300 \text{ cars} \cdot 3 \text{ min}}{60 \text{ min}} \cdot 2 \frac{\text{persons}}{\text{car}} = 30$ persons on highway
Railway users	Average: $\frac{2 \text{ trains} \cdot 3.75 \text{ min}}{60 \text{ min}} \cdot 100 \frac{\text{persons}}{\text{train}} = 12.5$ persons on railway

The numbers from Tables 13.1, 13.2 and 13.3 can be used to compute how many people are (in average) present at each object depending on the time and day of the week, see Table 13.4.

For example we explain the entry in the line “6 houses” and in the column “working day”: During the working day ($5 \cdot 9 \frac{\text{hours}}{\text{week}} = 45 \frac{\text{hours}}{\text{week}}$) 8 persons are

Table 13.4 Number of persons present at objects at different times of the day and at different days during the week (local exposure)

Object	Night	Working day	Evening/morning	Weekend
Magazine	0	$2 + 8 \cdot \frac{2h}{45h} = 2.36$	0	0
Church	1	1	1	$1 + 200 \cdot \frac{2h}{24h} = 17.67$
Plant	0	100	0	0
6 houses	30	$8 \cdot \left(1 - \frac{2h}{45h}\right) = 7.64$	$30 \cdot \left(1 - \frac{20h}{25h}\right) = 6$	$30 \cdot \left(1 - \frac{5h}{24h}\right) = 23.75$
Small farm	4	4	$4 \cdot \left(1 - \frac{20h}{25h}\right) = 0.8$	$4 \cdot \left(1 - \frac{2h}{24h}\right) = 3.67$
Big farm	15	12	15	$15 \cdot \left(1 - \frac{2h}{24h}\right) = 13.75$
Road	12.5	12.5	12.5	12.5
Highway	30	30	30	30
Railway	12.5	12.5	12.5	12.5
Soccer field	0	0	$34 \cdot \frac{20h}{25h} = 27.2$	0
Free field	0	3	0	$30 \cdot \frac{3h}{24h} = 0.38$

present in the house except for the 2 h where they go shopping. Hence in average there are $8 \cdot \left(1 - \frac{2h}{45h}\right) = 7.64$ persons in the house during a working day.

The average number of persons for any point in time during the week is

$$N_{\text{av pres}} = \frac{74 \text{ h}}{168 \text{ h}} N_N + \frac{45 \text{ h}}{168 \text{ h}} N_D + \frac{25 \text{ h}}{168 \text{ h}} N_E + \frac{24 \text{ h}}{168 \text{ h}} N_W \quad (13.5)$$

where N_N , N_D , N_E and N_W are the average numbers of persons during the night, working day, evening/morning and weekend, respectively. For example, the average number of persons in the free field is

$$\begin{aligned} N_{\text{avpresfield}} &= \frac{74 \text{ h}}{168 \text{ h}} N_{N,\text{field}} + \frac{45 \text{ h}}{168 \text{ h}} N_{D,\text{field}} + \frac{25 \text{ h}}{168 \text{ h}} N_{E,\text{field}} + \frac{24 \text{ h}}{168 \text{ h}} N_{W,\text{field}} \\ &= \frac{74 \text{ h}}{168 \text{ h}} \cdot 0 + \frac{45 \text{ h}}{168 \text{ h}} \cdot 3 + \frac{25 \text{ h}}{168 \text{ h}} \cdot 0 + \frac{24 \text{ h}}{168 \text{ h}} \cdot 30 \cdot \frac{3 \text{ h}}{24 \text{ h}} = 1.34 \end{aligned} \quad (13.6)$$

Remark It has to be kept in mind that taking averages always leads to a loss of detail and information. Regard the following example from Table 13.4:

- The average number of persons in the church is 17.67. However, there will never be close to 17.67 persons in the church, since we know that most of the time there is only one person and only in 2 h of the week (at a fixed time) there are a lot of people. So, one has to consider whether it makes sense to use this average or rather regard two different situations and their risks separately.
- In the contrary, for the magazine the computation of the average is more reasonable since one can expect that persons go shopping at different times (and might even change their behavior from one week to the other).

The numbers from Table 13.4 can be used to compute the average number of damaged persons for a given damage type for each building type, for example in case of an explosion in the plant during the evening:

$$\begin{aligned} N_{\text{avinj, small farm, E}} &= P(\text{damage occurring on the small farm}) \cdot 4 \text{ persons} \\ &\quad \cdot \left(1 - \frac{20 \text{ h}}{25 \text{ h}}\right). \end{aligned} \quad (13.7)$$

Remark These average numbers of persons can be used to compute the collective risk, for example

$$R_{\text{collinj,smallfarm,E}} = N_{\text{avinj,smallfarm,E}} \cdot P(\text{explosion in plant in evening}). \quad (13.8)$$

The computation of collective risks will be treated in more detail in Chap. 14.

13.3.6 Formalization

The Sects. 13.3.1–13.3.5 showed that a descriptive approach with sample numbers has limitations, mainly with respect to compactness and clarity. Therefore we summarize Sect. 13.3 in formulas to make it easier applicable to other, more complex situations.

We define a set of types of objects

$$O_k, \quad k = 1, \dots, N_k, \quad (13.9)$$

a set of time spans,

$$T_l, \quad l = 1, \dots, N_l, \quad (13.10)$$

and a set of persons,

$$P_m, \quad m = 1, \dots, N_m. \quad (13.11)$$

Let $N(P_m)$ be the number of persons of type P_m .

For simplicity we assume, that the time spans do not depend on the person type, i.e. we use the same time span intervals for all person types. In a similar way we do not assume that certain objects are only available for a certain persons, i.e. we have to specify for each person type the presence at each object type.

It is also assumed that each person belongs to exactly one person type and is at exactly one object in each time span.

For each type of person it is defined how much time it spends at which object,

$$T(P_m, O_k). \quad (13.12)$$

We assume that the following total time constraint holds for each person type (exposure of persons from a specific group at all object types)

$$T = T(P_m) = \sum_{k=1}^{N_k} T(P_m, O_k), \quad (13.13)$$

where T is the total time considered for all person types, i.e. the total time spans of each person type sum up to the same time.

The individual probability of a person to be exposed at a certain object reads

$$IP(P_m, O_k) = \frac{T(P_m, O_k)}{T}. \quad (13.14)$$

The local individual risk of a person at an object reads

$$ILR(P_m, O_k) = IP(P_m, O_k)P(\text{damage at } O_k \text{ in case of hazard event}) \\ \times P(\text{hazard event}). \quad (13.15)$$

The individual risk of a person reads (non-local individual risk)

$$IR(P_m) = \sum_{k=1}^{N_k} ILR(P_m, O_k). \quad (13.16)$$

The number of persons of given type, in given objects and time spans is denoted by

$$N(P_m, O_k, T_l). \quad (13.17)$$

Hence, for time spans of equal length, the average number of persons of given type at given object type reads

$$N(P_m, O_k) = \frac{1}{N_l} \sum_{l=1}^{N_l} N(P_m, O_k, T_l). \quad (13.18)$$

The total number of persons at a given object (absolute number of exposed persons) and given time span reads

$$N(O_k, T_l) = \sum_{m=1}^{N_m} N(P_m, O_k, T_l). \quad (13.19)$$

For time spans of equal length, the average number of persons (independent of the person type) at an object reads

$$N(O_k) = \frac{1}{N_l} \sum_{m=1}^{N_m} \sum_{l=1}^{N_l} N(P_m, O_k, T_l). \quad (13.20)$$

The average numbers can be used to compute average collective risks.

The average (averaged over person types) collective local risk reads

$$CLR(O_k) = \sum_{m=1}^{N_m} ILR(P_m, O_k)N(P_m). \quad (13.21)$$

$$CR = \sum_{k=1}^{N_k} CLR(O_k). \quad (13.22)$$

Similar and somewhat more general equations can be derived when assuming that the sets of time spans and/or objects depend on the person type. Also the considered

time span for each person type can be changed to depend on the person type, since (13.14), (13.21) and (13.22) only use exposure probabilities.

More elaborate formalizations of discrete object distributions and related risks can be found in Salhab et al. (2011).

13.4 Success Frequency of Avoiding Hazards

The description in Chap. 2 of this step in the process

This step considers the success frequency of organizational and training measures, of spontaneous reactions (for example flight) as well as the success rates of placing passive, reactive, or active physical barriers

already shows how difficult it is to generate numbers for these frequencies. We give some examples.

Example 1 Using sensors, explosive runaway reactions in a chemical reactor are detected, and typically the evacuation of the building is conducted successfully. We might assume that the occupation number for personnel is reduced to 10 % when compared to standard operation in the vicinity of the reactor.

Example 2 A general bombing alarm (public terror alert/warning level) is sounded for an embassy based on intelligence and surveillance data generated in the vicinity of the embassy. All workplaces close to the main road are evacuated in case the alarm is set. We might assume that the presence of personnel during real attacks is reduced to 50 %.

Example 3 In case of terror attacks with hand-held weapons, physical sight-protecting curtains are lowered in exposed areas. We might assume that physical consequences are reduced to 25 % (less impact close to exposed objects).

In general the definition of these counter measures change the scenario. So, the basic idea is that the steps where these changes has an influence on are reconsidered.

Example 4 The analyzed situation is the explosion of a gas tank on the property of a company. Now the analyzing team decides that a possible measure is to strengthen the walls of a building, e.g. by using blast walls, where dangerous chemicals are stored. What would change?

- The hazard source is still the same.
- The initial situation is mostly the same except for the different walls.
- The hazard propagation is different because the walls react different to blast and fragments do not go through as easily.
- The damage analysis is changed due to the changed hazard propagation. The damage in the building is (hopefully) reduced.
- The hazard event frequency is not changed, the explosion is as likely as before.
- The distribution of objects and persons is still the same.

All steps that have changed must be analyzed to determine the success frequency of this measure. In this case again, the impact is on physical consequences.

13.5 Summary and Outlook

In this chapter we have considered three steps of the risk analysis process. The hazard event frequency can be determined with different approaches: A database analysis can be used to see what has happened in similar situations in the past or system analysis methods like Fault Tree Analysis can be used to analyze the hazard event frequency of one specific situation or system in dependence of its parts or subsystems.

The step “distribution of objects” can be very time-consuming or relatively easy, depending how well the situation is known and how much material already exists. We presented a bootstrap example in a very basic discrete way showing that in discrete (with respect to locations and time table) cases all data is available for risk computations.

The success frequency of avoiding hazards is an important step towards the planning of mitigation measures but is difficult to generalize.

The next chapter will introduce the computation of individual and collective risks based on the classical risk formula $R = PC$. The computed risk can be visualized in different ways.

References

- American Institute of Chemical Engineers. (1999). *Guidelines for chemical process quantitative risk analysis*. New York: Wiley.
- Department of Transportation. (2014). *United States Department of Transportation*. Retrieved May 28, 2014, from <http://www.dot.gov/>
- National Consortium for the Study of Terrorism and Responses to Terrorism (START). (2011). *Global Terrorism Database [Data file]*. Retrieved January 20, 2012, from <http://www.start.umd.edu/gtd>
- Rübarsch, D., Dörr, A., & Gürke, G. (2003). *EMI Bericht E 36/03*. Efringen-Kirchen, Fraunhofer EMI.
- Salhab, R. G., Häring, I. & Radtke, F. K. F. (2011). Formalization of a quantitative risk analysis methodology for static explosive events.
- Schneier, B. (1999). *Attack Trees*. Retrieved May 28, 2014, from <http://tnlandforms.us/cns04/attacktrees.pdf>
- Yoon, E. S. (2012). *Event Probability and Failure Frequency Analysis*, from http://pssl.snu.ac.kr/korean/files/8th_class.pdf

Chapter 14

Risk Computation and Visualization

14.1 Overview

This chapter combines the measures for probability and damage in terms of various risk quantities. A schematic approach illustrates the distinction between individual and collective risks. Along with the discrete distribution and risk computation example of Chap. 13, this emphasizes the distinction between local and non-local risks, individual and group (collective) risks as well as time-dependent and time-independent risks as well as their various combinations.

Of particular importance are local individual annual risks, because they allow to compute non-local individual risks provided individual spatial (occupation) profiles are given or to directly compare with annual individual risks. Together with time-dependent exposure and protection level quantities they also allow to generate all types of collective risks. Furthermore they are well suited for risk visualization.

Taking up formal expressions of Chaps. 3, 4, 7, 8 and 10, this chapter also computes exemplarily the local risk due to fragments of single events, malicious events and blast hazards. This is exemplarily visualized for the last two cases. This shows that engineering approaches allow a much more detailed analysis, even if the exact locations of possible events are not known.

For risk visualization also the abstract risk matrix can be used. It is also suitable to support the determination of risks within expert rounds. The risk graph method is even more suitable to guide expert judgement. However, the design of the risk graph has already to take into account all key factors influencing the probability and risk quantities.

The different types of risk quantities of this chapter allow to systematically assess improvement and counter measures for all resilience management phases: protection, prevention, response and recovery. Such more detailed assessment measures typically are determined during the preparation phase. However, risk quantities can also be obtained up to real-time conditions. In particular

semi-quantitative risk quantitative risk quantities can be used for decision making in response and the initial recovery phase.

The risk quantities are key for the resilience capability of decision making and inference, action and implementation of counter and improvement measures.

Furthermore, risk and chance assessment can be used to asses all resilience capabilities, even for unknown events up to unknown events. Thus there are various options to use risk and chance quantities during resilience management, provided the objectives for which the risks/chances are determined are appropriately chosen.

The steps of the risk management process considered in the chapter are

- (9) **Risk computation and visualization:** This involves the computation of various risk quantities. The visualization options include risk maps, risk tables, and F-N-diagrams.
- (10) **Risk comparison with criteria:** The quantitie are compared to risk assessment criteria, for example risk matrices, critical values, and F-N criteria. For example, one checks whether the nonlocal annual individual risk is smaller than the de minimis risk.

These two steps will be treated in this chapter and will be extended in Chap. 17.

In Sect. 14.2 individual and collective risk are defined and discussed. Section 14.3 addresses risk computation and Sect. 14.4 local risk maps.

Then two tools are introduced to compute and visualize risks: Risk matrix (table) in Sect. 14.5, and risk graphs in Sect. 14.6. Another often used tool, the so called F-N-diagrams are also a common method to evaluate risks. They were introduced in Sect. 3.1.

The main sources for this chapter are Häring et al. (2009), International Electrotechnical Commission (2010), Salhab et al. (2011), Fischer et al. (2012), Thielsch (2012); Voss et al. (2012), Häring (2013a, b), Kaufmann and Häring (2013), Riedel et al. (2014, 2015).

14.2 Individual Versus Collective Risk

We have already seen the general formula of risk

$$R = PC, \quad (14.1)$$

where risk is defined as the product of probability/frequency and consequences several times. This can be computed for individual persons or groups. This results in the difference between individual and collective risk as we have already seen in the example in Sect. 15.2.2.

Individual risk is the expected damage (loss of money, injury, etc.) times a frequency/probability measure of an object or single person in or per time interval. The individual risk may consider a single location or all locations where the object or person is exposed.

An example for the average individual annual risk for injuries due to terror attacks on tunnels is

$$R_{\text{ind-inj}} \approx \frac{1000 \frac{\text{injured}}{\text{year}}}{6.514 \times 10^9 \text{ persons}} \approx 1.53 \times 10^{-7} \frac{\text{injured}}{\text{person year}}. \quad (14.2)$$

The examples show that the frequency/probability factor often is composed of several factors: scaling factors, basic probability, conditional probabilities, and further independent probabilities.

In a similar way the consequences may consist of sums of consequences. In the general case the individual risk is itself a sum of single risks, e.g. when considering all possible positions of personnel.

Collective or group risk is the expected damage (money, injury, ...) times a frequency/probability measure of a group of objects or persons per or within a time interval. Here it is important to clearly define the collective or group, e.g. the total population, company, city, country, world, etc.

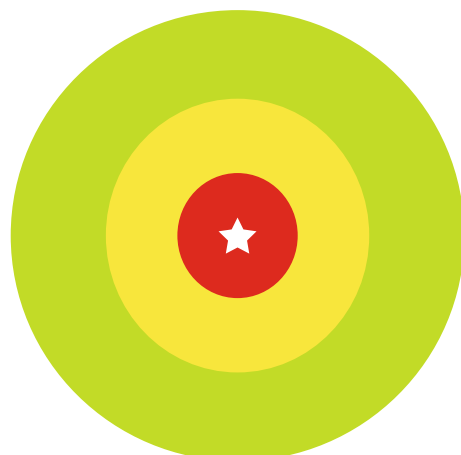
An example for the collective annual risk for damage due to terror attacks on tunnels reads

$$R_{\text{col-inj}} \approx 2.8 \frac{\text{attacks}}{\text{year}} \cdot \frac{\text{Euros damage}}{\text{attack}} \approx 2.8 \frac{\text{Euros damage}}{\text{year}}. \quad (14.3)$$

We note that the collective risk may be computed for the same scenario for very different groups, e.g. simultaneously for all buildings, all vehicles, all personnel of a fabrication side, the neighborhood and further third party. This risk quantity is very important to assess that catastrophes will not take place.

Why is it important to distinguish between those two forms of risk? Regard an explosion in an open area and assume that the damage effects have been determined in dependence of the distance to the explosion, see Fig. 14.1. For this vicinity of the

Fig. 14.1 Explosion and different levels of damage effects depending on the distance from the explosion



explosive source is divided in three (what-if) damage area zones: green, yellow and red in Fig. 14.1. The explosion is represented by the star in the middle. If the event frequency is known the color coding could also resemble the local individual risk.

Now we compare two situations. In the left situation in Fig. 14.2 a group of people is living in the yellow zone. In the right situation there is only one person living in that zone. All the people have the same individual risk, that is, by looking only at the individual risk there is no difference between those situations. However, the collective risk in the left situation is 5 times higher than in the right situation. So, it is important to also regard the collective risk.

Figure 14.3 shows the opposite case. Assume that the local risk of injury in the yellow zone is one third of the local risk of injury in the red zone. Then the

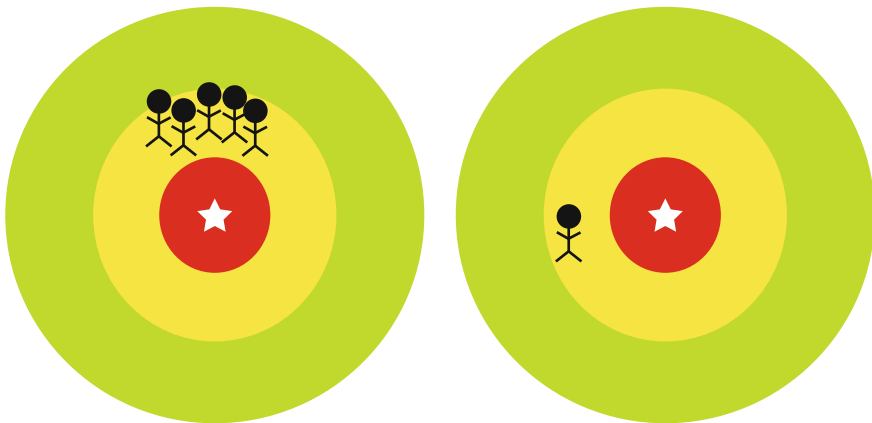


Fig. 14.2 Two situations with the same individual risk but different collective risks

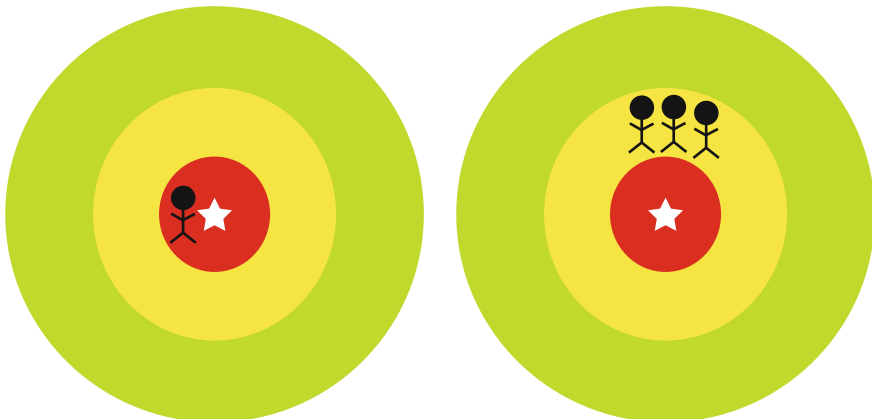


Fig. 14.3 Two situations with the same collective risk but different individual risks

collective risk of the two situations in Fig. 14.3 is the same. On the other hand, the individual local risk of the left person is higher than the individual risks of the 3 persons at the right hand side.

Hence, the example has shown that it is important to consider both forms of risk.

14.3 Risk Computation

In this section, four examples for risk computation are given.

14.3.1 Individual Local Risks Due to Single Stationary Hazard Source and Combination of Damage Effects

This section computes the local annual individual risks for persons due to a possible local stationary explosive event due to (a) fragments and (b) blast and (c) combined. It uses historical event data, experimental-analytical, physical-engineering and simulative approaches. This is a simplified and modified summary of Salhab et al. (2011).

The local individual risk of an object due to explosive fragments is given by

$$R_{l,m,l_s,j_{ES}}^{frag} = f^{ev} E_{j_{ES}} \left(\bar{r}_{j_{ES}}^{ES} \in V_{l,m}^{gr} \right) \mu_{l,m,l_s}^{frag}, \quad (14.4)$$

where l and m number the radial segments about the hazard source, l_s indicates the type of damage assessed and j_{ES} labels the exposed object (exposed site) considered. The logical bracket in (14.4) ensures, that the correct fragment density is used for the object at risk.

Due to its definition and computation, the local individual risk due to fragments is a discrete value for each combination of object type at risk, damage category and radial segment.

The annual frequency in (14.4) is given by the annual historical event frequency f^{ev} and the object exposure ratio at the exposed site

$$E_{j_{ES}} = \Delta t_{j_{ES}}^{\exp} / 365 \text{ days}. \quad (14.5)$$

The damage probability for the selected damage type and exposed object type within the radial segment is given by

$$\mu_{l,m,l_s}^{frag} = \min \left\{ \sum_{\underline{k}} \sum_j \left(\vec{r}_{\underline{k}}^{imp} \in A_{l,m}^{gr} \right) w_{\underline{k}} \cdot \frac{A_{\underline{k},j}^{ES,proj}(\alpha_{\underline{k}})}{A_{\underline{k},l,m}^{proj}(\alpha_{\underline{k}})} \Phi_{l_s,j} \left(v_{\underline{k}}^{imp}, m_{j_{sp}+1} \right), 1 \right\}, \quad (14.6)$$

where the multi index \underline{k} loops over all representative fragment initial launching conditions in terms of representative masses, launching directions and velocities (see Chap. 7) and the index j loops over all presented surfaces of the object j_{ES} at risk. The logical bracket ensures that only representative fragments are considered that impact the radial segment of interest.

The weighting factor $w_{\underline{k}}$ is the average (in general non-integer) number each representative fragment with mass $m_{j_{sp}+1}$ (upper bound of represented mass interval) and impact velocity $v_{\underline{k}}^{imp}$ is representing. The area $A_{\underline{k},j}^{ES,proj}(\alpha_{\underline{k}})$ is the representative (projected) partial (due to possible shadowing effects) area of the exposed three-dimensional object (see Sect. 12.3). In a similar way, $A_{\underline{k},l,m}^{proj}(\alpha_{\underline{k}})$ is the presented (projected) area of the radial surface segment.

The probability distribution $\Phi_{l_s,j}(v_{\underline{k}}^{imp}, m_{j_{sp}+1})$ determines the damage probability with respect to the damage category and the presented surface element of the object at risk and is assumed to depend on impact velocity and fragment mass.

The minimum function in (14.6) ensures that the damage probabilities add up to a maximum value of 1.

In summary, (14.4) sums up for each representative fragment the damage probabilities taking into account the geometrical probability of impact assuming a single object at risk on the radial surface element, the conditional probability of impacting presented surfaces as well as surface-specific damage models.

The individual local risk due to blast reads

$$R_{l_s,j_{ES}}^{blast} = f^{ev} E_{j_{ES}} \mu_{l_s}^{blast} \left(\vec{r}_{j_{ES}}^{ES} \right), \quad (14.7)$$

where μ_{l,m,l_s}^{blast} computes the blast damage for the damage category of interest using a direct or indirect approach as described in Sect. 10.2.

Assuming that blast and fragment damage effects (multiple damage effect assessment) are independent of each other, the combined individual local risk of objects is computed as

$$R_{l,m,l_s}^{comb} = f^{ev} E_{j_{ES}} \left(1 - (1 - \mu_{l,m,j_{ES}}^{frag})(1 - \mu_{j_{ES}}^{blast}) \right). \quad (14.8)$$

14.3.2 Possible Event Locations Distributed on 3D Line: F-N Curve Generation

This section reviews the generation of annual f-N and F-N curves in case of multiple possible locally distributed explosive events generating fragment hazard. They are distributed on a 3D line, e.g. street. This also covers the distribution in time of such events. They are computed using technical scenario data, physical-engineering and simulative approaches. See Häring et al. (2009) for a detailed derivation of such quantities.

For computing the f-N curve, the main idea is to compute for each possible event the expected damage numbers with an expression that is a little similar to (14.6). However, the average expected damage quantities are in general not integers. Therefore a binning is introduced. Furthermore, in cases where the average expected damage number in case of an event is below 1 before the binning a transformation is used. For instance, the frequency—average damage pair (1.E-5, 0.1) is interpreted as (1.E-6, 1.0). In this way, the frequency for all events with fractional damage number below 1.0 is transformed.

The computation of the F-N curve is similar to Sect. 17.2.7, i.e. obtained by cumulating the binned f-N curve.

14.3.3 Local Annual Risk in Case of Multiple Threats: Object-Wise Empirical-Analytical Approach

This section computes the annual local risk of terror events for all terror attack types on buildings and infrastructure based on statistical analysis of historical terror event data, see Voss et al. (2012) for a detailed derivation.

The local individual annual risk of a building or infrastructure object \vec{b}_k with respect to consequence type $T_n^{\text{consequence}}$ as computed from empirical database data from the past time interval $[t_1, t_2]$ reads

$$\begin{aligned} R\left(\vec{b}_k, T_n^{\text{consequence}}, [t_1, t_2]\right) \\ = \sum_{i=1}^{n_{\text{threat}}} F\left(T^{\text{building}}(\vec{b}_k), T_i^{\text{threat}}, [t_1, t_2]\right) w_{ik} C\left(T_i^{\text{threat}}, T^{\text{building}}(\vec{b}_k), T_n^{\text{consequence}}, [t_1, t_2]\right). \end{aligned} \quad (14.9)$$

In (14.9) the empirical-historical event frequency for the threat type T_i^{threat} and building type combination enters,

$$\begin{aligned} F(T_i^{threat}, T_l^{building}, [t_1, t_2]) &= \frac{\text{number of events of type } T_i^{threat} \text{ on building type } T_l^{building}}{\text{time period} \cdot \text{number of buildings of type } T_l^{building}} \\ &= \frac{N(T_i^{threat}, T_l^{building}, [t_1, t_2])}{(t_2 - t_1)N_l^{building}}, \end{aligned} \quad (14.10)$$

as well as the local probability and consequence scaling factor for the combination of building and threat w_{ik} , e.g. due to physical, organizational or societal effects (access control, fast response, etc.).

Furthermore, in (14.9) enters the empirical consequence measure

$$\begin{aligned} C(T_i^{threat}, T_l^{building}, T_n^{consequence}, [t_1, t_2]) \\ = \frac{\text{total number of } T_n^{consequence} \text{ for } T_l^{building} \text{ and } T_i^{threat} \text{ within } [t_1, t_2]}{\text{number of } T_i^{threat} \text{ events on } T_l^{building} \text{ within } [t_1, t_2]}, \end{aligned} \quad (14.11)$$

where the total number of $T_n^{consequence}$ is, e.g., the total number of objects destroyed or the number of injuries.

14.3.4 Local Risk in Case of Multiple Possible Event Types and Locations

The section presents local risks for (a) persons on places and streets, (b) buildings and infrastructure in case of a terror attack event within an urban quarter based on historical terror event data, analytical-empirical and engineering-simulative approaches, see Voss et al. (2012) for a detailed derivation.

The local individual risk at the positions \vec{r}_o due to all types of terroristic threats at all possible event locations r_j^{event} reads

$$R_{ind}(\vec{r}_o, T_n^{consequence}) = \sum_{j=1}^{n_{locations}} \sum_{i=1}^{n_{threat}} F(A_j^{event}, T_i^{threat}) C(H(r_j^{event}, T_i^{threat}; P), \vec{r}_o, T_n^{consequence}). \quad (14.12)$$

In (14.12)

$$H\left(r_j^{event}, T_i^{threat}; P\right) \quad (14.13)$$

is the hazard field parametrized by the local hazard parameters P due to a threat type at a possible event location and hence

$$C\left(H\left(r_j^{event}, T_i^{threat}; P\right), \vec{r}_o, T_n^{consequence}\right) \quad (14.14)$$

is the consequence quantity for the consequence type of interest at the position of interest. The event grid and the assessment grid are in general independent of each other. When assuming that a terror event takes place in an urban area or urban quarter in a given time span also local individual what-if terror risks can be computed.

The frequency for a given event type for the area A_j^{event} represented by the event location r_j^{event} considers the contributions of event frequencies from all buildings (infrastructure) within the scenario,

$$F\left(A_j^{event}, T_i^{threat}\right) = \sum_{k=1}^{n_{building}} w_{ik} F\left(A_j^{event}, T_i^{threat}, \vec{b}_k\right), \quad (14.15)$$

using a spatial distribution density, typically localized around the buildings (infrastructure)

$$F\left(A_j^{event}, T_i^{threat}, \vec{b}_k\right) = \iint_{A_j^{event}} f(\vec{b}_k, T_i^{threat}, \vec{r}) dr_x dr_y, \quad (14.16)$$

which has to fulfill the normalization condition

$$F\left(T^{building}(\vec{b}_k), T_i^{threat}, [t_1, t_2]\right) = \sum_{j=1}^{n_{location}} \iint_{A_j^{event}} f(\vec{b}_k, T_i^{threat}, \vec{r}) dr_x dr_y. \quad (14.17)$$

Equation (14.17) means that the event frequency is distributed around possible event locations around the building (infrastructure) entries.

In summary, in this case the threats on all buildings (infrastructure) in the neighborhood is considered for computing local event frequencies. The hazard effects are propagated for multiple weighted events using engineering models.

Finally, damage models are used. The risk assessment combines the frequency and consequence quantities.

14.4 Examples for Risk Mapping

The challenge of selecting appropriate implementation designs for the interaction with the user, risk computation and visualization for risk analysis and management processes, in particular for tools that use 3D visualizations is discussed for a representative set of tools in Kaufmann and Häring (2013). These tools also cover all the 3D visualization examples given in the present Sect. 14.4. A much more generic overview is given in Häring (2013a).

The determination of averaged and cumulated risks with respect to terrorism for whole urban areas based on empirical-historical data is introduced in Voss et al. (2012). See Fig. 14.4 for a sample application of empirical-historical local individual frequencies (susceptibilities) according to (14.10).

In a similar way, consequences (vulnerabilities) according to (14.11) and averaged risks according to (14.9) can be visualized. It is interesting to observe, that in practical applications these three quantities generate for most urban objects distinct input for urban scenario assessment. Furthermore, the susceptibility (frequency) component of risk in most cases dominates the averaged risk quantities.

As shown in Sect. 14.3, the idea is to start out with empirical-statistically sound estimates for frequency and consequences for combinations of threat type and building/infrastructure type, which are further averaged and cumulated. The implementation of the approach is shown, e.g., in Fischer et al. (2012).

Figure 14.4 is also an example of a geo-referenced risk map, since the housing block visualizations use GIS data as input.

In Voss et al. (2012) also the use of empirical hazard event density distributions is introduced, which take account of the urban geometry and physical accessibility according to (14.17), see Fig. 14.5 for a sample implementation.

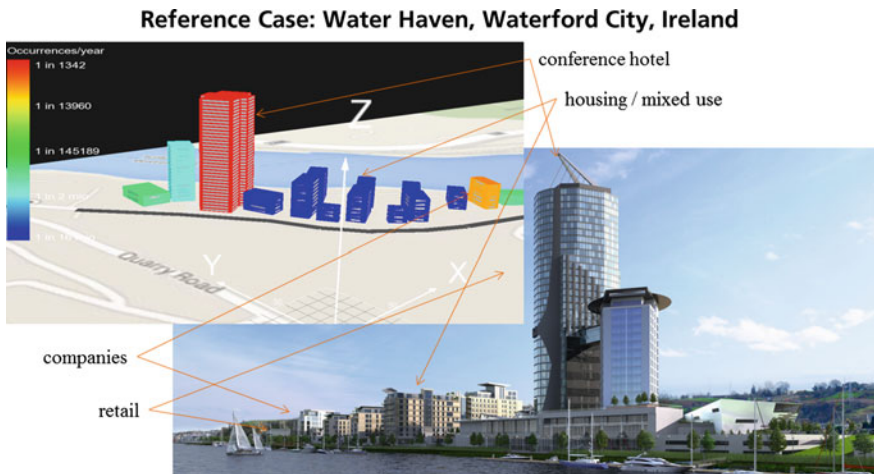


Fig. 14.4 3D model and empirical frequencies of terror events on the Water Haven site plan at Waterford City, Ireland (courtesy Bolster Group) (Riedel et al. 2015)

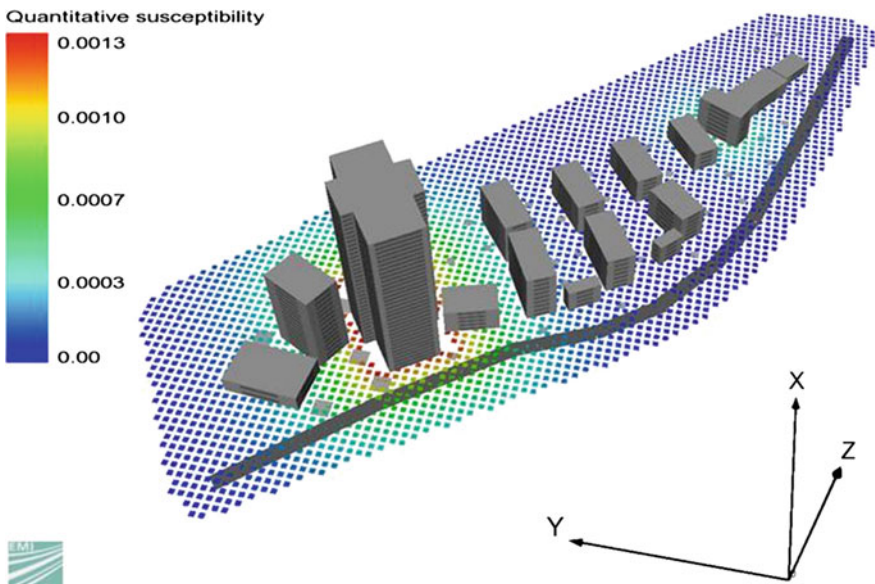


Fig. 14.5 Local event frequency distributed in a quarter normalized to 1: what-if event distribution (Riedel et al. 2015): The vicinity of the conference hotel and the international cooperation shows increased frequency (susceptibility), also for neighboring urban assets

Furthermore, along with the refined local event distributions, quantitative hazard propagation models, realized with empirical-analytical, engineering or simulative approaches are used to determine the hazard propagation of multiple of events, see (14.14). Finally, damage models for personnel and objects determine the damage effects with respect to different damage categories, see e.g. Riedel et al. (2014).

Examples of locally resolved what-if damage maps, that assess the what-if risks due to a set of explosive threats, for which a multitude of possible threat locations within the quarter is assumed are shown in Riedel et al. (2015), see Fig. 14.6. When determining what-if risks, in (14.12) only the relative empirical distribution of threat events is used rather than the absolute annual frequency.

Other examples that could be visualized include the plum shaped dispersion pattern of a gaseous hazard source and complex risk maps in case of physical barriers, shielding and venting effects, e.g. for blast or fragment sources.

14.5 Risk Matrix

An established method for the evaluation of risks is the so called risk matrix (risk assessment table, risk map) which has already been shortly introduced in Sect. 3.3. We also consider it as a visualization option. For instance all risks considered can

Quantitative Risk Evaluation: Threat Aspects

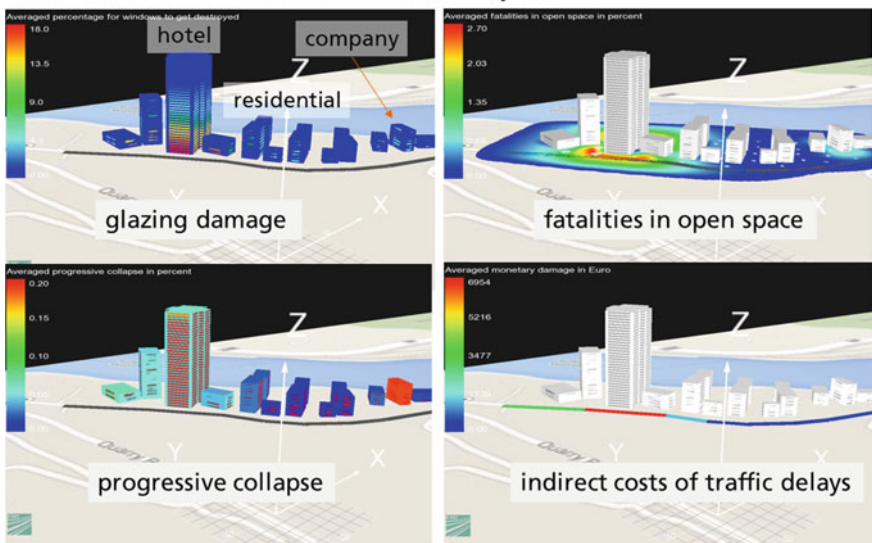


Fig. 14.6 Quantitative what-if risks in case of a terroristic explosive event within the quarter (Riedel et al. 2015). **a** Glazing damage risk. **b** Local fatality risk outside buildings. **c** Progressive collapse risk of buildings. **d** Overall average monetary risk due to local traffic delays caused by road damage, taking into account repair times

be positioned in the risk matrix as dots or using a contour plot based on the cumulated numbers for each matrix field.

A semi-quantitative risk matrix was shown in Table 4.1. Each combination of damage and probability of occurrence leads to one risk class. The acceptance level of each class is marked with a color. Red is a non-acceptable risk, yellow is a borderline risk area where the risk should be reduced by appropriate measures. The color green stands for acceptable risks.

14.6 Risk Graph

Risk graphs are a semi quantitative method to evaluate risks. The risk is estimated with a decision tree typically using three or four risk parameters (depending on which norm is used).

The IEC 61508 uses the four risk parameters to determine technical reliability requirements for safety functions. At least the first two and the last decision options can be used for the assessment of any risk.

(C) Consequence risk parameter

- (F) Frequency and exposure time risk parameter
 (P) Possibility of failing to avoid hazard risk parameter
 (W) Probability of the unwanted occurrence (event frequency of triggering (initial) hazard event)

resulting in the risk graph shown in Figs. 14.7 and 14.8.

“a, b, c, d, e, f, g, h represent the necessary minimum risk reduction. The link between the necessary minimum risk reduction and the safety integrity level is shown in Table 14.1” (International Electrotechnical Commission 2010, part 5, p. 34).

Tables 14.2 and 14.3 show examples of calibrations of the parameters C, F, P and W for the example in Fig. 14.8 and the generic risk graph in Fig. 14.7, respectively.

The present risk graph is a visualization option for the successive consideration of influencing factors relevant for the frequency/probability and the consequences. Typically each level means an increase or decrease by an order of magnitude (factor of 10 or 0.1). The risk graph implicitly executes an individual as well as collective risk criteria. Typically it uses a single individual risk criterion with some deviations for large consequence numbers. In the present case we have

$$R = WFPC \leq R_{crit} \quad (14.18)$$

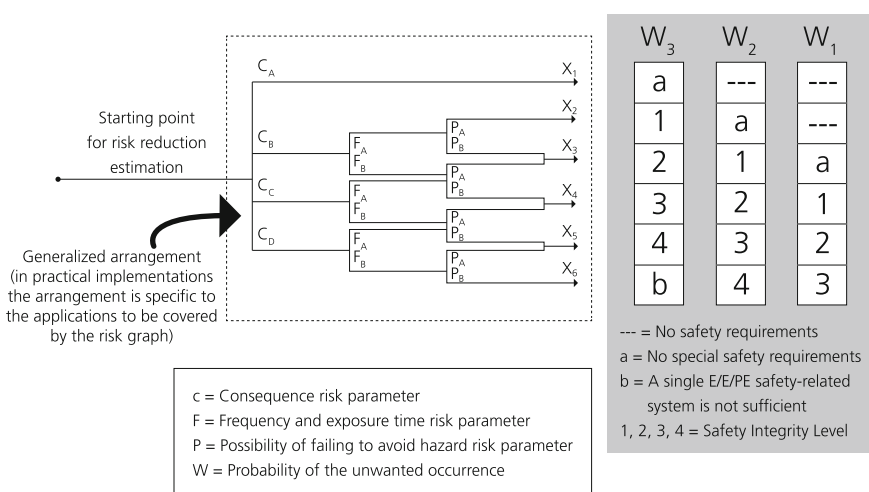


Fig. 14.7 Risk graph: general scheme (International Electrotechnical Commission 2010, part 5, p. 33). Reprinted from IEC 61508-5 with permission of IEC (Geneva), transferred through the division DKE of the VDE e.V. Relevant are the standards with the latest date of issue, which can be purchased at www.iecnormen.de. The German translation is published as DIN EN 61508-5 (VDE 0803-5) and can be purchased at www.iec-normen.de

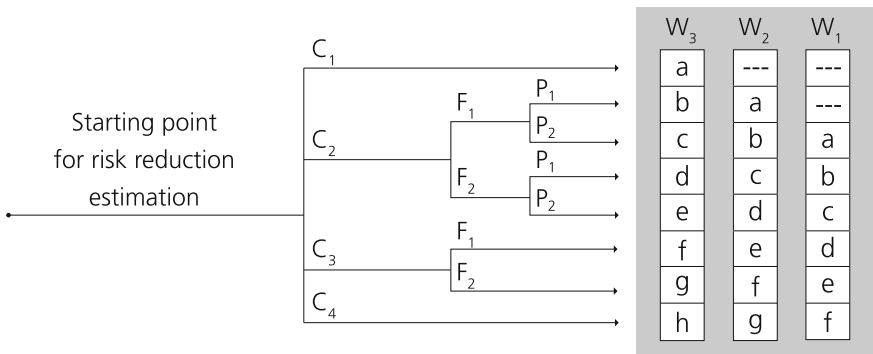


Fig. 14.8 Risk graph—example (illustrates general principles only) (International Electrotechnical Commission 2010, part 5, p. 34). Reprinted from IEC 61508-5 with permission of IEC (Geneva), transferred through the division DKE of the VDE e.V. Relevant are the standards with the latest date of issue, which can be purchased at www.iec-normen.de. The German translation is published as DIN EN 61508-5 (VDE 0803-5) and can be purchased at www.iec-normen.de

R_{crit} can be derived for each combination of the risk graph. Typically it is the same for small consequence numbers and decreases for larger consequence numbers. Often the factor C rates fatalities 10 times more than injuries. Another option to use the same risk criterion is to rate for instance 10 fatalities 100 times more than 1 fatality, thus implementing risk aversion.

The IEC 61508 is not the only norm using risk graphs. An extract of an overview of norms and standards treating risks graphs from Thielsch (2012) is shown in Table 14.4.

The presented risk graph approach is very generic and can also be applied to safety and security critical systems, e.g. if the safety risks originate from security hazards. However, an even more generic approach would be to assess the resiliency of technical systems rather than only their safety and security.

This would allow to take into account in a more explicit and systematic way not only the effects of the resilience (catastrophe, disruptive event) management phases preparation, prevention and protection on risks quantification but also of the phases response and recovery. On top level, this outlines a possible way to resilient technical systems (Häring 2013b).

14.7 Summary and Outlook

The general formula of risk as the product of frequency and consequences was already introduced at the beginning of the course. Most of the course dealt with steps necessary for the determination of those two parameters: frequency and consequences, their generalization and suitable combinations in various ways.

Table 14.1 Explanation of the parameters in Fig. 14.8 (International Electrotechnical Commission 2010, part 5, p. 34). Reprinted from IEC 61508-5 with permission of IEC (Geneva), transferred through the division DKE of the VDE e.V. Relevant are the standards with the latest date of issue, which can be purchased at www.iec-normen.de. The German translation is published as DIN EN 61508-5 (VDE 0803-5) and can be purchased at www.iec-normen.de

	Necessary minimum risk reduction	Safety integrity level
C = Consequence risk parameter	–	No safety requirements
F = Frequency and exposure time risk parameter	a	No special safety requirements
P = Possibility of avoiding hazard risk parameter	b, c	1
W = Probability of unwanted occurrence	d	2
a, b, c ... h = Estimates of the required risk reduction for the safety-related systems	e, f	3
	g	4
	h	An E/E/PE safety-related system is not sufficient

Table 14.2 Example of data relating to risk graph (Fig. 14.8) (International Electrotechnical Commission 2010, part 5, p. 35). Reprinted from IEC 61508-5 with permission of IEC (Geneva), transferred through the division DKE of the VDE e.V. Relevant are the standards with the latest date of issue, which can be purchased at www.iec-normen.de. The German translation is published as DIN EN 61508-5 (VDE 0803-5) and can be purchased at www.iec-normen.de

Risk parameter	Classification		Comments
Consequence (C)	C_1	Minor injury	1. The classification system has been developed to deal with injury and death to people. Other classification schemes would need to be developed for environmental or material damage 2. For the interpretation of C_1 , C_2 , C_3 and C_4 the consequences of the accident and normal healing shall be taken into account
	C_2	Serious permanent injury to one or more persons; death to one person	
	C_3	Death to several people	
	C_4	Very many people killed	
Frequency of, and exposure time in, the hazardous zone (F)	F_1	Rare to more often exposure in the hazardous zone	3. See comment 1 above
	F_2	Frequent to permanent exposure in the hazardous zone	

(continued)

Table 14.2 (continued)

Risk parameter		Classification	Comments
Possibility of avoiding the hazardous event (P)	P_1	Possible under certain conditions	<p>4. This parameter takes into account</p> <ul style="list-style-type: none"> • Operation of a process (supervised (i.e. operated by skilled or unskilled persons) or unsupervised) • Rate of development of the hazardous event (for example suddenly, quickly or slowly) • Ease of recognition of danger (for example seen immediately, detected by technical measures or detected without technical measures) • Avoidance of hazardous event (for example escape routes possible, not possible or possible under certain conditions) • Actual safety experience (such experience may exist with an identical EUC or a similar EUC or may not exist)
	P_2	Almost impossible	
Probability of the unwanted occurrence (W)	W_1	A very slight probability that the unwanted occurrences will come to pass and only a few unwanted occurrences are likely	<p>5. The purpose of the W factor is to estimate the frequency of the unwanted occurrence taking place without the addition of any safety-related systems (E/E/PE or other technology) but including any other risk reduction measures</p> <p>6. If little or no experience exists of the EUC, or the EUC control system, or of a similar EUC and EUC control system, the estimation of the W factor may be made by calculation. In such an event a worst case prediction shall be made</p>
	W_2	A slight probability that the unwanted occurrences will come to pass and few unwanted occurrences are likely	
	W_3	A relatively high probability that the unwanted occurrences will come to pass and frequent unwanted occurrences are likely	

Table 14.3 Example of calibration of the general purpose risk graph (International Electrotechnical Commission 2010, part 5, p. 36)

Risk parameter		Classification	Comments
Consequence (C)	C_A	Minor injury	
Number of fatalities	C_B	Range 0.01–0.1	
This can be calculated by determining the numbers of people present when the area exposed to the hazard is occupied and multiplying by the vulnerability to the identified hazard	C_C	Range >0.1–1.0	
The vulnerability is determined by the nature of the hazard being protected against. The following factors can be used:	C_D	Range >1.0	<p>1. The classification system has been developed to deal with injury and death to people. Other classification schemes would need to be developed for environmental or material damage</p> <p>2. For the interpretation of C_A, C_B, C_C and C_D, the consequences of the accident and normal healing shall be taken into account</p>
$V = 0.01$ Small release of flammable or toxic material $V = 0.1$ Large release of flammable or toxic material $V = 0.5$ As above but also a high probability of catching fire or highly toxic material $V = 1$ Rupture or explosion			
Occupancy (F)	F_A	Rare to more often exposure in the hazardous zone. Occupancy less than 0.1	3. See comment 1 above
This is calculated by determining the proportional length of time the area exposed to the hazard is occupied during a normal working period Note 1: If the time in the hazardous area is different depending on the shift being operated then the maximum should be selected Note 2: It is only appropriate to use F_A where it can be shown that the demand rate is random and not related to when occupancy could be higher than normal. The latter is usually the case with demands which occur at equipment start-up or during the investigation of abnormalities	F_B	Frequent to permanent exposure in the hazardous zone	

(continued)

Table 14.3 (continued)

Risk parameter		Classification	Comments
Possibility of avoiding the hazardous event (P) if the protection system fails to operate	P_A	Adopted if all conditions in column 4 are satisfied	4. P_A should only be selected if all the following are true: <ul style="list-style-type: none">• facilities are provided to alert the operator that the SIS has failed• independent facilities are provided to shut down such that the hazard can be avoided or which enable all persons to escape to a safe area• the time between the operator being alerted and a hazardous event occurring exceeds 1 h or is definitely sufficient for the necessary actions
	P_B	Adopted if all the conditions are not satisfied	
Demand rate (W) The number of times per year that the hazardous event would occur in absence of a the E/E/PE safety related system To determine the demand rate it is necessary to consider all sources of failure that can lead to one hazardous event. In determining the demand rate, limited credit can be allowed for control system performance and intervention. The performance which can be claimed if the control system is not to be designed and maintained according to IEC 61508, is limited to below the performance ranges associated with SIL 1	W_1 W_2 W_3	Demand rate less than 0.1 D per year Demand rate between 0.1 D and 1.0 D per year Demand rate between 1.0 D and 10 D per year For demand rates higher than 10 D per year higher integrity shall be needed	5. The purpose of the W factor is to estimate the frequency of the hazard taking place without the addition of the E/E/PE safety related systems If the demand rate is very high the SIL has to be determined by another method or the risk graph recalibrated. It should be noted that risk graph methods may not be the best approach in the case of applications operating in continuous mode (see 3.5.16 of IEC 61508-4) 6. The value of D should be determined from corporate criteria on tolerable risk taking into consideration other risks to exposed persons

Note This is an example to illustrate the application of the principles for the design of risk graphs. Risk graphs for particular applications and particular hazards will be agreed with those involved, taking into account tolerable risk, see Clauses E.1 to E.6

Table 14.4 Overview of norms and standards treating risk graphs, translated extract of Table 10.3 in Thielsch (2012)

Standard	Title	Year
ISO 13849-1	Safety of machinery—safety-related parts of control systems—Part 1: General principles for design	2008
IEC 61508	Functional safety of electrical/electronic/programmable electronic Safety-related systems	2010
IEC 61511	Functional safety—safety instrumented systems for the process industry sector	2005
VDI/VDE 2180	Safeguarding of industrial process plants by means of process control engineering	2010

In this chapter we emphasized on the combination options for these quantities resulting in individual and collective risk quantities. We also gave arguments why both of them should be considered explicitly.

We summarized some of the most common visualization options for risks: risk map, risk matrix and risk graph. The last two can also be considered as fast methods to determine and assess risks.

In further chapters this will be extended: Risk will be compared to criteria from the literature and F-N-curves will be explained in much more detail. It will be discussed how the computed risks are treated in the further steps of the risk management process, for example how they are communicated, how they are evaluated or how mitigation measures are determined.

References

- Fischer, K., Riedel, W., Häring, I., Nieuwenhuijs, A., Crabbe, S., Trojaborg, S., et al. (2012). Vulnerability identification and resilience enhancements of urban environments. In N. Aschenbruck, P. Martini, M. Meier & J. Tölle (Eds.), *7th Security Research Conference, Future Security 2012*. Germany: Bonn.
- Häring, I. (2013a). Sorting enabling technologies for risk analysis and crisis management. In B. Katzy & U. Lechner (Eds.), Civilian crisis response models, Dagstuhl seminar 13041.
- Häring, I. (2013b). Workshop research topic resilient systems. In B. Katzy & U. Lechner (Eds.), Civilian crisis response models, Dagstuhl seminar 13041, pp. 86–87.
- Häring, I., Schönherr, M., & Richter, C. (2009). Quantitative hazard and risk analysis for fragments of high explosive shells in air. *Reliability and System Safety Engineering*, 94(9), 1461–1470.
- International Electrotechnical Commission. (2010). IEC 61508 Edition 2.0. *Functional safety of electrical/electronic/programmable electronic safety-related systems*. Retrieved from <http://www.iec-normen.de>
- Kaufmann, R., & Häring, I. (2013). Comparison of 3D visualization options for quantitative risk analyses. In R. D. J. M. Steenbergen, P. H. A. J. M. van Gelder, S. Miraglia & A. C. W. M. Vrouwenvelder (Eds.), *European Safety and Reliability Conference (ESREL)*. Amsterdam, Netherlands: Taylor and Francis Group.

- Riedel, W., Fischer, K., Stoltz, A., Häring, I., & Bachmann, M. (2015). Modeling the vulnerability of urban areas to explosion scenarios. In M. G. Stewart and M. D. Netherton (Eds.), *3rd International Conference on Protective Structures (ICPS3)*. Australia: Newcastle.
- Riedel, W., Niwenhuijs, A., Fischer, K., Crabbe, S., Heynes, W., Müllers, I., et al. (2014). Quantifying urban risk and vulnerability—a toolsuite of new methods for planners. In K. Thoma, I. Häring & T. Leismann (Eds.), *9th Future Security Research Conference (Future Security)*, Berlin, Germany.
- Salhab, R. G., Häring, I., & Radtke, F. K. F. (2011). *Formalization of a quantitative risk analysis methodology for static explosive events*.
- Thielsch, P. (2012). *Risikoanalysemethoden zur Festlegung der Gesamtssicherheitsanforderungen im Sinn der IEC 61508 (Ed. 2)*. Thesis. Hochschule Furtwangen.
- Voss, M., Häring, I., Fischer, K., Riedel, W., & Siebold, U. (2012). Susceptibility and vulnerability of urban buildings and infrastructure against terroristic threats from qualitative and quantitative risk analyses. In *11th International Probabilistic Safety Assessment and Management Conference and the Annual European Safety and Reliability Conference*. Helsinki: Finland. pp. 5757–5767.

Chapter 15

Simple Examples of Risk Analysis

15.1 Overview

This chapter, rather than focusing on a single or few risk management and analysis steps or suitable methods for such steps, gives an overview on two complete risk analyses and sorts the conducted steps in the risk management and analysis scheme. This is continued with a more elaborate example comprising multiple methods in Chap. 16.

To assess risks for public underground traffic systems, annual worldwide event frequencies and collective risks are computed. It is argued how to determine individual annual risk frequencies. Further, this chapter discusses how this information can be used to derive most critical and relevant threat scenarios, which are candidates for more detailed analysis. The example is summarized by listing how the 14 risk management and analysis steps are or could be supported by the conducted analyses. In this way it becomes obvious, which steps have been covered: in the present case, it is the identification, description and finally computation of well-defined threat scenarios, along with a generic discussion based on the insights obtained.

A further example is much different to all examples considered so far. It shows that the defined risk management and analysis steps are generic and can be applied also with benefit to the example credit card fraud. A basic ad hoc sample risk assessment and management process is set up and compared and extended with the 14 step risk analysis and management process. It turns out that even rather basic terms are difficult to define, e.g., can a local individual annual risk per card (e.g. for credit card users in vivid urban areas in contrast to rural areas) be defined or is this a too advanced approach asking for too much data in the present context?

The rather basic but complete risk analyses presented in this chapter can be linked in various ways to resilience management and resilience engineering concepts. The typical first approach is to link probability quantities mainly with options for prevention and response, whereas consequence and damage quantities with

means of protection and improvement of response and to a lesser extend also with recovery.

In a similar way, typical resilience capabilities that can be improved with the help of risk analysis results and quantities include to improve or even enable situation awareness, sensing and modelling with the help of the event analysis results; to improve inference, implementation and action resilience capabilities based on risk and chance quantities; finally to improve adaption and learning based on long term avoidance of critical risks and by taking up the best chances.

This chapter shows two examples for risk analysis. The first example in Sect. 15.2 exemplifies how database analysis can be used as a method to compute risks for the underground public transportation system due to terroristic attacks.

Section 15.3 describes the example of analyzing cases of credit card fraud in a fictitious country. Again, the example is compared to the risk analysis and management process.

The main source of this chapter is (SKRIBT 2010). Further Fraunhofer EMI sources are (Siebold and Häring 2009; Fischer and Millon 2010; Fischer et al. 2014). The main author of the EMI sources are K. Fischer and U. Siebold supplemented with work by O. Millon, A. Stolz and I. Häring.

15.2 Database Analysis: Terrorist Threat to Underground Traffic Systems

The first example uses a database analysis which was done in a project to define exposure scenarios for terrorist attacks on underground traffic systems (Fischer and Millon 2010). The database which was used for this analysis was TED, the Terrorist Event Database developed at the Fraunhofer EMI (Siebold and Häring 2009). Social and economic effects were not regarded in the analysis.

Section 15.2.1 describes the extraction of relevant data out of the database and the statistical results. Section 15.2.2 computes the collective and individual risk for the population with the frequencies from Sect. 15.2.1. Potential risks are analyzed in Sect. 15.2.3 and five appropriate scenarios derived. Section 15.2.4 compares the example with the risk analysis and management process from Chap. 1. The section is based on (Fraunhofer EMI et al. 2010).

15.2.1 Database Analysis for Worldwide Underground Traffic Systems

The following Figs. 15.1 and 15.2 were created with the data from TED.

Figure 15.1 shows attacks on bridges registered in TED in the time from 1997 to 2007. Two of those attacks included attacks on tunnels.

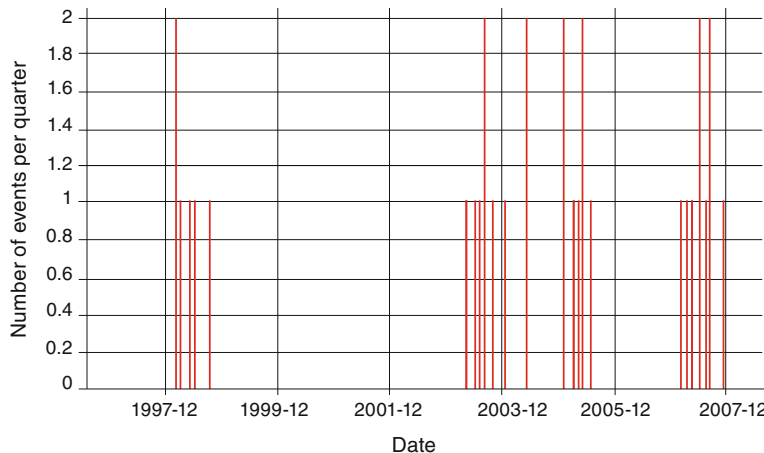


Fig. 15.1 Number of events per quarter on tunnels and bridges, worldwide (Fischer and Millon 2010)

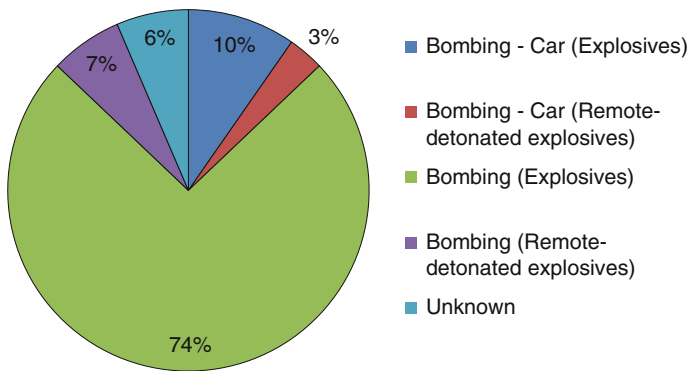


Fig. 15.2 Sort of attack on bridges worldwide between 1997 and 2007

In total there were 31 attacks in 11 years which results in the average annual worldwide attack frequency on bridges and tunnels

$$\frac{31 \text{ attacks}}{(2007 - 1997 + 1)\text{years}} = \frac{31 \text{ attacks}}{11 \text{ year}} \approx 2.8 \frac{\text{attacks}}{\text{year}}. \quad (15.1)$$

Figure 15.2 shows that most attacks on bridges were done with explosives by showing the percentage of each attack type.

15.2.2 Quantitative Risk Evaluation

The frequencies computed in Sect. 15.2.1 could be used to compute collective and individual risks if average consequences were known.

To show, how the collective and individual risks are computed, we arbitrarily assume (without using sensible data) that 310 persons died in the 31 attacks and 31,000 were injured. Using the assumed average consequences we find using (15.1) the average collective risk of fatalities

$$R_{\text{col-fat}} \approx 2.81 \frac{\text{attacks}}{\text{year}} \cdot 10 \frac{\text{fatalities}}{\text{attack}} \approx 28.1 \frac{\text{fatalities}}{\text{year}} \quad (15.2)$$

and of injuries due to attacks on bridges and tunnels

$$R_{\text{col-inj}} \approx 2.81 \frac{\text{attacks}}{\text{year}} \cdot 1000 \frac{\text{injured}}{\text{attack}} \approx 2810 \frac{\text{injured}}{\text{year}}. \quad (15.3)$$

To compute the average worldwide individual risk due to terror attacks on tunnels one needs the size of the population. According to the UN, the worldwide population in 2005 was 6.514×10^9 people (United Nations Department of Economical and Social Affairs 2013), yielding the averaged worldwide individual fatal and casualty risks

$$R_{\text{ind-fat}} \approx \frac{28.10 \frac{\text{fatalities}}{\text{year}}}{6.514 \times 10^9 \text{ persons}} \approx 4.3 \times 10^{-9} \frac{\text{fatalities}}{\text{person year}} \quad (15.4)$$

and

$$R_{\text{ind-inj}} \approx \frac{1000 \frac{\text{injured}}{\text{year}}}{6.514 \times 10^9 \text{ persons}} \approx 1.5 \times 10^{-7} \frac{\text{injured}}{\text{person year}}. \quad (15.5)$$

One might argue that one should only consider the population in urban regions, or even better only the fraction of urban population that uses public subsurface transport. This would, however not change the order of magnitude of the individual risks. The used consequence numbers lead to individual annual average risks that are even for non-fatal risks below or of the order of the standard de minimis annual individual risk of 10^{-6}a^{-1} (Proske 2008).

15.2.3 Potential Risks and Derived Scenarios

This section regards potential hazardous terroristic events for underground traffic systems. The goal is to define a worst case scenario and several significant other scenarios in terms of the risks associated with each scenario.

Figure 15.2 shows that in most attacks explosives were used. Hence, the scenario should be an attack using explosives. The amount of explosive is a relevant parameter for the damage of structures. From the amount of explosive one can estimate how the explosive is transported to the target place.

The further aspects of the scenarios derived from the database analysis are not elaborated here due to their sensitivity. This includes in particular an analysis of the averaged consequence effects and the combination of frequencies and consequences in terms of risks.

Economic and social effects are not regarded in the present context. Under consideration of these effects, the scenarios could be described in further detail.

15.2.4 The Given Example and the Risk Management Process

We want to see how the example fits into the risk management process defined in Chap. 1. First we defined the situation as attacks on transportation lines, especially tunnels (step 1 in the risk analysis process). We did not define one hazard source but a whole list of possible hazards in Fig. 15.2 (step 3). The database analysis elaborated in the present text can be seen as an analysis of the hazard event frequency (step 6). We did not present the consequence assessment based on the empirical data (step 4). We also did not present the empirical risk analysis.

Risks were computed (step 9) but not visualized. The other steps were not done. So, only a few steps of the risk analysis were executed. How can this be a good example?

In the end, the data from the database analysis was used to define typical scenarios. How does this fit into the process? The scenario itself can be seen as the initial situation and hazard source. So, what really happened here is that the empirical database approach only did a coarse analysis in preparation of a more detailed risk analysis that fulfills all steps of the risk analysis and management process. The detailed analysis was conducted only for the preselected scenarios.

Table 15.1 gives an example how a pre-defined scenario from Sect. 15.2.3 can be analyzed with the risk management process from Chap. 1. For this we assume that in the scenario the following values were defined:

- (a) Country
- (b) Geometry of the tunnel
- (c) Attack type, e.g. a bomb with x kg TNT
- (d) Container transporting the bomb

Table 15.1 shows that based on a given scenario, computer simulations can be used to execute the whole risk management process. An example for such evaluation expert tool is shown in (Fischer et al. 2014).

Table 15.1 Example how a defined scenario can be analyzed with the risk management process

Step	Name (abbreviated)	Example of what happens in the step
1	Background	Information about the country, e.g. risk criteria
2	Initial situation	Geometry of the tunnel, a model of the tunnel
3	Hazard source	A model of the hazard source
4	Hazard propagation	Computer simulation, for example simulating blast from the bomb
5	Damage analysis	Using the model of the tunnel to simulate the damage that would happen to it
6	Analysis of hazard even frequency	Refinement of the database analysis from this section for the given scenario or similar ones
7	Distributions of objects	Statistic about the number of cars in the tunnel
8	Success frequency of avoiding hazards	E.g. consequences of using stronger, protective materials in the tunnel
9	Risk computation and visualization	Risk computation based on simulation. Visualization in charts
10	Risk comparison with criteria	Comparison with criteria determined in step 1
11	Risk assessment	Comparison with individual and collective risk criteria
12	Risk communication	E.g. using a local risk map
13	Risk evaluation	Considerations based on step 10 and 11. In addition, for example consideration of the public response to a recent attack in that country
14	Mitigation measures	For example recommendation of the protection measures simulated in step 8

15.3 Credit Card Example

Figure 15.3 shows a simple example of how probabilistic risk analysis can be used to make decisions. The fictitious numbers cover the number of credit cards issued within a small country, the number of frauds per year, the average loss per fraud and a collective risk criterion.

15.3.1 The Given Example and the Risk Management Process

As for the example with tunnels in Sect. 15.2.4, we see in Table 15.2 how the credit card example fits into the risk management process from Chap. 1.

The simple example does not cover steps 1, 7, 8, 11 and 12. Examples of what they could look like in the given example are shown in Table 15.3.

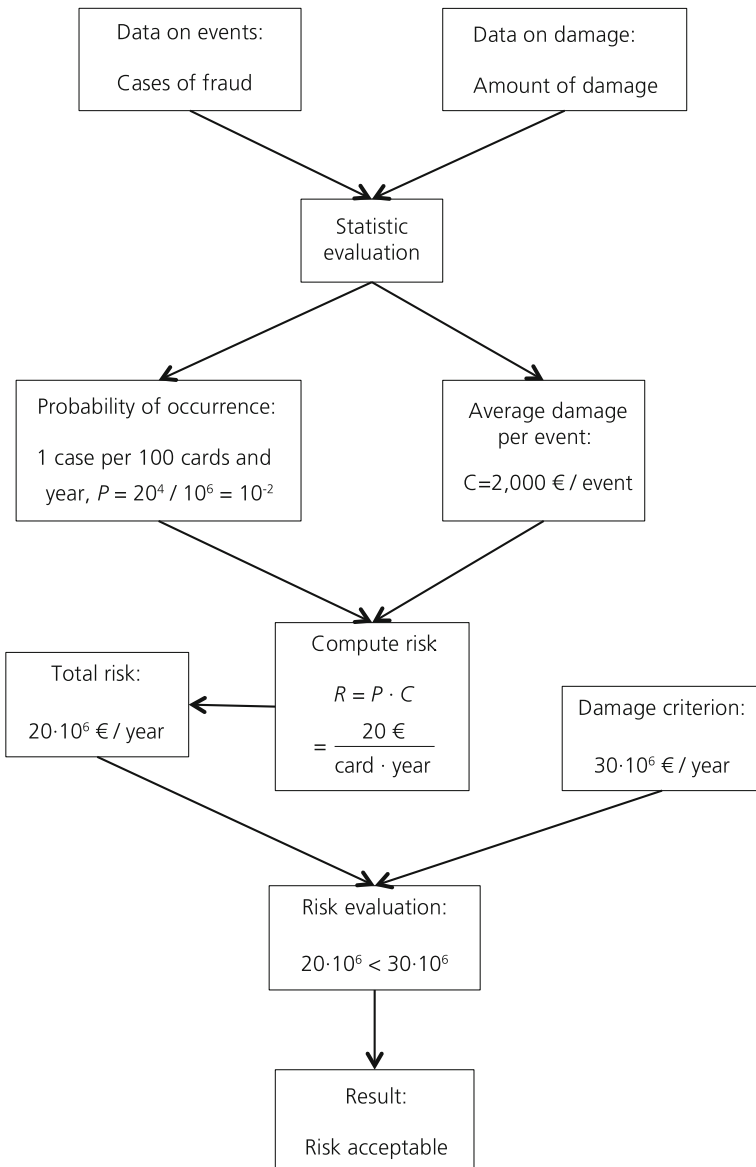


Fig. 15.3 Example for risk analysis in the case of fraud with debit cards

Table 15.2 Comparison of the credit card example and the risk management process

Step	Name (abbreviated)	Credit card example
1	Background	–
2	Initial situation	Credit card system in a fictitious country where one million cards are used every year
3	Hazard source	Credit card fraud
4	Hazard propagation	Fictitious number that 10,000 cases of fraud occur every year
5	Damage analysis	Total damage from (fictitious) statistic 20,000,000 €
6	Analysis of hazard event frequency	Average damage per event 2000 €/event
7	Distributions of objects	–
8	Success frequency of avoiding hazards	–
9	Risk computation and visualization	$R = 20 \text{ €/(card and year)}$, total risk 20,000,000 €/year
10	Risk comparison with criteria	Comparison with fictitious damage criterion
11	Risk assessment	–
12	Risk communication	–
13	Risk evaluation	Risk is acceptable (based on step 10)
14	Mitigation measures	Not necessary

Table 15.3 Examples for missing risk analysis and management steps in the credit card example

Step	Name (abbreviated)	Credit card example
1	Background	Statistic on country how well accepted credit cards are, including society's attitude towards credit card fraud, social value of credit cards, etc.
7	Distributions of objects	Statistic on distribution on manipulated ATMs (automated teller machines) and on web sites with credit card fraud
8	Success frequency of avoiding hazards	Statistic on successful credit card blocking or avoidance of credit card use
11	Risk assessment	Considering recent assessments of credit card fraud
12	Risk communication	Communication strategy based on steps 1 and 11

15.4 Summary and Outlook

This chapter gave an example where database analysis of worldwide terror events was used to determine relevant threat scenarios based on various empirical risk quantities. For these scenarios more detailed numerical assessment was performed.

The second part of the chapter showed an example that goes further. The risks are not only computed based on sample data. The example also shows the decision process based on an economic assessment.

Both examples were compared with the risk analysis and management process schemes from Chap. 1. We showed how missing steps could be covered by further investigations.

Easily accessible further reading on the topics of this chapter are (Ganz 2014) and (Mössner 2012).

15.5 Questions

- (1) Take the scheme from Fig. 15.3. To which boxes can you assign the steps of the 5-step risk analysis scheme?
- (2) Use the Global Terrorism Database (<http://www.start.umd.edu/gtd/>) to answer the following questions:
 - (a) Why is it not possible or very much work to do the same analysis (terrorist attack on bridges/tunnels) with GTD?
 - (b) Instead, we analyze attacks on airports and airlines between 1997 and 2007. How many occurred? Do you have explanations for the two peaks? What is different between the two peaks when you look at the individual attacks in more detail?
 - (c) How can the collective risk for fatalities be estimated? What would be necessary to compute it precisely?
 - (d) Compute the individual risk of death in an airport or airplane based on the world population of 6.514×10^9 !
 - (e) Instead of the time period 1997 to 2007 now look at the total time period of the database. How does that change your view on the decade from (b)? Is the collective risk bigger or smaller when it is based on the longer time period?

15.6 Answers

- (1) The 5 step scheme:
 - (a) 1 is before the scheme, cannot be assigned
 - (b) 2 is “cases of fraud”, “amount of damage” and “statistic evaluation”
 - (c) 3 is “probability of occurrence”, “average damage per event”, “total risk” and “compute risk”
 - (d) 4 is “damage criterion” and “risk evaluation”
 - (e) 5 is not necessary because the risk is acceptable

- (2) With the Global Terrorism Database (<http://www.start.umd.edu/gtd/>) and the settings “Only incidents where there is essentially no doubt of terrorism” and “Including only successful attacks” one gets the following results:
- Bridges or tunnels are not a category in the target choices in the advanced search of GTD. One can only use “transportation” which yields very many results that could be manually searched for attacks on bridges and tunnels.
 - 85 incidents (Search on 2014-06-17). Peaks in 1997 and 2001. 1997 very few fatalities, peak might not mean too much. 2001 was the year of 9/11.
 - Chart results-fatalities-bar chart (upper right corner): We take the middle of the ranges as an estimate. So the estimated total number of fatalities is $55 \cdot 0 + 17 \cdot 0.5(1+10) + 8 \cdot 0.5(11+50) + 0 \cdot 0.5(51+100) + 3 \cdot 101 = 640.5$. Hence, the average of fatalities per attack is $640.5/85 = 7.54$. The average of attacks per year is $85/11 = 7.73$. The resulting estimated collective risk is $R_{col} = 7.54 \times 7.73 \approx 58.28$ fatalities/year worldwide.
 - $R_{ind} \approx \frac{58.28}{6.514 \times 10^9} \approx 8.95 \times 10^{-9}$ which is not very high. The computed risk would probably much higher if the third world countries were left out.
 - The total number is 963 incidents.
Both peaks from (c) are not significant in this larger time scale. Since the time period from (b) has the smallest numbers of fatalities in the whole time period, it is obvious that the collective risk is bigger when computed over the total time period.

References

- Fischer, K., & Millon, O. (2010). *Risikobewertung von terroristischen und nicht-terroristischen Ereignissen gegen Bauwerke der kritischen Infrastruktur. Bericht E 22/10*. Efringen Kirchen: Fraunhofer EMI.
- Fischer, K., Siebold, U., Häring, I., & Riedel, W. (2014). Empirische analyse sicherheitskritischer Ereignisse in urbanisierten Gebieten. *Bautechnik*, 92(4), 262–273.
- SKRIPT (2010). Protection of critical bridges and tunnels in the course of roads. *Verbundprojekt SKRIPT—Schutz kritischer Brücken und Tunnel im Zuge von Straßen*. Retrieved November 19, 2015, from <http://www.skribt.org/home.htm>
- Ganz, C. (2014). *Die Risikoanalyse mittels Konsequenz und Eintrittswahrscheinlichkeit Methodik am Beispiel des Druckbehälterversagens im Erdgasfahrzeug*. Retrieved August 14, 2015, from <http://elpub.bib.uni-wuppertal.de/servlets/DocumentServlet?id=2627>
- Mössner, T. (2012). *Risikobeurteilung im Maschinenbau*. Retrieved August 14, 2015, from http://www.baua.de/de/Publikationen/Fachbeitraege/F2216.pdf?__blob=publicationFile&v=9
- Proske, D. (2008). *Catalogue of risks—natural, technical, social and health risks*. Berlin Heidelberg: Springer.
- Siebold, U., & Häring, I. (2009). *Terror event database and analysis software* (pp. 85–92). Karlsruhe, Germany: Future Security.
- United Nations Department of Economical and Social Affairs. (2013). *Population division, population estimates and projections section*. Retrieved June 14, 2013, from <http://esa.un.org/unpd/wpp/unpp/p2k0data.asp>

Chapter 16

Risk Analysis and Management Example for Increasing Harbour Security in Case of Bulk Scanning of Containers

16.1 Overview

This chapter comprises a rather broad set of methods which are composed to a risk analysis of a facility for fast bulk scanning of containers in large container harbors. The aim of the facility is to detect illicit and dangerous goods of outgoing containers. Possible events are relevant for the harbor and possibly much larger areas.

As in most of the past examples, first a database-driven event analysis on malicious or terroristic events in harbors is conducted. It turns out that the number of historic events is very small, some of them even seem to happen in harbors by accident rather than on purpose. Furthermore, some of the most critical events are clearly not relevant for the present context, e.g. suicide attacks on navy ships.

When taking account of the massive potential for malicious events, contrasted with the historic numbers, the decision was taken to use expert estimates to cover all kinds of possible threat events. It is shown how such an approach can be structured using 7 hazard description categories ranging from disguise and detection options, minimum quantities sufficient for detection devices over range of effects to risk-based relevance. This potpourri is used for semi-quantitatively ranking the most relevant and technologically controllable risks in the present project context.

The approach can be understood as a kind of multi criteria risk-informed decision making, since the key attribute for selection was the periodization according to likelihood and severity of the potential hazard events. It resulted in 5 scenarios comprising hazard sources in a single container: nuclear/radiologic hazard, explosives, “dirty bomb”, chemical/biological hazard and illicit weapons. The risk assessment was conducted for a massive container explosion and the “dirty bomb” scenario.

The what-if risk analysis determines the expected damage in case of the two events. First, the hazard propagation and resulting hazard fields are computed. Taking up and extending approaches from Chaps. 6 and 8, the free field reflected

and side-on overpressure are computed based on an assumed explosive material quantity appropriate for the present geometry.

In addition, the thermal heat radiation field is determined. However, for the far field the most critical parts are debris throw of container walls and further material close to the explosive source (fragments).

The debris throw of containers is explained using initial launch velocities for the walls, horizontal and vertical launch distributions as well as mass distributions for all debris. In the sample experiments, even the effect of wind is visible. It is indicated how the hazard distribution depends quantitatively on the hazard source characteristics. The indicated hazard modelling rests on parameterizations of experiments.

For the dispersion of radiological material, the analytical and numerical modelling options are discussed as well as the types of hazards and their interactions with humans. Within the presented approach, non-proprietary software was used to determine the dispersion of radiological substances based on a plume model.

For the damage analysis, a free parametrized empirical damage assessment is used, which is particularly suited for larger net explosive quantities. It determines the expected local damage for the built environment in terms of 5 damage levels. The input are scaled distances.

The damage assessment for personnel uses as input the side-on and reflected overpressures, which are processed with a variety of probit functions that determine respective local probabilities for discrete damage levels. It is argued why in the present context the consideration of overpressures is sufficient.

In the case of the fire ball, the absorbed heat radiation power and heat radiation duration at given distances is computed from the radiation power of the source, its radiation duration and the distance. This hazard is compared with critical time-dependent heat flow power absorption thresholds for different injury levels.

In case of the dispersed radioactivity, the damage assessment considers the different types of damage mechanisms corresponding to α , β , γ and neutron radiation. Their effects can be cumulated using the dose equivalent, for which critical thresholds are available. Furthermore critical doses for the damage assessment of toxicity as well as critical values for the radioactive activity are used.

Risk quantities are computed by combining the statistical-empirical frequency assessment with the expected damage for personnel and objects, which arise from the computed hazard potentials for the assumed two sample scenarios. Assuming to some degree fictitious numbers, sample individual local and collective risks for personnel and objects are computed for illustration.

Furthermore, this chapter introduces a section that provides a heuristic to characterize risk computations. It is applied to the presented combination of methods as well as the critical evaluation of the results, in particular their uncertainty.

The presented sample risk analysis of hazard events in harbor container scanning systems gives an overview of methods ranging from qualitative, semi-quantitative, engineering, and simulative to experimental. They allow to systematically analyse

and improve prevention, protection, response and recovery steps to enhance resilience. Even more as in Chap. 15, key resilience capabilities become evident. Examples include detection options of potential hazard source; physical means of protection for key areas close to the detection site; rather differentiated decision making processes for the assessment of alert levels.

This chapter gives an example of the application of the risk analysis process to a specific example. The main aim of the project “Increase of container security by applying contactless inspections in port terminals” (ECSIT) (Ziehm et al. 2011) was to show that bulk inspection of all containers is feasible to improve security in harbor terminals. The idea was to prevent the passing in and out of illicit and dangerous goods, e.g. bombs, by new scanning installations.

The risk analysis was supposed to identify hazards that might occur now and in the future in or close to the harbor, in particular at scanning devices, and to quantify their possible consequences. This was supposed to enable the decision makers to choose appropriate counter measures and to decide on a reasonable use of (financial) resources as well as to improve their logistic and scanning design.

Against the background of the concrete reference to the harbor in Bremerhaven, Germany, the steps of the risk analysis process and their theoretical background were explained and displayed. An event analysis, a hazard analysis and a damage analysis of selected sample events were executed. The focus lay on the damage to persons.

The database analysis [using the databases TED (Siebold and Häring 2009) and GTD (National Consortium for the Study of Terrorism and Responses to Terrorism (START) 2011)] did not yield any attacks on harbors involving containers (bombs etc. placed in a container) as dreaded by the USA and their “H.R. 1 (House Resolution)” law (Ziehm et al. 2011).

The risk analysis was hence executed on a prognostic basis. Potential hazards were identified in cooperation with Smith Heimann (Smiths detection 2014) and the Fraunhofer Development Center for X-ray technique EZRT (Fraunhofer IIS 2014) and scenarios were derived from this. These scenarios were regarded during the risk analysis and in the end collective risks were determined to be able to evaluate the severity. In this chapter we cover representative events without giving the complete results nor the final ranking obtained by the analyses.

First an event analysis based on a database analysis was executed, see Sect. 16.2. For this, relevant potential events in harbors were identified and their probability of occurrence was determined. The identification of relevant events was used to define scenarios and hazards. The hazard analysis, see Sect. 16.3, determined the physical hazards which originate in a specific event. Section 16.4 describes the damage analysis where the damage related to a specific event was regarded.

This chapter summarizes, translates and paraphrases (Ziehm et al. 2011). The main sources of the figures is (Tatom and Conway 2010). Further Fraunhofer EMI sources include (Dörr 2003; Sauer 2005; Dörr et al. 2007b; Siebold and Häring 2009; Ziehm 2009). The main author of the EMI source is J. Weissbrodt (under her birth name Ziehm) supplemented with work by S. Moser, N. Echterling, T. Leismann, Smith Heimann and Fraunhofer EZRT. It is further supplemented with work by A. Dörr, G. Gürke, D. Rübarsch, M. Voss and M. Sauer.

16.2 Event Analysis

In this section we show the database analysis to identify relevant hazards and events and to determine the probability of occurrence of sample events.

In cooperation with the project partners a list (“table of hazards”) was developed with potential hazard sources or threat (hazardous) events in the future. This was necessary because search criteria for the container scanning methods had to be developed and because of the small number of empirical attacks on harbors. The empirical evidence was too small to justify it as sole basis of the identification of possible hazard sources and threat events (Ziehm et al. 2011).

16.2.1 Database Analysis

For the database analysis, the EMI-internal database TED (Terrorist Event Database) with at that time approximately 35,000 entries and the GTD (Global Terrorism Database) (National Consortium for the Study of Terrorism and Responses to Terrorism (START) 2011), with at that time approximately 80,000 entries were used.

Figure 16.1 shows the number of attacks on harbors from 1970 to 2006. The 42 attacks on harbors are relatively few compared to the total number of events in the databases but should still be considered. The high number of attacks in the 1980s can generally be seen in the databases, not only for harbors.

For none of the attacks for which details were available containers were used. Also, none of the attacks was meant to destroy the infrastructure of the harbor and cause economic damage. The attacks were meant for specific persons or ships in the harbor. Additionally, not every harbor was a commercial harbor. Fishing harbors and marinas were also counted in the statistic.

Most attacks were of explosive type (bombs, mines). Some attacks were planned or executed with rockets or firearms. None of the attacks was nuclear or biological. There was one attack with Adamsit (chemical weapon) in a harbor in Belgium.

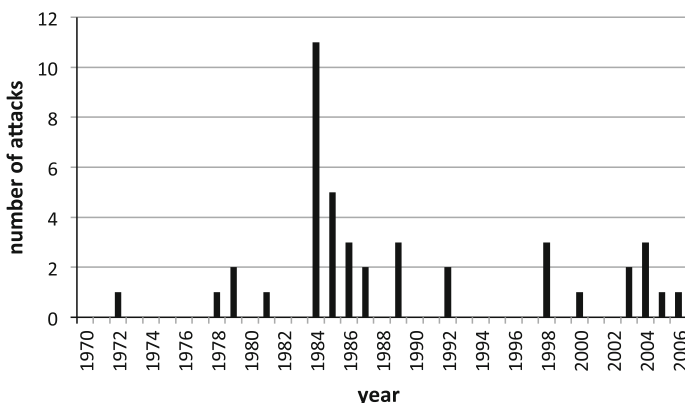


Fig. 16.1 Number of attacks on harbors per year from 1970 to 2006 (Ziehm et al. 2011)

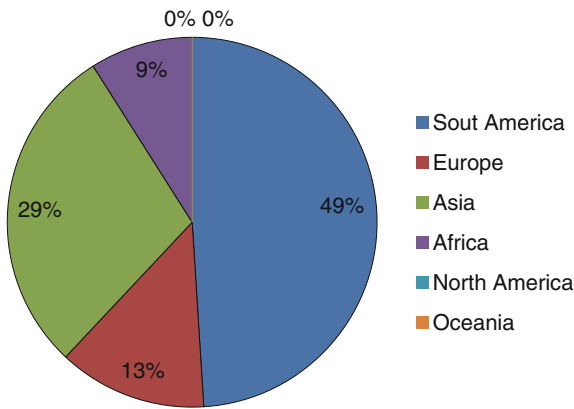


Fig. 16.2 Distribution of the attacks on harbors by continent (Ziehm et al. 2011). The classification of the continents follows (Ziehm 2009)

Figure 16.2 shows the number of attacks on harbors for the different continents. Most attacks were in South America, followed by Asia.

At the workshop “Bau Protect 2010” the German Federal Office of Criminal Investigation said that the terrorists’ focus still lies on western targets, especially on so-called “soft targets” (Ziehm et al. 2010). Simultaneous attacks (shortly after each other), as in Stockholm (Spiegel-Online 2010), are nowadays characteristic. Here, the classical firearms are mostly used for self-protection; for the attack itself Improvised Explosive Devices (IED) are used.

A harbor is seen as an unlikely target when the goal is to hit as many persons as possible. However, the location of the harbor must be considered, it could lie in a populated area. Also, the primary targets of the terrorists may change, see the following example.

In 2010, in an attack with parcel bombs from Yemen sent to the US via air freight, the explosion of the bombs could be prevented but there was an enormous economic damage. Afterwards the Al Qaida announced that this is a new tactic to weaken the West (Kronen Zeitung 2010). Hence, attacks to cause economic damage rather than to harm persons are also possible in the future.

A potential target can be a ship in the harbor because historically this kind of attack has happened. The goal behind it was probably not to cause damage to the shipping company but to the country the ship was from, for example in the attack on the “USS Cole” (Wikipedia 2011b).

The relatively small number of historic attacks on harbors makes some further systematic investigations of hazards and scenarios necessary. The following section describes the procedure of identifying hazards and the hazards themselves (Ziehm et al. 2011).

16.2.2 Table of Hazards

The table of hazards lists hazards of five different types:

- Nuclear/radiologic
- Conventional (explosives)
- Chemical/biological
- Firearms
- Possible support by customs (Discovering smuggled goods)

It was created during the project together with the project partners. Its content is not explained here in more detail for security reasons.

Table 16.1 shows the categories that are used in the hazard table to describe a hazard more precisely. The table also gives explanations of the different categories. Each potential hazard source or threat event was semi-quantitatively assessed using the categories. The aim was to obtain an indication of their relevance for different types of activities in the harbor, in particular for scanning and mitigation objectives.

In the project, hazards were prioritized from 1 (very important) to 10 (rather unimportant) following two criteria:

- Danger of the hazard: The higher the consequences of an attack based on the hazard, the higher the prioritization is chosen.
- Probability of the hazard: The more likely it is that the hazard is placed in a container, the higher the prioritization is chosen.

The evaluation of the two criteria was based on literature research and expertise.

Table 16.1 General explanations of the content of the hazard table, translated from (Ziehm et al. 2011)

Category	Explanation
Camouflage/signature	How can the hazard be disguised during transportation? Does this indicate a signature?
Examples and sources	Precise description of possible executions, explanatory background information or “links”
Terroristic background	Classification of hazards in a broader context, potential goals/motivation
Amount of substance	Information about the quantity which is necessary to achieve the described effect
Effect/damage/victims	Information about the expected effect, damage and numbers of victims
Possibilities of detection	Possible ways to detect the hazard with contactless procedures and screening
Prioritization and consequences for the project	Which role does this hazard scenario play in the project? Prioritization from 1 (very important) to 10 (rather unimportant)
Remarks	Additional information

This semi-quantitative assessment is an example of ranking possible events with respect to their risk without taking potential counter measures into account.

For the table, the analysis of terroristic attacks in the past was used and possible hazards in the future were identified. The list of potential hazards covers the hazards which have been valued most important at this time but it cannot cover all possible hazards. Hence, the table does not claim completeness (Ziehm et al. 2011).

16.2.3 Derived Scenarios

Five scenarios were derived from the table of hazards during the project. One scenario for each of the categories nuclear/radiologic hazard, explosives, “dirty bomb”, chemical/biological hazard and weapons was developed and described. Here, all hazard sources were transported in containers.

16.3 Hazard Analysis

During the hazard analysis, physical parameters of an attack are quantified, comprised and displayed. During the project, explosive events (Sect. 16.3.1) and the propagation of a substance (Sect. 16.3.8) were regarded.

16.3.1 Explosions Under Free Field Conditions

Explosions in the free field always create danger through a fireball, blast, ground shock, debris (e.g. from buildings), fragments (e.g. from the cover of the explosives) and crater formation for surrounding buildings, vehicles or persons, see Fig. 16.3.

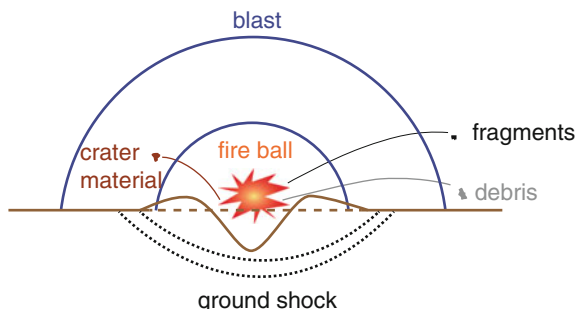


Fig. 16.3 Explosion hazards (Ziehm et al. 2011)

In the following we will describe blast hazard and fragment hazards (debris (earth, concrete, building material, etc.) and (metal) fragments (fragments generated out of (casing) material close to explosive material or within explosive material (e.g. nails)). Fireballs and ground shock are only relevant for big amounts of explosives (Ziehm et al. 2011).

16.3.2 Blast Hazard

When initiating an explosive charge, hot gas mixtures (3000–4000 °C) (Smith and Hetherington 1994) at pressures between 100 and 300 kbar occur. (For comparison, the air pressure at sea level is approximately 1 bar). A detonation front runs through the explosive. The detonation front can have a velocity between 1500 and 9000 m/s (Mays 1995), for example approximately 7000 m/s for TNT (Smith and Hetherington 1994).

When the detonation front reaches the surface of the explosive, the gas mixture expands (gaseous detonation produces, detonation waft) into the surrounding air and, under the formation of a compressed air layer (blast front), pushes the air ahead. Finally, the longitudinal (along the direction of the expansion) compression wave goes from the detonation waft into the air (blast waves frees itself from the detonation products). The blast front moves with a relatively high velocity (bigger than the velocity of sound in the air) but with a velocity significantly smaller than the one of the detonation front in the explosive.

The intensity of the blast is determined by the parameter overpressure P_s and the specific blast impulse I of the positive overpressure phase (short: blast impulse). The units are pressure and pressure multiplied with time (impulse per area), respectively. Hence, blast pressure is a measure for the force impact per surface area or alternatively impulse per surface area.

Figure 16.4 shows an example of a pressure-time-curve for a given distance r to the location of the detonation: After a time t_1 the blast front reaches the location with the distance r . The pressure p suddenly rises from the pressure of the surrounding P_0 to the overpressure P_s . Then it decreases fast, almost exponentially, and (during the so-called suction phase) goes below the original pressure P_0 , before it asymptotically goes back to P_0 (normally oscillatingly).

The blast impulse is the red hatched area in Fig. 16.4 and can be computed by

$$I = \int_{t_1}^{t_1 + T_s} p(t) dt. \quad (16.1)$$

The maximal *overpressure* and the *blast impulse* decrease when the distance r increases. The duration of the positive overpressure phase T_s and the arrival time t_1 increase when r increases.

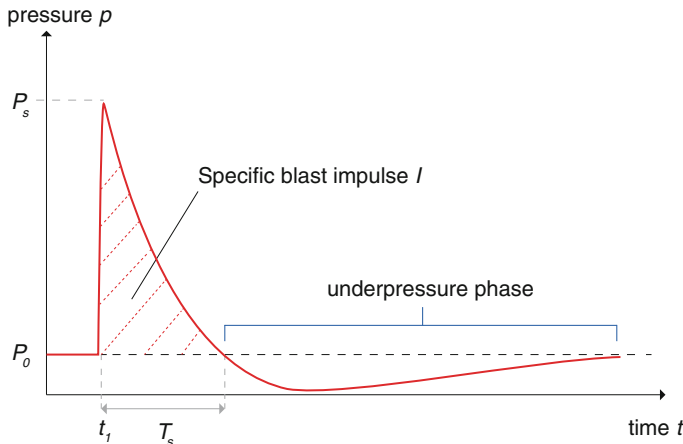


Fig. 16.4 Example of a pressure-time curve or history $p(t)$ (red curve) for an explosion under free field conditions. Pressure of the surroundings P_0 , overpressure P_s , suction, underpressure or negative phase, specific blast impulse I (hatched area) and duration of the positive overpressure phase T_s

The effects of free field explosions have been intensively studied by C.G. Kingery and G. Bulmash (Swisdak 1994) and have been well described by their polynomials. For areas with a high density of buildings, the situation is much more complex. Developing models for that type of situation would be very time-consuming. This was not reasonable for the building structure of the harbor in Bremerhaven and a first coarse analysis. Hence, free field explosions were assumed (Ziehm et al. 2011).

16.3.3 Side-on and Reflected Pressure and Impulse

For the overpressure and the impulse, one distinguishes between two different situations:

- The pressure and impulse when passing by an object.
- The pressure and impulse when hitting a surface.

The resultant parameters are the “*side-on*”-pressure P_s , the “*side-on*”-impulse I_s , the *reflected pressure* P_r and the *reflected impulse* I_r , see Fig. 16.5. Here, for the same distance, the reflected pressure and impulse are bigger than the “*side-on*”-pressure and impulse. The scheme of Fig. 16.5 allows to explain the difference. In the case of a locally reflected blast wave, the blast overpressure is higher and the blast impulse transferred as well because of the impulse (momentum) inversion (Ziehm et al. 2011).

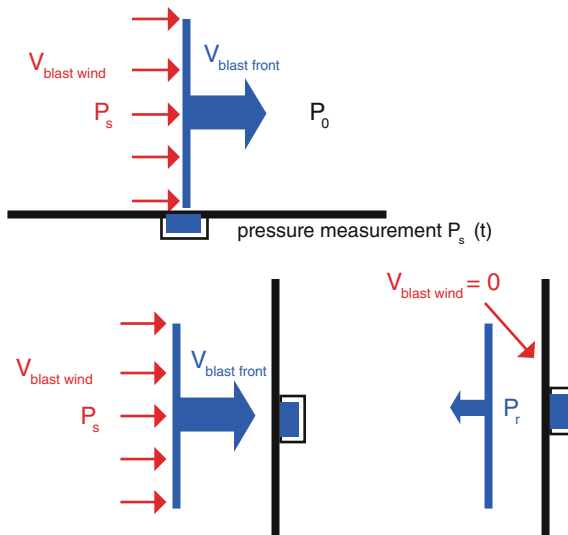


Fig. 16.5 Upper diagram: Measurement for the “side-on”-pressure P_s and “side-on”-impulse I_s . Lower diagram: Measurement for reflected pressure P_r and reflected impulse I_r . $V_{\text{blast wind}}$ velocity of the blast wind, $V_{\text{blast front}}$ velocity of the blast front (Ziehm et al. 2011)

16.3.4 TNT Equivalent

Blast parameters depend on the explosive used. With the TNT equivalent one calculates the mass of the explosive which is needed to get the same blast parameters as in an explosion with TNT. Overpressure and impulse are two such parameters for which TNT equivalents can be used. Their TNT equivalents are not equal but very similar.

TNT equivalents are based on many experiments with TNT. Table 16.2 shows the TNT equivalent for some explosives in comparison to TNT.

16.3.5 Overpressure

The computation of the “side-on” overpressure is based on data from four big explosion tests in Canada between 1959 and 1964 (Swisdak 1994). The formula for the computation contains the *scaled distance*

Table 16.2 TNT equivalents of some explosives for overpressure (Ziehm et al. 2011)

Explosive	Name/components	TNT equivalent
TNT	Trinitrotoluene	1
ANFO	Ammonium nitrate fuel oil	0.8
APEX/TATP	Acetone peroxide	0.83
RDX/cyclonite	Cyclotrimethylenetrinitramine	1.6
Comp B	63 % RDX, 36 % TNT, 1 % wax	1.35
C-4	Among others 91 % RDX	1.35
Amatol 80/20	80 % TNT, 20 % ammonium nitrate	1.17
Dynamite	75 % glycerin trinitrate, 24 % kieselguhr	0.8
HBX	Among others RDX, TNT, aluminum	1.43
HMTD	Hexamethylene triperoxide diamine	1.25
HMTD	Hexamethylene triperoxide diamine	1.53
Black powder	75 % potassium nitrate, 15 % charcoal, 10 % sulfur	0.25–0.55
Chlorate explosives	Chlorates	2.2
PETN	Nitropenta	1.66
Semtex A	94.3 % PETN, 5.7 % RDX	1.66

$$Z = \frac{r}{Q^{1/3}} \quad (16.2)$$

where r is the distance between the loading and the object/measuring point and Q is the mass of the explosive. The scaled distance has the dimensions m/kg^{1/3} which is proportional to a dimensionless quantity when taking into account that the volume equals mass times density.

The overpressure is computed by Swisdak (1994, 2001) and Dörr (2007a)

$$P = P_s - P_o = \exp\left(\sum_{j=0}^4 c_j (\ln Z)^j\right) \text{kPa}, \quad Z \in [a_i, b_i] \quad (16.3)$$

with $i = 1, 2, 3$. The values of c_j depend on which of the three intervals Z lies in. The different a_i and the matching c_j can be found in Table 16.3.

To get the correct explosive mass for the computation of the overpressure, one has to convert the explosive mass to the TNT equivalent mass as studied in Chap. 8. For this one has to consider the scaling factors for the TNT equivalent of the explosive, see Table 8.3.

Since for most damage criteria for personnel only the maximum overpressure is used we do not give the empirical-analytical expression for the blast impulse.

Table 16.3 Constants c_j in dependence of the interval where Z lies in Swisdak (1994)

i	$[a_i, b_i]$	c_0	c_1	c_2	c_3	c_4
1	[0.2, 2.9]	7.2106	-2.1069	-0.32290	0.1117	0.0685
2	[2.9, 23.8]	7.5938	-3.0523	0.40977	0.0261	-0.01267
3	[23.8, 198.5]	6.0536	-1.4066	0	0	0

16.3.6 Projection Hazard: Debris Throw

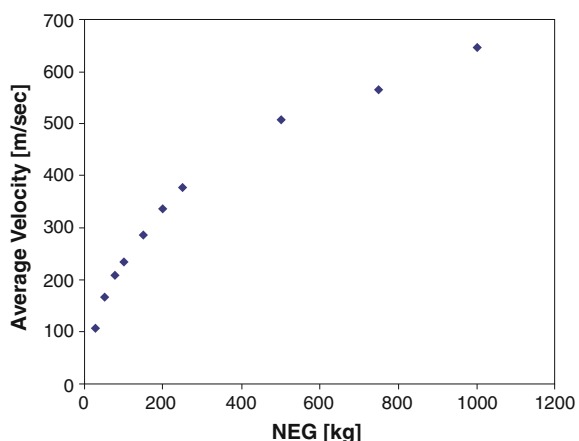
The hazard due to debris and fragments from explosions in containers is determined for selected examples. During the project, qualitative results from works on explosion behavior of containers (Tatom and Conway 2010) by the “Klotz Group”, an international expert circle with regard to explosion safety, were used.

16.3.6.1 Launch (Initial) Speed of Debris and Fragments

The dependency of the velocity distribution of the debris and fragments on the net explosive quantity (NEQ) was analyzed using numerical simulation and high speed videos of previous ISO container tests.

The numerical simulation does not only distinguish between the container walls and the container frame but also between the different areas such as side, top, front since they are differently far away from the detonation assumed to be situated in the center of the container. The assumed failure criterion was 20 % strain of the material. The measurement of the velocities and exit angles was done by several hundreds of fictitious pressure sensors within the discretized geometry and spread over the whole container. An example of results is shown in Fig. 16.6.

Fig. 16.6 Average velocity of the side wall of a container after an explosion at the container ground in the center. Taken from Robert T. Conway, John Tatom. ISO Container Source Function Development for the Klotz Group Engineering Tool. DDESB, Explosives Safety Seminar. Portland. USA. With permission



For the empirical determination of the exit speeds, high speed videos of a container explosion were analyzed. Fragments and debris from a specific part of the container were not only regarded for different time intervals after the explosion but also for different vertical exit angles. The angles were divided in three sectors and the exit speeds compared between those three sectors (Ziehm et al. 2011).

16.3.6.2 The Mass of Debris and Fragments

Estimating the mass of debris and fragments is more challenging. Numerical simulation was not used in the project because it is difficult to characterize with continuum mechanical models the breaking of a structure due to an explosion and hence the number and size of generated metal fragments. Instead, empirical results from previous projects were used to estimate the mass and number of fragments.

The problem is the so-called mass loss: One never finds all the fragments and debris after an explosion in an experiment, in particular fragments and debris of small mass. So, a method must be developed to estimate the mass of fragments which are not found.

Tatom and Conway (2010) do this with the data of three ISO container tests. They do not consider their data sets as final. They distinguish between the wall and the frame of the container which, as in other situations, turns out to be important. Figure 16.7 shows the number of fragments over their mass for different fitted models for three tests with an ISO container (1000 kg NEQ).

One can see that for “total container” the small fragments get counted well, but the big ones are neglected. The red curve “wall + frame/skin + brace” also allows

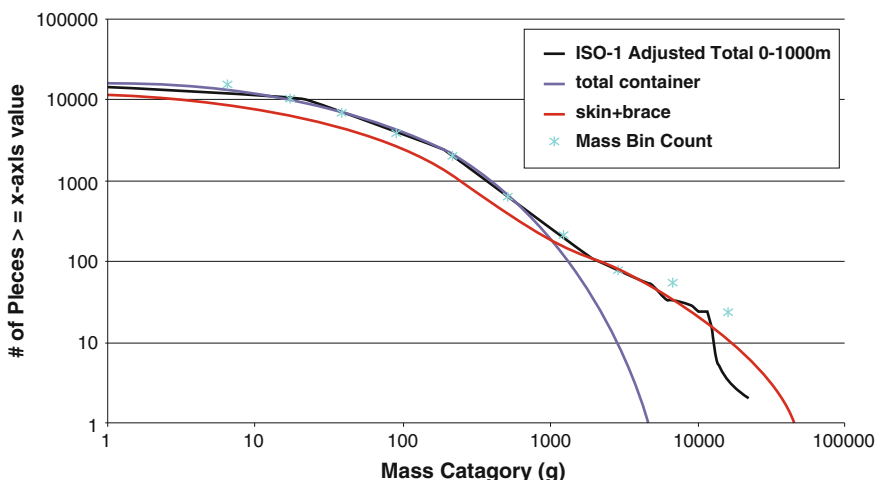


Fig. 16.7 The number of fragments over their mass for different fitted models for three tests with an ISO container (1000 kg NEQ). Taken from Robert T. Conway, John Tatom. ISO Container Source Function Development for the Klotz Group Engineering Tool. DDESB, Explosives Safety Seminar. Portland. USA. With permission

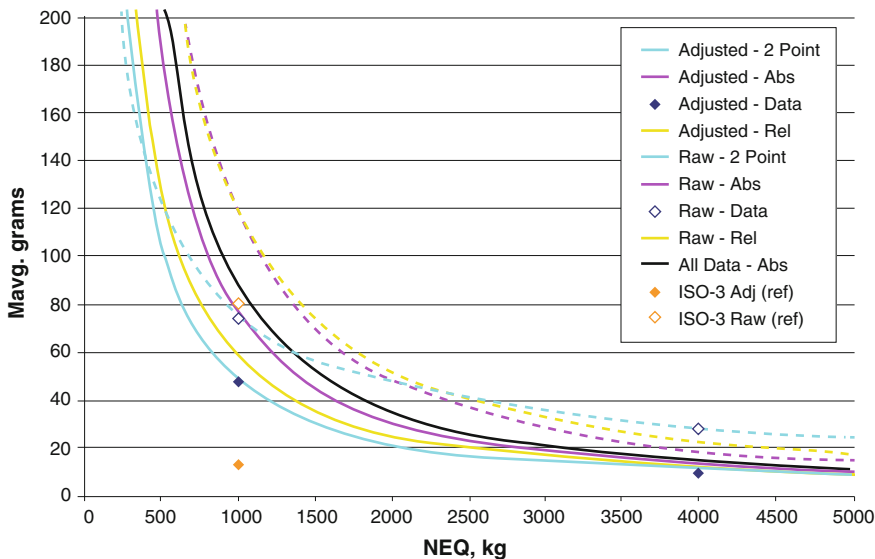


Fig. 16.8 Different functions describing the mass distribution as a function of the NEQ. Taken from Robert T. Conway, John Tatton. ISO Container Source Function Development for the Klotz Group Engineering Tool. DDESB, Explosives Safety Seminar. Portland. USA. With permission

few, big fragments. Figure 16.7 is a mass—cumulated number diagram, since it always count the number of fragments with more than the given mass. This leads to significant smoothing of the curves.

The curves in Fig. 16.7 are empirical data from three tests with an ISO container that were adjusted (for example by analyzing video material) because not all fragments are found after an explosion. The blue and the red curve show the different interpretations depending on whether the whole container is considered or just parts. For the mass bin count the fragments are divided into classes by weight. The black curve is an approximation without the interpretation of the blue and the red curve.

Figure 16.8 shows different functions which describe the average mass (m_{avg}) of the fragments as a function of the NEQ. The non-filled points show the raw data from experiments. If they are from the same experiment, such a point would be the average weight of a fragment in Fig. 16.7, for example

$$m_{avg} = \frac{\sum_i m_i N_{m_i}}{\sum_i N_{m_i}} \quad (16.4)$$

where m_i are the average masses of the mass bins and N_{m_i} the number of fragments in the mass bin (Ziehm et al. 2011).

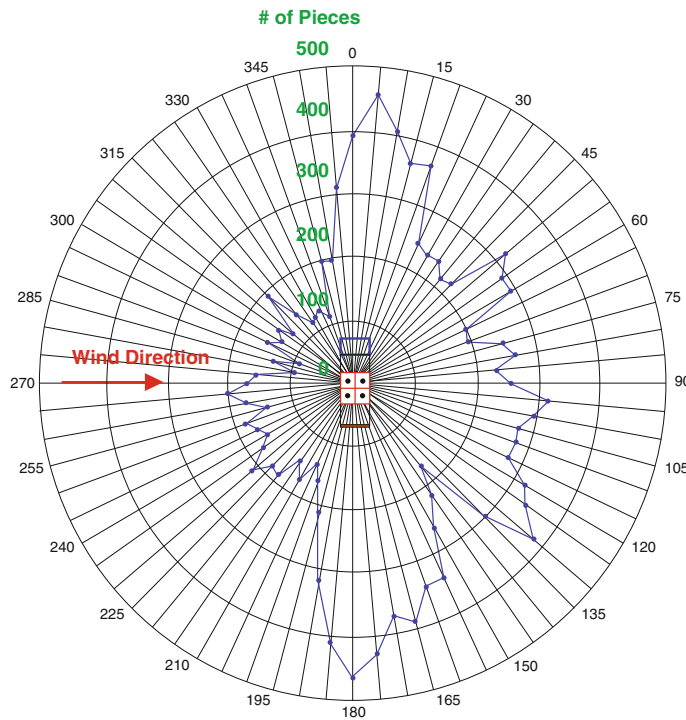


Fig. 16.9 Horizontal angle distribution of fragments for a container explosion (4000 kg NEQ) on a truck (*in the middle*) with a distance of more than 100 m. Taken from Robert T. Conway, John Tatton. ISO Container Source Function Development for the Klotz Group Engineering Tool. DDESB, Explosives Safety Seminar. Portland. USA. With permission

16.3.6.3 Horizontal Exit Angle

The horizontal exit angle was determined numerically and empirically.

An example of the determination of exit angles from the literature is shown in Figs. 16.9 and 16.10.

In both cases areas are visible that belong to the four wall sides of the container. The influence of the wind is nicely visible. There seems to be one small side wall of the container that generates more and more heavy fragments (that are less prone to wind drift and fly over longer distances). Typically this corresponds to the door part of the container.

Vertical exit angles were also analyzed.

16.3.7 Hazard Through Thermal Radiation

The following describes the physical hazard potential of heat radiation and its quantification in terms of emission and absorption/transmission quantities. In case

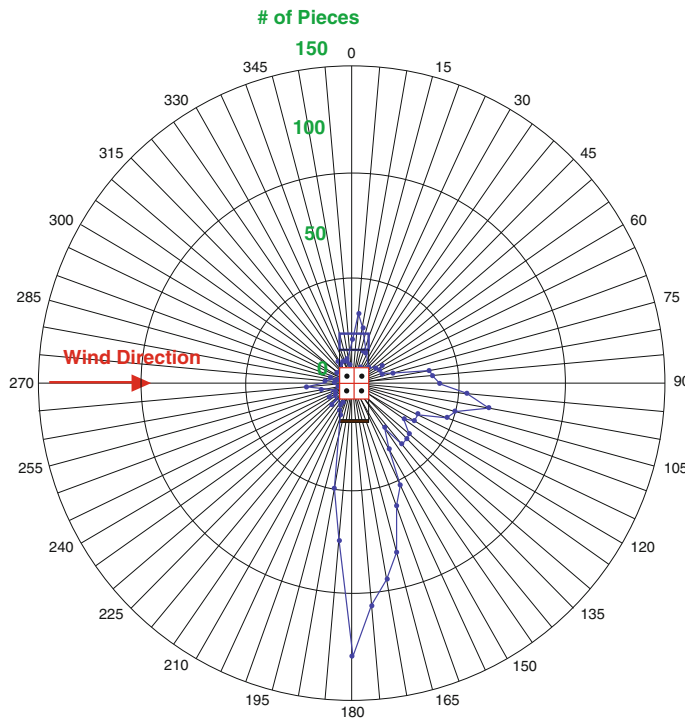


Fig. 16.10 Horizontal angle distribution of fragments for a container explosion (4000 kg NEQ) on a truck (*in the middle*) with a distance of more than 250 m. Taken from Robert T. Conway, John Tatom. ISO Container Source Function Development for the Klotz Group Engineering Tool. DDESB, Explosives Safety Seminar. Portland. USA. With permission

of an empirical-analytical or numerical computation, time-dependent local radiation absorption/transmission profiles are computed. This is the bases for effects of thermal radiation on persons.

Dermal burns due to an explosions can be caused by the following effects, where all effects result from the hot gas clouds or the heated air due to the fire ball (mostly for nuclear explosions) within the first minute of the explosion (Homann 2010):

- Absorption of thermal radiation by the skin.
- Heating or ignition of the clothes.
- By fire started by the thermal pulse.

Secondary effects of blast and ground shock also include resulting fire leading to secondary fires.

The radiated emission power P_e of a body is proportional to its surface area A , to the fourth power of its absolute temperature T , to its emissivity e (between 0 and 1 depending on the surface structure) and the Boltzmann constant $\sigma = 5.6703 \times 10^{-8} \text{ Wm}^{-2}\text{K}^{-4}$ (Tipler 1994):

$$P_e = e\sigma AT^4. \quad (16.5)$$

There are two effects of heat flow in the skin which influence the skin's temperature:

- **Absorption:** Absorption depends on the angle of the skin to the irradiating source, the surrounding temperature T_0 , the body's surface area A and the absorption capacity of the skin itself (depending on its emissivity e , structure and color) (van Dongen et al. 1998). The absorbed radiated power P_a is computed by Tipler (1994)

$$P_a = e\sigma AT_0^4. \quad (16.6)$$

- **Transmission:** Transmission is responsible for the conductivity of the skin and depends on the different conductivities and thermic capacities of the skin layers. With this property the warmth is conducted to the inside and leads to internal heating (van Dongen et al. 1998).

One often only regards the absorption of thermal radiation by the skin to quantify the damage of the skin. In the "User Guide" of "Hot Spot" (Homann 2010), which is used to determine the expected damage to persons by thermal radiation the model used is not described.

16.3.8 Radioactive Material After an Explosion

Radioactive material causes different hazards:

- Toxic effects (chemical property, no correlation with radioactivity; for example heavy metal)
- α -radiation (helium-4-nucleus)
- β -radiation (electrons and positrons)
- γ -radiation (photons)
- Neutron radiation

The hazards vary depending on the sort of interaction. In general, one distinguishes between three types of interaction:

- Radiation from the air
- Interaction after deposition onto the soil
- Absorption by the human body

Absorption by the human body normally is the most dangerous form of interaction. Additionally, most radioactive materials are toxic for the human body.

Two steps are necessary to estimate the hazard from an explosively released radioactive material. They correlate with the steps hazard and risk analysis:

- Simulation of the geographical distribution
- Simulation of the consequences on humans

There are two dominant models to simulate the geographical distribution: the empirical-analytical Gaussian Plume Model and the numerical Lagrange-particle-model, see for example (Carrascal et al. 1993). An example for a simulation tool is Hotspot (Homann 2010).

16.4 Damage Analysis

Damage analysis describes the damage to buildings, parts of buildings and persons caused by the physical hazards during free field explosions and the propagation of material (after an explosion) described in the previous section.

For free field conditions damage to buildings caused by blast is described, see Sect. 16.4.1.1. It is followed by a description of the damage to persons in Sect. 16.4.1.2. In Sects. 16.4.2 and 16.4.3 only the damage to persons is analyzed, first the damage caused by thermal radiation and then the one caused by the propagation of radioactive material.

16.4.1 *Blast in Explosions Under Free Field Conditions*

16.4.1.1 Damage to Buildings

The estimation of damage to buildings is done by the models mentioned in Dörr (2003) which are linked to the “Jarrett”-model (Jarrett 1968; Smith and Hetherington 1994; Mays 1995) through the detonation location and the loading.

The classification of damage reaches from 0 (little damage) to 5 or 6 (complete destruction). For each damage class the distance to the detonation location is given below which at least the damage level of the damage class is expected (e.g. broken windows for level 1),

$$R_{ai} = a_i \cdot Q^{b_i}, \quad (16.7)$$

where Q is the loading mass. For the factor a_i and the exponent b_i exist, depending on the loading and the explosive, three different values.

Table 16.4 shows the damage classification for residential buildings and other buildings in lightweight construction. More specifically, one regards residential buildings and smaller office buildings in brickwork or industrial buildings in lightweight construction at distance R from the hazard source (Ziehm et al. 2011).

Big office, hotel or residential buildings often have a reinforced concrete frame construction. This is probably also the case in the harbor of Bremerhaven. The damage classification for this type of building is shown in Table 16.5.

Table 16.4 Damage classes for residential buildings and other buildings in lightweight construction

Damage class	Description
Damage class 0	Damage which restricts the usage of the building is not expected. Possibly windows are destroyed
Little damage to buildings	
Damage class 1	Damage to windows and roofs is expected and visible, harmless cracks in the building are visible
Minor damage to buildings	
Damage class 2	In simple residential buildings all windows are destroyed, tiled roofs and lightweight facade elements are dented, walls, suspended ceilings and furniture are damaged, the building is still habitable or can be easily made habitable
Significant damage to buildings	
Damage class 3	The buildings are not in danger of collapse but inhabitable. All windows are destroyed, the roofs and two outer walls have partly collapsed and critical cracks are visible
Serious damage to buildings	
Damage class 4	The buildings are in danger of collapse. One expects that the buildings have partly collapsed; supply lines and connections are torn off. The buildings are inoperative and have to be torn down
Buildings inoperative	
Damage class 5	Buildings in this area are without load-bearing capacity
Buildings without load-bearing capacity	
Damage class 6	It is expected that simple, unreinforced buildings lie in ruins
Buildings collapsed	

Windows normally are the weakest component in a building with regard to blast because window glass is a relatively brittle material. It breaks as soon as the elastic stress limit is exceeded. For large blast stress, shear failure of the glass can occur at the window frames. The computation for window glass is done with so-called probit functions (Aschmoneit et al. 2009a) based on log-normal distributions. Probit functions normally are of the form

$$\Pr(x) = a \pm b \cdot \ln(x) \quad (16.8)$$

where $b > 0$ and a are parameters and x the variable. The probit value can be used to determine a probability for the regarded case (an example case is: glass breaks).

For our case, let Z be the scaled distance defined by

$$Z = \frac{r}{Q^{1/3}} \quad (16.9)$$

where r is the distance between loading and object/measuring point and Q the mass of the explosive.

Then the probit function is

$$\Pr(Z) = a - b \cdot \ln(Z). \quad (16.10)$$

Table 16.5 Damage classes for reinforced concrete frame construction

Damage class	Description
Damage class 0	At distances bigger than R_{ai} damage which restricts the usage of the building is not expected
No damage to buildings	
Damage class 1	Only damage to windows is expected
Minor damage to buildings	
Damage class 2	Many destroyed windows and dented lightweight facade elements are expected. The furniture is damaged but the building is still habitable
Significant damage to buildings	
Damage class 3	It is expected that all windows and lightweight facade elements are destroyed. The building is still habitable if absolutely necessary, although first cracks in reinforced concrete ceilings and walls can appear
Serious damage to buildings	
Damage class 4	It is expected that only the skeleton of the building still stands and that all supply lines, connections, windows, lightweight components and intermediate walls are destroyed
Buildings inoperative	
Damage class 5	It is expected that some reinforced concrete skeleton components (e.g. columns, ceilings) are destroyed. For small loadings close to components local damage at the total skeleton is expected: For $Q = 100 \text{ kg}$ one expects that columns within a radius of $R = 2 \text{ m}$ are destroyed and for $Q = 1000 \text{ kg}$ within a radius of $R = 10 \text{ m}$. For bigger loadings more load-bearing components can be damaged which can lead to a total loss of the building
Buildings with damage to load-bearing components	

Influence of Buildings (Shading, Focusing)

In the case of free field explosions on the ground, it is assumed that the blast wave expands hemispherically from the explosion location (Mays 1995). The blast parameters like overpressure and duration of the positive overpressure phase vary with the distance from the detonation location. The material of the explosive and its geometry are also considered (Mays 1995). For the computation of the scenarios regarded in the project, TNT equivalents are given.

Since the arrangement of objects in a container is not known, this will not be considered and a hemispheric expansion is assumed. For free field explosions, it is assumed that there are few (or no) buildings, that is, no urban structure. In urban areas the close arrangement of buildings can cause focusing and reflecting effects which influence the blast parameter (additionally to the distance).

In the project these effects were not regarded because the buildings in the Bremerhaven harbor do not resemble an urban structure. The few buildings that exist are relatively far apart and are not arranged like buildings along a street.

It also is not regarded that the blast waves go around and over buildings. If this happens at several buildings, canalization and shading effects can cause a very different stress situation behind the buildings. It can happen that buildings in the “shade” of other buildings are hit by the blast waves due to whirls caused by the effects mentioned above (Sauer 2005).

16.4.1.2 Damage to Persons

Blast can have different effects on persons. One distinguishes between primary, secondary and tertiary effects. Primary effects are caused directly by blast, for example lung and ear injuries. Secondary effects are indirect injuries caused by blast, for example injuries through debris or fragments of buildings. Tertiary effects are injuries caused by blow down. In the project debris and fragments were only regarded exemplarily and only up to hazard analysis, hence only primary and tertiary effects on persons were analyzed in detail.

Primary Injuries by Blast

Ear and eardrum injuries

For the analysis of possible injuries of eardrums and ears, probit functions are used (Dörr 2003; Sauer 2005). With growing distance from the explosion location not only the number of ear and eardrum injuries decreases but also their severity. The assessed injuries are permanent and not fully reversible.

There exist three different probit functions of the form (16.10) for three different categories of injuries. They all hold for loadings in the interval $1 \text{ kg} \leq Q \leq 100 \text{ t}$.

Deadly lung injuries

The overpressure and the blast impulse are mainly responsible for the degree of seriousness of lung injuries, see Fig. 16.4. In the case of loadings of at least 1000 kg only the overpressure is decisive for the lethality because the overpressure is changing relatively slowly when compared to smaller loading quantities. For small loadings of less than 1000 kg the influence of the duration of the positive excess pressure phase has to be considered (Dörr 2003, 2007b).

Probit functions of the form (16.10) can be used again in both cases: For larger loadings in terms of the quantity, for smaller loadings in terms of the overpressure.

16.4.2 Damage to Persons by Thermal Radiation

The presented damage models can also be used for urban and forest fires.

The skin is the outermost protection layer. It is sensitive to thermal radiation and at the same time protects us from it. It consists of 2 to 3 layers (epidermis, dermis and subcutis).

If the skin is exposed to thermal radiation, this can lead to damage of the skin layers, depending on the intensity and duration of the radiation. From the medical perspective, one distinguishes between four grades of burns where grade 1 is the weakest form of burn and burns of grade 4 do not only damage the skin but also muscles, bones, tendons, and joints (Onmeda 2010). Damage to the eyes (up to blindness) is also possible. In this case the retina is damaged by the light flash of a bigger explosion.

The project (scenario-dependently) regarded burns up to grade 3.

Fig. 16.11 Degree of injury from different models with regard to the incident thermal flux and the exposure time (Hymes 1983). Reprinted from Ian Hymes, The physiological and pathological effects of thermal radiation, Report N. SRD R 275, UK Atomic Energy Authority, Warrington, UK, with permission of Nuclear Decommissioning Authority

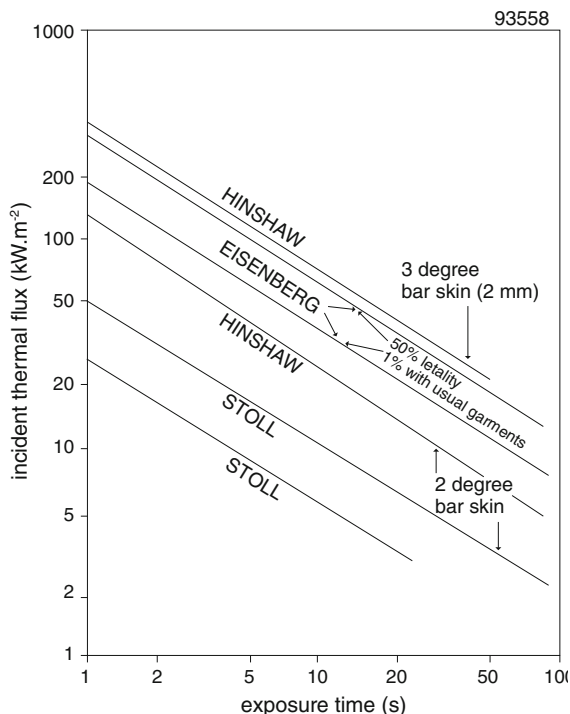


Figure 16.11 shows the relation between incident thermal radiation per square meter, the exposure time and the degree of injury, as it was developed in different literature sources. The figure gives a relationship between physical hazard and damage of the skin. The differences of the burns of grade 2 are due to the different views of the authors: Hinshaw concentrates on grade 2b, Stoll on grade 2a.

As for FN-curves, the criteria are of the form $ift(t) = ab^t$ where ift is the incident thermal flux and t the exposure time. For example, the line for pain by Stoll is roughly $ift(t) = 5.1 \times 1.1^t$.

Given the absorbed thermal energy, which is obtained by integrating the absorbed thermal radiation power over time, typically critical thresholds are used to generate damage levels, taking the distance from the radiating source into account, i.e. taking into account that the power is reduced by a factor defined by the ratio of absorbing surface over the total surface of the sphere at the considered distance (Ziehm et al. 2011).

16.4.3 Damage to Persons by Propagation of Radioactive Material

In the free field, radioactive material mostly spreads according to the direction of the wind. Damage occurs when it interacts with the human body.

16.4.3.1 Damage Through Radioactivity

Radioactive material creates four different hazards:

Toxic Effects

Whether toxic effects have to be regarded depends on the material. For very toxic plutonium (Plutonium-239) an intake of 40 ng is enough to reach the tolerable yearly limit for radioactivity but the chemical-toxic effects of such small amounts can be neglected. For other materials such as uranium they have to be considered and can cause damage to lung and liver (Helmers and Pade 2014).

α -Radiation

α -radiation consists of highly energetic helium-4-nucleuses, that is, two protons and two neutrons which are joint in a double positively charged nucleus. The exit speed usually is between 15,000 and 20,000 km/s or 2–5 MeV.

In the air, the reach of α -radiation under normal pressure normally is approximately 10 cm. A thin rubber layer already shields the radiation successfully.

The effect on the human body strongly depends on the sort of interaction. From the outside, α -radiation is harmless, as it enters only the outermost, dead skin layer. If the body absorbs material that sends out α -radiation when it decays, the high interaction with the material and the resulting short range effects leads to very high damage.

The radiation weighting factor of α -radiation is 20 while β -radiation and γ -radiation each have factor 1. The radiation weighting factor shows the relative biological effectiveness of certain radiation. For the same released energy per mass (1 Gray = 1 J/kg), 20 times as much effective energy per mass (Sievert, in Si) is absorbed (Bundesamt für Strahlenschutz 2010).

Typical α -radiators are uranium, thorium and elements which they decay into, like radium and radon (Ziehm et al. 2011).

β -Radiation

β -radiation consists of electrons and positrons. Positrons are the positively charged antiparticles of electrons.

β -radiation also has an ionizing effect. The range is strongly dependent of the energy at emission. For example, Phosphor-31 emits electrons with an energy of 1.7 GeV which have a range of approximately 7 m in air. Tritium, on the contrary, emits electrons with an energy of 19 keV which lead to a range of approximately 8 cm in the air (Wikipedia 2012b).

β -radiation can be shielded by appropriate material. Here, it has to be considered that β -particles are slowed down by shocks in a material and bremsstrahlung is produced. From the way bremsstrahlung is produced (collisions lead to most momentum transfer if colliding objects are of the same mass), it follows that atoms as light as possible should be used to absorb as much energy as possible in the shielding material. Examples for such materials are aluminum and glass. The bremsstrahlung can be stopped with a heavy metal layer such as lead.

If β -radiation hits the human skin, it leads to burnings of the skin. These can lead to skin cancer later on. Contact with the eyes is especially dangerous. It can lead to blindness.

β -radiation is also very dangerous when taken into the body. The most famous is iodine-131 which accumulates in the thyroid gland and can cause cancer there. To prevent this, iodine pills are often distributed after an accident. The accumulation of non-radioactive iodine in the thyroid gland prevents the accumulation of the radioactive isotope.

The radiation weighting factor (which will be used later) of β -radiation is 1 (Ziehm et al. 2011).

γ -Radiation

γ -radiation consists of particles seen as quanta of a very highly energetic electro-magnetic radiation. As such, its velocity of propagation is the speed of light and the energy content is directly related to the frequency and the wavelength.

In general, photons with an energy of more than 200 keV are called γ -radiation. The term X-radiation is often only used for the range of 100 eV–250 keV. There is no generally accepted definition. For comparison, visible light consists of photons with an energy between 1.91 eV (red) and 3.26 eV (purple).

In contrary to α - and β -radiation, γ -radiation decreases exponentially in matter. The decrease is described by the mass attenuation coefficient which depends on the material and the radiation's energy. Hence, no specific range can be assigned to γ -radiation. Instead, one speaks of so-called half-value layer which a material must have to decrease the intensity of radiation by 50 %. For example, the half-value layer of lead regarding 2 MeV radiation is 1.3 cm, the one of air would be 120 m (Wikipedia 2012a).

If γ -radiation penetrates into the human body from the outside, it has ionizing effects and splits chemical bonds. On the one hand, this leads to direct damage to the cells. On the other hand, it leads to damage to the genetic material. Due to the damage to the genetic material, either not enough cells are produced (especially blood cells) or they are uncontrollably reproduced (leading to tumors).

If γ -radiators penetrate the human body over the nutrition or breathing, they have a bigger effect due to their closeness to the tissue and the fact that they are surrounded by tissue.

The radiation weighting factor of γ -radiation is 1 (Ziehm et al. 2011).

Neutron Radiation

The natural decay of radioactive material does not normally cause *neutron radiation*. An exception is, for example, the rare californium-252 with a half-life period of 2.65 years. In nuclear reactors, neutron radiation leads to chain reactions.

Radioactive materials in combination with other material often are indirect neutron radiators. For example, radium-beryllium-neutron sources are common. Radon emits α -radiation which releases neutrons when it hits beryllium.

Neutron radiation is distinguished by fast and thermal neutrons. “Thermal” means that neutrons have an energy which corresponds to the surrounding temperature. Fast neutrons have a higher energy. Similar to the γ -radiation, neutrons are electrically neutral and hence have a relatively big range.

When interacting with the human body, fast neutrons scatter on light atoms such as hydrogen. Free protons are produced by the recoil which have a strongly ionizing effect.

Thermal neutrons, on the contrary, are caught by the hydrogen-atoms. Afterwards the energetically excited atoms emit γ -radiation.

Both fast and thermal neutrons can be converted from stable to radioactive elements by nuclear reactions. This is the process which causes the surrounding of a neutron radiator to be radioactive itself (for example in nuclear power plants).

The radiation weighting factor of neutron radiation is between 5 and 20 (Ziehm et al. 2011).

Meaning of the Dose Equivalent

The *dose equivalent H* is computed by multiplying the radiation weighting factor w_D with the energy absorbed by the ionization D :

$$H = w_R \cdot D. \quad (16.11)$$

To emphasize the difference to the absorbed dose (Gray), a new unit was defined: Sievert (Sv). Earlier, Rem was used instead which stands for “roentgen equivalent in man”. 1 Sv = 100 Rem.

The maximal dose per year for persons working in the corresponding areas is not allowed to exceed 20 mSv. During the total working life, the maximum does that is allowed to be absorbed is 400 mSv. For persons who do not work in the area, the limit per year is 1 mSv (Bundesamt für Strahlenschutz 2012).

Which doses lead to different levels of radiation sicknesses can be found in Bundesregierung (2008, 2012) and Bhushan and Katyal (2002). A dose of 0.0001 mSv per hour is seen as harmless (Bundesamt für Strahlenschutz 2010).

Meaning of Surface Contamination

Surface contamination refers to radiation which originates from surfaces. It is increased by radioactive rain or dust. For example, in Germany outside of radiation protection areas measures must be taken for a cesium-137-contamination of more than 10 KBq/m² (Bundesamt für Strahlenschutz 2010).

16.5 Damage Analysis of the Scenarios

After the collection of general information about damage analysis, the damage of the defined scenarios was analyzed. It was determined how people were injured at which distance. The damage of the building in terms of distance from the explosion was also determined.

Since these are project results, they are not displayed here.

16.6 Risk Analysis

There are four different heuristic types of risk which can be determined during a risk analysis (Fritzsche 1986):

- **Actual risk:** The risk results from a long observation period and can only be determined afterwards, normally under the not-fulfilled assumption that all circumstances in the hazard situation stayed the same. The actually occurring damage is analyzed in a methodically systematic way.
- **Statistical-actuarial risk:** The risk is determined using available data and statistical methods. Here, data can be analyzed which was systematically collected: for example data on accidents, terroristic events and natural disasters. The computation requires simple statistical methods, for example averaging.
- **Prognostic risk:** When determining the prognostic risk, the idea is to estimate the risk of a hazard which is new or has not appeared in this form before. This is done by comparing to similar scenarios or by using models.
- **Perceived risk:** The perceived risk is the risk (subjectively) perceived by a person or a group. This evaluation of the risk (risk perception) can be based on objective knowledge of the hazard but also depends on the personal willingness to take a certain risk or to have the feeling that a situation is under control or that the damage is acceptable and repairable (Bundesamt für Bevölkerungsschutz und Katastrophenhilfe 2005). Risk perception also plays an important role when defining tolerable risks because these are influenced psychologically, socially, sociologically and legally.

The first three types of risk are determined in an objective way, the last type of risk is subjective and subject to societal consents. The border between the first two

types of risk is fluid. The last type of risk can mostly be determined with systematical sociological methods.

In this project it is difficult to determine the risk by looking at hazards from the past because the attacks for which details are known did not involve containers. Hence, the risk has to be determined as prognostic risk (Ziehm et al. 2011).

16.6.1 Probability of Occurrence

The database analysis in Sect. 16.2.1 showed 42 attacks on harbors from 1970 to 2007, that is

$$\frac{\text{number of attacks}}{\text{years}} = \frac{42}{2007 - 1970 + 1} \approx 1.11 \frac{\text{attacks}}{\text{year}}. \quad (16.12)$$

By expert judgment, the number of attacks on harbors will stay about the same during the next years but due to the scenarios from Sect. 16.2.3 one believes that in the future between 1 and 10 % of the attacks will use containers. For the 10 % this would mean that an attack with a container is expected every $\frac{1}{0.1 \times 1.1053} \approx 9.05$ years and for 1 % every $\frac{1}{0.01 \times 1.1053} \approx 90.47$ years.

According to Wikipedia (2011a) there are approximately 651 harbors in the world. Assuming that the probability of a terrorist attack is the same for every harbor (homogeneous distribution), the probability for a specific harbor to be hit by a terrorist attack is

$$\frac{\frac{\text{attacks}}{\text{year}}}{\text{Number of harbors}} \approx \frac{1.1053}{651} \approx 0.00170 = 1.7 \times 10^{-3}. \quad (16.13)$$

Again assuming the 1 and 10 % from above, the probability of a specific harbor to be hit by a terrorist attack using a container is between 1.7×10^{-5} and 1.7×10^{-4} .

Remark It is not distinguished whether one of the scenarios is more likely than the others.

16.6.2 Damage

Two types of damage are relevant: damage to persons and damage to objects. The expected damage is explained in detail in Sect. 16.4.

Remark We change the numbers from the project in this subsection to show the computations that are necessary but not the project results. Fictitious numbers are chosen instead of parameters to make the computations easier to understand.

One expects that such a scenario takes place close to one of the “scanning”-machines which could be installed. Their location is not known yet, though. Hence, it is difficult to predict which buildings will be influenced. Also, the value of the buildings is not known. Therefore it is not possible to compute the financial damage due to the damaging of objects. In the following only the risk of persons is regarded.

A person density of 2 persons per hectare (ha) is assumed. There are parts of the harbor where almost no people are located but also areas where the person density is higher. The land area of the harbor is 1884 ha (Bremenports 2010), so one assumes that there are not much more than 4000 persons working in the harbor. A non-verifiable source from the internet states that there are 400 workers in the harbor terminal.

Using the conservative estimated number of persons, the expected numbers of non-fatal and fatal injured persons were computed for the different scenarios. For example, this includes injuries caused by blown down (blast), ear injuries, burns, radiation sickness, injuries through fragments (Ziehm et al. 2011).

16.6.3 Collective Risk (Societal Risk)

For the following computations we assume that 2 expected fatally injured persons and 10 injured persons with burns of grade 3 and 20 injured persons with ear injuries were computed in this step.

The *collective risk* is the risk that a group (e.g. the population of a country, workers in a company, ...) is exposed to. For example, for a company it is enough to show that the collective risk of the workers and the persons in the surrounding area is low enough.

In the most general case, the collective whom the risk refers to is not the immediate effected group, e.g. the persons working in a nuclear power plant, but a bigger group, e.g. the population of the whole area. Hence, the collective risk is not useful for an individual person. Instead it can for example be used by the government to decide on appropriate measures, e.g. evacuation.

In the project, only the average number of injuries was determined. One often also computes the probability of N or more deaths/injuries for different values of N. That results in so-called F-N curves, which were introduced in Chap. 4 and will be explained in more detail in Sect. 17.2.7.

For a longer period of time (e.g. hour, year, decade), the total damage is computed. Here the probability P is the reciprocal time in which the total damage is regarded, C_t is the total damage:

$$R_{coll} = PC_t = \left[\frac{1}{\text{time span}} \right] [\text{total damage}] = \left[\frac{\text{total damage}}{\text{time span}} \right]. \quad (16.14)$$

The collective risk can also be computed using the event frequency F and the average damage C_e for a single event. Then,

$$R_{coll} = FC_e = \frac{\text{number of events}}{\text{time span}} \cdot \frac{\text{damage}}{\text{event}}. \quad (16.15)$$

For the fictitious numbers given at the beginning of this subsection and the results from Sect. 16.6.1

$$R_{coll(1\%-\text{injured})} = 1.7 \times 10^{-5} \cdot 30 = 5.1 \times 10^{-4} \text{ a}^{-1} \quad (16.16)$$

and

$$R_{coll(10\%-\text{injured})} = 1.7 \times 10^{-4} \cdot 30 = 5.1 \times 10^{-3} \text{ a}^{-1}. \quad (16.17)$$

The collective risk of fatal injuries is described by

$$R_{coll(1\%-\text{fatal})} = 1.7 \times 10^{-5} \cdot 2 = 3.4 \times 10^{-5} \text{ a}^{-1} \quad (16.18)$$

and

$$R_{coll(10\%-\text{fatal})} = 1.7 \times 10^{-4} \cdot 2 = 3.4 \times 10^{-4} \text{ a}^{-1}. \quad (16.19)$$

So, in this case the collective risk of fatal injuries about one amplitude lower than for all injuries. The computed risks could be compared to risk criteria as a next step (Ziehm et al. 2011).

16.7 Summary

The chapter showed the steps of a risk analysis work package of a research project for harbor security. The threat event and hazard source analysis wants to identify relevant hazards and hazards that might be relevant in the future. For an efficient use of the (financial) resources for counter measures it is also important to determine the consequences of the hazards.

First, a database analysis was executed to identify hazards in the past and draw conclusions for the future. 42 attacks were found between 1970 and 2007, using the internal database TED of the Fraunhofer EMI institute and the public database GTD. The attacks for which details were available did not involve containers.

Due to the small amount of data, systematic considerations with the project partner were made to identify further potential hazards. The result were five types of hazards with multiple scenarios. Three of those scenarios were regarded in the further analysis: the nuclear scenario, the scenario with explosives and the “dirty

bomb” scenario. For these scenarios, a hazard analysis, a damage analysis and a risk analysis were executed.

During the hazard analysis the general physical hazards of an explosion and of radioactive material were described. For an explosion these are blast, fire ball, ground shock, debris and fragments. If radioactive material is involved, the radioactive cloud has to be considered.

The expected damage for the defined scenarios was computed.

Finally, the collective risk was derived from the expected damage and the event frequency.

The risk analysis does not include an evaluation of the results and does not present suggestions for counter measures. These decisions are left to the decision makers.

16.8 Questions

- (1) Which of the 9 steps of the risk analysis process (background to risk computation) were described in the chapter? If they were described, in which sections/subsections?
- (2) What is necessary to compute individual risks from the collective risks?
- (3) What is necessary to compute individual risks from the collective risks?
- (4) Formalize the heat radiation hazard propagation.
- (5) Formalize the heat radiation damage assessment.
- (6) Assuming a radial distribution of radioactive material of different types, formalize the hazard propagation modelling.
- (7) Compare the dispersion model of (5) with a simple plum dispersion model!
- (8) Set up the damage modelling for (5) and (6).

References

- Aschmoneit, T., Richter, C., Gürke, G., Brombacher, B., Ziehm, J., & Häring, I. (2009a). Damage assessment modeling for explosion effects. In *13th ISIEMS*. Brühl, Germany.
- Bhushan, K., & Katyal, G. (2002). *Nuclear, biological and chemical warfare*. New Delhi: S.B. Nangia A.P.H Publishing Corporation.
- Bremenports. (2010). *Zahlen, Daten, Fakten—bremenports (Bremen, Bremerhaven)*. http://www.bremenports.de/1973_1. Bremerhaven, bremenports GmbH & Co. KG: 2.
- Bundesamt für Bevölkerungsschutz und Katastrophenhilfe. (2005). *Problemstudie: Risiken in Deutschland*. From http://www.bbk.bund.de/SharedDocs/Downloads/BBK/DE/Publikationen/Wissenschaftsforum/Bd6_Risiken-fuer-D_Teil1.pdf?__blob=publicationFile
- Bundesamt für Strahlenschutz. (2010). *Verordnung über den Schutz vor Schäden durch ionisierende Strahlen*. From http://www.bfs.de/de/bfs/recht/rsh/volltext/1A_Atomrecht/1A_8_StrlSchV.pdf

- Bundesamt für Strahlenschutz. (2012). *Grenzwerte*. Retrieved September 24, 2012, from http://www.bfs.de/de/ion/beruf_schutz/grenzwerte.html
- Bundesregierung. (2008). Auszüge aus: ‘Radiologische Grundlagen für Entscheidungen über Maßnahmen zum Schutz der Bevölkerung bei unfallbedingten Freisetzungen von Radionukliden’. From http://www.verwaltungsvorschriften-im-internet.de/bsvvbund_27102008_RSII51593013.htm
- Bundesregierung. (2012). *Grenzwerte*. Retrieved September 24, 2012, from http://www.bfs.de/de/ion/beruf_schutz/grenzwerte.html
- Carrascal, M. D., Puigcerver, M., & Puig, P. (1993). Sensitivity of Gaussian plume model to dispersion specifications. *Theoretical and Applied Climatology*, 48, 147–157.
- Dörr, A. (2003). *EMI Bericht E 46/03*. Fraunhofer EMI: Efringen Kirchen.
- Dörr, A., Voss, M., & Gürke, G. (2007a). *Technisches Handbuch ESQRA-GE Version 2.0. Bericht E 21/07*. Efringen-Kirchen, Fraunhofer EMI.
- Dörr, A., Gürke, G., & Rübartsch, D. (2007b). The German explosive safety code ESQRA-GE. Department of Defense Explosive Safety Board (DDES) Seminar.
- Fraunhofer IIS. (2014). *Entwicklungszentrum Röntgentechnik*. Retrieved July 18, 2014, from <http://www.iis.fraunhofer.de/de/abt/ezrt.html>
- Fritzsche, A. F. (1986). *Wie sicher leben wir? Risikobeurteilung und -bewältigung in unserer Gesellschaft*. Köln: publisher TÜV Rheinland.
- Helmers, H., & Pade, H. J. (2014). *Radioaktivität*. Retrieved July 16, 2014, from <http://www.uni-oldenburg.de/physik/forschung/ehemalige/physikalische-umweltanalytik/radioaktivitaet/>
- Homann, S. G. (2010). *HotSpot Computer Program Version 2.07.1*. From <https://narac.llnl.gov/HotSpot/HotSpot.html>
- Hymes, I. (1983). *The physiological and pathological effects of thermal radiation*. Warrington, UK: UK Atomic Energy Authority. Report N. SRD R 275.
- Jarrett, D. E. (1968). Derivation of the British explosives safety distances. *Annals of the New York Academy of Science* (and Ministry of Defence, United Kingdom), 152, 18–35.
- Kronen Zeitung. (2010). *Al Kaida: Westen soll durch neue Taktik Geld bluten*. Kronen Zeitung, http://www.krone.at/Welt/Al_Kaida_Westen_soll_durch_neue_Taktik_Geld_bleiben-Paketbomben-Story-231621
- Mays, G. C. (1995). Blast effects on buildings. London: Thomas Telford Publications.
- National Consortium for the Study of Terrorism and Responses to Terrorism (START). (2011). *Global terrorism database [data file]*. Retrieved January 20, 2012, from <http://www.start.umd.edu/gtd>
- Onmeda. (2010). *Verbrühungen und Verbrennungen—Symptome*. Retrieved March 29, 2011, from <http://www.onmeda.de/krankheiten/verbrennung-symptome-5486-4.html>
- Sauer, M. (2005). Interaktion von Detonationswellen und Gebäuden. 9. Dresden Baustatik Seminar, 14. Oktober 2005. Dresden: 25.
- Siebold, U., & Häring, I. (2009). *Terror event database and analysis software* (pp. 85–92). Germany: Future Security. Karlsruhe.
- Smiths detection. (2014). *Why use Smiths Detection?*. Retrieved July 18, 2014, from <http://www.smithsdetection.com/>
- Smith, P. D., & Hetherington, J. G. (1994). *Blast and ballistic loading of structures*. Oxford: Butterworth-Heinemann.
- Spiegel-Online. (2010). *Stockholm entgeht knapp der Terrorkatastrophe*. Spiegel-Online, <http://www.spiegel.de/politik/ausland/0,1518,734168,00.html>
- Swisdak, M. M. J. (1994). Simplified Kingery airblast calculations. In *Proceedings of the 26th Department of Defense (DoD) Explosives Safety Seminar, Miami, Florida, US*.
- Swisdak, M. M. (2001). The Determination of Explosion Yield/TNT Equivalence from Airblast Data, Indian Head Devision/Naval Surface Warfare Center.
- Tatom, J., & Conway, R. (2010). *ISO container source function development for the Klotz Group Engineering Tool*. Portland, USA: DDES, Explosives Safety Board Seminar.
- Tipler, P. A. (1994). Physik, Spektrum Akademischer Verlag.

- van Dongen, P., Absil, L. H. J., & Kodde, H. H. (1998). *Inventory of damage and lethality criteria for HE explosions*. TNO report PML 1998-C21. Rijswijk, Netherlands: TNO.
- Wikipedia. (2011a). *List of seaports*. http://en.wikipedia.org/wiki/List_of_seaports.
- Wikipedia. (2011b). *USS Cole*. [http://de.wikipedia.org/wiki/USS_Cole_\(DDG-67\)](http://de.wikipedia.org/wiki/USS_Cole_(DDG-67))
- Wikipedia. (2012a). *Abschirmung (Strahlung)*. Retrieved September 24, 2012, from http://de.wikipedia.org/wiki/Abschirmung_%28Strahlung%29
- Wikipedia. (2012b). *Betastrahlung*. Retrieved September 24, 2012, from <http://de.wikipedia.org/wiki/Betastrahlung>
- Ziehm, J. (2009). Verbundprojekt «Flughafen Sicherungssystem FluSs» AP 2.2: Ereignisanalyse für konventionelle Bedrohungen an Flughäfen. Bericht E 19/09. Efringen-Kirchen, Fraunhofer EMI.
- Ziehm, J., Mayrhofer, C., & Häring, I. (2010). Ereignis- und Schadensanalyse für terroristische Anschläge auf einen deutschen Flughafen. Workshop BAU-Protect. Ed.: K. Thoma, N. Gebekken. pp. 269–281.
- Ziehm, J., Moser, S., Echterling, N., & Fraunhofer EZRT. (2011). Increase of container security by applying contactless inspections in port terminals. ECSIT: Erhöhung der Containersicherheit durch berührungslose Inspektion im Hafen-Terminal. Efringen-Kirchen, Fraunhofer Ernst-Mach-Institut. Report 21/11.

Chapter 17

Risk Acceptance Criteria

17.1 Overview

This chapter reviews a variety of risk assessment criteria (models) that can be presented together with risk visualizations of computed risks. The risk computation itself has to take account of the intended risk visualization and risk comparison as well as which risk criteria should be applied.

This chapter emphasizes that for all applications it must be guaranteed that individual and collective risks are acceptable for persons and objects. Often this can also be assessed by using criteria for the combination of probability and consequence of risks, since low consequences tend to represent events relevant for single persons and objects, whereas high consequences tend to represent events relevant for multiple persons and objects. For instance, referring back to Chap. 16, using the classical definition of risk, criteria can be introduced for single persons, and various group sizes.

For instance, in case of storage or production of dangerous goods, the individual risks of persons taking their exposure history into account must be acceptable, the local individual risks (to take account of unknown exposure histories), the local collective risks as well as the overall collective risks. With some effort, and taking account of the accumulation of similar events, this could be mapped onto a risk matrix to employ risk acceptance criteria. However, this chapter shows that it is more straightforward to use for each assessment established assessment criteria.

This chapter first presents some basic concepts underlying risk acceptance criteria, including absolute critical values, balancing of costs and chances, comparison with already commonly accepted risks in given domains and contexts. These concepts can also be applied to the combination of probabilities and consequences that determine the risks. The principles can also be combined, e.g. when asking for as low as reasonable practicable risks (ALARP principle).

In general, it can be observed that there are no generally accepted absolute risk acceptance criteria, that the assessment context has to be taken account of as well as already established risk acceptance criteria in the given context.

This chapter introduces and relates the fatal accident rate to the frequency of events. Both are also related to the (quality adjusted) lost life-years.

It is shown how the local risks introduced in Chap. 14 and used in Chap. 16 can be compared with local individual risk criteria.

F-N curves are derived from f-N curves. It is discussed how the most common F-N criteria take into account risk aversion. This takes up discussions of Chap. 4. The difference between consequence-probability plots of risks in risk maps (matrices) as used in Chap. 14 and FN curves is mentioned. This takes up discussions of Chap. 4.

As an example, risk acceptance criteria of the UK Health and Safety Executive are given, which mainly cover individual risks for selected (working) groups of the society.

A set of examples from different applications shows how individual and collective risk criteria in terms of F-N criteria are combined for overall assessment. The following examples are covered: landslides, liquefied gas, and explosive storage.

Reference risk tables of Proske are reviewed for different types of risk events, and for individual risks.

This chapter summarizes risk acceptance criteria for different countries, it emphasises the differences of the approaches, resulting in the lack of absolute quantitative criteria. Most countries use individual risk criteria and collective risk criteria that can be presented in terms of F-N criteria.

As an application example that is difficult to classify with respect to country, industry and group of persons affected, the status quo of risk acceptance criteria for humanitarian demining is reviewed. Based on the overview of Chap. 17, risk acceptance criteria are recommended.

Risk acceptance criteria can be used for rational and informed decision making in all resilience management phases. In particular, they can be used to decide whether intended or unintended frequencies (probabilities) or consequences should be increased or decreased, respectively or both. In particular, different risk criteria may be used in different resilience management phases for resilience engineering.

Risk criteria are in particular an important input for the decision making resilience capability. The distinction of the textbook between the risk management steps assessment of risks using risk criteria and the final risk evaluation or risk decision, see Chap. 2, highlights the need of careful use of risk criteria within capability-based resilience engineering approaches.

After computing risks, it has to be decided whether they are acceptable or not. For this, often risk acceptance criteria are used. We assume that risk criteria support risk evaluation and risk assessments rather than enforcing a deterministic decision.

“Introducing the language of mathematics is a trial to improve objectivity. As shown, this can only be done partially; nevertheless the application of parameters might be useful for risk-informed decisions” (Proske 2008), based on Arrow et al. (1996)

Risk acceptance criteria can take different forms. Some of these forms, for example individual and collective risks, fatal accident rates, lost life-years, risk contours, the ALARP principle and FN-curves, are introduced in the method Sect. 17.2.

Sections 17.3–17.5 give different examples of risk criteria defined in the literature. Concrete numbers are presented based on the concepts of Sect. 17.2. They are divided by working sectors (landslides, liquefied natural gas crew, ammunition storage workers, humanitarian demining) and countries (mostly the different countries from the European Union are compared).

As an exemplary application we relate the presented risk criteria to the context of humanitarian demining.

The information collected in this chapter were also used in Schäfer and Rathjen (2014). The main sources are Health and Safety Executive (2001), Trbojevic (2005), Proske (2008) and Johansen (2010). The main author of the part of Schäfer and Rathjen (2014) used here was S. Rathjen supplemented with work by J. Schäfer.

17.2 Concepts and Methods

Based on the classical formula of risk, where risk is the product of frequency and consequences $R = PC$, the simplest form of a risk comparison is to compare the computed risk with a number that is considered a tolerable risk per year, for example $10^{-6}a^{-1}$.

The standard procedure is then as follows. If the computed risk is below the identified tolerable risk, the risk is acceptable. If it is higher than that number, mitigation measures are necessary. Of course, this has to be further specified with respect to the nature of risk considered, e.g. individual versus collective, local versus non-local, etc.

Instead of defining the risk per year, other metrics can be chosen, for example the Fatal Accident Rate(FAR) which defines risks per hours of exposure or lost life years (LLY) which is the difference between the average life expectancy without the considered risk and the average life expectancy with the considered risk.

Other more advanced concepts do not base risk acceptance criteria on single numbers. These concepts include F-N curves, risk contours and ALARP-areas. An F-N curve is typically a function that relates acceptable probabilities to respective minimum numbers of expected fatalities.

Risk contours define local areas with different risks around a hazard source.

ALARP-areas extend the concept of a hard boundary between acceptable and non-acceptable risks by defining a risk interval where risk should be kept as low as reasonably practicable (ALARP).

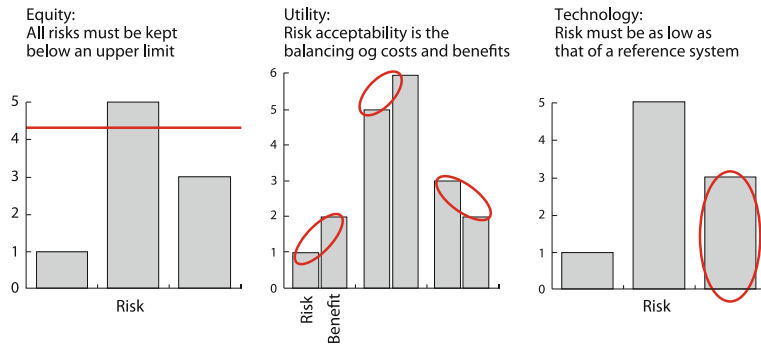


Fig. 17.1 Three lines of reasoning as visualized by Johansen (2010). The y-axis is abstract and can be any reasonable measure of risks, for example €/year or injuries/year

17.2.1 *Three Principles of Defining Risk Acceptance Criteria*

Risk acceptance criteria are defined to distinguish between acceptable and non-acceptable risks. The decision of what is acceptable can be based on different principles. Three principles to motivate risk criteria are introduced in Fig. 17.1: equity, utility and technology (Johansen 2010).

The principle of equity means that a fixed boundary is defined for risks, independent of the situation or the circumstances. An example is the de minimis risk for the countries.

Utility relates the risk to its benefits. For instance, in the area of humanitarian demining this can mean that a higher risk is tolerable for farmers working also as deminers (with the benefit of making their farming area safer) than deminers without such a perspective, or more general societies with the perspective of improving the development options of their area dramatically.

The technology principle compares risks of a system to risks of a reference system or the average risk of comparable systems. For instance, if the risk of dying in an air plane of a certain airline or airplane manufacturer is above the risk of another airline or manufacturer. A similar argument holds respectively if the references are the averages.

In practical approaches these principles are often combined, for example by defining limits (equity principle) for different groups of persons (utility principle).

17.2.2 Individual and Collective Risks Based on the Classical Formula of Risks

The commonly used definition of risk is from Blaise Pascal:

“Risk should be proportional to the probability of occurrence as well as to the extent of damage.” (Blaise Pascal 1623–1662)

Formalized this reads as follows.

Risk is proportional to a measure for the probability P of an event (frequency, likelihood) and the consequences C of an event (impact, effect on objectives):

$$R = PC. \quad (17.1)$$

This can be computed for individual persons or groups. This results in the difference between individual and collective risk.

Individual risk is the expected damage (e.g. money, injury) of a person per year. In addition it is assumed that the person is located at a certain local position or if this is not assumed and the individual risk of the person is averaged over all its expected positions. Examples were given in Sect. 16.6.3.

In the case of averaged collective risks for a collective or group of persons, again with assumptions about their position, the average risk per time interval is computed. Collective risk is the expected damage, or money lost, or expected injuries of the group per time interval. Here it is important to clearly define the group considered (e.g. employees of company, city, country, world). See Sect. 17.4 for examples.

17.2.3 Fatal Accident Rate

The idea of the Fatal Accident Rate (FAR) is to introduce a standardized time of exposure. For this time the number of expected number of fatalities is given. This number is dimensionless. It is defined as the “statistically expected number of fatalities resulting from accidents per 10^8 exposed hours [100 million hours]” (Johansen 2010).

Example 1 To get acquainted we compute the FAR corresponding to working with the individual annual de minimis risk of 10^{-6} assuming an average full time job in Germany corresponding to 1760 h/a:

$$FAR = \frac{10^{-6} \cdot 10^8}{1760} = 0.05 \frac{\text{accidents}}{10^8 \text{ working hours}} \quad (17.2)$$

Example 2 In this example we want to show the advantage of FAR. It is able to distinguish between situations with very different durations of exposure.

According to Proske (2008) the individual mortality risk m of a person living in a house for one year and of using a motorbike for 2 h/year is the same!

Now we want to show how different the FAR for those two situations is. That is, we compute by which factor the Fatal Accident Rate varies. The Fatal Accident Rate of living in a house for one year (assuming the person spends the complete year there) is

$$FAR_{house} = \frac{m \cdot 10^8 \text{ h}}{365 \cdot 24 \text{ h}} \approx 11415.53 \text{ m} \quad (17.3)$$

where m is the individual mortality risk.

And the Fatal Accident Rate of using a motorbike for 2 h/year is

$$FAR_{motorbike} = \frac{m \cdot 10^8 \text{ h}}{2 \text{ h}} = 5 \times 10^7 \text{ m.} \quad (17.4)$$

Hence the Fatal Accident Rate of using a motorbike is $\frac{5 \times 10^7}{11,415.53} \approx 4380$ times bigger than the Fatal Accident Rate of living in a house.

17.2.4 Lost Life-Years

The individual risk and the Fatal Accident Rate do not consider the age when a person dies. Proske (2008) follows the general line of argument when he writes that age might not be considered important at first glance. However, only death at a certain (older) age seems to be ‘natural’. “For instance, if young people die by a car accident, it is very much considered to be risk that should be controlled. Therefore, the age information has to be considered for risk comparison” (Proske 2008).

The formula often used reads

$$LLY = e' - e, \quad (17.5)$$

where e' is the average life expectancy without the considered risk and e is the average life expectancy with the considered risk. LLY stands for lost life-years.

The concept of lost life-years has another advantage besides considering the age of persons. It also makes it possible to consider long term health effects. For example, people’s life expectancy sinks if they eat food contaminated in a nuclear disaster. So, the catastrophe causes long time fatalities which are not considered in the most simple computation of individual risk that only consider the risk of injury or fatality in a very short time interval after the accident.

It is also possible to distinguish between quality adjusted life-years (QALY) and disability adjusted life-years (DALY). For this, the degree of disability for different kinds of injuries must be defined. For example, deafness has a degree of disturbance

of 0.241–0.360 and paraplegia a degree of disturbance of 0.501–0.700 (Proske 2008).

17.2.5 Localized Individual Risk and Risk Contours

In contrast to the individual risk per year, the Fatal Accident Rate and the lost life-years which are all based on the activity or profession of a person, the localized individual risk per annum (LIRA) depends on the geographical position.

It is defined as the “annual probability that an unprotected, permanently present individual dies due to an accident at a hazardous site” (Jongejan 2008). We introduced the notion of an individual local risk in Sect. 17.2.2.

“Helpful is in this regard the use of iso-risk contour maps, displaying lines that connect locations with the same value of LIRA” (Johansen 2010). They can be used to divide an area into risk contours, similar to the schematic contours in Chap. 14.

Although the definition is simple, the calculation can be difficult if for example meteorological conditions are considered. In such cases one averages over all possible wind directions.

17.2.6 ALARP

The basic idea behind the ALARP (as low as reasonably practicable) principle is to divide the risk into three regions (unacceptable, tolerable, broadly acceptable) instead of only unacceptable and acceptable.

“Unlike the upper [unacceptable] and lower [broadly acceptable] zones, risks in this mid region cannot be claimed tolerable just because they happen to fall within the limits. The crucial point is that a risk must have been reduced to a level as low as reasonably practicable to serve this designation. What constitutes reasonable practicability is given by the ratio between the costs and benefits of reducing a specific risk” (Johansen 2010).

The ALARP principle is most common in the UK where the Health and Safety Executive (HSE) has prepared a series of guidance documents on the principle.

The ALARP principle can also be considered to take account of the fact that the computation of risks is challenging and that risk decisions should not depend on sharp boundaries, but rather on orders of magnitude.

17.2.7 F-N Curves

An F-N curve is a function to show the frequency of N or more fatalities. “It can be used for presenting accident statistics and risk predictions, as well as drawing

criterion lines for acceptable levels of societal risk. Mathematically, it is derived from the commonly used expression of risk being a product of frequency and consequence, [which is in total] denoted [as] number of fatalities per year” (Johansen 2010).

The functions can be “plotted in either of two fashions:

Non-cumulative frequency basis: For these graphs, called *f-N curves*, the value plotted on the y-axis is the discrete frequency of experiencing exactly N fatalities.

Cumulative frequency basis: For these graphs, called *F-N curves*, the value plotted on the y-axis is the cumulative frequency of experiencing N or more fatalities.” (Center for Chemical Process Safety 2009)

The resulting diagram is called an F-N diagram.

17.2.8 Construction of an F-N Curve in Practice

An F-N-curve is constructed in four steps:

- Collect data of relevant events in a table
- Sort the events by the number of accidents (from low to high)
- Compute the cumulative probabilities of N or more fatalities
- Display results in a diagram

The following example to explain the four steps is described in Tables 3.23–3.25 and Fig. 3.12 in Proske (2008), which is based on Ball and Floyd (2001).

The first step is to collect relevant data, for example of accidents. Proske does this in Table 3.23 which is displayed here as Table 17.3.

Remark Non-integers for the numbers of fatalities are generated when considering the degree of disturbance as explained in Sect. 17.2.4.

Table 17.2 shows the same data as Table 17.1 but here the data is sorted by the number of fatalities (left column).

Table 17.1 Original accident data including frequencies and number of fatalities (Proske 2008) based on Ball and Floyd (2001). With permission of Springer Science and Business Media

Event no.	Number N of fatalities	Probability f of events per year
1	12.1	4.8×10^{-3}
2	123	6.2×10^{-6}
3	33.4	7.8×10^{-3}
4	33.2	9.1×10^{-4}
5	29.2	6.3×10^{-3}
6	15.6	7.0×10^{-4}
7	67.3	8.0×10^{-5}
8	9.5	4.0×10^{-3}
9	52.3	1.2×10^{-6}
10	2.7	3.4×10^{-4}

Table 17.2 Sorted accident data with respect to number of fatalities, corresponding cumulative frequencies and the contributing events (Proske 2008) based on Ball and Floyd (2001). With permission of Springer Science and Business Media

Number N of fatalities	Probability f of events per year	Event no.
2.7	3.4×10^{-4}	10
9.5	4.0×10^{-3}	8
12.1	4.8×10^{-3}	1
15.6	7.0×10^{-4}	6
29.2	6.3×10^{-3}	5
33.2	9.1×10^{-4}	4
33.4	7.8×10^{-3}	3
52.3	1.2×10^{-6}	9
67.3	8.0×10^{-5}	7
123	6.2×10^{-6}	2

Table 17.3 Rearranged accident data (Proske 2008) based on Ball and Floyd (2001). With permission of Springer Science and Business Media

Number N of fatalities	Probability f of events per year	Event no.
1 or more	2.49×10^{-2}	1–10
3 or more	2.46×10^{-2}	1–9
10 or more	2.06×10^{-2}	1–7, 8
30 or more	8.80×10^{-3}	2–4, 7, 9
100 or more	6.20×10^{-6}	2
300 or more	—	—

Table 17.3 shows the cumulative probabilities. They are computed by adding all probabilities of all events in one category. For example, the numbers of fatalities of the events 2, 3, 4, 7 and 9 are at least 30. All other events have numbers of fatalities which are smaller than 30. Hence, to compute the probability belonging to “30 or more fatalities”, one has to add up the probabilities of events 2, 3, 4, 7 and 9, that is

Fig. 17.2 Sample for empirical F-N curve. Display of the data in Table 17.1

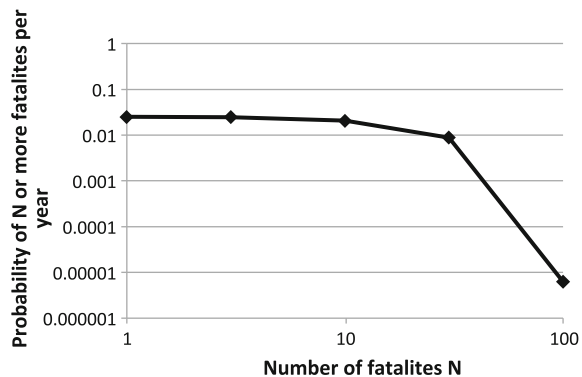


Fig. 17.3 Display of the cumulative probabilities without forming classes

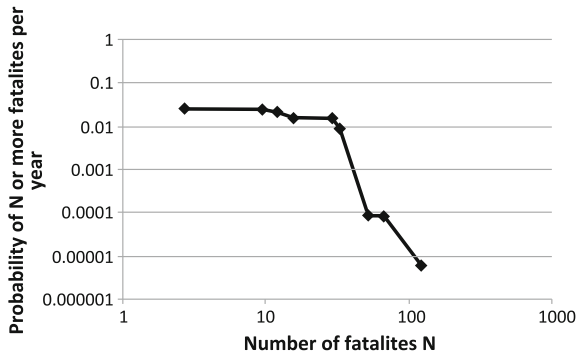
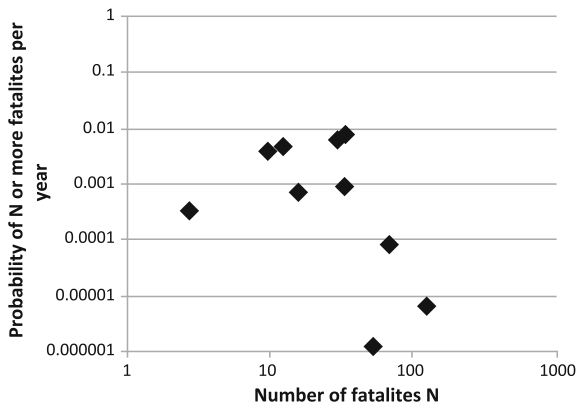


Fig. 17.4 fN diagram belonging to Table 17.1



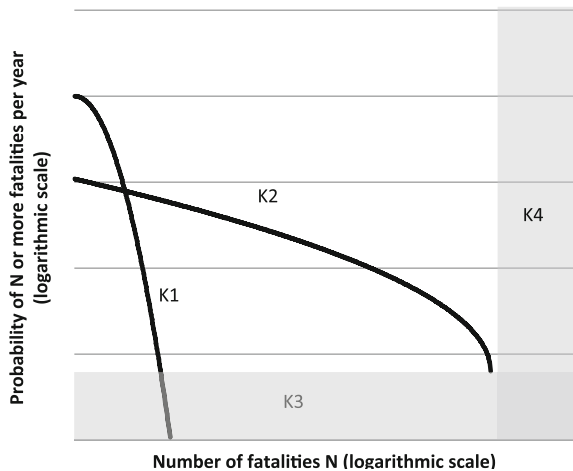
$$p = 6.2 \times 10^{-6} + 7.8 \times 10^{-3} + 9.1 \times 10^{-4} + 8.0 \times 10^{-5} + 1.2 \times 10^{-6} \\ = 8.8 \times 10^{-3}/a. \quad (17.6)$$

Figure 17.2 shows the F-N-diagram belonging to Table 17.1. Both axes are scaled logarithmically.

The FN-diagram in Fig. 17.2 was based on the decision by Proske to divide the numbers of fatalities in the classes 1, 3, 10, 30, 100 and 300. Another possibility is to use the numbers from the events, that is “2.7 fatalities or more”, “9.5 fatalities or more”, “12.1 fatalities or more”, etc. The resulting FN-diagram is shown in Fig. 17.3. Instead of connecting the points by straight lines, it is also common to find a smooth graph to approximate the points or to draw step functions to connect the points.

Instead of using the cumulative probabilities in the diagram, the probabilities from Table 17.1 can also be used. The resulting diagram is an fN-diagram, see Fig. 17.4. It is difficult to combine the points in this diagram to a reasonable curve.

Fig. 17.5 Modified illustration of the classification of risk by van Breugel (2001)



17.2.8.1 Classification of Risks in Terms of FN-Curves

Proske (2008) introduced 4 types (K1–K4) of risks based on van Breugel (2001):

- Risks of type K1 are events that have a high frequency but low severity, for example car accidents.
- Risks of type K2 are events that have a low frequency but high severity, for example tsunamis.
- Risk of type K3 are theoretically known but have not been experienced, so statistical data is not available.
- Finally, risks of type K4 are so severe that the number of fatalities is bigger than the size of the population.

The four types are illustrated in Fig. 17.5, adapted from Fig. 3-14 in Proske (2008).

The grey areas can be seen as the boundaries of the diagram where a statistical analysis is not reasonable.

17.2.8.2 Risk Aversion Criteria Using F-N-Curves

In F-N diagrams risks can be compared to F-N acceptance measures that take risk aversion into account, see Fig. 4.1. A typical risk aversion criterion reads

$$\begin{aligned}
 F(N) &= \text{Acceptable probability of } N \text{ or more fatalities} \\
 &= aN^{-b}, \\
 a, b &> 0.
 \end{aligned} \tag{17.6}$$

One can compare this risk criterion with single points in the F-N diagram or with a whole F-N curve calculated from data from several given events. “If any portion of the calculated F-N curve exceeds the criterion line, the societal risk is said to exceed that risk criterion” (Center for Chemical Process Safety 2009). See Fig. 2.10 for an example.

Example for calculating a risk aversion criterion F-N curve: Given two values for a F-N acceptance measure of collective risk in England

$$\begin{aligned} F(10) &= 10^{-3}, \\ F(100) &= 10^{-4}, \end{aligned} \quad (17.7)$$

we can determine the parameters a and b in the risk aversion criterion F-N curve $F(N) = aN^{-b}$.

Substituting the values for N and $F(N)$ in the equation yields

$$\begin{aligned} 10^{-3} &= a \cdot 10^{-b}, \\ 10^{-4} &= a \cdot 100^{-b}. \end{aligned} \quad (17.8)$$

Hence,

$$\begin{aligned} a &= 10^{-3+b}, \\ a &= 10^{-4+2b}. \end{aligned} \quad (17.9)$$

Comparing the exponents yields

$$-3 + b = -4 + 2b. \quad (17.10)$$

That is, $b = 1$, $a = 10^{-3+1} = 10^{-2}$ and $F(N) = 10^{-2}N^{-1}$.

F-N curves can be visualized in so called F-N diagrams as shown in Fig. 4.1. The computed curve $F(N) = 10^{-2}N^{-1}$ for example is the blue line in the diagram.

Remark As risk is defined by $R = PC$, combinations of P and C with the same resulting risk lie on a hyperbola in a coordinate system with N (as a measure of the consequences C) and F (as a measure for P) on the axes. In a double logarithmic scale this becomes a straight line with gradient -1 .

$$\begin{aligned} const &= NF \\ \Rightarrow F &= \frac{const}{N} \text{ (hyperbola)} \\ \Rightarrow \log F &= \log const - \log N \text{ (straight line in double log scale).} \end{aligned} \quad (17.11)$$

The more general formula $F(N) = aN^{-b}$ becomes a straight line with gradient $-b$ in double logarithmic scale (Fig. 17.6):

Fig. 17.6 Example of an FN-curve and a criterion line (both axes in logarithmic scale)

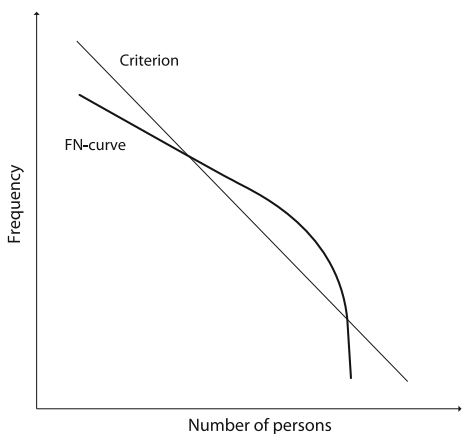
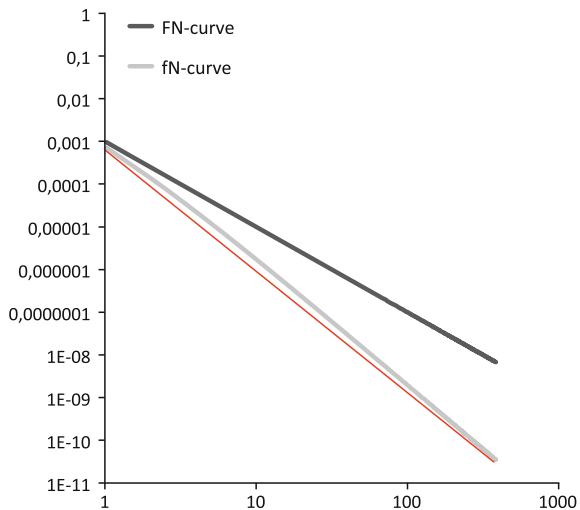


Fig. 17.7 Comparison of F-N-curve and f-N-curve. The thin red line shows that the fN-curve is not a straight line in double-log scale



$$\begin{aligned} F(N) &= a N^{-b} \\ \Rightarrow F &= \frac{a}{N^b} \text{ (hyperbola)} \end{aligned} \tag{17.12}$$

$\Rightarrow \log F = \log a - b \log N$ (straight line in double log scale).

Last, we want to compare F-N-curves and f-N-curves of risk aversion criteria. We have seen that F-N-risk aversion criteria are often displayed as straight lines in double-logarithmic scale. Looking closely at Fig. 17.7 one can see that the corresponding f-N-curve is not a straight line.

Table 17.4 Computation of an f-N-curve from an F-N-curve: spreadsheet application example

	P	Q	R
1	a	0.001	
2	b	2	
3	$F(N) = aN^{-b}$		
4			
5	N	F-N-curve	f-N-curve
6	1	$\$Q\$1 * P6^{(-\$Q\$2)}$	Q6-Q7
7	2	$\$Q\$1 * P7^{(-\$Q\$2)}$	Q7-Q8
8	3	$\$Q\$1 * P8^{(-\$Q\$2)}$	Q8-Q9

This can be derived as follows in the situation where we only have integer numbers of fatalities.

$F(N)$ is the frequency of N or more fatalities and $F(N + 1)$ the frequency of $N + 1$ or more fatalities. Hence, the frequency of exactly N fatalities $f(N)$ can be computed by $f(N) = F(N) - F(N + 1)$. This was done for the curve $F(N) = 0.001N^{-b}$ in Table 17.4.

The computed fN-curve and the original FN-curve are the once displayed in Fig. 17.7.

17.2.9 Risk Map/Matrix

An established method for the evaluation of risks is the so called risk matrix, see Sect. 14.5.

17.3 Health and Safety Executive Boundaries

The Health and Safety Executive (2001) presents some statistics to show average risks in the UK, see Tables 17.5 and 17.6.

As risk criteria, the Health and Safety Executive gives boundaries between broadly acceptable, tolerable and unacceptable risks:

- “HSE believes that an individual risk of death of one in a million per annum for both workers and the public corresponds to a very low level of risk and should be used as a guideline for the boundary between the broadly acceptable and tolerable regions” (Health and Safety Executive 2001).
- “[I]n our document on the tolerability of risks in nuclear power stations, we suggested that an individual risk of death of one in a thousand per annum should on its own represent the dividing line between what could be just tolerable for

Table 17.5 Annual risk of death from industrial accidents to employees for various industry sectors (Health and Safety Executive 2001)

Industry sector	Annual risk	Annual risk per million	Basis of risk and source
Fatalities to employees	1 in 125,000	8	GB 1996/97–2000/01 ^a
Fatalities to the self-employed	1 in 50,000	20	GB 1996/97–2000/01 ^a
Mining and quarrying of energy producing materials	1 in 9200	109	GB 1996/97–2000/01 ^a
Construction	1 in 17,000	59	GB 1996/97–2000/01 ^a
Extractive and utility supply industries	1 in 20,000	50	GB 1996/97–2000/01 ^a
Agriculture, hunting, forestry and fishing (not sea fishing)	1 in 17,200	58	GB 1996/97–2000/01 ^a
Manufacture of basic metals and fabricated metal products	1 in 34,000	29	GB 1996/97–2000/01 ^a
Manufacturing industry	1 in 77,000	13	GB 1996/97–2000/01 ^a
Manufacture of electrical and optical equipment	1 in 500,000	2	GB 1996/97–2000/01 ^a
Service industry	1 in 333,000	3	GB 1996/97–2000/01 ^a

^aHealth and Safety Commission, Health & Safety Statistics (1996/97, 1997/98, 1998/99 & 1999/2000) published by HSE Books. Figures used for 2000/2001 are provisional

Table 17.6 Average annual risk of injury as a consequence of an activity (Health and Safety Executive 2001)

Type of accident	Risk	Basis of risk and source
Fairground accidents	1 in 2,326,000 rides	UK 1996/7–1999/00 ^a
Road accidents	1 in 1,432,000 km travelled	GB 1995/99 ^b
Rail travel accidents	1 in 1,533,000 passenger journeys	GB 1996/97–1999/00 ^c
Burn or scald in home	1 in 610	UK 1995–1999 ^d

^aTilson and Butler (2001)

^bDepartment of Environment, Transport and the Regions—Transport Statistics (2000)

^cHealth and Safety Executive (2001)

^dDepartment of Trade and Industry and Office of National Statistics (2001)

any substantial category of workers for any large part of a working life, and what is unacceptable for any but fairly exceptional groups. For members of the public who have a risk imposed on them ‘in the wider interest of society’ this limit is judged to be an order of magnitude lower—at 1 in 10,000 per annum” (Health and Safety Executive 2001).

One can see that most industries in Table 17.5 lie in the defined ranges.

Table 17.7 Tolerable risks for engineered slopes (Australian Geomechanics Society 2000)

Situation	Suggested tolerable risk for loss of life
Existing engineered slopes	10^{-4} /a person most at risk
	10^{-5} /a average of persons at risk
New engineered slopes	10^{-5} /a person most at risk
	10^{-6} /a average of persons at risk

17.4 Examples for Risk Criteria by Sectors

17.4.1 Risks for Landslides

Fell et al. (2005) describe risk acceptance criteria within their risk management process for landslides. They define tolerable risk as “[a] risk within a range that society can live with so as to secure certain net benefits. It is a range of risk regarded as non-negligible, and needing to be kept under review and reduced further if possible” (Fell et al. 2005).

They present tolerable risks from the Australian Geomechanics Society (see Table 17.7) but also note that “the AGS (2000) guidelines do not represent a regulatory position” (Fell et al. 2005).

For the collective/societal risk they introduce an F-N curve “which has been trialled on an interim basis to assist landslide risk management of natural hillside hazards” (Fell et al. 2005), see Fig. 17.8.

An important question is whether those criteria are acceptable, depending on the country and its legal system. For landslides Fell et al. (2005) state: “In some societies, e.g. Australia, Hong Kong, and the United Kingdom, the use of such criteria for Potentially Hazardous Industries, and to a lesser extent dams and land-slides is gaining acceptance. In others, such as France, the legal framework currently precludes the use at least in absolute terms.”

17.4.2 Risks for Liquefied Natural Gas Crew

The individual and societal risk acceptance criteria for crew members of LNG (liquefied natural gas) carriers presented by Vanem et al. (2008) are shown in Table 17.8 and Fig. 17.9. They are similar to the HSE boundaries for workers in nuclear power stations from Sect. 17.3.

The individual risk criteria in Table 17.8 cannot be compared to the risk criteria for landslides in Sect. 17.4.1 because here the ALARP principle is used which Fell et al. (2005) only used for the societal risk acceptance criteria.

The societal risk criteria shown in Fig. 17.9 can be compared because here both authors use F-N curves and distinguish between negligible, ALARP and intolerable risks. The slope of the F-N curves in double logarithmic scale are approximately the

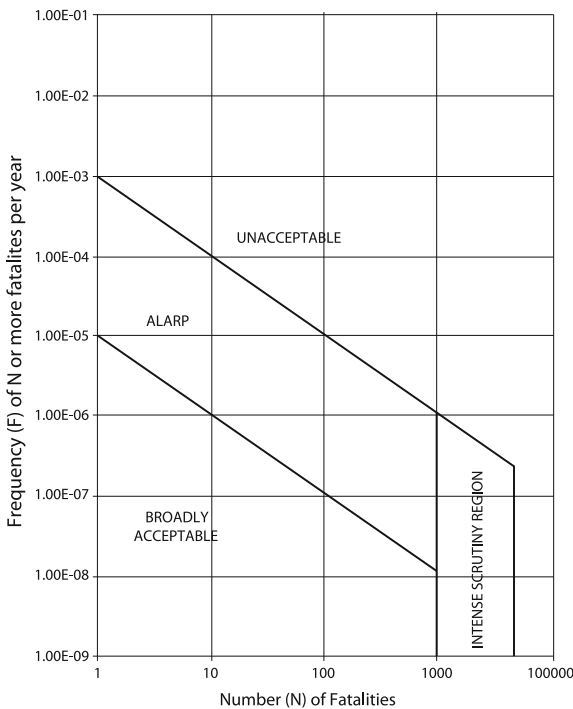


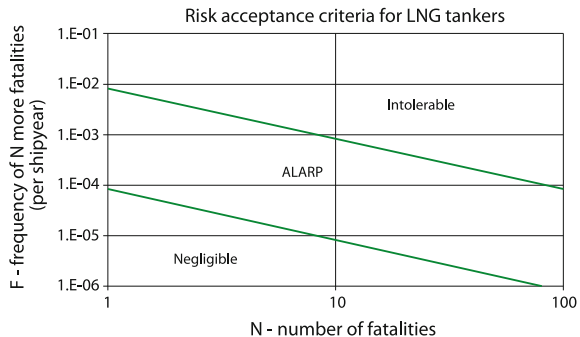
Fig. 17.8 Interim societal risk tolerance criteria (Geotechnical Engineering Office 1998). With permission

Table 17.8 Individual risk acceptance criteria for LNG crew (Vanem et al. 2008), based on Skjøng et al. (2005)

Intolerable risk per year	$>10^{-3}$
ALARP area per year	$10^{-6} - 10^{-3}$
Negligible risk per year	$<10^{-6}$

same in both diagrams ($b \approx 1$ in (17.6), the neutral risk aversion factor from HSE). The major difference are the different values for a in (17.6). The frequencies in the F-N curves for LNG are almost 10 times higher than for the comparable F-N curves for landslides. For example frequencies of 1 or more fatalities that are bigger than 10^{-3} are not acceptable for landslides but still in the ALARP area for LNG carrier crews as long as they are below approximately 10^{-2} .

Fig. 17.9 Societal risk acceptance for crew (Vanem et al. 2008). With permission from Elsevier



17.4.3 Risks for Ammunition Storage Workers

For the tolerable individual risks for workers in Explosives Facilities, the International Ammunition Technical Guideline (UN OAD 2012) says that the level of tolerable risk should depend on the country but also says that it should not be higher than in manufacture or industry and gives suggestions.

The standard suggests maximum tolerable risks levels of $10^{-3}/a$ (occasional exposure) and $10^{-4}/a$ (regular exposure) for workers and $10^{-5}/a$ for the general public. The suggested acceptable limit for both groups is $10^{-6}/a$. This is stricter than the HSE boundaries from Sect. 17.3 where the limit for workers in the nuclear sector was $10^{-3}/a$ instead of the division in $10^{-3}/a$ and $10^{-4}/a$. The other values are identical to the HSE boundaries.

17.4.4 Risk Criteria by Proske

The “Catalogue of Risks” (Proske 2008) sees itself as “an encyclopedia for the topic of risk” (Proske 2008). It was first published in German. The English version from 2008 we introduce here is not only a translation. “Not only are many updated examples included in chapter ‘Risks and disasters’ but also new chapters have been introduced, such as the chapter ‘Indetermination and risk’” (Proske 2008).

We give a short overview of the topics treated in Chaps. 2 and 3 of his book here. In his book, Proske collects data from many different sources. All these sources are not listed here but can be found in Proske (2008).

17.4.4.1 Types of Risk

The second chapter of the book is called “Risks and Disasters”. He divides the risks he lists on the 194 pages of the chapter in 4 categories:

- “Natural (volcano, earthquake, flood, storm)
- Technical (dam failure, airplane crash, car accident)
- Health (AIDS, heart attack, black death ...) and
- Social (suicide, poverty, war, manslaughter)” (Proske 2008)

The most relevant category in our context are the technical risks but the other categories can also be important depending on the event that is analyzed. He collected data for 85 figures and 103 tables from approximately 420 references. Examples for the collected and created statistics are among many others (Proske 2008)

- “The 40 most deadly disasters from 1970 to 2001”
- “Number of recorded natural disasters since 1900”
- “Distribution of natural hazards in the US”
- “Return period of meteorite impacts”
- “Prognosed regions of water deficiency in 2025”
- “Frequency of tornados worldwide”
- “List of major debris flows, rock avalanches or landslides”
- “Statistics of killings by bears in Europe”
- “Mortalities and accident frequencies for different means of transport”
- “Frequency of airplane crashes”
- “Accident numbers for the Frankfurt airport (Germany)”
- “Probability of errors during design and construction of structures”
- “International Nuclear Event Scale (INES)”
- “Probability of fire for different building types”
- “Risk of cancer during lifetime”
- “Development of homicide rate in the US from 1900 to 1980”
- “Fatality rates for people climbing different mountain peaks”.

17.4.4.2 Individual Risk

The third chapter “Objective Risk Measures” is the most relevant in the context of risk criteria, especially Table 3.19. Here he collected the “Mortality per year” for 189 situations. The mortality per year can be seen as the individual risk of persons. He sorted them by the numbers in the column “Mortality per year” from high to low. The references are listed in Proske (2004). An extract is shown in Table 17.9.

Also interesting is Table 3.20. It lists “[a]ctions that increase the chance of death by one in a million” (Proske 2008). Here, one can read that living 2 days in New York and Boston (cause of death: air pollution) increases the risk as much as living 2 months with a cigarette smoker or eating 40 tablespoons of peanut butter (case of death for both: cancer). “This value of increased mortality by one in a million is of great importance since it is included in many regulations as ‘permitted maximum additional risk’ or as so-called ‘de minimis risk.’ However, the origin of this value

Table 17.9 Extract from Table 3.19 in Proske (2008)

Causes of death	Mortality per year	Literature
German soldier in World War II	7.0×10^{-2}	Overmans (1999)
Smoking (US 1999)	3.6×10^{-3}	Ellingwood (1999)
Smoking (US)	3.0×10^{-3}	James (1995–1996)
Heart disease in the US (1975–1995)	2.9×10^{-3}	Parfit (1998)
Cancer every age (UK)	2.8×10^{-3}	Kafka (1999)
Acceptable risk in the British heavy industry (new value)	2.0×10^{-3}	Paté-Cornell (1994)
Workers on off-shore platform (UK 1990)	1.3×10^{-3}	Bea (1990)
Acceptable risk for British off-shore platform	1.0×10^{-3}	Paté-Cornell (1994)
Acceptable risk for Norwegian off-shore platform	1.0×10^{-3}	Paté-Cornell (1994)
Firefighters (US)	8.0×10^{-4}	James (1995–1996)
Fatalities during police actions in the US	8.6×10^{-5}	Parfit (1998)
Workers in agriculture industry	7.9×10^{-5}	Mathiesen (1997)
Acceptable risk by General Motors in the 1990s	1.2×10^{-5}	Stern (1999)

remains uncertain; even some indications for [its] development in the 1960s have been found” (Proske 2008), originally from Kelly (1991).

Similar to Table 17.9 there is also a table listing Fatal Accident Rates. Here the values vary depending on the source. For example, the FAR for traveling by car varies from 15 to 70. Proske also lists some risk criteria in terms of FAR, for example 15 for the oil industry based on Randsaeter (2000) and an FAR of 0.04 to 0.12 for fire risks in the public in Switzerland.

Proske also uses the concept of lost life-years introduced in Sect. 17.2.4. In the text he refers to poverty and comparing the lost life-years with respect to 1000 life-years. In the table he lists different values for lost life-years in the literature, however, without mentioning in all cases the total number of expected life-years, respectively.

17.4.5 Examples for Risk Criteria by Country

17.4.5.1 Risk Contours for Third Party in Land Use Planning

Okstad and Hokstad (2001) present safety measures for 3rd party from different countries. “In the Netherlands, UK and Canada the location of [a] new activity in the vicinity of existing establishments is based on risk contours” (Okstad and Hokstad 2001), as shown in Table 17.10.

Here, the individual annual local risk (IR) is the “the probability that an average unprotected person permanently present at a specific location is killed due to an accident at the hazardous activity” (Bottelberghs 2000; Okstad and Hokstad 2001)

Table 17.10 Risk contours in Land use Planning (Z = zone) (Okstad and Hokstad 2001)

Z	The Netherlands ^a	Z	Canada	Z	UK
1	$IR < 10^{-6}$ housing, schools, hospitals allowed	i	$IR < 10^{-6}$ every activity allowed	A	$PED < 10^{-6}$ insignificant risk area
2	$10^{-6} < IR < 10^{-5}$ offices, stores, restaurants allowed	ii	$10^{-6} < IR < 10^{-5}$ commercial activity only	B	$10^{-6} < PED < 10^{-5}$ risk assessment required
3	$IR > 10^{-5}$ only by exemption	iii	$10^{-5} < IR < 10^{-4}$ only adjacent activity	C	$PED > 10^{-5}$ high risk area
		iv	$IR > 10^{-4}$ forbidden area		

All risks have the unit 1/a

^aValues for siting of new establishments

and PED is “[t]he [annual] probability of exposure of a dangerous dose (at a specific location) due to an accident at the hazardous activity” (Health and Safety Executive 1992; Okstad and Hokstad 2001).

“Germany, France, Sweden and Norway have developed a set of Safety distances to separate new activity from hazardous installations. Such generic safety distances may have been derived from expert judgments, including consideration of historical data, or from experience through operating similar plants” (Okstad and Hokstad 2001).

17.4.5.2 Risk Criteria for the EU

Trbojevic (2005) compares risk criteria from different European countries. He classifies them by three categories:

- “Risk based, goal setting criteria where [the] safety goal is specified and not the means of achieving it (UK)” (Trbojevic 2005).
- “Prescriptive, risk based criteria where a prescribed maximum level of risk is used for risk control (The Netherlands, Hungary, Czech Republic) and some form of risk reduction may be specified but not necessarily implemented” (Trbojevic 2005).
- “Prescriptive, consequence based criteria where the prescribed level of impact is used for control (France) or no risk is allowed outside the boundary of the facility (Germany)” (Trbojevic 2005).

For four countries in the first two categories he presents risk criteria, see Table 17.11. The HSE boundaries from Sect. 17.3 can be among others found in the column for the UK. The risk contours from Table 17.10 also do not contradict the entries in Table 17.11 although they cannot be precisely compared due to a different focus. Comparing the individual criteria to the criteria for engineered slopes in Table 17.7 shows that the limits for an average person at risk coincide with the

Table 17.11 Comparison of individual risk criteria (Trbojevic 2005). Copyright 2005 CRC Press. Permission of Taylor & Francis Books UK

IRPA	UK	The Netherlands	Hungary	Czech Republic
10^{-4}	Intolerable limit for members of the public			
10^{-5}	Risk has to be reduced to the level as low as reasonably practicable (ALARP)	Limit for existing installations. ALARA principle applies.	Upper limit	Limit for existing installations. Risk reduction must be carried out
3×10^{-6}	LUP limit of acceptability (converted from risk of dangerous dose of 3×10^{-7})		Lower limit	Limit for the new installations
10^{-6}	Broadly acceptable level of risk	Limit for the new installations and general limit after 2010. ALARA applies		
10^{-7}	Negligible level of risk			
10^{-8}		Negligible level of risk		

LUP land use planning, ALARA as low as reasonably achievable, IRPA individual risk per annum

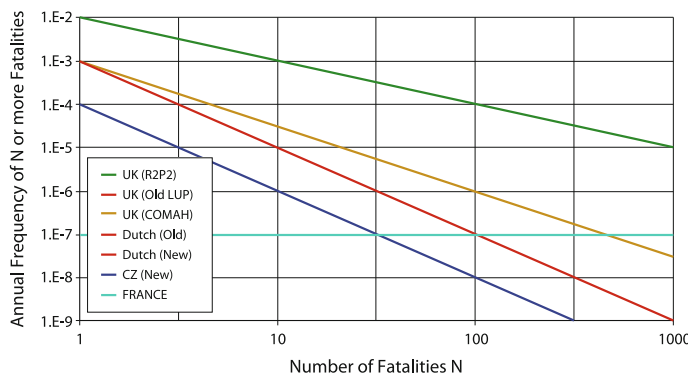


Fig. 17.10 Comparison of F-N curves generated from the risk criteria presented in his paper (Trbojevic 2005). R2P2 = (Health and Safety Executive 2001), COMAH = (Health and Safety Executive 2004). Copyright 2005 CRC Press. Permission of Taylor & Francis Books UK

limits for the Netherlands and Czech Republic for existing and new installations. The criteria for LNG carrier crews from Sect. 17.4.2 allow higher risks than all limits presented in Table 17.11.

Trbojevic (2005) also compares societal risk criteria in the form of FN-curves for different countries, see Figs. 17.2 and 17.10. The F-N curves for landslides and LNG carriers from Sects. 17.4.1 and 17.4.2 are different because they each consist of two F-N curves to show the ALARP area. One can still notice that they have a neutral risk aversion (slope -1) while here the risk aversion is higher for most of the

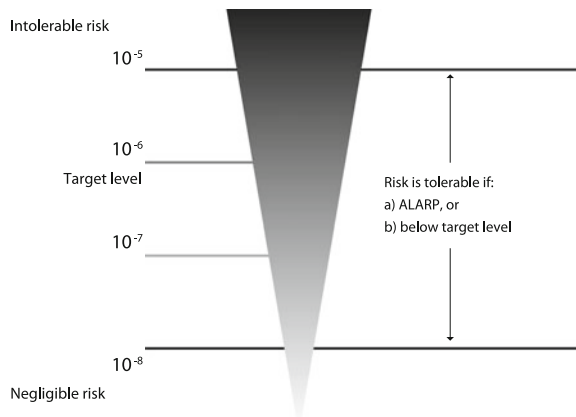


Fig. 17.11 Proposed individual risk criteria (Trbojevic 2005). Copyright 2005 CRC Press. Permission of Taylor & Francis Books UK

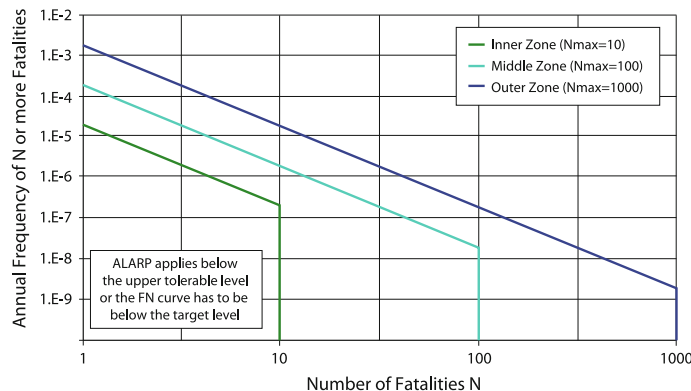


Fig. 17.12 Proposed societal risk criteria (Trbojevic 2005). Copyright 2005 CRC Press. Permission of Taylor & Francis Books UK

F-N curves. Only the old HSE slope has the same risk aversion (slope -1 , see Fig. 17.10).

Interesting is his approach to find risk criteria that hold for the whole European Union. For the individual risk he suggests a mixture of the ALARP principle and a fixed target level, the two concepts used in different countries. This is shown in Fig. 17.11.

He also tries to find common societal risk criteria. Here it is difficult to find a common risk aversion factor. Trbojevic (2005) suggests the slope -2 in double logarithmic scale (see Fig. 17.12) but he also admits difficulties: “This will be

Table 17.12 Risk criteria in Häring et al. (2009). Copyright 2009. With permission from Elsevier

Description	Individual risk	Citation
Negligible level of risk in The Netherlands	10^{-8}a^{-1}	[62]
Negligible level of risk in the UK	10^{-7}a^{-1}	[62]
Traditional de minimis risk (per life cycle)	10^{-6}	[63]
Individual fatality risk per mission for the general public	10^{-6}	[21]
Broadly acceptable level of risk in UK	10^{-6}a^{-1}	[62, 64]
Limit for new installations in The Netherlands and Czech Republic after 2010		
Sport accidents in Germany in 2006	$2.5 \times 10^{-6} \text{a}^{-1}$	[65]
Accident at work in Germany in 2006	$6.1 \times 10^{-6} \text{a}^{-1}$	[65]
Upper limit for (existing) hazardous installations in EU	10^{-5}a^{-1}	[62]
Fatalities in road traffic in Germany in 2006	$6.3 \times 10^{-5} \text{a}^{-1}$	[65]
Accident at work in Austria	$8.7 \times 10^{-5} \text{a}^{-1}$	[66]
Intolerable limit for members of the public in UK	10^{-4}a^{-1}	[62]
Fatalities in road traffic in Austria in 2006	$1.8 \times 10^{-4} \text{a}^{-1}$	[66]
Total accident risk in Germany in 2006	$2.4 \times 10^{-4} \text{a}^{-1}$	[65]

In this table, the quotations on the right (in the order that they occur) are [62] = (Trbojevic 2005), [63] = (Sandin 2005), [21] = (STANDARD 321-07 2007), [64] = (Bykov and Akimov 2004), [65] = (Statistisches Bundesamt Deutschland 2007) and [66] = (Leitner 2007)

acceptable by the Netherlands and Czech Republic and perhaps by the UK as well” (Trbojevic 2005).

Statements as “It seems that there are no societal risk criteria in use in Hungary” (Trbojevic 2005) and “In the absence of any other anchor points for the F-N criterion, the risk matrix from the HSE guidance on ALARP demonstration in HSE 2004, has been used to define [the F-N curve for the UK]” (Trbojevic 2005) show that the concept of F-N curves is not totally accepted. Hence, it might be to communicate his suggestion from Fig. 17.12 all over Europe. He also sees that with Fig. 17.12 “[a]n example of such criteria based on the same level of individual risk and the same level of expected fatalities across hazard zones has been presented as the first step” (Trbojevic 2005) and not as a final solution.

Table 17.12 shows individual risk criteria used in a “hazard and risk analysis [...] for personnel from primary fragments of fast moving and variably oriented high-explosive sources with spatially distributed event probability of a single event” (Häring et al. 2009). Here the values from Trbojevic (2005) are set into relation with statistics from different countries, for example “accidents at work in Australia” or “sport accidents in Germany”. This gives an impression of how high or low the defined limits are.

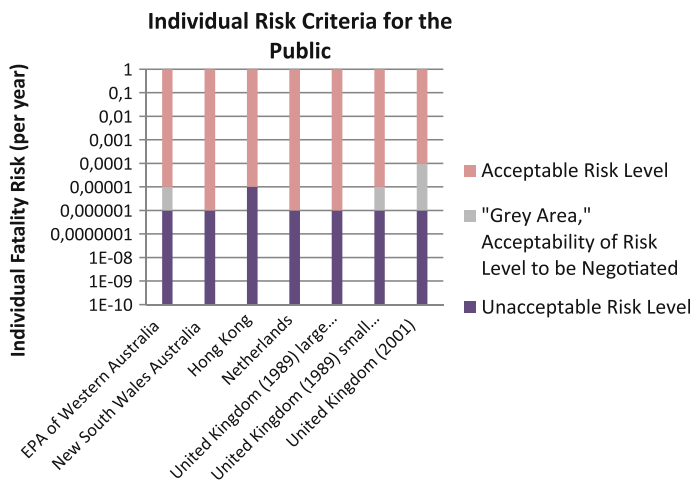


Fig. 17.13 Comparison of individual risk criteria (Cornwell 2015). EPA = Environmental Protection Agency (Cornwell and meyer 1997). With permission from Quest Consultants

17.4.5.3 Risk Criteria for Australia, Hong Kong, UK and the Netherlands

Cornwell (2015) also compares individual risk criteria for different countries outside of Europe, see Fig. 17.13. The acceptable risk level is equal in all countries but Hong Kong. The countries vary in the definition of when the acceptability of the risk level is to be negotiated.

17.5 Risk Criteria for Humanitarian Demining

Different from the examples from Sect. 17.4, most sources about risk criteria for humanitarian demining do not give precise risk criteria:

- “In Humanitarian demining, the aim is not only to allow others to use a path in relative safety, they must be able to do so in complete safety. [“Complete safety” may be impossible to guarantee, but it must be the aim.] Furthermore, the process of clearance itself must also be safe. While it may be acceptable for combat personnel to be injured while making a passage through a danger-area, there is no such thing as an “acceptable loss” during Humanitarian Mine Action activity” (Smith 2005).
- “The tolerance of the local community may vary from place to place and people in one area may be prepared to accept a higher level of risk than people in another. The level of tolerable risk needs to be continually reassessed, because, for example, an economically feasible improvement in technology or knowledge

may be achievable, meaning that a higher level of safety can be achieved. [...] The tolerance levels of the affected community may also change. If, for instance, someone is injured due to a missed mine in a supposedly cleared area, the people in the area may call for a lower level of risk. [...]

- This is the most subjective phase of risk assessment because it is based on the perception of risk held by local people as well as the responsibility of the demining industry to ensure the relative safety of its product or service. So, even after a demining organization has deemed an area to be tolerably free of landmines and UXO [unexploded ordnance], if the people in the area refuse to use the land because of the perception of risk is still too high and the demining organization may need to increase the perception of safety by implementing a further demining technique. Alternatively, the local people may be using an area that the demining industry cannot yet confirm to be tolerably free from mines and UXO" (Bach 2004).

The International Mine Action Standards (IMAS) and the national demining standards of Turkey, Sri Lanka and Herzegovina (these three countries were exemplary regarded) also do not give individual or societal risk criteria. The closest that they introduce to risk criteria are (Bosnia and Herzegovia Mine Action Centre 2004; National Steering Committee for Mine Action 2010; Turkish Ministry of National Defence 2012; United Nations Mine Action Service 2013):

- safety distances between workers and between the demining activity and buildings (IMAS, Turkey, Sri Lanka, Bosnia Herzegovina),
- land release criteria in terms of how many dangerous parts are still allowed to be found by extern testers after the demining activity (Sri Lanka, Bosnia Herzegovina),
- a residual risk (Sri Lanka) that remains after all reasonable efforts to remove the hazards are executed to a specific depth.

Obviously, the reviewed literature does not give absolute numbers for individual and societal risks for humanitarian demining. Therefore we recommend to use the broadly accepted concepts of risk criteria for individual and collective risks summarized in Sects. 17.3 and 17.4.

17.6 Risk Evaluation and Communication

The three steps of the risk management process

- (8) risk assessment
- (9) risk communication
- (10) risk evaluation

are for example treated in the (German) publications Gigerenzer (2007), Hensel (2007) and Gandenberger et al. (2013, pp. 125–136).

17.7 Summary

In this chapter we have seen how different risk concepts and different risk visualization forms can be applied to define and demonstrate risk criteria. In the following it was shown how those methods were applied in different countries and different work sectors to define their risk criteria. As different methods were applied, not all risk criteria are comparable but comparisons were drawn where possible.

In the following we want to show how the methods and presented criteria can be summarized with regard to their applicability to one work field, in this case humanitarian demining.

Risk criteria are a widely used form of trying to find objective ways to decide whether a risk is acceptable. For humanitarian demining however not very many precise information on risk criteria could be found.

The argument of the UN in case of ammunition storage that the workers should not be exposed to bigger risks than workers in manufacturing or industrial processes can also be used for humanitarian demining. Comparing the HSE boundaries, the risks for people most at risks for landslides and the risks for workers in explosives facilities shows that the tolerable individual risk of $10^{-4}/a$ for workers and $10^{-5}/a$ for the general public and the acceptable individual risk of $10^{-6}/a$ are consistent with all three examples and are a good first approach for humanitarian demining.

Another approach is to compare with the annual risk of workers in agriculture, some of which are listed in Table 17.9.

Even a further approach is to compare with historic broadly accepted risks related to demining activities. However, those are difficult to find in the literature, see Sect. 17.5.

Besides the international and national standards for demining which define important risk reducing measures such as safety distances, the risk criteria of all countries involved (where the demining takes place and where the workers are from) should also be regarded. Section 17.4.5 has shown that different countries have different risk criteria and that they are not always consistent.

At last, “it is important to recognize that there is a degree of uncertainty in the analysis of risk, and that the individual and societal risk criteria are only a mathematical expression of the tolerance of society to risk. They are not precise, and should be used only as a general guide” (Dai et al. 2002).

17.8 Questions

- (1) In Fig. 17.7 we have seen that the f-N-curve belonging to an F-N-criterion of the form $F(N) = aN^{-b}$ is not a straight line in double-logarithmic scale and hence not of the form $f(N) = cN^{-d}$. Now we want to confirm this in a computation, especially because the difference between the f-N-curve and a

straight line was not very big and hard to see. In the following we assume that N only takes integer values.

- (a) Write out $F(1)$, $F(2)$, $F(3)$, $F(4)$. From this compute $f(1)$, $f(2)$, and $f(3)$.
- (b) Suppose $f(N) = cN^{-d}$ would hold. Compute c and d with the results from (a)
- (c) Compute $f(3)$ with the formula from (b) and show that is not the same for $b = 0.001$ and $b = 2$.

17.9 Answers

(2) As in the question we show the solution in three steps.

(a) $F(1) = a$, $F(2) = a2^{-b}$, $F(3) = a3^{-b}$ and, $F(4) = a4^{-b}$. With this $f(1) =$

$$F(1) - F(2) = a - a2^{-b}, f(2) = F(2) - F(3) = a2^{-b} - a3^{-b}, f(3) = a3^{-b} - a4^{-b}$$

(b) $c = f(1) = a(1 - 2^{-b})$.

$f(2) = c2^{-d} = a2^{-b} - a3^{-b}$ where the first $=$ is from the formula $f(N) = cN^{-d}$ and the second $=$ is from (a).

Plugging in $c = a(1 - 2^{-b})$ yields $a(1 - 2^{-b})2^{-d} = a(2^{-b} - 3^{-b})$. That is,

$$d = \frac{\log\left(\frac{1-2^{-b}}{2^{-b}-3^{-b}}\right)}{\log 2}.$$

$$(a) \quad f(3) = a(1 - 2^{-b})3^{-\frac{\log\left(\frac{1-2^{-b}}{2^{-b}-3^{-b}}\right)}{\log 2}} = a3^{-b} - a4^{-b}$$

$$\Rightarrow 3^{-\frac{\log\left(\frac{1-2^{-b}}{2^{-b}-3^{-b}}\right)}{\log 2}} = \frac{3^{-b} - 4^{-b}}{1 - 2^{-b}}$$

Plugging in a number for b shows that the two sides are not the same.

References

- Arrow, K. J., Cropper, M. L., Eads, G. C., Hahn, R. W., Lave, L. B., Noll, R. G., et al. (1996). Is there a role for benefit-cost analysis in environmental, health and safety regulations. *Science*, 272, 221–222.
- Australian Geomechanics Society. (2000). Landslide risk management concepts and guideline. *Australian Geomechanics*, 35, 49–92.
- Bach, H. (2004). A study of mechanical application in demining, Geneva International Centre for Humanitarian Demining.
- Ball D. J., & Floyd, P. J. (2001). Societal Risks. Final Report. School of Health, Biological/ Environmental Sciences. Middlesex University, London.
- Bea, R. G. (1990). Reliability criteria for New and Existing Platforms. In *Proceedings of the 22nd Offshore Technology Conference*, pp. 393–408.
- Bosnia and Herzegovina Mine Action Centre. (2004). Standard for mine clearance and EOD operations in Bosnia and Herzegovina.
- Bottelberghs, P. H. (2000). Risk analysis and safety policy developments in the Netherlands. *Journal of Hazardous Materials* 71.
- Bykov, A. A., & Akimov, V. A. (2004). Normative and economic models of risk management. *Issues of Risk Analysis*, 1(2), 125–137.
- Center for Chemical Process Safety. (2009). *Appendix A: Understanding and Using F-N Diagrams. Guidelines for Developing Quantitative Safety Risk Criteria*. NJ, USA.; Wiley, Inc. Hoboken. doi:[10.1002/9780470552940.app1](https://doi.org/10.1002/9780470552940.app1)
- Cornwell, J. B. (2015). Individual risk criteria for the public. Personal Communication.
- Cornwell, J.B., & Meyer, M. M. (1997). Risk acceptance criteria or “how safe is safe enough?”. In *II Risk Control Seminar*, Petróleos de Venezuela, Puerto La Cruz, Venezuela.
- Dai, F. C., Lee, C. F., & Ngai, Y. Y. (2002). Landslide risk assessment and management: an overview. *Engineering Geology*, 64(1), 65–87.
- Ellingwood, B. R. (1999). Probability-based structural design: Prospects for acceptable risk bases. *Application of Statistics and Probability (ICASP 8)*, 1, 11–18.
- Fell, R., Ho, K. K. S., Lacasse, S., & Leroi, E. (2005). State of the art paper 1-A framework for landslide risk assessment and management. In *International Conference on Landslide Risk Management*, Vancouver, Canada.
- Gandnerberger, C., Lüllmann, A., Lüninck, B., Freiherr von, A. P., & Tettenborn, F. (2013). Schlussbericht zum Teilvorhaben: “Sozioökonomische Ansätze zur Bewertung und Kommunikation von Maßnahmen zur Verbesserung der Sicherheit der Wasserversorgung”, Fraunhofer-Institut für System- und Innovationsforschung ISI, http://publica.fraunhofer.de/eprints/urn_nbn_de_0011-n-2777595.pdf
- Geotechnical Engineering Office (1998). Landslides and boulder falls from natural terrain: interim risk guidelines. GEO Report No.75, Geotechnical Engineering Office, The Government of the Hong Kong Special Administrative Region.
- Gigerenzer, G. (2007). Ursachen gefühlter Risiken. Rechtfertigen “gefühlte“ Risiken staatliches Handeln? Festveranstaltung zum 5-jährigen Bestehen des Bundesinstituts für Risikobewertung (BfR), http://www.bfr.bund.de/cm/350/rechtfertigen_gefuehlte_risiken_staatliches_handeln_tagungsband.pdf
- Häring, I., Schönherr, M., & Richter, C. (2009). “Quantitative hazard and risk analysis for fragments of high explosive shells in air.” *Reliability and System Safety Engineering*, 94(9): 1461–1470.
- Health and Safety Executive. (1992). Preliminary report on land use planning controls for major hazard installations in the European community.
- Health and Safety Executive. (2001). Reducing risks, protecting people; HSE’s decision-making process. Technical report. HMSO, Norwich.
- Health and Safety Executive. (2004). Guidance on ‘as low as reasonably practicable’ (ALARP) decision in control of major accident hazards (COMAH), SPC/Permissioning/12.

- Hensel, A. (2007). Wissenschaft in der Gesellschaft - Wissenschaft für die Gesellschaft: Wem kann man heute noch glauben? Rechtfertigen „gefühlt“ Risiken staatliches Handeln? Festveranstaltung zum 5-jährigen Bestehen des Bundesinstituts für Risikobewertung (BfR), http://www.bfr.bund.de/cm/350/rechtfertigen_gefuelt_risiken_staatliches_handeln_tagungsband.pdf
- James, M. L. (1995–1996). Acceptable transport safety, research paper 30. Department of the Parliamentary Library.
- Johansen, I. L. (2010). *Foundations and Fallacies of Risk Acceptance Criteria*. Trondheim: Norwegian University of Science and Technology.
- Jongejan, R. (2008). How safe is safe enough? The government's response to industrial and flood risks. PhD thesis, Technische Universiteit Delft.
- Kafka, P. (1999). *How safe is safe enough? An unresolved issue for all technologies*. Rotterdam: Balkema.
- Kelly, K. E. (1991). The myth of 10–6 as a definition of acceptable risk. In *84th Annual Meeting of the Air & Waste Management Association*, Vancouver, Canada.
- Leitner, B. (2007). *Jahrbuch der Gesundheitsstatistik 2006*. Wien: Statistik Austria.
- Mathiesen, T. C. (1997). Cost benefit analysis of existing bulk carriers. DNV paper series no. 97-P008.
- National Steering Committee for Mine Action. (2010). Sri Lanka national mine action standards (SLNMAS).
- Okstad, E., & Hokstad, P. (2001). Risk assessment and use of risk acceptance criteria for the regulation of dangerous substances. Retrieved Apr 2, 2014, from <http://citeserx.ist.psu.edu/viewdoc/download?doi=10.1.1.195.4993&rep=repl&type=pdf>
- Overmans, R. (1999). Deutsche militärische Verluste im Zweiten Weltkrieg. Beiträge zur Militärgeschichte Band 46, R. Oldenbourg Verlag, München.
- Parfit, M. (1998). Living with natural hazards. *National Geographic*, 194(1), 2–39.
- Paté-Cornell, M. E. (1994). Quantitative safety goals for risk management of industrial facilities. *Structural Safety*, 13, 145–157.
- Proske, D. (2004). *Katalog der Risiken, Risiken und ihre Darstellung*. Dresden: Eigenverlag.
- Proske, D. (2008). *Catalogue of Risks—Natural, Technical, Social and Health Risks*. Berlin, Heidelberg: Springer.
- Randsaeter, A. (2000). Risk assessment in the offshore industry. Promotion of technical harmonization on risk-based decision-making, Stresa, Italy.
- Sandin, P. (2005). Naturalness and de minimis risk. *Environmental Ethics*, 27(2), 191–200.
- Schäfer, J., & Rathjen, S. (2014). Risk acceptance criteria, deliverable D6.5 for the D-BOX project (which has received funding from the European union's seventh framework programme for research, technological development and demonstration under grant agreement no 284996).
- Skjøng, R., Vanem, E., & Endresen, O. (2005). Risk evaluation criteria, SAFEDOR report D.4.5.2.
- Smith, A. (2005). Why military demining is not humanitarian demining. Retrieved Apr 24, 2014, from <http://www.nolandmines.com/militarydemining.htm>
- STANDARD 321-07. (2007). Common risk criteria standard for national test ranges: Supplement. White sands missile range, range safety group, risk committee, range commander council.
- Statistisches Bundesamt Deutschland. (2007). Todesursachen in Deutschland 2006, Gestorbene in Deutschland an ausgewählten Todesursachen, Fachserie 12 Reihe 4. Wiesbaden.
- Stern (1999). Eiskalte Rechnung.
- Trbojevic, V. M. (2005). Risk criteria in EU. In K. Kolowrocki (Ed.), *European Safety and Reliability Conference (ESREL 2005)*. Tri City, Poland, CRC Press, Taylor and Francis UK.
- Turkish Ministry of National Defence. (2012). Syrian border mine clearance standards (SBMCS).
- UN OAD. (2012). International ammunition technical guideline. Introduction to risk management principles and processes.
- United Nations Mine Action Service (2013). International Mine Action Standards (IMAS).
- van Breugel, K. (2001). Establishing performance criteria for concrete protective structures. In *fib-Symposium: Concrete & Environment*. Berlin, Germany.
- Vanem, E., Antao, P., Ostvik, I., & Del Castillo de Comas, F. (2008). Analysing the risk of LNG carrier operations. *Reliability Engineering and System Safety*, 93:9, 1328–1344.

Chapter 18

Risk Mitigation and Chance Enhancement

Measures for Improving Resilience

18.1 Overview

This chapter gives an overview of a range of possible mitigation and counter measures to reduce risks, mainly for malicious explosive events. Some of the measures are also relevant for natural hazards (e.g. earthquake, hail impact, wind effects, flooding), accidental events (e.g. dust explosion, chemical accidents, dispersion of dangerous substances) and other malicious events (e.g. CBRN events).

Mitigation measures discussed include organizational measures mainly focusing on access control measures, building design and topology, physical barriers at different positions, secondary facades as a holistic innovative potential approach and various reinforcement measures.

This chapter emphasizes the need to assess the countermeasures and to repeat the risk analysis and management process, in case counter measures are applied. Two schemes are presented for a quick assessment of risks in given contexts before implementation. In addition, for an urban security improvement application example, the reassessment of existing risks and the identification of secondary risks is given. In general, one has to repeat all risk management steps in case mitigation or improvement measures have been implemented.

Risk mitigation measures contribute to improve prevention, protection, response and recovery resilience management phases. They are typically implemented in the prevention phase.

Risk mitigation measures can also be implemented in any other resilience management phase. In the latter cases, they require as well pre-event or (fast) post-event planning. In particular it is interesting to ask for which resilience capabilities and resilience management layers are necessary to implement risk mitigation measures on demand, even more when asking for soft or even hard real time mitigation resilience response.

When the result of the risk analysis is that the risk should be reduced, risk mitigation measures are necessary. As the methods of risk analysis and

management can be applied to many different situations, mitigation measures can be very different. In this chapter we focus on mitigation measures for risks resulting from explosive hazards but also give other examples.

The mitigation measures presented here for explosive risks can be divided into four categories:

- Organizational measures
- Building design
- Barriers
- Secondary facades
- Structural reinforcement systems

The measures can be taken as retrofit measures or be implemented for new designs.

Some of this classifications can also be used for other contexts, for example floods. In general, other measures are often also feasible, for example new technical systems that maintain the safety of a system or facility thus reducing the event frequency. Other systems might reduce the consequences of hazardous events.

The Sects. 18.2–18.6 regard the three types of mitigation measures listed above. Sections 18.7 and 18.8 discuss the reasons for the choice of a certain mitigation measure. Mitigation measures might cause new risks, so called secondary risks. These risks are regarded in an example in Sect. 18.9.

The chapter presents extracts of Schäfer (2014). Schäfer (2014) himself bases his work on Mayrhofer (2010), Stolz (2012).

Further references include FEMA (2003a, b, c), Unified Facilities Criteria (UFC 2003), Lohn (2005), Fischer and Stolz (2011).

This section only gives an overview of physical protection measures, which are dealt in much more detail in the courses Structural Protection.

The main sources of the chapter are Stolz (2012), Schäfer (2014). Further EMI sources are Fischer and Stolz (2011), Brenneis and Millon (2012), Baumann et al. (2014), Finger (2014), Siebold et al. (2015). The main authors of the EMI sources are J. Schäfer, Chr. Mayrhofer (supplemented with work by C. Brand, B. Brombacher, A. Dörr, J. Frick, S. Sutter and M. Voss) and A. Stolz. It is further supplemented with work by D. Baumann, U. Siebold, S. Hasenstein, J. Finger and K. Fischer.

18.2 Organizational Mitigation Measures

Examples for organizational mitigation measures are:

- surveillance (e.g. cameras),
- control (e.g. admission control),
- emergency plans and
- standoff distance implemented by organizational means.

18.3 Building Design

Schäfer (2014) discusses organizational measures for IEDs. His argumentation also holds for other explosive hazards.

“The increase of the standoff distance is probably the most efficient and effective mitigation measure. It is typically applied to protect buildings against the effects of vehicle-born IEDs. By decreasing the mobility, vehicles carrying IEDs are prevented from approaching vulnerable buildings within a certain distance. To achieve this, metal or reinforced concrete barriers such as bollards and Jersey barriers or safety fences can be used. However, the increase of standoff distances is often difficult or impossible, especially in urban environments” (Schäfer 2014)

One can see that one often does not choose between organizational measures or barriers but uses a combination of both.

The design of a building comprises decisions on geometry and materials used. For example, in case of an explosion in the streets, a building is safer when most windows are directed towards the back of the house. Against the risk of burglary, windows in the upper floors are safer than on the bottom floor.

Fig. 18.1 shows some examples how to implement the principle security-by-design in case of buildings and structures. “The consideration of the

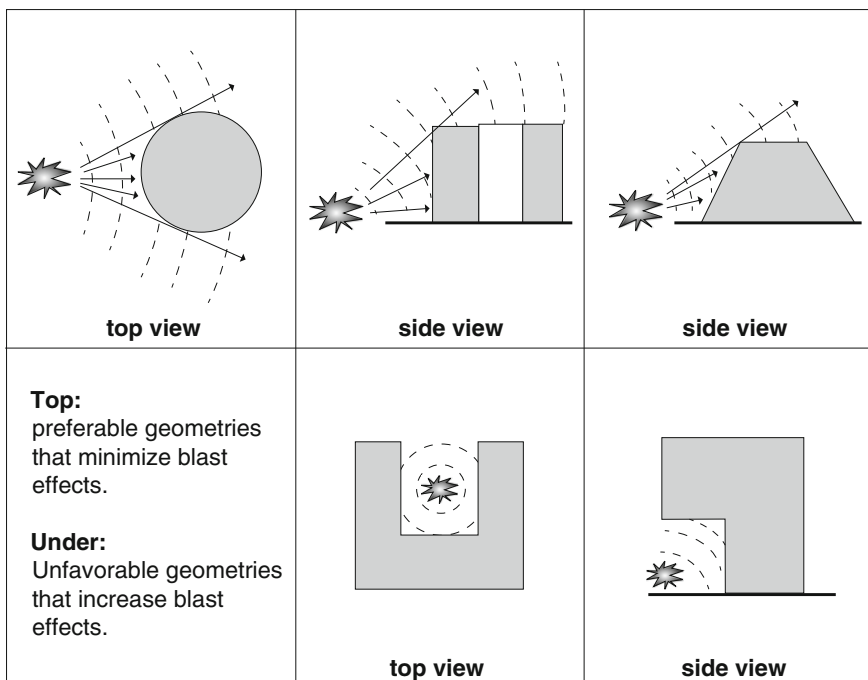


Fig. 18.1 Advantageous (upper row) and disadvantageous (lower row) building shapes in the case of an explosion (Mayrhofer 2010)

following guidelines in the design of new buildings can improve their resistance to blast waves considerably and reduce the damage in case of an explosion. Regarding the shape of buildings, internal corners should be avoided which reflect blast waves and ‘store’ the blast energy (see Fig. 18.1). [Such geometries prevent the “venting effects” present in urban areas.] A purposeful arrangement of windows which minimises the number of windows facing the street can also mitigate the damage. Furthermore, the use of redundant static systems can prevent the progressive collapse of buildings” ([Schäfer 2014](#))

18.4 Barriers (Far-Out and Close-In)

When a hazard is known and the original building and organizational measures are not enough, different forms of barriers can be used to create a distance of the building and its surrounding. Examples are:

- barriers,
- fences,
- bollards,
- protective walls,
- standoff distance implemented by physical means (barriers).

An example is the embassy area in Berlin. After 09/11, many roads in front of the embassies were closed by barriers. Police men supervised the barriers.

[Schäfer \(2014\)](#) summarizes the use of barriers for the risk of attacks with IEDs which again can be generalized for risks resulting from explosions:

“A barrier provides a spatial separation of a suspected IED from the environment. It is placed between the IED and people or objects to be protected such as buildings and infrastructure. Barriers mitigate the threat of an IED by reducing the physical effects of an explosion through absorption or redirection. Typically but not exclusively, they reduce the peak overpressure and impulse of a blast wave and decelerate or retain flying fragments.

Barriers can be employed in the near field of the suspected IED as well as in the far field to vulnerable objects to be protected. In the near field, barriers are used for a total or a partial containment of a suspected IED. In case of a partial containment, they usually have an opening at the top for a vertical redirection of the blast wave. In the far field, barriers are applied as temporary or permanent protective structures. They are either placed close to or directly mounted on vulnerable objects to be protected” ([Schäfer 2014](#)).

“Barriers can be made of many natural or synthetic materials. Widely spread and easily available natural materials which are commonly used to mitigate the physical effects of explosions are listed below.

- Water is used for example in commercial waterwall products or in containers such as flexitanks or intermediate bulk containers.
- Sand or earth are used for example in containers such as flexible intermediate bulk containers (big bags) or in the form of embankments.
- Straw is used for example in the form of bales” (Schäfer 2014).

The following commercial techniques and research topics are examples for barriers (Schäfer 2014):

- Waterwall blast suppression systems,
- Mobile protective wall.

18.5 Secondary Facades: Multifunctional Hulls

Secondary facades protect a building from the outside but are non-bearing and do not strengthen the structure of the building. They are typically not intended for structural reinforcement of the object. Their purpose is to mitigate the blast impact loading.

“Flexible secondary facades can consist of different elements and materials. Examples include wire meshes, ropes, chains, membranes and woven structures made of metal, plastic or fabric. Combinations of several elements are also possible. Materials, size, geometry and weight of secondary facades are adapted to the size of the building to be protected an the anticipated threat level.

Due to the flexible construction, energy and impulse can be transferred from the blast wave to the secondary facade through friction. The secondary facade reacts on this effect with a clearly visible temporary displacement as illustrated in Fig. 18.2. In this manner, energy of the blast wave is dissipated and the peak overpressure and the impulse are considerably reduced behind the protective structure. In addition, fragments are decelerated or retained. Consequently, the combined loading on the



Fig. 18.2 Example of a barrier (Stolz 2012)

building—resulting from the blast and fragment effects of an explosion—is reduced” (Schäfer 2014).

“At Fraunhofer EMI, the protective effect of a flexible secondary facade against the blast wave of an explosion of 100 kg TNT at 34 m standoff was investigated in full-scale shock tube experiments. Using a construction made of a membrane, a wire mesh and ropes, the peak overpressure und impulse of the simulated blast wave was reduced to a 1/3 and a 1/10, respectively, at a distance of 3 m behind the protective structure, which showed a very ductile behaviour. This means that such a flexible secondary facade suspended 3 m in front of a building can reduce the loading of a blast wave on the building by 67 % and 90 % in terms of overpressure and impulse, respectively.” Schäfer (2014), based on Stolz (2012).

18.6 Structural Reinforcement Systems

A way to protect buildings against explosions from the inside and outside is reinforcement.

In the case of earth quakes, brick walls are endangered. They can be protected by a bracing with reinforced concrete (Bundesamt für Umwelt 2006).

Reinforcement is also a good method to reduce damage in case of an explosion:

“Reinforcement systems mitigate the damage on existing structures caused by an explosion by increasing the resistance of the structures to the physical effects of the explosion. The protective effect of the reinforcement is regardless on which side of the structure the explosion occurs. [However, it can be different effective.]

This category comprises all technologies which are designed and suitable for

- a temporary or a permanent reinforcement, and
- new building designs or retrofit applications.

A typical example is the reinforcement of walls, roofs and windows.

However, also less common applications—such as the freezing of the ground soil using for example liquid nitrogen to increase the soil stability, reduce the cating and prevent the collapse of nearby buildings [in case of e.g. explosive disposal activities]—fall into this category” (Schäfer 2014).

Another possibility are structural measures which are added to a building, for example curtain-wall facings.

Other structural measures are for example

- Reinforced/retrofitted masonry,
- safety glass,

Structural measures are one of the main topics in the course Structural Security (Fig. 18.3).

Fig. 18.3 Example for a structural damping mitigation measure (Brenneis and Millon 2012)



18.7 What Do the Mitigation Measures Reduce?

We have seen different types of mitigation measures. Generally, mitigation measures are supposed to reduce risk. This can mean that they reduce the frequency of an undesired event, that they reduce the damage or both. We give examples in Table 18.1.

The classification is not always precise for these very short examples. It should be understood as an illustration for the different effects of mitigation measures. For example, a tsunami warning system does not reduce the frequency of a tsunami. It does however reduce the frequency of a person being exposed to a tsunami. Hence,

Table 18.1 Exemplary categorization of mitigation measures (Fischer and Stolz 2011)

Measure	Against which risk	Reduces frequency	Reduces damage
Surveillance (camera)	burglary	X If camera is not hidden (deterrent)	X If burglar gets caught because of the video
Emergency plan	Person injured by fire		X
Barriers in form of bollards in the street	Dangerous person/object placed in front of building	X	
Tsunami warning system	Injuries and financial damage by tsunami	X Frequency of exposure of personnel	X
Reinforcement of brick wall	Earthquake		X
Weather forecast	Being in the woods during thunder and lightning	X	

whether it reduces only the damage or also the frequency depends on whether one regards the exposure in the calculation of the average damage or the frequency.

18.8 Decisive Factors

At the end of a risk management process, appropriate mitigation measures (counter measures) are chosen. But which measures are appropriate?

In Baumann et al. (2014) and Siebold et al. (2015) a quick ad hoc generic assessment of counter measures as proposed by Stadt (2013) of is presented within a generic risk assessment process, see Fig. 18.4.

For instance, persons typically do not like to feel supervised and hence often do not approve mitigation measures such as surveillance cameras or police men in the streets. On the other hand, they want to live in a safe urban space. This is an example where informed decision making involving all stakeholders has to be practiced taking account of all constraints is necessary. Sample constraints include, political, social, legal, ethical, psychological and religious. They should have been identified in the context risk management phase, see Chaps. 2 and 5.

In particular legal regulations also have to be considered when installing mitigation measures. For example, a private household in Germany does not have the right to install surveillance cameras that show the sidewalk or the street (MBW-Electronic 2014).

It is also important to analyze whether the planned mitigation deliver the intended risk reduction. This assessment is obtained by repeating the risk management process with the mitigation measures in place.

Fig. 18.4 Evaluation of risk mitigation measures (Siebold et al. 2015)

Evaluate measure:		
Impact:	high	▼
Feasibility:	medium	▼
Readiness:	high	▼
Duration of effect:	medium	▼
Acceptance:	medium	▼
Cost:	high	▼
Evaluation result:	OK	
	OK	

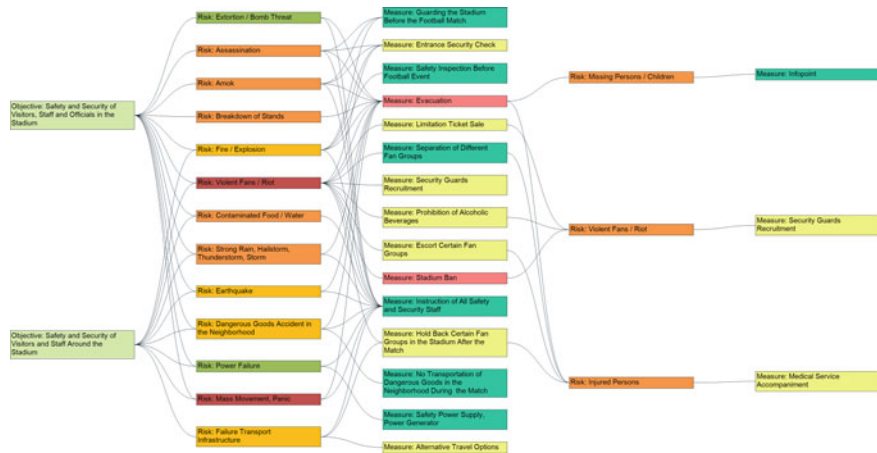


Fig. 18.5 Overview of overall risk management as generated by the tool IDAS: objectives, risks (including their color-coded evaluation), measures (including their color coded assessment), secondary risks and measures (Siebold et al. 2015). With permission from Taylor and Francis

18.9 Secondary Risks

The execution of mitigation measures changes the situation. Hence, the results of the preceding risk analysis have to be reconsidered. In particular, it must be assessed, whether the intended risk reduction occurs.

In addition, secondary risks may arise. We give an example from a research project BESECURE (2014). In the project risks in urban areas are regarded. One risk are glass fragments on a popular public square at weekends. A mitigation measure is to ban alcohol from this place. Then one of the secondary risks is that the people drink in several other places throughout the city, see Fig. 18.5. This is an example of relocation of risks.

18.10 Summary and Outlook

In this chapter we have seen different forms of mitigation measures. Examples are organizational measures such as emergency plans, a change in the city law or surveillance, barriers to separate areas or as physical protection against hazards, secondary facades to protect buildings against blast from the outside, and reinforcement of buildings to strengthen the structure against explosions inside and outside the building.

When deciding upon a mitigation measure, several questions arise such as

- Does it minimize the intended parameters?
- Does it reduce the risk significantly?

- Is it socially acceptable?
- Is it legal to install?
- Is it manageable to install?
- Do the benefits legitimate the costs?

After a mitigation measure is chosen, it has to be checked for secondary risks and the original risk analysis must be reconsidered, as indicated by the circular risk management scheme in Fig. 1.11 of Chap. 1.

References

- Baumann, D., Häring, I., Siebold, U., & Finger, J. (2014). A web application for urban security enhancement. In K. Thoma, I. Häring & T. Leismann (Eds.), *9th Future Security Research Conference 2014*. Berlin, Germany.
- BESECURE. (2014). Besecure - best practice enhancers for security in urban regions. Retrieved Oct 09, 2014, from <http://www.besecure-project.eu/>
- Brenneis, C., & Millon, O. (2012). Entwicklung eines Verfahrens zum Herstellen von Polymerbeton aus nachwachsenden Rohstoffen. Fraunhofer EMI Bericht E 31/12.
- Bundesamt für Umwelt. (2006). Erbebsicheres Bauen in der Schweiz. Retrieved Oct 14, 2014, from <http://www.news.admin.ch/NSBSubscriber/message/attachments/3683.pdf>
- FEMA (2003a). US federal emergency management agency. Primer for design of commercial buildings to mitigate terrorist attacks.
- FEMA (2003b). Primer for design safe school projects in case of terrorist attacks.
- FEMA (2003c). Reference manual to mitigate potential terrorist attacks against buildings.
- Finger, J. (2014). Screenshot of the software IDAS (Besecure).
- Fischer, K., & Stolz, A. (2011). Verbundprojekt SKRIBT - Schutz kritischer Brücken und Tunnel im Zuge von Straßen. F. EMI. E 61/11.
- Lohn, T. (2005). *Ballistic Protection*. Diplom, Universität Stuttgart.
- Mayrhofer, C. (2010). Städtebauliche Gefährdungsanalyse - Abschlussbericht Fraunhofer Institut für Kurzzeitdynamik, Ernst-Mach-Institut, EMI, Bundesamt für Bevölkerungsschutz und Katastrophenhilfe, http://www.emi.fraunhofer.de/fileadmin/media/emi/geschaeftsfelder/Sicherheit/Downloads/FiB_7_Webdatei_101011.pdf
- MBW-Electronic. (2014). Videoüberwachung - Legalität und Datenschutz. Retrieved Oct 09, 2014, from <http://www.mbw-electronic-online.de/Videoueberwachung-Legalitaet-und-Datenschutz>
- Schäfer, J. (2014). Classification of mitigation measures. S. Rathjen, Personal Communication.
- Siebold, U., Hasenstein, S., Finger, J., & Häring, I. (2015). Table-top urban risk and resilience management for football events. In *European Safety and Reliability Conference ESREL 2015*. Zürich, Switzerland. pp. 3375–3382.
- Stadt, L. (2013). Sicherheitsbericht Stadt Luzern 2013. Retrieved Aug 21, 2015, from http://www.stadtluzern.ch/dl.php/de/523c180e2d6b7/2013-07-22_Sicherheitsbericht_Stadt_Luzern_2013.pdf
- Stolz, A. (2012). Sonderlösungen - Brücken, Tunnel, integrierte Sensorik. Carl-Cranz-Gesellschaft, Presentation.
- Unified Facilities Criteria (UFC). (2003). DoD minimum antiterrorism standards for buildings. UFC 4-010-01.

Index

A

- Abbreviated Injury Scale, 201. *See also* Normal distribution
Absolute annual frequency, 91, 261
Absolute scale, 27
Absorption, 282, 295–297, 346
Acceptable, 15, 21, 63, 76, 79, 81, 102, 262, 278, 279, 306, 313–316, 319, 320, 323, 328, 330, 332, 336, 337, 339, 352. *See also* LIRA
Accident data, 320, 321. *See also* F-N curve
Accidental explosions, 118–120, 133. *See also* Explosion
Accumulation, 304, 313
Ad hoc risk analysis, 20, 271
Adamsit, 284
Administration, 102
Admission control, 344
Airbag, 119, 124
Airline, 54, 57, 104, 279, 316. *See also* Protective structure
Airplane, 279, 316, 331 *See also* Protective structure
Airplane accidents, 215. *See also* Storm
Airport security, 1, 4, 92, 94
AIS, 201. *See also* Abbreviated Injury Scale
AIS level, 201 *See also* Abbreviated Injury Scale
Al Qaida, 285
Alarm level, 248
ALARP, 313, 315, 319, 328, 329, 334–336. *See also* As low as reasonable practicable
ALARP-area, 315. *See also* Fatal accident rate
Alpha-radiation, 297, 303
American Institute of Chemical Engineers, 238
Analytical approach, 215, 257
Analytical-empirical methods, 5, 137, 155, 257, 258, 261, 291, 296, 298
ANFO, 159, 291
Angular sector, 147. *See also* Fragment
Annual accident rate, 102. *See also* Fatal Accident Rate
Annual attack rate on airports, 95
Annual local risk, 332. *See also* F-N curve
Annual local risk of terror events. *See* Collective
Annual probability of exposure of a dangerous dose, 333. *See also* Annual local risk
Annual risk. *See* Collective
Annual risk of death for industry sectors, 327. *See also* F-N curve
Annual risk of injury, 13, 327. *See also* F-N curve
Annual risk per million, 327. *See also* F-N curve
Applicability, 236, 339
Application of analysis methods, 27
Applied research, 2
Area density, 216, 217
Arithmetic mean, 88, 31
Arson, 98. *See also* IED
As low as reasonable practicable, 313
Asymptotic limiting cases, 130. *See also* Side-on pressure
Asymptotic loading types, 116. *See also* Explosion
ATM, 278
Atmospheric ambient conditions, 129. *See also* Side-on pressure
Atmospheric explosion, 117. *See also* Explosion
Attack event, 98, 258
Attack locations at European airports, 97
Attack tree, 233, 237
Attack type distribution, 96
AURIS, 97, 98
Australia, 328, 336, 337
Autocorrelation, 61, 67

- Autocorrelation coefficient, 31, 68
 Autocorrelation function, 31, 32, 61, 68, 75, 84
 Autocovariance, 31, 71
 Availability, 34, 110
 Average full time job, 317. *See also* FAR
 Average life expectancy with the considered risk, 315, 318. *See also* FAR
 Average maximum velocity of fragments, 143. *See also* Presented surface
 Average number of persons at an object, 247
 Average number of persons in the scenario, 243
 Average number of persons of given type at given object type, 247
 Average worldwide individual risk due to terror attacks on tunnels, 274. *See also* Terrorist Event Database
 Averaging, 201, 216, 306
 Aviation, 3, 92, 109
- B**
- Background/context analysis, 21
 Back side, 162, 164
 Backward data analysis, 29, 30
 Baker, 115, 117–120, 123, 124, 126–131, 168, 199
 Ball, 115, 120, 141, 150, 225, 282, 296, 310, 320, 321
 Bank, 26, 46, 50, 98, 100, 104
 Barrier, 21, 52, 138, 147, 234, 248, 268, 343–347, 349, 351. *See also* Fragment
 Base rate, 233
 Basic event rate, 233, 234
 Basic statistical approaches, 27
 Benchmark, 2, 187
 Berlin, 6, 105, 106, 346
 Beta-radiation, 282, 297, 303, 304
 Binary choice approach, 188, 192, 213
 Binning, 257
 Biological effect, 198, 303
 Biological hazard source, 115, 281, 287
 Black powder, 291
 Blaise Pascal, 11, 12, 317
 Blasting, 118, 119
 Blast propagation, 116, 122, 155, 187
 Blast wall, 127, 200, 248, 347
 Blast wind, 115, 290
 BLEVE, 118
 BMBF, 3, 4, 94
 Body, 13, 27, 61, 93, 141, 143–145, 151, 198, 199, 201, 296, 297, 302–305
 Bolland, 345, 346, 349
 Boltzmann constant, 296
- Bomb, 15, 33, 36, 96, 97, 99, 112, 115, 120–122, 138, 139, 142, 146, 147, 149–152, 198, 275, 276, 281, 283–285, 287, 310. *See also* IED
 Bootstrap example, 249
 Boston, 133, 331
 Bounce and roll, 122
 Bremsstrahlung, 304
 Brickwork, 298
 Bridge, 4, 93, 94, 98, 100, 111, 112, 235, 272–274, 279, 280
 Broadly acceptable, 25, 319, 326, 334, 336
 Building bomb, 120, 138
 Building cost estimate, 108
 Building design, 343–345, 348
 Build-up of blast wave, 125
 Bulk scanning, 281
 Bulmash, 156–158
 Burning material, 198
 Burst, 126, 150
- C**
- Calibration of risk graph, 263, 267
 Californium-252, 305
 Camouflage, 286
 Canada, 290, 332, 333
 Cancer, 304, 331, 332
 Car bomb, 97, 99, 112, 115, 120–122. *See also* IED
 Car bomb fragments, 142. *See also* Fragment
 Cardan angles, 167, 179, 180
 Cartesian coordinate system, 139, 140.
See also Coordinate system
 Case study, 2, 209
 Catastrophic event, 98
 Categorization of explosions, 115. *See also* Explosion
 Categorization of mitigation measures, 349
 Cauchy Theorem, 141, 143
 Cavity, 139
 CBRN, 4, 343
 CBRNE, 4
 Centralized standardized normal distribution, 193. *See also* Normal distribution
 Cesium-137, 306
 Characteristic dimension, 128. *See also* characteristic length scale
 Characterization of explosions, 117, 119, 124, 133
 Chemical accidents, 343
 Chemical energy release, 117. *See also* Explosion
 Chemical hazard source, 115

- Chemical industry, 119
 Chemical properties of the hazard source, 93
 Chi-squared test, 205
 Chlorates, 291
 Citizen, 2, 3
 City, 50, 55, 101, 103–106, 108, 163, 237, 253, 260, 317, 351
 Civil, 3, 4, 7, 102, 103, 109, 111
 Club, 36, 102
 Clustering, 27, 34, 35, 102
 Collatz, 146
 Collective, 1, 2, 13, 63, 216, 234, 245, 247, 249, 251–255, 263, 269, 271, 272, 274, 276, 279, 280, 282, 283, 308–310, 313–315, 317, 328, 338
 Collective local risk, 2, 247
 Collective risk criteria, 63, 263, 276, 308, 314
 Collective total risk, 2, 13
 Collision, 98, 215, 304
 Combination of methods, 282
 Combined blast and fragment damage effects, 256
 Combustible dusts, 119
 Combustion, 11, 118, 124, 198
 Complete safety, 337
 Completeness, 199, 236, 287
 Complex blast engineering scaling factors, 162
 Complex blast propagation, 116, 187
 Composition, 3, 159
 Computer algebra, 194
 Computer center, 98
 Concentration distribution, 216
 Concrete frame construction, 298, 300
 Conditional probability, 234, 256
 Conditional risk, 13
 Confined explosion, 120
 Confinement, 118, 127, 128, 160
 Consequence, 2, 3, 9–12, 15, 16, 20, 21, 24, 26, 27, 50, 52, 53, 64, 76, 92, 94, 101, 107, 116, 120, 122, 123, 134, 189, 198, 199, 209, 234, 235, 248, 249, 252, 253, 257–260, 262–264
 Consequence risk parameter, 262, 265, 267
 Construction, 98, 298–300, 320, 327, 331, 347, 348
 Contained explosion, 118, 120
 Container, 4, 146, 147, 275, 281–284, 286, 287, 292–296, 300, 307, 347
 Container explosion, 281, 293, 295, 296
 Container security, 4, 283
 Context, 1, 3, 13, 15, 21, 22, 28, 40, 42, 61, 92, 93, 94, 111, 117, 179, 234–237, 275, 281, 282, 286, 313–315, 331, 343, 344, 350
 Context analysis, 15
 Continental distribution of historic airport attacks, 95
 Continuous mode, 268
 Continuous risk, 13
 Continuum-mechanical, 137, 293
 Controlled explosions, 117, 120. *See also* Explosion
 Control system, 266, 268, 269
 Convex Hull, 138, 141, 143
 Conway, 283, 292–296
 Coordinate system, 64, 66, 76, 133, 137, 138–141, 167, 179, 217, 218, 225, 239, 324
 COPRA, 109
 Coriolis force, 138
 Correlation, 61, 65, 66, 75
 Correlation map, 61
 Correlogram, 32, 68, 71, 79, 80, 81, 84, 85
 Cost of rebuilding, 62
 Country-specific resolution of events, 104
 Crater formation, 120, 151, 287. *See also* Cratering
 Cratering, 119. *See also* Crater formation
 Credible hazard event, 92, 93
 Credit card fraud, 235, 271, 272, 278
 Crisis, 264
 Crisis management, 264. *See also* International Electrotechnical Commission
 Critical energy, 200, 230, 231
 Critical risk, 12, 92, 272
 Critical value, 21, 52, 188, 192, 200, 252, 282, 313
 Crossing, 160, 161
 Cross section, 141, 145, 221. *See also* Presented surface
 Culture, 102
 Cumulated number diagram, 294
 Cumulative risk, 260
 Cumulative frequency of experiencing N or more fatalities, 62, 320.
See also F-N curve
 Cumulative probability distribution, 167, 191
 Cycle detection, 61

D

- DALY, 318. *See also* disability adjusted life-years
 Damage, 1–4, 9, 11, 15, 18, 20, 28, 30, 36, 38, 39, 50, 52, 93, 98, 101, 107–109, 116, 120, 123, 130, 134, 138, 139, 149, 155, 157, 159, 167, 168, 170, 187–192, 196–200, 202, 205, 209, 212–216, 231, 234, 234, 245, 248, 251–257, 259, 261, 262, 265, 267, 271, 275, 278, 281–286, 291, 297–310, 317, 346, 348–350

- Damage analysis, 9, 16, 20, 24, 97, 109, 111, 165, 167, 180, 188–191, 198–200, 248, 276, 278, 282, 283, 298, 306, 310
 Damage category, 255, 256
 Damage class, 298, 299, 300
 Damage criterion, 168, 278, 279
 Damage Decreases with increasing argument, 188
 Damage Increases with increasing argument, 188
 Database, 20, 41, 235, 284
 Data acquisition, 30, 33, 34
 Database analysis, 25, 28–30, 32, 42, 46, 51–53, 61, 62, 94, 95, 98, 99, 102, 272, 275, 276, 283, 284, 307
 Database analysis scheme, 28, 30, 62
 Database design, 36
 Database-driven, 28, 233, 281
 Database notation, 40, 41, 54, 56, 57
 Data-driven risk quantity, 27
 Data collection, 20
 Data-gathering, 27, 33, 34
 Data management, 5, 27, 62
 Data preparation, 43, 75
 Data selection, 27, 42, 75
 Data spotting, 34
 D-BOX, 4
 Dead-end street, 160
 Deafness, 318
 Debris, 11, 115, 120, 121, 122, 137, 138, 146, 150, 151, 215, 216, 282, 287, 288, 292, 293, 301, 310, 331. *See also* Fragment
 Debris throw, 146, 147, 150, 282, 292.
See also Fragment
 Decision maker, 20, 283, 310
 Decision making, 3, 252, 281, 283, 314, 350
 Decision process, 15, 35, 279
 Defense, 3, 141
 Definition of explosion, 123. *See also* Explosion
 Deflagration, 118, 123
 Degree, 80, 124, 139, 140, 282, 301, 302, 318, 319, 320, 339
 Demand rate, 267, 268
 Demining, 338, 341. *See also* IMAS
 Demolition of buildings, 119
 Density function, 167–172, 182
 Density of air, 145
 Department of transportation, 236
 Dependencies of risk management steps, 10, 23–25
 Derived scenarios, 97, 274, 287
 Dermal burn, 296
 Detection, 116, 147, 281, 283, 286, 311
 Determination of parameters of distributions, 205
 Detonation, 116, 124
 Detonation products, 11, 122, 126, 127, 288
 1D expansion, 160
 Diagram, 27, 32, 63, 66, 68, 71, 76, 79, 80, 82, 85, 107, 239, 294, 320, 322–324. *See also* Visualization
 Differential equation, 131, 145, 152
 Dimensionless, 102, 129, 134, 145, 291, 317.
See also Scaling laws
 Direct damage assessment, 187, 189
 Dirty bomb, 281, 287
 Disability adjusted life-years, 318. *See also* DALY
 Discrete damage model, 216
 Discrete grid integration method, 228
 Discrete object distribution, 235, 239, 248
 Discrete object locations, 233
 Discrete occupation number, 234
 Dispersion, 20, 52, 115, 116, 137, 261, 282, 343
 Dispersion of dangerous substances, 343
 Dispersion of material, 137. *See also* Fragment distribution
 Disruptive, 3, 155, 188, 264
 Distance, 15, 85, 124, 128–130, 139, 148, 156, 158–160, 162, 163, 168, 170, 180, 188–191, 196, 197, 199, 210, 220, 225, 239, 241, 253, 263, 282, 288, 290, 291, 295, 296, 298, 299, 301, 302, 306, 333, 338, 339, 344–346, 348
 Distribution of attacks, 95, 98, 102
 Distribution type determination, 205
 3D line, 257
 Dose equivalent, 282, 305
 DOT, 236. *See also* Department of Transportation
 Double integral, 226
 3D plane equation, 167
 Drag coefficient, 145, 146
 Drag force, 145
 Drilling, 119
 Drone, 121, 152, 215
 Drone accidents, 215
 3D rotation, 167
 Duration of overpressure phase, 128
 Dust explosion, 343
 3D visualization options for quantitative risk analyses, 260
 Dynamite, 291

E

- Ear, 199
Eardrum injury, 301
Earthquake, 56, 98, 100, 115, 137, 331, 343, 349
Earth's surface, 11, 127, 137
ECSIT, 4, 283
EDEN, 4
Education, 3, 4, 6, 94, 102
E/E/PE safety-related system, 265
Eigen period of structure, 132, 133
Electro-magnetic radiation, 304
Emergency plan, 344
Emissivity, 296
Empirical, 187
Empirically parametrized analytical expressions, 155
Empirical risk quantity, 278
Empirical-statistical analysis, 91
Empirical-statistical damage models, 215
ENCOUNTER, 4
End user, 20
Energy, 11, 98, 99, 117, 118, 123, 124, 127, 130, 131, 150, 200, 216, 230
Energy density, 124
Energy distribution in case of an explosion, 127
Energy release, 124
Engineering approach, 91
Engineering risk assessment, 3. *See also* Security research
England, 63
Environment, 4, 14, 20, 120, 160, 163, 265, 267, 282, 337, 341, 345, 346
Equator, 139. *See also* Coordinate system
Error estimation for parameters, 205
Ersatz model, 130–132, 232
Estimator, 211
Ethical group, 106
Euler angles, 167, 179. *See also* Coordinate transformation
Europe, 41, 50, 95, 96, 104–106, 108, 112, 331, 336, 337
European security research, 1
Event, 233, 234, 235, 236, 237, 243, 247, 248, 249, 251, 252, 254, 255, 257–270
Event attribute, 27
Event avoidance frequency analysis, 21
Event frequency, 233
Event frequency analysis, 20
Event prevention rate, 233
Event probability, 233
Events per quarter, 273
Event type analysis, 27
Event type ratio analysis, 91
Expectation, 171
Expectation value, 167
Expert assessment, 92. *See also* Expert estimate
Expert estimate, 212, 281. *See also* Expert assessment
Expert round, 251
Explosion, 93, 281, 285, 287, 289, 290–310
Explosive forming, 118
Explosively formed or shaped IED, 120
Explosive mass, 189
Explosive material, 117, 120, 123, 147, 282, 288
Explosive sources, 18, 118, 120, 127, 129, 336
Explosive storage, 13, 314
Explosive welding, 118
Exponential loading, 130, 131
Exposed, 19, 21, 52, 101, 301, 308, 317, 339, 349
Exposed object, 216, 248, 255
Exposed site, 19, 255
Ex-post risk analysis, 20
Exposure, 9, 10, 15, 21, 52, 102, 217, 233, 234, 239, 241, 244, 246, 248, 251, 255, 263, 265, 267, 272, 302, 313, 315, 317, 330, 333, 349, 350
Ex-post risk analysis, 20
Extensive risk quantity, 27
Extreme snow loading, 98

F

- Failure rate, 233, 236, 237
FAR, 101, 102, 315–319, 332. *See also* Fatal accident rate
FAR, 101, 102, 315, 317, 318, 332
Far-field, 116, 120, 125, 126, 134, 282, 346
FAR for living in a house, 318
FAR for motorbike driving, 318
Fast methods to determine and assess risks, 269
Fatal accident rate, 101, 102, 314, 315, 317–319, 332. *See also* FAR
Fatality, 101, 102, 152, 262, 264, 318, 331, 336
Fatality rate, 102, 331
Fault tree analysis, 233, 237, 238, 249
Fence, 338, 345, 346
FEMA, 344, 352
Finance, 98, 99, 102, 104
Financial damage, 93, 308, 349
Fire, 98, 100, 115, 120, 121, 198, 267, 282, 287, 296, 301, 310, 331, 332, 349
Firearm, 96, 99, 284–286

- Fire ball, 115, 120, 121, 282, 287, 288, 296, 310
 Fischer, 6, 92, 117, 131, 252, 260, 272, 273, 275, 344, 349
 Fixed structures, 127
 Flood, 98, 187, 331, 343, 344
 Flooding, 187, 343
 FluSs, 4, 37, 94
 F-N curve assessment for multiple locally distributed events, 62–64, 257, 314, 315, 319, 320, 323–329, 335
 F-N diagram, 21, 52, 61–64, 252, 320, 322–324
 f-N diagram, 61, 62, 257, 314, 320, 325, 326
 F-N risk criteria, 325, 334
 Forensic risk analysis, 20
 Formalization, 234, 235, 246, 248
 Forward data analysis, 29
 Fragment, 1, 11, 115, 121, 122, 137, 141–150, 198, 200, 215, 255, 287, 293
 Fragment density, 148, 149, 152, 255. *See also* Fragment distribution
 Fragment effects, 198, 200, 348
 Fragment hazard, 144, 150, 188, 257, 288
 Fragment launch, 122, 137
 Fragment matrix, 143–145, 150
 Fragment trajectories, 138, 145
 France, 43, 68, 328, 333
 Fraud, 235, 271, 272, 276–278
 Fraunhofer EMI, 4, 6, 7, 10, 28, 62, 92, 98, 101, 117, 138, 167, 189, 206, 216, 235, 239, 272, 283, 348
 Free parameterization, 188, 198, 200, 202, 215
 Frequency, 11, 20, 105, 233, 235, 248
 Frequency and exposure time risk parameter, 263, 265
 Front side, 162, 163
 Functional safety, 3, 269
 Future aviation, 109
- G**
 Gabion, 148–150
 Gamma-radiation, 282, 297, 303–305
 Gaseous hazard source, 261
 Gas transmission, 236
 Gateway, 148, 149
 Gauge, 160–164
 Gaussian, 172, 192, 298. *See also* Normal distribution
 Gaussian plume model, 298
 Generalized fragment point source, 143, 145. *See also* Point source
 Geneva International Centre for Humanitarian Demining, 338, 341
 Geographical scenario data, 93
 Geo-location, 54, 137
 Geometrical 3D bodies, 216
 Geometrical scenario data, 93
 Geometry information, 187, 215
 Geometry of hazard source, 93. *See also* Hazard source
 Germany, 65, 70
 GIS, 260. *See also* Geo Information System
 Glass sphere, 126
 Glazing damage, 262
 Goodness, 61, 205, 210
 Goodness of fit, 205, 206, 210, 213
 Grade of burn, 301
 Graham, 168
 Graphical method, 205, 207
 Gravity force, 145
 Gray, 22, 303, 305
 Great Britain, 79–82, 84, 85
 Ground shock, 115, 120, 287, 288, 296, 310
 Ground zero, 122, 147, 152
 Group, 1, 13, 251, 253, 308, 317. *See also* Collective
 GTD, 41, 57, 235, 280, 283, 284, 309
 Gürke, 189, 194, 206, 209, 210, 212, 283
- H**
 Hail impact, 115
 Hands-on approach, 234
 Harbor, 281
 Harbor security, 4, 309
 Häring, 41, 272, 275, 283
 Hazard density, 138, 150
 Hazard effects, 115
 Hazard field, 115, 187
 Hazardous event, 92
 Hazardous zone, 265, 267
 Hazard potential, 187
 Hazard potential propagation, 115
 Hazard propagation, 20
 Hazard source, 2, 9, 15, 20–22, 52, 93, 115, 137–139, 145, 148, 149, 155, 167, 187, 234, 235, 239, 248, 255, 261, 275, 276, 278, 282, 283, 286, 298, 309, 315
 Hazard source characterization, 9, 20, 155
 Hazard source description, 9, 93, 137, 187. *See also* Hazard source
 HBX, 159, 291
 Health and safety executive, 7, 123, 314, 315, 319, 326, 327, 334. *See also* HSE
 Health risks, 331
 Hearing damage, 168. *See also* Ear injury
 Heat absorption, 296
 Heat absorption thresholds, 282

- Heat radiation, 120
Heat radiation hazard, 295
Heat transmission, 297
Heavy wind, 215. *See also* Storm
Helmet, 200
Hemispherical charges, 156
High explosion, 116, 123
High frequency but low severity risk, 323
High pressure vessels, 119. *See also* Liquefied petroleum gas
High-speed video, 122
Historical event frequency, 233
Historical frequency, 236
Hit function, 225, 226, 230
Homogeneity, 139
Homogeneous integration, 216
Hong Kong, 7, 328, 337
Hook's constant, 131, 132
Hopkinson-Cranz scaling, 128. *See also* Scaling law
Horizontal exit angle, 295
Hot Spot tool, 297
HSE, 7, 319, 326, 328–330, 333–336, 339
Hull, 138, 139, 141, 147, 150, 347
Humanitarian demining, 3, 314–317, 337–339
- I**
Ice rain, 215
Ideal explosion, 124
IEC, 268. *See also* International Electrotechnical Commission
IEC 61508, 262–265, 268, 269
Illicit goods, 281
IMAS, 338. *See also* International Mine Action Standard
Impact loading, 120
Improvised explosive device, 4, 16, 18, 120, 237, 285
Impulse equivalent mass, 159
Impulsive loading, 130, 132
Incident, 236
Incident thermal flux, 302
Incomplete analysis, 91
Independence, 236
Indirect damage assessment, 187
Individual, 251
Individual local risk, 2
Individual risk, 2
Individual risk acceptance criteria, 329
Individual risk criteria, 314, 328, 334–337
Individual versus collective risk, 252
Industrial research, 2
Information extraction, 34
- Infrastructure, 3, 20, 27, 94, 97, 101, 105, 108–110, 116, 188, 257–259
Initial situation, 20
Injury, 13, 170, 201, 210, 252–254, 283, 302, 317
Insurance, 15, 35, 98, 99, 102
Integrity level, 263, 265
Intentional explosion, 117, 118
Interaction with radiation, 297
Interdisciplinary, 2
International Electrotechnical Commission, 252, 263, 264, 265, 267. *See also* IEC
International mine action standards, 338.
See also IMAS
Internet, 100
Intersection, 30, 40, 42, 46, 141, 144
Involuntary risk, 13
Iodine-131, 304
Ionizing effects, 304
IR, 332, 333. *See also* Individual risk
ISO container, 292
- J**
Jarrett model, 298
Johansen, 7, 315–317, 319, 320
Justice, 102
- K**
Kinetic energy, 127, 132, 133, 201, 202, 231.
Kingery, 156–158, 190, 289
Kinney, 168
Klotz Group, 292–296
Knowledge Discovery, 28. *See also* Data mining
Kolmogorov-Smirnov test, 205
- L**
Lack of data, 205
Landslide, 314, 315, 328, 329, 331, 334
Latitude, 139. *See also* Coordinate system
Latitude bands, 143
Launch, 122
Launch velocities of container walls, 282
Least squares, 66
Legal, 350
Length scale of the explosive, 125
Lethal, 201. *See also* Abbreviated injury scale
Lethality, 200–202, 301
Life expectancy without the considered risk, 315, 318
Life threatening, 201. *See also* Abbreviated injury scale
Lightweight construction, 298
Likelihood, 20

- Likelihood method, 205
 Limiting cases of blast loading, 130
 Linear trend, 73, 87
 Liquefied gas, 314
 Liquefied petroleum gas, 119
 Liquid fuel tanks, 119
 LIRA, 319. *See also* Localized individual risk per annum
 LLY, 315. *See also* Lost life-years
 Loading mass, 298
 Local acting substances, 198
 Local coordinate system, 139. *See also* Coordinate system
 Local individual risk, 246
 Localization of hazard source, 115
 Localized individual risk per annum, 319.
See also LIRA
 Locally distributed event locations. *See* Collective
 Local risk, 13
 Location of event, 32
 Logarithmic scale, 64
 Logical bracket, 31, 221, 228, 255, 256
 Logit distribution, 188
 Lognormal distribution, 167, 172, 187, 188,
 197–199, 202, 205, 207, 209, 211, 213
 Longitude, 139. *See also* Coordinate system
 Longitudinal shock wave, 127
 Long term health effects, 318. *See also* LLY
 Loss of money, 252
 Lost life-years, 318. *See also* LLY
 Low explosion, 123
 Low frequency but high severity risk, 323
 LPG, 119. *See also* Liquefied petroleum gas
 Lung, 13, 198, 199, 209, 301, 303
 Lung injury, 301
- M**
- Mach number, 145, 146
 Malicious explosion, 115, 120
 Management-system, 94, 97
 Man-made threat, 1
 Manufacture, 102, 119, 316, 327, 330
 Mapping, 156
 Mass attenuation coefficient, 304
 Mass bin count, 294
 Mass distribution for fragments, 293
 Mass interval, 143, 144, 151, 256
 Mass loss, 293
 Mass of hazard source, 93
 Maximum blast overpressure, 155
 Mayrhofer, 344
 Mean, 167, 171. *See also* Expectation value
 Media, 7, 33, 77, 101, 102, 117, 133, 320, 321
- Membrane, 347
 Mercx, 199, 202
 Meridian, 139. *See also* Coordinate system
 Meteorological scenario data, 93
 Method, 2
 Micro cracks, 139
 Military, 16, 18, 102, 117, 118
 Mine clearance, 341. *See also* Humanitarian demining
 Minimum risk reduction, 263, 265
 Ministry, 94, 98, 99, 338
 Mitigation measure, 15, 20, 21, 24, 52, 53, 93,
 343–345, 349–352
 Mixed/Iterative data analysis, 30
 Momentum conservation, 132
 Momentum method, 205
 Monte Carlo computation of presented surfaces, 223
 Monte Carlo integration, 215, 216, 226, 227
 Mortality per year, 331, 332
 Movable structure, 127
 Multidisciplinary, 20
 Multifunctional hull (facade), 347
 Multinational, 20
 Multiple degree of freedom model, 133
 Multiple weighted events, 259
 Multiplicative trend removal, 71, 73
- N**
- Natural explosions, 117, 118
 Natural risks, 13, 331
 Natural-technical threat, 1
 Natural threat, 1
 Near field, 125, 137, 346
 Neighborhood, 253, 259
 Net explosive quantity, 282
 Netherlands, 63, 332–334, 336, 337
 Neutron radiation, 282, 305
 Newspaper, 100
 Newton's second law, 145
 N-like blast wave, 125
 Non-cumulative, 62
 Non-local individual risk, 247
 Non-local risk, 13
 Non-modular analysis approach, 91
 Non-parametric approach, 212
 Non-proprietary software, 282
 Normal distribution, 171, 182, 188, 192, 193,
 194, 199, 207, 210. *See also* Gaussian
 Normalization condition, 150, 259
 Normal vectors of the plane, 220
 Norway, 18, 333
 Nuclear, 118, 123, 281, 284, 286, 287, 296,
 302, 305, 308, 318, 326, 328, 330, 331

- Number of persons of given type, in given objects and time spans, 247
Numerical integration, 215
Numerical Lagrange-particle-model, 298
Numerical simulation, 5, 97, 160, 292, 293
- O**
Object distribution, 21, 93
Object exposure densities, 216
Objective, 11
Objective risk, 13
Occupancy, 267
Occupational safety, 3
Occupation pattern, 242
Octol, 159
Office building, 98, 99, 298
One-dimensional probability distribution, 198, 213
Organizational measures, 234, 344
Orientation of hazard source, 93
Orthogonal projection, 220, 223
Outside of 3D object, 220
Overload, 98
Overpressure, 288
- P**
Parameterization of the blast hazard, 116
Paraplegia, 319
Particle motion, 127
Peak pressure equivalent mass, 159
PED, 333. *See also* Probability of exposure of a dangerous dose
Pentolite, 159
Perceived risk, 13
Preformed fragment, 151
Permitted maximum additional risk, 331
Person damage, 107
PETN, 121, 148, 152, 158, 159, 291
Phases of explosive material, 117
Phenomenological characterization, 133
Phosphor-31, 303
Physical accessibility, 260
Physical consequences of explosions, 116, 134
Physical-engineering modelling, 215
Physical hazard, 2, 187
Physical hazard analysis, 189
Physics based analysis, 190. *See also* Indirect damage assessment
Picratol, 159
Pipe, 236
Pipe bomb, 139
Pipeline, 236
Point estimator, 211
Point fragment source, 116
Point source, 116, 124, 125, 133, 139, 143, 145
Polar geocentric coordinates, 139. *See also* Coordinate system
Policy, 16
Politics, 20, 102, 104
Position, 20, 52, 93, 127, 131, 133, 139, 144, 145, 147, 150, 162, 179, 191, 216, 217, 239, 253, 258, 259, 262, 317, 319, 328, 343
Position of hazard source, 93
Position of objects, 217
Possibility of failing to avoid hazard risk parameter, 263. *See also* Averaging
Possible event, 91
Potential energy, 127, 131
Power plant, 99, 305, 308
Power supply, 102. *See also* Power plant
Prediction model, 61
Preparation, 1
Presented surface, 141, 188, 213, 215, 216, 218, 220, 221, 222, 223, 224, 226, 228–232
Presented surface of a cylinder, 222
Presented surface of a sphere, 221
Presented surface of cuboid, 218
Pressure-impulse diagram, 101
Pressure loading, 132, 133
Pressure range, 159
Pressure-time history, 127
Pressure-time loading history, 116
Prevention, 1
Preventive risk analysis, 20
Primary injuries by blast, 301
Priorization, 110
Private housing, 102
Probabilistic, 93
Probabilistic damage assessment, 167
Probability, 11, 167, 170. *See also* Cumulative probability distributions
Probability density function, 167, 168
Probability of event pre-assessment, 92
Probability of the unwanted occurrence, 263, 266
Probability paper, 207
Probit, 187
Process plants, 269
Process step, 20
Progressive collapse, 97–99, 262, 346
Propagation of fragment trajectory, 225
Propagation of multiple trajectories, 152
Proske, 280
Protection, 1
Protective structure, 149, 151, 276, 346–348.
See also Protective material
Protective wall, 346
Public places, 102

- Public transport, 272
 Public underground traffic system, 271
- Q**
QALY, 318. *See also* Quality adjusted life-years
 Quadratic trend, 71
 Qualitative risk levels, 44, 108
 Qualitative methods, 5, 146
 Quality adjusted life-years, 318. *See also* QALY
 Quantitative risk analysis, 3, 16, 26, 139.
See also QRA
 Quasi-random distribution, 228. *See also* Storm
 Quasi-static loading, 130
 Quick assessment of counter measures, 350
- R**
 Radiated emission power, 296
 Radiation, 282
 Radiation field, 282
 Radiation weighting factor, 303
 Radiologic hazard, 281
 Radiological material, 282
 Radium, 303
 Radon, 303
 Random point, 226, 227
 Random variable, 180, 192
 Range Commander Council, 201
 Rathjen, 7, 167, 235, 315
 Raw data, 27, 199, 206, 294
 RDX, 159
 Real distance, 159
 Real time risk analysis, 20
 Real word scenario, 233
 Recovery, 1
 Reduction factor, 145
 Reduction of effects of hazards, 234
 Reflected, 127
 Reflection, 162. *See also* Tunnel
 Regression, 207
 Regulation, 350
 Reinforced concrete, 300
 Reinforcement measures, 343
 Relational database, 27, 54. *See also* Database
 Relative biological effectiveness, 303
 Relative blast impulse, 155
 Relevant surface, 216, 228
 Religion, 37, 102
 Rem, 305
 Repair time, 262
 Representative fragment, 144, 150, 152, 256
 Resampling method, 205
- Research, 1–7, 33, 34, 76, 92, 94, 99, 100, 102, 194
 Research program, 3
 Research project, 6
 Residential buildings, 298
 Residual energy, 127
 Resilience, 1
 Resilience engineering, 2
 Resilience enhancement, 4, 252
 Resilience quantity, 252
 Resiliency, 6, 92, 155, 264. *See also* Resilient systems
 Resilient systems, 252
 Resonance, 160
 Response, 1
 Retail, 102, 106
 Retrofit, 348
 Reversible, 201. *See also* Abbreviated Injury Scale
 Riedel, 7, 252, 261, 269, 280
 Risk analysis, 2, 13
 Risk analysis examples, 271
 Risk analysis modeling steps, 17
 Risk and equity, 316
 Risk and state of practice of technology, 316
 Risk and utility, 316
 Risk assessment, 1, 21
 Risk assessment criteria, 313
 Risk aversion, 63, 79, 264, 314, 324, 329, 334
 Risk aversion and F-N curve, 63, 323
 Risk aversion criterion, 63, 79, 323, 324.
See also F-N curve
 Risk classification, 13
 Risk communication, 1, 21
 Risk comparison, 21
 Risk computation, 9, 13, 15, 21, 108, 215, 251, 255, 276, 282, 310
 Risk contour, 315, 319, 332, 333. *See also* Risk map
 Risk criteria based on prescribed maximum level of risk, 333
 Risk criteria based on risk goals, 333
 Risk criteria based on tolerated consequences, 333
 Risk criteria by sectors, 328
 Risk criteria for humanitarian demining, 337
 Risk criterion, 63, 264, 276, 324
 Risk diagram, 61
 Risk evaluation, 1, 15, 21
 Risk graph, 251, 263, 264, 268, 269
 Risk identification, 1, 15
 Risk management, 1, 13
 Risk management context, 1
 Risk management process, 13

- Risk management step, 13
Risk map, 76, 108
Risk matrix, 251, 262, 269, 261, 313, 336
Risk mitigation, 15
Risk of death of 1 in 10,000 per annum, 327
Risk of death of one in a million per annum, 326
Risk of death of one in a thousand per annum, 326
Risk on demand, 13
Risk per time, 13
Risk quantity, 12, 253
Risk table, 21, 52, 252, 314
Risk treatment, 15
Risk visualization, 21, 313
Risk zones, 308. *See also* Collective
Risk-based decision, 18
Risks for explosives storage, 330
Risks per event, 13
Risks with very high fatality numbers, 323
Road damage, 262
Rocket, 284
Roentgen equivalent in man, 305
Runaway reaction, 248
Runge-Kutta, 146
- S**
Sach's scaling law, 129. *See also* Scaling law
Safety distance, 333, 338, 339
Safety engineering, 4, 6, 17
Safety factor for humans, 198
Safety function, 234
Safety glass, 348
Safety of machinery, 269
Safety research, 2
Sailing effect, 147. *See also* Fragment trajectory
Sauer, 283, 300, 301
Scale, 7, 27, 28, 64, 65, 79, 110, 129, 134, 160, 162, 191, 331
Scale factor, 129
Scaled blast impulse, 157
Scaled distance, 129, 130, 134, 156, 190, 290, 299
Scaled experiments, 155
Scaling factor, 155
Scaling law, 128, 129
Scaling laws for explosions, 116
Scanner, 283
Scenario, 93
Scenario data, 189
Scenario-based approach, 15, 94
School, 105, 106
Second order effect, 20
Secondary facade, 344, 347
Secondary risks, 344
Security by design, topological security design, 345
Security concept, 109
Security research, 2, 3
Security technology, 94
Semi-quantitative assessment, 286
Semi-quantitative ranking, 281
Semi-quantitative risk assessment, 13
Semi-quantitative risk matrix, 262
Semtex, 291
Sensitive presented surface, 230
Separation of blast wave, 125
Severity of event, 27
Set of types of objects, 246
Shelter, 138, 128, 216
Shielding material, 304
Shock front, 123
Shock wave in air, 116
Side-on overpressure, 157
Side-on-pressure, 127, 289
Siebold, 6, 7, 28, 41, 44, 62, 64, 66, 74, 272, 280, 344, 351
Sievert, 303
Sight-protecting curtains, 248
Signature, 286
Simulative approach, 187, 255, 257, 258, 261. *See also* Simulation
Simultaneous attacks, 285
Single degree of freedom, 130
Single degree of freedom model, 116, 130, 133
Skin, 297
SKRIBT, 4
Smoothing, 61, 62, 65, 73–75
Smuggled goods, 286
Social institutions, 102, 106
Social risks, 13, 331
Societal risk criteria, 328, 335, 338, 339
Societal risk tolerance criteria, 329
Societal security research, 2, 3. *See also* Security research
Society's attitude, 278
Software application tool, 5
Software support, 20
Soil, 147, 297, 348
Solid angle, 143
Spatial distribution density, 259
Spatial exposure profile, 251
Specially shaped fragments, 146
Specific blast impulse, 116. *See also* Blast impulse
Speed, 124, 145, 292, 293, 303
Speed of sound, 145

- Sport, 102, 237, 336
 Sports event, 237
 Spreadsheet applications, 194, 205
 Squip, 119
 Stadium, 98, 100
 Stakeholder, 20
 Standard deviation, 167, 171, 172, 180
 Standard normal distribution, 171, 194.
See also Normal distribution
 Standardized, 20
 Standoff distance, 344
 START, 235
 Static loading, 14, 116, 130, 131
 Static loading of structures, 116
 Statistical historic risk, 13
 Statistical time series model, 61
 Statistical-empirical methods, 5, 282
 Step, 187
 Step-wise approach, 233
 Stochastic linear correlation, 208
 Stock exchange, 98
 Stockholm, 311
 Stoltz, 92, 272, 344, 347–349
 Storage of explosives, 119
 Storm, 93, 98, 331
 Straight street, 160
 Streblow, 119, 123, 124, 127
 Strong wind, 115
 Structural loading, 120
 Structural reinforcement, 344
 Sub system, 233
 Subjective risk, 13, 306
 Substitution, 181, 182, 195
 Suicide bomb, 96, 120. *See also* IED
 Suitcase bomb, 96. *See also* IED
 Super bomb, 120
 Superficial, 201. *See also* Abbreviated Injury Scale
 Superposition, 160
 Surface discretization, 218
 Surrounding media of an explosion, 117.
See also Explosion
 Surveillance, 344
 Susceptibility, 260, 261. *See also* Probability
 Susceptible, 101, 106
 Sweden, 333
 Swisdak, 156
 Symbolic value, 106, 107
 Symmetry, 139
 Systematically acting toxic substance, 198
- T**
 Table of hazards, 284, 286, 287
 Tabular approach, 235
- Tactic, 32, 36, 38, 41, 43–46, 50, 94, 96, 285.
See also Terrorist event
 Tamed explosion, 117, 118
 Tank, 93, 97, 119, 248, 347
 Target resolution, 103, 104, 105
 Target systems, 38, 101
 Tatom, 283, 292–296
 Technical development, 2
 Technical risk, 13, 331
 Technical safety, 234
 Technogenic hazard, 115
 Tensile energy, 127
 Terminal, 4, 96, 97, 283, 308
 Terror, 3, 28, 75, 92, 98, 109, 248, 257–260,
 274, 278
 Terror attacks with hand-held weapons, 248
 Terror event, 1, 3, 28, 37, 41, 65, 76, 92, 94,
 98, 108, 160, 257–260, 278
 Terror event attribute, 27, 32
 Terror event localization around building
 entries, 15, 98, 259
 Terrorist attack, 93, 94, 96, 99, 109, 235, 272,
 279, 307
 Terrorist event, 32, 34, 41, 43, 96, 101, 111,
 235, 272, 284
 Terrorist Event Database (TED), 27, 28, 33, 34,
 36–38, 41, 42, 50, 54, 57, 62, 96, 98–101,
 109, 112, 272, 283, 284, 309. *See also*
 Terror event database (TED)
 Terroristic explosion, 115, 120
 Test, 75, 116, 120, 121, 122, 126, 141, 142,
 146–153, 162, 198, 205, 206, 209, 210,
 213, 264, 290, 292, 293
 Tetryl, 159
 Tetrytol, 159
 Theoretical models describing explosive
 sources, 118
 Theoretical risk, 323
 Thorium, 303
 Threat event tactic analysis, 94, 284, 286, 309
 Threat scenario, 11, 271
 Throw, 120
 Time, 20
 Time-dependent risk, 91, 138, 233, 251, 282,
 303
 Timeframe, 110
 Time rate of energy release, 124
 Time series analysis, 61, 62, 75, 76, 79
 Time-independent risk, 251
 T-junction, 160
 TNT equivalent, 100, 124, 145, 155, 158, 164,
 189, 290, 291, 300
 Tolerable, 303, 316, 319, 334
 Tolerable risk, 268, 306, 315, 330, 337

- Tool, 4, 5, 16, 25, 28, 39, 51, 62, 138, 180, 252, 260, 275, 293, 351
Topological scenario data, 50, 93
Total damage, 278, 308
Total number of fragments, 150
Total population, 253
Total time constraint, 246
Tourism, 70, 76, 102, 106, 108
Toxicity, 282
Toxic substance, 198
Training, 234
Training of models, 61
Trajectory, 122
Trajectory-based hazard assessment, 167
Transformation, 188
Transport, 4
Transport infrastructure, 94
Travel, 102, 327
Trend detection, 61
Trend polynomial, 68, 75, 80, 86
Tritium, 303
Truck, 223
Tube, 11, 160, 348
Tumbling of fragements in air, 141
Tunnel, 4, 98, 128, 275. *See also* Tube
Type of explosive, 124, 139
Type of injury, 199
Type of threat event, 91
- U**
UFC, 352. *See also* Unified facilities criteria
UK Health and Safety Executive, 314.
See also HSE
UN, 274, 330, 339
Unacceptable, 319, 326, 327. *See also* LIRA
Uncertainty, 11, 282, 339. *See also* IMAS
Underground explosion, 117
Underwater explosion, 117
Unexploded ordnance, 338. *See also* UXO
Unified Facilities Criteria, 344, 352
Union, 4, 30, 31, 40, 315, 355
Unknown parameters, 209, 216
Upper bound of interval, conservative assessment, 143, 144, 256
Uranium, 303
Urban asset, 261
Urban geometry, 2, 127, 155, 156, 160, 162, 260
Urban risk, 101
Urban risk and resilience analysis, 101
Urban security, 92, 343
- US, 285, 331, 332
USS Cole, 285
UXO, 338. *See also* Unexploded ordnance
- V**
Validation, 20, 115, 155, 165, 236
Validation of computational approaches, 116, 155
Value of increased mortality, 331
Vapor, 118, 119
Variance of the estimator, 227
VBIED, 120
Vector length, 173, 176, 177, 180, 184
Vector scalar product, 167, 172, 173, 180
Vehicle born IED, 120, 345
Velocity of hazard source, 20, 52, 93
Venting, 122, 128, 160, 261, 346
Vertical exit angles, 293, 295
Virtual environment, 20
Visualization, 5, 9, 20, 21, 24, 35, 51, 75, 252, 260, 261, 269, 276
Voluntary risk, 13
Vulnerability, 4, 109, 267, 267. *See also* Damage
Vulnerability of urban areas, 259, 260
- W**
Water supply, 54, 102, 106
Waterwall, 347
Weibull distribution, 199, 205–212
Weighted backward SMA, 65
WGS84, 140, 141. *See also* Coordinate system
What-if damage, 254
What-if hazard zone, 281
Wind effect, 138, 343
Window, 71, 73, 116, 142, 148, 230, 298–300, 345, 346, 348
Wire mesh, 347, 348
Worldwide, 95, 96, 105, 106, 109
Worst-case, 20, 100
Woven structure, 347
- Y**
Yemen, 285
- Z**
Zero forecast, 72, 74, 75, 80, 87, 88
Ziehm, 92, 94–97, 109, 110. *See also* Weissbrodt